Identification and Characterisation of Post-Translational Modifications that Regulate Human PrimPol

A thesis submitted to the University of Sussex for the degree of Doctor of Philosophy

Rebecca Teague

June 2021

I hereby declare that this thesis has not been and will not be submitted in whole or in part to another University for the award of any degree.

Rebecca Teague

University of Sussex

Rebecca Teague

Doctor of Philosophy, Genome Stability

Identification and Characterisation of Post-Translational Modifications that regulate Human PrimPol

Summary

DNA replication is hindered by lesions and obstacles arising both endogenously and exogenously, which stall the replication machinery, leading to DNA replication fork stalling or collapse. DNA damage tolerance (DDT) pathways allow the replisome to bypass impediments without impairing replication. One such DDT pathway involves repriming DNA synthesis and is mediated by Primase-Polymerase (PrimPol) in human cells. How this pathway is regulated and deployed during the cell cycle or following damage is poorly understood.

This thesis investigates the regulation of PrimPol by post-translational modifications. We establish that PrimPol is phosphorylated at key amino acid residues in PrimPol's C-terminus by cell-cycle kinases. Chapter 3 investigates the role of serine 538 phosphorylation. We establish that this modification is performed by Polo-like kinase 1, with increasing phosphorylation occurring in G2 and mitosis and its delay or reversal in response to replication stress. When this residue was mutated to prevent phosphorylation, cells exhibited increased sensitivity to genotoxic agents, aberrant recruitment of PrimPol to chromatin, and increased genomic instability.

Chapter 4 investigates serine 499 phosphorylation, establishing that this modification is performed by cyclin-dependent kinase 1 (CDK1) and regulated during the cell cycle. S499 phosphorylated and unphosphorylated PrimPol is maintained across G1 and S phase and prevention of this modification induces sensitivity to UV-C damage and replication stress induced by aphidicolin, camptothecin and olaparib.

Finally, Chapter 5 describes the generation of a cell line, expressing endogenous levels of PrimPol tagged with a fluorescent label, as a tool for enabling a better understanding of the localisation and recruitment of PrimPol protein.

Together, these studies establish the critical role of post-translational modifications in the regulation of PrimPol's activities and recruitment during the cell cycle and in response to DNA damage. This study defines important regulatory pathways and reveals the deleterious consequences that deregulated repriming has on cell survival and genome stability.

Acknowledgements

The first and most important thank you must go to my supervisor, Professor Aidan Doherty. Working on this project, with the excellent group of scientists he has assembled, was a real privilege, and I'm extremely grateful for the opportunity. I also wish to thank the members of my committee, Dr Helfrid Hochegger, Dr Jon Baxter and Dr Chris Chan, for their help over the last four years.

I am grateful to all the members of the Doherty lab for their help and guidance. Special thanks go to Dr Laura Bailey, for sharing the human PrimPol project with me, teaching me everything I know, and for never once ignoring my questions, no matter how inane or annoying.

This thesis, and the last four years, would not have been possible without my friends, family, and partner. To my parents, thank you for your support. It's okay if this is the only page of this thesis you read. Thank you to Adrijana Crncec for reading this whole thesis and keeping me sane, even from 10,000km away. Finally, to my partner, Billy: thank you for making me coffee in Starbucks 9 years ago, and for everything that has happened since.

Table of Contents

Abbreviations

6-4PP	Pyrimidine (6-4) pyrimidone photoproduct
8-oxo-dG	8-oxo-2'-deoxyguanosine
aa	Amino acid
AEP	Archaeo-eukaryotic primase
AND-1	Acidic nucleoplasmic DNA-binding protein
A-NHEJ	Alternative non-homologous end joining
APS	Ammonium persulphate
ATM	Ataxia telangiectasia mutated
ATP	Adenosine triphosphate
ATR	Ataxia telangiectasia and Rad3-related kinase
ATRIP	ATR-interacting protein
BER	Base excision repair
BLM	Bloom syndrome helicase
BPDE	Benzo(a)pyrene diol epoxide
BRCA1	Breast cancer Type 1 susceptibility protein
BRCA2	Breast cancer Type 2 susceptibility protein
CDK	Cyclin-dependent kinase
CDT1	CDC10 target 1
Chk1	Checkpoint kinase 1
CldU	5-chloro-2'-deoxyuridine
Cm	Chloramphenicol
CMG	CDC45, MCM2-7, GINS helicase
CPD	Cyclobutane pyrimidine dimer
CPT	Camptothecin
CRISPR	Clustered regularly interspaced short palindromic repeat
CTD	C-terminal domain
C-terminus	Carboxyl-terminus
Ctf4	Chromosome transmission fidelity protein 4
CTNA	Chain-terminating nucleotide analogue
DDT	DNA damage tolerance
DMEM	Dulbecco's modified eagle's medium
DMSO	Dimethyl sulfoxide
DNA	Deoxyribonucleic acid
DNA2	DNA replication helicase/nuclease 2
DNAPK	DNA-dependent protein kinase

dNTP	Deoxynucleoside triphosphate
Dox	Doxycycline
DSB	DNA Double-strand break
DSBR	DNA Double-strand break repair
dsDNA	Double-strand DNA
E. coli	*Escherichia coli*
EDTA	Ethylenediaminetetra-acetic acid
EGTA	Ethyleneglycoltetra-acetic acid
Exo1	Exonuclease 1
FACT	Facilitates chromatin transcription
FANCJ	Fanconi anemia group J protein
FANCD2	Fanconi anemia group D protein 2
FCS	Fetal calf serum
FEN1	Flap endonuclease 1
FWD	Forward
G1-phase	Growth-phase 1
G2-phase	Growth-phase 2
GINS	Go-ichi-ni-san
H3	Histone H3
HEK293	Human embryonic kidney cell line 293
HIV	Human immunodeficiency virus
HLTF	Helicase-like transcription factor
HR	Homologous recombination
ICL	Inter/intra-strand crosslink
Indel	Insertion-deletion
IR	Ionising radiation
Kb	Kilobase pair
LIG	Ligase
LRR1	Leucine-rich repeat protein 1
MCM	Mini-chromosome maintenance
MMEJ	Microhomology-mediated end joining
MMR	Mismatch repair
MMS	Methylmethanesulfonate
mRNA	Messenger RNA
MS	Mass spectrometry
MRC-5	Medical Research Council cell line 5
MRN	MRE11-RAD50-NBS1

mtDNA	Mitochondrial DNA
MTS	Mitochondrial targeting sequence
mtSSB	Mitochondrial single-strand binding protein
NER	Nucleotide excision repair
NHEJ	Non-homologous end-joining
NTD	N-terminal domain
N-terminus	Amino-terminus
OLP	Olaparib
ORC	Origin recognition complex
P-S538	Phosphorylated Serine 538
P-S499	Phosphorylated Serine 499
PAGE	Polyacrylamide gel electrophoresis
PARP	Poly(ADP-ribose) polymerase
PAXX	Paralogue of XRCC4 and XLF
PBS	Phosphate-buffered saline
PCNA	Proliferating cell nuclear antigen
PCR	Polymerase chain reaction
PFAH	Paraformaldehyde
Pi	Inorganic phosphate
PIPES	Piperazine-N,N'-bis(2-ethanesulfonic acid)
Pol	Polymerase
PPL	PrimPol-like protein
Pre-IC	Pre-initiation complex
Pre-RC	Pre-replication complex
PriL	DNA primase large subunit (archaeal)
Prim1	DNA primase small subunit (eukaryotic)
Prim2	DNA primase large subunit (eukaryotic)
PrimPol	Primase-Polymerase
PriS	DNA primase small subunit (archaeal)
Rad	Radiation (gene)
RBD	RPA-binding domain
RBM	RPA-binding motif
Rev	Reversionless (gene)
RFC	Replication factor C
RNA	Ribonucleic acid
rNTP	Ribonucleotide triphosphate
ROS	Reactive oxygen species

RPA	Replication protein A
SCJ	Sister chromatid junction
SDM	Site-directed mutagenesis
SDS	Sodium dodecyl sulfate
S-phase	Synthesis-phase (cell cycle stage)
SSB	Single-strand break
SSBR	Single-strand break repair
ssDNA	Single-stranded DNA
TDP1	Tyrosyl-DNA phosphodiesterase 1
TdT	Terminal transferase
TEMED	N,N,N',N'-Tetramethylethylenediamine
TLS	Translesion synthesis
Tm	Melting temperature
Tof1	Topoisomerase 1-associated factor 1
TOP	Topoisomerase
TOPRIM	Topoisomerase-primase fold
TRAIP	TRAF-interacting protein
TS	Template switching
UBM	Ubiquitin-binding motif
UBZ	Ubiquitin-binding zinc finger
UFB	Ultra-fine bridge
UV	Ultraviolet
WRN	Werner syndrome helicase
WRNIP1	WRN-interacting protein 1
XLF	XRCC4-like factor
XP	Xeroderma pigmentosum
XPV	Xeroderma pigmentosum variant
XRCC	X-ray cross complementation protein
ZnKO	Zinc finger knockout
ZnF	Zinc finger

List of Tables

List of Figures

Chapter 1

Introduction

In all living cells, hereditary information is stored in the form of complementary double-stranded DNA (dsDNA). This information provides specific instructions to the cell, which control everything from cell growth to programmed death, and the processes in between. In order to pass this genetic information down to new daughter cells, genome duplication must be performed to faithfully copy the complete set of instructions (the genome) from each parental cell. This is achieved by a biochemical process called DNA replication. This process has to be highly accurate and must happen only once per cell division: any perturbation must be rectified quickly and with minimum disruption to the replication process or to the integrity of new DNA strand. This thesis focuses on the mechanisms employed to maintain genomic integrity, while preventing the disruption of DNA replication. To understand this, however, we will first discuss the general process of DNA replication and the cell cycle, followed by the conventional DNA repair mechanisms employed outside of DNA replication. Additionally, we will discuss DNA damage tolerance mechanisms – the pathways utilised when repair mechanisms have failed, to tolerate obstacles that impede the DNA replication process. Finally, we will discuss a newly discovered replicase called **Prim**ase-**Pol**ymerase (PrimPol), our current understanding of its role in maintaining ongoing DNA replication, and outstanding questions regarding its place in the DNA damage tolerance landscape.

1.1 DNA polymerases and DNA replication

1.1.1 The DNA polymerases

Human cells encode 16 different DNA polymerase enzymes (Johansson and Dixon, 2013). The primary function of these enzymes is to ensure that cells can replicate their DNA; it is vital that this copying process occurs with high fidelity to ensure that mistakes are not made or propagated. Polymerases can be crudely divided into those responsible for the bulk of replication, and those with more specialised roles. Replicative polymerases, including Pol ε, δ and γ, duplicate the bulk of the genome. The fidelity of this process relies on the nucleotide selectivity and proofreading ability of these polymerase (Bębenek and Ziuzia-Graczyk,

2018). Based on sequence homology and structural similarities, DNA polymerase enzymes can be further categorised into six groups: A, B, C, D, X and Y (Acharya et al., 2020). The C family are only present in bacteria and share no sequence homology with any of the other DNA polymerase families (Lamers and O'Donnell, 2008), and family D polymerases are present in archaea, but not in eukaryotes, and therefore will not be discussed further (Burgers et al., 2001).

Members of the A, B, X and Y families and their specific roles are summarised in Table 1.1. All DNA polymerases generally conform to a conserved general structure, and act using a similar two metal ion-dependent catalytic mechanism (Steitz and Steitz, 1993). Briefly, DNA polymerases extend the DNA from primers in the 3’ direction, using a single-stranded (ss) DNA template. These RNA primers, in most cases, must be made by a separate class of replicase enzymes known as primases, which are DNA-dependent RNA polymerases. The extension from the primer involves deoxynucleotide triphosphates (dNTPs) being paired to their partner templating base (adenine with thymine, cytosine with guanine) using hydrogen bonds (Watson and Crick, 1953). DNA polymerases then catalyse - using two metal ion-dependent catalytic mechanism - the nucleophilic attack of the 3’ hydroxyl moiety on the α-phosphate group of the dNTP, which allows a phosphodiester bond to form between the backbone of the primer and the new nucleotide (Rothwell and Waksman, 2005).

Table 1.1. Eukaryotic DNA polymerases

A table presenting four DNA polymerase families and their 15 DNA polymerases (excluding PrimPol), and their role in human cells. Information obtained from (Goodman and Woodgate, 2013; Lujan et al., 2016).

Polymerase Family	**Polymerase name**	**Role**
A	Pol θ	Alternative end joining
	Pol ν	Homology directed repair at strand crosslinks
	Pol γ	Replication of the mitochondrial genome
B	Pol α	Replication initiation
	Pol δ	Replication of lagging strand
	Pol ε	Replication of leading strand
	Pol ζ	Translesion synthesis, homologous recombination
X	Pol β	Base excision repair
	Pol μ	Non-homologous end joining, base excision repair, translesion synthesis
	Pol λ	Non-homologous end joining
	TdT	Antibody gene recombination
Y	Pol η	Translesion synthesis
	Pol ι	Translesion synthesis
	Pol κ	Translesion synthesis
	Rev1	Translesion synthesis, TLS regulation by polymerase switching

1.1.2 Eukaryotic DNA replication

During the synthesis phase (S phase) of the eukaryotic cell cycle, genome duplication is performed by the replisome. This multi-protein complex consists of the major replicative enzymes required to accurately duplicate DNA. Replisome proteins include the DNA polymerases α, δ and ε, the Cdc45-MCM-GINS (CMG) DNA helicase complex, as well as additional proteins such as AND-1 (*Saccharomyces cerevisiae* Ctf4), Timeless (Tof1), Claspin (Mrc1), Tipin (Csm3), Topoisomerase I, Mcm10, Replication protein A (RPA) and FACT (Baretić et al., 2020; Gambus et al., 2006).

Replisome assembly begins in G1 phase with the binding of the minichromosome maintenance (MCM) complex to defined loci known as origins of replication (Lei, 2005). Loading of the MCMs to origins is dependent on prior binding of the Origin Recognition Complex (ORC), comprised of ORC1-6, and the proteins Cdc6 and Cdt1 (Wohlschlegel et al., 2000). The MCM replicative helicase is loaded onto DNA as an inactive, double hexamer structure (Evrin et al., 2009), and is activated when DNA replication begins at the beginning of S phase (Deegan and Diffley, 2016). The activation process remodels the MCM complex into two active CMG complexes, one for each direction of synthesis. Encircling each leading DNA strand, the active complex moves away from the centre of the origin and allows for the assembly of the remaining replisome components on the resulting single-stranded DNA (ssDNA) (Fu et al., 2011). These complexes are activated by the activity of CDC7 and cyclin-dependent kinase enzymes (CDKs) (Takeda and Dutta, 2005). This process is summarised in Figure 1.1A. The DNA replication fork describes the site at which DNA unwinding and DNA replication occur, through the activity of the replisome.

While the bulk of synthesis is completed by the major replicative polymerases, these enzymes lack the ability to initiate DNA synthesis *de novo*. Therefore a short ribonucleotide primer is required, from which 3’ extension can be continued by the replicative polymerases (Kuchta and Stengel, 2010). In the conventional model, the initiating primers on both the leading and lagging strand are generated by the Pol α-primase complex. The primase subunit synthesises a short RNA primer de novo, from which Pol α extends using dNTPs to create an RNA-DNA

primer. This is then further extended by a primary replicative polymerase with proofreading capacity, to ensure high fidelity synthesis. Initial extension is performed by Pol δ, which then either hands off to Pol ε to replicate the leading strand, or Pol δ continues to synthesise the lagging strand (Figure 1.1B) (Clausen et al., 2015). However, Pol δ has also been shown to conduct synthesis on both strands in yeast, both during bulk replication and following recombination-mediated replication restart (Guilliam and Yeeles, 2020; Miyabe et al., 2015). All polymerases exclusively synthesise DNA in a 5' to 3' direction. For this reason, the lagging strand is synthesised in short, discontinuous fragments known as Okazaki fragments, as the DNA is unwound to allow coupled unidirectional replication to occur (Lujan et al., 2016; Miyabe et al., 2011). These discontinuous fragments are processed when Pol δ meets the primer and displaces it, leaving it as a flap which Fen1 will instantly digest. The nick is then ligated by Ligase 1, with displacement and ligation occurring in iterative cycles (Figure 1.1C).

Termination of DNA replication occurs either when converging replication forks meet or when the end of the chromosome is reached (Dewar and Walter, 2017). The replication machinery is then unloaded by the ATPase p97 (Cdc48 in *Saccharomyces cerevisiae*), to prevent re-replication of DNA (Franz et al., 2011). Unlike replication initiation, which is well studied in eukaryotes, replication termination has received significantly less attention. The mechanisms for human DNA replication termination are not well characterised, and the current understanding of replication termination somewhat incomplete. Briefly, termination occurs in eukaryotes through the action of two pathways, one consigned to S phase and the other taking place in mitosis. S phase termination occurs whenever replication forks converge, and this pathway is dependent on the polyubiquitylation of K48 of Mcm7, a subunit of the CMG (Maric et al., 2014; Moreno et al., 2014). It is not clear what performs this polyubiquitylation in humans; in *Saccharomyces cerevisiae*, it is performed by SCF-Dia2 (Maric et al., 2014), in metazoans it is linked to Cullin2-LRR1 (Dewar et al., 2017; Sonneville et al., 2017) (Figure 1.1D). The termination that occurs in mitosis is controlled differently, through ubiquitylation of Mcm7 by TRAIP (Moreno et al., 2019). In both pathways, polyubiquitylation serves as a signal for degradation of the replisome from chromatin by the segregase VCP (p97). It is unclear which

proteins are responsible for replication termination in humans, though both TRAIP and Cullin2-LRR1 are conserved and essential for cell viability – though, as TRAIP has been shown to play a role in both mitosis and DNA repair (Chapard et al., 2014; Harley et al., 2016), this may be due to their activity in these pathways and not replication termination.

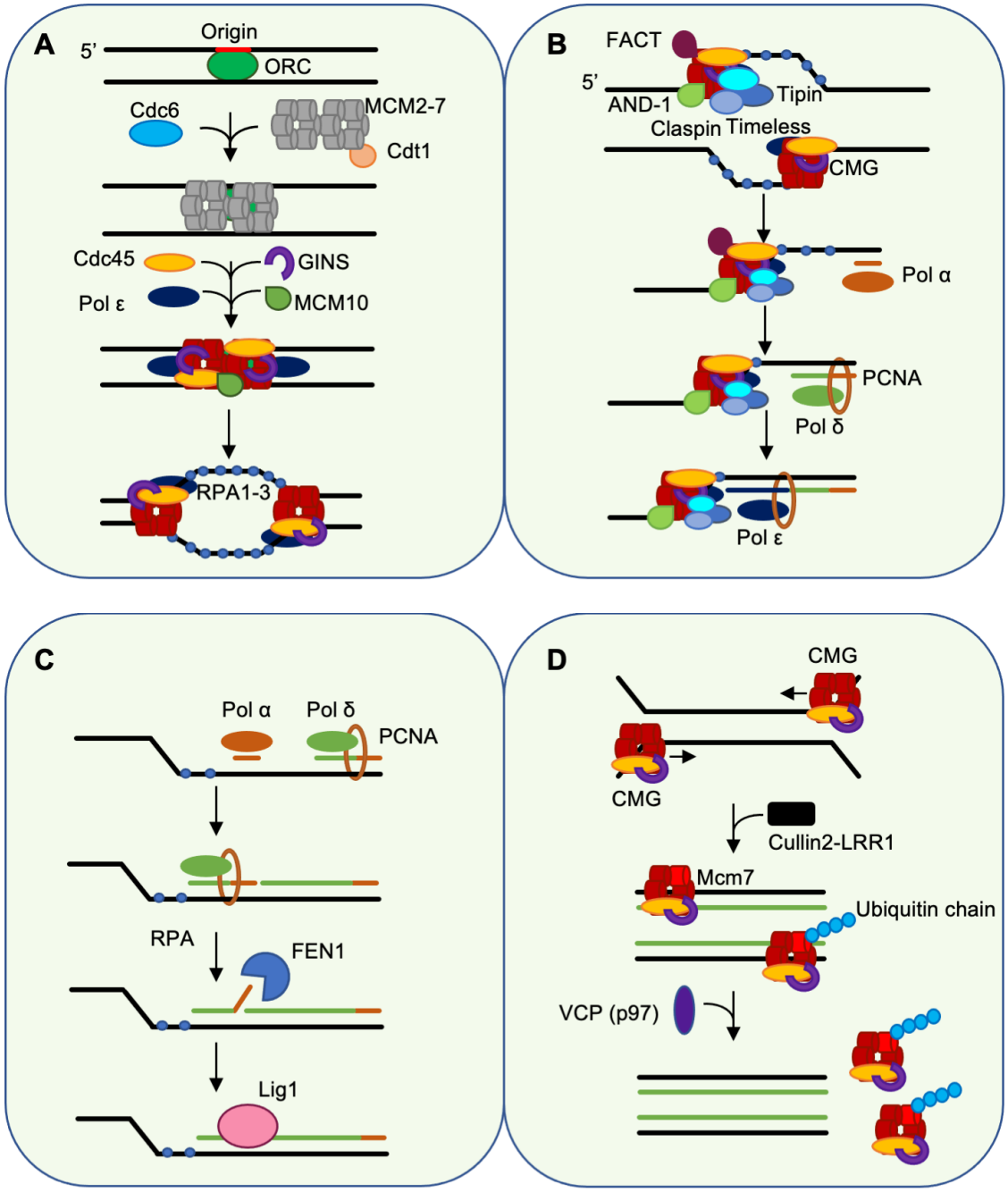

Figure 1.1. A brief summary of eukaryotic DNA replication

A. DNA replication initiation begins when the ORC binds to nucleosome free regions in the genome, which mark origins of replication. ORC recruits CDC6 and CDT1, which direct loading of MCM2-7 as an inactive double hexamer. The inactive MCM recruits other factors to form the CMG complex, which unwinds the parental DNA, leading to initiation of replication. **B.** Parental DNA is unwound by CMG. This produces ssDNA, which is bound by RPA, AND-1, Timeless, Claspin,

Tipin, Topoisomerase I, Mcm10, and FACT to form the replication progression complex. Pol α is also recruited and initiates DNA synthesis on the ssDNA template. Current literature suggests that primer elongation on the leading strand is initiated by Pol δ before replication is transferred to Pol ε. **C.** Elongation of the lagging strand is discontinuous and consists of repeated priming by Pol α and extension by Pol δ and PCNA. Extension continues until Pol δ reaches the primer of the preceding Okazaki fragment downstream. Pol δ displaces the RNA primer, generating a flap which is removed by FEN1. The nick in the DNA is then ligated by LIG1. **D.** DNA replication termination promotes recruitment of Cullin2-LRR1 to the terminated CMGs, leading to ubiquitylation of Mcm7 with K48-linked ubiquitin chains. The ubiquitylated replisome is subsequently disassembled by p97, in conjunction with Ufd1 and Npl4 (not shown). Figure 1.1D adapted from (Moreno and Gambus, 2020).

1.1.3 The eukaryotic cell cycle

Replication of DNA occurs in S phase. This is preceded by a gap phase known as G1 during which the cell is prepared for DNA synthesis, and followed by a second gap phase, G2, during which DNA replication is completed and the cell prepares to undertake mitosis. DNA replication takes around 8 hours in mammalian cells, with stagged origin firing so as to balance the number of active replication forks with the number of replication proteins and DNA precursors (Alberts et al., 2002). Mitosis is the cell division phase, where the parental cell divides into two daughter cells, each containing a complete copy of the genome.

1.1.3.1 Kinases and their regulation of the cell cycle

Cyclin-dependent kinases (CDKs) control entry and exit of cell cycle stages. The mammalian genome contains over 20 CDKs, and there is widespread redundancy between these proteins, evident if one of these is absent (Malumbres and Barbacid, 2009). In G1, D type cyclins bind to CDK4 and CDK6 (Kato et al., 1994), allowing for the inactivation of pocket proteins such as retinoblastoma protein (Rb). This allows for the expression of E-type cyclins, which in turn activate CDK2 (Harbour et al., 1999). Cyclin E-CDK2 is required to initiate S phase, in addition to Cyclin A (Livneh and Shachar, 2010). However, the above-mentioned kinases are all non-essential for life in mice, inducing developmental defects or infertility but not affecting viability (Malumbres et al., 2004; Ortega et al., 2003; Rane et al., 1999). However, CDK1 is essential and plays important roles in both mitosis and S phase (Hochegger et al., 2007; Santamaría et al., 2007). Mitosis is initiated by the activation of CDK1 through its binding to a cyclin protein – cyclin A or cyclin B. CDK1 phosphorylates over 1000 phosphorylation sites to trigger mitotic entry, in conjunction between PLK1 and the Aurora kinases (Dephoure et al., 2008).

PLK1 controls the timing of mitotic entry and is required for the assembly of functional mitotic spindles (Sumara et al., 2004). It also plays a role in the regulation of centrosome maturation, kinetochore attachment, and chromosome segregation (Liu et al., 2012). PLK1 is initially expressed in basal amounts in cells in G1 and S phase (Lee et al., 2008). PLK1 protein then accumulates at the end of S phase but does not become fully activated until just prior to the onset of

mitosis (Akopyan et al., 2014; Gheghiani et al., 2017). PLK1 protein must be degraded at the onset of anaphase to allow mitotic exit (Lindon and Pines, 2004). The role of PLK1 and CDK1 in the phosphorylation of DNA damage repair or damage tolerance proteins will be discussed in 1.3.1.3.4.

1.2 DNA damage and replication stress

1.2.1 Sources of DNA damage

A wide range of processes can inflict DNA damage, which can have a marked impact on genome replication and stability. Approximately 30,000 DNA lesions are spontaneously generated in every cell per day (Lindahl and Barnes, 2000). Damage to a cell's genetic information is a threat to both the cell's survival and its ability to faithfully transmit this information to daughter cells. To maintain genomic integrity, cells must repair damage to their DNA, or if repair is not possible, tolerate damage so it does not impair DNA replication or cell division.

Damage to DNA can come from endogenous sources. For example, DNA can be altered by spontaneous alterations, such as degradation of cytosine to uracil by deamination (Ciccia and Elledge, 2010). The metabolism of the cell itself can produce reactive oxygen species (ROS) or reactive nitrogen and carboxyl species, alkylating agents and estrogen, all of which can damage DNA (Hoeijmakers, 2009). DNA can also be damaged by exogenous environmental factors, such as UV light or ionising radiation (IR) (Ciccia and Elledge, 2010).

1.2.2 Damage to DNA bases

The effect of these endogenous and exogenous sources of DNA damage are variable. While not an extensive list, this section details some of the most common forms of damage known to occur on DNA, to help provide context to the variety of DNA damage repair and tolerance mechanisms employed by cells. These types of damage are also depicted in Figure 1.2.

1.2.2.1 Oxidative damage

Oxidative damage leads to oxidised nucleobases, which can remain as damaged bases or result in single or double-strand breaks during replication (De Bont and

van Larebeke, 2004). The most common oxidative lesion is 8-oxo-7,8-dihydroguanine (8-Oxo-G), a modification of guanine bases that results in it resembling a thymine base. This leads to the mispairing with an adenine base during replication, resulting in the introduction of mutations. Other modifications to guanine are also possible (Cooke et al., 2003).

1.2.2.2 Abasic Sites

Exogenous damage such as IR, endogenous processes such as oxidation, or repair by mechanisms such as SSBR and base excision repair, can lead to the presence of abasic sites. These lesions are characterised by the absence of a base on the nucleotide (Dianov et al., 2003). These lesions are both potentially mutagenic, and can block both replication and transcription (Wang et al., 2018).

1.2.2.3 Pyrimidine Dimers

Two common types of pyrimidine dimer are found in cells, both caused by UV irradiation linking two consecutive bases together: the helix distorting 6-4 photoproducts (6-4PP), so named because they are linkages connecting the 6’ carbon of one base to the 4’ carbon of the next, and the less distorting cyclobutane pyrimidine dimers (CPDs), dimers made of bonds between two carbons on each pyrimidine nucleotide (Ravanat et al., 2001). CPDs occur more commonly than 6-4PP in the genome but the latter are more toxic to cells due to their helix distorting properties (Sinha and Häder, 2002).

1.2.2.4 Chain Terminating Nuclear Analogues

Chain terminating nuclear analogues (CTNAs) are nucleotides that typically lack a 3’ hydroxyl group, and therefore cannot be extended from. Some CTNAs have a fluorine group at the 2’ position that weakens the nucleophilic potential of the 3’OH moiety, thus similarly preventing bond formation. CTNAs are commonly used as treatments for viral infections, e.g. HIV therapy (Yamamoto et al., 2016), as they terminate DNA synthesis. Prematurely terminating DNA replication leads to substantial missing genetic information, often leading to cell death. In order to repair DNA containing CTNAs, these unextendible bases must be removed.

1.2.3 Strand crosslinking and DNA strand breaks

Strand crosslinking can occur between bases on the same strand (intra-strand crosslinks), resulting in result in significant distortion to DNA double helix (Gu et al., 2006). Examples include pyrimidine dimers (1.2.2.3). Bases on separate strands can also be linked, causing inter-strand crosslinks (ICLs). ICLs prevent the separation of the DNA strands, stalling both DNA replication and transcription (Noll et al., 2006). This damage can be caused by endogenously produced chemical species, such as aldehydes, and by drugs such as mitomycin C and cisplatin, which are routinely used in cancer therapeutics (Rajski and Williams, 1998).

Single-strand breaks (SSBs) are discontinuities in one strand of DNA, often with lesions on the 5' and 3' bases surrounding the nick or gap. SSBs can lead to the collapse of DNA replication (Kuzminov, 2001), and the stalling of transcription (Kathe et al., 2004). The end result of an unrepaired ssDNA break can be the dissolution of such a break into a double-strand break (DSB) (Kuzminov, 2001), with significant increases to the number of unrepaired SSBs leading to a saturation of DSB repair pathways (Caldecott, 2008). DSBs are instances where two SSBs appear, one on each strand of DNA, up to 20 base pairs apart. Double strand breaks are highly deleterious, and unrepaired DSBs can lead to cell death (Hoeijmakers, 2001; Sishc and Davis, 2017), making their immediate repair essential for survival.

1.2.4 DNA secondary structures

DNA secondary structures can impede replication and cause replication stress. Four-stranded G4 quadruplexes are structured DNA made up of regions of guanine-rich single or double-stranded DNA, which form secondary structures that impede fork progression (Todd et al., 2005). Additionally, other difficult to replicate sites in the genome, such as repetitive sequences which can form stable secondary structures, may induce replication stress (Zou and Nguyen, 2018).

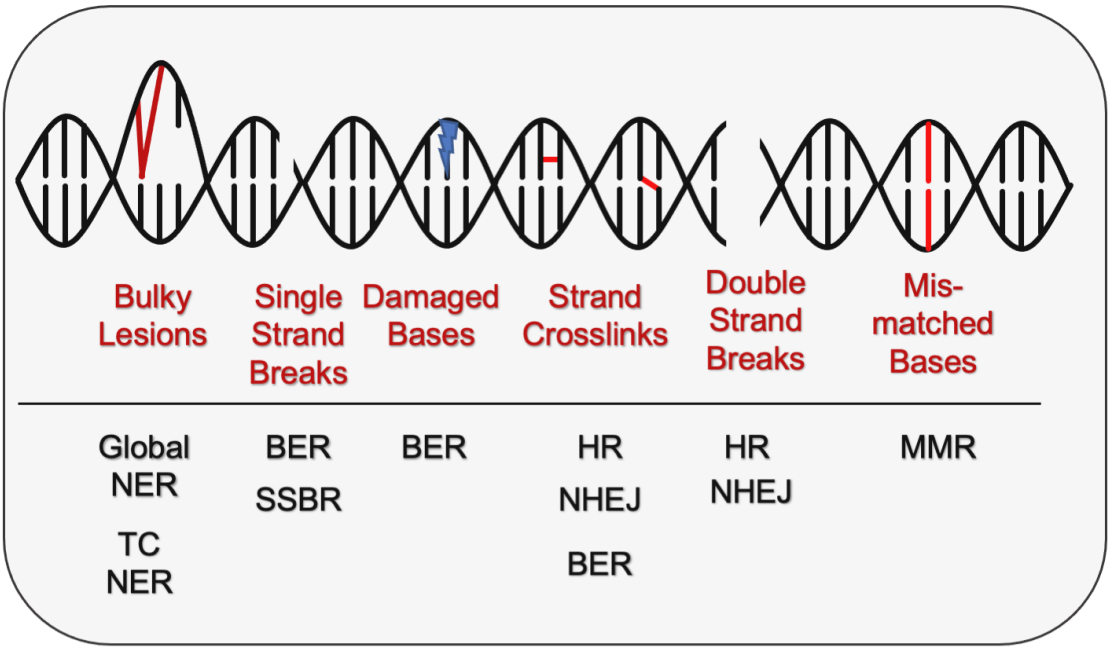

Figure 1.2. Damage to the DNA template can be a source of replication stress

A diagram of a DNA strand containing various kinds of DNA damage (red). These lesions include bulky lesions, often generated by UV damage, single strand breaks in the DNA, damage to the DNA bases, strand crosslinking, which can occur across strands (inter-strand) or on the same strand (intra-strand), double strand breaks, and mismatched bases (A to C/G, C to A/T etc). The lower half of the figure shows the main repair mechanisms (described in 1.3.2) utilised for each lesion type. If the DNA repair mechanism does not successfully detect or repair the lesions before the onset of DNA replication, it can cause replication stress.

1.2.5 Replication stress

During genome duplication, the replication fork encounters a myriad of conditions and obstacles that can affect the progression of DNA polymerases, resulting in replication stress. Causes of polymerase stalling can include unrepaired DNA lesions generated by both endogenous and exogenous sources, described above. In addition, DNA secondary structures such as G4 quadruplexes (Bryan, 2019), R loops – DNA:RNA hybrid structures – (Allison and Wang, 2019), proteins tightly bound to DNA (Carr and Lambert, 2013), repetitive sequences including common fragile sites (Debatisse et al., 2012), depletion of replication factors such as dNTPs and unfavourable replication conditions (Pai et al., 2019) can all induce replication stress. Replication stress occurs when the replisome encounters such features on the DNA template, causing slowing or stalling of the fork, which, in turn, can lead to slower or reduced synthesis, fork collapse, DNA breaks, and checkpoint activation (Muñoz and Méndez, 2017).

The consequences of stalling events vary, depending upon which strand the arresting structure or lesion resides on. It is generally accepted that the constant cycles of priming during discontinuous synthesis reduces the impact of lagging strand lesions on fork progression, as a downstream primer can readily be synthesised as part of the canonical replication process. Providing the replicative helicase is not impaired by a lagging strand barrier, the lagging strand polymerase (Pol δ) can dissociate and restart replication from a new primer, bypassing the impediment (McInerney and O'Donnell, 2004). In fact, overall fork progression is hardly affected by lagging strand damage in reconstituted replisome collisions (Taylor and Yeeles, 2018). The repair of stalling lesions on this template strand can subsequently be conducted in a post-replicative manner. In contrast, large stretches of ssDNA are generated by leading strand polymerase stalling caused by the continued unwinding of the DNA template by the replicative helicase. This process is known as helicase-polymerase uncoupling (Byun et al., 2005). ssDNA is fragile and prone to breakage. It can be protected by the binding of RPA, which binding acts as a marker of replication stress and can trigger the S phase checkpoint response by activating the ATM and Rad3-related (ATR)-mediated DNA damage response cascade.

1.3 DNA damage response

1.3.1 Recognition of stalled replication forks

The cellular DNA damage response to stalled replication forks requires a complex network of proteins to be activated, which lead to the stalling of the cell cycle and downregulation of gene transcription. Defects in these maintenance systems can lead to additional genome instability, which can cause the onset of cancer and developmental defects (O'Driscoll, 2012), as well as premature aging (Garinis et al., 2008).

1.3.1.1 RPA and its role as a first responder

RPA is a ssDNA-binding protein expressed in high levels in the cell. It is present across all eukaryotes and shows a strong affinity for single stranded DNA (Wold, 1997). RPA is a heterotrimer of three subunits: RPA70 (encoded by the *RPA1* gene), RPA32 (*RPA2*) and RPA14 (*RPA3*), with the numbers of the protein subunits representing their size in kilodaltons (Figure 1.3). These three subunits have six OB fold domains. Four of these (70A, 70B, 70C, and 32D) act as ssDNA-binding domains. 32D, 70C, and RPA14 help assemble the RPA trimer, while 70N acts as a protein-interaction domain. In addition to these OB-folds, RPA32 has a winged-helix C-terminal domain (RPA32C) that is involved in mediating protein interactions. RPA uses modular domain architecture to facilitate dynamic DNA and protein interactions.

The primary role of RPA in DNA replication and repair is to protect the transiently generated ssDNA stretches from degradation and secondary structure formation (Chen et al., 2013). It also coordinates the recruitment of other repair and replication factors, including PrimPol, to the DNA, through its protein interaction domains (see Figure 1.3). RPA is regulated by phosphorylation, including by CDKs that regulate its ability to bind DNA (Oakley et al., 2003), or by ATR after UV damage that facilitates adaption of the replication fork and prevents accumulation of ssDNA (Cruet-Hennequart et al., 2006; Vassin et al., 2009). Similarly, genotoxic stress responsible for increased DSBs stimulates the phosphorylation of RPA by DNAPK (Liaw et al., 2011). Specifically regarding its role in the DNA damage response, the binding of RPA to ssDNA is required for

ATRIP binding, which in turn recruits and stimulates ATR activation (Cortez et al., 2001), and for BLM binding for its role in replication stress response and fork restart, but not for its activity during HR (Shorrocks et al., 2021). Independently, RPA recruits Rad17 to chromatin, which is phosphorylated by ATR and allows formation of the Rad9-Rad1-Hus1 (9-1-1) checkpoint clamp.

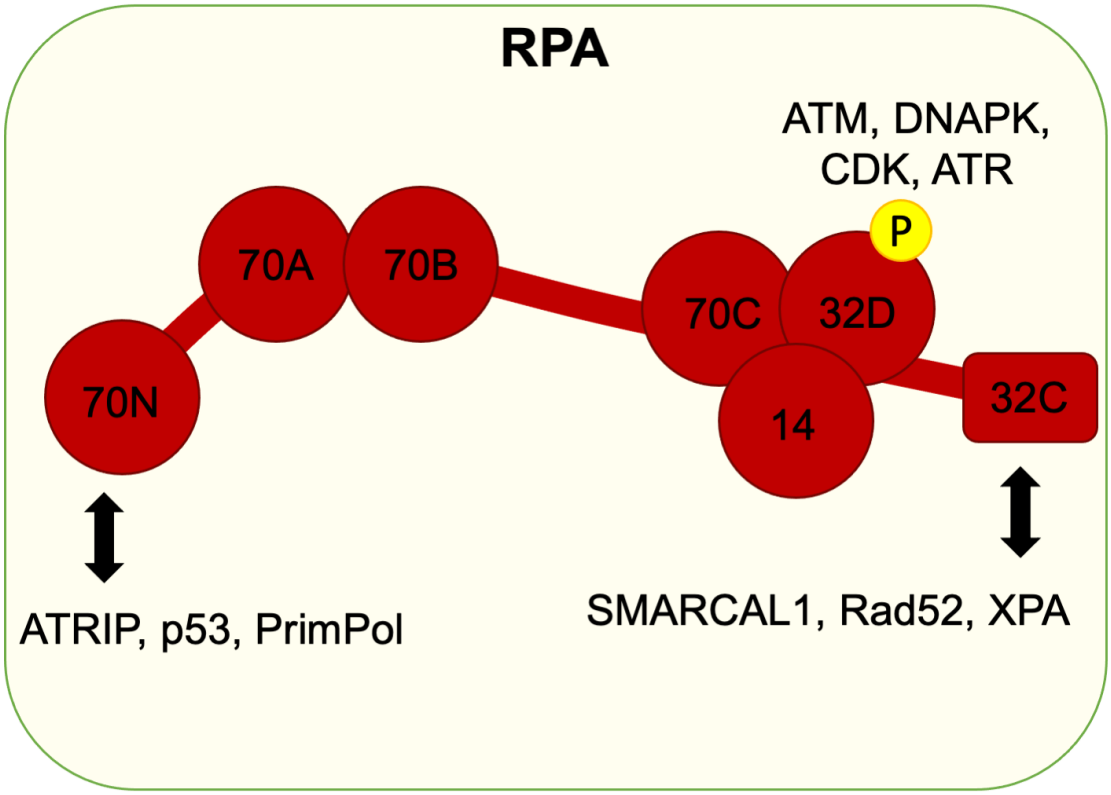

Figure 1.3. Replication protein A

Diagram showing the structure of RPA. The major protein–protein interaction domains with example binding partners are shown below, and example kinase enzymes, which regulate RPA binding and activity, are shown above. Figure adapted from (Bhat and Cortez, 2018).

1.3.1.2 Kinase signalling and DNA damage recognition

The cellular response to DNA damage is orchestrated by three key kinases: the ATM and ATR kinases, and DNA-dependent protein kinase (DNA-PK) (Blackford and Jackson, 2017) (Figure 1.4). In response to DNA damage, these kinases together phosphorylate over 700 proteins to co-ordinate DNA repair (Matsuoka et al., 2007). Interestingly, hundreds of proteins are phosphorylated by ATM or ATR, whereas DNA-PKcs appears to regulate a smaller number of targets and play a role primarily in non-homologous end joining (NHEJ). In undamaged conditions, these kinase enzymes exist in inactive forms (Bakkenist and Kastan, 2003; Gottlieb and Jackson, 1993; Zou and Elledge, 2003). These kinases activate several downstream proteins through phosphorylation, such as BRCA1 and p53. ATM and ATR also activate the checkpoint kinases Chk1 and Chk2, triggering a signalling cascade. While Chk2 is expressed continuously throughout the cell cycle and kept inactive in undamaged cells, Chk1 expression is predominately restricted to S phase and G2 and is expressed in its active form (Bartek and Lukas, 2003). Other kinase enzymes, as well as ATM and ATR, phosphorylate DNA repair and DNA damage tolerance enzymes during these processes.

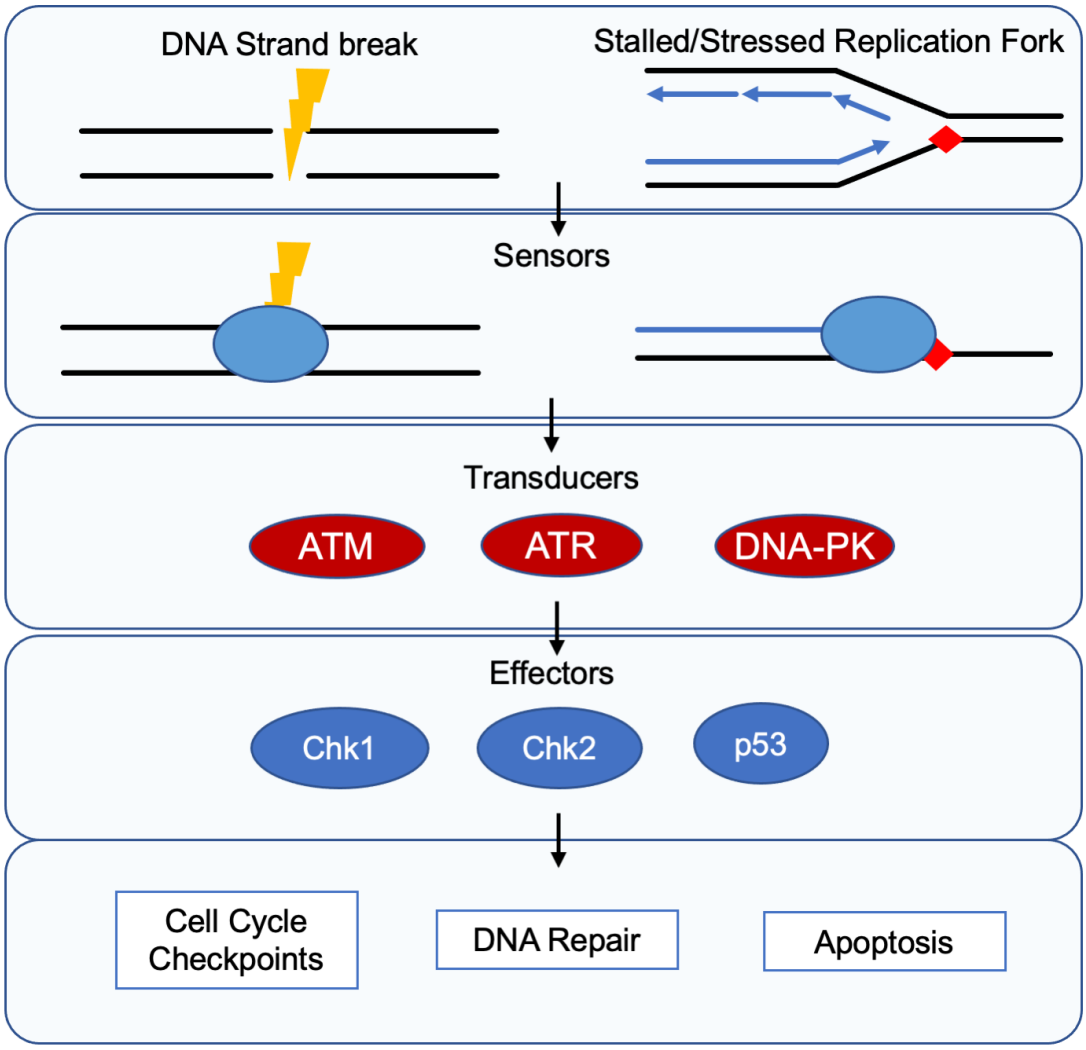

Figure 1.4. A brief overview of key cellular response pathways in response to replication forks stalling or strand breaks

A schematic showing the cellular response to replication stalling or strand breaks and the downstream consequences. DNA strand breaks or stalling replication forks require recognition from the cell before they can be dealt with. The pathway consists of signal sensors (such as RPA), transducers (ATM/ATR), and effectors (Chk1, Chk2). Figure adapted from (Maréchal and Zou, 2013).

1.3.2 Cell cycle arrest and the cell cycle checkpoints

The cell cycle is driven by cyclin proteins bound to cyclin-dependant kinases (CDKs) (1.1.3.1). Cell cycle arrest can occur to allow repair of DNA lesions, and in response to stalled replication forks that have encountered damage or double strand breaks. Nutrient depletion or dNTP depletion can also cause arrest. This arrest aims to prevent DNA synthesis or mitotic entry of cells with damaged DNA.

1.3.2.1 G1/S Checkpoint

The G1/S checkpoint allows cells to pause entry to S phase, either by remaining in G1 or entering a senescent G0 phase, to prevent proliferation of cells with a high damage load, or repair DNA damage before replication. There are two main pathways of G1/S checkpoint activation. The rapidly activated pathway involves ATR/ATM mediated activation of Chk1/Chk2, which both independently phosphorylating Cdc25A, marking it for degradation and preventing its activity on the Cyclin E:Cdk2 complex (Hoffmann et al., 1994; Mailand et al., 2000). G1 arrest also requires the activity of p53, p38 and p21 proteins (Mikule et al., 2007).

1.3.2.2 Intra-S checkpoint

This checkpoint is activated during S phase when DNA damage or replication stress are detected. The cell relies on this checkpoint to mediate DNA repair during S phase. The activation of this checkpoint centres heavily on the activity of ATM and ATR, and is activated by both stalled replication forks and the intermediate structures of several repair pathways (Iyer and Rhind, 2017). ATR/Chk1 responds to a more diverse range of lesions, including stretches of RPA bound ssDNA generated by fork stalling, while ATM/Chk2 predominately responds to DNA double strand breaks, but cross-talk between these proteins is vital for proper checkpoint activation (Jazayeri et al., 2006). ATM is also responsible for the phosphorylation of SMC1, which leads to activation of the S phase checkpoint in a pathway that requires BRCA1 and NBS1 but is independent of Chk2 (Kitagawa et al., 2004; Yazdi et al., 2002). Checkpoint activation also suppresses origin firing, preventing new forks from meeting damage or replicating under stress (Costanzo et al., 2003).

1.3.2.3 G2/mitosis checkpoint

Damage that is undetected by the S phase checkpoint and proceeds into G2 unrepaired, or damage that occurs in G2, can be detected by the cell before it enters mitosis. Both ATM and ATR are required for this checkpoint to be activated. In unperturbed cells, progression from G2 to mitosis involves the activation of the inhibited complex of Cyclin B and CDK1 by CDC25. When DNA damage is detected, ATR and ATM activate Chk2 and Chk1 respectively, leading to the phosphorylation of CDC25 (Sørensen et al., 2003). Phosphorylated CDC25 is sequestered in the cytoplasm and unable to remove the Cyclin B: Cdk1 inhibition (Peng et al., 1997). The activation of the checkpoint can involve different proteins depending on the source of the damage: for example, after UV damage induces checkpoint activation, the p38 MAP kinase is vitally important for phosphorylating CDC25 (Bulavin et al., 2001). Additionally, when DNA is damaged, the p53 tumour suppressor and the Rb family of transcriptional repressors work together to downregulate transcription of a number of genes which encode essential proteins for mitosis (Stark and Taylor, 2006).

1.3.2.4 DNA damage recognition by cell cycle kinases

Cell cycle kinases, such as the cyclin-dependent kinases (CDKs), Aurora kinases or Polo-like kinases (PLKs), play roles in the detection of DNA damage and the activation of repair factors (Hyun et al., 2014). Examples include CDK1 phosphorylation of BRCA2 to prevent association with Rad51 (Esashi et al., 2005), and phosphorylation of repair proteins after DNA damage leading to activation of the G2/M checkpoint (Cho et al., 2013). PLK1 has also been shown to play a role in the regulation of DNA damage proteins such as Rad51 and BRCA2, and PLK1 phosphorylation can lead to inhibition of protein loading to sites, such as in the case of MRE11 (Lee et al., 2004; Li et al., 2017; Yata et al., 2012). The Aurora kinases have roles in the DNA damage checkpoints, but also in regulating BRCA1/2 expression, and inhibiting Rad51 binding (Ma and Poon, 2020).

1.3.3 Mechanisms of DNA repair

Once lesions have been detected they must be repaired. There are several key DNA damage repair mechanisms, with each repair pathway specific to a particular lesion type. These are listed below (Iyama and Wilson, 2013).

1.3.3.1 Mismatch repair

Nucleotide misincorporation leads to mismatched DNA bases; if uncorrected, this can lead to mutations in the DNA produced by subsequent replication. As mentioned previously, replicative DNA polymerases contain 3'-5' proof-reading domains, which allow the enzyme to edit out misincorporated bases before moving on. Any mistakes that are missed by the proof-reading mechanisms are therefore repaired by MMR mechanisms (Iyer et al., 2006). MMR works only on the newly synthesised strand of DNA during DNA replication; when this strand is first created it will contain small nicks that have yet to be ligated, where PCNA will accumulate. This will then recruit MutL to begin MMR (Pluciennik et al., 2010). This pathway has been exploited in certain chemotherapy drug treatments, such as cisplatin (Kothandapani et al., 2013).

1.3.3.2 Base excision repair

Base excision repair (BER) is employed to correct damaged DNA bases, such as modifications caused by oxidation or deamination. BER occurs in five key steps: excision of the damaged base by a lesion-specific DNA glycosylase, removal of the remaining abasic site - either by DNA glycosylase or APE1 – modification of the exposed 5' and 3' ends of the DNA break, DNA nucleotides insertion and end ligation by DNA ligase (Nemec et al., 2010). These repair steps require the cooperation of many different enzymes, including the previously mentioned DNA glycosylase enzymes, as well as endonucleases, phosphatases, kinase enzymes and polymerases (Kim and Wilson, 2012). Deficiencies or mutations in any of these enzymes leaves cells open to elevated mutation rates and hypersensitivities to DNA damage agents.

1.3.3.3 Nucleotide excision repair

NER can be used to resolve distortions to DNA that affect the helical structure, including cyclobutene pyrimidine dimers (CPDs) and 6-4PP, as well as reactive oxygen species induced base modifications, such as cyclopurines (Iyama and Wilson, 2013). The classic pathway involves recognition of the damage, incisions to remove the damaged bases, synthesis of new bases to fill the gap, and ligation of the new DNA. This process involves approximately 30 different proteins (Spivak, 2015). The bulk of nucleotide lesions are repaired by global genomic NER (GGR) but those detected during transcription are repaired by a sub-pathway called transcription-coupled NER (TC-NER). Defects in components of these NER pathways can lead to the development of syndromes such as Xeroderma pigmentosum (XP), Cockaynes syndrome and trichothiodystrophy (TTD) (McKinnon, 2009).

1.3.3.4 Single-strand break repair

Thousands of single-strand breaks (SSBs) occur in genomic DNA every day (Moore et al., 2000). The causes of these breaks are varied: the damage can come from reactive oxygen species (ROS) damage, or as an intermediate in other DNA damage repair pathways, such as BER (Iyama and Wilson, 2013). The improper dissociation of Topoisomerase I can also generate increased SSBs: when trapped on the DNA, the breaks Topo I induced to reduce topological stress are not re-ligated.

The repair of most SSBs occurs in four main steps: SSB detection, DNA end processing, gap filling and ligation. PARP1 is involved in detecting SSBs, including those generated by BER, and this protein recruits XRCC1, a protein which acts as a scaffold for subsequent repair proteins. End-processing is performed by a variety of enzymes depending on the specific repair required for the 5’ and 3’ ends. For example, the repair of abortive SSBs – those generated by the improper dissociation of Topo I, either through chemical inhibition or mutation – requires TDP1 to remove Topo I before DNA synthesis can resume (Pommier et al., 2006). The gap is then repaired, either by a specialist polymerase, Pol β, or the replicative polymerases ε and δ (Caldecott, 2007). The final step is ligation by LIG1 or LIG3 (Abbotts and Wilson III, 2017). Slow or

incomplete repair of these lesions can lead to collision with the replication fork, which can lead to the formation of a DNA DSB. This would be repaired as described below.

1.3.3.5 Non-homologous end-joining

When DSBs occur, they must be repaired quickly and accurately to prevent serious consequences, including apoptosis. Upon formation of a DSB, phosphorylated histone H2AX, termed 'γH2AX', mediates the chromatin response. γH2AX is a specific and efficient coordinator of the subsequent break repair (Kinner et al., 2008); this phosphorylation can be detected in the human cell up to 2 million base pairs away from the site of the damage (Rogakou et al., 1998). There are two classical mechanisms for repairing DSBs: non homologous end-joining (NHEJ) and homologous recombination (HR). NHEJ does not require a sister chromatid and is therefore of particular importance during G1 phase of the cell cycle. NHEJ is problematic as information may be lost around the site of the break during repair. Briefly, the ring shaped Ku70/Ku80 heterodimer detects and binds to the DNA ends generated by the break (Frit et al., 2019). This allows for the recruitment of proteins such as PAXX (Ochi et al., 2015) and recruitment and activation of DNA-PK. This kinase stimulates end-processing by polymerases (e.g. Pol μ and λ) and nucleases (e.g., Artemis), if required. Finally, the XLF-XRCC4-DNA ligase IV complex interacts with the bound Ku and ligates both broken strands to repair the DSB (Grawunder et al., 1997). Both NHEJ and HR utilise the MRN complex (MRE11-RAD50-NBS1) to sense DSBs, activate checkpoints, and as an effector in repair.

A subtype of NHEJ, alternative-NHEJ does not require the Ku proteins or DNA ligase IV and instead repairs the DSB by annealing 2–20-bp stretches of overlapping bases flanking the break using the MRN complex, Pol θ, PARP1, ATM among others (Seol et al., 2018). The further subtype of this repair that requires small regions of homology is termed microhomology-mediated end joining (MMEJ).

1.3.3.6 Homologous recombination

Homologous recombination (HR) is another mechanism by which cells repair DSBs. It can also be used to repair ICLs (Li and Heyer, 2008). To perform HR, cells must be in either S or G2 phase, as they require access to a sister chromatid to use as a template. When cells do not possess a sister chromatid, DSBs must be repaired using canonical NHEJ, or alternative NHEJ pathways. To prevent NHEJ when undertaking HR, the cell quickly employs methods to remove the fast-binding Ku heterodimer, inferring that the process of end-resection is the centre of DSBR pathway choice (Chanut et al., 2016).

There are two key stages of homologous recombination repair: homology searching and strand invasion. Either side of the break is bound by the MRN complex, which recruits helicase (BLM) and nucleases (Exo1/DNA2) to resect by a few hundred bases; this stretch of ssDNA is then bound by RPA (Wold, 1997). The RPA is then replaced by Rad51 in combination with other proteins, and this ssDNA-protein complex then begins searching for homologous regions to perform strand invasion. Strand-invasion, where the 3' invading end is extended by a DNA polymerase, leads to formation of a D loop structure. In most cases, double strand breaks are repaired using a synthesis dependent strand-annealing pathway, though Holliday junction can also be formed. Human cells have two mechanisms for Holliday junction processing: the first is performed by the BTR complex (BLM helicase/Topoisomerase IIIα/RMI1/RMI2), whereas the second involves endonucleases such as MUS81/EME1 (Boddy et al., 2001) and GEN1 (Rass et al., 2010), and can produce crossover products depending on the orientation of cleavage (Sarbajna and West, 2014).

1.4 DNA damage tolerance

If lesions remain unrepaired during S phase, collisions of the replisome with lesions or secondary structures can result in stalling or collapsed replication forks, leading to stretches of under-replicated DNA. Therefore, the cell has processes it can employ to bypass lesions / structures and allow replication to proceed; these are collectively known as DNA damage tolerance (DDT). Such

mechanisms include template switching, fork reversal, dormant origin firing, translesion synthesis (TLS), and repriming (Figure 1.5).

1.4.1 Fork reversal

Fork reversal is a mechanism by which replication of a damaged template can be avoided by using the newly synthesised nascent strand as a template (Figure 1.5). Fork reversal leads to the formation of a regressed fork, which is commonly referred to as a 'chicken foot' structure (Lopes et al., 2001; Neelsen and Lopes, 2015). This provides the cell with the opportunity to return the DNA lesion to a double-stranded context, to aid in lesion removal. Lesion removal occurs after fork regression but before replication restart. Alternatively, fork reversal also allows the cell to bypass the lesion through template switching once the fork restarts. Reversed forks can also converge with oncoming replication forks, bypassing the need for fork restart (McGlynn and Lloyd, 2002). Intriguingly, fork reversal has also been implicated in the resolution of specific ICLs (Amunugama et al., 2018)

The onset of fork reversal occurs through the recruitment of fork remodelling factors. These include the translocases SMARCAL1, HLTF and ZRANB3 (Taglialatela et al., 2017). SMARCAL1 is recruited to RPA bound ssDNA, and therefore will directly compete with PrimPol (1.6.3). Additionally, the binding of Rad51 to RPA covered ssDNA has been shown to be an essential step in fork reversal, though this is independent of Rad51's strand exchange activity (Mason et al., 2019). Following fork reversal, the replication fork will use proteins such as the helicase RECQ1 to allow for efficient restart; this pathway carefully balances the need for timely fork restart with the necessary restraint required to allow DNA lesion removal to occur before replication continues (Berti et al., 2013).

While fork slowing is implicated in DNA lesion tolerance, the majority of remodelled forks are not directly challenged by lesions (Mutreja et al., 2018). As fork reversal mechanisms have only recently been reported, further studies are required to fully elucidate the molecular mechanisms underpinning this process, and their interactions with other tolerance pathways remains to be elucidated.

1.4.2 Dormant origin firing

An additional method employed by cells to tolerate replication stress is dormant origin firing (Figure 1.5), a mechanism by which the dormant origins distributed throughout the genome are activated. In G1, when the MCM complex is loaded onto origins, significantly more origins are loaded with complexes than are initially activated. The remaining origins can then be activated in response to replication stress, despite the activation of the ATR-dependent S phase checkpoint, which decreases late-stage origin firing (Ge et al., 2007). In fact, Chk1, required for the suppression of origin firing, is paradoxically required for the dormant origin activation by distinguishing between origins within currently active replication factories and those outside (Ge and Blow, 2010).

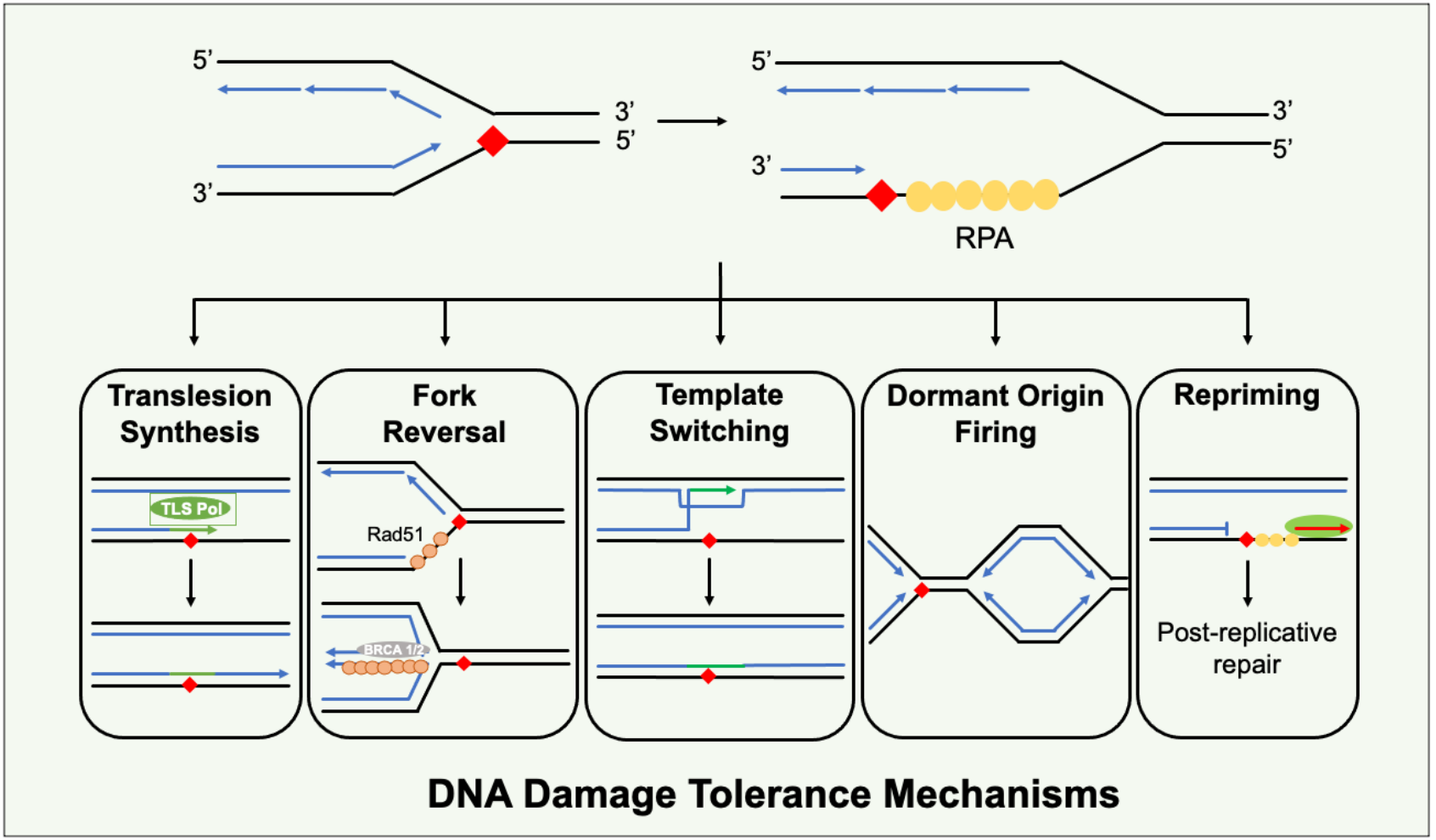

Figure 1.5. A summary of DNA damage tolerance mechanisms

Obstacles on the DNA template (red diamond) block ongoing replication (blue arrows) and lead to fork stalling. This leads to helicase/polymerase uncoupling, generating tracts of ssDNA which is bound by RPA (yellow circles). DNA damage tolerance mechanisms include translesion synthesis, fork reversal, template switching, dormant origin firing and repriming. They allow DNA replication to continue in the presence of such impediments.

1.4.3 Translesion DNA synthesis

Virtually all DNA polymerases are able, to some degree, to perform synthesis across damaged sections of DNA, but replicative polymerases are the least adept at this process due to their high fidelity. Lower fidelity polymerases are better able to bypass lesions, and less likely to stall. This bypass is known as translesion synthesis (TLS) and is predominately performed by Y family TLS polymerases: Pol k, Pol ι, Pol η and Rev1, in addition to Pol ζ from the B family (Vaisman and Woodgate, 2017) (Figure 1.6). TLS polymerases are characterised by low processivity, fidelity and efficiency: while their large active site allows them to accommodate damaged bases, it is therefore too large to securely interact with DNA (Vaisman and Woodgate, 2017). Further, their low fidelity is explained by the lack of 3'-5' exonuclease activity. Lack of proofreading allows the polymerase to avoid enzymatic idling, where the proofreading exonuclease can remove any incorrect bases that the polymerase has incorporated (Khare and Eckert, 2002).

Pol ζ and the Y family TLS polymerases do not share significant primary amino acid sequence homology, and beyond a general structural similarity, the domain architecture and structural complexity of Y family polymerases does not match that of Pol ζ (Steitz and Steitz, 1993). However, both are efficient TLS polymerases suited to specific lesion types. Despite their inherent low fidelity, each specialised polymerase can bypass at least one specific kind of DNA damage with high fidelity. For example, Pol η is able to accurately replicate over UV-induced CPD lesions but is unable to efficiently bypass 6-4PP *in vitro* (Masutani et al., 2000). Rev1 is able to bypass abasic sites by incorporating deoxycytidine bases (Lin et al., 1999). To properly co-ordinate bypass, TLS polymerases often work together (Livneh and Shachar, 2010).

1.4.3.1 Regulation of TLS

All the above-mentioned TLS polymerase enzymes interact with PCNA, though this interaction has been well established for some, such as Pol η, while it remains

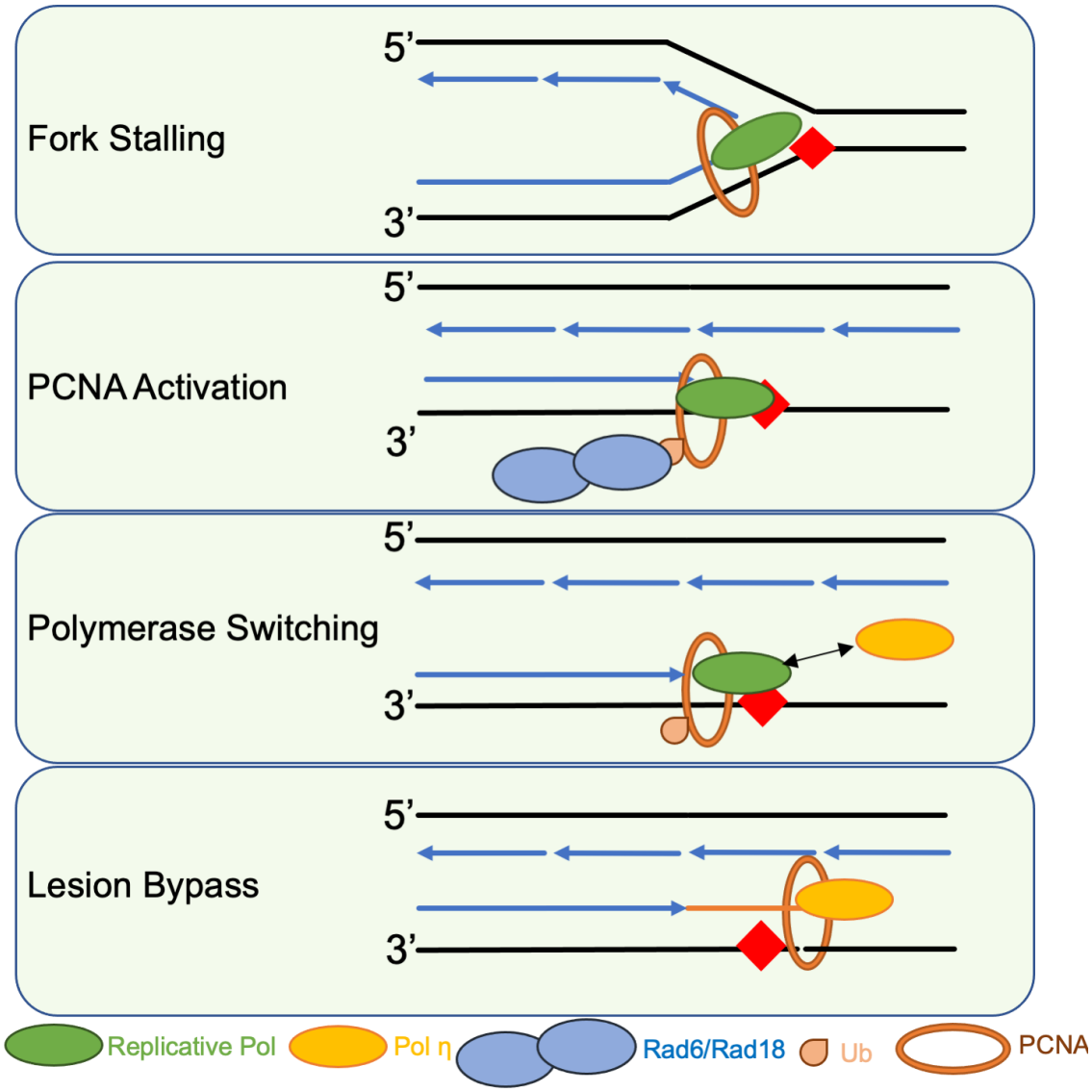

Figure 1.6. The process of translesion synthesis by Pol η

DNA damage lesions can be directly overcome by the action of TLS polymerases which are able to replicate over the lesion. Monoubiquitination of PCNA is performed by Rad6/Rad18, which signals for the recruitment of a TLS polymerase. The TLS polymerase will replicate over the stalling lesions, before its low processivity leads to dissociation and the strand is once again transferred to the replicative polymerase.

unclear for others, such as Pol ζ. PCNA acts as a scaffold for both replicative and specialised polymerases, as well as recruiting other secondary proteins; the proteins that interact with PCNA contain a PCNA-interacting peptide (PIP) box (Warbrick, 1998). For its role in DNA damage tolerance, PCNA is monoubiquitinated by Rad6-Rad18 to stimulate TLS (Waters et al., 2009). Rev1 has also been implicated in the recruitment of TLS polymerases to stalled forks, through its CTD interaction with various polymerases, such as Pol κ and Pol η (Guo et al., 2003). After damage stalls replication, RPA protein binds ssDNA surrounding a stalled fork, and changes conformation to allow interaction with Rad18. This stimulates the ubiquitination of PCNA, leading to polymerase switching (Hedglin et al., 2019).

In addition to protein interactions, post-translational modifications (PTMs) are important in regulating the recruitment and residence time of each TLS polymerase at the replication fork. For example, the chromatin binding of all Y family polymerases has been shown to be regulated by ubiquitination (Sale et al., 2012). Additionally, alongside promoting PCNA ubiquitination, RAD18 also associates with Pol κ and Pol η, helping chaperone these polymerases to a stalled replication fork. RAD18 can be phosphorylated at S409 after UV-C radiation, which resides in the Pol η binding domain of Rad18. This phosphorylation helps the recruitment of Pol η to stalled forks (Day et al., 2010).

1.4.3.2 The function of Pol η and its role in the cell

Pol η is a DNA polymerase transcribed from the *POLH* gene. Mutation of this gene causes the inherited disorder Xeroderma pigmentosum variant (XP-V), associated with increased incidence of sunlight-induced skin cancers, due to errors in the repair of UV induced DNA lesions. While its main role is in the tolerance of these lesions during S phase, XP-V cells lacking Pol η show more chromosome breaks than cells with competent Pol η, suggesting it also plays a role in allowing replication to occur unimpeded, especially across common fragile sites (Rey et al., 2009).

Pol η is recruited to stalled replication forks. It first interacts with monoubiquitinated FANCD2 after UV-C damage, though the precise role of this interaction is unknown (Fu et al., 2013). It then interacts with monoubiquitinated

PCNA, an interaction which allows polymerase switching to occur (Lau et al., 2015). Interestingly, human studies have since shown that Pol η's DNA synthesis and binding ability are independent of PCNA K164 ubiquitination (Hedglin et al., 2016), though this ubiquitination still being required for optimum levels of TLS to occur (Hendel et al., 2011). While ubiquitination of PCNA by Rad6/Rad18 is required for efficient TLS, it does not appear to be necessarily required for TLS polymerase recruitment; it is unclear what precise role it plays (Yoon et al., 2015).

1.4.3.3 The regulation of Pol η

Pol η is a low fidelity polymerase which can replicate across CPDs with high fidelity. However, it has been shown to introduce mutations when replicating undamaged DNA (Matsuda et al., 2000). Pol η can also play a role in the bypass of lesions caused by exogenous DNA damaging agents, such as cisplatin-induced intra-strand crosslinks (Masutani et al., 2000), but it is not proficient at replicating over most other kinds of damage. As such, its recruitment must be tightly controlled. While Pol η's low expression works to moderate its activity somewhat, the post-translational modifications of both the polymerase and its interacting partner PCNA will be the focus of the next section, as they provide an interesting model framework for how PrimPol could be regulated.

Some of the PTMs applied to Pol η inhibit its activity. A small amount of Pol η is ubiquitinated in undamaged cells, on sites K682, K686, K694, and K709 of its C-terminus (Bienko et al., 2010). The ubiquitinated C-terminus of Pol η can bind the UBZ in the centre of the protein, causing a conformational change, blocking the PIP box located between the UBZ and K682. The PIP box is the PCNA interacting protein box, and its blockage prevents Pol η from associating with chromatin and forming replication foci (Bienko et al., 2010).

In contrast, some PTMs have stimulatory effects. ATR-dependent phosphorylation has been shown to play a role in recruitment of Pol η. The change in phosphorylation state that occurs after UV-C damage is dependent on the ATR kinase, and one site specifically, S601 is phosphorylated by ATR (Bertoletti et al., 2017; Göhler et al., 2011). Protein kinase C (PKC) has also been shown to phosphorylate Pol η at S587 and T617 (Chen et al., 2008), and the mutation of both sites to alanine induces an increased sensitivity to UV-C

damage, suggesting these phosphorylation sites play a role in the utilisation of Pol η. The phosphorylation of these residues, in combination with phosphorylated S601, have been shown to regulate Pol η's interaction with ubiquitinated PCNA: Phosphorylation at these sites leads to stronger binding with PCNA, and this phosphorylation is sufficient to overcome Pol η's binding to PolDIP2, which sequesters it in undamaged cells (Peddu et al., 2018).

1.4.4 Template switching

Template switching is a recombination-mediated mechanism of fork restart and is therefore significantly more accurate than using TLS polymerases, as the correct sequence can be copied from an undamaged template (Figure 1.6) (Lehmann et al., 2020). The process of template switching involves the initial steps of TLS, including recruitment of Rad18 by RPA and chromatin remodelling by INO80. Along with ubiquitination of PCNA, Rad18 may also recruit MMS2-UBC13 and HTLF/SHPRH, which polyubiquitinates K164 to stimulate template switching (Fan et al., 2020; Hoege et al., 2002; Kanao and Masutani, 2017; Ulrich and Jentsch, 2000). The 9–1–1 clamp is then loaded to the 5′ end of the ssDNA, leading to Exo1 recruitment (Karras et al., 2013), and Rad51/BRCA2/Dss1 mediated strand invasion of the sister chromatid (Holloman, 2011). This facilitates the synthesis of the unreplicated sequence opposite the damaged template by Pol δ. After replication has been completed, the newly synthesised strand switches back to its original position, leaving no unreplicated DNA but instead a sister chromatid junction (SJC) that requires resolution by BLM (Sgs1)/TOP3α (Top3)/RMI1/2 (RMI1) (Fasching et al., 2015). Unlike TLS, this process is considered to be error-free.

1.5 Repriming – a DNA damage tolerance mechanism

As discussed above (1.4), cells can tolerate DNA damage during replication by using translesion synthesis – replicating over damaged bases using specialised polymerases – or fork reversal, a complex process where forks anneal in a four way structure with newly synthesised strands, and proceed in the opposite direction to avoid DNA damage (Quinet et al., 2017). However, there is another possible mechanism that takes a much more simplistic and intuitive approach –

simply restarting replication by generating a new primer downstream of the DNA lesion. This restart mechanism was first proposed by Rupp and Flanders in a seminal paper published over 50 years ago (Rupp and Howard-Flanders, 1968).

Repriming pathways exist across all domains of life but are performed by different replicative enzymes. In *E.coli,* both leading and lagging strand repriming are performed by the replicative primase DnaG (Bouché et al., 1975; Heller and Marians, 2006). The roles of DnaG (primase) and DnaB (helicase) in this repriming process have now been established (Yeeles and Marians, 2013; Yeeles and Marians, 2011). In yeast, *in vitro* evidence suggests that the Pol α complex performs leading and lagging strand repriming (Georgescu et al., 2015). In the absence of this process, cells show increased stretches of ssDNA, fork uncoupling, and error prone annealing events, and cells default to using TLS polymerases, specifically mutagenic pol ζ (Fumasoni et al., 2015).

In humans, as described in 1.1, the Pol α / primase complex generates and extends primers during the repeated cycle of Okazaki fragment generation on the lagging strand, but also only once at the origin for the leading strand (Burgers and Kunkel, 2017). There is currently no substantial evidence to suggest that human Pol α can reprime to play a role in DNA damage tolerance on the leading strand during DNA replication. However, there was suggestions of a repriming enzyme present in human cells. The supporting evidence for such a mechanism came in the form of ssDNA gaps left behind after replication resumed, with initial papers suggesting that this was a by-product of a repriming event (Bainbridge et al., 2021; Elvers et al., 2011; Lehmann, 1972; Lopes et al., 2006). The discovery and cementation of repriming as a canonical DNA damage tolerance pathway are reviewed in Bainbridge *et al.,* (2021, Appendix A). It is clear now that repriming in human cells is dependent on the recently discovered primase polymerase, PrimPol.

1.6 Eukaryotic PrimPol

PrimPol (Primase-Polymerase) is a eukaryotic enzyme from the archaeo-eukaryotic primase (AEP) superfamily involved in DNA damage tolerance in both the mitochondria and the nucleus (Bianchi et al., 2013; García-Gómez et al., 2013; Keen et al., 2014b; Mourón et al., 2013; Wan et al., 2013). Its ability to act as both a TLS polymerase and a DNA-dependent DNA primase allows it to maintain DNA replication by potentially synthesising over or bypassing DNA lesions and structures and allowing continuation of stalled DNA synthesis by the replicative polymerases. PrimPol can overcome a variety of lesions, and its loss induces several clear phenotypes in cells, which are exasperated by the loss of other DDT pathways, such as Pol η. Recent work on the cellular role of PrimPol has revealed that the specific application of DNA-damaging agents promotes PrimPol-mediated DNA damage tolerance, and that PrimPol-mediated repriming leaves behind products that activate HR pathways. The absence of PrimPol induces both mitochondrial defects and phenotypes indicative of genomic instability. This section will discuss the catalytic activities and domain architecture of PrimPol that enable it to rescue stalled forks. It will also describe PrimPol's interaction with partner proteins that assist in its recruitment to stalled forks. Finally, we will discuss the collated evidence of PrimPol's contribution to the DNA damage tolerance landscape during replication in eukaryotic cells.

1.6.1 Discovery of PrimPol and an overview of its domain architecture

In 2005, 13 families of archaeo-eukaryotic primase (AEP) enzymes were classified from *in silico* analyses and organised into 3 major families: the AEP proper clade, the nucleo-cytoplasmic large DNA virus (NCLDV)-herpesvirus primase clade, and the Prim-Pol clade (Iyer et al., 2005). Mammalian PrimPol (previously called CCDC111 / FLJ33167 / hPrimPol1) was assigned to the NCLDV clade, which includes enzymes present in eukaryotic viruses. It was renamed Primase-Polymerase (PrimPol) to more accurately describe its biochemical activities as a bifunctional replication enzyme (Bianchi et al., 2013; García-Gómez et al., 2013; Mourón et al., 2013; Rudd et al., 2013; Wan et al., 2013). Orthologues of PrimPol are found in vertebrates, higher and more primitive eukaryotes, and plants, with a few notable absences (e.g. *Drosophila*

melanogaster, *C. elegans*, *S. pombe*, *S. cerevisiae*), which indicates that PrimPol has likely been lost at multiple, separate instances throughout evolution. Sequence analysis revealed that PrimPol enzymes, including human PrimPol, contain an AEP domain (101-240) and a UL52-like zinc finger domain (392-470) as described in Iyer et al., (2005).

In the initial computational study of PrimPol proteins, several conserved motifs were discovered, including three conserved motifs that make up the AEP domain, motif I, II and III (Iyer et al., 2005) (Figure 1.8). The metal ligands in AEP primases are normally aspartates and form a DxD motif. In the case of human PrimPol, this domain – motif I – is DxE, with a glutamic acid residue at 116 replacing the standard aspartate. Another AEP protein with a glutamate in the final position is ORF904, a prokaryotic replicative protein found on the pRN1 plasmid in *Sulfolobus islandicus* (Sanchez et al., 2009). Motif I and motif III, which includes Asp280, contain the key residues responsible for metal ion coordination and are therefore essential for the catalytic activity of these enzyme (Bianchi et al., 2013; Keen et al., 2014b). These motifs are specific to AEP enzymes, and are highly conserved (Figure 1.8).

Amino acids 201-260 are an unstructured region of human PrimPol (Rechkoblit et al., 2016). The crystal structure of a human PrimPol truncation contains only the AEP domain. The structure shows the enzyme in complex with template DNA and a Ca^{2+} ion occupying the metal B position, as well as an incoming nucleotide. There is no metal ion in the metal A position (Rechkoblit et al., 2016). This structure suggests that the AEP domain has no contacts with the primer strand, only binding to the template strand. This structure reveals only the conformation of PrimPol in its polymerase mode – elongating a pre-existing primer - and that the structure of the enzyme when acting as a primase may be significantly different, particularly in the regions missing from this structure.

PrimPol is monomeric (Keen et al., 2014b); this differs from traditional replicative AEP enzymes, which form heterodimers, such as the eukaryotic replicative primase complex Pri1/Pri2 (Arezi and Kuchta, 2000). PrimPol contains a UL52-like zinc finger domain downstream of the AEP catalytic domain. Zinc finger domains often contain cytosine and histidine residues that co-ordinate binding of

the zinc ion: PrimPol's zinc finger domain contains one histidine and three conserved cytosines (C2HC). UL52 domains are zinc finger primase motifs, found in the Herpes simplex virus type 1 and 2 (HSV-1/2) (Chen et al., 2005). PrimPol's zinc finger domain is similar to this type of zinc finger (Bianchi et al., 2013). This domain is essential for primase activity but not polymerase activity, though PrimPol's specific polymerase activity, along with its fidelity and processivity were decreased in the zinc finger KO mutant (Keen et al., 2014b). PrimPol mutated at this site is also unable to bind ssDNA in assays performed by the Doherty lab, though in a recent publication, data was obtained to suggest that its ssDNA-binding ability is entirely conferred by the its catalytic core (Martínez-Jiménez et al., 2018), independently of the catalytic residues (Calvo et al., 2019). The zinc finger domain has been proposed to be required for selecting and binding the first nucleotide that initiates the synthesis of the new primer strand, with a preference for triphosphate-containing nucleotides. A similar preference for triphosphate-containing nucleotides has been seen in a DNA primase recently discovered in the deep-sea vent phage NrS-1 (Zhu et al., 2017).

Two acidic RPA binding motifs (RBMs) are present in the C-terminus of PrimPol. PrimPol interacts through these two motifs, RBM-A (aa 510-528) and RBM-B (aa 542-560) in human PrimPol, with the basic cleft of RPA 70N (Guilliam et al., 2017; Guilliam et al., 2015). These sites bind independently and competitively, with the removal of either site individually not impeding RPA binding, but the removal of both totally abrogating it. The *in vivo* consequences for the mutation of either of these sites will be discussed in 1.6.4.2.

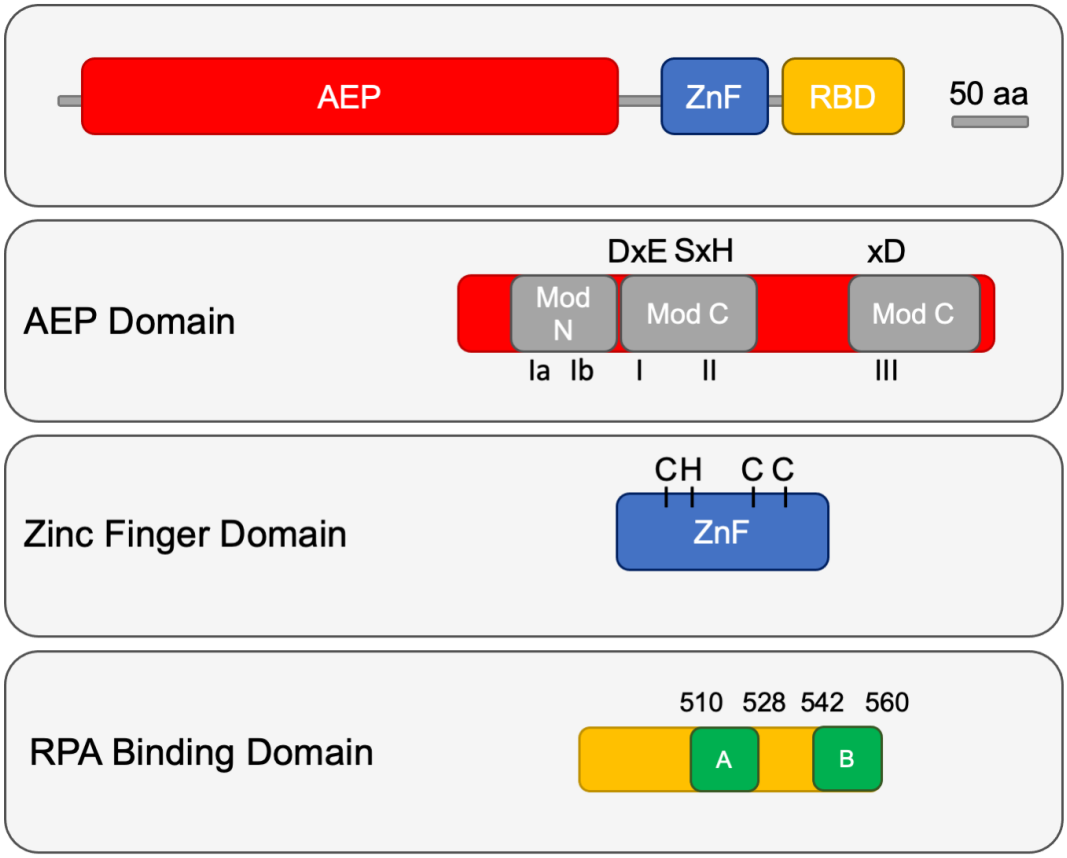

Figure 1.7. The domain architecture of human PrimPol

The domain architecture of PrimPol is depicted in the top panel. The second panel shows only the AEP domain (red). ModN and ModC (labelled) comprise the archaeo-eukaryotic primase (AEP) domain and contain motifs Ia, Ib, I, II, and III, required for template binding and catalytic activity. The zinc finger (ZnF) (blue) contains three conserved cysteines and a histidine which coordinate a zinc ion and are required for primase, but not polymerase, activity. The RPA binding motifs (RBD) (yellow) containing RPA binding motif-A (RBM-A) and RBM-B (green) is located at the C-terminus. A 50 amino acid (aa) scale bar is shown to the right of the top panel.

1.6.2 PrimPol's catalytic activities

1.6.2.1 PrimPol's polymerase activity

PrimPol can act as a DNA-dependent DNA polymerase, with low processivity and low fidelity (Keen et al., 2014b). It is a distributive polymerase, inserting between 1 and 4 nucleotides before dissociating, a similar level of processivity compared to other TLS polymerases. This is probably explained by its open active site and limited contacts with the primer-template strands (Rechkoblit et al., 2016). TLS polymerases are characterised by modified finger and thumb domains which make fewer DNA contacts than traditional replicative polymerases such as Polymerase δ, meaning the stability of the enzyme on the DNA is decreased (Sale et al., 2012). For example, Pol ι can only insert 2-3 nucleotides before dissociating (Tissier et al., 2000).

Interestingly, Keen *et al.,* (2014b) showed that PrimPol's low processivity was due to the zinc finger, and while mutated protein - with the primase domain present but inactive - had decreased processivity, a truncated version of the protein lacking this domain entirely had increased processivity and extension activity. This suggests that the zinc finger domain, independent of its primase activity, regulates PrimPol's processivity. This is one of the first suggestions of a strong auto-regulatory mechanism that controls the synthesis activity of the PrimPol protein.

PrimPol will on average insert the wrong base during DNA synthesis every 10^4 – 10^5 bases (Guilliam et al., 2015), a similar fidelity to other TLS polymerases (Matsuda et al., 2000). However, PrimPol's main mutagenic signature is a propensity to introduce insertion-deletion (indel) mutations (Guilliam et al., 2015; Keen et al., 2014b). The presence of manganese, though required for a number of PrimPol's activities including processive TLS activity, has been shown to decrease PrimPol's fidelity (Zafar et al., 2014).

PrimPol's ability to perform nucleotide transfer, to extend DNA using dNTPs was recently shown to be dependent on the metal cofactor provided. PrimPol's usage of Mn^{2+} and Mg^{2+} ions as metal cofactors has been a point of interest since PrimPol's discovery, and as mentioned previously, Mn^{2+} has been found to

stimulate the enzymatic activity of PrimPol and is required for the formation of the enzyme:DNA:dNTP complex, independent of the ZnFD (Martínez-Jiménez et al., 2018). PrimPol can catalyse DNA synthesis using with Mn^{2+} or Mg^{2+} metal ions, though it shows a preference for the former (Zafar et al., 2014). However, mutating Glu116 to the standard aspartate negatively affects PrimPol's ability to use manganese as a cofactor, and leading to instability in the formation of the PrimPol:ssDNA:base complex, its formation becoming undetectably low (Calvo et al., 2019).

PrimPol has also been shown to act as a TLS polymerase *in vitro*, bypassing a number of lesions such as 8-Oxo-G and 6-4PP. Although it is unable to bypass CPD lesions (Bianchi et al., 2013; García-Gómez et al., 2013), the truncated catalytic core alone can do so, suggesting a level of regulation in the protein's activity outside of its active site (Keen et al., 2014b). PrimPol is able to both bypass and extend from 8-Oxo-G residues and 6-4PP (Zafar et al., 2014), and has been suggested in some contexts to "loop out" the damaged bases instead of synthesising opposite them, resuming synthesis at a later undamaged base (García-Gómez et al., 2013; Mourón et al., 2013). This form of pseudo-TLS is enhanced by the presence of manganese (Mourón et al., 2013).

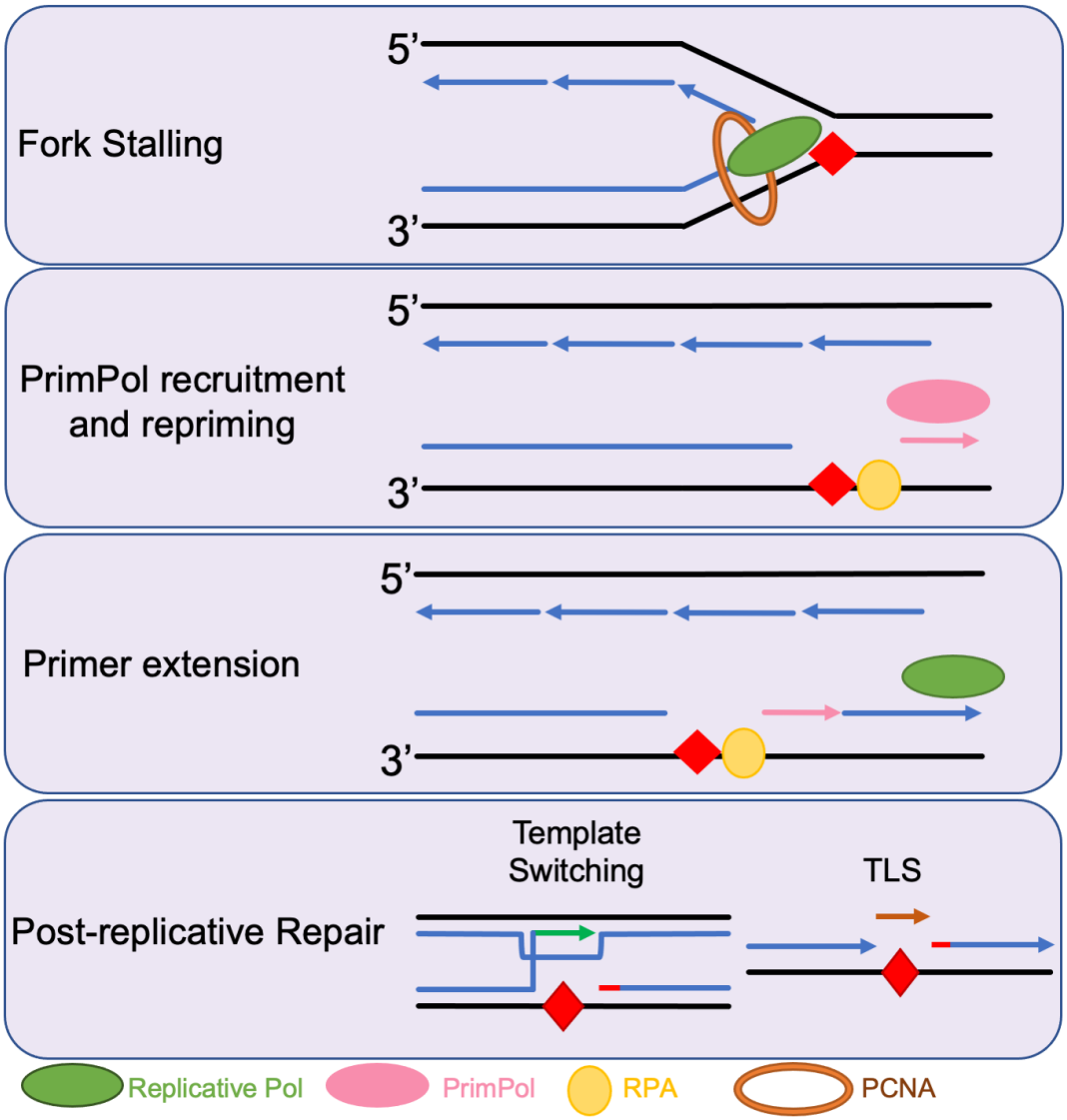

Figure 1.8. An overview of PrimPol mediated repriming after template lesion

The replicative polymerase is stalled on the leading strand by a lesion, secondary structure, or CTNA. Parental DNA unwinding and lagging strand replication continues, subsequently generating ssDNA on the leading strand. This ssDNA is bound by RPA. The generation of RPA-bound ssDNA leads to PrimPol's recruitment, facilitated by the interaction between RPA70 and PrimPol's C-terminus. Following recruitment, PrimPol reprimes the leading strand. After repriming and some extension by PrimPol, the primer is handed off to the replicative polymerase, and replication resumes.

1.6.2.2 PrimPol's primase activity

Human PrimPol is also able to instigate *de novo* synthesis by acting as a DNA primase. Primer synthesis is typically initiated using NTPs; while PrimPol does require an initiating NTP, unlike canonical replicative primases (Pri1/S) it prefers to generate primers using dNTPs (Bianchi et al., 2013; García-Gómez et al., 2013). PrimPol is therefore classed as a DNA-dependent DNA primase. The ability to synthesise primers using both NTPs and dNTPs makes PrimPol unique among eukaryotic polymerases. PrimPol's increased use of dNTPs is due to the zinc finger domain, which shows a preference for triphosphate containing nucleotides (Bianchi et al., 2013). The zinc finger domain in human PrimPol is essential for the primase activity, both *in vivo* and *in vitro*. However, it is fully dispensable for the polymerase and TLS activities (Keen et al., 2014b). PrimPol's primase activity can therefore be abrogated by the mutation of key sites within the domain, specifically C419A and H426A (Keen et al., 2014b). This primase ability has been suggested to initiate from a specific sequence (GTCC) (García-Gómez et al., 2013). *In vivo* evidence for PrimPol's role as a primase will be discussed in 1.6.4.2.

1.6.3 PrimPol's interaction with partner proteins

A number of additional proteins have been shown to impact upon PrimPol's primase and polymerase activities. One of the first studies on human PrimPol found that it interacts with the ssDNA-binding RPA complex (Wan et al., 2013). This initial analysis showed an interaction between RPA1 (but not RPA2 or RPA3), which would be further examined by Guilliam *et al*. (2015, 2017). PrimPol also interacts with mtSSB, the mitochondrial ssDNA-binding protein (Guilliam et al., 2015), which will likely play a role in its recruitment in the mitochondria in a similar way to RPA. The C-terminus of PrimPol contains two separate acidic motifs responsible for binding RPA called the RPA-binding motifs (RBMs), both of which bind to the cleft of RPA1 70N domain (Guilliam et al., 2017). In the case of Pol α, RPA binding increases the processivity and stimulates the polymerase activity (Maga et al., 2001). Although both RPA and mtSSB strongly inhibit PrimPol's ability to synthesise primers with either dNTPs or rNTPs on short oligonucleotide templates (Guilliam et al., 2015), in experiments using longer M13

ssDNA – used to mimic the stretches of ssDNA found *in vivo* after fork stalling – PrimPol is able to extend primers with improved processivity at concentrations of RPA approximating 500nM (Guilliam et al., 2017; Martínez-Jiménez et al., 2017). At higher concentrations (> 2 μM), RPA becomes inhibitory, preventing priming, likely by simply binding to the entire stretch of ssDNA and blocking access to the template. On the same template, the addition of Pol ε lead to the highest level of products synthesised, implying the increased primer synthesis by PrimPol creates primers for Pol ε/δ to extend. However, on short templates (14-50nt) PrimPol is unable to displace other binding proteins in order to extend further, leaving it able to contribute only a few bases of DNA synthesis. The role of the RPA binding motifs *in vivo,* particularly as they pertain to chromatin binding in the cell, will be discussed in 1.6.4.2.

Polymerase-δ interacting protein 2 (PolDIP2) was first discovered as a binding partner of Pol δ and PCNA (Liu et al., 2003). It has also been shown to bind to PrimPol, as well as other TLS polymerases such as Pol η (Tissier et al., 2010). PrimPol's precise PolDIP2 binding domain is not yet known, though it has been shown to bind to the catalytic fragment (1-354) of PrimPol, inferring it does not require the C terminus to bind. When the rate of primer extension after the titration of PolDIP2 was plotted, it showed a sigmoidal shape, from which the authors deduced that PrimPol may bind two PolDIP2 molecules at once (Guilliam et al., 2016). PrimPol's interaction with PolDIP2 increased both the rate of primer formation and primer length, and PrimPol's ability to bind DNA by forming a DNA-bound complex with PrimPol. PolDIP2 also increases PrimPol's processivity by approximately 4-fold. PolDIP2 also interacts with mtSSB (another PrimPol partner) (Cheng et al., 2005), and the three proteins may interact together in some way during PrimPol's activity in the mitochondria.

PCNA interacts with Y family TLS polymerases and allows them to perform polymerase switching – the act of removing Pol delta, stalled at a lesion, and replacing it with a TLS polymerase that can replicate over the lesion. However, PrimPol has been shown to have no interaction with either ubiquitinated or non-ubiquitinated PCNA indicating that it is not regulated by the Rad18 epistasis group. PrimPol's activity was inhibited by the presence of PCNA, and when the

reaction contained both PCNA and PolDIP2 – shown to stimulate PrimPol's activity and processivity - this inhibition was maintained (Guilliam et al., 2016).

In cells, PolDIP2 depletion caused a decrease in replication fork speed, but an additional decrease was not observed when PrimPol was knocked down as well, inferring that the two function together in an epistatic way as the combined loss of the two is equivalent to loss of either one (Guilliam et al., 2016). Additionally, the knockout of PolDIP2 did not induce any significant sensitivity to UV-C damage, similar to the lack of sensitivity seen when PrimPol is knocked out (Tsuda et al., 2019). Whether this interaction between PrimPol and PolDIP2 leads to TLS activity or repriming by PrimPol remains unclear; though it has been shown that the depletion of PolDIP2 leads to decreased TLS and increased template switching, this model does not account for the third means of DDT, namely repriming using PrimPol. This raises questions, such as why the absence of PolDIP2, if required for both PrimPol's activity and the activity of other TLS polymerases, did not induce a more significant DNA damage sensitivity when tested in colony survival assays (Tsuda et al., 2019). Regardless, current research indicates that PolDIP2 and PrimPol act together in at least one DDT pathway.

PrimPol has also been suggested to interact with WRNIP1. WRNIP1 is a highly conserved DNA-dependent ATPase enzyme, which interacts with the WRN helicase (Kawabe et al., 2001). Its role in human cells remains somewhat obscure. It contains a ubiquitin-binding zinc finger (UBZ) domain similar to that of Rad18, and an ATPase domain. After previously implicating WRNIP1 in the recruitment of Pol η to sites of UV damage, and inferring that PrimPol responded to this damage if either WRNIP1 or Pol η were absent, Yoshimura and colleagues showed that endogenous levels of PrimPol protein increased when WRNIP1 was downregulated, and decreased in a proteasome dependent manner when WRNIP1 is overexpressed (Yoshimura et al., 2019). Their model suggests that WRNIP1 binds to PrimPol to allows for its degradation, to prevent its association with UV induced DNA lesion, in contrast to previous work suggesting UV damage leads to PrimPol's interaction with chromatin (Bianchi et al., 2013; Kobayashi et al., 2016).

Finally, PrimPol has very recently been shown to interact with USP36, a deubiquitinase enzyme. USP36 is deubiquitinated following DNA replication stress, leading to increased protein levels and increased interaction with PrimPol. This, in turn, is hypothesised to stabilise the PrimPol protein and prevent its degradation. Conversely, knockdown of USP36 was implicated in the sensitisation of cells to agents such as UV-C and HU, which the authors imply is due to instability of PrimPol protein in the absence of USP36 (Yan et al., 2020).

1.6.4 PrimPol's function in eukaryotic cells

Tagging and overexpression of human PrimPol showed that the majority of PrimPol was found in the cytoplasmic and the mitochondrial compartments in human cells (Sean Rudd, PhD thesis; Bianchi et al., 2013). Supporting this, an estimation of the precise distribution suggested that only 19% of PrimPol protein is found in the nucleus in undamaged cells, with 47% of PrimPol found in the cytoplasm and 34% in the mitochondria (García-Gómez et al., 2013). These numbers, while giving an overall picture of the distribution of PrimPol, do not account for differences in localisation across the cell cycle – one potential reason for the increased PrimPol levels in the mitochondria is that mitochondrial DNA replication occurs throughout the cell cycle, and PrimPol may play a role in this replication. Nuclear localisation may, therefore, increase during S phase, consistent with its role in general fork progression (Bailey et al., 2019).

1.6.4.1 PrimPol in the nucleus

To date, most studies on PrimPol's role in the cell have focused on its nuclear role. PrimPol has been shown to be recruited to sites of DNA damage *in vivo* (Bianchi et al., 2013; García-Gómez et al., 2013; Wan et al., 2013). The initial characterisation of PrimPol in cells found that while PrimPol is predominately cytoplasmic in undamaged cells, the protein localised to the nucleus after the application of UV damage, and formed detergent resistant foci, implying that UV damage causes PrimPol to bind to chromatin (Bianchi et al., 2013).

A number of studies, in both human and avian cells, has greatly expanded our knowledge of PrimPol's importance in cells. PrimPol knock-out DT40 avian cells showed pronounced sensitivity to UV-C damage, 4NQO (a UV-C mimetic),

cisplatin, CTNAs and MMS, but no greater sensitivity to X-rays, camptothecin, γ-rays or IR (Bailey et al., 2016; Bianchi et al., 2013; Kobayashi et al., 2016). DT40 cells also showed that, compared to Pol η knock-out cells, there is no loss in post-replicative bypass of UV-C damage, but that fork speeds and general fork progression decreased in PrimPol's absence. (Bailey et al., 2016; Keen et al., 2014b). This suggests a role for PrimPol is the maintenance of fork progression after UV-C damage.

Further investigation of PrimPol's role in damage recovery revealed that, when damaged by UV-C, PrimPol$^{-/-}$ DT40 cells stalled in G2, and were prevented from entering mitosis (Bailey et al., 2016). This phenotype was more pronounced in PrimPol$^{-/-}$ cells than Pol η$^{-/-}$ cells. The addition of a Chk1 inhibitor did not alleviate this stalling entirely, suggesting that in the absence of PrimPol, DT40 cells are stalled in G2 and unable to enter mitosis in a manner somewhat dependent on Chk1 but maintained by other pathways. Further investigation revealed that the G2 stalling after damage could be prevented by the addition of a p38 inhibitor, but could not be reversed by this inhibitor, suggesting initial activation of the checkpoint may rely on p38 but maintenance of the G2 stalling does not require it. It's clear from these data that in DT40 cells, PrimPol plays a vital role in DNA damage tolerance, potentially one that cannot be fulfilled by Pol η or other TLS polymerases. Interestingly, in the absence of Pol η lesions remain unrepaired, and this leads to cell death. However, in the absence of PrimPol, cells do not die, but instead remain stalled in G2 – unable to proliferate, but still alive. The reasons for this specific phenotype are currently unknown but it suggests that PrimPol plays a key role in the tolerance of a specific lesions, the presence of which leads to robust activation of checkpoint pathways as opposed to apoptosis.

The importance of PrimPol in DNA damage tolerance was further elucidated by the study of PrimPol$^{-/-}$ MRC-5 cells (Bailey et al., 2019), which once again showed decreased fork speeds, increased fork stalling after damage, though the UV sensitivity observed in DT40 cells was not seen in the human knock-out (or knock down) cells (Bianchi et al., 2013). This suggests that in human cells, while the recovery is slower, cells do recover from DNA damage, likely by employing another DDT mechanism. This discrepancy is likely due to the significantly faster doubling time of DT40 cells compared to human cells – 11 hours compared to 24

hours (Cervera et al., 2011; Orlowska et al., 2013). Human PrimPol$^{-/-}$ cells also exhibit a variety of phenotypes that indicate the important role the protein plays in genetic stability. These include increases in micronuclei, sister-chromatid exchanges and mutation frequency (Bailey et al., 2019). PrimPol$^{-/-}$ cells also show a decrease in fork speed, even when no exogenous damage was applied, indicating a role for PrimPol in maintaining efficient DNA replication in unperturbed cells.

Furthermore, PrimPol$^{-/-}$ Pol η $^{-/-}$ human cells are more sensitive to UV, cisplatin, 4NQO and zeocin than either PrimPol$^{-/-}$ or Pol η $^{-/-}$ cells. These cells also experience more pronounced stalling in S phase than the single knock-out lines, suggesting further slowing of replication forks in response to the absence of two damage tolerance proteins (Bailey et al., 2019). These phenotypes indicate that PrimPol's role in the cells is non-epistatic to the role of Pol η.

1.6.4.2 PrimPol in the mitochondria

Unlike nuclear DNA replication, mitochondrial DNA synthesis is less tightly coupled to the cell cycle, and replication can occur in any cell cycle stage. Additionally, replication is not initiated by Pol α primase complex, but instead by POLRMT (Tiranti et al., 1997). Replication of the mitochondrial genome is performed by Pol γ (Bebenek and Kunkel, 2004). There are approximately 1000 copies of the mitochondrial genome in a mammalian cell, and mitochondrial copy number indicates the efficiency with which the cell has replicated this genome (Legros et al., 2004). It is known that PrimPol does not perform essential priming activity on the mitochondrial replisome, as both knock-out cells and mice are viable (Bailey et al., 2019; García-Gómez et al., 2013). However, more oxidative damage is thought to occur in mitochondrial DNA than on nuclear DNA (See 1.2.2.1). Pol γ, the mitochondrial polymerase, has trouble bypassing oxidative damage, and while bypass of 8-oxo-G has been seen, albeit in an error-prone manner (Hanes et al., 2006), Pol γ completely stalls when encountering abasic sites (García-Gómez et al., 2013).

As PrimPol acts as both a primase and TLS polymerase *in vitro*, and is found to localise to the mitochondria, it was expected it would perform both functions to allow lesion bypass in the mitochondria. However, recent work infers that PrimPol

is not able to act as a TLS polymerase, at least in the case of bypass of oxidative lesions in the mitochondria, as the addition of PrimPol to *in vitro* experiments using Pol γ and the mitochondrial replisome proteins, including PrimPol partner protein mtSSB, had no effect on the bypass of DNA damage (Bailey and Doherty, 2017).

Notably, the presence of the mitochondrial helicase Twinkle did stimulate PrimPol's enzymatic activity, but this was independent of DNA damage on the template (Stojkovič et al., 2016). The role of PrimPol in the mitochondria, therefore, seems to be as a repriming enzyme, as a decrease in replication reinitiation was observed in in the mitochondria after replication stalling in PrimPol deficient cells (Torregrosa-Muñumer et al., 2017).

The most extensive work studying PrimPol's role in the mitochondria was found in studies performed by Bailey et al., (2019). This research utilised human PrimPol$^{-/-}$ cells to analyse specific mitochondria phenotypes, such as mitochondrial copy number, membrane potential and replication after stalling of the mitochondrial polymerase Pol γ, and replication intermediates indicative of replication stalling. PrimPol knock-out cells were found to have significant mitochondrial copy number increases, which was consistent across human cell lines treated with siRNA, DT40 PrimPol$^{-/-}$ cells and mouse embryonic fibroblasts (MEFs) (Bailey et al., 2019; Torregrosa-Muñumer et al., 2017). This coincided with an increase in mitochondrial nucleoid number, but not nucleoid size. Mitochondria function, as determined by mitochondrial membrane potential, was not significantly impacted by the loss of PrimPol. Interestingly, despite the increase in copy number, DNA replication speed, or the abundance of replication forks, was seen to decrease in PrimPol$^{-/-}$ cells, with additional signs of replication stalling at later stages of replication. It is possible that an increase in copy number reflects the need for more copies to maintain functionality. It is likely that PrimPol is only one of several players involved in mtDNA damage response, and works in conjunction with the mitochondrial polymerase, and other enzymes, to promote DNA damage tolerance (Copeland et al., 2016).

1.6.4.3 The importance of PrimPol's primase activity in cells

As mentioned previously, PrimPol can act as both primase and a TLS polymerase *in vitro*. However, it is important to understand how PrimPol acts in a cellular environment. Data obtained thus far suggests that in vertebrate cells, PrimPol primarily acts as a primase. The importance of PrimPol's repriming activity was first demonstrated in Keen *et al.* This paper showed that fork speed decreases observed in PrimPol$^{-/-}$ avian cells could be complemented by expression of either primase- or polymerase-deficient PrimPol, but that the fork stalling observed when PrimPol is absent was not recovered by expression of primase-deficient PrimPol (Keen et al., 2014b). PrimPol's primase activity has been shown to allow the tolerance of specific DNA replication impediments. For example, PrimPol is able to restart replication and allow bypass of G-quadraplex structures on the leading strand of avian DT40 cells (Schiavone et al., 2016). While unable to replicate over the G4 blockage, PrimPol was able to reprime downstream of the lesion by "close-coupled" repriming – which occurs close to the stalling structure – and restart DNA synthesis *in vivo*. This bypass was determined to be specific to the primase activity of PrimPol, as both AxA mutants (catalytic inactive) and Zinc finger mutants (primase inactive) lead to a loss of expression in the reporter assay, indicating extensive uncoupling of the helicase and the replication fork. Schiavone *et al*., propose a model whereby PrimPol is recruited, by means of its interaction with RPA, to sites where a G4 quadraplex has stalled leading strand replication. PrimPol then reprimes downstream of the blockage to allow replication to continue. Rev1, a TLS polymerase, has also been shown to play an important role in the *in vivo* tolerance of G4 quadraplexes, particularly those with longer single stranded loops (Schiavone et al., 2014), while PrimPol appears to be primarily utilised in the bypass of shorter, more thermodynamically stable G4 quadraplexes (Schiavone et al., 2016).

Repriming mediated by PrimPol is also required for cells to tolerate GAA repeats, found commonly in the genome, that can potentially form secondary structures such as R-loops: DNA:RNA hybrid structures. Specifically, using both primase and polymerase separation of function mutants, they found that PrimPol's primase ability was required to resolve the replication stalling at these sites (Šviković et al., 2019). Overexpression of RNase H1 compensates for the lack of

PrimPol by degrading these DNA:RNA hybrid structures. The model for PrimPol's role in this system relies on PrimPol's ability to reprime after the replication machinery stalls at an R-loop, generated when GAA(10) repeats are transcribed. When the machinery stalls, the helicase continues unimpeded, leading to ssDNA stretches which are bound by RPA. This in turn recruits PrimPol, which reprimes after the R-loop to allow replication to continue. In cells without PrimPol – or, one would imagine, cells without PrimPol capable of binding RPA - the fork will collapse into potentially deleterious DNA damage. The limit of PrimPol's interaction with these R-loops may, as the authors pose, depend on the fate of the RNA polymerase that transcribed the repeat – if the polymerase never completed transcription and remains stalled on the DNA, it will collide with the replication machinery; it is unlikely PrimPol's repriming capacity would help in this scenario.

Further evidence for the important role of PrimPol-mediated repriming events comes from a study using Chain-Terminating Nuclear Analogues (CTNAs, reviewed in 1.2.2.4). Since bypass by extending from the CTNA is impossible, repriming remains the only DNA damage tolerance pathway available to resume replication. Experiments performed in DT40 cells showed that, after fork stalling induced by CTNA incorporation, cells lacking PrimPol showed dramatically decreased survival. This decrease in survival could be complemented by WT PrimPol, but not truncated PrimPol lacking the zinc finger domain, or PrimPol with zinc finger knockout mutations (Kobayashi et al., 2016; Schiavone et al., 2016). This is supported by *in vitro* evidence showing that PrimPol can reprime DNA synthesis downstream, close to the site of the replication terminating CTNA. Together, these data establish PrimPol's additional role in maintaining active DNA replication after forks encounter CTNAs or similar lesions.

While most evidence suggests PrimPol primarily acts as a primase in human cells, it's possible that PrimPol has secondary activity as a TLS polymerase. However, it may act in this capacity only in certain circumstances, possibly when other pathways such as canonical TLS mechanisms are prevented from operating.

1.6.4.4 PrimPol's interaction with other DNA repair pathways

BRCA proteins are known to protect replication forks undergoing reversal from degradation, meaning that BRCA null cells are susceptible to the increased genomic instability brought on by extensive fork degradation (Quinet et al., 2017). Interestingly, while one dose of cisplatin applied to BRCA null cells lead to reversed fork degradation, two doses of cisplatin – a small pre-dose followed, 24 hours later, by a challenging dose - upregulates PrimPol protein levels, and increases this proteins propensity to bind chromatin, leading to rescue of the fork degradation phenotype characteristic of the BRCA1$^{-/-}$ cells. This was also observed after "pre-doses" of other DNA damaging agents such as UV-C or HU. These data, coupled with experimental evidence from Bailey *et al.* and Tsuda *et al.,* suggests that cells are able to dynamically switch between DDT mechanisms depending on protein availability, and that pre-doses of damage or stress can lead to an adaptive response (Quinet et al., 2020).

The increase in PrimPol protein observed after pre-doses of cisplatin is dependent on the ATR pathway. ATR activation occurs in response to RPA binding ssDNA, and the subsequent binding to ATRIP (Zou and Elledge, 2003). Quinet *et al.* suggest PrimPol overexpression is linked to decreased replication fork reversal and that the suppression of traditional fork reversal proteins such as Rad51 and SMARCAL1 leads to an increase in ssDNA tracks, indicative of PrimPol repriming events (Quinet et al., 2020). In undamaged cells, levels of PrimPol protein remain consistent throughout the cell cycle, though protein binding to chromatin is only observed in G1 and S phase (Mourón et al., 2013).

The repriming role of PrimPol has been examined further in recent work, where it was found that Rad51 foci formation was induced both by small and high doses of the environmental carcinogen BPDE, but in the lower doses, foci formation was independent of HR activation, suggesting the foci were forming in response to another repair pathway (Piberger et al., 2020). This pathway was shown to be PrimPol repriming-mediated DNA damage tolerance and Rad51 was seen to bind to ssDNA left behind by such repriming events. These Rad51-bound stretches of ssDNA are then repaired by HR. In PrimPol depleted cells, or cells expressing primase-deficient PrimPol, low doses of BPDE induced fork speed decreases, a

decrease in ssDNA gaps and prevented Rad51 foci formation. At high BPDE concentrations, which induced the recruitment of DSB repair factors, the formation of Rad51 foci was PrimPol independent. Interestingly, WRNIP1 has been shown to stabilise Rad51 binding to ssDNA, which is now thought to be an intermediate of a PrimPol-mediated repriming event in some instances, though while WRNIP1 is posited to form a complex with PrimPol, it is unclear how these pathways interact, as Yoshimura *et al.,* (2019) propose WRNIP1 stimulates the degradation of PrimPol.

1.6.5 PrimPol-like polymerases in Trypanosomes

T. brucei is a protozoan parasite that is the cause of the human disease African trypanosomiasis (Ponte-Sucre, 2016). In this organism – which, as one of the earliest diverging organisms from the eukaryotic tree, is an interesting model to analyse – there are two PrimPol-Like proteins (PPL): PPL1 and PPL2. PPL1 and PPL2 share ∼16% and ∼11% homology with human PrimPol, respectively, and ∼10% homology with each other (Rudd et al., 2013). However, these two proteins both share the catalytic capabilities of human PrimPol; both PPL1 and PPL2 contain the characteristic AEP domain found at the N terminus of PrimPol and a UL52-like zinc finger domain, and both show polymerase activity. This polymerase activity allows them to bypass 8-oxo-G and 6-4PP and extend from templates containing a mismatched base opposite a CPD lesion (Rudd et al., 2013).

As with human PrimPol, PPL1 possesses both primase and polymerase activity. However, although PPL2 retains polymerase activity, primase activity was not evident. This is likely due to the poor quality of the protein used in this study as it is a difficult protein to purify and prone to fragmentation. While the absence of PPL1 has a minimal effect, depletion of PPL2 induces stalling in G2, leading to cell death (Rudd et al., 2013). Interestingly, this stalling occurs after the bulk of DNA replication has been completed, suggesting a role for PPL2 in assisting in the completion of DNA synthesis. PPL2's absence also induced significant increases in DNA damage markers, e.g., γH2AX foci and Rad51 foci. Additionally, after the DNA damaging agent MMS was applied, PPL2 relocalised to the nucleus and formed foci co-localising with γH2AX foci. These findings suggest an

essential role for the polymerase activity of PPL2 in trypanosomes in damage repair or DDT in late S / G2 to prevent replication fork stalling. In the absence of PPL2, excessive fork stalling is potentially leading to checkpoint activation and stalling in G2. This is remarkable as no DNA-damaging agents were applied, suggesting that PPL2 is required to bypass replication impediments caused by endogenous stressors. Only Pol ζ, a TLS polymerase, has been shown so far to be essential for unchallenged DNA replication (Bemark et al., 2000; Esposito et al., 2000; Wittschieben et al., 2000). These data suggest that PPL2 may possibly also fulfil a similar role in *Trypanosomes* as Pol ζ does in yeast.

1.6.6 PrimPol's possible connections with human disease

Due to PrimPol's role in the tolerance of a diverse range of DNA lesions, and its role in both the mitochondria and nucleus, mutations to PrimPol that alter its activity may be involved in many pathologies. An example of such a mutation is Y89D, a mutation found to be potentially linked to the incidence of high myopia (Keen et al., 2014a; Zhao et al., 2013). Tyrosine 89 is located close to motif I in the AEP domain and is highly conserved across domains of life. The mutation decreases both polymerase and primase activity of PrimPol through abolishing the enzymes ability to use rNTPs in DNA synthesis (Keen et al., 2014a). The ability to use dNTPs is retained, and while its processivity is slower, the fidelity of PrimPol's insertion remains the same. In experiments performed by Keen *et al.,* this mutant cannot complement UV-C sensitivity induced by the loss of PrimPol, (though in Kobayashi *et al.,* (2016) it did complement the reduction in survival seen at lower UV doses). The mutant also leads to slower fork rates. The Y89D mutation, in combination with other mutations in other proteins, may induce some of the phenotypes typical of myopia. In tandem with this, the Y89R mutation showed a 10-fold higher RNA-dependent priming activity when compared to the wild type protein (Agudo et al., 2017). However, it is still not clear whether this mutation of PrimPol is a significant contributor to myopia in these patients.

Additionally, a mutation to Y100H, found in a specific type of lung cancer, still displays primase and polymerase activity but this tyrosine to histidine substitution was sufficient to alter the balance of nucleotide insertion, favouring the insertion of NTPs over dNTPs (Díaz-Talavera et al., 2019). In cells, this mutant enhances

the cell's ability to withstand dNTP depletion, leading to a decrease in DSB formation after prolonged exposure to hydroxyurea (Díaz-Talavera et al., 2019). Additionally, mutations to the RPA-binding domains of PrimPol (F522V and I554T) have been found in cancer patient cell lines (Guilliam et al., 2017). PrimPol's role in the onset or progression of cancers has not yet been established but remains an area of significant interest.

PrimPol has also been suggested to act to prevent the accumulation of mutagenic activity at abasic sites. A PrimPol deficiency in some tumours was shown to correlate with increased mutations, and an inverse correlation was seen between single point mutations and PrimPol protein expression (Pilzecker et al., 2016). PrimPol's specific role is thought to be to counter the mutagenic effect of APOBEC3B (Apolipoprotein B MRNA Editing Enzyme Catalytic Subunit 3B), a gene overexpressed in cancers and thought to cause specific mutations in cancer genomes - referred to as APOBEC mutations (Burns et al., 2013). The authors' model suggests that PrimPol reprimes at stalling lesions on the leading strand, correlating to the decreased mutations observed on this strand when PrimPol is present. Following repriming, a PrimPol-dependent repair mechanism would be employed, specifically one known to be high fidelity – the authors suggest this must be homology-directed repair as TLS polymerases are known to introduce mutations. This supports a recent study that reported that, post-PrimPol repriming, Rad51 binds to the ssDNA left behind and this is repaired by HR, an inherently high-fidelity repair mechanism (Piberger et al., 2020). These data support previous work by Bailey *et al*., which suggests that PrimPol$^{-/-}$ MRC-5 cells show an increase in mutation frequency after damage by UV-C or 4NQO, specifically an increased accumulation of transversion mutations (Bailey et al., 2019).

1.7 Objectives of this doctoral thesis

DNA repair is a complex process, with a variety of pathways each responsible for the repair of specific lesions, ready to be employed under different circumstances. However, genome repair is not infallible and therefore, in instances where replication is impeded by unrepaired or misrepaired DNA, damage tolerance mechanisms are vital for proper replication to occur. Both DNA repair and damage tolerance pathways require proper regulation to allow for activation or inactivation depending on the circumstance. Key examples, such as the regulation of TLS polymerases or the activation of the ATM/ATR pathways of DNA repair, show that this regulation can be performed by sequestration, degradation or increased synthesis of proteins and post-translational modifications such as phosphorylation or ubiquitination.

Although PrimPol is an important player in replication fork progression in eukaryotic cells, its precise roles, and how it is regulated, remain to be established. Recent work has examined the interplay between competing DNA damage tolerance pathways, but there has been minimal examination of the regulation of repriming pathway itself. There is specifically very little work examining the post-translational modification of the protein, and none that points to severe phenotypes in human cells. This thesis primarily focuses on studying post-translational mechanisms that regulate the DNA damage tolerance protein PrimPol, a primase-polymerase enzyme known to play a key role in repriming DNA synthesis in human cells. Specifically, the aims of this project are as follows:

Aim One: To investigate the cellular regulation of PrimPol by specific phosphorylation pathways in human cells.

Objective 1: Characterise the cellular phenotypes associated with mutating a number of prominent PrimPol phosphorylation sites and identify the kinases responsible for producing these PTMs.

Objective 2: Assess the pattern of phosphorylation of these sites during the cell cycle and in response to replication stress and DNA damage. Identify how PTMs regulate PrimPol-related damage tolerance pathway in cells.

Aim Two: To characterise the role of repriming in untransformed human RPE-1 cells.

Objective 1: Generate and characterise PrimPol$^{-/-}$ RPE-1 cell lines and investigate their cellular phenotypes.

Objective 2: Generate, through CRISPR-mediated genome editing, an RPE-1 cell line expressing endogenously PrimPol tagged with a fluorescent marker.

Aim One focuses on the regulation of human PrimPol; this research is particularly important now given the current focus on DNA damage tolerance pathways, and in particular mechanisms of pathway choice. PrimPol is a relatively new player in the field, and given difficulties working with endogenous PrimPol protein and limited phenotypes associated with its absence, its mechanism of regulation remains to be established. The residues analysed in this work are novel phosphorylation sites, and an improved understanding of these would aid in the general study of DNA damage tolerance overall. For scientists working specifically on PrimPol-mediated repriming, this research's focus on cell cycle mediated modifications will allow for more focused experimental design.

Additionally, a comprehensive analysis of the cellular phenotypes present after mutation of key residues will allow for these defined phenotypes to be explored in other systems. This will allow for investigation into the overlapping cellular roles of PrimPol with other DTT pathways and the phenotypes associated with co-depleting these DTT pathways. It also lays the groundwork for research to establish the extent to which PrimPol, and other pathways, facilitate replication restart following stalling across S-phase and better define the interplay and deployment of these DTT mechanisms according to cell cycle stage.

Aim two focuses on generating new cell lines to benefit PrimPol research in the untransformed RPE-1 cell line. Investigating PrimPol's absence in these stable, immortalised diploid cells, through the creation of a knockout cell line, provides more data to support previous published work on the phenotypes associated with a lack of repriming, along with a resource for future work. The generation of a novel cell line expressing fluorescent tagged PrimPol under its endogenous promoter will additionally allow for complex visualisation experiments to be conducted. With several outstanding questions surrounding the recruitment, localisation, and dissociation of PrimPol protein to stalled replication forks, this cell line will be a valuable resource for future work.

Chapter 2
Materials and Methods

2.1 Preparation of plasmid DNA

2.1.1 Transformation of competent *E. coli*

To prepare DNA, DH5α *E. coli* was transformed with the plasmid of interest by adding 100ng of DNA from either a Miniprep (2.1.2) or the product from a PCR Clean reaction (NEB) to 50 µl competent cells. Cells were defrosted on ice before the addition of DNA and incubated on ice for 30 minutes. The cells were then heat shocked for 45 seconds at 42 °C, left on ice for a further 3 minutes, before 1 ml of lysogeny broth (LB) media was added and cells were incubated, shaking, at 37 °C for 1 hour. The cells were then plated on LB agar plates with or without antibiotics and incubated overnight at 37 °C. Ampicillin was used at 100 µg/ml and kanamycin at 30 µg/ml final concentrations.

2.1.2 Plasmid DNA amplification and purification

If a larger quantity of DNA was required, or DNA was required to be transfection grade, 5 ml of LB was inoculated with a single colony of transformed *E. coli* and grown at 37 °C for 8 hours, before 1 ml of this culture was removed and added to 100 ml fresh LB containing the appropriate antibiotic. This was then incubated overnight, shaking at 37 °C. Cells were then lysed and DNA extracted using Qiagen Midiprep columns (Qiagen). DNA concentration was determined using a NanoDrop spectrophotometer (Thermo Scientific). DNA was stored at -20 °C.

2.2 Molecular cloning

2.2.1 Polymerase Chain Reaction (PCR)

PCR was performed using either Phusion or OneTaq as the DNA polymerase. For instances where the PCR product would be used to generate plasmid DNA, Phusion High Fidelity DNA Polymerase (NEB) was used due to its higher fidelity. When a PCR product would not be used further, OneTaq 2x master mix with standard buffer (NEB) was used. Reactions of 25 µl was assembled in 0.2 ml tubes, using 10 ng plasmid DNA or approximately 200 ng genomic DNA, 0.5 µM forward and reverse primers, and either 1 U Phusion, or 12.5 µl OneTaq master mix solution. PCR primers were designed using SnapGene, ordered from Sigma Aldrich (Merck) and annealing temperatures predicted using the NEB TM

Calculator. PCR primers used in this thesis are provided in Table 2.1. In a Techne TC3000G thermocycler, the samples were denatured for 3 minutes at 98 °C, before 25-30 cycles of 98 °C for 15 seconds, annealing temperature for 15 seconds, and elongation at 72 °C for 15-30 seconds per kb, and a final elongation of 72 °C for 10 minutes. Optimisation of the reaction often required testing a range of annealing temperatures, the utilisation of a gradient PCR protocol, or inclusion of DMSO or $MgCl_2$ in the reaction. To determine if a PCR was successful, 5 µl of the reaction was run on an appropriate percentage agarose gel as described in 2.2.3. If a PCR product was required further, it was PCR cleaned using Monarch PCR and DNA cleanup kit (NEB) according to manufacturer's instructions.

During cloning or site directed mutagenesis, a small quantity of DNA would be required for sequencing. For this purpose, 5 ml of LB containing the appropriate antibiotic was inoculated with a single colony of transformed *E. coli* and grown at 37 °C, shaking, for 16 hours. This culture was then spun down at 3700 x g for 10 minutes, and DNA was extracted using Qiagen Miniprep kit (Qiagen) and sent for sequencing (Eurofins/GATC).

2.2.2 Site directed mutagenesis via PCR

To perform site directed mutagenesis on plasmid DNA, a PCR reaction with semi-complimentary primers was performed. Primer designed followed the protocol previously described (Zheng et al., 2004), which is a modified form of QuickChange site-directed mutagenesis protocol. Oligonucleotide primer pairs that carry the desired mutation were designed and PCR was performed as described in 2.2.1 using the Phusion polymerase (NEB). If modified DNA was visible when visualised by gel electrophoresis (2.2.3) it was then further treated with an excess (10-20 U) of DpnI (NEB) in a 30 µl reaction for ~4 hours at 37 °C.

Table 2.1. Primers used for sequencing, site directed mutagenesis, PCR screening or plasmid generation in this thesis.

Primers designed and used in this thesis. Primers for PrimPol RBMA/B were described previously in Guilliam et al. (2017). Primers for PrimPol ZnKO were described previously in Keen et al. (2014a). Primers for PrimPol AxA were described previously in Bianchi et al. (2013).

Primer Name	F/R	Description	Sequence
SDM S499E	Forward	SDM 499E	GAATCCTCATAAACCAGAACCTAGCAGGCTGTCAACAGGTG
SDM S499A	Forward	SDM 499A	GAATCCTCATAAACCAGCACCTAGCAGGCTGTCAACAGGTG
SDM S499E/A	Reverse	SDM 499A/E	CTGGTTTATGAGGATTCTGGGTTTCATTGCTCCTAGTTTC
SDM S538E	Forward	SDM 538E	CAGAGAACGAGCTTCTCAGTTATAACAGTGAAGTG
SDM S538E	Reverse	SDM 538E	CTGAGAAGCTCGTTCTCTGCAGCTTCAGC
SDM S538A	Forward	SDM 538A	CAGAGAACGCTCTTCTCAGTTATAACAGTGAAGTG
SDM S538A	Reverse	SDM 538A	CTGAGAAGAGCGTTCTCTGCAGCTTCAGC
PrimPol RBMA	Forward	PrimPol D519R/F522A FWD	GGCATTGATCGTGCTTATGCTTTAGAAGCTACTGAAGATGC

PrimPol RBMA	Reverse	PrimPol D519R/F522A REV	GCTTCTAAAGCATAAGCACGATCAATGCCATTATCCCAGAC
PrimPol RBMB	Forward	PrimPol D551R/I554A FWD	GAAATTCCTCGTGAACTAGCTATAGAAGTATTACAAGAG
PrimPol RBMB	Reverse	PrimPol D551R/I554A REV	CTTCTATAGCTAGTTCACGAGGAATTTCATCCACTTCAC
PrimPol ZnKO	Forward	C419G H426Y	GTAAATATCGGTGGGGTGAAAACATTGGAAGAGCCCCTATAAGAGTAATAA TATAATG
PrimPol ZnKO	Reverse	C419G H426Y	CATTATATTATTACTCTTATAGGCTCTTCCAATGTTTTCACCCCACCGATATT TACAAATATC
PrimPol AxA	Forward	D114A/E116A	AGCTTTATTTTGCTTTGGCATTTAACAAACC
PrimPol AxA	Reverse	D114A/E116A	GGTTTGTTAAATGCCAAAGCAAAATAAAGCT
SDM Guide 3	Forward	SDM.GRNA3.F	CCATCTATATGGAGGCTGTTTCATCGACAAGCTCAAGCTTTTAATTTTG
SDM Guide 3	Reverse	SDM.GRNA3. R	TGGTTCTTCTGGCTTGGACAATCTTGAACAGCCTCCATATAGATGG

PCR Test 1	Reverse	Tag Test 1	CTTCGGGCATGGCGGACTTGAAGAAG
Peter's Vector	Forward	Vector Test 1	GTTGAGAGAGAAGAGGAGACATGGACAG
Peter's Vector	Reverse	Vector Test 2	CTCCTACTTGCTTACTGTGTTG
Intron2/3 PP	Forward	Intron Test 1	GCAATTCCTTGGTTCTTTTCCATGTGGG
Intron2/3 PP	Reverse	Intron Test 2	GCTCCTCGCCCTTGCTCACCAT
Full Length PrimPol	Forward	Sequencing	ATGAATAGAAAATGGGAAGCAAAACTG
Full Length PrimPol	Reverse	Sequencing	CTCTTGTAATACTTCTATAATTAGTTCATCAGG

2.2.3 Cloning gRNA into Cas9 cassette

Generation of the co-expression vector utilised for Crispr/Cas9 genome engineering, containing both the chosen guideRNA and Cas9 protein cDNA, was performed as described previously (Ran et al., 2013). Briefly, the guideRNA utilised here were designed using the Zhang lab guideRNA design tool (http://crispr.mit.edu, now defunct). The sequence is TTGTCCTCAGTGTATAGACC. It was purchased from Sigma. 100 µM of the forward and reverse guideRNA oligos were annealed together in T4 ligation buffer (NEB) and phosphorylated using 10 U T4 PNK (NEB), using a thermocycler protocol with the following parameters: 37 °C for 30 minutes, 95 °C for 5 minutes, followed by a ramp-down protocol of 5 °C per minute until 25 °C. 50 nM of the annealed guideRNAs were cloned into the co-expression vector (pSpCas9(BB)) in the following reaction: 100 ng pSpCas9(BB), 10x Fast Digest buffer (NEB), 10 mM ATP, 10 mM DTT, 10 U BpiI, 1500 U T7 ligase, diluted to a final volume of 20 µl with ddH_2O. The ligation was incubated for 1 hour using a thermocycler protocol with the following parameters: 37 °C for 5 minutes, 21 °C for 5 minutes, repeated 6 times. A no insert control was also performed, and 2-4 µl of each reaction was transformed into *E.Coli.*

2.2.4 Agarose gel electrophoresis

DNA was typically resolved on a 1% (w/v) agarose TAE (0.4 M Tris-Acetate pH 8, 1 mM EDTA) gel containing approximately 0.3 µg/ml ethidium bromide (Sigma). The gel was run at 120 V until samples appropriately separated. Samples were loaded in DNA loading buffer which was supplied in a 6x stock (New England Biolabs), and resolved alongside a 1 kb DNA ladder (New England Biolabs). DNA was visualised using a UV illuminator (Syngene InGenius Gel Documentation System).

2.2.5 Sequencing

Sequencing of plasmid DNA or PCR products was performed by GATC biotech (Eurofins) using universal primers or gene specific primers (listed in Table 2.1). Sequencing results were analysed using SnapGene.

2.3 Protein electrophoresis and western blot analysis

2.3.1 2D-Gel analysis

2D gel electrophoresis was performed with the equipment and procedure according to Eravci et al. (2007). Pharmalytes, IPG buffers and IPG strips were purchased from GE Healthcare. All other reagents were acquired from Sigma Aldrich. Briefly, cell extract from approximately 1x10^7 cells was diluted with rehydration buffer (7 M urea, 2 M thiourea, 5% CHAPS, 10 mM DTT, 0.4% Pharmalyte 3–10 (GE-Healthcare), 0.5% Triton X-100, 0.025% bromophenol blue and 2% IPG-buffer (GE-Healthcare) to a volume of 360 µl per sample and 340 µl was applied to each IPG dry strip (18cm pH 3–10 L, GE-Healthcare) for passive rehydration overnight at room temperature. IEF (isoelectric focussing) was carried out for 65 kVh, using a Multiphor II Unit and an EPS3501 XL Power Supply (GE Healthcare Biosciences). After the IEF, IPG strips were first equilibrated for 15 min in equilibration solution (6 M urea, 250 mM Tris-HCl pH 6.8, 30% glycerol, 1% SDS) with 1% DTT, followed by a second equilibration for 15 min in equilibration solution containing 9% iodoacetamide in the dark. SDS-PAGE for the 2nd dimension, was carried out, beginning with a low current of 20 mA/gel for 1 h, followed by 120 mA/gel overnight. The SDS-PAGE was stopped when the bromophenol blue marker reached the bottom of the gel. This gel was transferred in Triple-Wide Mini-Electrophoretic Blotting System (CBS Scientific), at 10V for 16 hours at 4 °C.

2.3.2 Sodium dodecyl sulphate polyacrylamide gel electrophoresis

Protein was analysed by sodium dodecyl sulphate polyacrylamide gel electrophoresis (SDS-PAGE). Protein samples were prepared to 30 µg total protein, resuspended in 5x Laemmli sample buffer (0.01% Bromophenol Blue,

62.5 mM Tris-HCL pH 6.8, 7% w/v SDS, 20% w/v sucrose and 0.1% 2-mercaptoethanol). Samples were boiled at 95 °C for 5 minutes.

SDS-polyacrylamide gels were prepared in 1mm Novex Gel cassettes (Invitrogen), and consisted of a resolving layer of gel made with different concentrations of polyacrylamide (8, 10, 12 or 15%), 375 mM Tris HCl (pH 8.8), 0.1% (w/v) SDS, 0.1% ammonium persulphate and 0.04 (v/v) % TEMED.

This was then followed, after the resolving layer had set, by a layer of stacking gel containing 5% polyacrylamide, 375 mM Tris HCl (pH 6.8), 0.1% (w/v) SDS, 0.1% ammonium persulphate and 0.04 (v/v) % TEMED. The XCell SureLock Mini-Cell Electrophoresis System was used to run the gel. Samples were loaded alongside 3 µl Precision Plus Dual Marker (Bio-Rad) or 2 µl Colour Prestained Protein Standard (NEB). The gel was initially run at 120V until samples had passed through the stacking gel, then increased to 200V until the dye front reached the bottom of the gel.

2.3.3 Western blotting

Proteins to be analysed by western blotting were initially resolved using SDS gel electrophoresis (See 2.3.2). Prior to the transfer of the protein from the gel to a membrane, PVDF membrane was activated using methanol and washed using ddH_2O. Transfer was performed in the XCell II Blot Module according to the manufacturer's instructions, in the presence of transfer buffer (20 mM Tris, 50 mM glycine, 10% (v/v) methanol), at 25V for 70 minutes. Following transfer, the membrane was blocked using 5% milk powder or 3% BSA (Sigma) supplemented PBS + 0.1% (v/v) Tween for 1 hour at room temp. Primary and secondary antibodies were diluted blocking buffer (Antibodies and approximate dilutions shown in Table 2.2). Primary antibodies were either incubated at room temperature for 1 hour, or at 4 °C overnight. Between the primary and secondary antibody incubations, the membrane was washed three times with PBS + 0.1% (v/v) Tween. Following antibody exposure, chemiluminescent detection with Amersham ECL Western Blotting Detection reagent (GE Healthcare) was performed according to the manufacturer's instructions. Light emission was

captured with Amersham Hyper film (GE Healthcare) autoradiography film and developed using a Xo-graft compact X4 developer.

2.3.3.1 Phospho-specific antibody generation

Phospho-specific polyclonal antibodies were generated by Eurogentec. Firstly, two antigens were designed per antibody – one containing the phosphorylated serine, and an identical peptide lacking the phosphorylation. These peptides were ELAEAAEN**S**LLSC and CNPHKP**S**PSRLST for S538 and S499 respectively. The antigen containing the PTM is then coupled to a carrier and inoculated into host rabbits. The immune system of a host immunised with a PTM peptide will raise antibodies specifically targeting that antigen. However, as some epitopes will likely be located within the peptide sequence outside the PTM, the host serum will contain a complex mixture of polyclonal antibodies, some recognizing the PTM, some others recognizing a non-modified part of the peptide. A double affinity purification is then performed against the PTM containing peptide, with non-peptide related antibodies collected in the flowthrough. All antibodies specific to the PTM peptide were eluted using 100mM glycine (pH 2.5). This elution was then additionally passed through a column containing the non-PTM peptide, with PTM-specific antibodies collected in the flowthrough: this is the final phospho-antibody. The antibodies efficiency was additionally tested by ELISA.

Table 2.2. Primary and secondary antibodies used in this study.

Primary antibodies used in this thesis for western blot or FACS analysis against human proteins. Supplier and dilution are provided. Rabbit anti - PrimPol P-S499 and P-S538 are custom antibodies generated as described in 2.3.3.1.

Antibody	**Supplier**	**Dilution**
Rabbit anti - PrimPol	Antibodie Genie (#PACO0022224-100)	1:6000
Rabbit anti - PrimPol P-S538	Custom, Eurogentech	1:1000
Rabbit anti - PrimPol P-S499	Custom, Eurogentech	1:1000
Mouse anti - tubulin	Merck (TS168)	1:10000
Rabbit anti - H3	Abcam (ab1791)	1:10000
Rat anti - P-H3 (HTA28)	Abcam (ab10543)	1:5000
Mouse anti - RPA2	Calbiochem (Na 18)	1:500
Mouse anti - RPA1	Calbiochem (Na 13)	1:2000
Rabbit anti - P-Chk1 (345)	Cell Signaling (2341S)	1:1000
Rabbit anti - Chk1	Cell Signaling (2360S)	1:1000
Rabbit anti - P-P38 (T180/T182)	Cell Signaling (9211S)	1:1000
Rabbit anti - P38	Cell Signaling (9212S)	1:1000
Mouse anti - GFP	Invitrogen (C163)	1:1000
Anti - rabbit HRP	Abcam (ab6721)	1:10000
Anti - rat HRP	Sigma (A9037)	1:10000

Anti - rat 488 green	Invitrogen (A-21208)	1:2000
Anti - mouse HRP	Abcam (ab6728)	1:10000

2.4 Culture of human cells

2.4.1 Cell lines

RPE-1 cells were obtained from Helfrid Hochegger (University of Sussex). These cells were hTERT RPE-1 cells which had been modified by Crispr/Cas9 to no longer express the puromycin resistance cassette. RPE-1 cells were cultured in DMEM F-12 media, supplemented with 10% FCS and 1% Pen-Strep.

Human embryonic kidney (HEK) 293 cells (including HEK-293 Flp-In T-REx cells) were cultured in DMEM media, supplemented with 10% FCS, 1% L-Glutamine and 1% Pen-Strep. MRC-5 cells and XP30RO cells (obtained from Alan Lehmann, University of Sussex) were cultured using MEM media, supplemented with 15% FCS, 1% L-Glutamine and 1% Pen-Strep. Cells were grown in a 37 °C incubator in 5% CO_2. Where applicable, cells were selected using antibiotics. Puromycin was used at 2 µg/ml and G418 at 1 mg/ml. Blasticidin was used at 15 µg/ml, Hygromycin at 10 µg/ml and Zeocin at 100 µg/ml. The cell media, supplements, and antibiotics were purchased from Gibco Invitrogen.

2.4.2 Cell maintenance

Cells were maintained in a 75 cm^2 cell culture flask with 10 ml media containing their selection antibiotics where required. For removal of adherent cells such as RPE or MRC-5 cells, 1 ml Trypsin EDTA was used to detach cells from the plate. 4mls of relevant media was added, and cells were then spun down (1500 x g for 3 mins) and resuspended in 1 ml of fresh media. For less adherent cells such as HEK-293 cells, 5 ml of PBS was used to wash the cells off the dish, and these cells were spun down and resuspended as before. For passage, 10% of cells were then replated in 10 ml fresh media, plus any relevant antibiotics at the above concentrations. Cells were passaged when approximately 80% confluent. To generate cell stocks, cells were processed as before, but resuspended in 1 ml media containing 10% DMSO, before being decanted to a cryo-tube and stored in controlled rate freezing apparatus, designed to allow the temperature to decrease at close to 1°C per minute. Cells were then stored at -80 °C or liquid nitrogen for long term storage. To restart a cell line, cells were warmed from -80

°C in a 37 °C water bath, added to 4 mls of relevant media before being centrifuged at 3700 x g for 3 mins. The cell pellet was then resuspended in 10 ml media and plated in a 75 cm^2 cell culture flask.

2.4.3 Transfection of human cells

2.4.3.1 Transfection of MRC-5 and XP30RO cells

To transfect plasmid DNA into MRC-5 or XP30RO cells, Lipofectamine 2000 was used according to the manufacturer's instructions. In summary, cells were plated to be 70-80% confluent on the day of transfection in 6 well plates. On the day of transfection, tube A (1.5 µg plasmid DNA in 320 µl Opti-MEM media) was mixed with tube B (3.6 µl Lipofectamine in 320 µl Opti-MEM) and incubated at room temperature for 20 minutes, before addition to cells. Cells were incubated at 37 °C for 4 hours before 600 µl of MEM media containing no antibiotics was added. 24 hours after transfection, the transfection media was aspirated and replaced with normal MEM media. Selection was added 48 hours after transfection, and cells were grown in this selection for several days, with media changes where necessary due to cell death. These cell lines were expanded from a pool population, with FACS used to check for the presence of GFP in all cells.

2.4.3.2 Transfection of HEK-293 cells

pCDNA5 containing N-terminally flag tagged PrimPol was used to express PrimPol in HEK-293 cells as has been described previously (Guilliam et al., 2017). For the generation of stable inducible N-terminal FLAG-tagged PrimPol HEK293 Flp-In T-REx, cells were grown in medium containing 15 µg/mL Blasticidin and 100 µg/ml Zeocin prior to transfection with pcDNA5 and pOG44 at a 9:1 ratio. The pcDNA5 vector encoded either WT FLAG-PrimPol, or PrimPol containing several mutations. Primers utilised to generate these mutations are listed in Table 2.1. Transfection of pcDNA5 and pOG44 was performed using calcium phosphate transfection method documented previously (Kingston et al., 2003). Briefly, DNA was added to calcium chloride in a buffered phosphate containing solution, which is then added to the cells. 24 hours after transfection, media was replaced to include 15 µg/ml Blasticidin and 10 µg/ml Hygromycin. Cells were selected using antibiotics until resistant clones appeared. These

clones were then expanded and checked for doxycycline inducible PrimPol expression.

2.4.3.3 Transfection of RPE cells

For generating the cell line containing endogenous PrimPol tagged with Clover-GFP, RPE-1 cells were transfected using the Neon electroporation kit (ThermoFisher), as per manufacturer's instructions. For the knock in cell lines, $1x10^6$ cells were resuspended in 30 µl R buffer, and electroporated with Cas9 plasmid containing gRNA and the donor vector, in 10 µl increments at 1350 V at 20 ms for 2 pulses, before plating in 2 ml media. 24 hours later, media was changed, and a further 24 hours later G418 selection was added. Cells were grown as a pool for approximately 72 hours under selection before being split out to single cells in a 96 well plate. Single cell clones were grown for 2-3 weeks before expansion to a 24 well plate, from which genomic DNA was extracted to perform PCR screening. Primers for PCR screening are provided in Table 2.1. Genomic DNA extraction was performed in 500 µl DNA extraction buffer (75 mM NaCl, 7.5 mM EDTA, to 15 ml ddH_2O, 2% SDS 0.8 U proteinase K (NEB)) for 2 hours at 50°C, before 500 µl isopropanol was added and cells incubated at 4°C overnight. Solution was then centrifuged to pellet DNA (13,000 x g, 20 minutes), washed with 70% ethanol, and pellet left to try before resuspension in appropriate amounts of TE.

For the $PrimPol^{-/-}$ RPE cell line, commercial gRNAs were used as per manufacturer's instructions (Synthego). In summary, 1-2 x 10^6 cells were trypsinised, centrifuged at 500 x g and washed once, before being resuspended into 50µl R buffer. 5µl of the cell suspension was used per transfection reaction and was added to the previously assembled RNP complexes (90 pmol sgRNA:10 pmol Cas9, resuspended in R buffer). 10 µl of cell/RNP solution was electroporated at 1350 V at 20 ms for 2 pulses. 72 hours post electroporation, cells were split out to single cells in a 96 well plate and grown into clonal cell lines. PCR was then used to detect whether a deletion had taken place (primers in Table 2.1). Cell lines which were positive for a deletion were expanded, frozen down, and used for further experiments.

RPE-1 cell lines were also generated using the Lipofectamine LTX reagent. These include the transfection of RPE-1 PLK1-as cells to overexpress wild type PrimPol, and generation of the Sleeping Beauty cell lines. In brief, the sleeping beauty transposon system is a non-viral vector that can induce the integration of transgenes into the mammalian genome in the presence of the highly active transposase SB100X (Wu et al., 2016). This was done through the co-transfection of a sleeping beauty expression vector containing WT PrimPol and SB100X. To summarise, cells were seeded in a 24 well plate with 1 ml of DMEM-F12 media, to be 80% confluent on the day of transfection. For transfection, 4 µl of LTX reagent was diluted in 50 µl Opti-MEM media. Separately, both SB100X and the Sleeping Beauty expression vector containing PrimPol were diluted in 50 µl Opti-MEM, tor a total amount of 500 ng at a ratio of 10:1 expression vector:SB100X. These dilutions were then mixed and incubated for 5-10 minutes, before dropwise addition to cell media. Cells were incubated for 24 hours before media was changed to include selection by Puromycin (2 µg/ml) and incubated for a further 48-72 hours. The pool population was split out to single cells, expanded, and tested for overexpression of PrimPol by western blot. Successful clonal lines were further expanded, frozen down, and used for subsequent experiments.

2.4.4 Cell synchronisation

To synchronise cells to the G1/S border, a double thymidine synchronisation was performed as described before (Chen and Deng, 2018). Briefly, HEK-293 cells or RPE-1 cells were plated and left to attach in media containing doxycycline to induce protein expression. Cells were treated with 4 mM thymidine for 18 hours. This media was then removed, cells were washed 3x with PBS, and fresh media replaced. Cells were released for 9 hours before reapplication of 4 mM thymidine for 18 hours. Unreleased cells were harvested to represent a 0 hour population, otherwise cells were released for defined timepoints for 0-12 hours.

To synchronise cells in anaphase, RPE-1 cells were treated with 0.5 µM nocodazole for 16 hours before release for 90 minutes. For general synchronisation in mitosis, 1 µM nocodazole was applied for 16 hours before mitotic cells were obtained by mitotic shake off. Cells from this shake-off were

harvested directly for the 0h timepoint. Cells were then washed in PBS, resuspended and replated in media containing 4 mM thymidine to prevent S phase entry and harvested at defined timepoints between 0-24 hours.

Table 2.3. A list of the drugs, antibiotics and inhibitors used in this study and their supplier.

Concentrations can be found in the relevant methods section or relevant figure legend.

Drugs and Inhibitors	Supplier
3-MB-PP1	Abcam
Thymidine	Sigma
Doxycycline	Sigma
Hydroxyurea	Sigma
Aphidicolin	Sigma
Olaparib	Stratech
Camptothecin	Sigma
BI2536 (PLK1i)	Cayman Chemical/Stratech
Nocodazole	Sigma
Hygromycin	Sigma
Blasticidin	Fisher Scientific
G418	Sigma
Puromycin	Fisher Scientific
RO-3306 (CDK1i)	Sigma

2.5 Human cell analysis

2.5.1 Flow cytometry

Cell cycle populations were analysed using flow cytometry. To analyse cell cycle stage or confirm synchronisation. Cells were trypsinised or washed with PBS and collected by centrifugation, washed with PBS, then resuspended in a small volume of PBS and fixed with ice cold 70% (v/v) ethanol added dropwise with gentle agitation, before storage overnight at -20 °C. Cells were then washed twice with PBS to remove the ethanol and resuspended in PBS containing 5 µg/ml propidium iodide (PI) and 150 µg/ml RNAse A, and transferred to FACS tubes (BD Biosciences) for subsequent analysis using FACS Accuri (BD Biosciences). To label replicating DNA, cells were treated with 10 µM EdU 25 minutes prior to collection. EdU positive cells were then labelled using Click chemistry and sulfo-CY5 azide in addition to PI (Jena Biosciences) as described previously (Bailey et al., 2019; Jia et al., 2015). To follow progression into mitosis samples were additionally stained for P-H3. After fixation cells were permeabilised with 0.2% triton in PBS for 10 mins before blocking in 3% BSA in PBS-T and staining with antibodies to P-H3 followed by anti-Rat 488 green (Antibody table). Cells were then stained for EdU and PI as above. Samples were analysed using a BD Accuri C6 flow cytometer and approximately 10,000 cells were quantified using BD CSampler Software.

2.5.2 Cell growth assay

On day 0, 500 cells from each cell line were plated and left to attach, before being harvested and counted every 24 hours. The doubling time of the cell line was determined from these four points and calculated using https://www.doubling-time.com.

2.5.3 Colony survival assay

100 cells, or a serial expansion dependent on expected toxicity, were plated and allowed to attach for approximately 16 hrs. For HEK-293 cells where PrimPol protein expression required induction, 10 ng/µl doxycycline was applied to cells at plating. For RPE-1 cells where PrimPol protein expression required induction,

500 ng/µl was applied at plating. For plating efficiency experiments, cells were left untreated and compared to no doxycycline controls. For colony survival experiments, cells were treated 16 hours after plating. Table 2.3 shows the stressor applied, the doses used, and the cell dilutions used for this stressor. For aphidicolin, camptothecin, olaparib or low HU treatment, drugs were applied continuously. For high HU, the drug was applied for 24 hours before cells were washed, and fresh media applied. Colonies were allowed to form for approximately 10 days. To quantify colony formation, cells were stained with 1% methylene blue for counting. Sensitivity was measured in relation to plating efficiency calculated from undamaged controls.

2.5.4 Chromosome breaks

Chromosome spreads were performed as described previously (Bailey et al., 2016). To analyse the occurrence of chromosome breaks, cells were first grown for 96 hrs in the presence of 10 ng/ml doxycycline. 1 µM nocodazole was added for the final 16 hrs to stall cells in mitosis before the cells were collected. Cells were swollen in 75 mM KCl at 37°C for 10 minutes before being fixed in 3:1 methanol: acetic acid. Cells were then dropped onto glass slides. After drying, chromosomes were stained with giemsa (Merck) and mounted in Eukitt Quick-hardening mounting medium (Merck). Slides were analysed on a Nikon E400 fluorescent microscope. While a number of chromosomal aberrations can be detected using metaphase spreads, only strict breaks in chromosomes – either where the fragment was missing or visible nearby – were counted.

2.5.5 Chromatin binding analysis

DNA bound protein populations were analysed by chromatin assay as described previously (Bianchi et al., 2013). Approximately 7 x 10^6 cells were grown in 10 ng/ml doxycycline for at least 16 hrs before being treated with 0, 6 or 20 J/m^2 UV-C and allowed to recover for 6 hrs. Cells were collected and 25% were resuspended in 50 µl NETN buffer (150 mM NaCl, 5 mM EDTA, 50 mM Tris pH 7.5, 0.5 % NP-40). The remaining 75% was incubated in 150µl CSK buffer (100 mM NaCl, 300 mM sucrose, 3 mM MgCl2, 10 mM PIPES pH 6.8, 1 mM EGTA, 0.2 % (v/v) Triton X-100) on ice for 10 minutes, before being pelleted at 4°C with

the supernatant containing soluble proteins. The pellet containing chromatin bound proteins was washed twice in PBS and resuspended in 50 µl Laemmli sample buffer and boiled for 10 minutes. Proteins were analysed by western blotting relative to whole cell fraction using antibodies.

2.5.6 Micronuclei assay

Cells were trypsinised if strongly adherent, or washed off if not, and resuspended in PBS before being cytospun at 8000 rpm for 3 minutes onto glass slides. Cells were then fixed with 4% paraformaldehyde in PBS at RT for 10 minutes. Cells were then washed with PBS, permeabilised with 0.2% Triton X-100 for a further 10 minutes, washed again in PBS before being mounted using Vectorshield DAPI mounting media. Slides were imaged on an Eclipse E400 microscope (Nikon). A micronucleus was defined as being round or oval in shape and having the same DAPI staining intensity as the main nuclei. Micronuclei were counted if they were fully separated from the main nucleus.

Table 2.4. Stressors applied in colony survival experiments, their doses, and cell numbers plated for each dose.

Cell numbers were kept consistent across cell lines.

Drug	Concentrations	Cell Number
Aphidicolin	0 μM	100
	0.1 μM	100
	0.2 μM	200
	0.4 μM	500
UV-C	0 J/m^2	100
	2 J/m^2	100
	4 J/m^2	200
	6 J/m^2	500
High HU	0 mM	200
	0.5 mM	400
	1 mM	1000
	3 mM	2000
Camptothecin	0 nM	150
	2 nM	150

	4 nM	300
	6 nM	1500
	10 nM	3000
Olaparib	0 μM	150
	0.5 μM	300
	1 μM	1500
	2 μM	3000
Low HU	0 μM	100
	50 μM	100
	100 μM	200
	200 μM	400

2.5.7 Kinase inhibition

To analyse the effect of kinase enzymes on PrimPol's phosphorylation, the kinase inhibitors BI2536 (Stratech/Selleck) and RO-3306 (Sigma) were used. As both kinases are required for proper mitotic entry or exit, nocodazole was used as a control for mitotic stalling. Where not stated, BI2536 was added at 100 nM concentration. These inhibitors were added for 8/16 hours, before cells were harvested for FACS analysis or protein analysis by western blot.

2.6 Microscopy

2.6.1 Live cell imaging

Cells were grown in glass bottom microwell dishes for live cell imaging. Zeiss LSM880 confocal microscope was used to image the endogenously tagged line. For nuclear staining in live cell experiments, Hoechst 33342 (Thermofisher) was applied 20 minutes prior to imaging. A stock solution was prepared at 1 mg/ml, and cells were incubated for 10 minutes at 37 °C with 1 µg/ml.

2.6.2 Fixed imaging

RPE cells were grown on coverslips in a 24 well plate for 16 hours, before the addition of any drugs or treatments. Mitotracker Deep Red was used at 1 µM and left for 20 minutes before removal. Cells were then washed with PBS, fixed with 4% paraformaldehyde for 10 minutes, then mounted using Vectorshield DAPI mounting media. Zeiss LSM880 confocal microscope was used to image the endogenously tagged line.

2.7 Reproducibility and data analysis

Unless otherwise stated in the figure legend, all charts, including colony survivals, show the average of 3 independent biological repeats, with error bars showing standard deviation. Significance was determined using a Students T-test. $P \leq 0.05$ *, ≤ 0.01 **, ≤ 0.001 ***. Unless otherwise identified, western blots are representative images of at least two biological repeats. Data analysis and presentation was carried out using Microsoft Excel and images were quantified with Image J/FIJI.

Chapter 3

The Role of S538 Phosphorylation in the Regulation of Human PrimPol

3.1 Introduction

3.1.1 Phosphorylation of the C-terminus of human PrimPol

PrimPol has previously been shown to interact with RPA, specifically the RPA70 subunit (Guilliam et al., 2017). The two domains that interact with RPA – the RPA binding motifs (RBMs) – are denoted as RBM-A and RBM-B and encompass residues 510-528 and 542-560 respectively (Figure 3.1A). The phosphorylation site that is the focus of this chapter, serine 538, resides between these two motifs, though other phosphorylation sites, such as S499 and S501, are found just prior to the first RPA binding motif. S538 is highly conserved across species (Figure 3.1B). Previous data has shown the equivalent serine residue was phosphorylated in *Xenopus laevis* cell free egg extract, a model system previously used to study PrimPol (H. Lindsay, University of Lancaster, unpublished data). *Xenopus* PrimPol protein contains one RBM-A site, and five RBM-B sites. This protein was shown to contain equivalent phosphorylation sites to S538 at each of its RBM-B domains, with phosphorylation detectable at S551, S576, S601, S623, and S648,

3.1.2 The generation of an antibody specific to phosphorylated S538

On the basis of the *Xenopus* analysis, we proceeded with the generation of an antibody specific to phosphorylated S538. This antibody was generated as described in 2.3.3.1 of Methods. The specificity of this antibody to phosphorylated S538 was fist examined. For the majority of experiments in this chapter, unless otherwise denoted, HEK-293 cells were utilised. Due to issues detecting endogenous levels of PrimPol protein by western blot with commercial antibodies, including the custom phospho-antibody used here, we generated cell lines that allowed for controlled overexpression of mutant PrimPol. HEK-293T Flp-In TREx cells, a derivative human embryonic kidney cell line, contain a stably integrated FRT site at a transcriptionally active genomic locus. We utilised the Flp recombinase-mediated integration (Flp-In) Tetracycline-regulated expression (TREx) system (described in 2.4.3.2). In these cells, endogenous PrimPol was disrupted using CRISPR/Cas9 to generate several PrimPol$^{-/-}$ clones. This work was performed by Dr Laura Bailey. The PrimPol knockout cell line was then

transfected with a pcDNA5 vector containing FLAG-tagged wildtype PrimPol, the expression of which was controlled by the addition of doxycycline. We first assessed the specificity of the antibody to phosphorylated PrimPol by treating cell lysate from HEK-293 cells overexpressing wildtype PrimPol with λ phosphatase (Figure 3.1C) and then by testing the antibody against S538A mutant protein, with the alanine substitution rendering the protein unable to be phosphorylated at this site (Figure 3.1D). This verified that the antibody was specific to phosphorylated S538. PrimPol presents on a low percentage gel as two bands, the causes of which are discussed further in Chapter 4. Detection of PrimPol protein phosphorylated at S538 using the phosphoantibody showed both the higher and lower band, suggesting the electrophoretic shift in PrimPol is independent of S538 phosphorylation (Figure 3.1D).

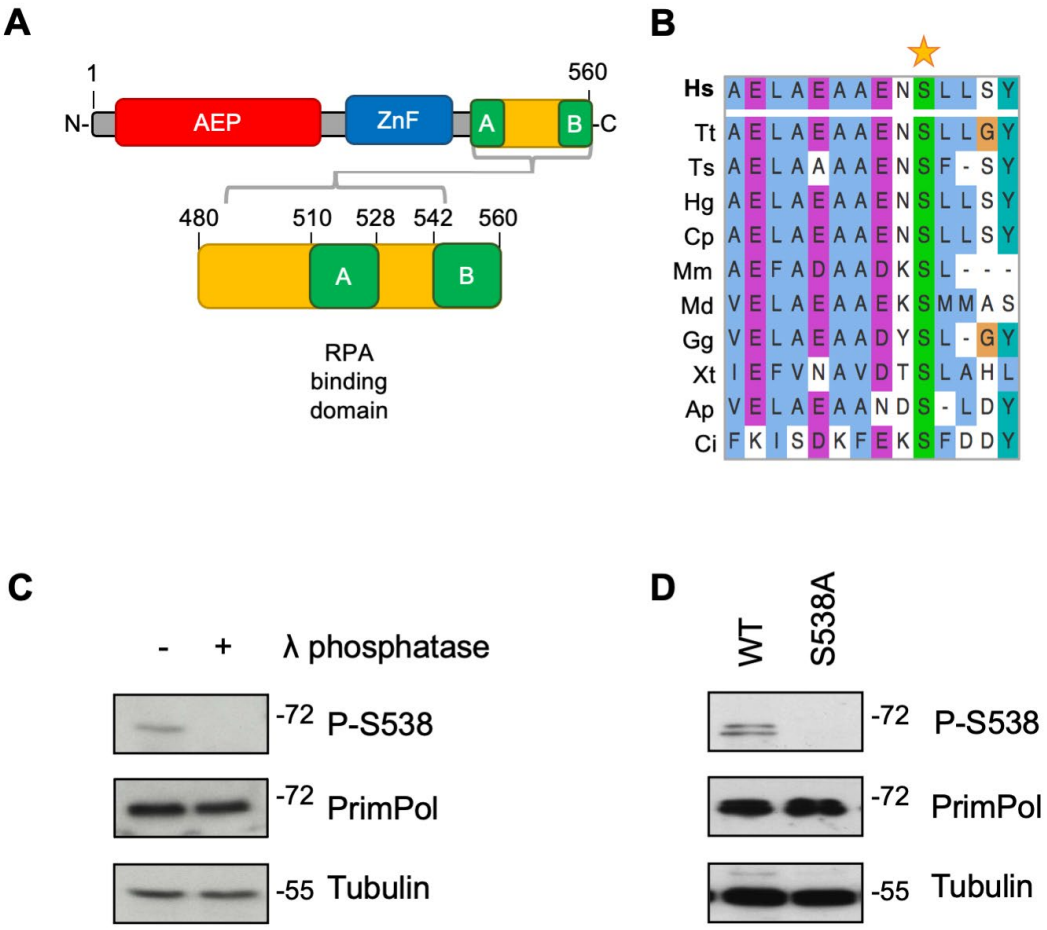

Figure 3.1. A summary of PrimPol S538 and the generation of a phospho-specific antibody

A. A schematic describing PrimPol's key domains; the AEP domain, zinc finger domain (ZnF) and RPA binding domain. The RPA binding domain is expanded to show the two RPA binding motifs, A and B. **B.** Amino acid alignment of residues 529-542 across multiple species of PrimPol. *Hs, Homo sapiens (Human); Tt, Tursiops truncatus (Bottle-nosed dolphin); Ts, Tarsius syrichta (Philippine tarsier); Hg, Heterocephalus glaber (naked mole rat); Cp, Cavia porcellus (guinea pig); Mm, Mus musculus (mouse); Md, Monodelphis domestica (gray short-tailed opossum);* Gg, *Gallus Gallus* (chicken); Xt, *Xenopus tropicalis* (Western clawed frog); Ap, *Anas platyrhynchos* (Northern mallard); Ci, *Ciona intestinalis* (vase tunicate*).* Yellow star highlights S538 of human PrimPol*.* **C.** Western blot of cell lysate from HEK-293 cells overexpressing WT PrimPol protein, mock or λ phosphatase treated and probed with antibodies specific to phosphorylated S538

(P-S538), PrimPol and tubulin. **D.** Western blot of protein from HEK-293 cells expressing either WT or S538A PrimPol protein, probed with antibodies specific to P-S538, PrimPol and tubulin.

3.2 S538 is phosphorylated by PLK1

To determine which protein kinase (PK) was responsible for the phosphorylation of PrimPol S538 in human cells, eukaryotic linear motif (ELM) was used to predict phosphorylation sites (Kumar et al., 2020). This analysis suggested that the phosphorylation of S538 may be performed by a polo-like kinase enzyme, such as PLK1. The first reported consensus sequence of PLK1 is D/E – X – **S/T** – θ – X – D/E, where θ is any hydrophobic amino acid and X is any amino acid without restriction (Nakajima et al., 2003). However, subsequent to this discovery it was suggested that the consensus sequence of PLK1 may be broader than this – while a new predicted consensus sequence was suggested, this motif still does not match all known PLK1 phosphorylation sites (Santamaria et al., 2011). The region surrounding S538 is E N **S** L L S (Figure 3.2A), which matches the first predicted PLK1 motif at 5/6 residues.

Additionally, preliminary work from the Doherty lab had suggested that the CTD of PrimPol was phosphorylated by PLK1 (P. Hentges and A. Doherty, data not shown), so initial experiments worked to determine if a PLK1 was required for S538 phosphorylation. To verify if PLK1 was able to specifically phosphorylate S538, an *in vitro* kinase assay was performed by Dr Laura Bailey using purified recombinant PrimPol, incubating this protein with PLK1 and ATP. Using the P-S538 specific antibody, we showed that PrimPol was specifically phosphorylated by PLK1 at residue S538 *in vitro*. PrimPol with a S538A mutation was not seen to interact with PLK1 (Figure 3.2B).

We therefore hypothesised that PLK1 would also perform the phosphorylation of S538 *in vivo*, and to that end, we utilised the inhibitor BI2536 to determine if S538 phosphorylation was prevented by the inhibition of PLK1 (Lénárt et al., 2007). HEK-293 cells were treated with BI2536 for 16 hours before WT PrimPol protein expression was induced by doxycycline. Cells were harvested and subject to western blot analysis, with S538 phosphorylation levels detected using the P-S538 antibody. As seen in Figure 3.2C, S538 phosphorylation was absent in cells treated with either 2 or 10 nM of BI2536, though PrimPol expression levels remain unchanged. Interestingly, treatment with BI2536 also led to PrimPol presenting

as a single higher band instead of two bands. This will be discussed further in Chapter 4, as it relates to the phosphorylation of S499 and cell cycle stage.

To further verify that the inhibition of PLK1 prevented phosphorylation of S538, we utilised a modified RPE1 cell line. This cell line contains a mutant form of PLK1, which can be inactivated using an ATP analogue (Burkard et al., 2012). Cells were stably transfected to express PrimPol before treatment with the ATP analogue 3-MBPP1. In the absence of active PLK1, S538 phosphorylation was not detected, establishing a specific role for the PLK1 kinase in the phosphorylation of PrimPol (Figure 3.2D).

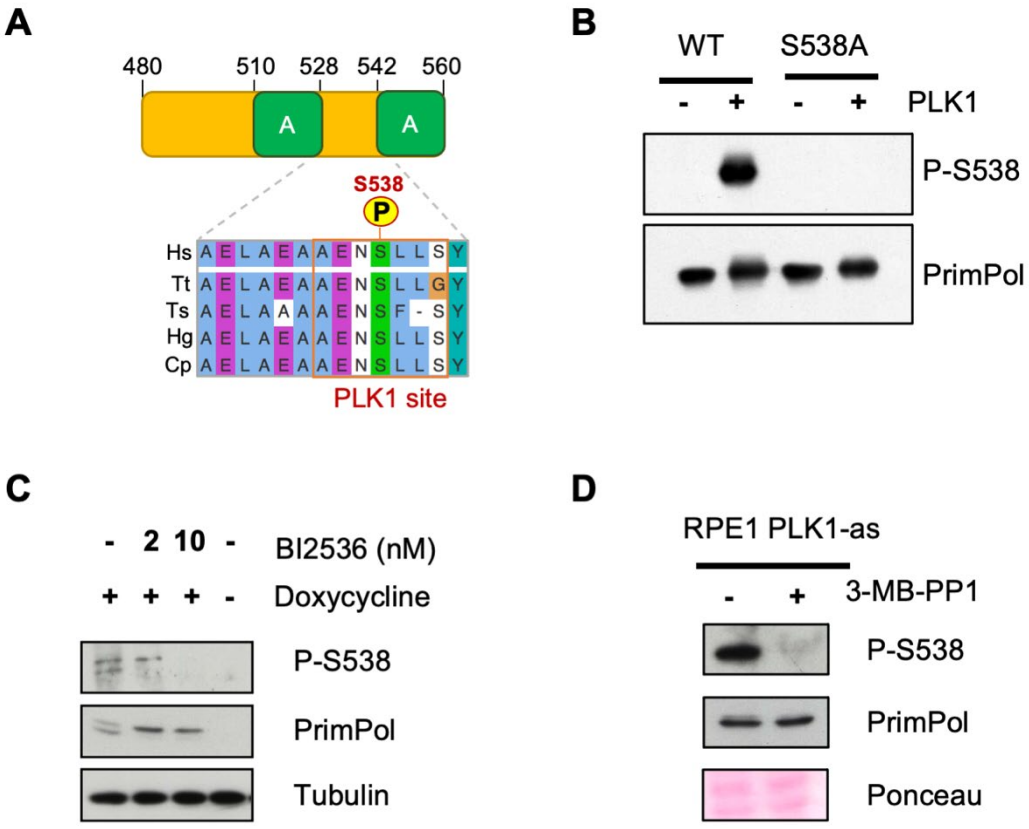

Figure 3.2. PLK1 mediates S538 phosphorylation of human PrimPol

A. A schematic describing the region of the C terminus of PrimPol that closely matches the known PLK1 consensus motif. *Hs, Homo sapiens (Human); Tt, Tursiops truncatus (Atlantic bottle-nosed dolphin); Ts, Tarsius syrichta (Philippine tarsier); Hg, Heterocephalus glaber (naked mole rat); Cp, Cavia porcellus (guinea pig).* **B.** *In vitro* kinase assay performed on recombinant PrimPol protein incubated with ATP and PLK1 (Bailey et al., 2021, Appendix B). **C.** Cells were treated for 16 hours with 2 or 10 nM BI2536 before protein expression was induced by doxycycline addition. Protein from these cells was then analysed for S538 phosphorylation, total PrimPol and tubulin. **D.** RPE1 PLK1-as cells (Burkard et al., 2012) expressing WT PrimPol were treated with with 3-MB-PP1. Protein was then probed for P-S538, total PrimPol, and loading confirmed by ponceau stain.

3.3 Phosphorylation of serine 538 changes throughout the cell cycle

As described in 1.1.3.1, the activity of PLK1 changes throughout the cell cycle. PLK1 plays an essential role in mitosis (Lane and Nigg, 1996) and it is at its most active in that stage of the cell cycle (Lemmens et al., 2018). However, PLK1 has also been implicated in the transition to mitosis, and is active in G2 in order to promote mitotic entry (Gheghiani et al., 2017). Additionally, while current thinking suggests that PLK1 is activated at the S/G2 boundary (Lemmens et al., 2018), there is evidence for phosphorylation by PLK1 taking place in S phase (Li et al., 2008), and a role for PLK1 at the centrosome in regulating DNA replication, though this is independent of its kinase activity (Shen et al., 2013).

We hypothesised that S538 phosphorylation may be either consistently maintained throughout the cell cycle, as PrimPol protein levels are, or follow the pattern of PLK1 levels – low in G1/S, increasing after S phase throughout G2 to a peak in mitosis. To investigate this, cells were arrested at the onset of S phase with 4 mM thymidine, and then left unreleased or released for 2, 4, 8, or 14 hours, before being harvested for FACS and western blot analysis (Figure 3.3A). This was to obtain populations in early S (2h), mid-late S (4h), G2/M (8h) and G1 (14h), or stalled at the start of S phase (0h). Figure 3.3B shows the FACS profiles, along with quantification of the cell cycle stage of these cell populations, based on gating according to PI and EdU incorporation, which was added 30 minutes prior to collection (Figure 3.3C). Samples were probed by western blot for PrimPol S538 phosphorylation using the phospho-specific antibody, with total PrimPol levels and tubulin levels detected as a control (Figure 3.3D). These data show that cells stalled by thymidine at the G1/S boundary have no S538 phosphorylation, while cells in early to mid S phase have low levels. The highest levels of phosphorylation occurred at 8h. Finally, in an unstalled G1 population (14h), phosphorylation is present at higher levels than in the 0h G1/S population, suggesting that dephosphorylation occurs between early G1 and the G1/S boundary.

These data suggest that phosphorylation of S538 does follow the pattern of activity of PLK1, with increasing levels from late S phase to mitosis. However, the

presence of phosphorylation in G1 and the absence of phosphorylation at the G1/S boundary, suggests the presence of a phosphatase working in tandem with PLK1 to control S538 phosphorylation levels after mitotic exit.

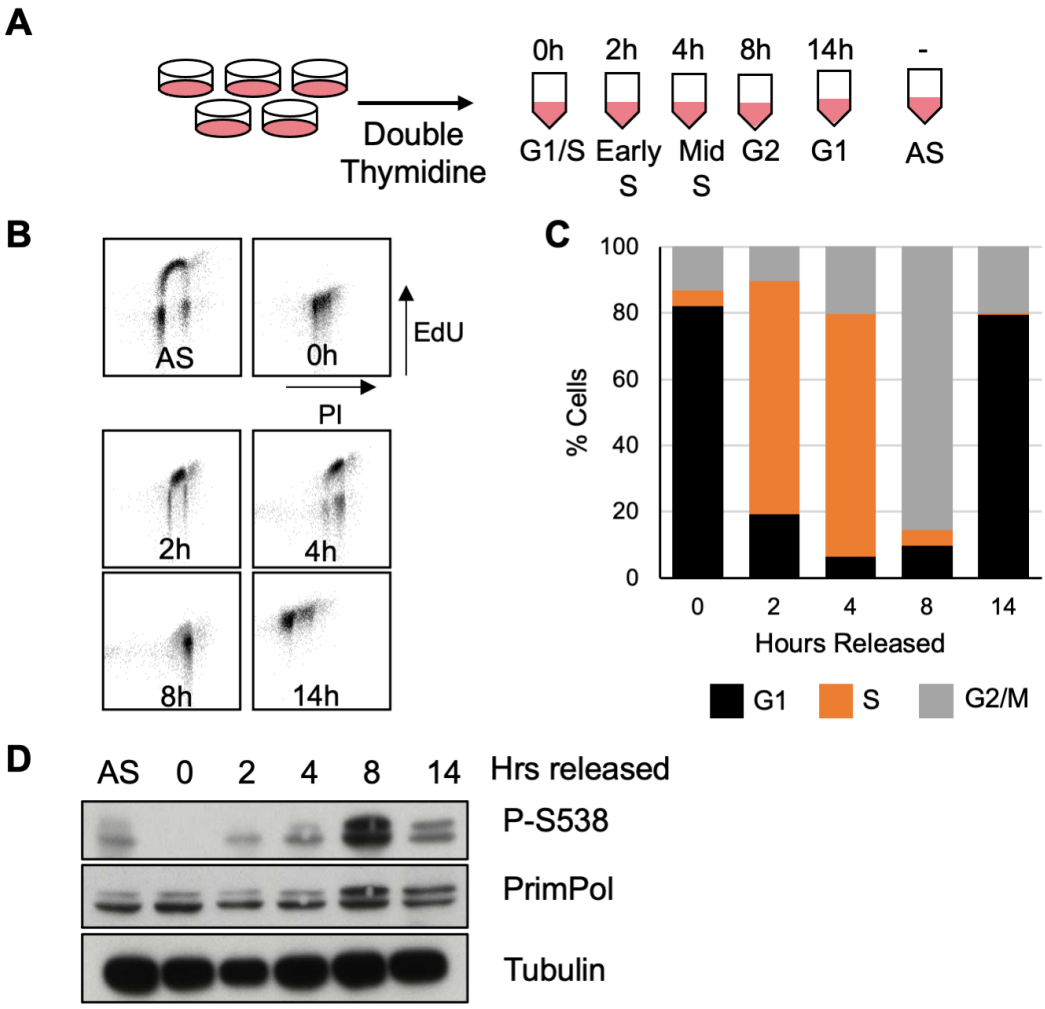

Figure 3.3. PrimPol S538 phosphorylation changes across the cell cycle

A. A schematic describing the experimental protocol. Cells were stalled by 4 mM thymidine at the G1/S boundary, before being released into fresh media. Samples were taken at defined timepoints for FACS and western blot analysis. AS is an asynchronous control. **B.** FACS analysis of HEK-293 cells expressing WT PrimPol after thymidine release. Approximately 10,000 cells were analysed per sample. **C.** Quantification of cells in each cell cycle stage at each timepoint. **D.** Western blot analysis of protein from HEK-293 cells expressing WT PrimPol. Samples from denoted timepoints were probed for P-S538, total PrimPol and tubulin.

To look more closely at S538 phosphorylation across the cell cycle, cells were released from a thymidine stall for 0, 2, 4, 6, 8, 10 or 12 hours into media containing nocodazole (Figure 3.4A). Nocodazole is a microtubule poison, which prevents completion of mitosis. At each timepoint, cells were harvested for protein analysis by western blot, and FACS analysis with EdU staining. FACS analysis shows that cells enter S phase and begin DNA synthesis quickly after release from thymidine. Cells had completed DNA replication at 8 hours, at which point EdU signal was no longer detected (Figure 3.4B,C). Western blot analysis of these samples (Figure 3.4D) shows that phosphorylation is detectable at 6 hours post-thymidine release, at which point cells are 52% S phase and 42% G2, and steadily increases to a peak at 12 hours (83% G2). These data suggest that phosphorylation occurs in late S/early G2 and is maintained until mitosis.

The western blots in Figure 3.4 also show that, as cells progress towards mitosis, the two-band distribution of PrimPol becomes one, upper band (Figure 3.4D, compare 2 hours to 12 hours). The change in the distribution of PrimPol is discussed further in Chapter 4 and is unrelated to the phosphorylation of S538.

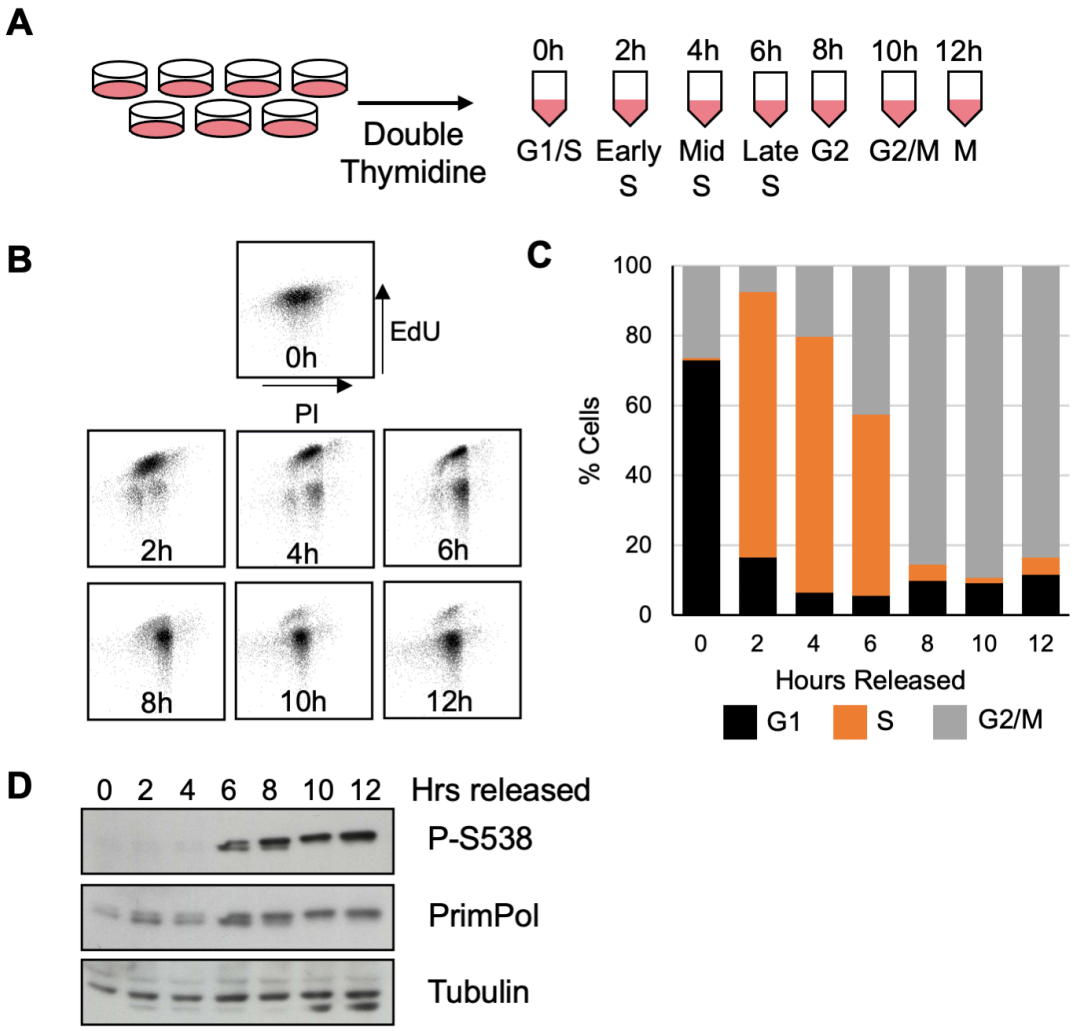

Figure 3.4. Phosphorylation of PrimPol S538 occurs as cells move into late S/G2

A. A schematic describing the cell synchronisation protocol. HEK-293 cells expressing WT PrimPol were stalled by 4 mM thymidine to the onset of S phase, before being released into fresh media. Samples were taken every 2 hours for FACS and western blot analysis. **B.** FACS analysis of each sample after thymidine release. Approximately 10,000 cells in total were analysed per sample. **C.** Quantification of the number of cells in each cell cycle stage at each timepoint. **D**. Western blot analysis of protein from HEK-293 cells expressing WT PrimPol. Samples from denoted timepoints were probed for P-S538, total PrimPol and tubulin.

3.3.1 S538 Phosphorylation decreases across G1

Low levels of phosphorylation in the G1/S stalled and early S phase samples, in contrast to the high levels of phosphorylation in mitosis, suggested that PrimPol S538 phosphorylation decreased during G1 before the start of DNA replication. We therefore analysed the presence of S538 phosphorylation throughout G1, by synchronising cells to mitosis using the microtubule poison nocodazole. After mitotic stalling, cells were detached by mitotic shake-off, replated, and left to reattach for defined timepoints in the presence of 4mM thymidine to prevent S phase entry. A schematic describing the experimental procedure is shown in Figure 3.5A. To determine the efficiency of mitotic release, cells from 0h (unreleased), 2h and 6h post nocodazole release were harvested and assessed for condensed chromosomes to determine percentage cells mitotic. This confirmed that cells had largely exited mitosis 2 hours after nocodazole release.

Protein was harvested from these cells at the denoted timepoints and subject to western blot analysis. This showed that S538 phosphorylation decreased as cells progressed through G1, though PrimPol protein levels remained equal across all timepoints. The decrease occurs by 2 hours, and continues until 4 hours post-nocodazole release, at which point phosphorylation is no longer detectable. As cells accumulate at the G1/S boundary, phosphorylation remains low as seen previously. Mitotic exit was additionally confirmed by western blot analysis of phospho-H3 (S10), which served as a mitotic marker as it is only present when cells have condensed chromosomes. (Figure 3.5C).

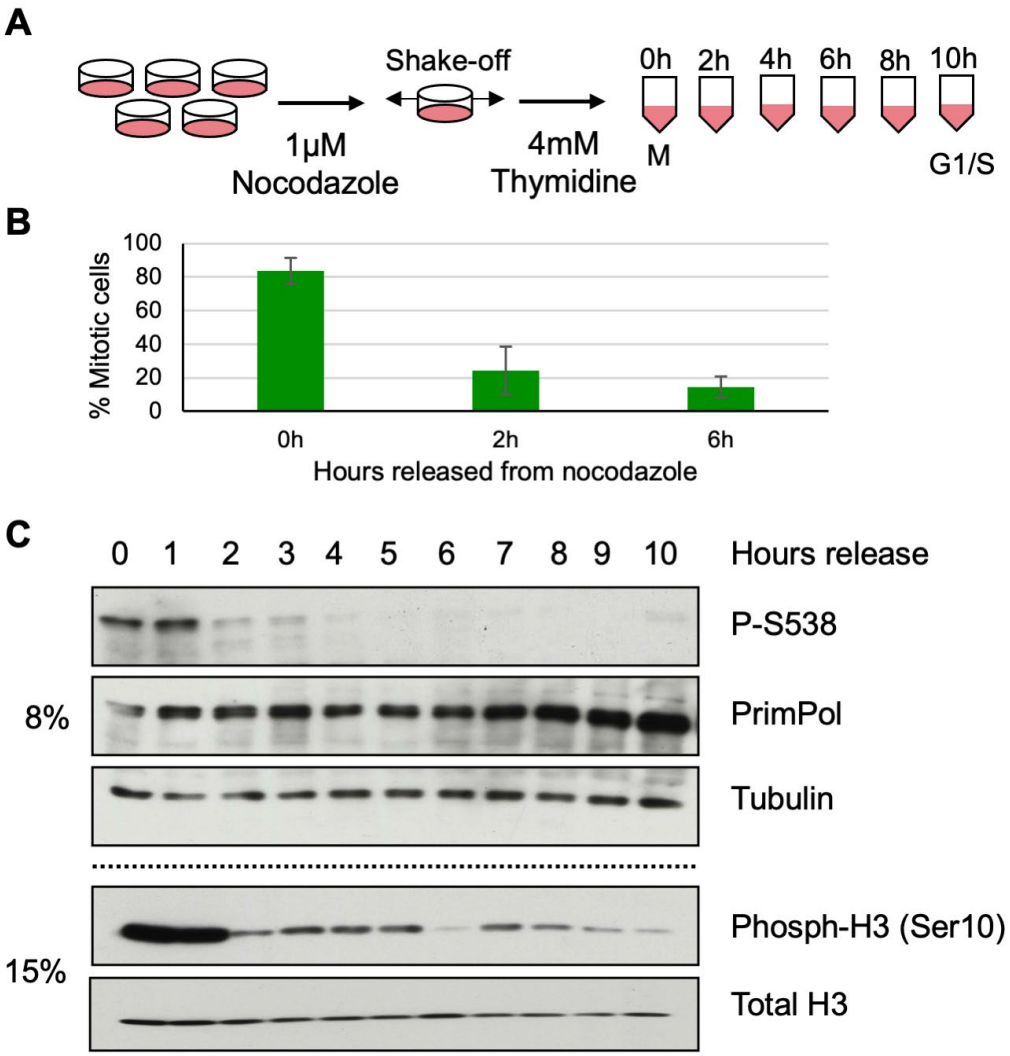

Figure 3.5. PrimPol S538 phosphorylation decreases after release from mitosis

A. A schematic describing the experimental protocol. Cells were stalled in mitosis by nocodazole. Mitotic cells were harvested and replated in fresh media to progress through mitosis into G1. Samples were taken at defined timepoints for western blot analysis. **B.** Quantification of cells in mitosis at defined release points after 16-hour treatment with 1 μM nocodazole. **C.** Western blot analysis of S538 phosphorylation. Lysate from defined timepoints was probed for P-S538, total PrimPol, tubulin (upper blot, 8%), or P-Histone H3 (Ser10) or total H3 (lower blot, 15%).

3.4 DNA damage and replication stress in S phase, and its effect on PrimPol S538 phosphorylation

3.4.1 Changes in PrimPol S538 phosphorylation levels are undetectable in asynchronous cells after UV-C damage

In previous experiments using MRC-5 cells, 6 J/m^2 UV-C damage induced a slowing of S phase progression in cells lacking PrimPol leading to S phase accumulation, which could be complemented by overexpression of WT PrimPol. (Bailey et al., 2019). To determine if S538 phosphorylation changed after UV damage, as is true in the case of Pol η (Göhler et al., 2011), asynchronous populations of HEK-293 cells expressing WT PrimPol were treated with 6 J/m^2 UV-C and left to recover for increasing amounts of time. These cells were then harvested, and protein was analysed by western blot to determine the level of PrimPol S538 phosphorylation. After both short recovery times (between 10 and 30 minutes, Figure 3.6A) and longer recovery times (1 and 6 hours, Figure 3.6B), there was no visible shift in phosphorylation levels in asynchronous cells.

3.4.2 Increasing doses of hydroxyurea induces S phase stalling and a decrease in PrimPol S538 phosphorylation in asynchronous cells

As HU treatment has previously been shown to induce PrimPol foci formation (Bianchi et al., 2013), we investigated whether HU treatment may lead to a detectable shift in phosphorylation of PrimPol at S538 in asynchronous cells. We therefore applied hydroxyurea (HU), which induces replication stress by dNTPs depletion. It is a stressor specific to DNA replication and has minimal effect on cells when they are outside of S phase. Low doses of hydroxyurea lead to replication stress and slower DNA synthesis, while higher doses lead to full dNTP depletion and fork stalling. In both the 1 and 4 hour treatments, at the highest dose of HU (2 mM), S538 phosphorylation was absent, suggesting that the hydroxyurea treatment impacted the phosphorylation levels (Figure 3.6C). However, while it is possible this is due to fork stalling, it is also likely that unintentional synchronisation of cells to the start of S phase plays a role in the decreased phosphorylation.

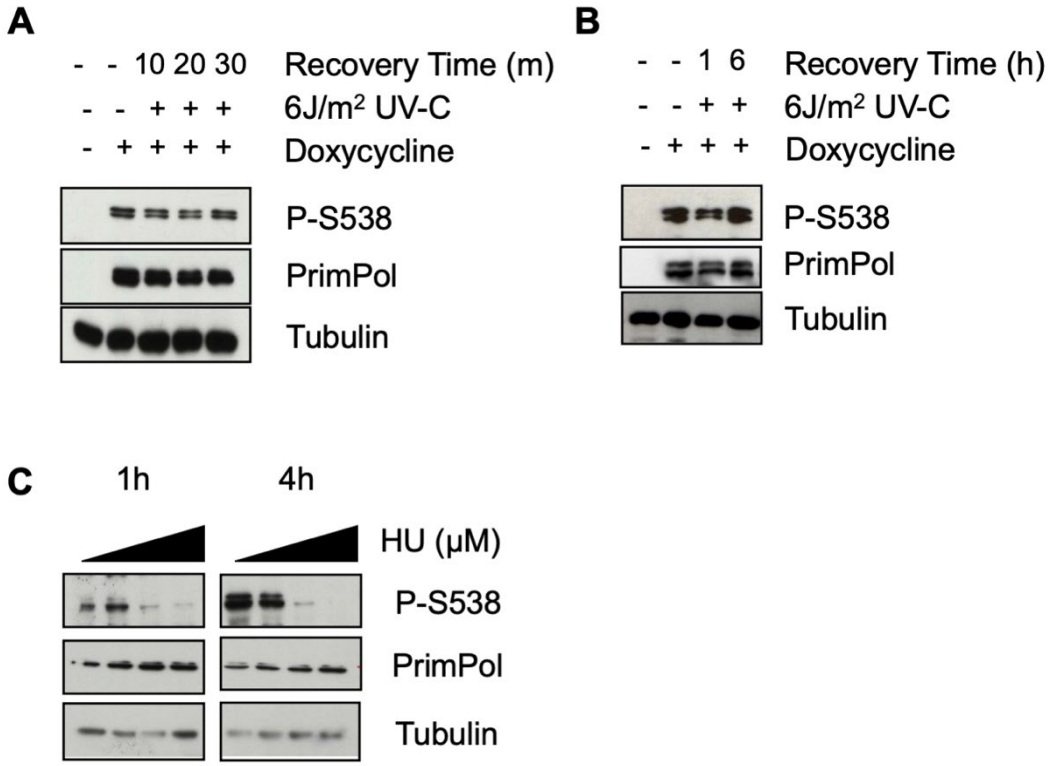

Figure 3.6. Treatment with hydroxyurea, but not UV-C damage, decreases PrimPol S538 phosphorylation when applied to asynchronous cells

A. HEK-293 PrimPol$^{-/-}$ cells expressing WT PrimPol were treated with 6 J/m^2 UV-C and left to recover for 0, 10, 20 or 30 minutes before harvest and analysis by western blot. Samples from denoted timepoints and treatment conditions were probed for P-S538, total PrimPol and tubulin. **B.** HEK-293 PrimPol$^{-/-}$ cells expressing WT PrimPol were treated with 6 J/m^2 UV-C and left to recover for 0, 1 or 6 hours before harvest and analysis by western blot. Samples from denoted timepoints and treatment conditions were probed for P-S538, total PrimPol and tubulin. **C.** HEK-293 PrimPol$^{-/-}$ cells expressing WT PrimPol were treated with 0, 50, 500 or 2000 μM HU and left to recover for 1 or 4 hours before harvest and analysis by western blot. Samples from denoted timepoints and treatment conditions were probed for P-S538, total PrimPol and tubulin.

3.4.3 DNA damage or replication stress applied to cells in early S phase delays PrimPol S538 phosphorylation

As PLK1 is responsible for phosphorylating S538, we considered whether replication stress or DNA damage during DNA replication would affect this phosphorylation. PLK1 has previously been shown to phosphorylate 53BP1 and XRCC4 (Benada et al., 2015; Terasawa et al., 2014) to prevent NHEJ in mitosis, and has recently been shown to be recruited to broken replication forks in S phase to inhibit the recruitment of DSB repair factors (Nakamura et al., 2021). We therefore considered whether S538 phosphorylation by PLK1 was involved in the regulation of repriming.

3.4.3.1 Olaparib treatment delays phosphorylation of PrimPol S538

Recent work has shown that olaparib treatment in human cells leads to an increase in PrimPol-mediated repriming (Genois et al., 2021). Olaparib is a poly (ADP ribose) polymerase (PARP) inhibitor. The application of PARP inhibitors prevents the repair of ssDNA breaks, and without this repair, these lesions convert into DSBs. PARP proteins detect ssDNA breaks, and initiate their repair (Abbotts and Wilson III, 2017), as well as recruiting repair proteins to DSB sites (Haince et al., 2008), and fork stabilisation factors during S phase (Liao et al., 2018). In S phase, PARP inhibition by olaparib will lead to both the trapping of PARP proteins and catalytic inactivation of PARP at ssDNA breaks (Murai et al., 2014). The reason for increased PrimPol-mediated repriming after PARP inhibition is not yet clear, and it is not obvious what PrimPol is responding to, though RPA-bound ssDNA could be a potential substrate for the recruitment of PrimPol.

To investigate the role of increased PrimPol dependence and increased ssDNA gaps on the phosphorylation of PrimPol, we monitored the change in phosphorylation after thymidine release in cells treated at point of release with 10μM olaparib. We found that, while in undamaged cells phosphorylation is detectable 6 hours after thymidine release (late S/G2), S538 phosphorylation remains low until 10 hours post-thymidine release in cells treated with olaparib (Figure 3.7A).

FACS analysis shows that, when cells were released from G1/S stall into media containing olaparib, a greater number of cells were still replicating at 8 hours (46% EdU positive, Figure 3.7B), when undamaged cells had ceased replication (4.7%, Figure 3.4C). This suggests that exit from S phase is delayed by the addition of olaparib, as described before (Prasad et al., 2017). These data infer that the phosphorylation of S538 is closely associated with the end of DNA synthesis. However, along with previously mentioned phenotypes associated with PARP inhibition, olaparib has also been shown to increase replication fork speed, which is suggested to trigger the replication stress response (Maya-Mendoza et al., 2018). It is unclear whether the delay in S phase completion or the replication stress induced by olaparib were the cause of the phosphorylation delay.

3.4.3.2 Treatment with camptothecin delays the S/G2 phosphorylation of S538

DNA Topoisomerase I (Topo I) is a DNA relaxer, responsible for removing DNA supercoils in front of the fork to allow DNA replication and transcription to take place. Camptothecin inhibits this DNA relaxation, by preventing the removal of Topo I from the DNA after it has performed the nick. The cell can remove Topo I from the DNA using a complex of proteins including Tyrosyl-DNA Phosphodiesterase 1 (TDP1) and PARP (Pommier et al., 2006). However, until this process is completed, forks remain stalled, and replication cannot continue from this site.

To determine if this fork stalling and an increase in ssDNA breaks caused a similar delay in PrimPol phosphorylation to olaparib treatment, cells were released from a thymidine induced G1/S stall into media containing 20nM camptothecin. FACS analysis of cells treated with camptothecin showed that 6 hours post-thymidine release, approximately 70% of cells are undergoing DNA replication, and by 8 hours this has dropped to 4% (Figure 3.7D). This is similar to undamaged cells, where at 6 hours 52% of cells are undergoing DNA replication, and by 8 hours this has dropped to 4.7%, suggesting in both cases that DNA replication has been largely completed. In undamaged cells, phosphorylation is clearly strongly detectable at 6 hours; however, in cells treated with camptothecin, this phosphorylation is almost undetectable at 6 hours,

instead only occurring in the 8 hour sample onwards (Figure 3.7C). This suggests that the completion of S phase is unimpeded by the addition of camptothecin, but S538 phosphorylation is still delayed.

To summarise, these data suggest that replication stress induced at the start of S phase leads to a shift in the timing of PrimPol S538 phosphorylation. In the case of olaparib treatment, this delay corresponds to a delay in the completion of S phase. However, the cell cycle does not appear to be significantly impeded by the application of camptothecin. This may indicate that phosphorylation is related to the completion of the bulk of DNA synthesis, and the EdU positive cells remaining at 8/10 hours after olaparib or UV-C treatment may only be completing small amounts of replication. It may also suggest that the replication stress itself may be the cause of phosphorylation delay after drug treatment.

3.4.3.3 UV-C Damage in early S phase delays S538 phosphorylation

To determine if damage to the DNA template can also delay the phosphorylation of S538, as replication stress has been shown to do, we analysed the effect of UV-C damage on cells in early S phase. To have a greater effect on the replication fork, 20 J/m^2 UV damage was applied to cells once they were already replicating (2 hours after release from the G1/S boundary) and harvested after a further 0.5, 2, 4, 6 and 8 hours. FACS analysis showed that UV damage applied 2 hours after thymidine release (with 76% of cells in S phase) delayed S phase completion when compared to undamaged cells: 10 hours post-thymidine release, the undamaged population had only 1.7% of cells still replicating, while after UV-C damage, 52% of cells incorporated EdU at 10 hours (Figure 3.7F). As in previous experiments, UV-C damage also delayed phosphorylation of S538 (Figure 3.7E). These data suggest that DNA damage occurring in early S phase delays the PLK1-dependent phosphorylation of S538 through a similar mechanism to the delay caused by replication stress. In cells treated with UV-C, as with olaparib, this delay in phosphorylation also correlated with a delay in the completion of S phase, suggesting that S538 phosphorylation is tightly controlled by the cell cycle and the stage of DNA replication. We additionally tested 20 J/m^2 UV-C damage on cells released for 4 hours and found that this corresponded

with the earlier experiments where damage was applied at 2 hours, or stress at point of release (data not shown).

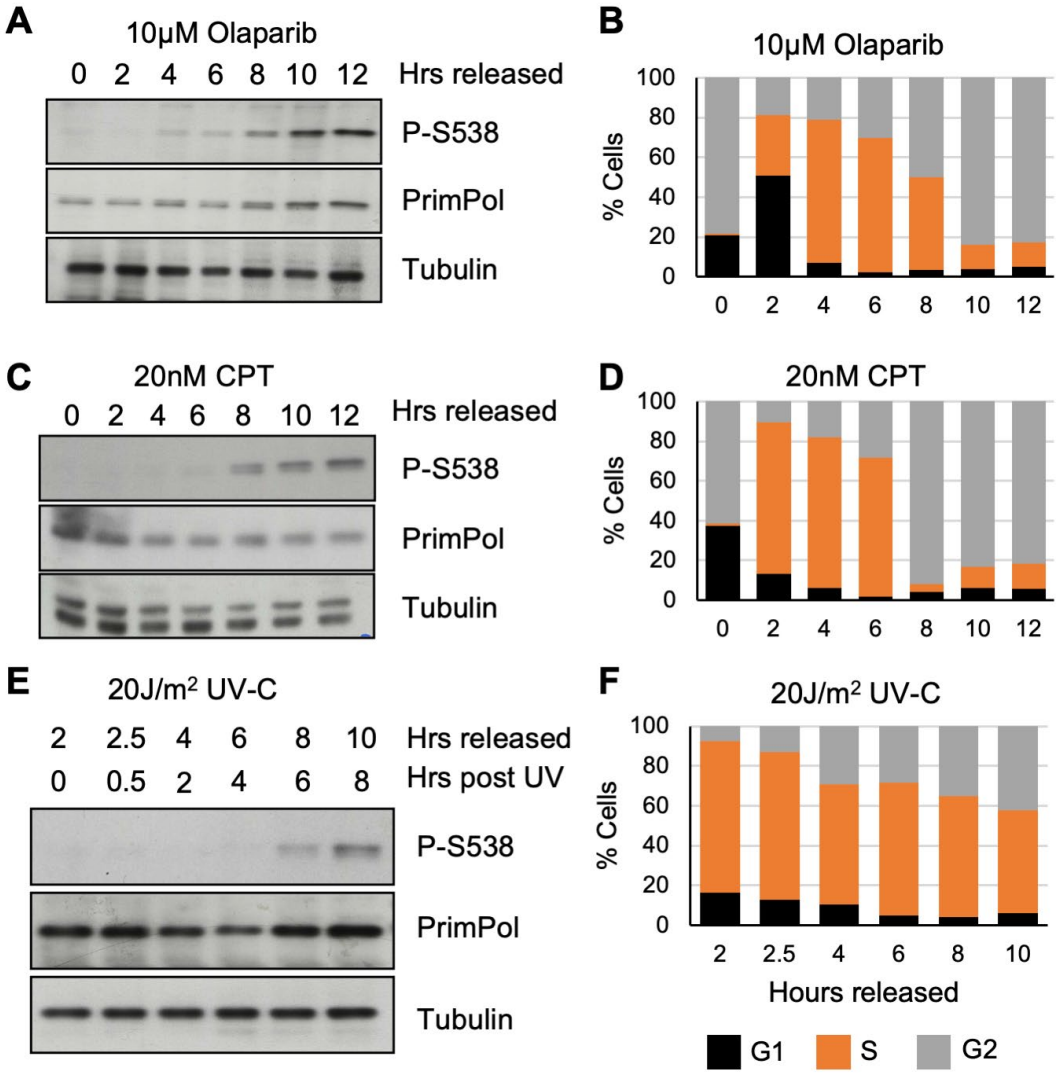

Figure 3.7. The addition of olaparib or camptothecin to cells released from a G1/S stall delays PrimPol S538 phosphorylation

A. Western blot analysis of protein from HEK-293 cells expressing PrimPol. Cells were released from thymidine block into media containing 10 μM Olaparib. Samples from denoted timepoints were probed for P-S538, total PrimPol and tubulin. **B.** Cell cycle quantification at each timepoint after treatment with olaparib. **C.** Analysis of protein from cells expressing PrimPol released from thymidine block into media containing 20 nM camptothecin. **D.** Quantification at each timepoint after treatment with camptothecin **E.** Analysis of protein from cells damaged with 20 J/m^2 UV-C, 2 hours after thymidine release. **F.** Quantification at each timepoint after treatment with UV-C.

3.4.4 The effect of DNA damage on PrimPol S538 phosphorylation in late S phase

3.4.4.1 Replication stress alters the phosphorylation of S538 in late S phase

The suggestion that phosphorylation of S538 was delayed in cells damaged by DNA damaging agents, or when replication stress was applied, raised the question of whether active dephosphorylation could occur in response to replication stress, to reverse S538 phosphorylation. We therefore altered the experimental protocol previously applied to early S phase cells and applied it to cells that had progressed into late S/G2 before damage was applied. We aimed to determine if the high levels of phosphorylation present in late S phase would decrease in response to replication stress or DNA damage.

We initially applied damaging agents to cells that had been released from thymidine and allowed to progress through S phase for 6 hours, at which point 54% of cells were actively replicating and 39% were in G2 (Figure 3.8B). As seen in Figure 3.4D, 6 hours after thymidine release there is strong S538 phosphorylation clearly detectable by western blot. Cells were allowed to progress through late S phase into G2/M, and harvested at 6, 6.5, 7, 8, 10 and 12 hours total post-thymidine release. To aid in interpretation of the data, cells were also stained for phospho-H3 to allow for analysis of mitotic entry – 1μM nocodazole was present in the media to prevent exit from mitosis into G1. At 7 hours, the majority of cells (82%) were in G2/M (Figure 3.8B) and 35% of these cells were mitotic – this increased to 72% by 12 hours (Figure 3.8C). Western blot analysis of these samples showed that PrimPol phosphorylation increases as cells increasingly progress into G2/M (3.8D). While total PrimPol levels may visibly appear to slightly increase over time, we attributed this to bleed through of S538 antibody signal from reprobing of the blot, and therefore presented the ratio of S538 phosphorylation:total PrimPol (Figure 3.8E) for clarity.

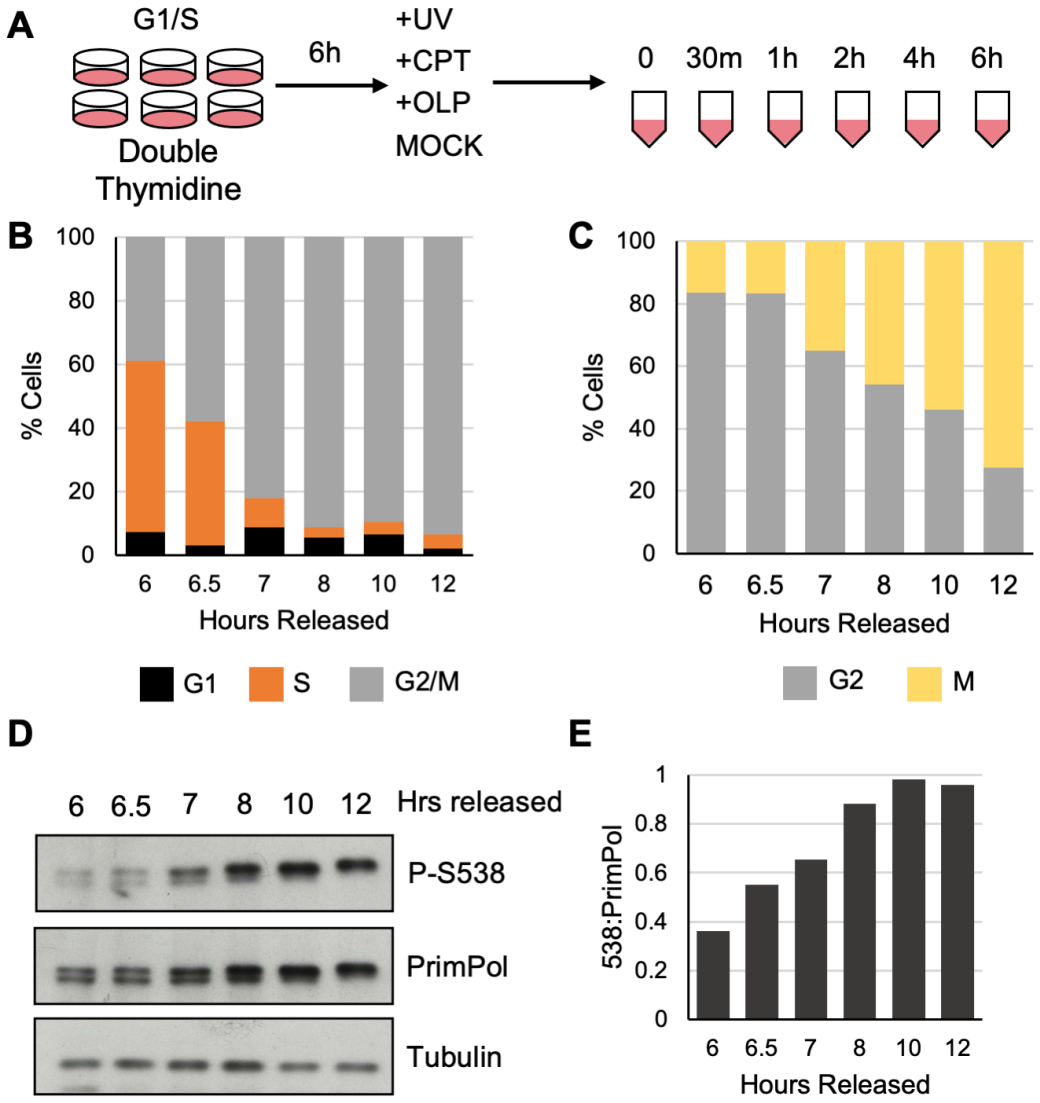

Figure 3.8. PrimPol S538 phosphorylation increases as cells progress into G2/M in undamaged cells

A. A schematic describing the cell synchronisation protocol. Cells were stalled by 4mM thymidine, then released for 6 hours before harvest at the denoted timepoints for FACS and western blot analysis. When damaged was applied, this was performed after the 6 hour release but before harvest. **B.** Cell cycle quantification of undamaged cells based on PI and EdU at each timepoint. **C.** Cell cycle quantification of p-H3 positive undamaged cells at each timepoint. **D.** Western blot analysis of protein from undamaged HEK-293 cells expressing WT PrimPol. Samples from denoted timepoints were probed for P-S538, total PrimPol and tubulin. **E.** Quantification of the western blot shown in D.

After verifying the phosphorylation pattern in undamaged cells, we next treated cells at the late S phase timepoint with a panel of replication stress inducing or DNA damaging agents, in order to determine if they had an effect on PrimPol S538 phosphorylation. We initially assessed the effect of 20 nM camptothecin and 10 μM olaparib, the same doses used in experiments described in Figure 3.7A. Treatments were added 6 hours after thymidine release and cells were harvested at the above timepoints. In the instance of camptothecin, we found this dose insufficient to alter cell cycle progression, and there was no detectable effect on S538 phosphorylation (data not shown). We therefore increased the dose utilised in late S phase experiments.

50 nM camptothecin and 10 μM olaparib were applied to cells 6 hours after thymidine release and cells were harvested at subsequent defined timepoints. FACS analysis determined that the addition of both 50 nM camptothecin and 10 μM olaparib significantly impaired S phase progression, with EdU positive cells at 6.5 hours decreasing from 39% of cells in undamaged conditions to 5.5% and 5.7% respectively (Figure 3.9B, E). These drug treatments also delayed mitotic entry, with a smaller number of cells with detectable phospho-H3 signal at 12 hours after camptothecin or olaparib treatment compared to undamaged cells. Western blot analysis (Figure 3.9A,D) showed a small decrease in S538 phosphorylation signal relative to total PrimPol one/two hours after treatment with both olaparib and camptothecin. Quantification of two experiments revealed this decrease was reproducible, but in all cases mild and resolved by 12 hours. We hypothesise that this is due to the mixed population, with cells closer to the end of S phase moving on to G2 and becoming phosphorylated and masking the dephosphorylation of those unable to complete DNA replication. These data do suggest, however, that S538 phosphorylation can undergo active dephosphorylation, as opposed to simple regulation by PLK1 activation.

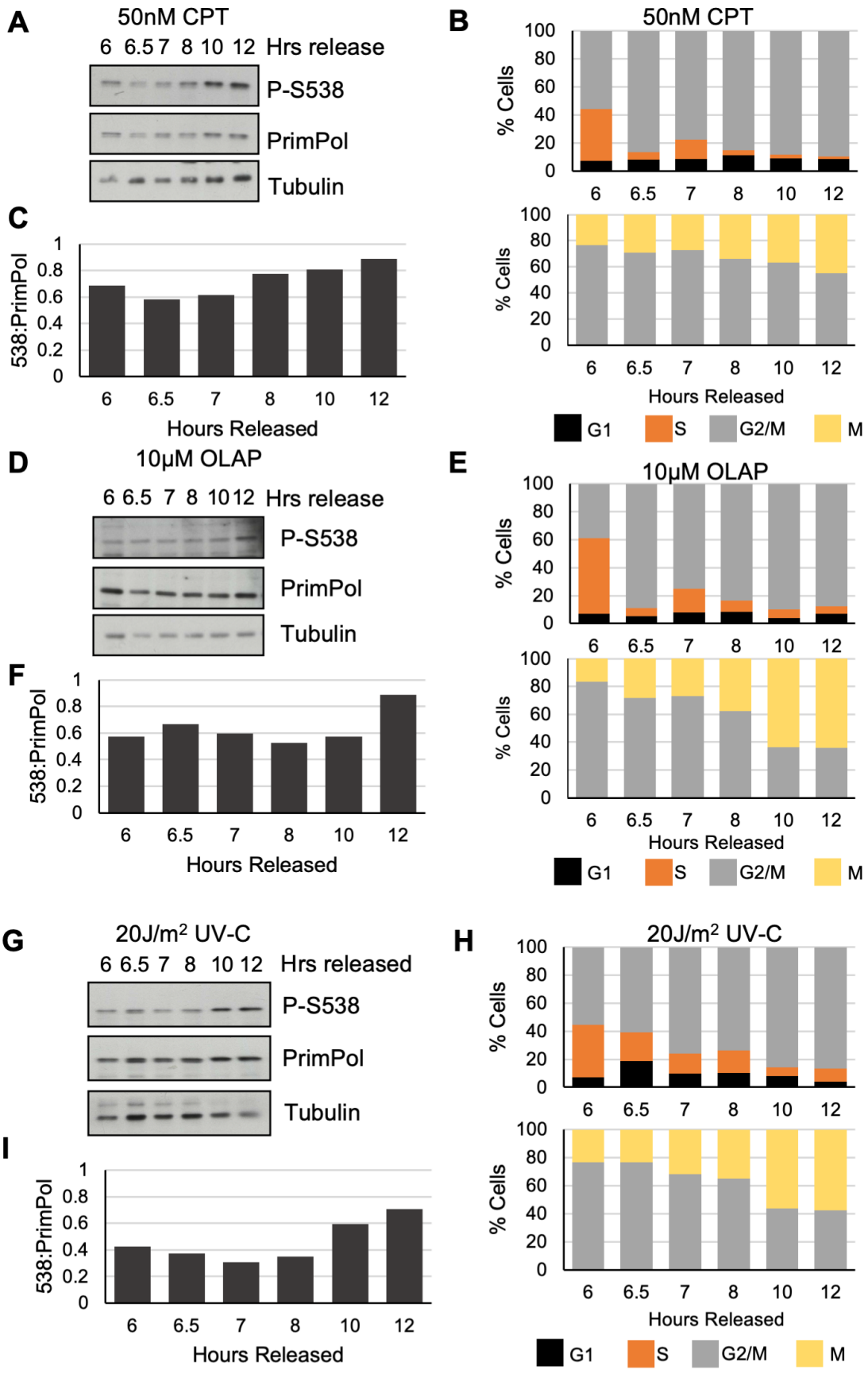
A
50nM CPT
6 6.5 7 8 10 12 Hrs release
P-S538
PrimPol
Tubulin
B
50nM CPT
% Cells
100
80
60
40
20
0
6 6.5 7 8 10 12
Hours Released
G1
S
G2/M
M
C
538:PrimPol
1
0.8
0.6
0.4
0.2
0
6 6.5 7 8 10 12
Hours Released
D
10μM OLAP
6 6.5 7 8 10 12 Hrs release
P-S538
PrimPol
Tubulin
E
10μM OLAP
F
G
20J/m2 UV-C
6 6.5 7 8 10 12 Hrs released
P-S538
PrimPol
Tubulin
H
20J/m2 UV-C
I

Figure 3.9. The effect of olaparib, camptothecin and UV-C treatment on S phase completion, mitotic entry and PrimPol S538 phosphorylation 6 hours after release from thymidine

A. Western blot analysis of protein from cells expressing WT PrimPol treated with 50nM Camptothecin. Samples from denoted timepoints were probed for P-S538, total PrimPol and tubulin. B. Cell cycle quantification of cells treated with 50 nM camptothecin using gating based on PI and EdU (top panel) or P-H3 (lower panel) at each timepoint. **C.** Quantification of P-S538 signal relative to total PrimPol signal over time (n=2). **D.** Western blot analysis of protein from cells expressing WT PrimPol treated with 10 μM Olaparib. Samples from denoted timepoints were probed for P-S538, total PrimPol and tubulin. **E.** Cell cycle quantification of cells treated with 10 μM olaparib using gating based on PI and EdU (top panel) or P-H3 (lower panel) at each timepoint. **F.** Quantification of P-S538 signal relative to total PrimPol signal over time (n=2). **G.** Western blot analysis of protein from cells damaged with 20 J/m^2 of UV-C. Samples from denoted timepoints were probed for P-S538, total PrimPol and tubulin. **H.** Cell cycle quantification of cells treated with 10 μM Olaparib using gating based on PI and EdU (left panel) or P-H3 (right panel) at each timepoint. **I.** Quantification of P-S538 signal relative to total PrimPol signal over time (n=2).

Given the minor changes in phosphorylation observed 6 hours after treatment with replication stress, we additionally tested 20 J/m^2 UV-C damage to determine if this had an effect on phosphorylation levels. Cells were damaged 6 hours post-thymidine release, then left to recover until 6.5, 7, 8, 10 and 12 hours total post-thymidine release, before each sample was harvested and subject to western blot analysis of P-S538 levels (Figure 3.9G). Western blot analysis after UV-C treatment determined that phosphorylation decreased across 6.5-8 hours (Figure 3.9I), but minimal perturbation of S phase completion or mitotic entry was observed (Figure 3.9H). These data suggest that the decrease in phosphorylation after replication stress induced by olaparib and camptothecin can also be induced by DNA damage caused by UV.

The data obtained from UV-C, olaparib or camptothecin treatment support the notion of an active dephosphorylation pathway in cells. However, the decrease is small, potentially due to differences in progression after thymidine release. All treatment conditions induced a similar, small decrease that was resolved as cells begun to enter mitosis, suggesting any phosphorylation overcame any dephosphorylation when cells were undergoing division, likely due to the high activity of PLK1. We theorised cells that had largely completed DNA replication to a sufficient degree to progress to G2 at the 6 hour timepoint did not undergo significant dephosphorylation, while those with significant DNA replication left to complete may undergo active dephosphorylation.

Given that, largely, cells in the 6 hour population appeared to enter G2/M as normal, we altered the experimental protocol (Figure 3.10A) to damage cells 5 hours after thymidine release, when 55% of cells were EdU positive (Figure 3.10B). Cells were left undamaged or treated with 50 nM camptothecin or 10 μM olaparib at 5 hours, and harvested at 5, 5.5, 6, 7, 8, 10 and 12 hours post-thymidine release. Cells were also stained for phospho-H3 to detect mitotic entry. In undamaged cells, phosphorylation increased as cells progressed through S phase and into G2/M, reaching a peak 8 hours post-release. However, olaparib treated cells show a small delay in this phosphorylation, and camptothecin treated cells show a decrease in phosphorylation (6 hours compared to 5.5) (Figure 3.10). A similar phenotype is seen after UV-C damage, though in all cases

cells still progress into G2 and mitosis at approximately the same rate as undamaged cells, indicating the absence of significant stalling.

Olaparib applied at 5 hours appears to generate a similar response to olaparib applied at 6 hours – while a decrease in phosphorylation is observed, it is not immediate, and there remains an increase in S538 phosphorylation levels between 5 and 5.5 hours, and 6 and 6.5 hours. However, this does not necessarily suggest that the PrimPol response to olaparib induced stress is slow, but rather may reflect the competitive nature of S538 dephosphorylation during a cell cycle stage where PLK1 is known to be highly active. A much more significant increase is seen at 5.5 hours in the camptothecin treated cells, which was not observed 0.5 hours after treatment at 6 hours. It is not clear what would cause a significant increase in phosphorylation followed by a significant increase, but discrepancies could be attributed to the low number of cells that were EdU positive at 5.5 hours in the camptothecin sample (34%), compared to undamaged cells (46%), and cells treated with olaparib (44%). It could also represent a specific response to the stress caused by camptothecin, which would first stall all ongoing replication by inhibiting strand unwinding - replication stress which would not be helped by PrimPol mediated repriming. This may promote phosphorylation until the Top1 blockage has been removed, at which point PrimPol may be utilised to restart ongoing replication, resulting in a dephosphorylation signal.

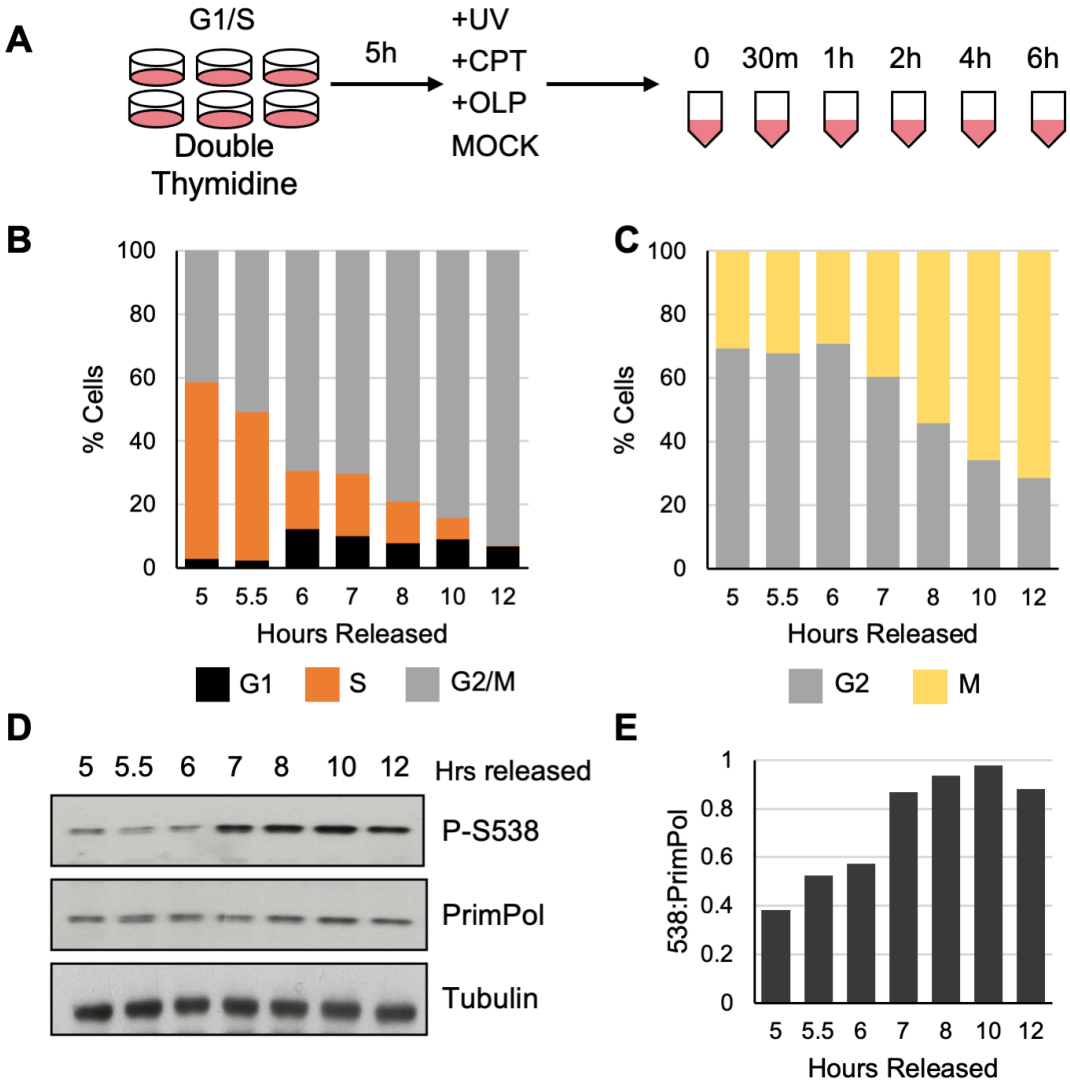

Figure 3.10. Undamaged cells released from thymidine for 5 hours show increasing PrimPol S538 phosphorylation

A. A schematic describing the experimental protocol. Cells were stalled by 4mM thymidine to the G1/S boundary, then released into fresh media for 5 hours. Samples were taken at defined timepoints for FACS and western blot analysis. **B.** Cell cycle quantification of undamaged cells using gating based on PI and EdU at each timepoint. **C.** Cell cycle quantification of undamaged cells using gating based on P-H3 signal at each timepoint. **D.** Western blot analysis of protein from HEK-293 cells expressing WT PrimPol. Samples from denoted timepoints were probed for P-S538, total PrimPol and tubulin. **E.** Quantification of the blot shown in D.

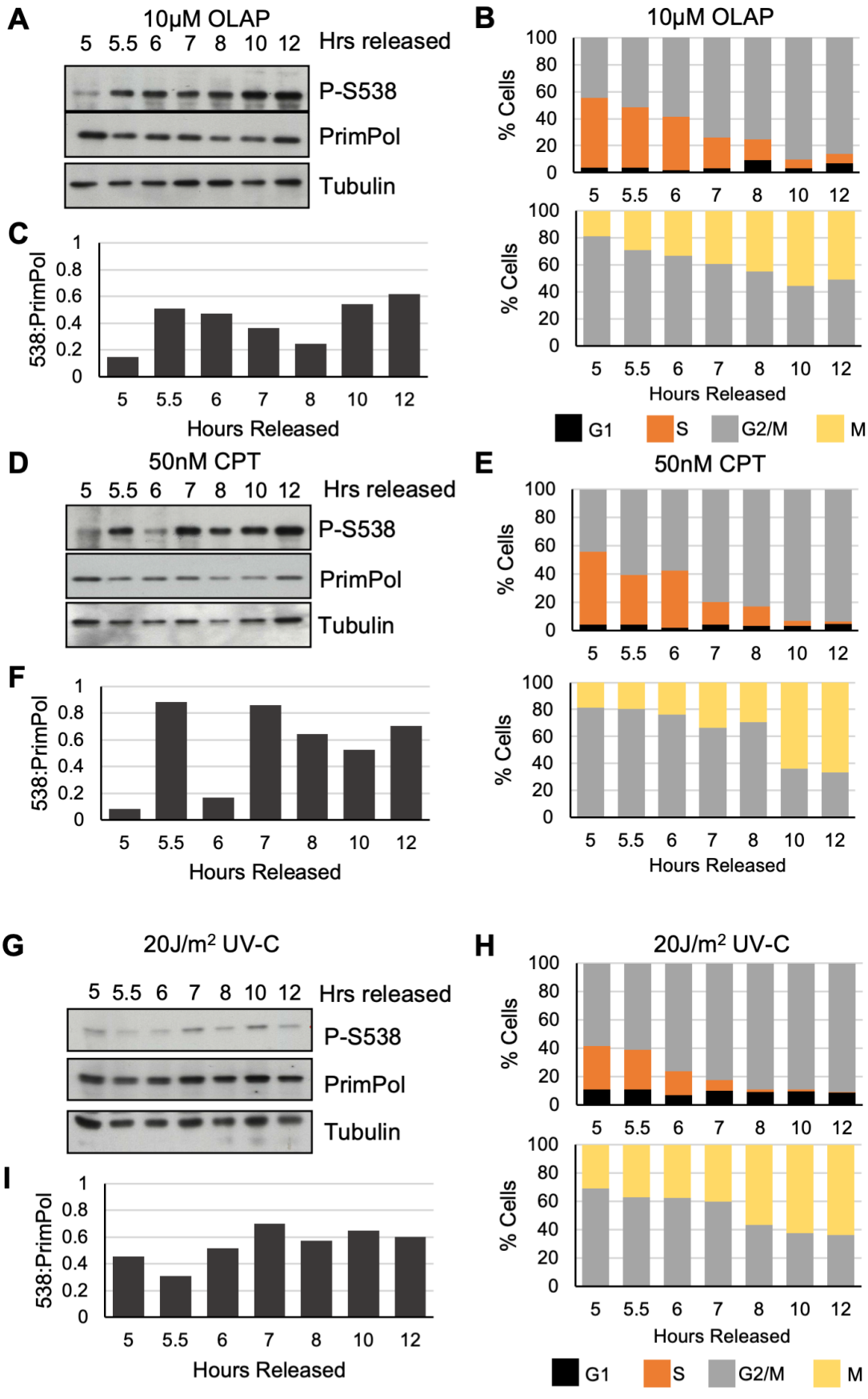
A
10μM OLAP
5 5.5 6 7 8 10 12 Hrs released
P-S538
PrimPol
Tubulin
B
10μM OLAP
% Cells
100
80
60
40
20
0
5 5.5 6 7 8 10 12
Hours Released
G1
S
G2/M
M
C
538:PrimPol
1
0.8
0.6
0.4
0.2
0
5 5.5 6 7 8 10 12
Hours Released
D
50nM CPT
5 5.5 6 7 8 10 12 Hrs released
P-S538
PrimPol
Tubulin
E
50nM CPT
F
G
20J/m2 UV-C
H
20J/m2 UV-C
I

Figure 3.11. The effect of olaparib, camptothecin and UV-C treatment on S phase completion, mitotic entry and PrimPol S538 phosphorylation 5 hours after release from thymidine block

A. Western blot analysis of protein from HEK-293 cells expressing WT PrimPol, after treatment at 5 hours post-thymidine release with 10 μM Olaparib (OLAP). Samples from denoted timepoints were probed for P-S538, total PrimPol and tubulin. **B.** Cell cycle quantification of cells treated with 10 μM olaparib using gating based on PI and EdU (upper graph) or PI and P-H3 (lower graph) at each timepoint. **C.** Quantification of P-S538 signal after olaparib treatment relative to total PrimPol signal over time (n=2). **D.** Western blot analysis of protein from HEK-293 cells expressing WT PrimPol, after treatment at 5 hours post-thymidine release with 50 nM Camptothecin (CPT). Samples from denoted timepoints were probed for P-S538, total PrimPol and tubulin. **E.** Cell cycle quantification of cells treated with 50 nM camptothecin using gating based on PI and EdU (upper graph) or PI and P-H3 (lower graph) at each timepoint. **F.** Quantification of P-S538 signal after camptothecin treatment relative to total PrimPol signal over time (n=2). **G.** Western blot analysis of protein from HEK-293 cells expressing WT PrimPol, after damage at 5 hours post-thymidine release with 20 J/m^2 UV-C. Samples from denoted timepoints were probed for P-S538, total PrimPol and tubulin. **H.** Cell cycle quantification of cells damaged with 20 J/m^2 UV-C using gating based on PI and EdU (upper graph) or PI and P-H3 (lower graph) at each timepoint. **I.** Quantification of P-S538 signal after UV damage relative to total PrimPol signal over time (n=2).

Data described to this point suggests that the phosphorylation of S538 is closely linked to the completion of DNA synthesis, and can be regulated in response to replication stress or DNA damage. However, each FACS sample, as shown in their cell cycle quantification, is a mixed population. While generally a population of cells may be “mid-S phase”, the inherent variability of each population, even in synchronised cells, led us to conclude that if dephosphorylation was occurring in S phase, it may be partially masked by S538 phosphorylation in cells which had progressed into G2. For this reason, we constructed an experiment to allow us to determine more clearly if dephosphorylation did occur after stress or damage, by using the PLK1 inhibitor BI2536 to prevent subsequent G2 phosphorylation.

At 5 hours post-thymidine release, 56% of cells are EdU positive and 42% are G2/M. At this stage, when there are detectable levels of PrimPol S538 phosphorylation, cells were treated with BI2536 and either left undamaged or treated with 50 nM camptothecin, 10 μM olaparib or 20 J/m^2 UV-C.

With all further phosphorylation inhibited by inhibition of PLK1, phosphorylation would either remain the same or, if dephosphorylation occurred, phosphorylation levels would decrease. Interestingly, we found that in undamaged cells treated with the inhibitor, phosphorylation levels are maintained. This suggests that dephosphorylation of S538 does not occur in late S/G2 in the absence of replication stress or damage. However, when cells were treated with olaparib, camptothecin or damaged by UV-C, S538 phosphorylation levels were undetectably low, suggesting full dephosphorylation of S538.

To summarise, these data suggest that in undamaged cells, PrimPol S538 phosphorylation is primarily regulated by the cell cycle. Phosphorylation is low at the start of S phase due to the dephosphorylation of PrimPol throughout G1. When cells reach late S/G2, phosphorylation of S538 occurs (Figure 3.12). This phosphorylation of S538 remains high through G2 and mitosis. However, if the cell experiences replication stress in early S phase, the completion of DNA synthesis is delayed by a slowing of the cell cycle, and this in turn delays phosphorylation of S538. When replication stress is introduced at the end of S phase, when phosphorylation of S538 has already occurred, this phosphorylation can be removed by a phosphatase enzyme.

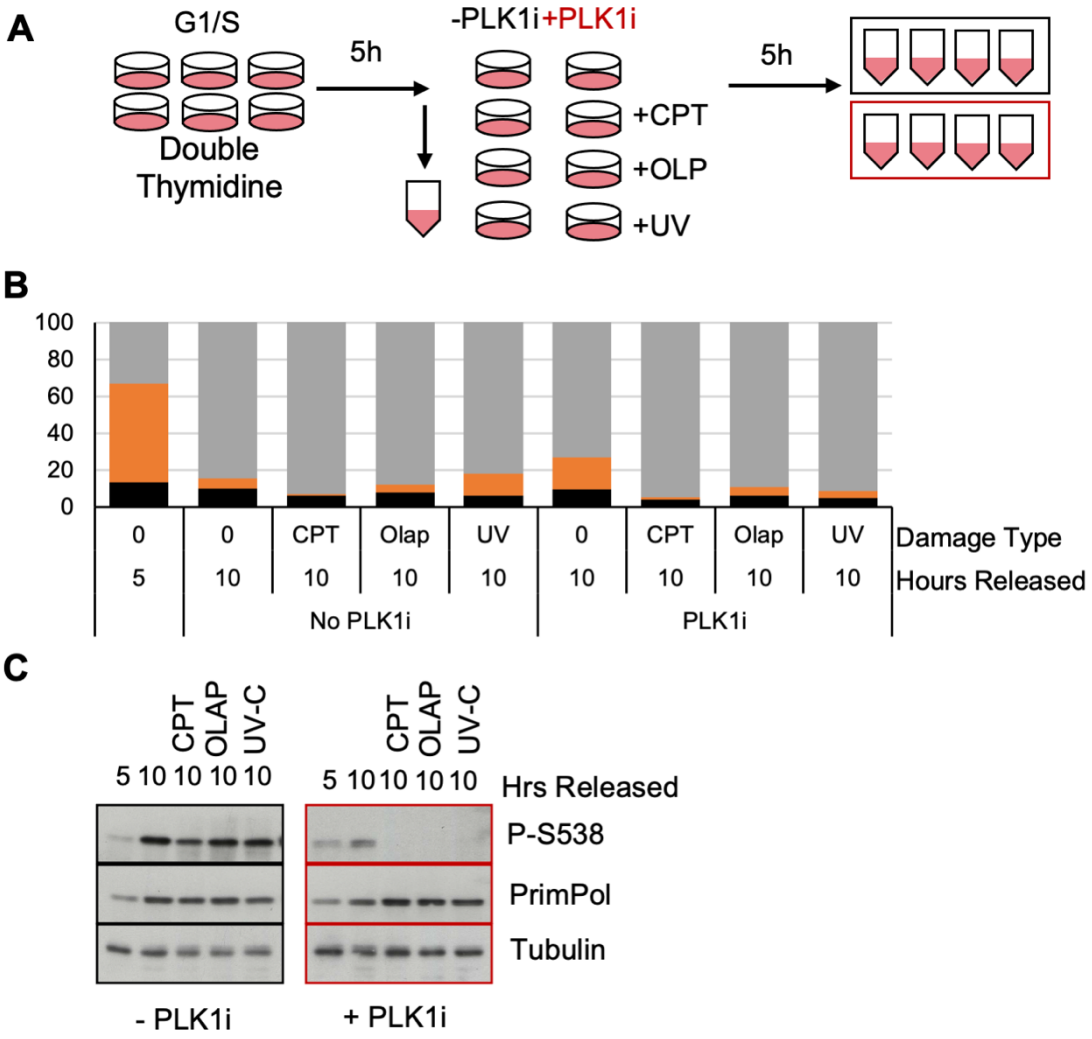

Figure 3.12. Inhibition of PLK1 reveals that PrimPol S538 is dephosphorylated after treatment with olaparib, camptothecin or UV-C damage

A. A schematic describing the experimental protocol. Cells were stalled by 4 mM thymidine to the G1/S boundary, then released into fresh media for 5 hours. Cells were then either incubated with 1 μM BI2536 to inhibit PLK1, or left untreated, and were also mock damaged, treated with 10 μM Olaparib, 50 nM Camptothecin or damaged with 20 J/m^2 UV-C at 5 hours, and left to recover for a further 5 hours. Cells were harvested at 10 hours post-thymidine release for FACS and western blot analysis. **B.** Cell cycle quantification of undamaged cells using gating based on PI and EdU at each timepoint and treatment condition. **C.** Western blot analysis of cell lystate from each treatment condition and timepoint. Samples from denoted timepoints were probed for P-S538, PrimPol and tubulin.

3.5 Disruption of PrimPol S538 phosphorylation leads to catastrophic effects on cell viability and genome stability

3.5.1 Generation of HEK-293 cell lines expressing S538 phospho-mutant PrimPol

To generate cell lines that allowed for controlled expression of mutant PrimPol, the Flp recombinase-mediated integration (Flp-In) Tetracycline-regulated expression (TREx) system was again employed (described in 2.4.3.2). The PrimPol knockout cell line was transfected with a pcDNA5 vector containing FLAG-tagged PrimPol. This vector was mutated to contain either wild type, S538A – a phosphonull substitution at S538 – or S538E – a phosphomimic substitution within PrimPol. Figure 3.13A shows western blot analysis of WT, S538A and S538E cell lines, showing that while doxycycline induced expression of protein in all three lines, only WT protein was bound by the phospho-S538 antibody, and no PrimPol protein was detected without the addition of doxycycline.

Generation of these cell lines revealed that, on initial study, the S538A mutant line grew more slowly, with significantly higher average doubling time when compared to wild type cells (Figure 3.13B) and showed a plating deficiency when cells were grown in the presence of doxycycline (Figure 3.13C), indicating that the overexpression of this mutant in undamaged cells was detrimental to their growth when compared to wild type protein. These mutant cell lines were additionally subject to FACS analysis 24 hours after protein expression, which determined that despite slower doubling time, the cell cycle distribution was unchanged (Figure 3.13D).

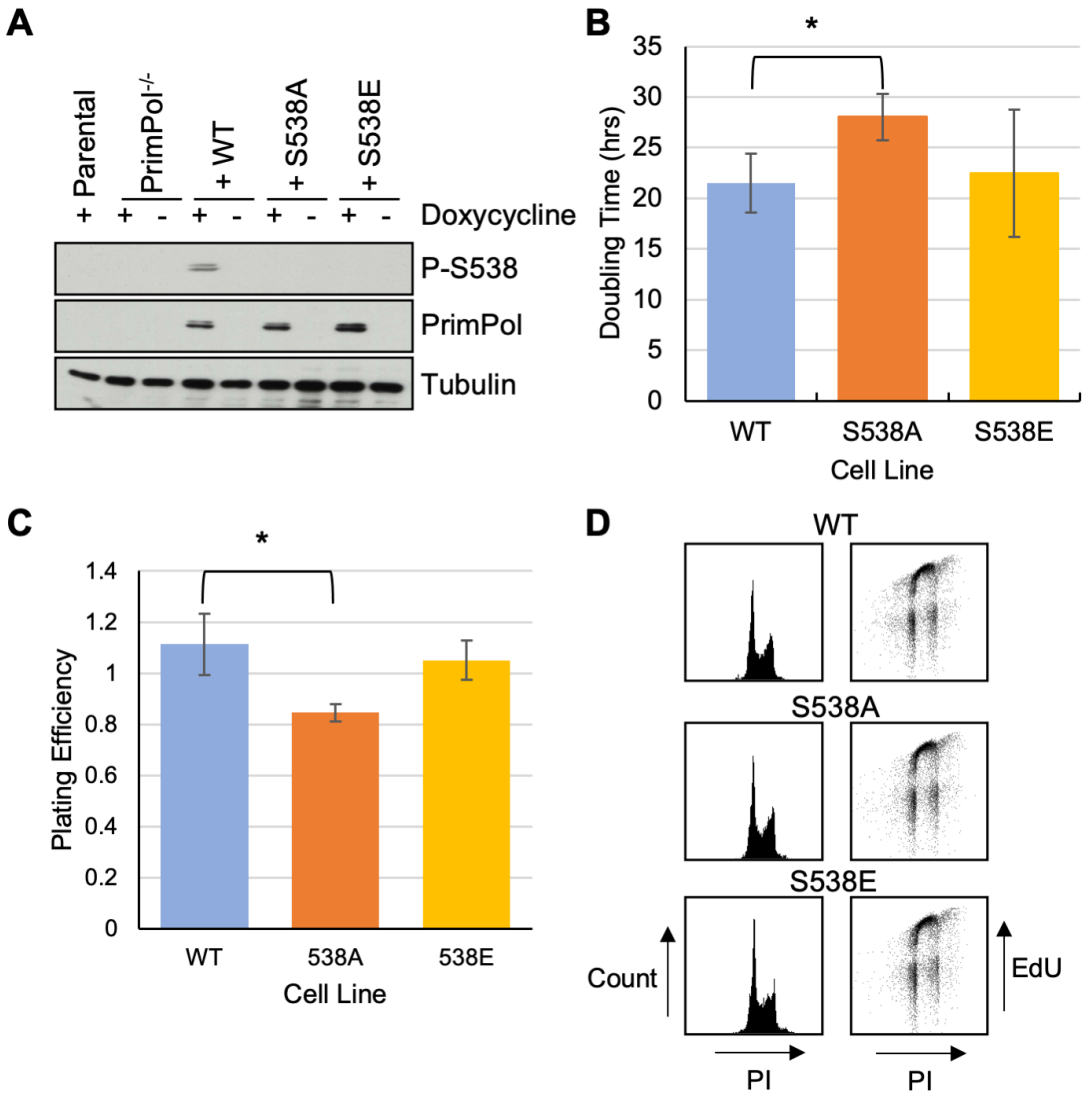

Figure 3.13. Analysis of S538 phospho-mimic and phospho-null mutant PrimPol in HEK-293T Flp-In T-REx cell lines

A. Western blot analysis of HEK-293 PPKO cells expressing WT, S538A or S538E PrimPol. **B.** Doubling time of cells expressing WT, S538A or S538E PrimPol (n=3). **C.** Plating efficiency of WT, S538A and S538E cell lines compared to no doxycycline controls (n=3). **D.** FACS analysis of WT, S538A and S538E cells with PI and EdU staining.

3.5.2 Mutation of S538 of PrimPol induces cellular phenotypes, including mitotic aberrations

We assessed the propensity for cells expressing S538 mutant PrimPol protein to develop phenotypes indicative of genomic instability. Micronuclei are small nuclear bodies, entirely separate to the nucleus but contained within the cell body, formed when a chromosome or fragment of a chromosome is not incorporated into the nucleus of the daughter cell after cell division (Krupina et al., 2021). Micronuclei form during anaphase, caused by either lagging chromosomes, extra chromosomes or chromatid fragments, or as the result of unrepaired or misrepaired DNA breaks. Cells expressing WT, S538A or S538E mutant protein were initially assessed for the presence of micronuclei. Undamaged cells expressing S538A had significantly more micronuclei than cells expressing S538E or wildtype protein (Figure 3.14A). Cells were then treated with 5J/m^2 UV-C and left to recover for 72 hours; this caused an increase in micronuclei in all cell lines. However, the expression of S538A mutant PrimPol lead to a significant increase in the number of cells with one or more micronuclei compared to cells expressing wildtype protein (Figure 3.14B). Additionally, when assessed by metaphase spread experiments, cells expressing S538A had significantly more chromosome breaks than cells expressing WT or S538E protein (Figure 3.14C).

3.5.3 Mutation of S538 of PrimPol alters cell cycle-dependent chromatin exclusion

PrimPol's recruitment to DNA is mediated by an interaction between RPA and PrimPol's C terminal RBD (Guilliam et al., 2017). Given that S538 is located between PrimPol's two RPA binding domains, we considered that it may play a role in regulating chromatin binding. Previous work has shown that PrimPol is recruited to chromatin in response to UV damage (Bianchi et al., 2013), and we therefore analysed the binding of PrimPol to chromatin in undamaged and damaged conditions and examined whether this was altered in the S538A or S538E mutant lines. Figure 3.14D shows that in both undamaged conditions, and after 6 J/m^2 UV-C damage, there was no significant difference in the amount of protein bound to chromatin across each cell line. This experiment was, however,

performed in asynchronous cells, meaning that any cell cycle specific changes may not be detectable.

Additionally, the S538A and S538E mutations to PrimPol were studied *in vitro* to determine if these mutations had any effect on the enzyme's activity. There was no detectable effect on the primase or polymerase activity of the protein after mutation of S538 to either alanine or glutamic acid (Bailey et al., 2021, Appendix B).

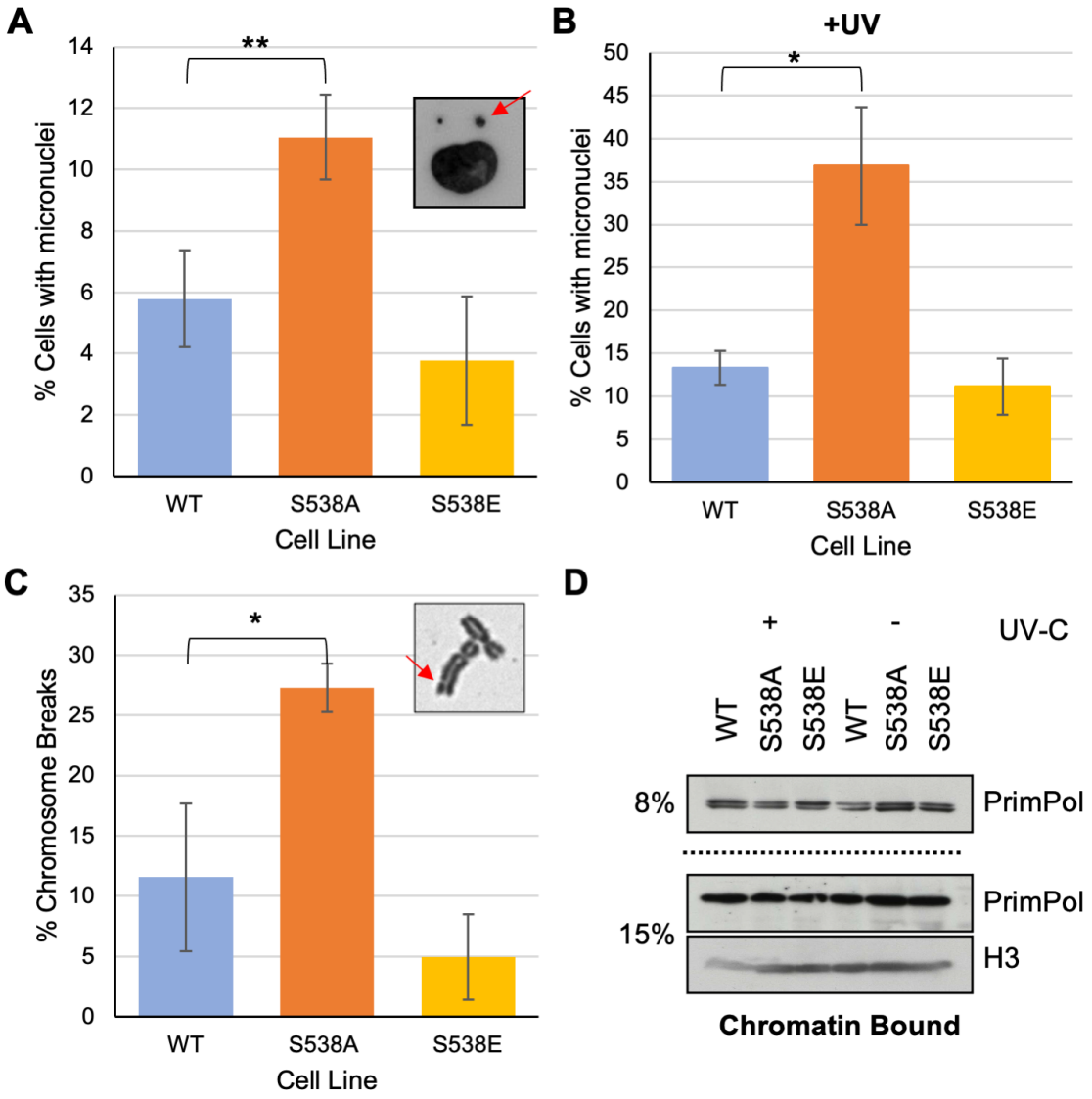

Figure 3.14. Expression of S538A mutant PrimPol causes genomic instability but does not induce an overt change in chromatin binding in asynchronous cells

A. Cells with 1 or more micronuclei were counted 72 hours after PrimPol protein expression was induced by doxycycline. **B.** Cells with 1 or more micronuclei were counted 72 hours after 5 J/m^2 UV-C damage (3 biological repeats with n>400). **C.** Cells with one or more chromosome breaks were counted 96 hrs after PrimPol protein expression was induced by doxycycline (3 biological repeats, n>100). **D.** HEK-293 cells expressing WT, S538A or S538E PrimPol were harvested 4 hours after mock or 5 J/m^2 UV-C damage. Detergent resistant chromatin fractions were separated from soluble proteins before analysis by western blot using both 8% and 15% SDS-PAGE gels. Samples were probed for PrimPol and Histone H3.

Previous work has shown that, when expressed at an endogenous level, PrimPol does not associate with chromatin during G2 (Mourón et al., 2013). As discussed in 3.3, PrimPol S538 phosphorylation increases in S/G2, with high levels of phosphorylation in G2 and mitosis, and decreasing levels across G1 into early S phase. We hypothesised that the increased S538 phosphorylation and the decreased chromatin association occurring in G2 may be related, and therefore investigated the chromatin binding of PrimPol across different stages of the cell cycle. Cells were synchronised to G1, S or G2, before being damaged by 0, 6 or 20 J/m^2 and left to recover for one hour (Figure 3.15A). Chromatin binding was assessed by probing the chromatin fraction for PrimPol protein. FACS analysis determined the efficacy of cell synchronisation and protein expression was verified by analysis of the whole cell component (Figure 3.15B,C).

In undamaged cells, PrimPol was observed to bind chromatin in G1 and S phase, regardless of S538 mutation. However, while protein was expressed in the G2 sample, no PrimPol protein was seen bound to chromatin, supporting previous assertations that PrimPol is excluded from chromatin in G2 (Mourón et al., 2013) (Figure 3.15D). This was also the case when cells were damaged with 6 J/m^2 of UV – G1 and S phase binding was maintained across all lines, but PrimPol was excluded from chromatin in G2. However, at the highest dose of UV damage, S538A mutant PrimPol was recruited to chromatin, while S538E and WT PrimPol remained excluded. This suggests that the recruitment dynamics of PrimPol are altered by mutation of S538 to prevent phosphorylation, indicating phosphorylation may play a role in regulating PrimPol recruitment.

Alongside this work, experiments were conducted to determine if the S538A mutant protein interacted differently with RPA, explaining increased recruitment to chromatin in G2. When we analysed the binding of the C-terminal region of wild type or mutant PrimPol with RPA70N by analytical gel filtration, we observed no overt changes in the interactions between PrimPol and RPA *in vitro*. We also found no changes in PrimPol and RPA interaction *in vivo* after mutation of the S538 residue when analysed by immunoprecipitation (Bailey *et al.,* 2021, Appendix B).

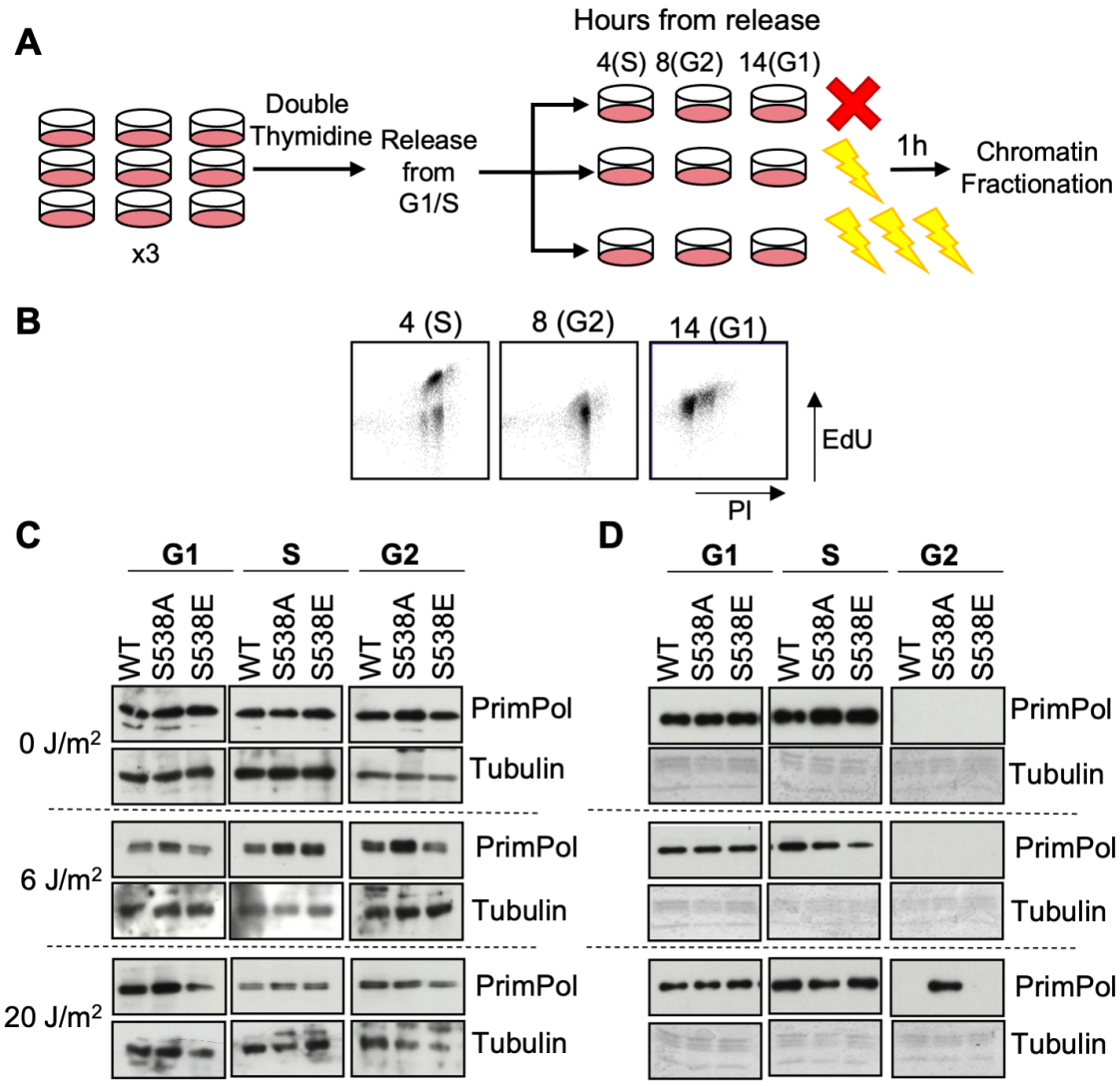

Figure 3.15. Mutation of PrimPol S538 to alanine dysregulates G2 chromatin exclusion and allows for chromatin binding after UV-C damage

A. A schematic describing the experimental protocol. HEK-293 cells expressing WT, S538A or S538E protein were stalled by 4mM thymidine, before being released into fresh media. Samples were damaged at the defined timepoints and left to recover for an additional hour before being harvested for FACS and chromatin fractionation. **B.** FACS profiles of the 4, 8 and 14 hour timepoints used to obtain synchronised S, G2 and G1 cell cycle populations. **C.** Protein from the whole cell fraction was subject to western blotting and probed for total PrimPol and tubulin. **D.** Detergent resistant chromatin fractions were separated from soluble proteins before analysis by western blot. Samples were probed for PrimPol and InstantBlue stained histones were used as a loading control.

3.5.4 S538 mutation does not affect PrimPol recruitment after HU treatment

Previous data has shown treatment with the nucleotide-depleting drug hydroxyurea (HU) leads to a decrease in S538 phosphorylation (3.4.2), though it is unclear whether dephosphorylation occurred in response to dNTP depletion or due to synchronisation at the G1/S boundary. In addition, we have shown that mutation of S538 to alanine dysregulates the recruitment of PrimPol to chromatin. To expand on this, we analysed the differences in chromatin binding and unloading of mutant protein during a HU block and during the release.

To analyse the recruitment of PrimPol during fork stalling by HU, cells were treated with 2mM HU for 2 hours, and either left unreleased (Figure 3.16A, far left panel) or released for 2 hours (centre-left panel). Whole cell extracts probed for PrimPol protein shows that in every tested condition, PrimPol protein levels were largely unchanged. As seen in Figure 3.17A, cells were no longer replicating after the 2 hour HU stall, but quickly resumed DNA synthesis after release. Chromatin fractionation and western blot analysis showed that PrimPol binds chromatin at the same rate during the 2 hour HU application and the short release when compared to undamaged cells.

Previous work has shown that forks stalled for 16-24 hours collapse and are unable to directly restart (Ercilla et al., 2020; Petermann et al., 2010). To analyse the recruitment of PrimPol to collapsed forks, cells were treated with 2mM hydroxyurea for 16 hours, then harvested or released for a further 8 hours before harvest. The 16 hour arrest led to stalled replication (Figure 3.16A, centre-right panel) and chromatin fractionation of these cells showed that PrimPol is recruited to chromatin at similar levels to those observed in undamaged cells. However, after an 8 hour release, at which point cells have resumed replication (Figure 3.17A, far right panel), PrimPol binding decreased. As previous data suggests recovery from fork collapse is primarily mediated by dormant origin firing, this process cannot conceivably require PrimPol (Petermann et al., 2010). Its exclusion from chromatin may therefore suggest a mechanism by which PrimPol association is prevented, either as a result of cellular signals, a lack of ssDNA, or

due to cell cycle stalling. This decrease was observable in all cell lines, suggesting this exclusion is independent of S538 phosphorylation (Figure 3.16B).

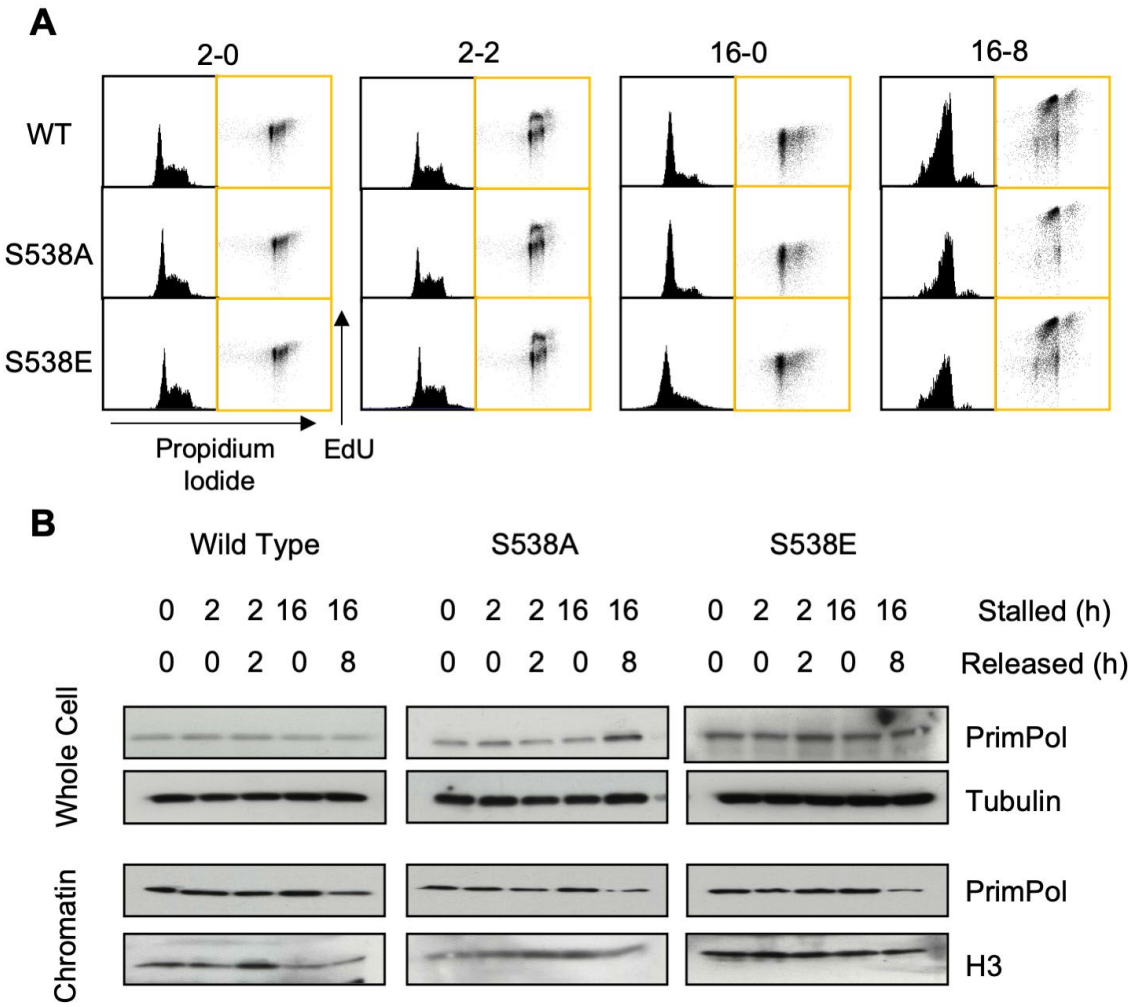

Figure 3.16. Recruitment of PrimPol changes during and after hydroxyurea-mediated fork stalling, but is independent of S538 phosphorylation

A. FACS plots of cell cycle progression during and after HU treatment. Representative images of 0-0 timepoint are not shown as they are untreated and asynchronous. **B.** Western blot analysis of whole cell or chromatin fractions of cells stalled at the above timepoints after HU treatment and release. Whole cell lysate was probed with PrimPol and tubulin antibodies, and the chromatin fraction was probed with PrimPol and H3 antibodies.

3.5.5 Expression of S538A PrimPol protein reduces cell survival after DNA damage

Mutation of PrimPol S538 to alanine has been shown to induce increased chromatin binding in G2 after cells have been damaged by high levels of UV-C, when WT protein is known to be largely excluded from chromatin. We next assessed whether S538A protein expression influenced cell recovery after damage. Cells expressing mutant or WT PrimPol were plated in the presence of doxycycline to induce protein expression and treated with increasing doses of UV-C. Cells were left to recover for 10 days before colony formation was assessed in relation to the number of cells plated and the plating efficiency of the undamaged control. Cells expressing S538A showed decreased survival after UV-C damage when compared to cells expressing WT or S538E (Figure 3.17A).

To ensure that the clonal cell line expressing S538A was not itself sensitive to DNA damage independent of PrimPol expression, we further repeated the experiment with no doxycycline. Without doxycycline, each of these cell lines is effectively a PrimPol$^{-/-}$ line, which have previously been shown to not have significant sensitivity to UV-C damage (Bailey et al., 2019., L. Bailey, unpublished data). We found there was no significant difference in survival across all cell lines without doxycycline after increasing UV-C doses (Figure 3.17B).

3.5.6 Expression of S538A PrimPol protein reduces cell survival after replication stress

We have shown that treatment with olaparib and camptothecin alters the phosphorylation of S538, indicating that dynamic control over S538 phosphorylation was important for PrimPol-mediated recovery after replication stress. We tested the mutant cell lines to determine if either line was more sensitive to olaparib or camptothecin and found that cells expressing S538A mutant protein survived less well at high doses of both olaparib (Figure 3.17C) and camptothecin (Figure 3.17D) compared to WT. PrimPol$^{-/-}$ cells were not any more sensitive to these drugs than cells overexpressing WT protein, suggesting that expression of S538A protein is more harmful to cells under stressful conditions than the absence of PrimPol entirely.

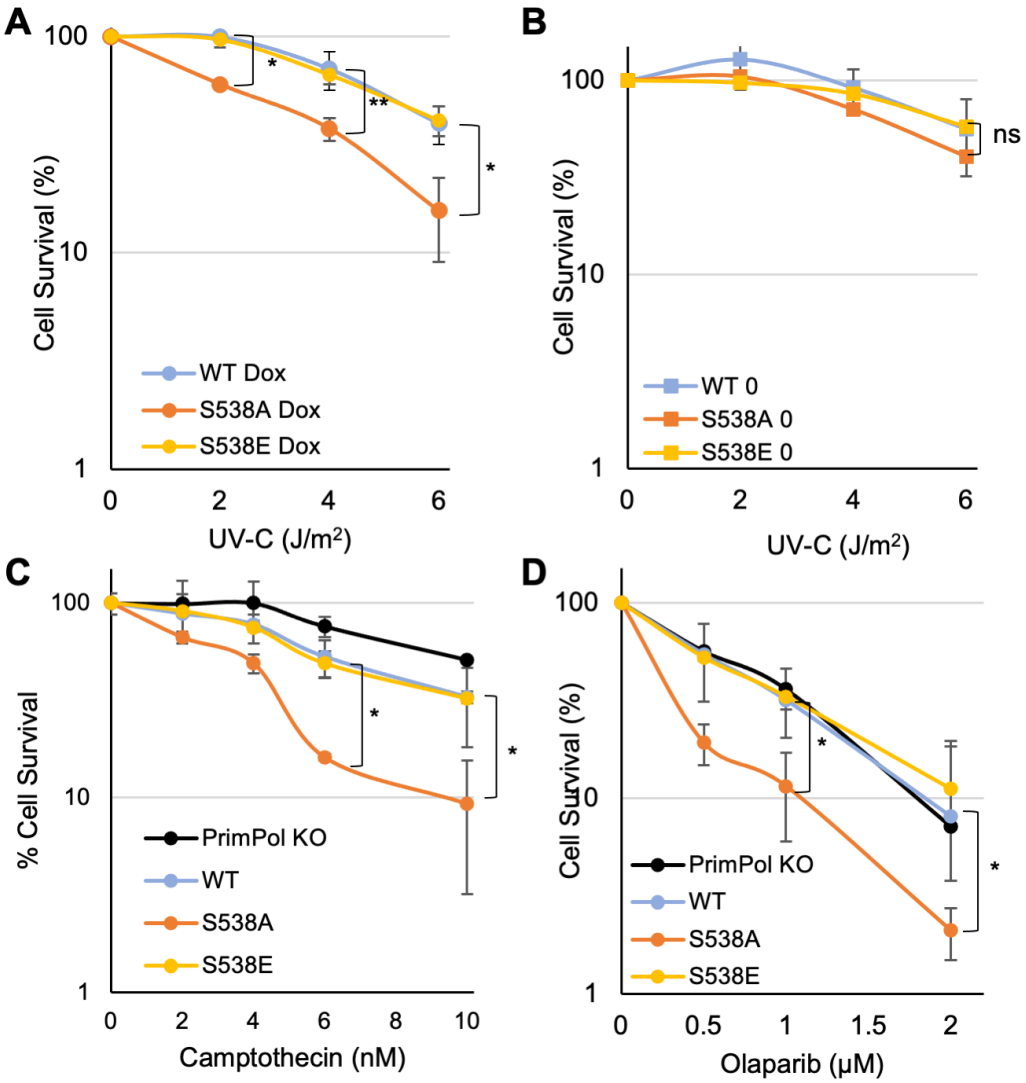

Figure 3.17. Cells expressing S538A PrimPol protein are sensitive to UV-C damage

A. Colony survival assay measured sensitivity to increasing doses of UV-C damage. WT, S538A and S538E cells were plated in media containing doxycycline to induce protein expression. **B.** Colony survival assay to measure sensitivity to increasing doses of UV-C damage. WT, S538A and S538E cells were plated in media without doxycycline, so protein was not expressed. **C.** Colony survival assay to measure sensitivity to increasing doses of camptothecin. WT, S538A and S538E cells were plated in media containing doxycycline to induce protein expression. **D.** Colony survival assay to measure sensitivity to increasing doses of olaparib. WT, S538A and S538E cells were plated in media

containing doxycycline to induce protein expression. Significance is shown between WT and S538A.

3.5.7 Expression of S538 mutant PrimPol does not affect cell cycle progression after replication stress or checkpoint activation

As previously described, undamaged cells expressing S538A or S538E mutant PrimPol progressed through the cell cycle normally, with the distribution across the cell cycle appearing unchanged when compared to WT cells (Figure 3.13D). However, cells expressing S538A had a longer doubling time than cells expressing WT protein (Figure 3.13B). We therefore determined if replication stress, in the form of fork stalling induced by camptothecin treatment, led to a greater delay in S phase completion in cells expressing mutant S538 protein. Asynchronous cells were assessed initially, confirming previous observations that S538 mutant PrimPol did not significantly alter cell cycle. FACS analysis and quantification based on EdU and P-H3 labelling determined that the proportion of cells in S phase 4 hours after 10 nM camptothecin treatment increased equally across each cell line. 24 hours of 10 nM camptothecin treatment induced cell accumulation in G2, but no significant difference was seen across cell lines. While 20nM camptothecin induces a full G2 stall as opposed to a partial accumulation; this too appears to be independent of S538 phosphorylation (Figure 3.18B,C).

As camptothecin induces fork stalling in S phase and accumulation of cells in G2, we also measured activation of the intra-S and G2 checkpoints. The intra-S checkpoint is activated as DNA replication forks interact with lesions (as opposed to the presence of lesions alone), and activation leads to slower DNA replication, through the inhibition of origin firing and slowing of active replication forks (Iyer and Rhind, 2017). ATR mediated phosphorylation of S345 of Chk1 relieves inhibition of the protein, rendering it active and inducing S phase arrest (Liu et al., 2000; Zhao and Piwnica-Worms, 2001). At the tested doses of camptothecin in this experiment, we observed neither Chk1 phosphorylation nor S phase arrest. Additionally, we looked at the phosphorylation of Tyr180/Tyr182 of P38, which indicates P38 activation, which has previously been implicated in the activation of the G2/M checkpoint in PrimPol$^{-/-}$ DT40 cells (Bailey et al., 2016). We hypothesised that there may be increased G2 checkpoint activation in cells expressing S538, as this led to improper recruitment of PrimPol in G2. However, we saw no significant difference in the presence of these markers after expression of mutant PrimPol (Figure 3.18D).

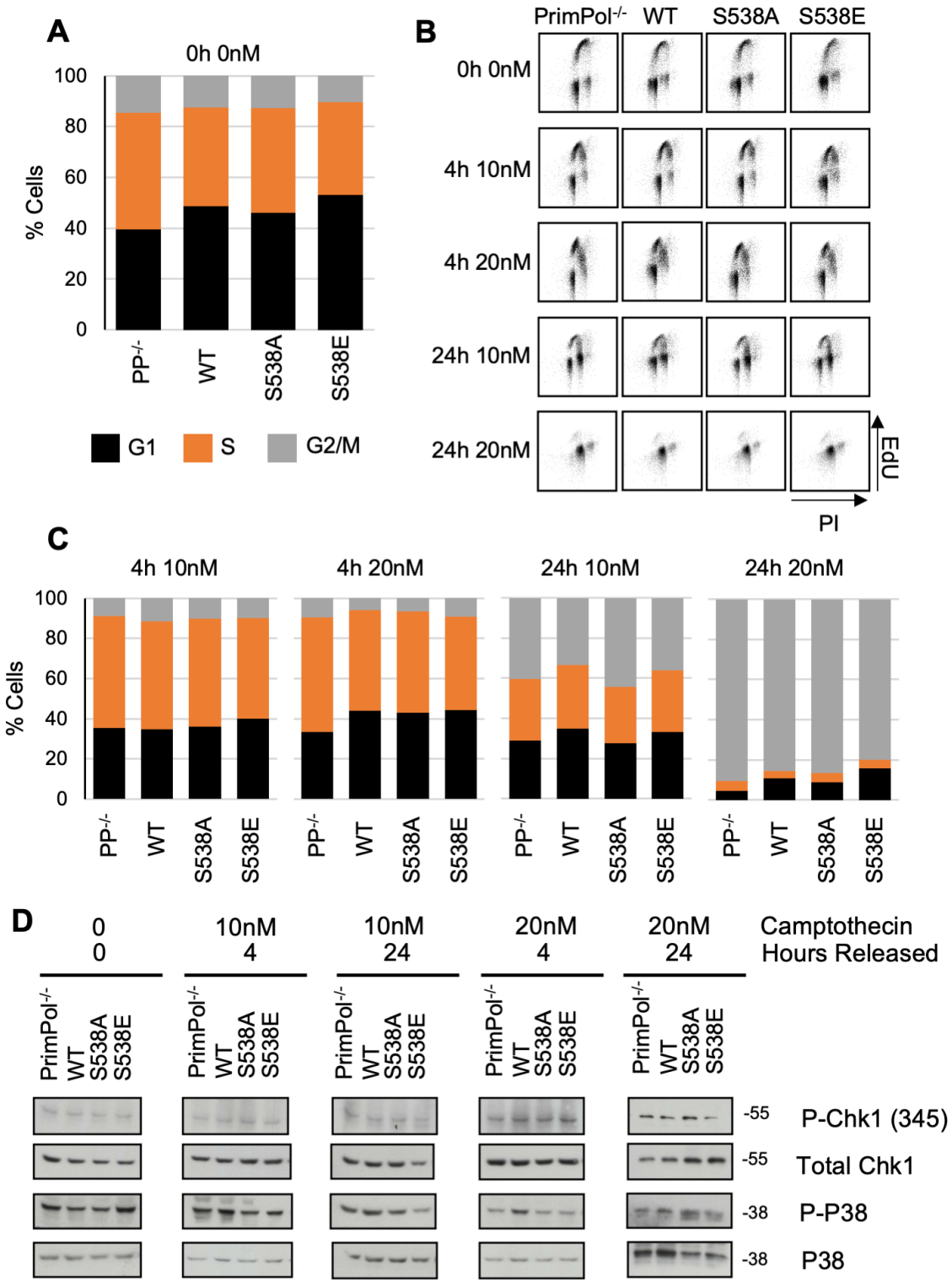

Figure 3.18. PrimPol S538 mutation does not lead to a change in the expression of markers indicative of checkpoint activation or cell cycle stalling

A. Cell cycle profile quantification of asynchronous undamaged cells. **B.** Cells were stained with PI and EdU and cell cycle stage was measured by FACS analysis. **C.** Quantification of cell cycle stage was performed across each condition and cell line. **D.** Western blot analysis of protein harvested from each cell line after treatment with 10/20 nM Camptothecin, and a defined recovery period (4/24 hours). Protein was analysed for phosphorylated S345 of Chk1, phosphorylated T180 and T182 of P38, and total Chk1 and P38 levels to control for loading.

3.6 Key mutations to PrimPol's catalytic domains affect the phenotype of cells expressing PrimPol S538A

The phenotypes observed after mutation of S538 are conditional on expression of the protein, as verified by experiments performed in the presence and absence of doxycycline (Chapter 3.5.5). However, beyond this, it is not clear which activity of PrimPol – its primase activity, its polymerase activity, or potentially, actions independent of activity, such as RPA binding – are required for this toxicity. Separation of the functional domains of PrimPol has been studied extensively by the Doherty lab, and mutations have been utilised to inactivate the catalytic domain (D114A/E116A), the zinc finger primase domain (C419A/H426E) and the RPA binding domain (D519R/F522A in motif A, D551R/I554A in motif B). We therefore utilised these mutations to generate functional mutant cell lines, disrupting PrimPol's ability to bind RPA (RAB), to act as a primase by disrupting the zinc finger domain (ZnKO) and to perform catalytic activity entirely (AxA).

A schematic to describe these mutations is shown in Figure 3.19A. Their ability to perform activity or binding functions is described in Figure 3.19B. These cell lines were generated as before (Chapter 2.4.3.2), and subject to western blot analysis, which determined that disruption of these functions did not totally prevent the phosphorylation of S538 in the WT line (Figure 3.19C). Although not clear from Figure 3.19C, the introduction of the zinc finger mutations did alter the presence of the slower migrating, phosphorylated form of the protein (discussed further in chapter 4), but did not alter S538 phosphorylation.

As phosphorylation is maintained in these cell lines, it suggests that the dynamic regulation performed by phosphorylation/dephosphorylation of S538 is still active, and that this regulation is not dependent on either the catalytic activity of the protein, or the interaction between PrimPol and RPA70. We therefore next assessed whether phenotypes associated with S538 mutation were maintained in the functional mutant cell lines, or if preventing primase/polymerase activity or RPA binding alleviated the phenotypes associated with S538A.

A

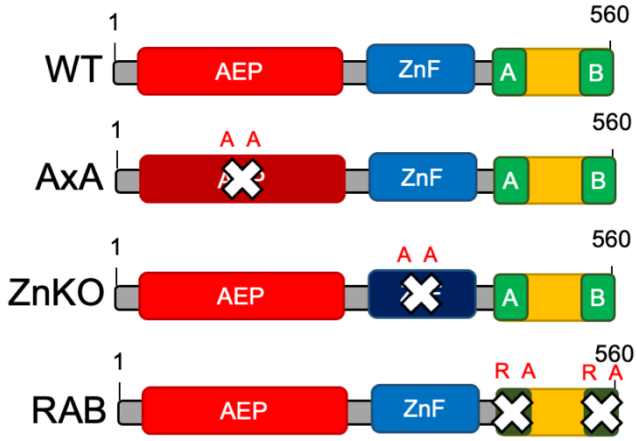

B

Mutant	AxA	ZnKO	RAB
Primase	N	N	Y
Polymerase	N	Y	Y
RPA Binding	Y	Y	N

C

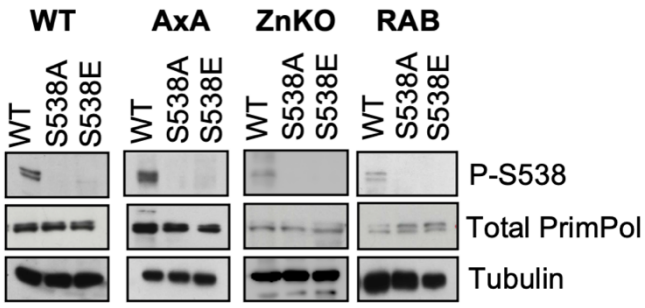

Figure 3.19. Mutation of the functional domains of PrimPol in a S538 mutant background

A. A diagram of the functional domains of PrimPol, showing the AEP domain, the ZnF domain and the RPA binding domain. The AxA (D114A/E116A), ZnKO (C419A/H426E), and RAB (D519R/F522A, D551R/I554A) mutations are shown below. **B.** A table showing the competency of each mutant protein for the key activities of PrimPol. **C.** Western blot analysis of the functional mutant cell lines from WT, S538A and S538E backgrounds. Protein was harvested from these cells and subject to analysis with antibodies to P-S538, total PrimPol and tubulin.

3.6.1 Mutating the RPA binding domains of PrimPol fully rescues the UV sensitivity phenotype of cells expressing S538A

To determine if the toxicity of S538A mutant PrimPol was dependent on chromatin binding, vectors containing wild type, S538A or S538E mutant PrimPol were mutated to RAB, transfected into HEK-293 Flp-In cells, and grown to stable cell lines. These cell lines will be referred to as RAB, RAB 538A and RAB 538E. Protein expression was induced in these cell lines by 10 ng/µl doxycycline, before cells were fractionated into chromatin enriched, soluble or whole cell fractions for chromatin association assay. As seen previously, while protein expression levels were comparable across mutants, and soluble levels of the protein consistent, none of the lines bound to chromatin (Figure 3.20A).

The sensitivity of RAB cells to UV-C was comparable to that of cells expressing wild type protein (Figure 3.20B). While PrimPol protein is expressed and functional in these cells, the prevention of the RPA70 interaction prevents its recruitment to chromatin, effectively rendering the cells unable to reprime. Therefore, as in PrimPol knockout cells, we hypothesise that the minimal sensitivity is due to the utilisation of other DDT methods such as TLS. Rendering PrimPol unable to bind chromatin led to a statistically significant increase in survival after all doses of UV-C damage in the S538A cell line, while cells with intact RPA binding domains showed extensive UV-C sensitivity (Figure 3.20C). There was no change in the survival of S538E cells when the RPA binding domains were mutated (Figure 3.20D).

Similarly, the number of micronuclei in S538A cells after treatment with UV-C damage decreased following the mutation of the RPA binding domains, as seen in Figure 3.20E, and there was a significant decrease in number of chromosome breaks in RAB S538A cells compared to S538A cells (Figure 3.20F). These data suggest that the toxicity of S538A mutant PrimPol is dependent on PrimPol's ability to associate with chromatin.

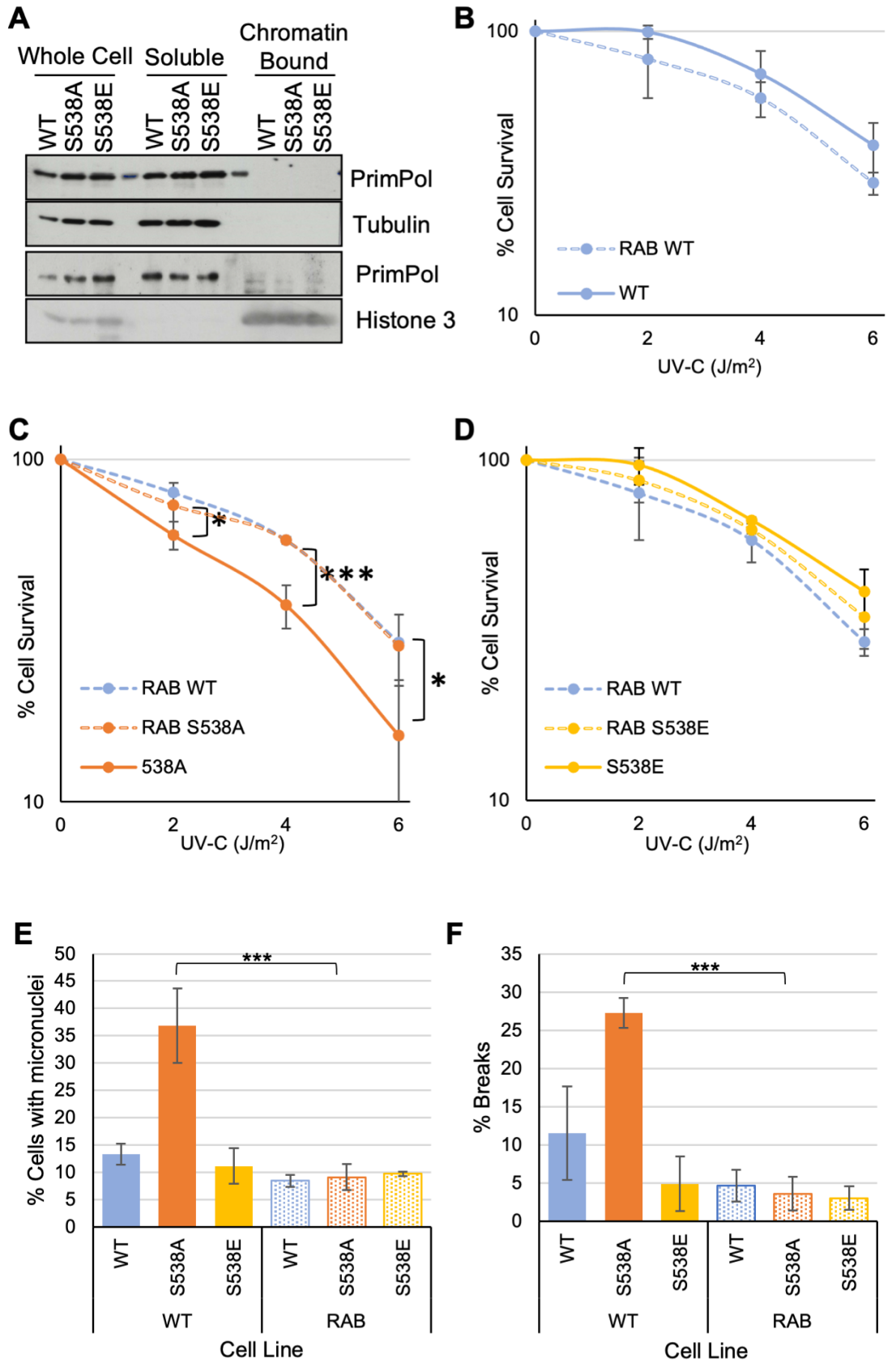

Figure 3.20. Mutation of PrimPol's RPA binding domain disrupts S538A-mediated toxicity

A. Cells expressing RAB, RAB 538A and RAB 538E were fractionated into whole cell, soluble and chromatin bound (insoluble) fractions. Samples were then run on an 8% gel (upper half) and were probed for PrimPol and Tubulin, and on a 15% gel and probed for PrimPol and Histone 3. **B.** Colony survival assays compared the sensitivity of WT and RAB cells to UV-C damage. **C.** Colony survival assays compared the sensitivity of RAB, 538A and RAB 538A cells to UV-C damage. **D.** Colony survival assays compared the sensitivity of RAB, 538E and RAB 538E cells to UV-C damage. **E.** Cells expressing various mutant PrimPol proteins were stained with DAPI 72h after 5 J/m^2 UV-C damage, and number of cells with one or more micronuclei were counted as a percentage of the total cell population. **F.** Cells with one or more chromosome breaks were counted 96 hrs after WT or mutant PrimPol expression was induced by doxycycline.

3.6.2 Mutating the zinc finger domain of PrimPol largely rescues the phenotype of cells expressing S538A mutant PrimPol protein

Mutation of the UL52-like zinc finger domain of PrimPol has previously been shown to prevent the primase activity of the protein. PrimPol's zinc finger is also thought to be important for stabilisation of the incoming nucleotide, primer translocation and extension (Keen et al., 2014b; Martínez-Jiménez et al., 2018). We wanted to examine if loss of PrimPol's primase activity was able to rescue the toxicity of S538A, thereby inferring that the toxicity is dependent on PrimPol's repriming activity. Unlike the AxA mutant, which prevents all catalytic activity of PrimPol, the zinc finger mutations only prevent primase activity, and polymerase activity is maintained (Keen et al., 2014b). It is not known whether the zinc finger mutations, or other mutations for that matter, affect protein stability.

To determine if the S538A phenotypes were rescued by the ablation of primase activity, the zinc finger mutations C419A and H426A were introduced into vectors containing either the normal serine residue, or alanine or glutamic acid substitutions, at 538. These vectors were then stably expressed in HEK-293 PrimPol$^{-/-}$ cells. These lines will subsequently be referred to as ZnKO, ZnKO S538A and ZnKO S538E. There was no change in cell survival after UV-C damage after ZnKO expression compared to WT cells. Interestingly, the sensitivity of cells expressing ZnKO S538A to UV-C was less than cells expressing S538A alone (Figure 3.21A), though survival did not reach the level of cells expressing WT or ZnKO protein. This suggests that the S538A mutation is still having some effect. There was no change in survival in the S538E cell line after the introduction of the ZnKO mutations (data not shown).

Additionally, the statistically significant increase in doubling time in S538A cells was not present in ZnKO S538A cells (Figure 3.21B), suggesting the delay in cell cycle completion was prevented. Similarly, cells expressing ZnKO S538A showed an increase in chromosome breaks, with significantly more breaks than cells expressing ZnKO or WT PrimPol, though fewer breaks than cells expressing S538A (Figure 3.21C). These data suggest that largely, the toxic effect of S538A expression can be rescued by mutations to the zinc finger domain that prevent

repriming, though several genomic instability phenotypes remain in ZnKO S538A cells that are not present when wildtype or ZnKO PrimPol is expressed.

We additionally verified that ZnKO mutant PrimPol was still phosphorylated at S538 in a cell cycle dependent manner by synchronising cells at the G1/S border as before, releasing into S phase, and harvesting every 2 hours for 10 hours (Figure 3.21D). Phosphorylation was detectable at 6 hours, as in cells expressing WT PrimPol. We hypothesised that, separate to its role in repriming, the zinc finger domain may confer stability to PrimPol's interaction with RPA, or its binding to DNA, and therefore the mutations in this domain may lead to weaker binding of PrimPol to DNA or chromatin. We therefore analysed chromatin binding of protein in asynchronous cells through chromatin fractionation and western blot. Having previously shown that WT, S538A and S538E mutant protein all bound chromatin at the same rate in undamaged cells, we found that the ZnKO equivalents also bound chromatin largely similarly compared to cells expressing wildtype protein both before and after UV-C damage (Figure 3.21E). This infers that chromatin binding of PrimPol protein is maintained regardless of that protein's ability to reprime, though the small reduction in binding could contribute to the decrease in phenotype.

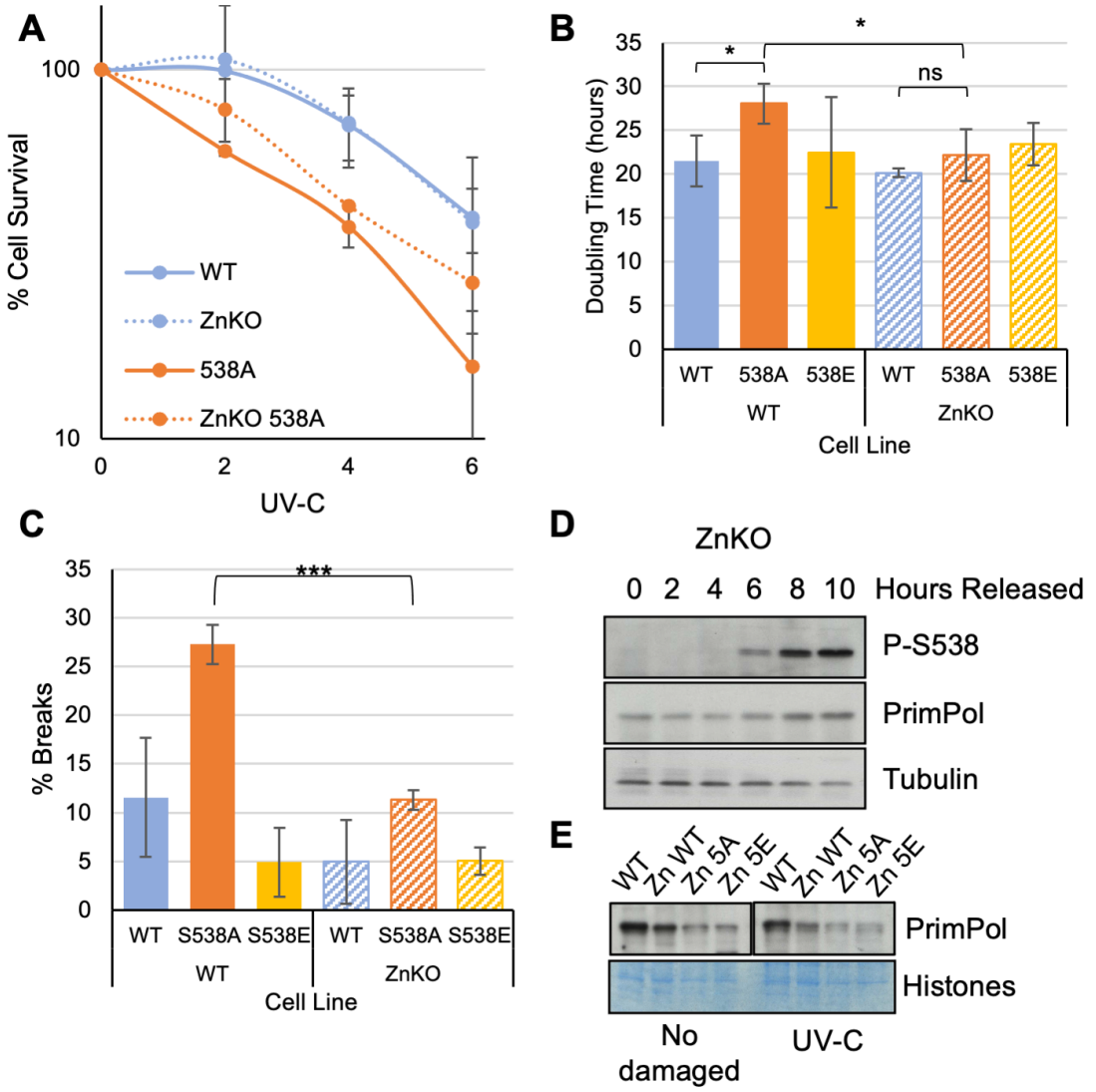

Figure 3.21. Mutation of PrimPol's zinc finger domain partially prevents genomic instability phenotypes associated with S538A expression

A. Colony survival assays compared the sensitivity of WT, ZnKO, 538A and ZnKO 538A cells to UV-C damage. **B.** Doubling time of cells expressing WT, S538A, S538E, ZnKO, ZnKO 538A or ZnKO 538E mutant PrimPol. **C.** Cells with one or more chromosome breaks were counted 96 hrs after WT or mutant PrimPol expression. **D.** Western blot assay of S538 phosphorylation in cells expressing ZnKO protein. Protein was probed for P-S538, total PrimPol and tubulin. **E.** Chromatin fractionation of WT, ZnKO, ZnKO 538A or ZnKO 538E cells was performed before and after UV damage, and the insoluble fraction probed for total PrimPol binding. InstantBlue stained histones provided as control.

3.6.3 Mutating metal binding residues in PrimPol's catalytic domain reduces survival and induces genomic instability

Mutation of the conserved active site metal binding residues D114 and E116, which form PrimPol's DxE motif, ablated both primase and polymerase activity in previous studies (Bianchi et al., 2013; García-Gómez et al., 2013). These mutations (hereafter referred to as AxA mutations) were performed on WT, S538A or S538E mutant PrimPol constructs and expressed in HEK-293 Flp-In cells. These lines are further referred to as AxA, AxA S538A, and AxA S538E.

As before, we tested the sensitivity of AxA, AxA S538A, and AxA S538E cells to UV-C damage. However, in this instance, we found that the AxA mutations did not rescue toxicity from S538A, and in fact made cells significantly more sensitive to UV-C than either AxA or S538A alone (Figure 3.22A). Furthermore, cells expressing AxA protein were found to be more sensitive than cells expressing WT PrimPol, indicating that expression of mutant PrimPol that is unable to perform catalytic activity, but is still able to bind RPA, leads to poor recovery from UV damage. This is interesting and unexpected, as mutation of the zinc finger domain to abrogate primase activity did not induce this effect.

Additionally, we assessed whether the AxA mutations in the S538A mutant background alleviated the genomic instability phenotypes in S538A cells, such as chromosome breaks. Figure 3.22B shows that in cells expressing S538A, there is greater incidence of chromosome breaks, and this is not rescued by the AxA mutation. Similarly, the decrease in plating efficiency seen when S538A protein expression is induced in cells, while rescued by the ZnKO mutations, was not rescued by the AxA mutations (Figure 3.22C). Instead, cells once again appeared more sensitive to AxA S538A than AxA or S538A alone.

The phenotype associated with the AxA mutations, along with the inability to rescue the S538A phenotype, was unexpected. Understanding what causes these phenotypes required significantly more investigation than could be undertaken during this project. For this reason, the AxA phenotype and its relationship to PrimPol's regulation through phosphorylation was not examined further.

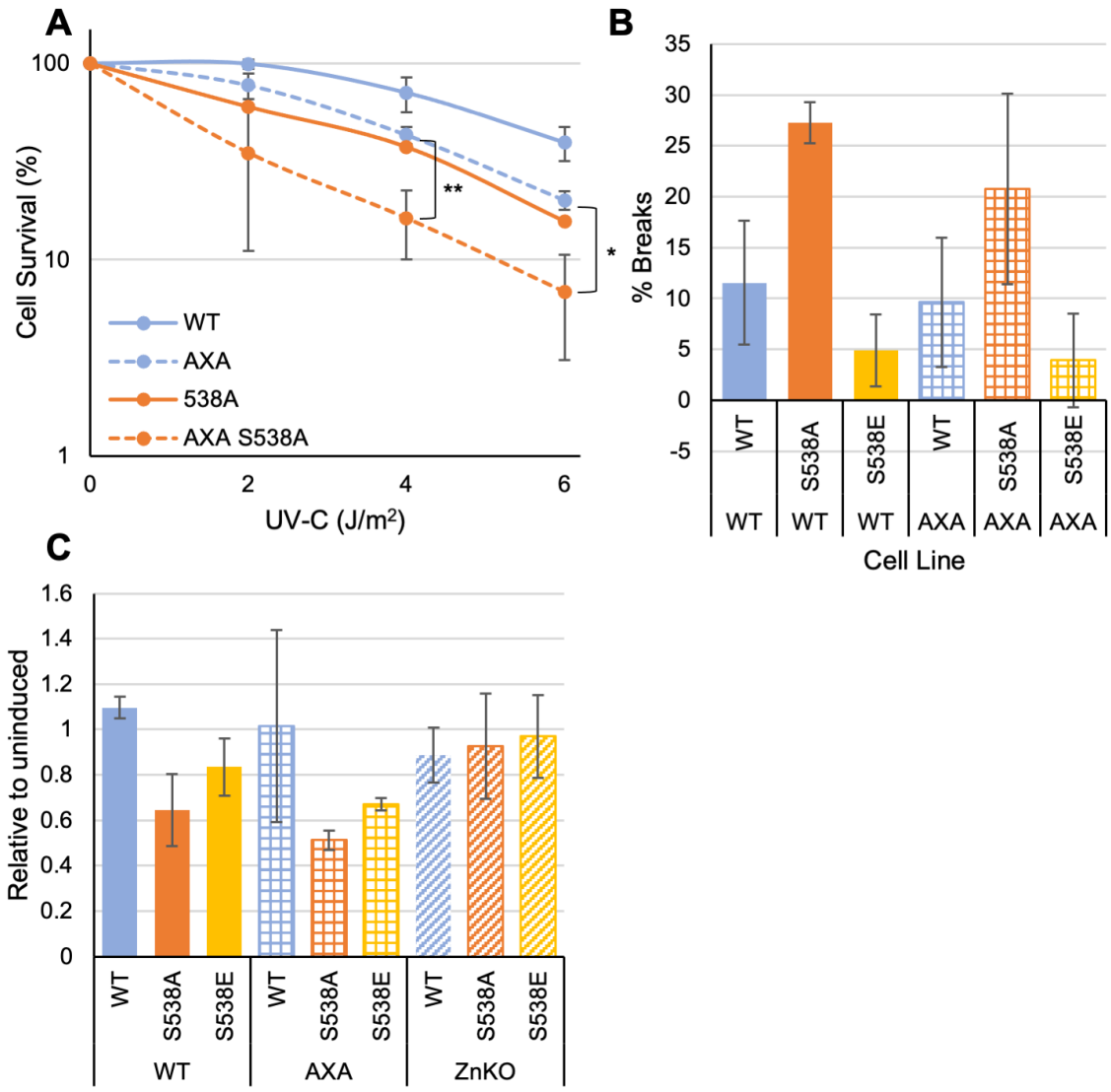

Figure 3.22. Mutation of the catalytic domain of PrimPol does not rescue the decreased cell survival, increased chromosome breaks or plating deficiency associated with S538A expression

A. Colony survival assays compared the sensitivity of WT, AxA, 538A and AxA 538A cells to UV-C damage (n=3). Significance is shown between S538A and AxA S538A. **B.** Cells with one or more chromosome breaks were counted 96 hrs after WT or mutant PrimPol expression (3 biological repeats, n>400). **C.** Plating efficiency of WT, S538A and S538E cell lines compared to AxA, AxA 538A and AxA 538E, and ZnKO, ZnKO 538A and ZnKO 538E (n=3).

3.7 Phenotypes of MRC-5 cells expressing S538 mutant PrimPol

Prior to utilising the HEK-293 T-REx system to allow for inducible expression of mutant PrimPol, we transfected MRC-5 PrimPol$^{-/-}$ cells with GFP-tagged PrimPol constructs containing either WT PrimPol, or S538A or S538E mutant PrimPol. PrimPol tagged with GFP was previously studied and determined to be functional and utilised as normal (Bailey et al., 2019) We also introduced the mutations described in 3.6, namely the AxA, ZnKO and RAB mutants.

Phenotypes of these cells differed from those seen in HEK-293 cells. While expression of S538A did induce phenotypes indicative of genomic instability, including reduced survival after UV-C damage and micronuclei (Figure 3.23A,B), S538E was the more toxic mutation. Specifically, PrimPol$^{-/-}$ cells expressing GFP-tagged PrimPol S538E could not survive under selection, in the absence of damage, for more than 10 days before failing to replicate and dying (Figure 3.24C). The death of these cells could be rescued by addition of the primase-deficient ZnKO mutants, or by mutating the RPA binding domains of S538E mutant PrimPol, rendering it unable to associate with chromatin. However, as with S538A expression in the HEK-293 cells, mutation of the AxA domain did not prevent cell death. The cell death phenotype was not plasmid-specific, as the same GFP-PrimPol S538E plasmid could be expressed in HEK-293 (Figure 3.24C, last row) U2OS or RPE-1 cells (data not shown) with no effect. The specific cause for such serious toxicity in MRC-5 cells is unclear, though the consistency between which mutations to the catalytic domains of PrimPol are able to rescue S538A toxicity in HEK-293 cells and S538E toxicity suggests they may exert their effect in the same way.

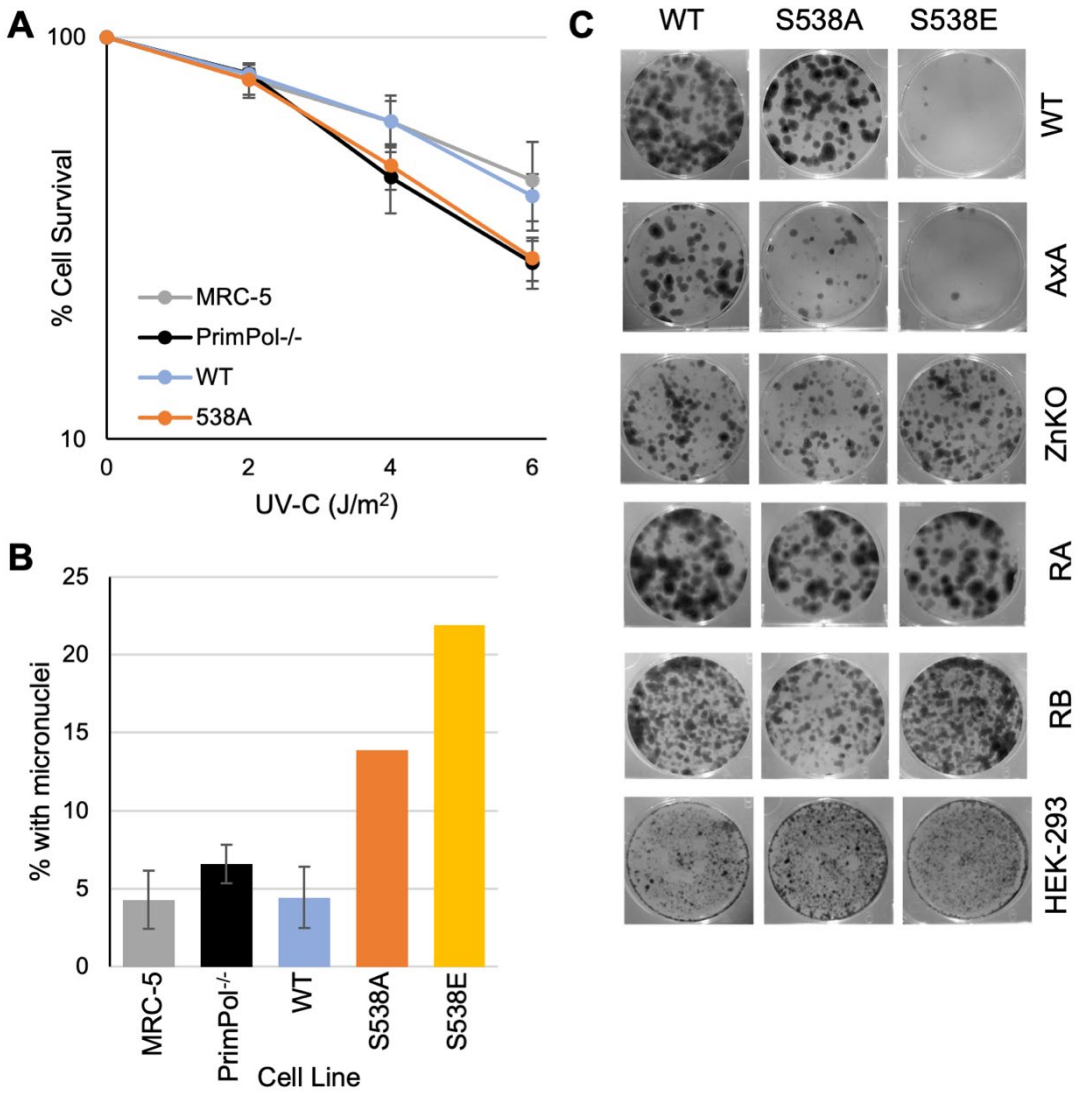

Figure 3.23. Phenotypes of PrimPol S538 mutation found in HEK-293 cells can be partially reproduced in MRC-5 cells

A. Colony survival of MRC-5 parental cells, or PrimPol$^{-/-}$ cells, or PrimPol$^{-/-}$ cells expressing GFP tagged WT or S538A mutant PrimPol After increasing doses of UV damage. **B.** Cells expressing various mutant PrimPol proteins were stained with DAPI 72h after 5 J/m^2 UV-C damage, and number of cells with one or more micronuclei were counted as a percentage of the total cell population. For MRC-5, PrimPol$^{-/-}$ and WT, 3 repeats were performed (n>400). For S538A and S538E, two repeats were performed (n>400). **C.** Colony formation of undamaged MRC-5 PrimPol$^{-/-}$ cells expressing WT, S538A or S538E PrimPol alone, or in addition to AxA, ZnKO, RA or RB mutations. The WT vectors were also transfected into HEK-293 cells as a control.

3.8 Discussion and future work

This chapter focuses on the role of S538 phosphorylation in regulating PrimPol's activity within the cell. S538 phosphorylation was found to change across the cell cycle: phosphorylation levels are high when are in G2 and mitosis, with levels decreasing as cells proceed through G1 into early S phase. Phosphorylation is entirely absent in mid/late G1, and this persists if cells are stalled at the G1/S boundary. Phosphorylation of S538 increases as cells progress into late S phase. The phosphorylation of S538 is dependent on the mitotic kinase PLK1, working in tandem with one or more unidentified phosphatases. S538 phosphorylation in late S phase can be delayed by the application of damaging agents, or reversed if phosphorylation has already occurred. Prevention of this phosphorylation by mutating S538 to alanine prevents proper regulation of PrimPol's chromatin binding, allowing PrimPol to bind to chromatin in G2 after UV-C damage. In turn, loss of phosphorylation causes phenotypes associated with genomic instability, including micronuclei and chromosome breaks, as well as sensitivity to DNA damaging agents like UV-C and replication stress inducing agents such as olaparib and camptothecin. Many, but not all, phenotypes associated with S538A mutation are suppressed by the mutation of the zinc finger domain, which prevents priming, and fully abolished by the mutation of the RPA binding domain, preventing chromatin association. However, they are not alleviated by the mutation of the AEP catalytic domain.

3.8.1 PrimPol S538 phosphorylation across the cell cycle

This work follows a previous study which showed that PrimPol's association with chromatin changes across the cell cycle. However, it is the first to indicate how this may take place. Phosphorylation by PLK1, a kinase expressed in high amounts in G2/M, is one half of this regulation. However, as cell cycle regulation appears to respond to DNA damage signals or replication stress and leading to dephosphorylation, a phosphatase is also implicated in this regulation. These data support a model whereby PrimPol usage at stalled replication forks is dynamically regulated by both phosphorylation and dephosphorylation.

The role of PLK1 as a highly conserved regulator of mitosis is well established (Barr et al., 2004). Outside of mitosis, PLK1 has been suggested to play a role in S phase, though recent evidence suggests that DNA replication itself suppresses PLK1 activity and PLK1 levels do not increase until the bulk of DNA synthesis is complete (Barr et al., 2004; Lemmens et al., 2018; Mandal and Strebhardt, 2013).

As the pattern of S538 phosphorylation closely aligns with PLK1's activity, we hypothesise that phosphorylation at the end of S phase may operate to keep PrimPol away from replication of common fragile sites and other repetitive elements, which are replicated in late S (Li and Wu, 2020). Following a similar pattern, PLK1 has also been shown to phosphorylate BRCA2 as cells complete S phase, with phosphorylation levels peaking during mitosis (Lee et al., 2004). As with PrimPol, the cell cycle-dependent phosphorylation of BRCA2 can be suppressed by the application of DNA damaging agents.

It is clear that the cell's requirements for PrimPol are likely to significantly change throughout the cell cycle. Loss of regulation could lead to inappropriate usage of PrimPol outside of S phase. Cell cycle-dependent phosphorylation provides an innate regulatory mechanism whereby proteins can be dynamically and reversibly regulated, without the need to be degraded and resynthesised.

Experiments examining the cell cycle distribution of PrimPol S538 phosphorylation invariably used thymidine, a nucleotide analogue, to synchronise cells to specific stages of the cell cycle (Chen and Deng, 2018). High concentrations of thymidine blocks DNA replication and could therefore induce replication stress. Data from these experiments show that S538 phosphorylation is low in mid/late-G1 and early/mid-S phase, timepoints correlating with stalling by thymidine. It therefore is important to note that the decreases in phosphorylation seen throughout the cell cycle highly correlate with the onset of stalling, and therefore potential replication stress, induced by thymidine application, and it is not impossible that the two are connected. Future experiments could utilise different synchronisation drugs, such as palbociclib, or sorting by FACS to obtain clean G1 and S populations from asynchronous populations, to verify cell cycle changes in PrimPol S538 phosphorylation.

3.8.2 Chromatin binding and the phosphorylation of PrimPol at S538

As PrimPol's primary mode of activity *in vivo* is repriming, it is clear why its action is largely restricted to S phase. While it can bind to chromatin in both G1 and S (Mourón et al., 2013), it is unclear what role, if any, PrimPol plays in G1, and the purpose of its chromatin association in this stage is unknown. PrimPol is excluded from chromatin in G2. However, we found that S538A mutant PrimPol protein is recruited to chromatin after cells are damaged by UV-C. It is possible that binding also occurs in undamaged conditions but at low levels, given the very small amount of ssDNA generated in undamaged conditions in G2, leading to minimal RPA recruitment and low levels of substrate for PrimPol binding.

While it is unclear precisely what PrimPol is directly responding to in G2 after UV damage, it is possible that repair through NER, particularly of lesions close together, generates sufficient ssDNA intermediates of NER after UV-C damage (Giannattasio et al., 2010; Ma et al., 2013). Additionally, given that replication does continue to some extent during G2, it could be responding to stalled replication forks generated in greater numbers after significant UV-C damage, as observed for BRCA1 (Pathania et al., 2011). Without any indication so far that PrimPol can act as a TLS polymerase, we discount that this is related to its recruitment in G2. We hypothesise that the phosphorylation of S538 may regulate PrimPol's association with RPA, chromatin or ssDNA. Given that genomic instability phenotypes induced by S538A expression are dependent on RPA binding, we hypothesise this is likely to be due to the aberrant recruitment of S538A protein to chromatin. Whether this aberrant binding can be mimicked using PLK1 inhibitors to prevent phosphorylation of S538 remains to be established but is a vital future experiment.

3.8.3 Mutating PrimPol's key domains, and its effect on the S538A phenotype

It is unsurprising that preventing PrimPol's association with RPA, in turn preventing PrimPol's binding to chromatin, prevented S538A's toxicity. If the toxicity of S538A was dependent on recruitment or repriming in the incorrect cell cycle stage, both are ablated by mutation of the RPA binding domains. However,

this is complicated by the fact that, while RPA interaction is clearly key for the toxicity of S538A, S538A protein interacts with RPA identically (Bailey *et al.,* 2021, Appendix B). It's likely that the cellular environment is significantly more complex than an *in vitro* experiment can model, and therefore there may be a yet unidentified factor influencing PrimPol's recruitment and binding to RPA bound ssDNA.

Primase-deficient PrimPol (ZnKO) can still be recruited to chromatin but cannot initiate *de novo* primer synthesis. However, it retains polymerase activity and can extend existing primers, though it is uncertain whether it would be recruited to do this. The partial rescue of the S538A phenotype by the zinc finger mutations, therefore, suggests that an aspect of S538A's toxicity is due to the primase activity of PrimPol. However, the zinc finger mutations may have other effects on the stability, recruitment or interactions of the protein that are as yet unknown.

While some genotoxicity was lost by the mutation of the zinc finger domain - these cells showed increased survival after genotoxic stress and decreased chromosome breaks - cells expressing ZnKO S538A are still more damage sensitive than ZnKO alone. This aligns with observations from other *in vivo* complementation studies, where it has been found that many phenotypes observed upon PrimPol depletion are not complemented by ZnKO PrimPol (Keen et al., 2014b; Kobayashi et al., 2016; Mourón et al., 2013). Interestingly, chromatin recruitment of ZnKO protein is largely similar to that of WT protein, though expression of all ZnKO mutant protein is lower generally and there is a small decrease in binding that is maintained after UV-C damage.

If the phenotypes associated with S538A expression are due to repriming, the aberrant recruitment of ZnKO S538A protein will not generate gaps in need of repair or reprime in improper places, but its recruitment to chromatin in G2 may block alternative mechanisms of DDT or repair and delay fork restart. Conclusive evidence of increased repriming in cells expressing S538A is required to solidify this model. It is also possible that the zinc finger mutations alter protein stability; this is supported by the decrease in protein expression, decreased chromatin binding and the absence of at least one phosphorylated isoform, and suggests a model where repriming is not the primary conveyor of S538A toxicity.

3.8.4 Future work

3.8.4.1 Replication stress and DNA damage levels

When cells were treated with camptothecin or olaparib, or UV-C damage, the cell cycle phosphorylation of S538 was delayed or reversed. However, while the role of PrimPol in DNA damage tolerance after UV damage is well studied (Bailey et al., 2019; Bailey et al., 2016; Bianchi et al., 2013; Keen et al., 2014b; Kobayashi et al., 2016), it is not clear what role PrimPol plays in recovery from Olaparib or Camptothecin induced replication stress, though recent work has highlighted a role for PrimPol in recovery from Olaparib induced stalling in the absence of proteins important for fork reversal (Genois et al., 2021). Experiments to determine what role PrimPol plays after these treatments are vital for our understanding of stress and damage tolerance during DNA replication. Additional microscopy experiments, including super-resolution experiments, may yield interesting results regarding foci formation during S phase. Additionally, while previous data strongly implies a specific role for PrimPol at stalled replication forks, additional work utilising other methods such as iPond could elucidate the specific dynamics of PrimPol recruitment to stalled or collapsed forks.

3.8.4.2 Expanding on PrimPol's effect in G2

We suggest in this chapter that the cause of the S538A induced toxicity is the aberrant recruitment of PrimPol to chromatin in G2. Additional work (Bailey et al., 2021, Appendix B) shows that this is concurrent with an increase in RPA foci in G2, suggesting an increase in ssDNA gaps indicative of increased repriming outside of S phase. However, conclusive evidence of increased repriming is required to solidify this conclusion. To show the ssDNA, a BrdU incorporation assay could be used on both undamaged and damaged cells on G2 cells to detect ssDNA.

3.8.4.3 The catalytic domain of PrimPol and its effect on S538A induced toxicity

An interesting discovery in the course of this work was the effect of expression of PrimPol containing the AxA mutations. These mutations render the protein unable to polymerise or prime, but still capable of binding RPA. The expression of this protein induced sensitivity to UV-C and did not rescue the phenotypes

associated with S538. Additionally, phenotypes associated with AxA protein appeared to be additive to phenotypes associated with S538A protein. A full examination was beyond the scope of this project, but this discovery does raise interesting questions. How does catalytically inactive PrimPol interact with stalled replication forks? How quickly is this protein removed from the fork, in order to allow a competent pathway to take over? Utilising chromatin fractionation to determine if catalytically inactive PrimPol is recruited to stalled forks, and how quickly this protein is able to dissociation upon failing to reprime, would be easy initial experiments, followed potentially by the addition of the AxA mutation to the RPA binding knockout background, to determine that association with RPA is also required for the toxicity of AxA PrimPol. It's tempting to speculate that part of AxA's phenotype hinges on its binding to chromatin – potentially, AxA PrimPol is recruited to the stalled fork, engages a dNTP for the repriming reaction, and then fails to perform catalysis, but remains associated with the DNA template, thereby preventing the recruitment of alternative factors, such as TLS polymerases. This, in turn, may exasperate the phenotype of cells expressing S538A, as PrimPol is now both incorrectly recruited to chromatin outside of S phase, and remaining associated with DNA for longer. Assessing whether AxA mutant cells accumulate markers of increased fork collapse may indicate that this occurs.

3.8.5 Model of the toxicity of PrimPol S538 mutation

In summary, this study establishes that PLK1-dependent phosphorylation of PrimPol prevents aberrant recruitment and repriming that could otherwise lead to genomic instability. Our data highlights the importance of appropriately regulating PrimPol's recruitment following DNA damage, and throughout the cell cycle. While this study identifies that PrimPol is specifically regulated by PLK1, it is likely that additional mechanisms also regulate PrimPol, and other DDT pathways, to ensure that cells respond appropriately in the immediate aftermath of replication stress. The discovery of PLK1's role in regulating PrimPol's deployment underscores other important functions this major cell cycle kinase undertakes outside of mitosis, emphasising its status as a key regulator of genome stability.

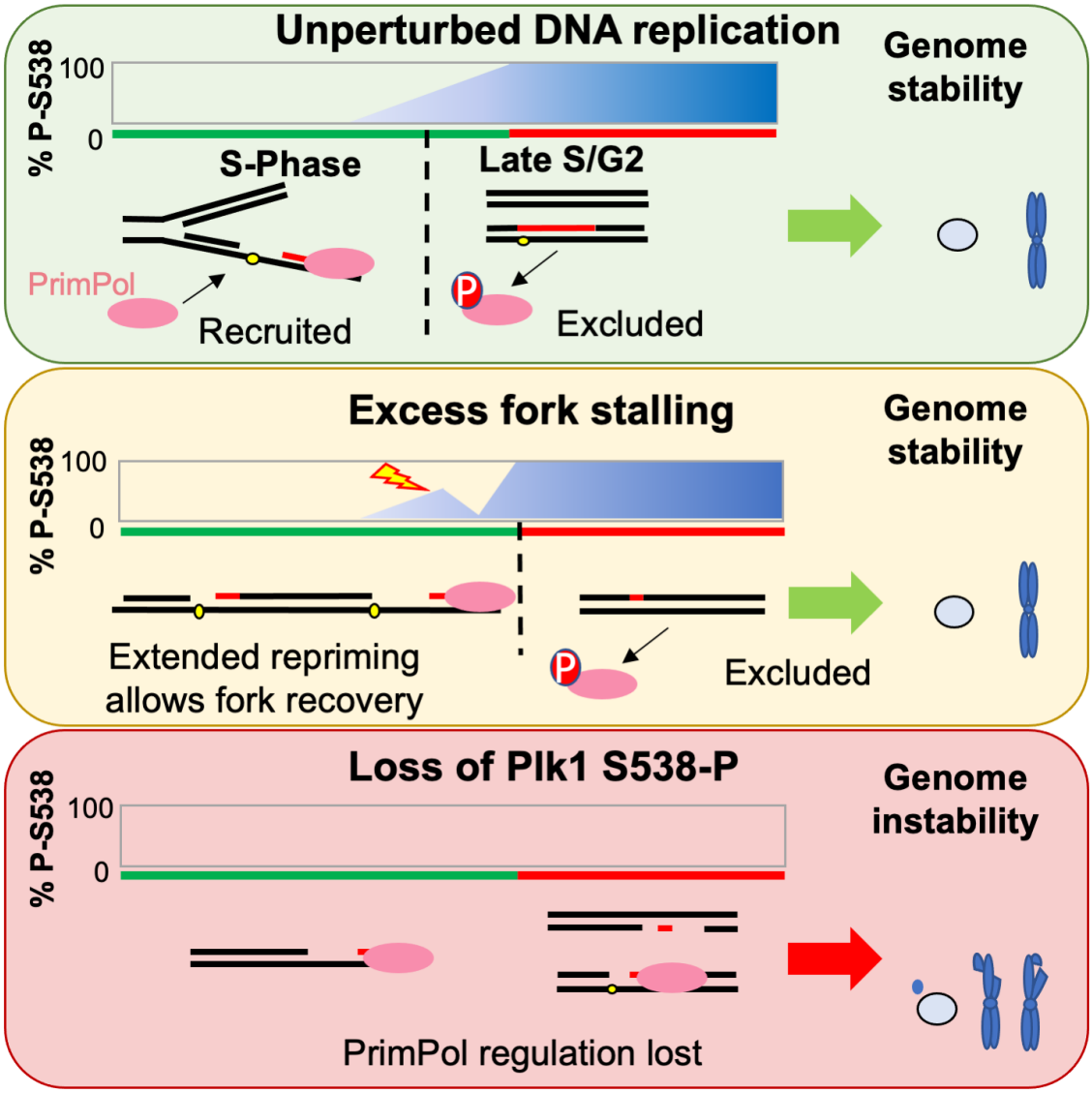

Figure 3.24. Model of PrimPol regulation by S538 phosphorylation and impact on genome stability

Model showing the role of S538 phosphorylation in the regulation of PrimPol throughout the cell cycle and in response to fork stalling damage.

Chapter 4
Investigation into the role and regulation of S499 phosphorylation

4.1 Introduction

The study of PrimPol, by the Doherty group and others, has shown that a major role for PrimPol in human cells is to overcome replication obstacles by restarting stalled replication forks through repriming DNA synthesis. *In vitro,* PrimPol also has the capacity to act as a TLS polymerase opposite certain lesions. However, very little is known about the regulation of PrimPol, either in its capacity as a repriming enzyme or as a TLS polymerase. There is no crystal structure of full-length PrimPol in a primase-proficient configuration, and it is not clear which modifications, if any, support primase-active PrimPol *in vivo*.

In addition to S538, PrimPol has been previously shown to be phosphorylated at other serine residues, including S499 and S501. Phosphorylation of these sites has been suggested to lead to an electrophoretic shift in the protein, generating the distinct double band presentation of PrimPol protein on low percentage SDS-PAGE (L. Bailey, S. Rudd, A. Doherty, unpublished data). This chapter describes investigation of the role of S499 phosphorylation, and its regulation.

4.2 The phosphorylation state of PrimPol in human cells

4.2.1 2D Gel analysis of charged isoforms of PrimPol

Initial investigation into the post-translational modifications of PrimPol was performed by two-dimensional (2D) gel electrophoresis. This separates proteins by charge in one dimension, before separating them again based on their molecular weight. HEK-293 cells expressing WT PrimPol were grown in culture in the presence of doxycycline to induce protein expression. Cells were then harvested and lysed to obtain protein before analysis by 2D electrophoresis. The gel was transferred onto a membrane and blotted with anti-PrimPol antibody, to reveal several specific dots at the size and expected isoelectric point (pI) of PrimPol. Four species were revealed in total, likely representing multiple modified isoforms of PrimPol (Figure 4.1A). After treatment with λ phosphatase, all but one of these isoforms were absent, though at least one charged isoform of PrimPol was maintained, indicating this was conferred by another modification, such as ubiquitination. These data suggest that PrimPol is significantly modified by multiple phosphorylations, and that these modifications accumulate.

Interestingly, mutation of S538 (Chapter 3) did not lead to a reduction in the number of detectable isoforms, suggesting that modification of other sites is maintained in the absence of S538 phosphorylation.

4.2.2 Phosphorylation of PrimPol at S499 induces a mobility shift

After determining that PrimPol exists in several charged isoforms within cells, including phosphorylated isoforms, we set out to determine which phosphorylation site led to the two species of PrimPol observed on 1D western blots (Figure 4.1B) When separated on a low percentage gel, PrimPol migrates as two distinct bands – this is maintained when PrimPol is expressed in both endogenous levels, and exogenously overexpressed (Bianchi et al., 2013). Previous work had suggested that the upper band represents protein which is shifted by phosphorylation; we verified this by treating protein from HEK-293 cells overexpressing PrimPol with λ phosphatase. This treatment led to the absence of the upper band of PrimPol, suggesting this band is dependent on phosphorylation. Mass spectrometry analysis had previously identified multiple phosphorylation sites on PrimPol, including S499, S501 and S504 (P. Kolesar and A. Doherty, unpublished work). These sites are found on the C-terminus of PrimPol, just prior to the CTD and the first RPA binding motif (Figure 4.1C). S499, one site of interest, was found to be conserved across species (Figure 4.1D). Mutation of these sites on PrimPol protein determined that S499 mutation prevented the formation of the upper, phosphorylated band of PrimPol (Figure 4.1B, lower panel).

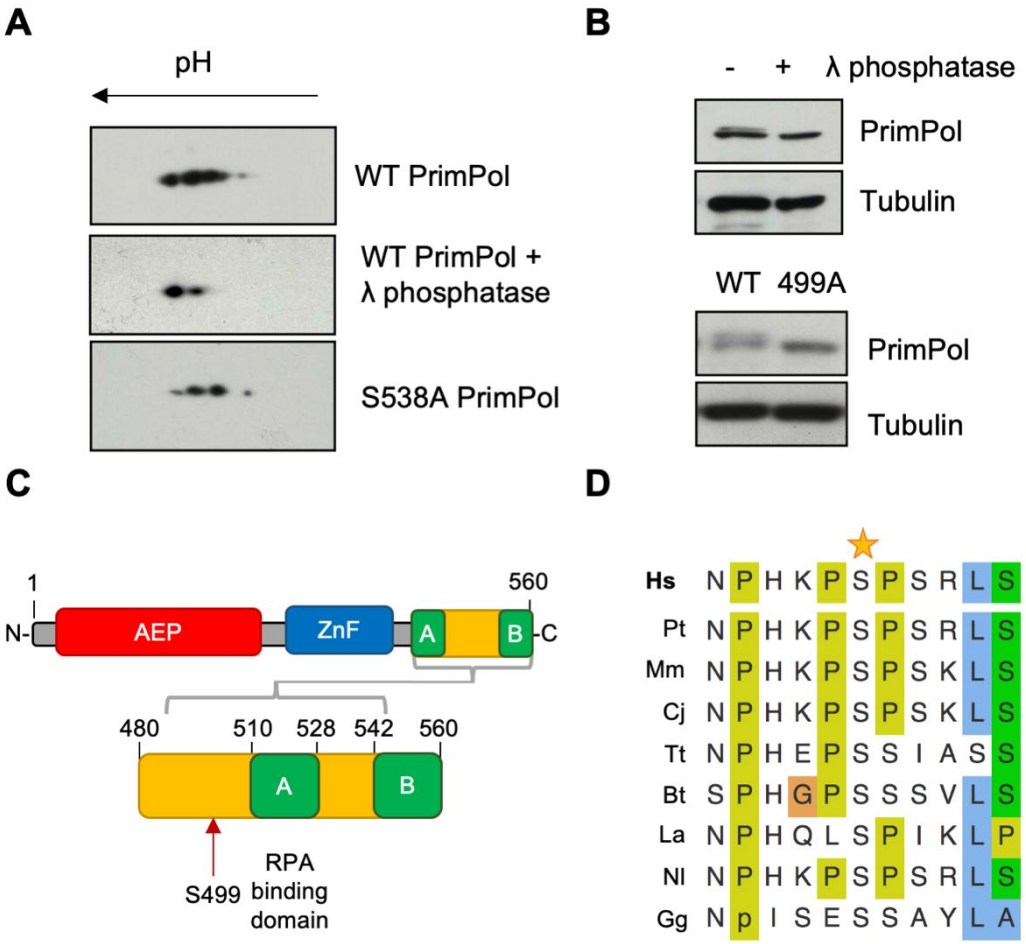

Figure 4.1. Multiple charged isoforms of PrimPol are found within cells, including isoforms dependent on S499 phosphorylation

A. WT or S538A PrimPol was analysed by 2D-Gel electrophoresis to identify the charged isoforms of human PrimPol. Protein treated with λ phosphatase enzyme showed several fewer isoforms. **B.** SDS-PAGE gel of PrimPol protein harvested from HEK-293 cells overexpressing WT PrimPol mock or phosphatase treated with 400U λ phosphatase, and overexpressing WT or S499A mutant PrimPol. Proteins were probed with antibodies for PrimPol and tubulin. **C.** Schematic outlining the location of S499 relative to the key domains of PrimPol. **D.** Amino acid alignment of residues 494-504 across multiple species of PrimPol. *Hs, Homo sapiens (human); Pt, Pan troglodytes (chimpanzee); Mm, Macaca mulatta (Rhesus macaque); Cj, Callithrix jacchus (common marmoset); Tt, Tursiops*

truncatus (Atlantic bottle-nosed dolphin); Bt, Bos taurus (cow); *La, Loxodonta africana (African bush elephant); Nl, Nomascus leucogenys (Northern white cheeked gibbon); Gg, Gallus gallus (chicken);* Yellow star highlights S499.

4.3 Cellular phenotypes of MRC-5 PrimPol$^{-/-}$ cells expressing phospho-micic and phospho-null mutant S499

4.3.1 Expression of S499 mutant PrimPol protein

Initial characterisation experiments were performed using MRC-5 PrimPol$^{-/-}$ cells transfected with constitutively expressed GFP-tagged WT, S499A or S499E PrimPol. Analysis was initially performed in these cells as phenotypes of MRC-5 PrimPol$^{-/-}$ cells are well characterised (Bailey et al., 2019). MRC-5 PrimPol$^{-/-}$ cells expressing WT PrimPol and the phospho-mutant PrimPol protein were harvested and subject to western blot analysis to confirm consistent protein levels. Overall, expression levels of the mutant proteins were consistent with wild type expression levels (Figure 4.2A). We additionally verified GFP signal was consistent across cell lines using FACS analysis, which also confirmed that cells did not accumulate in any cell cycle stage (Figure 4.2B). However, cells expressing S499E mutant protein completed the cell cycle faster on average than cells expressing WT or S499A protein (Figure 4.2D).

4.3.2 MRC-5 cells expressing S499 mutant protein have increased micronuclei

Cells were also tested for markers of genotoxic stress. When PrimPol is absent from MRC-5 cells, a small increase in micronuclei is observed, which is complemented by the expression of WT PrimPol (Bailey et al., 2019, Figure 4.2C). S499A or S499E mutant protein does not complement, instead inducing a further increase in cells with one or more micronuclei (Figure 4.2C). Additionally, after 5J/m^2 UV-C damage, cells expressing S499A or S499E mutant PrimPol show a significantly greater increase in cells with micronuclei than cells expressing wild type protein (Figure 4.3B).

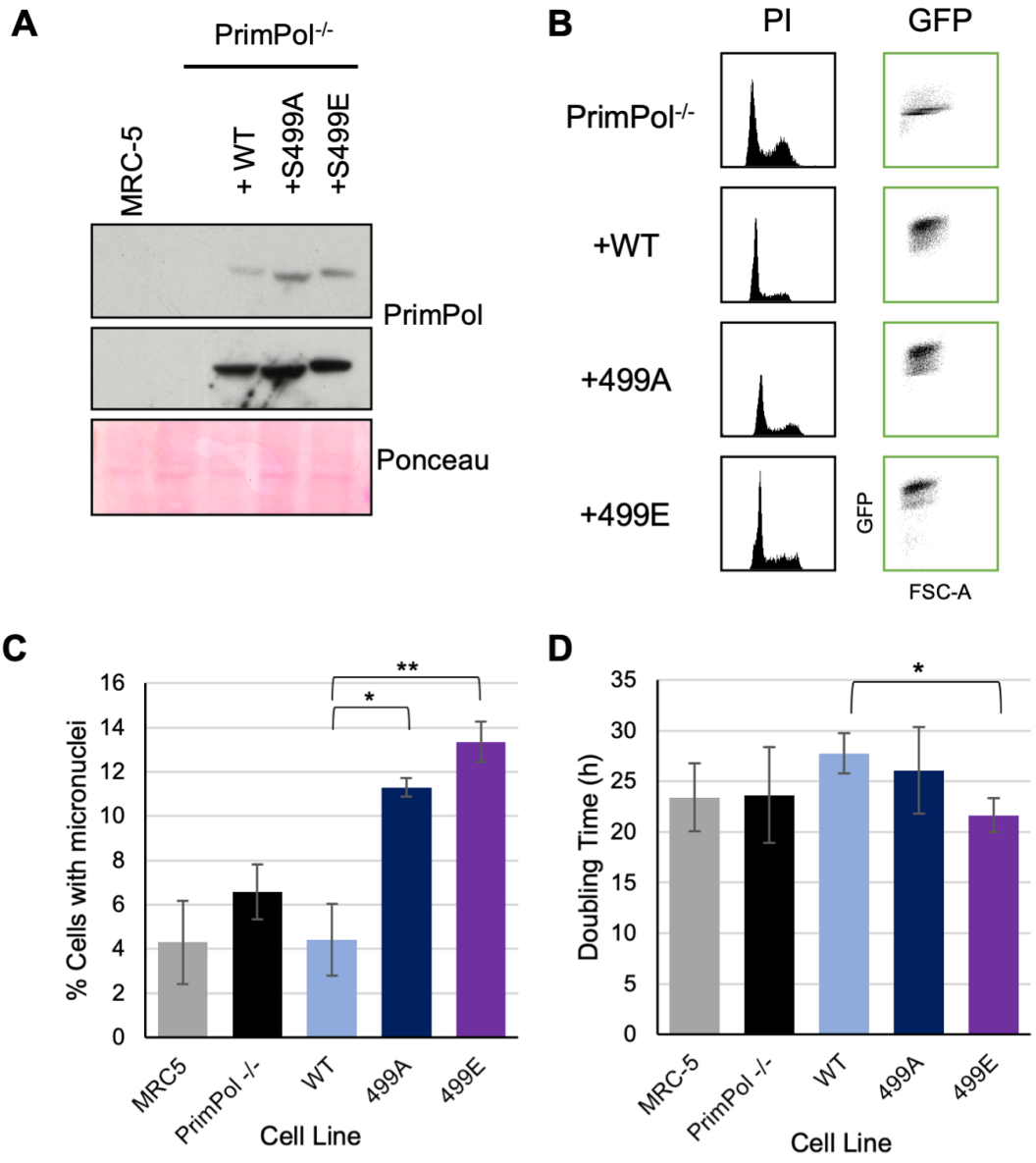

Figure 4.2. MRC-5 PrimPol$^{-/-}$ cells expressing GFP-tagged S499 mutant PrimPol protein have increased micronuclei

A. Western blot analysis of protein from MRC-5 PrimPol$^{-/-}$ cells expressing GFP-tagged WT, S499A or S499E mutant PrimPol. Ponceau stained membrane provided as a loading control. **B.** FACS analysis of MRC-5 PrimPol knockout cells, or PrimPol$^{-/-}$ cells expressing GFP-tagged WT, S499A or S499E mutant PrimPol. Gates were applied to measure GFP fluorescence (FL1-A/FSC-A) and cells were stained with PI to determine DNA content. **C.** MRC-5 cells with 1 or more micronuclei were counted 72 hours after plating. **D.** Doubling time of MRC-5 PrimPol$^{-/-}$ cells expressing GFP-tagged WT, S499A or S499E PrimPol (n=3).

4.3.3 MRC-5 cells expressing S499E mutant PrimPol protein are sensitive to UV-C

PrimPol has previously been shown to play a role in UV-C induced lesion bypass (Bianchi et al., 2013; García-Gómez et al., 2013). To assess for the mutant protein's proficiency in overcoming UV-C damage, we monitored the cells in a clonogenic survival assay after increasing doses of UV-C. S499A induced a small decrease in survival at the highest UV-C dose, which is not seen in cells expressing WT protein. This sensitivity is similar to that of PrimPol$^{-/-}$ cells. Mutation of S499 to glutamic acid also increased UV-C sensitivity, more significantly than the alanine substitution, with a survival rate of only 13.4% at 6 J/m^2. This sensitivity was moderately more severe than the PrimPol$^{-/-}$ sensitivity and mimicked the UV sensitivity observed in XPV (XP30RO) cells. The XPV cells are a patient fibroblast cell line that lack the TLS polymerase Pol Eta (η) (Lehman et al., 1975). Their sensitivity to UV-C damage is well documented (Lehman et al., 1975; Stary et al., 2003) and this sensitivity increases when PrimPol is also absent from the cell (Bailey et al., 2019). These data suggest that the S499A and S499E mutant proteins are unable to complement PrimPol knockout phenotypes and induce moderate sensitivity to UV-C, greater than is seen in the absence of PrimPol entirely.

4.3.4 Mutation of S499 alters PrimPol's ability to bind to chromatin

Initial experiments performed on MRC-5 PrimPol$^{-/-}$ cells expressing either wild type, S499A or S499E PrimPol investigated whether the S499 phosphorylation mutation altered the protein's ability to bind chromatin. To better visualise the difference in chromatin loading, cells were damaged with 20 J/m^2 UV-C damage and left to recover for 8 hours. Soluble and insoluble fractions were separated from harvested protein and compared by western blot against the whole cell fraction. These protein fractions were probed for total PrimPol and RPA70 to assess loading after damage across cell lines. The stringency of the preparation was confirmed by probing for histone H3, a nuclear chromatin bound protein, and tubulin, a soluble cytoplasmic protein (Figure 4.3C).

Despite being expressed at similar levels to wild type protein, S499E mutant protein bound chromatin in greater amounts than WT or S499A protein. Additionally, the levels of RPA70 bound to chromatin appeared different across each cell line, with S499E cells showing higher levels of chromatin-bound RPA. There was no change in the level of soluble RPA. Overall, this suggested that the mutation of S499 to glutamic acid, mimicking phosphorylation, led to changes in the protein's chromatin binding ability or frequency of recruitment. In tandem with increased RPA70 binding, we speculated it may indicate issues with dissociation of the protein. Additionally, it could relate to the activity of PrimPol or other pathways generating more ssDNA, leading to more substrate for both PrimPol and RPA to bind.

The MRC-5 cells showed interesting phenotypes worthy of additional study. To confirm these phenotypes in a second cell line, we next expressed the mutant PrimPol proteins in the HEK-293 cells. We utilised the doxycycline inducible T-REx system to more closely control protein expression of these cell lines, and to better visualise the two bands of PrimPol.

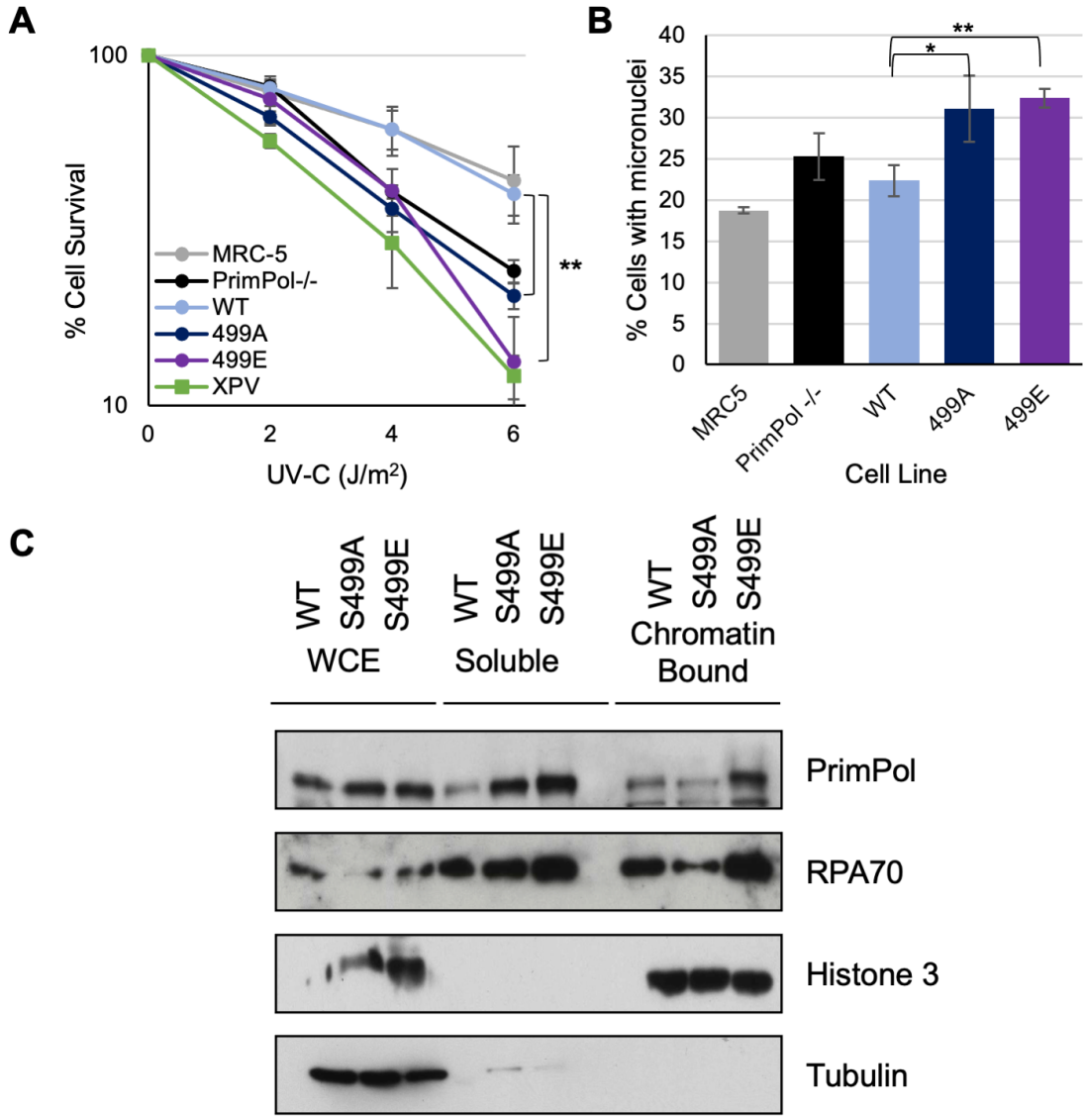

Figure 4.3. Mutation of PrimPol S499 alters chromatin binding and induces sensitivity to UV-C damage

A. Colony survival assay measured sensitivity of MRC-5 cells expressing WT, S499A and S499E PrimPol to increasing doses of UV-C damage (n=3). Significance shown between WT/S499A and WT/S499E. **B.** MRC-5 cells with 1 or more micronuclei were counted 72 hours after 5J/m^2 UV-C. **C.** Chromatin fractionation of MRC-5 PrimPol$^{-/-}$ cells expressing GFP-tagged WT, S499A or S499E PrimPol. Whole cell, soluble and insoluble fractions were analysed by western blot and probed with antibodies to GFP, RPA70, Histone H3 and tubulin.

4.4 Phenotypes of HEK-293 cell lines expressing S499 mutant PrimPol

4.4.1 Generation of cell lines expressing PrimPol S499 mutations in HEK-293 PrimPol$^{-/-}$ cells

HEK-293 T-REx PrimPol$^{-/-}$ cells expressing mutant PrimPol protein were generated as described before (2.4.3.2, L. Bailey, unpublished data). To ascertain the importance of S499 phosphorylation, we generated expression vectors using the plasmid pcDNA5 containing either WT PrimPol, or PrimPol with this site mutated to either the phospho-mimetic residue glutamic acid (E) or the phospho-null residue alanine (A). We introduced the PrimPol mutant variants in the HEK-293 PrimPol$^{-/-}$ T-REx cells, leading to doxycycline-inducible protein expression of WT, S499A and S499E PrimPol. Figure 4.4A shows that doxycycline induces approximately equal levels of S499A and S499E mutant protein expression when compared to each other, but lower when compared to WT protein levels. Interestingly, while S499A mutant protein was seen as a single lower band, the phospho-mimic protein S499E was a single higher band approximately equal in size to the upper band of PrimPol. This suggested that the S499E mutant PrimPol was a good equivalent to phosphorylated protein.

When compared to uninduced cells plated without doxycycline, cells induced to express either WT or S499A protein survived to form colonies at a similar rate. However, in the S499E line, the addition of 10ng/µl doxycycline to induce protein expression led to an observable difference in colony formation, with only 80% survival when compared to uninduced (Figure 4.4B), suggesting expression of this protein is harmful to cells.

We performed cell synchronisation on cells expressing WT, S499A or S499E mutant protein to monitor S phase progression in the presence of mutant PrimPol. Cells were stalled at the G1/S border before release and were harvested for FACS analysis at defined timepoints across the cell cycle. Cells expressing both S499A and S499E showed a delay in the completion of S phase compared to cells expressing WT protein, as determined by the percentage of cells still EdU positive at 12 hours (Figure 4.4C). We also monitored cells for the presence of

micronuclei as an indicator of genomic stability and found that cells expressing S499A and S499E protein also had more cells with one or more micronuclei than cells expressing WT PrimPol in the absence of damage (Figure 4.4D).

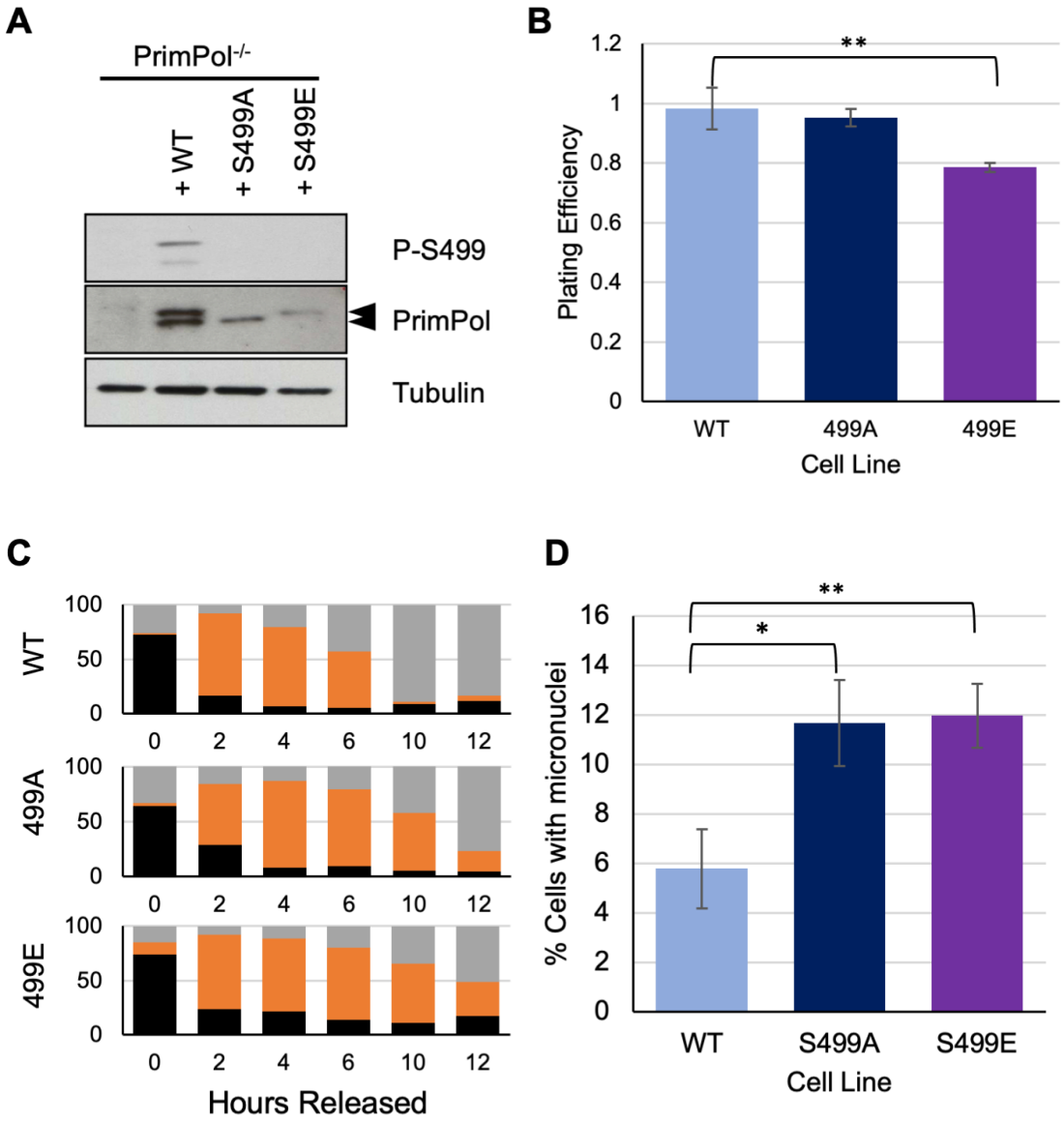

Figure 4.4. Expression of S499 mutant PrimPol affects S phase progression, decreases plating efficiency, and increase cells with micronuclei

A. Western blot analysis of HEK-293 PrimPol$^{-/-}$ cells, and cells expressing WT, S499A and S499E mutant PrimPol. Samples were probed for P-S499, total PrimPol and tubulin. **B.** Plating efficiency of WT, S499A and S499E cell lines compared to no doxycycline controls (n=3). **C.** FACS analysis quantification of WT, S499A and S499E cells with PI and EdU staining progressing through S phase from a thymidine stall. **D.** Cells with 1 or more micronuclei were counted 72 hours after PrimPol protein expression was induced by doxycycline (3 biological repeats with an n>400).

4.4.2 Expression of S499E mutant PrimPol protein reduces cell survival after DNA damage

UV-C damage induces the formation of helix distorting DNA lesions. PrimPol has been shown to respond to this damage during DNA replication (Bianchi et al., 2013), though previous work has shown that cells lacking PrimPol are not significantly UV-C sensitive (Bailey et al., 2019), suggesting other tolerance pathways can respond in PrimPol's absence. To determine the effect of UV-C damage on cells expressing the S499 mutant PrimPol protein, colony survival experiments were performed after increasing doses of UV-C damage. As described in 4.3.2, MRC-5 cells expressing either S499A or S499E mutant PrimPol were sensitive to the highest dose of UV-C damage. Figure 4.5A shows that, as in MRC-5 cells, HEK-293 cells expressing S499E were sensitive to UV-C damage. However, induction of S499A mutant protein expression did not induce sensitivity to UV-C damage, when compared to either PrimPol$^{-/-}$ cells or cells expressing WT protein. We also tested the sensitivity of these cells to UV-C in the absence of doxycycline-induced protein expression, to verify the cell lines themselves were not sensitive to UV-C. These cells, effectively PrimPol$^{-/-}$ lines, were not sensitive to UV-C damage (Figure 4.5B).

Chapter 3 describes the phenotypes induced by PrimPol S538 mutation; specifically, cells expressing S538A protein were sensitive to UV damage. As both S538A and S499E mutant PrimPol induced UV-C sensitivity, we utilised colony survival assays to determine if this sensitivity was additive; this would infer the sensitivity is non-epistatic and induced by different mechanisms. Figure 4.5C shows that, compared to cell lines expressing either S538A or S499E mutant PrimPol, the double mutant S499E/S538A was not any more UV-C sensitive. It is not clear which mutant is dominant in these cells. There are multiple possible explanations for this: either S499E sensitivity is induced through a similar mechanism to the sensitivity observed in S538A cells, making both mutations redundant with one another, or the mutation of one site prevents the mechanism by which the other induces sensitivity.

Additionally, the catalytic domain of PrimPol was mutated to inhibit its primase and polymerase activities in a S499E mutant background, generating AxA S499E

mutant protein. As previously described, the AxA mutations introduce sensitivity to UV-C that is independent to the sensitivity caused by S538A (3.6.3, Figure 3.23). However, interestingly, the sensitivity of AxA S499E cells to UV-C damage is less than S499E mutant protein alone, suggesting that S499E mutant PrimPol is less harmful for survival after mutation of the catalytic domain to block its activities (Figure 4.5D). This indicates that, to a large extent, the toxicity of S499E is dependent on PrimPol's activities as either a primase or polymerase, suggesting the toxicity is induced in a different manner to the S538A phenotypes. Additionally, given that AxA S499E mutant cells are less sensitive than the AxA mutations alone, it suggests that the S499E mutations prevent the mechanism by which the catalytic domain mutations induce toxicity also.

In addition to a sensitivity in colony survival assays, 5 J/m^2 UV-C damage also induced a significant increase in the number of micronuclei in cells expressing S499E mutant protein compared to cells expressing WT or S499A (Figure 4.5E), supporting previous data obtained in MRC-5 cells. Together, these data suggest that preventing S499 phosphorylation leads to decreased survival and decreased tolerance of DNA damage.

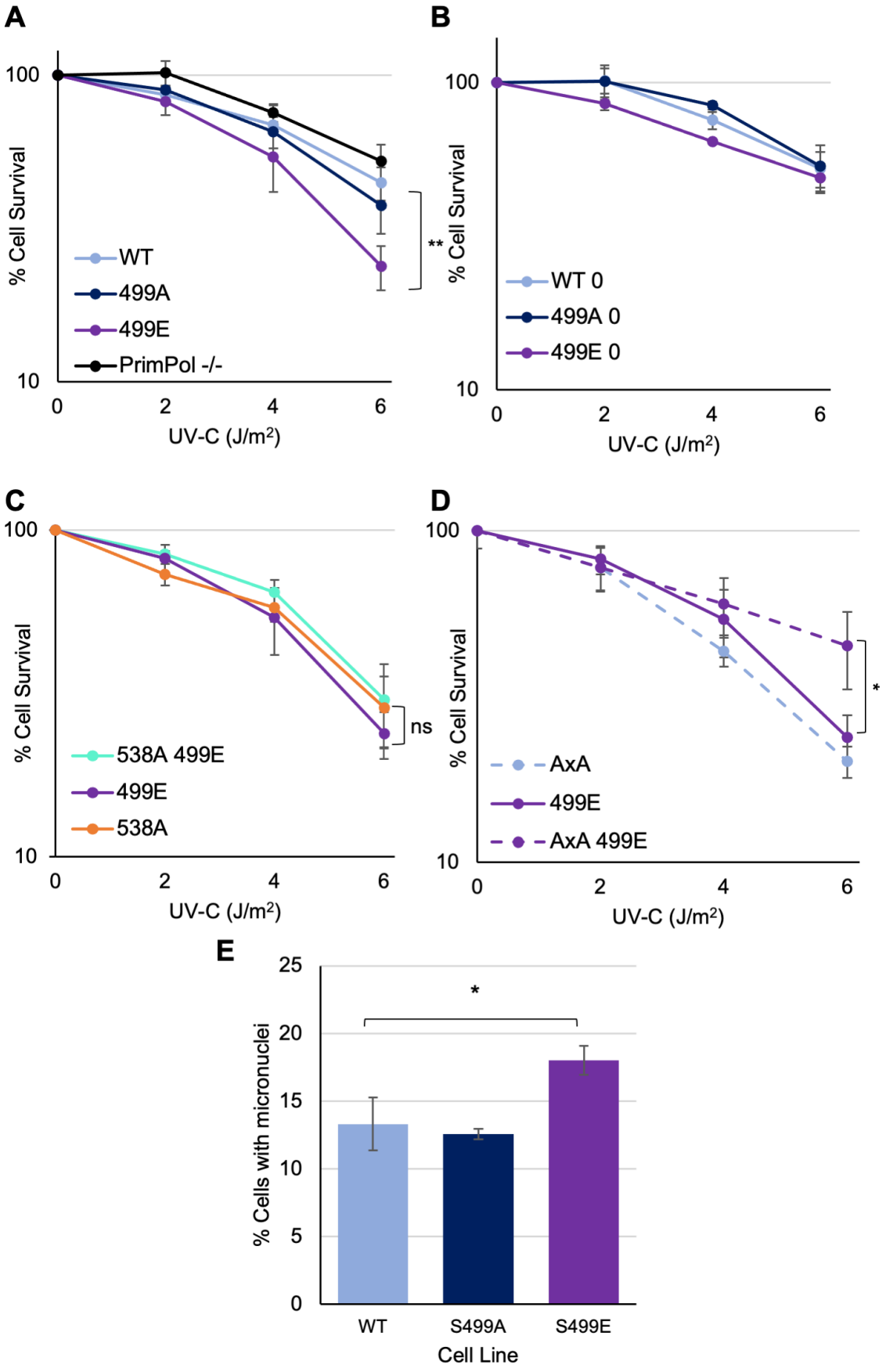
A
100
10
% Cell Survival
0
2
4
6
UV-C (J/m²)
WT
499A
499E
PrimPol -/-
**
B
100
10
% Cell Survival
0
2
4
6
UV-C (J/m²)
WT 0
499A 0
499E 0
C
100
10
% Cell Survival
0
2
4
6
UV-C (J/m²)
538A 499E
499E
538A
ns
D
100
10
% Cell Survival
0
2
4
6
UV-C (J/m²)
AxA
499E
AxA 499E
*
E
25
20
15
10
5
0
% Cells with micronuclei
*
WT
S499A
S499E
Cell Line

Figure 4.5. Cells expressing PrimPol S499E are sensitive to UV-C damage

A. Colony survival assay measured sensitivity of HEK-293 cells expressing WT, S499A and S499E PrimPol to increasing doses of UV-C damage. **B.** Colony survival assay measured sensitivity of HEK-293 cells containing WT, S499A and S499E PrimPol to increasing doses of UV-C damage in the absence of doxycycline. **C.** Colony survival assay measured sensitivity of HEK-293 cells expressing S499E, S538A and S499E/S538A mutant PrimPol to increasing doses of UV-C damage. **D.** Colony survival assay measured sensitivity of HEK-293 cells expressing S499E and AxA S499E mutant PrimPol to increasing doses of UV-C damage. **E.** HEK-293 PrimPol$^{-/-}$ cells expressing WT, S499A and S499E mutant PrimPol with 1 or more micronuclei were counted 72 hours after protein expression was induced by doxycycline (3 biological repeats with an n>400).

4.4.3 Cells expressing S499A and S499E mutant PrimPol are increasingly sensitive to hydroxyurea induced fork stalling and collapse

We next worked to determine what effect the S499 mutant PrimPol would have on resumption of DNA synthesis after fork collapse, thought to be the primary role for PrimPol *in vivo*. To appropriately mimic fork stalling, we utilised colony survival assays in the presence of hydroxyurea, which depletes dNTPs and leads to fork stalling and, after prolonged exposure to high doses, dissociation of replisome components and fork collapse. While both Rad51-mediated fork reversal and fork uncoupling have been implicated in the tolerance of replication stalling treatments (Ercilla et al., 2020; Zellweger et al., 2015), it is unclear what role, if any, repriming plays in the tolerance of this stalling. We tested the survival of parental HEK-293 cells, PrimPol$^{-/-}$ cells, and cells overexpressing WT PrimPol after a 24 hour treatment with 0, 0.5, 1 or 3mM HU (Figure 4.6A, parental and PrimPol$^{-/-}$ data obtained by Dr Laura Bailey). While both parental cells and PrimPol$^{-/-}$ cells showed similar survival, cells overexpressing WT PrimPol showed significantly better survival. On average, 38% of cells overexpressing WT PrimPol survived at the highest HU dose, compared to only 10.6% of parental cells and 12.6% PrimPol$^{-/-}$ cells (Figure 4.6A).

Interestingly, at the higher HU doses tested, cells expressing the S499 mutant protein showed lower survival than cells expressing WT protein, but higher than cells with no PrimPol at all. This suggests that, when appropriately regulated by S499 phosphorylation, higher PrimPol protein levels are advantageous to recovery, cell survival and colony formation after fork collapse. However, when misregulated due to the prevention of S499 phosphorylation, this protein does not aid as well in the resumption of DNA synthesis, leading to lower cell survival.

We additionally measured cell survival after treatment with lower doses of HU (50-200μM) which more closely mimic replication stress but do not cause total fork stalling or collapse. Previous work using similar doses has suggested that the primary form of tolerance to this stress was fork reversal, with PrimPol acting as a secondary pathway (Bai et al., 2020). In this instance, cells were incubated in the presence of HU for the duration of colony formation. We found that parental HEK-293 cells, PrimPol$^{-/-}$ and cells overexpressing WT PrimPol survived equally

well when treated with low doses of HU, indicating that overexpression of PrimPol does not increase survival after replication stress. It is possible that as fork slowing and transient fork stalling may not induce as much ssDNA as full fork stalling or collapse. Cells expressing S499 mutant showed significantly lower survival (Figure 4.6C). This implies that S499 mutant PrimPol is less adept at participating in both the recovery mechanism employed during mild replication stress, and after fork collapse: this leads to a decrease in cell survival. However, there was no concomitant increase in micronuclei after treatment with low doses of hydroxyurea, despite the significantly increased sensitivity. We hypothesise this is due to poor cell survival; cells which undergo extensive HU induced replication stress do not survive to progress through mitosis and generate a cell with micronuclei.

It is interesting that the cells with endogenous levels of PrimPol, cells with no PrimPol and cells over-expressing PrimPol respond similarly to low doses of HU, implying that PrimPol is not an essential component of the cell's response to this mild replication stress, yet S499 mutant cells survive so poorly. Due to the difference responses induced by high and low doses of hydroxyurea, we sought to mimic the replication stress response by another method.

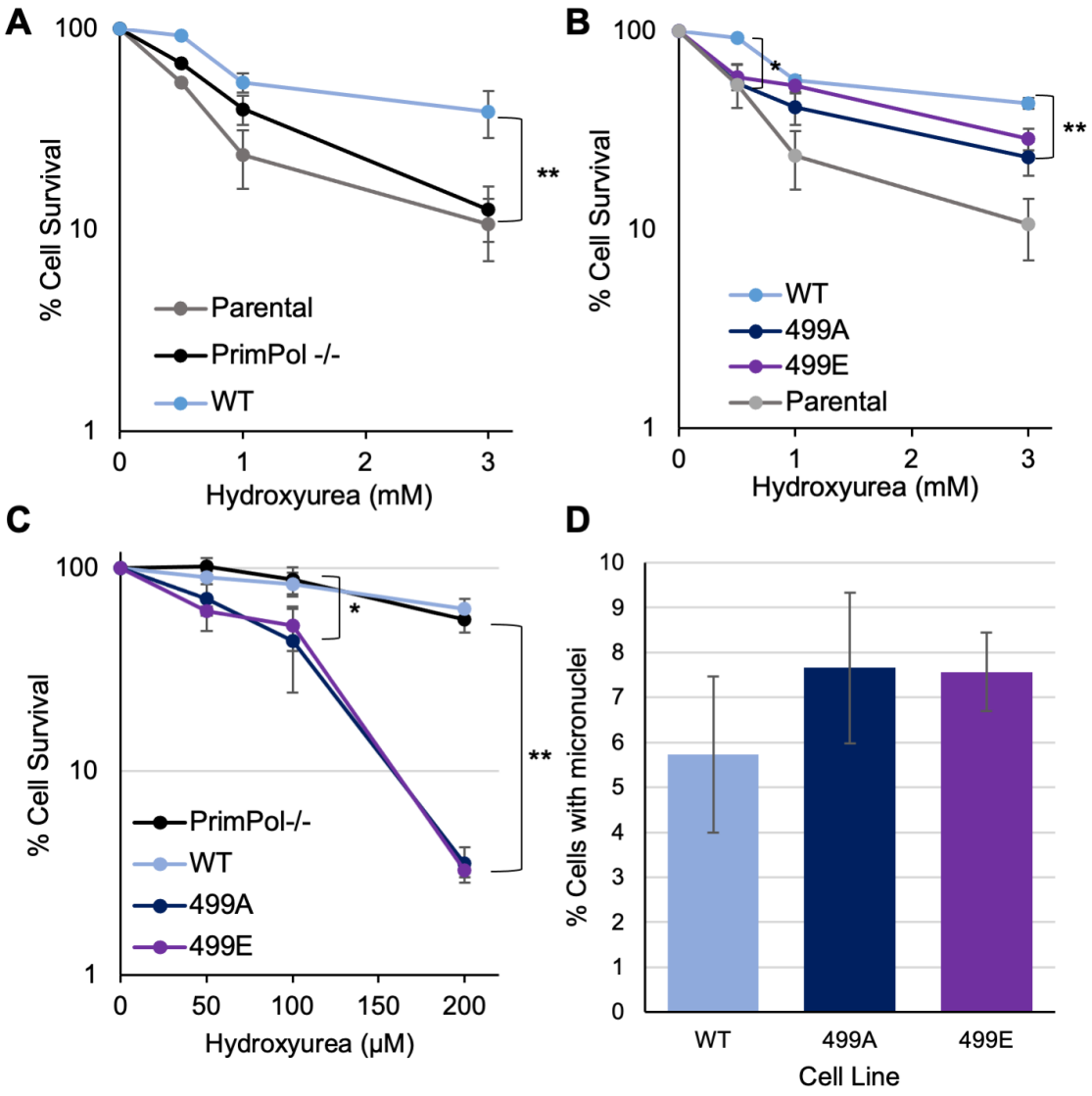

Figure 4.6. The effect of both PrimPol protein levels and S499 phosphorylation on cell survival after hydroxyurea treatment

A. Colony survival assay to measure sensitivity of parental HEK-293 cells, HEK-293 PrimPol$^{-/-}$ cells and cells expressing WT PrimPol to increasing doses of HU, applied for 24 hours. Significance is shown between WT and S499A. Significance is shown between WT and PrimPol$^{-/-}$. **B**. Colony survival assay to measure sensitivity of parental HEK-293 cells, and HEK-293 PrimPol$^{-/-}$ cells expressing WT, S499A or S499 PrimPol, to increasing doses of HU, applied for 24 hours. Significance is shown between WT and S499A. **C.** Colony survival assay to measure sensitivity of HEK-293 PrimPol$^{-/-}$ cells expressing WT, S499A or S499 PrimPol to increasing doses of HU applied continuously. Significance is shown

between WT and S499A/E. **D.** Cells with 1 or more micronuclei were counted 72 hours after PrimPol protein expression was induced and treatment with 200 μM HU (3 biological repeats with an n>400).

4.4.4 Cells expressing S499 mutant PrimPol are sensitive to replication stress induced by aphidicolin

Aphidicolin, a tetracyclic diterpene chemical first isolated from the fungus *Cephalosporum aphidicola* (Bucknall et al., 1973) inhibits DNA replication by inhibiting both Pol δ and Pol α. It also induces breaks and gaps at common fragile sites in human cells (Glover et al., 1984) and at low doses, replication stress (Wilhelm et al., 2019). We utilised this drug to assess the sensitivity of cells expressing the S499 mutants after showing they were significantly sensitive to low doses of hydroxyurea. To determine if this response was specific to hydroxyurea, colony survivals on HEK-293 cells expressing wild type, S499A or S499E PrimPol protein were performed in the continuous presence of increasing doses of aphidicolin to induce similar replication stress (Figure 4.7A,B). S499E cells were significantly more sensitive to aphidicolin than cells expressing S499A or WT PrimPol, but this sensitivity can be abrogated as before through the introduction of the AxA mutations, which prevent catalytic activity (Figure 4.7C). This supports the hypothesis that S499 toxicity is induced by the catalytic activity of PrimPol.

Additionally, treatment with aphidicolin induced significantly greater micronuclei formation in cells expressing S499A or S499E mutant PrimPol compared to cells expressing WT PrimPol (Figure 4.7D). Furthermore, cells expressing S499A and S499E showed a significant increase in cells undergoing an abnormal mitosis – defined as showing lagging chromosomes or bridges during anaphase, or tripolar spindles (Figure 4.7E).

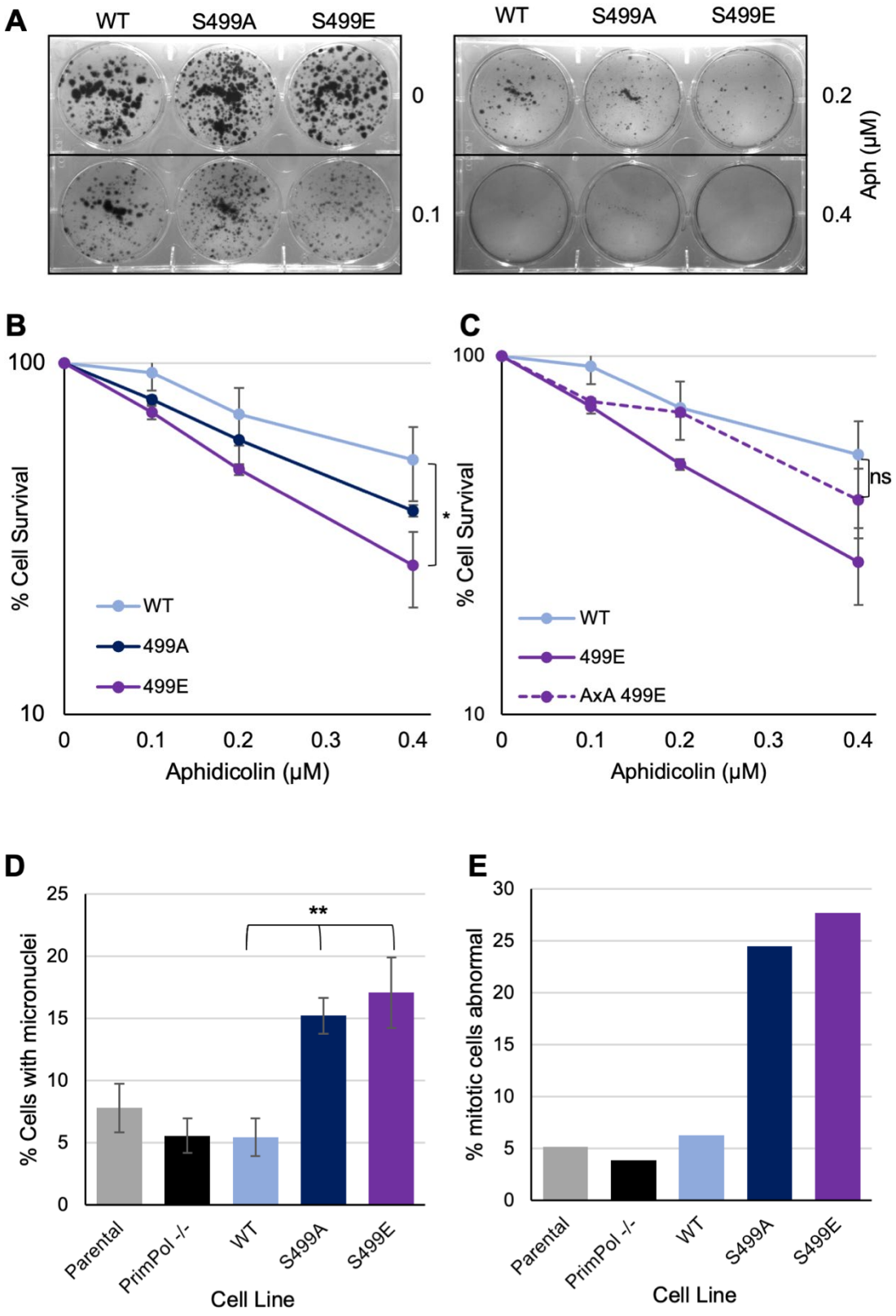

Figure 4.7. Cells expressing S499E mutant PrimPol are sensitive to the polymerase inhibitor aphidicolin, while both mutations lead to increased micronuclei and abnormal mitosis

A. Images of cell survival after methylene blue staining. HEK-293 cells expressing WT, S499A or S499E mutant PrimPol were subject to increasing doses of aphidicolin, before being left to grow for 10 days. **B.** Colony survival assay measuring sensitivity of HEK-293 cells expressing WT, S499A and S499E PrimPol to increasing doses of aphidicolin. **C.** Colony survival assay measuring sensitivity of HEK-293 cells expressing WT, S499E and AxA S499E PrimPol to increasing doses of aphidicolin. **D.** Cells with 1 or more micronuclei were counted 72 hours after PrimPol protein expression was induced and treatment with 0.4 μM aphidicolin (3 biological repeats with an n>400). **E.** Cells displaying abnormal mitosis were counted 72 hours after PrimPol protein expression was induced and treatment with 0.4 μM (3 biological repeats with an n>100).

4.4.5 Expression of S499 mutant PrimPol induces greater sensitivity to replication stress

Expression of S499 mutant protein also induced sensitivity to olaparib, a poly(ADP ribose) polymerase (PARP) inhibitor. The application of PARP inhibitors prevents the repair of ssDNA breaks by both inhibiting the activity of PARP and preventing its dissociation from breaks (Murai et al., 2014). We assessed sensitivity to this inhibitor through colony survival assays, which showed that both S499A and S499E expression reduced survival at all tested doses of olaparib compared to the expression of WT protein (Figure 4.8A). Additionally, treatment with 0.5 μM olaparib also increased the number of cells with micronuclei in cell lines expressing either of the S499 mutants (Figure 4.8B), suggesting that cells that do survive have evidence of genomic instability.

We additionally assessed sensitivity of cells expressing S499 mutant protein to camptothecin, a Topoisomerase I inhibitor. Inhibition of Topo I can lead to fork stalling, as DNA unwinding is prevented when the protein remains attached to the nicked DNA (Pommier et al., 2006). At higher concentrations, camptothecin induces DSBs, but at lower concentrations, fork slowing, stalling and reversal are also seen (Chaudhuri et al., 2012). We tested cell survival after treatment to assess the cell's recovery after replication stress. Cells overexpressing WT PrimPol were no better at surviving after this stress than cells without PrimPol or parental cells (data not shown), but the expression of S499 mutants reduced survival significantly. In WT cells, 39% of cells survive at 10 nM Camptothecin, compared to 11% and 6% in S499A and S499E cells, respectively (Figure 4.8C). This suggests that cells that are unable to regulate S499 phosphorylation of PrimPol are less tolerant of the replication stress induced by camptothecin. Shorter exposure to camptothecin for 72 hours, as with olaparib, also induced an increase in the number of cells with one or more micronuclei (Figure 4.8D).

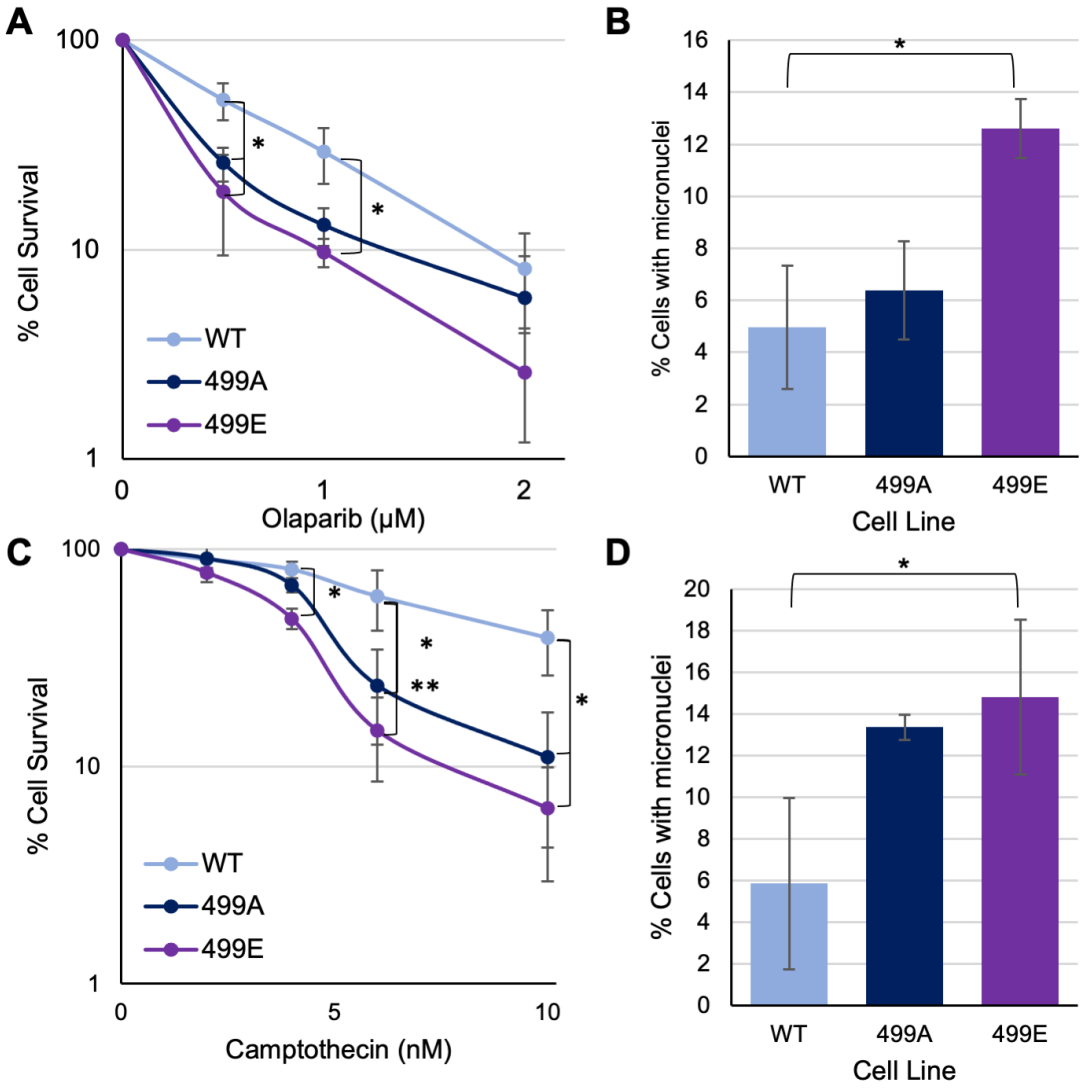

Figure 4.8. Replication stress induced by olaparib or camptothecin reduces survival of cells expressing S499 mutant PrimPol, and leads to an increase in micronuclei

A. Colony survival assay measuring sensitivity of HEK-293 cells expressing WT, S499A and S499E PrimPol to increasing doses of olaparib. **B.** Cells with 1 or more micronuclei were counted 72 hours after PrimPol protein expression was induced and cells were treated with 0.5 μM olaparib (3 biological repeats with an n>400). **C.** Colony survival assay measuring sensitivity of HEK-293 cells expressing WT, S499A and S499E PrimPol to increasing doses of camptothecin. **D.** Cells with 1 or more micronuclei were counted 72 hours after PrimPol protein expression was induced and treatment with camptothecin (3 biological repeats with an n>400).

4.4.6 The binding of S499 mutant PrimPol to chromatin

4.4.6.1 Chromatin binding of PrimPol mutated at S499 in asynchronous cells

Previous investigation, using the MRC-5 PrimPol$^{-/-}$ cell line, indicated that the binding of PrimPol to chromatin was altered by the mutation of the S499 phosphorylation site. Additionally, cells expressing S499E specifically showed increased binding of RPA70. However, protein in this instance was GFP-tagged, which prevented visualisation of the two bands of PrimPol, even on lower percentage SDS-PAGE gels. Protein expressed in the HEK-293 cells, without this bulky tag, showed the two bands of PrimPol clearly. We therefore wanted to determine if both bands bound chromatin, and whether any difference in binding was detected after mutation of S499.

Figure 4.9 shows that, in the whole cell fraction, the upper, phosphorylated band of PrimPol is present; while it is less clear in the undamaged, it is easily detectable in protein from the UV-C damaged cells. Cells were left to recover after 20J/m^2 for 24 hours before harvesting and were then fractionated to isolate soluble and insoluble fraction. In the chromatin fractionation, where no signal was detected for the soluble protein tubulin, both bands of WT PrimPol, and both S499A and S499E mutant protein, were recruited to chromatin, suggesting that both S499 phosphorylated and unphosphorylated protein is recruited to sites of UV induced damage, and in undamaged cells to endogenous stalls. Using quantification based on whole cell protein expression levels, it was determined that S499A protein bound chromatin in slightly lower amounts than both WT and S499E, but unlike in MRC-5 cells, S499E did not appear to accumulate on chromatin in greater amounts than WT PrimPol.

The changes in protein binding seen in Figure 4.9 could be attributed to small variations in both expression and chromatin binding, and UV damage did not appear to make the difference clearer. We therefore next tested PrimPol binding during S phase, to determine what if any effect the S499 mutations had on chromatin binding during replication.

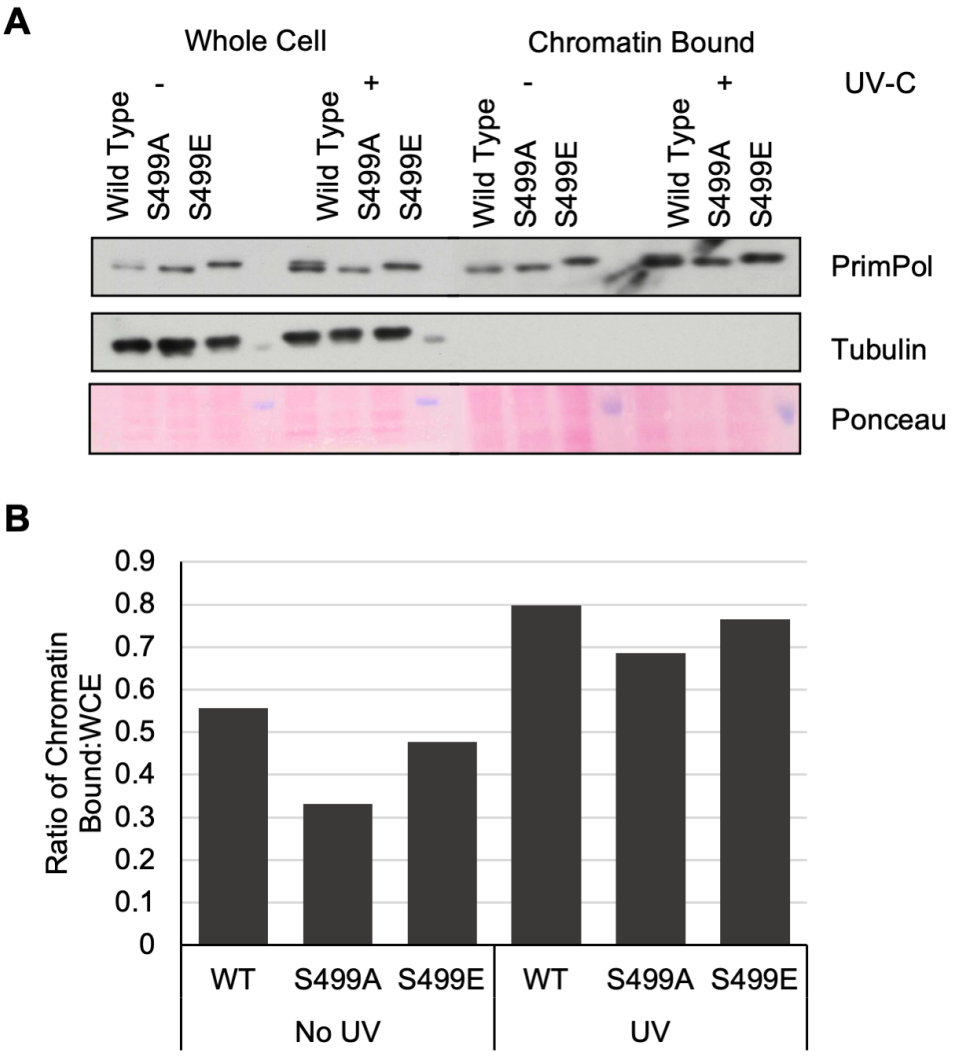

Figure 4.9. Chromatin fractionation of HEK-293 cells expressing WT or S499 mutant PrimPol

A. Protein from the whole cell fraction and detergent resistant chromatin fractions were subject to western blotting and probed for total PrimPol protein and tubulin. Ponceau stained membrane provided as a control for loading. **B.** Quantification of chromatin bound protein relative to whole cell extract. Note: this experiment is n=1.

4.4.6.2 Chromatin binding during DNA replication

We investigated whether any changes in the binding of the mutant proteins were observable in cells synchronised to S phase, the cell cycle stage where PrimPol is primarily utilised: we assessed PrimPol binding in asynchronous cells and in cells stalled to the G1/S border by thymidine block and then released for 4 hours. Figure 4.10A shows that whole cell protein expression was consistent in each cell line across these two samples. In the insoluble fraction, there was no significant difference in chromatin association between the mutant cell lines, suggesting that S499 mutant PrimPol bound as well as WT protein in S phase (Figure 4.10B). However, when insoluble protein was probed for chromatin bound RPA70, there was a small increase observed in both the asynchronous and S phase chromatin fraction from S499E cells that is not observed in the WT cells. When this blot was quantified, the amount of RPA bound to chromatin normalised to the amount of chromatin-bound PrimPol was higher in the S499E cells synchronised to S phase, compared to either WT or S499A cells in the same cell cycle stage. This indicates the RPA accumulation on chromatin in cells expressing S499E may be independent of PrimPol loading.

Additionally, we treated asynchronous cells with 0.4 μM aphidicolin or 200 μM hydroxyurea – doses which induced sensitivity in the colony survivals (Figures 4.6 and 4.7), and which would only induce stress in S phase – for 4 hours before chromatin fractionation. There was no change in the loading of S499E mutant PrimPol to chromatin in these cells after aphidicolin or HU induced damage (Figure 4.10D).

Overall, PrimPol that is either phosphorylated and unphosphorylated at S499 is able to associate with chromatin, indicating both are recruited and likely interact with DNA and RPA. We hypothesise, based on the accumulation of chromatin bound RPA70, that expression of S499E may in fact increase replication stress during S phase, leading to increased fork stalling and the generation of ssDNA bound by RPA. This may then lead to changes in recruitment of S499E mutant PrimPol, which could be more apparent in the MRC-5 cells due to their constitutive expression.

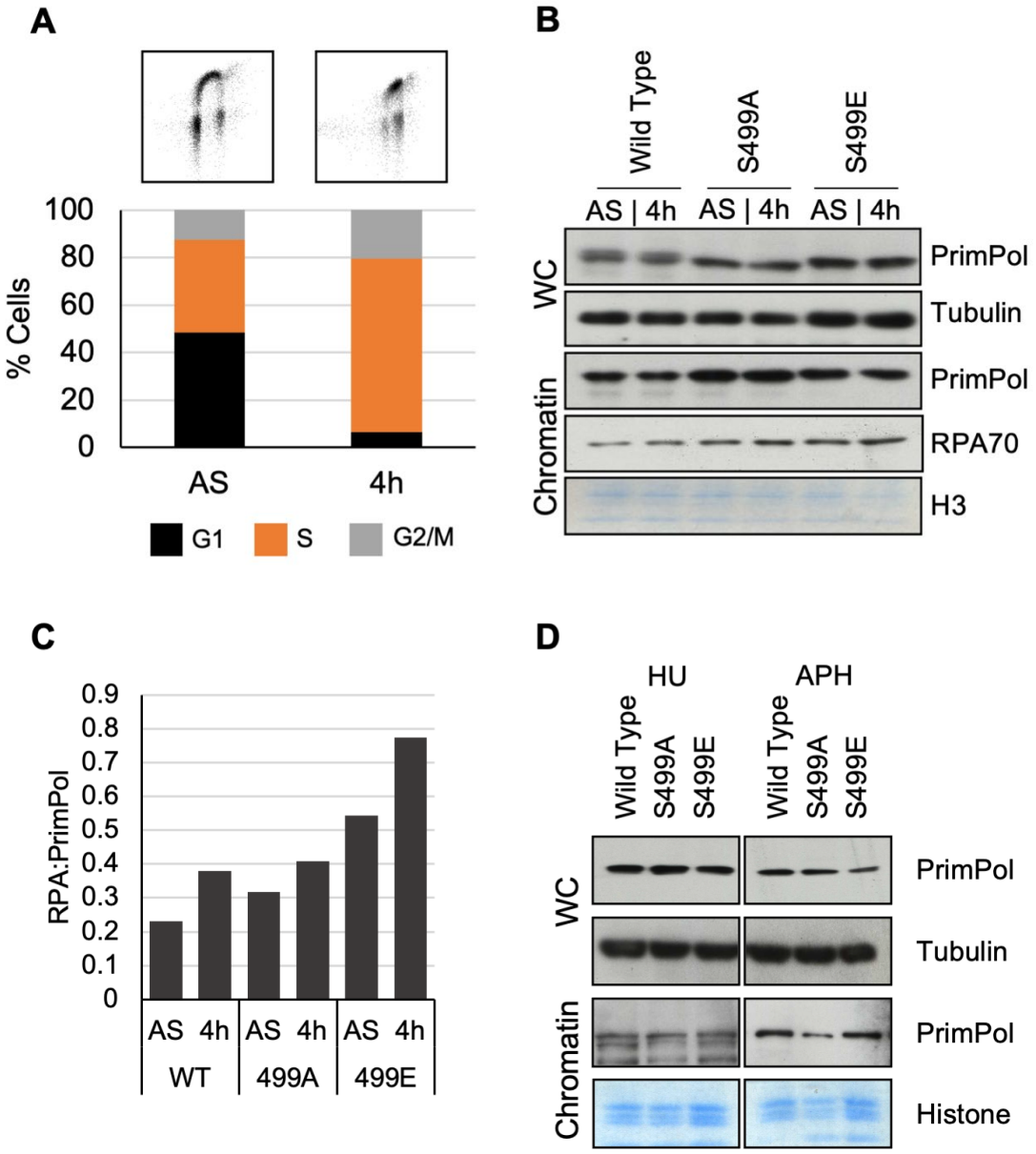

Figure 4.10. Chromatin binding of S499 mutant PrimPol does not change in S phase or after replication stress

A. Example FACS profiles and quantification of asynchronous HEK-293 cells (AS) and cells synchronised by thymidine stall and released for 4 hours to obtain a mid-S phase population (4h). **B.** Whole cell and chromatin fraction of HEK-293 cells expressing WT, S499A or S499E protein, synchronised as described in A. Protein from whole cell extract was probed for PrimPol and tubulin. Chromatin fraction was probed for PrimPol, RPA70, with InstantBlue stained histones used as a loading control. **C.** Quantification of the blot in B, with RPA70 signal normalised to PrimPol. **D.** Whole cell and chromatin fraction of HEK-293 cells

expressing WT, S499A or S499E mutant PrimPol, treated with 0.4 μM aphidicolin or 200 μM HU 4 hours before harvest. Protein was probed with PrimPol and tubulin antibodies with InstantBlue stained histones used as a control for chromatin loading.

4.5 Inhibiting RPA binding rescues phenotypes induced by PrimPol S499 mutation

To verify that differences in PrimPol's activity were not to blame for the phenotypes described so far, *in vitro* polymerase and primase assay experiments were performed and showed that S499A or S499E PrimPol had comparable activities as WT PrimPol (L. Bainbridge and A. Doherty, unpublished data).

We therefore next investigated whether phenotypes associated with the S499 mutants (sensitivity to replication stress and damage, and increased micronuclei) were dependent on RPA binding. We therefore mutated key residues within the RPA binding motifs (D519R, F522A, D551R and I554A) as previously described (3.6.1) to generated PrimPol RAB in a S499A/E mutant background. Previous work has shown that RAB mutant PrimPol does not associate with chromatin and cannot bind RPA (Guilliam et al., 2017). The cell lines are referred to as RAB, RAB 499A, and RAB 499E. Figure 4.11A verifies that PrimPol does not associate with chromatin in these cell lines, though protein expression is maintained and equal across the cell lines, as detected in the soluble fraction. The RAB mutations do not induce significant sensitivity to UV-C compared to WT cells (Figure 4.11B), as they mimic HEK-293 PrimPol$^{-/-}$ cell lines which are themselves not sensitive to these damaging agents (L. Bailey, unpublished work). In the cell line expressing S499A, which was not sensitive to UV-C damage, RAB mutation did not induce sensitivity (Figure 4.11C). Cells expressing S499E, which were sensitive to UV-C damage, showed a decrease in sensitivity when the RAB mutation was introduced, preventing the protein from associating with chromatin (Figure 4.11D).

Additionally, we verified that the plating deficiency observed after S499E expression was absent when RPA interaction was prevented (Figure 4.12A). Mutation of the residues within the RPA binding domain also worked to prevent the increase in micronuclei observed after aphidicolin, camptothecin or olaparib induced replication stress (Figure 4.12B,C,D). These data show that preventing PrimPol's association with chromatin alleviates phenotypes associated with S499 mutations.

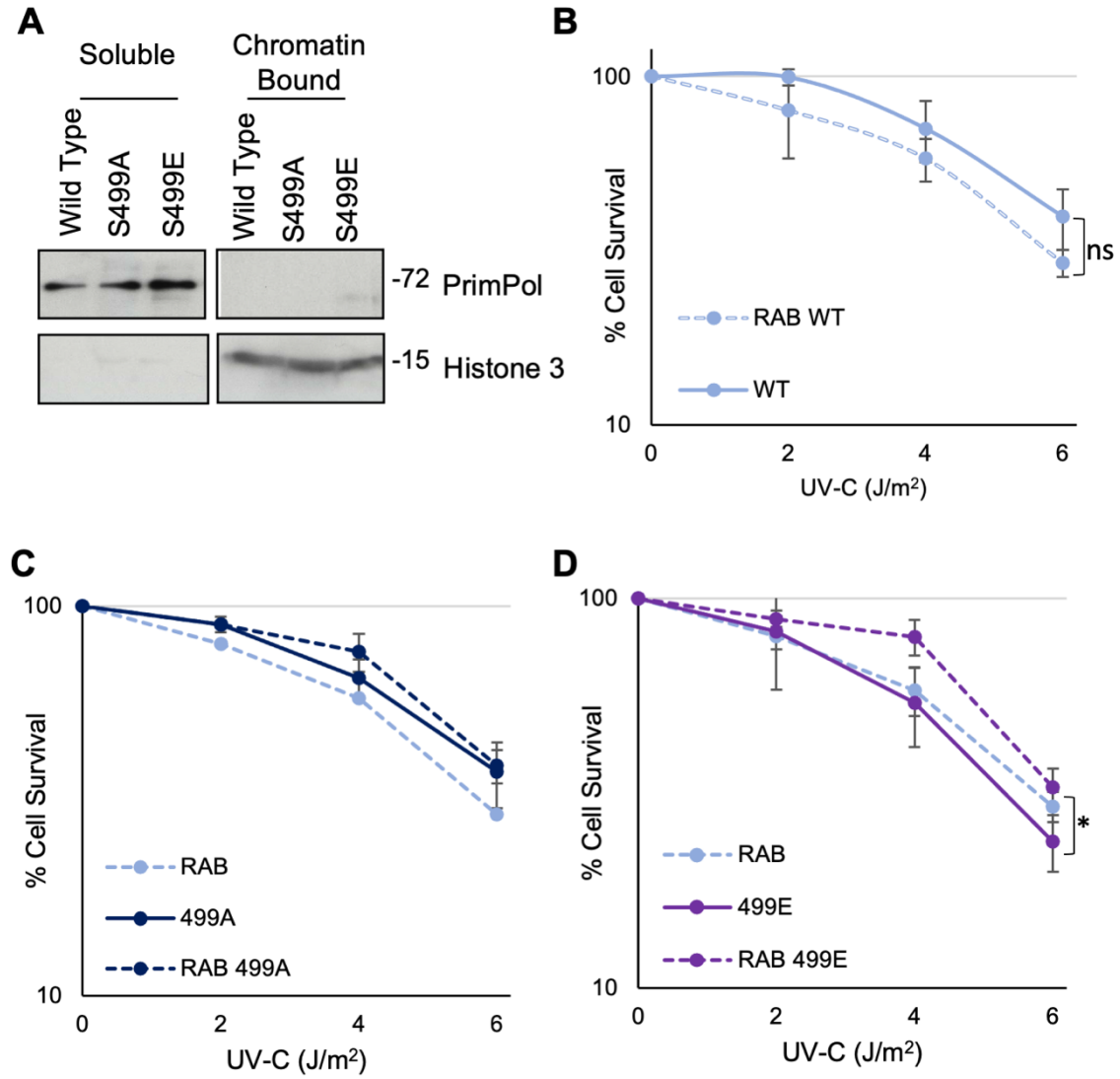

Figure 4.11. Mutating the RPA binding motif to prevent association with chromatin alleviates UV sensitivity in cells expressing S499 mutant PrimPol

A. Cells expressing RAB, RAB 499A and RAB 499E were fractionated into soluble and chromatin bound (insoluble) fractions. Samples were then resolved on a 15% SDS-PAGE gel and probed for PrimPol and Histone H3. **B.** Colony survival assay compared the sensitivity of WT and RAB cells to UV-C damage. **C.** Colony survival assays compared the sensitivity of RAB, 499A and RAB 499A cells to UV-C damage. **D.** Colony survival assays compared the sensitivity of RAB, 499E and RAB 499E cells to UV-C damage. Significance shown between 499E and RAB 499E.

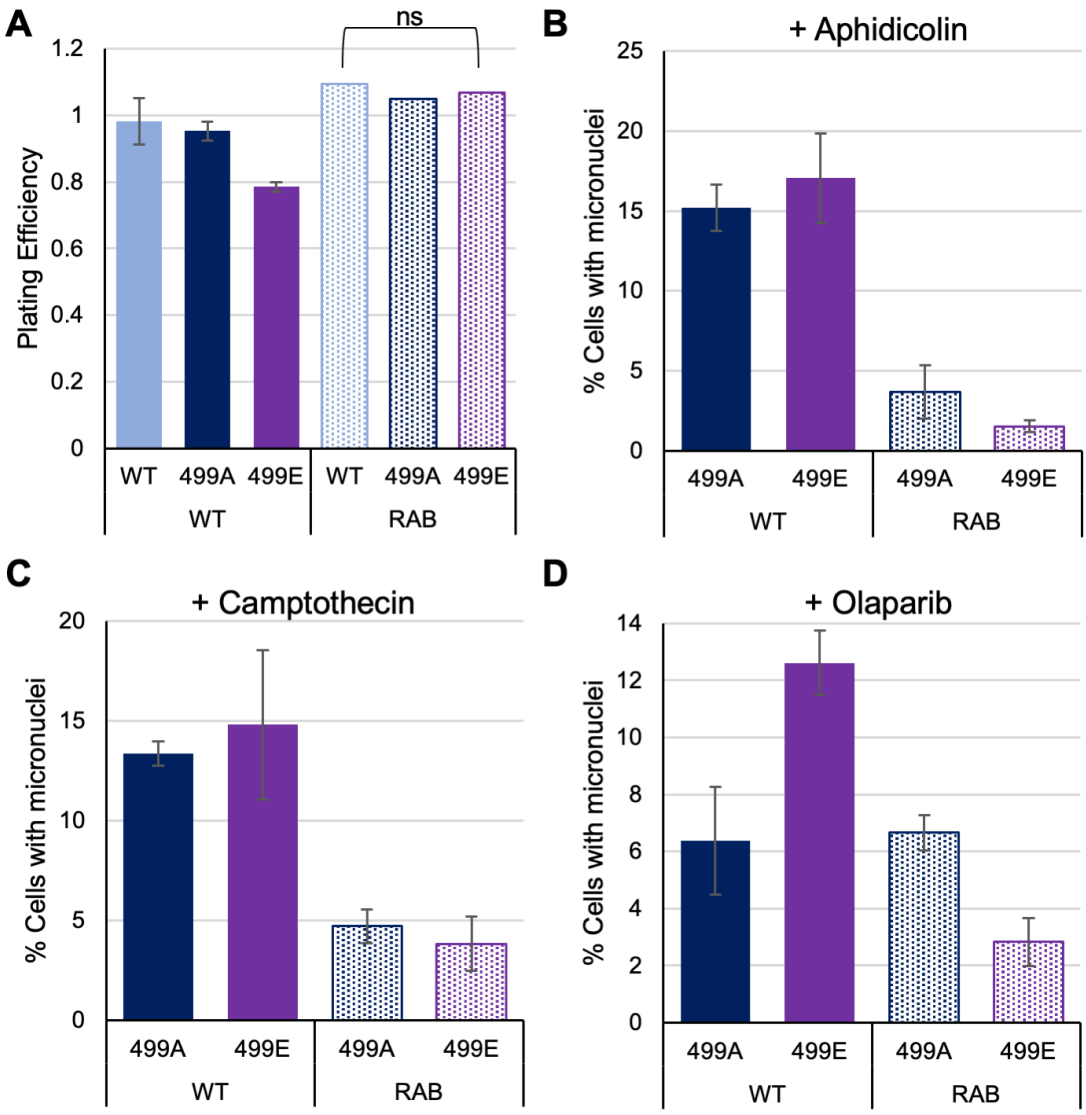

Figure 4.12. Mutation of the RPA binding motif reduces the plating deficiency of cells expressing S499E, and prevents PrimPol induced micronuclei accumulation after replication stress

A. Plating efficiency of RAB, RAB S499A and RAB S499E cell lines (n=2) compared to the plating efficiency of WT, S499A or S499E cell lines (n=3) after doxycycline induced protein expression. **B.** Cells with 1 or more micronuclei were counted 72 hours after PrimPol protein expression was induced and treatment with aphidicolin (3 biological repeats with an n>400). **C.** Cells with 1 or more micronuclei were counted 72 hours after PrimPol protein expression was induced and treatment with camptothecin (3 biological repeats with an n>400). **D.** Cells with 1 or more micronuclei were counted 72 hours after PrimPol protein

expression was induced and treatment with olaparib (3 biological repeats with an n>400).

To summarise, data obtained using HEK-293 cells supports previous work in the MRC-5 cells, with similar phenotypes including decreased survival and increased micronuclei after UV-C damage. Additional phenotypes observed in HEK-293 cells include a plating deficiency induced by expression of S499E protein in undamaged conditions, along with significant sensitivity to replication stress induced by aphidicolin, olaparib or camptothecin. This sensitivity is accompanied by increases in mitotic abnormalities and micronuclei, which suggest incomplete replication or incomplete repair of DNA damage (Fragkos and Naim, 2017). Phenotypes of cells expressing S499A protein, while occasionally milder, are largely the same, indicating that neither protein is adept at recovery from damage or stress.

This suggests that both S499 phosphorylated and unphosphorylated PrimPol are required by the cell and are important for PrimPol's activity. Whether one form is a by-product of the other – for example, repeated phosphorylation and dephosphorylation during repriming – or whether both forms are used independently is unclear. However, migration to the HEK-293 T-Rex system allows for doxycycline-inducible expression of mutant protein, and the absence of a bulky tag allows for easier and clearer detection of the two-band appearance of PrimPol on SDS-PAGE. To investigate the role of S499 phosphorylation further, we generated an antibody specific to S499 phosphorylation, which we utilised to investigate the cellular signals that regulate this phosphorylation *in vivo*.

4.6 Phosphorylation of S499 of PrimPol is associated with cell cycle stage

4.6.1 Detection of S499 phosphorylation using a phospho-specific antibody

An antibody specific to phosphorylated S499 was raised using a phospho-peptide approach (2.3.3.1). The antibody was verified to be specific to phosphorylated protein, as the antibody no longer bound to protein after λ phosphatase treatment (Figure 4.13A). Similarly, the antibody was tested against PrimPol protein mutated to express S499A or S499E, to determine if the antibody was specific to phosphorylation of S499 (Figure 4.13A). As before, there was no antibody binding observed when protein was unable to be phosphorylated at S499, further suggesting that the antibody is specific to phosphorylated S499 of human PrimPol. We next utilised this antibody to detect changes in S499 phosphorylation, to help elucidate the role of this phosphorylation in the regulation of human PrimPol.

4.6.2 Inhibition of CDK1 prevents S499 phosphorylation

Analysis of the amino acid sequence of PrimPol using the ELM server (Kumar et al., 2020) indicated that S499 lies within a putative CDK1 site. To test if PrimPol was a substrate for this kinase, preliminary *in vitro* kinase assays were performed, which showed that the CTD (aa 480-560) of PrimPol was phosphorylated by CDK1 (P. Hentges and A. Doherty, unpublished data). We decided to verify if CDK1 was phosphorylating S499 using the CDK1 inhibitor RO-3306. RO-3306 is a ATP-competitive inhibitor that blocks the ATP binding site of CDK1 (Vassilev et al., 2006). Increasing concentrations of RO-3306 were applied to HEK-293 PrimPol$^{-/-}$ cells that had been induced to over-express WT PrimPol (Figure 4.13B). In addition to the absence of phosphorylated S499, as indicated by phospho-antibody binding, the disappearance of the top band of PrimPol after RO-3306 also infers the absence of PrimPol phosphorylation at S499. This indicates that S499 is phosphorylated by CDK1, although there is a possibility that CDK2 or another CDK could also modify this site. Strikingly, the addition of nocodazole, added in this experiment to control for any change in

phosphorylation induced by mitotic accumulation, increased the amount of detectable phosphorylated S499 PrimPol. While full mitotic stalling was not induced by the nocodazole addition, as the drug was only applied for 8 hours to match the CDK1i treatment, the accumulation suggested that nocodazole treatment leads to increased S499 phosphorylation. No change was observed in S499A cells treated identically with nocodazole (Figure 4.13B).

4.6.3 PrimPol S499 phosphorylation increases after UV damage

Cells expressing S499E are sensitive to UV-C damage in both MRC-5 and HEK-293 cells (Figures 4.3A and 4.5A). Cells expressing S499E also developed increased micronuclei after UV damage compared to cells expressing WT protein (Figure 4.4D and 4.5E). We therefore investigated to see if UV damage affected S499 phosphorylation itself. Figure 4.9 shows an increase in the slower migrating isoform of PrimPol 24 hours after UV-C damage, indicating that S499 phosphorylation may increase after UV damage.

Asynchronous cells expressing WT PrimPol were damaged by 20 J/m^2 UV-C and left to recover for a short period, before cells were harvested for protein extraction and subject to western blot analysis for S499 phosphorylation (Figure 4.13C). Quantification was performed using ImageJ and calculated the ratio of S499 phosphorylated protein to total PrimPol protein, in order to take into account total protein expression. As shown in Figure 4.13D, phosphorylation increased slightly to a peak at 45 minutes before decreasing (n=1). An additional experiment, using recovery timepoints of 0, 10, 20 and 30 minutes post-UV, showed a similar increase in S499 phosphorylation (data not shown). This suggested that S499 phosphorylation levels could increase soon after UV induced DNA damage, before returning to pre-damage levels shortly after. The rapid phosphorylation and dephosphorylation may explain the sensitivity of both S499A and S499E cells, as it may indicate the importance of dynamic regulation of the protein. However, further experiments are required to fully assess whether this shift in phosphorylation, mild as it is, is truly dynamic phosphorylation or dephosphorylation, or simply experimental variance.

We additionally assessed S499 phosphorylation during longer recovery time-points after treatment with 20 J/m^2 UV-C. Phosphorylation did not vary significantly, except for a peak at 24 hours as before (Figure 4.13E). Cells additionally accumulated in G2 24 hours after UV-C damage, described previously in Bailey et al., (2019) (Figure 4.13F). This accumulation in G2, where S499 phosphorylation levels have been shown to be high, may account for the increase in phosphorylation.

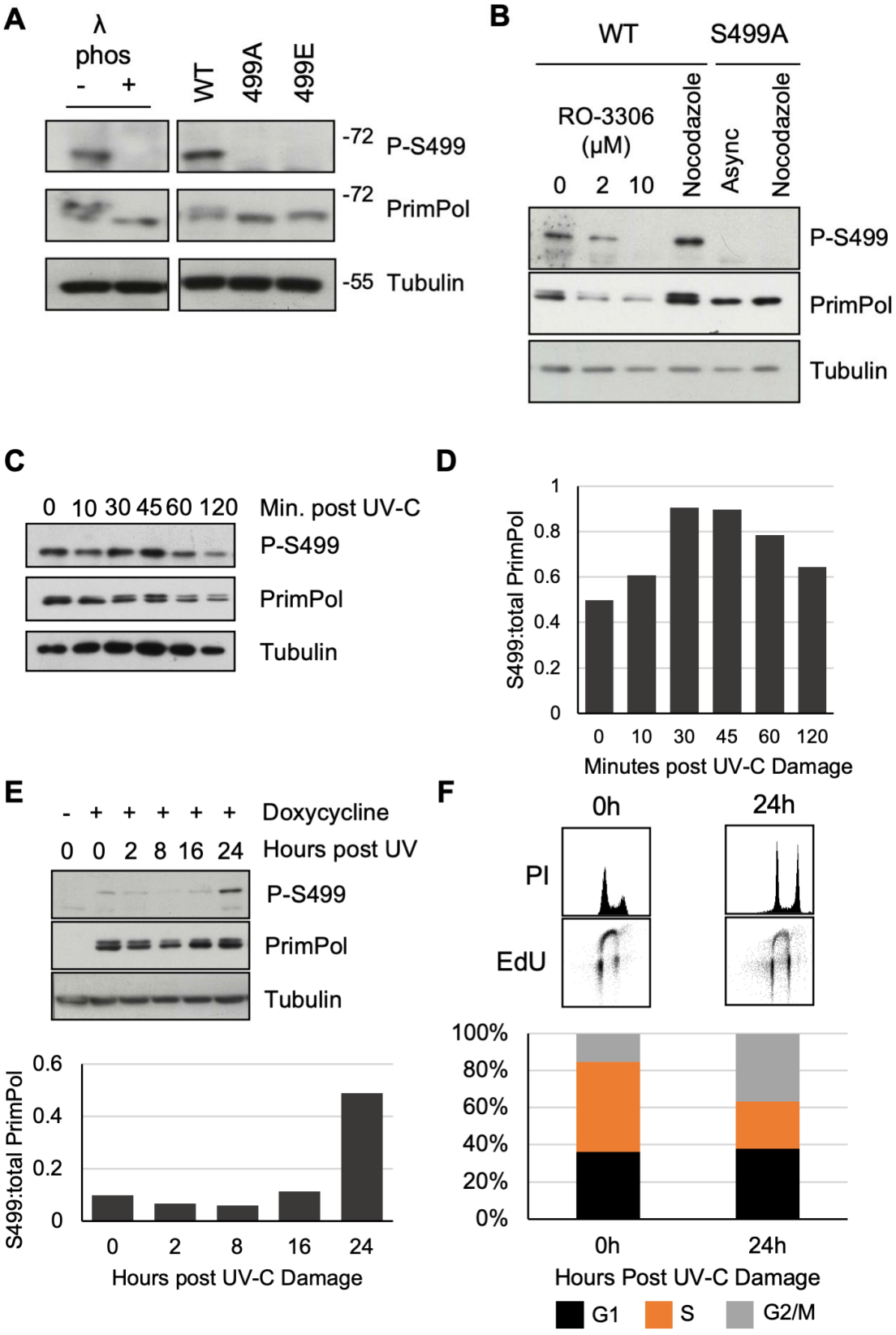

Figure 4.13. Inhibition of CDK1 decreases PrimPol S499 phosphorylation, while nocodazole treatment and UV damage increase S499 phosphorylation

A. Western blot analysis of HEK-293 cells expressing WT PrimPol. Left panel shows cells ± 400 U λ phosphatase, probed with P-S499, PrimPol and tubulin antibodies. **B.** Western blot analysis of HEK-293 cells expressing WT or S499A PrimPol. Cells were treated with 2 or 10 μM RO-3306, a CDK1 inhibitor, or 1 μM nocodazole, for 8 hours before harvest and analysis with P-S499, PrimPol and tubulin antibodies. **C.** Western blot analysis of protein from cells damaged by 20 J/m^2 UV-C over defined recovery periods. Note, this experiment is n=1. **D.** Quantification of western blot in A (n=1). **E.** Western blot analysis of protein from cells damaged by 20 J/m^2 UV-C over defined recover periods, and a quantification of this blot. **F.** FACS analysis of cells harvested 0 and 24 hours after UV-C damage. Cells were stained with EdU and PI for quantification of cell cycle stage.

4.6.4 Phosphorylation of PrimPol S499 changes across the cell cycle

CDK1 is an essential kinase responsible for cell cycle progression, particularly governing entry into mitosis and cell division (Santamaría et al., 2007). Since its discovery (Lee and Nurse, 1987), our understanding of its importance in cells has expanded to include roles in DNA replication (Liao et al., 2017), DNA damage repair (Ira et al., 2004), and the ability to compensate for other absent CDK enzymes, such as CDK2, a key regulator of S phase entry (Aleem et al., 2005).

CDK1 activity increases through late S phase, and is highest in G2 and mitosis, with low levels in G1 and early S (Bashir and Pagano, 2005). We considered that S499 phosphorylation may change according to the activity of the kinase. This model would explain changes in phosphorylation when cells accumulated in mitosis, such as after nocodazole treatment (Figure 4.13B), in addition to the increase in phosphorylation after UV-C damage, where cells accumulate in G2 (Figure 4.13E). To investigate this, cells were synchronised by double thymidine and released to defined timepoints (Figure 4.14A). Western blotting was performed on protein samples harvested from cells stalled at different stages of the cell cycle. Cell cycle stage of the samples was determined by FACS analysis from cells stained with both propidium iodide and the thymidine analogue EdU (Figure 4.14B). Samples were obtained from 4, 8 and 14 hours post-thymidine release to represent S, early G2 and G1 populations of cells respectively, as well as asynchronous cells and stalled cells (0h) as controls. Figure 4.14C shows that phosphorylation generally appears consistent across these cell cycle stages.

Additionally, to verify initial data that suggested nocodazole treatment led to an increase in S499 phosphorylation, cells were treated with 4 mM thymidine, 1 μM nocodazole or 1 μM BI2536, a PLK1 inhibitor, for 16 hours. Nocodazole and BI2536 treatment fully stalled cells in mitosis, while thymidine stalled cells at the G1/S border and was included to provide a control for cell cycle stalling outside of mitosis. After both BI2536 and nocodazole treatment, PrimPol migrated as a single higher mobility band as evaluated by western blotting, indicative of total S499 phosphorylation (Figure 4.14D). However, protein from cells subject to thymidine stalling remained as two bands, indicating this migration was specific to mitotic stalling, but not specific to nocodazole treatment.

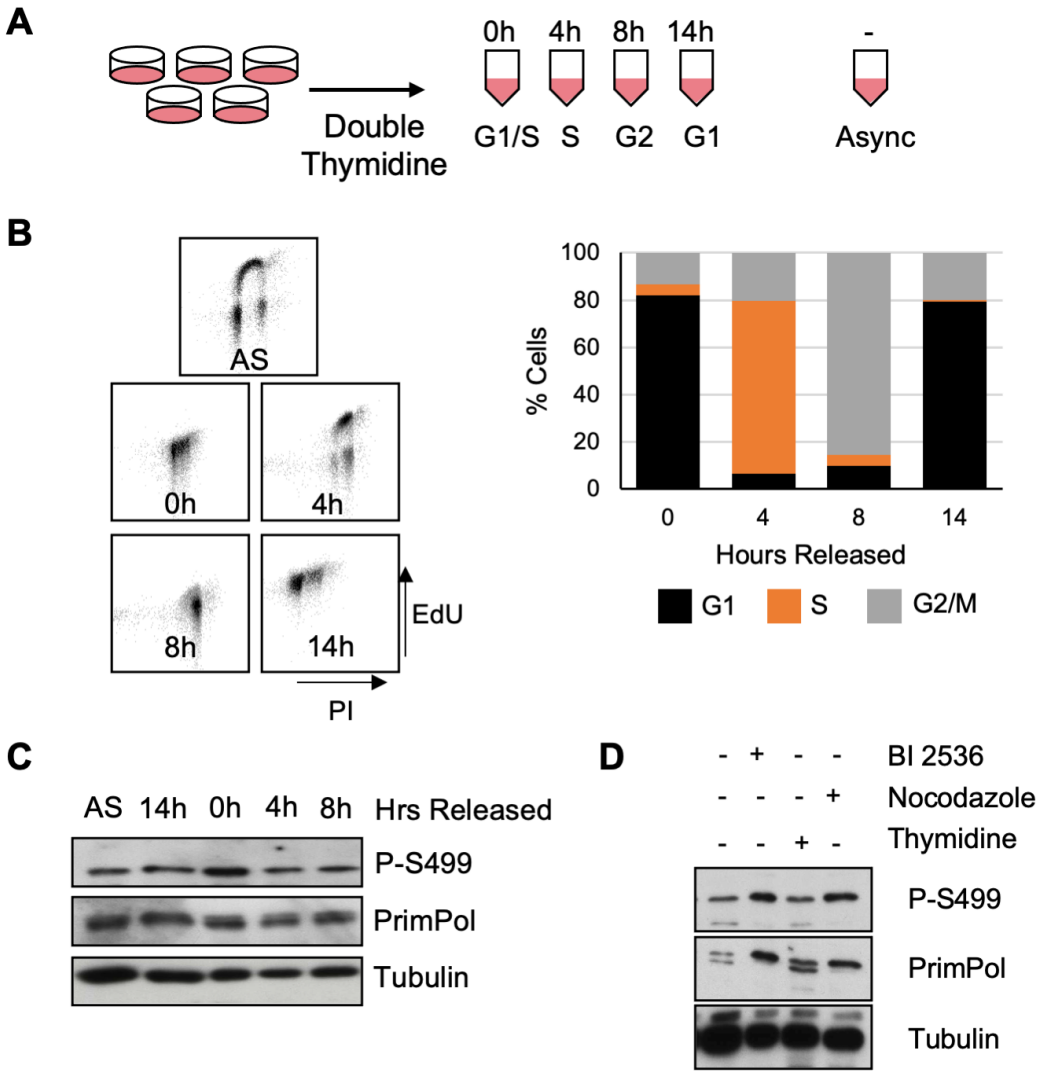

Figure 4.14. Phosphorylation of PrimPol throughout the cell cycle, and after mitotic stalling

A. A schematic describing the experimental protocol. Cells were stalled by 4mM thymidine at the G1/S boundary, before being released into fresh media. Samples were taken at defined timepoints for FACS and western blot analysis. AS is an asynchronous control. **B.** FACS profile and quantification of FACS from asynchronous cells and cells from defined timepoints. **C.** Western blot analysis of protein at defined timepoints post-thymidine release. **D.** Cells were treated with 1 μM BI2536 or 1 μM nocodazole to induce mitotic stalling, or 4 mM thymidine to induce G1/S stalling, before being harvested and subject to western blot analysis using P-S499, PrimPol and tubulin antibodies.

We further investigated the phosphorylation of S499 in mitosis by stalling HEK-293 cells expressing WT PrimPol at G1/S with 4mM thymidine. We then released the cells and harvested them at defined timepoints between 0-12 hours after release (Figure 4.15A). Nocodazole was present in the release media in order to stall cells in mitosis and prevent cell division. We analysed this thymidine release schedule to determine cell cycle distribution at each timepoint, using PI and EdU staining to detect G1, S and G2 cells (Figure 4.15B). As cells progressed through S phase into G2/M, there was both a visible increase in S499 phosphorylation, as detected by the p-S499 antibody, and a clear shift in the two bands of PrimPol. By 12 hours, PrimPol was appearing as a single band as opposed to the two equal bands observed at 0h (Figure 4.15C); as this band's size corresponded with upper of the two bands of PrimPol, this suggests PrimPol is entirely phosphorylated at S499 at 12 hours.

We additionally quantified the number of cells that had progressed into mitosis at the later timepoints, using PI and EdU staining in combination with staining for P-Histone H3, which is utilised as a mitotic marker as it indicates condensed chromosomes. Interestingly, at 12 hours, 27% of cells are still P-H3 negative, indicating they have not condensed their chromosomes. However, analysis of the doublet presentation of PrimPol by western blot (Figure 4.15C) shows that, at 12 hours, PrimPol protein is entirely S499 phosphorylated. This suggests that S499 phosphorylation occurs prior to chromosome condensation, likely in G2. This fits with the activity of CDK1, as it has been shown that CDK1 activity increases at the end of DNA replication (Lemmens et al., 2018).

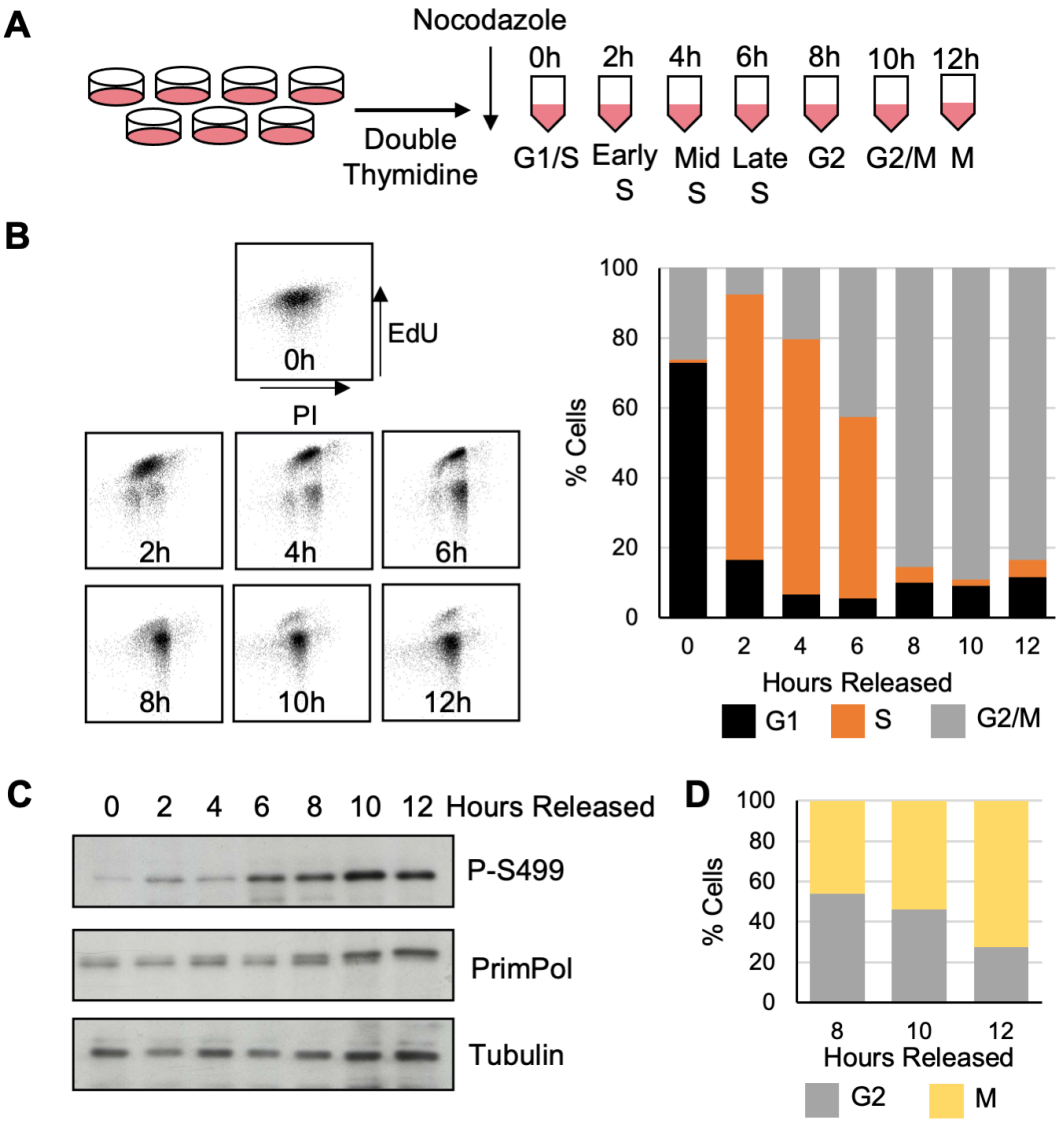

Figure 4.15. Phosphorylation of PrimPol S499 across S phase

A. A schematic describing the experimental protocol. Cells were stalled by 4 mM thymidine at the G1/S boundary, before being released into fresh media containing nocodazole to prevent mitotic exit. Samples were taken at defined timepoints for FACS and western blot analysis. **B.** FACS analysis of HEK-293 cells expressing WT PrimPol after thymidine release. Approximately 10,000 cells were analysed per sample. **C.** Western blot analysis of protein from HEK-293 cells expressing WT PrimPol. Samples from denoted timepoints were probed for P-S499, total PrimPol and tubulin. **D.** Cell cycle quantification of p-H3 positive undamaged cells was performed using FACs analysis at 8, 10 and 12 hours post thymidine release.

4.6.5 Dephosphorylation of PrimPol S499 after mitotic exit

As S499 phosphorylation was seen to increase dramatically during mitosis, we next investigated how this phosphorylation would change after mitotic exit. To assess this, cells were stalled for 16 hours with 1μM nocodazole before a mitotic shake-off was performed to obtain a mitotic population. Cells were then replated in media containing 4mM thymidine to prevent entry to S phase, and left to recover for 10 hours, with cells harvested every hour. Additionally, cells at the 0h, 2h and 6h timepoints were harvested for microscopy analysis to determine the effectiveness of the mitotic stall and release. Cells were classified as mitotic if they showed condensed chromosomes. Cells at the 0 hour timepoint were 84% mitotic, and this decreased to 14% by 6 hours (Figure 4.16B). Figure 4.16C shows western blot analysis of these samples. Phospho-H3 (S10) is utilised as a marker for mitosis, which decreases dramatically at 2 hours, and continues to decrease gradually until 10 hours. We next probed for S499 phosphorylated and total PrimPol protein on a low percentage gel (8%) to visualise the two bands of PrimPol, to see how they change across G1. Here we see that dephosphorylation is gradual, with 499 phosphorylation detectably decreasing until 6 hours before appearing to stabilise. While the blot of total PrimPol protein is not clear enough to closely examin the two bands of PrimPol across each timepoint, the lower band of PrimPol is detectable only 1 hour after nocodazole release, indicating a percentage of protein has been dephosphorylated at S499 (Figure 4.16C).

Based on the rapid reappearance of the lower band of PrimPol, we hypothesised that entry to G1 – where CDK1 levels are crucially very low to allow for pre-RC formation – leads to dephosphorylation of S499 by a phosphatase. Based on consistent PrimPol protein levels and previous work suggesting consistent mRNA levels (Mourón et al., 2013), it is unlikely the appearance of the lower band represents a sudden degradation of phosphorylated protein and resynthesis of new, unphosphorylated protein.

These findings highlight an important outstanding question. If we hypothesise that dephosphorylation of S499 occurs during mitotic exit/entry to G1, partly due to activity of a phosphatase and partly due to low CDK1 levels, we could anticipate that as cells progress to the G1/S border, phosphorylation would continue to

decrease. However, interestingly, full dephosphorylation does not occur. Instead, the cells quickly return to the approximately equal, 1:1 ratio of each isoform of PrimPol, and S499 signal stabilises. It is not clear what the importance of these two isoforms is, but as both are carefully maintained before the onset of S phase, it is implied both are required for full functionality of PrimPol during replication.

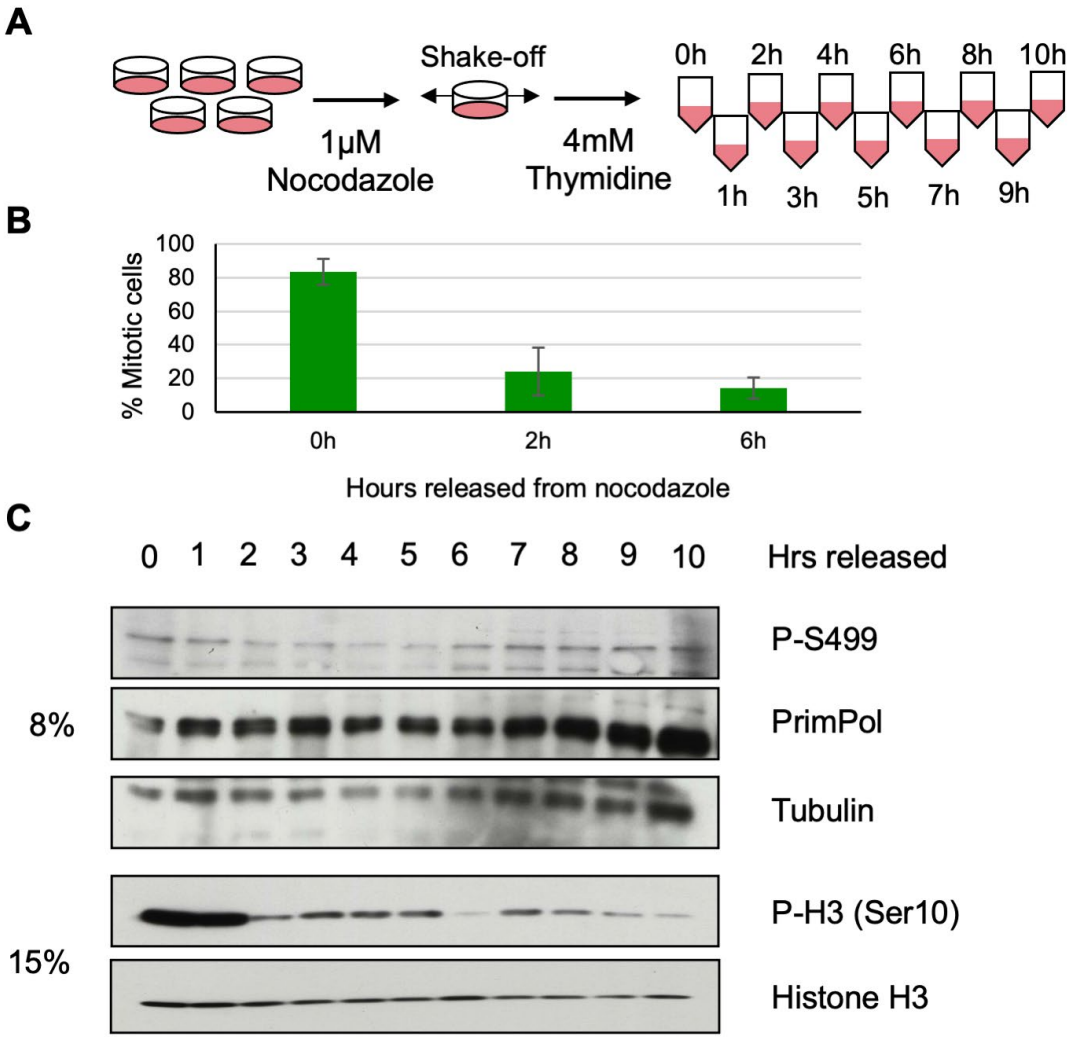

Figure 4.16. PrimPol S499 phosphorylation decreases, but does not disappear, as cells exit mitosis and progress through G1

A. A schematic describing the experimental protocol. Cells were stalled by 1μM nocodazole to anaphase, before being released into fresh media containing 4mM thymidine to prevent DNA replication. Samples were taken at defined timepoints for western blot analysis. **B.** Quantification of % mitotic cells from populations harvested at 0, 2 and 6 hours post nocodazole release. **C.** Western blot analysis of protein from HEK-293 cells expressing WT PrimPol, released from nocodazole synchronisation in mitosis for defined periods before harvest. Protein was probed with antibodies to P-S499, PrimPol and tubulin (8%), or P-H3 (S10) and total H3 (15%).

4.6.6 DNA damage during S phase does not induce a significant increase in PrimPol S499 phosphorylation

We hypothesised the increase in S499 phosphorylation detected in UV damaged asynchronous cells may be due to an increase in cells in G2. To clarify this, and specifically determine if any changes occurred in S phase, when PrimPol is primarily utilised, cells were synchronised by double thymidine to obtain a population stalled G1/S border. Cells were then released into S phase before damage was applied. Cells were released and harvested at defined timepoints: when damage was applied at 2 and 4 hours, they were harvested every two hours until 12 hours post-thymidine release, but when damage was applied six hours after thymidine release, an additional harvest 1 hour after damage was added.

When cells were treated with 20 J/m^2 UV-C damage two hours after release, at which point we hypothesised cells would largely be in early S phase, the completion of S phase and exit into G2 was delayed compared to undamaged cells (Figure 4.19C, right panel). The application of this damage also somewhat delayed the phosphorylation of S499, but an increase did occur. We hypothesised this was due to a delay in the cell cycle, as progression from two bands to one single, upper band indicative of mitosis was also prevented.

We also performed the UV-C treatment 4 and 6 hours after thymidine release, to damage cells in mid and late S phase respectively. This delay appeared to prevent the increase in S499 phosphorylation as detected by the phospho-specific antibody (Figure 4.19). UV-C damage 4 hours after release did not substantially impact the phosphorylation of S499 compared to undamaged cells, though again it did appear to delay the progression of PrimPol to a single, upper band (Figure 4.19C). This can be explained by the significant percentage of cells still replicating (37%).

UV damage applied 6 hours after release from thymidine, when 37% of cells were replicating (Figure 4.19E), did not significantly stall the cell cycle, and S499 phosphorylation increased similarly to undamaged cells, with strong detectable signal at 12 hours and a shift to one single band, the size of the slower migrating isoform indicative of S499 phosphorylation (Figure 4.19E).

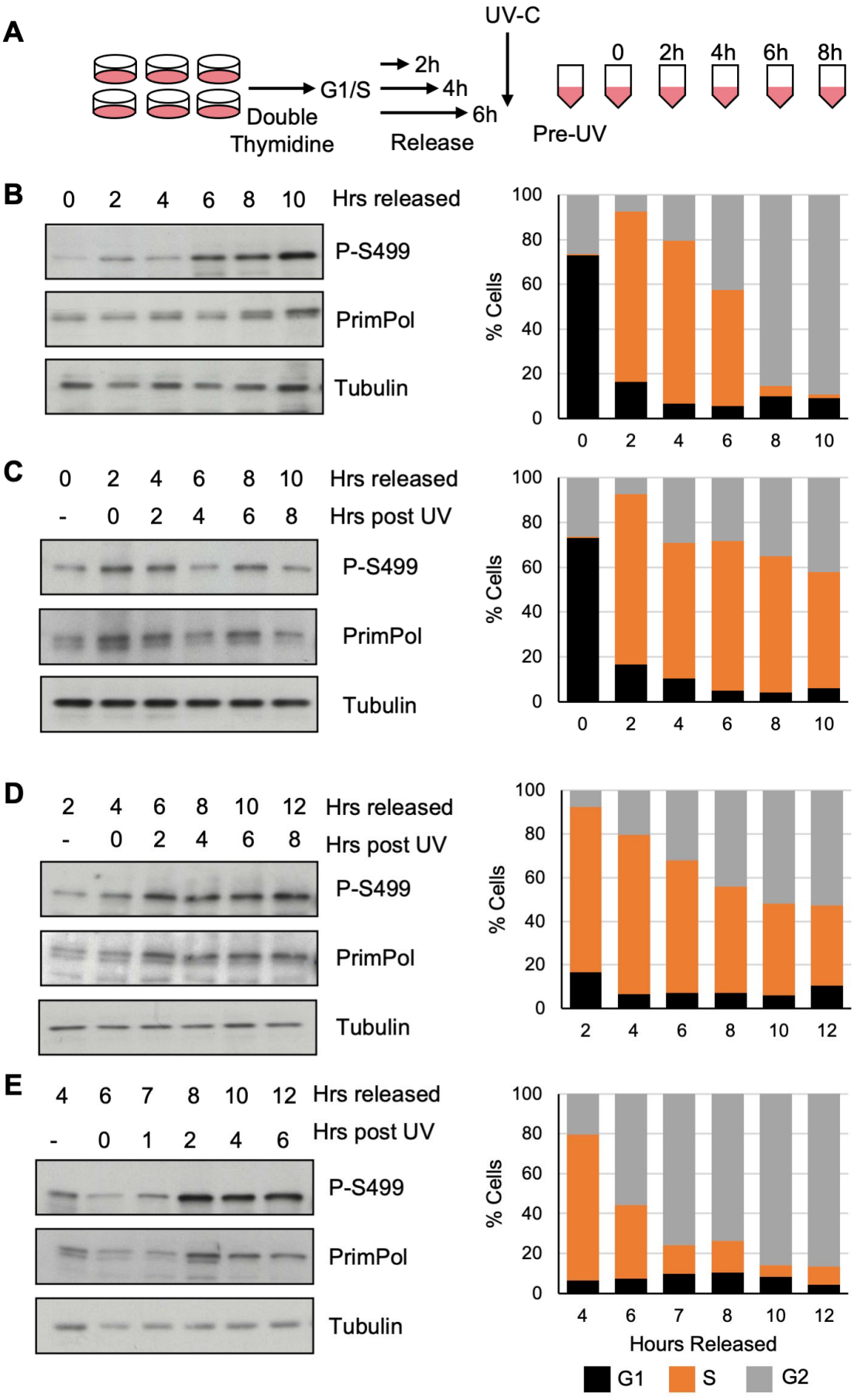
A
Double Thymidine
G1/S
2h
4h
6h
Release
UV-C
0
2h
4h
6h
8h
Pre-UV
B
0 2 4 6 8 10 Hrs released
P-S499
PrimPol
Tubulin
% Cells
C
0 2 4 6 8 10 Hrs released
- 0 2 4 6 8 Hrs post UV
P-S499
PrimPol
Tubulin
% Cells
D
2 4 6 8 10 12 Hrs released
- 0 2 4 6 8 Hrs post UV
P-S499
PrimPol
Tubulin
% Cells
E
4 6 7 8 10 12 Hrs released
- 0 1 2 4 6 Hrs post UV
P-S499
PrimPol
Tubulin
% Cells
Hours Released
G1
S
G2

Figure 4.17. UV-C damage in early and mid S phase delays PrimPol S499 phosphorylation, but has no effect when applied in late S phase

Western blot analysis of protein from HEK-293 cells expressing WT PrimPol; cells were released from thymidine block for two hours, **A**, four hours, **C**, or six hours, **E**, before being damaged by 20 J/m^2 UV-C and harvested at denoted timepoints. Samples probed for p-S499, total PrimPol and tubulin. **B,D,F** Cell cycle quantification of samples from each timepoint after damage by UV-C.

4.6.7 Mutating the zinc finger region of PrimPol prevents phosphorylation of S499

Previous work has shown that the primase activity of PrimPol is vitally important for its cellular functions. Mutating the zinc finger of PrimPol protein to render it primase inactive (ZnKO) does not complement several of the phenotypes of PrimPol$^{-/-}$ cells. For example, primase activity is required to restore replication fork rate after damage (Keen et al., 2014b), DNA replication restart after lesions or the incorporation of a chain terminating nuclear analogue (Kobayashi et al., 2016), or allow for fork recovery after UV or HU damage (Mourón et al., 2013).

To determine whether PrimPol's phosphorylation at S499 was dependent on its activity as a primase or polymerase enzyme, these activities were prevented through mutation as described before (3.6). PrimPol mutated to be primase inactive (ZnKO, C419A / H426A) or polymerase inactive (AxA, D114A / E116A) was purified from HEK-293 cells and subject to western blotting. Wild type protein was compared to AxA protein and ZnKO protein and probed for S499 phosphorylation and total PrimPol protein and the protein assessed for phosphorylation by western blot, using the antibody specific to phosphorylated S499. AxA protein maintained its two-band appearance, indicating that a proportion of PrimPol protein is phosphorylated at S499. However, ZnKO protein was not phosphorylated at S499 and was detected predominately as a single band (Figure 4.18A). Protein expression levels also appeared to decrease after the ZnKO mutations, suggesting a decrease in protein stability.

Previous work conducted during investigation of HEK-293 PrimPol$^{-/-}$ cells and their phenotypes found that cells over-expressing primase-deficient PrimPol were no more sensitive to UV-C damage than PrimPol$^{-/-}$ cells, or cells expressing WT PrimPol (Figure 4.18B, ZnKO data obtained by L. Bailey). While it is tempting to speculate that toxicity induced by S499 mutation may be related to primase activity, a full examination of the protein stability of ZnKO mutant PrimPol should first be performed, to determine if the absence of a phenotype is due to unstable protein. Future work could also examine if mutation of the zinc finger domain alleviates the phenotypes induced by S499 mutation.

We considered that S499 phosphorylation may still occur during repriming, and therefore be dependent on DNA or chromatin binding, nucleotide engagement or the process of dissociation. If this was the case, then mutation of the zinc finger may prevent these processes and therefore abolish S499 phosphorylation. We therefore tested PrimPol protein mutated to no longer bind RPA (RAB), hypothesising that abrogating RPA association – which would in turn prevent any of the steps of a priming reaction – may also block S499 phosphorylation. RAB protein showed detectable S499 phosphorylation, and two bands of PrimPol were clearly observable, indicating that S499 phosphorylation is not dependent on prior RPA binding (Figure 4.18C).

Finally we speculated that there may be a link between the phosphorylation of S499, which we have shown to be regulated by the cell cycle, to the phosphorylation of S538 of PrimPol (Chapter 3), given the similarities between the strong cell cycle regulation and the phenotypes observed in mutant cells. This theory would suggest that S499 phosphorylation by CDK1 may be a priming phosphorylation for subsequent PLK1 phosphorylation, or vis versa. However, the mutant cells unable to phosphorylate S499 were still positive for S538 phosphorylation, and cells unable to phosphorylate S538 were positive for S499 phosphorylation, indicating neither were dependent on each other (Figure 4.18D).

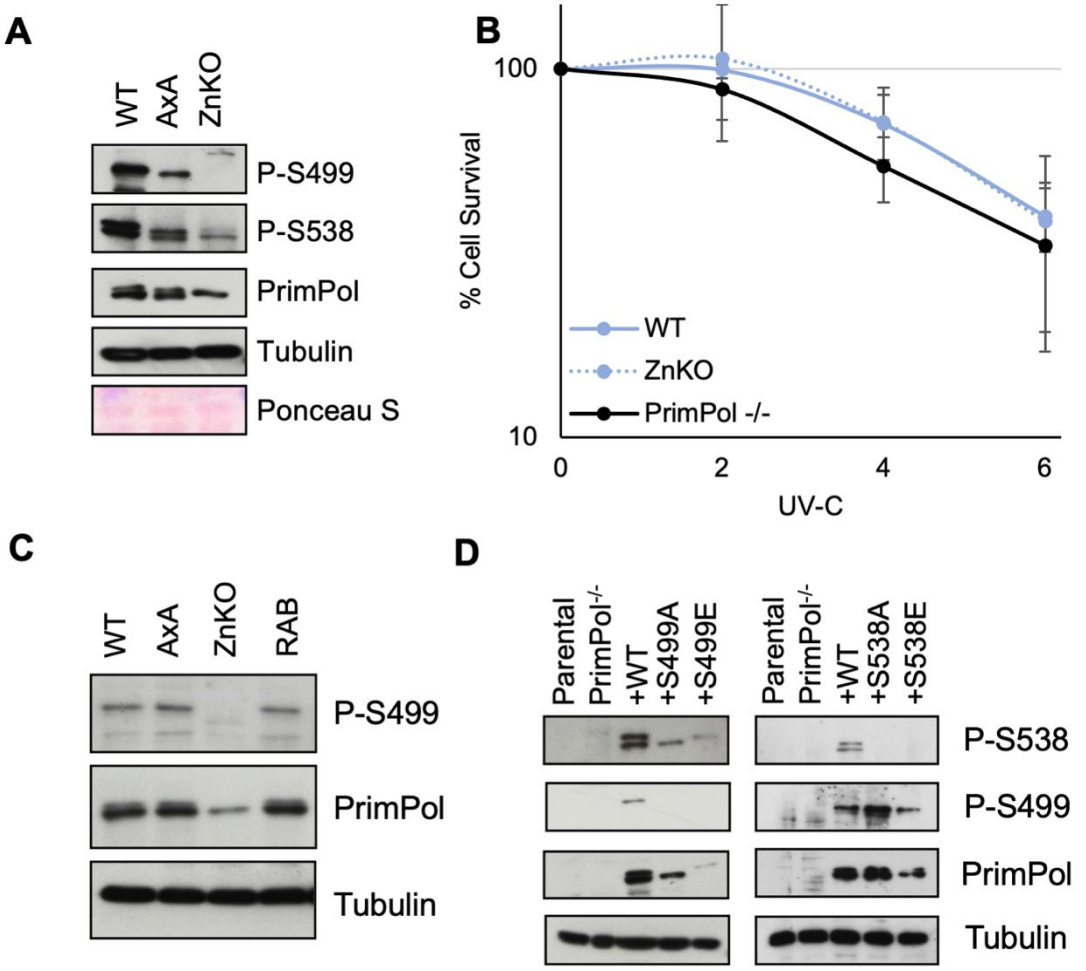

Figure 4.18. Mutation of the zinc finger domain of PrimPol to prevent primase activity disrupts the phosphorylation of S499 and decreases total PrimPol protein levels, but mutations to the catalytic domain and RPA binding domain have no effect

A. Western blot analysis of protein from HEK-293 PrimPol$^{-/-}$ cells expressing WT, AxA or ZnKO PrimPol, probed for P-S499, PrimPol and tubulin, with Ponceau provided as an additional loading control. **B.** Colony survival assays compared the sensitivity of PrimPol$^{-/-}$ cells expressing WT or ZnKO protein, or cells left uninduced (PrimPol$^{-/-}$) to increasing doses of UV-C damage. **C.** Western blot analysis of protein from HEK-293 PrimPol$^{-/-}$ cells expressing WT, AxA, ZnKO or RAB PrimPol, probed for P-S499, PrimPol and tubulin. **D.** Western blot analysis of protein from HEK-293 PrimPol$^{-/-}$ cells expressing WT, S499A or S499E PrimPol (left side), or S538A or S538E PrimPol (right side), probed for P-S499, P-S538, PrimPol and tubulin.

4.7 Discussion

4.7.1 Summary

Here, we have determined that phosphorylation of S499, a residue on PrimPol's C terminus, leads to the characteristic doublet appearance of the protein on SDS-PAGE gels. We have shown that multiple charged isoforms of PrimPol are observable in human cells, with many, but not all, dependent on the activity of kinase enzymes. The two bands of PrimPol, observed initially when detecting endogenous protein (S. Rudd and L. Bailey, unpublished work) are clearly observable when PrimPol is over-expressed, though the shift is obscured if PrimPol is tagged with a larger protein, such as GFP.

We have also described the impact of misregulation of S499 phosphorylation. To determine the importance of this site, we mutated it to either alanine (S499A) or glutamic acid (S499E) to serve as phospho-null or phospho-mimic substitutions, respectively. However, unlike S538 mutation, where only the phospho-null form induced toxicity (see Chapter 3), both 499 mutations appeared to introduce similar changes in survival. These include sensitivity to replication stress, induced by hydroxyurea, aphidicolin, camptothecin or olaparib, as well as indications of genomic instability including micronuclei and mitotic abnormalities. Additionally, while initially it appeared that mutation of S499 altered binding to chromatin, we also observed an increase in binding of RPA70 to chromatin in cells expressing S499E. It is therefore possible that S499E protein may itself contribute to replication stress, leading to increased or prolonged fork stalling or delays to restart, generating greater stretches of ssDNA as a result of helicase-polymerase uncoupling. The increase in S499E protein bound to chromatin in MRC-5 cells may have been induced by prolonged replication stress and continuous protein expression in these cells.

Additionally, we found that S499 phosphorylation itself is strongly regulated by the cell cycle, and that this phosphorylation is primarily mediated by the kinase CDK1. In G2 and mitosis, S499 phosphorylation increases, leading to PrimPol protein being fully phosphorylated at this site and presenting as a single (top) band. As PrimPol has no conclusive role in these stages of the cell cycle, it is

tempting to speculate that this phosphorylation is part of PrimPol's inactivation or sequestering. However, interestingly, dephosphorylation after mitosis is not complete, and instead, throughout both G1 and S phase, PrimPol is retained as two bands. Additionally, both isoforms are seen to bind chromatin, and there is no change in mutant protein binding during S phase, implying both isoforms are recruited to replication forks. With no direct effect on the protein's activity *in vitro*, (L. Bainbridge and A. Doherty, unpublished work) it is not yet clear what precise role this phosphorylation plays *in vivo.*

One caveat to consider here is the overexpression of PrimPol in the HEK-293 system. It is possible under unperturbed conditions, a regulatory system is in place that allows the two isoforms – protein phosphorylated at S499 and protein unphosphorylated at the same site – to perform fully separate functions or transition cleanly between the two forms. With PrimPol protein levels far in excess of endogenous levels, the cell may be unable to perform this regulation cleanly. However, endogenous PrimPol is still a doublet when run on low percentage SDS-PAGE gel (Martínez-Jiménez et al., 2018; Mourón et al., 2013), suggesting both isoforms are required and maintained even when protein levels are lower. Therefore, while more subtle shifts in protein phosphorylation may be difficult to ascertain using this system, the general ratio of isoforms appears to be maintained.

4.7.2 Differences and similarities between S499A and S499E.

Given the low levels of endogenous PrimPol protein in human cells, a system where the protein is overexpressed is required in order to allow for protein detection by western blot. It is worth noting, however, that endogenous PrimPol protein also presents as a doublet when run on low percentage SDS-PAGE gel (Martínez-Jiménez et al., 2018; Mourón et al., 2013), suggesting both S499 phospho-isoforms are required and maintained even when protein levels are lower.

The cell maintains both the unphosphorylated and phosphorylated isoforms of PrimPol throughout most of the cell cycle; of particular importance is the presence of both isoforms during replication, the cell cycle stage where PrimPol is surely

primarily utilised. However, expression of S499A or S499E, designed to mimic the expression of only one isoform, affects cell survival and genome stability. It is possible that both forms are required for damage tolerance during replication, potentially representing different active forms of PrimPol. For example, S499 phosphorylated protein is primase-active, while S499 unphosphorylated protein is only active as a TLS polymerase, or is entirely inactive. It is also possible that the protein transitions between phosphorylated and unphosphorylated, a transition that is impossible when either alanine or glutamic acid have been substituted at S499.

It is also possible that phosphorylation of S499 by CDK1 is only a priming phosphorylation, and subsequent phosphorylations depend on this. While S538 has been excluded from this, there are other potential nearby phosphorylation sites, such as S501. The role of S499 phosphorylation in priming for subsequent phosphorylation may lead to the similar phenotypes in S499A and S499E cells: as neither residue is a full copy of a phosphorylated serine, neither allow for further phosphorylation of the protein.

4.7.2.1 Cell line differences

It is interesting to hypothesise on the causes of the different phenotypes in the MRC-5 and HEK-293 cells after mutation of PrimPol S499. Some studies have worked to identify reasons for different replication stress responses across cell lines. Both p53 status and the expression levels of Lamin A/C have been implicated in altered stress responses (Lukášová et al., 2019), which could be measured in both HEK-293 and MRC-5 cells to determine if they are the cause of differences in sensitivity or protein recruitment. It may be worth studying phenotypes in another cell line, such as RPE-1, to determine which phenotypes are consistent. Overall, however, these discrepancies are minor, and may in fact be caused by the differences in protein expression methods: while the HEK-293 system is doxycycline inducible, MRC-5 cells constitutively express the protein. The high levels of S499E mutant PrimPol on chromatin after damage may reveal that protein accumulation builds up over time. It would not be detectable in the HEK-293 experiment because protein expression was induced a short time before damage induction and cell harvest.

4.7.3 PrimPol's activity and the toxicity of S499A and S499E expression

Mutation of the conserved active site metal binding residues D114 and E116, which form the DxE motif, ablate both primase and polymerase activity (Bianchi et al., 2013; García-Gómez et al., 2013). We utilised these mutations to examine the role of PrimPol's catalytic activity in regulating its post-translational modification. Chapter 3 first described the sensitivity induced by the AxA mutations: cells expressing this mutant protein showing decreased survival after UV-C damage and genotoxic stress. This sensitivity was independent of the sensitivity induced by S538A mutation, and introduced through separate mechanisms, as implied by the combined sensitivity of the double mutant (Chapter 3.6.3).

However, interestingly, we found that the addition of the AxA mutations to S499E mutant PrimPol increased survival after UV-C damage. This firstly suggests that abrogating PrimPol's catalytic activity can rescue toxicity related to S499E. Additionally, cells expressing both AxA and S499E were less sensitive to UV-C damage than either S499E or AxA alone. This indicates that mutation of S499 to glutamic acid can also rescue the toxicity of the AxA mutations. These results complicate our understanding of the S499E data and suggest that the mechanism by which S499E affects PrimPol's utilisation in cells prevents, directly or indirectly, AxA induced toxicity.

The cell lines expressing AxA and S499E provoke interesting questions about the overlap between post-translational modifications and the activity of PrimPol, and further studies are needed to clarify this. Additional characterisation, including survival assays in the presence of additional stressors and chromatin binding assays, may elucidate this further. The accumulation of RPA-bound ssDNA is a phenotype worth exploring further through IF analysis, to determine if an increase in replication stress can be attributed to the S499E mutant; if true, this would help expand our understanding of the role of post-translational modification of PrimPol, and the effects of its perturbation.

Additionally, we have shown that ZnKO mutant PrimPol protein is not phosphorylated at S499, while AxA and RAB mutant protein can be. It is possible

that this is due to the ZnKO mutations affecting the secondary structure of PrimPol: C419 and H426 are both positively charged residues which we mutate to alanine to abrogate primase activity; doing so may also change the folding of this region and may also affect protein stability. Without a crystal structure of this region, it is hard to predict what changes these mutations would induce, but it's possible that they alter the secondary structure or protein stability in such a way that CDK1 is no longer able to bind.

4.7.4 PrimPol S499, CDK1 and the cell cycle

The data presented in 4.6 suggests that regulation of S499 is controlled by both a phosphatase and a kinase, that this regulation strongly correlates with cell cycle stage, and that the kinase is CDK1. The role of CDK1 in the regulation of DNA repair processes is well studied, particularly in yeast, where it has been shown to control checkpoint activation, DNA end-resection and HR across multiple cell cycle stages (Ira et al., 2004). In human cells, however, its role during S phase is less clear. While its activity is lower during G1 and S phase, it is still playing an active role during replication, for example in regulating origin firing (Hochegger et al., 2007; Katsuno et al., 2009).

Our data shows that during G2/mitosis, S499 phosphorylation increases until all PrimPol protein becomes S499 phosphorylated, as indicated by the absence of a lower band. This remains throughout mitosis, likely due to high CDK1 activity (Lemmens et al., 2018). Shortly after (or possibly during) mitotic exit into G1, CDK1 activity is decreased due to the destruction of cyclins. At this point, dephosphorylation of PrimPol occurs. However, this dephosphorylation is only partial, and a subpopulation of phosphorylated PrimPol remains detectable by western blot. The doublet appearance of PrimPol is retained throughout G1 and into S phase. As cells progress through S phase, they remained detectable as two bands until G2, when they again become fully S499 phosphorylated. Interestingly, when cells have been stalled at the G1/S boundary for several hours, full dephosphorylation of S499 does not occur, suggesting that either some protein is sequestered and prevented from dephosphorylation, or that the minimal CDK activity found at the start of S phase is sufficient to keep PrimPol partially phosphorylated. Further investigation is required to determine if this is

an artifact, potentially induced by overexpression of PrimPol protein. If partner proteins or defined recruitment pathways are required for timely and accurate regulation of S499 phosphorylation, they may be exhausted or depleted by the high PrimPol protein levels. This could be clarified by monitoring S499 phosphorylation of endogenous protein across the cell cycle, though current experimental limitations, such as the low sensitivity of the p-S499 antibody, prevent this.

It is additionally possible that a second kinase maintains S499 phosphorylation levels throughout G1 and S phase, though the absence of detectable phosphorylation after RO-3306 treatment suggests this kinase would have to be one of the targets of this inhibitor, which include CDK2 and CDK4 (Vassilev et al., 2006). It is essential, therefore, to verify that CDK1 phosphorylates this site, to perform further *in vivo* and *in vitro* experiments. A repeat of the *in vitro* kinase has been performed suggesting that CDK1 can phosphorylate S499 *in vitro* (L. Bailey, L. Bainbridge and A. Doherty, unpublished results). This does not preclude additional phosphorylation by another kinase in order to maintain phosphorylation in CDK1's absence. An additional level of verification is currently underway using CDK1-as cells, transfected to over-express PrimPol, to determine whether S499 phosphorylation is not detectable when CDK1 activity is inhibited.

4.7.5 Theoretical models for the role of PrimPol S499 phosphorylation

One potential model for the role of S499 phosphorylation of PrimPol is that this modification changes depending on the localisation of the protein (Figure 4.19A). Potentially, PrimPol's S499 phosphorylation may regulate import into the nucleus or mitochondria, both areas PrimPol has been shown to act (Bailey et al., 2019; Bianchi et al., 2013). This would explain the phenotypes of genomic instability when this modification is prevented, as it may prevent transport mechanisms vital to PrimPol's correct utilisation. However, as both bands of PrimPol and mutant S499 protein bind chromatin, it does not appear to directly control import into the nucleus. Little is known about PrimPol's role in the mitochondria: S499 phosphorylation may relate to this. While mitochondrial DNA replication is only partially linked to the cell cycle, mitochondrial replication initiation is strongly liked to DNA replication, occurring predominately during G1 and S phase alongside

high nucleotide levels (Chatre and Ricchetti, 2013). Potentially S499 phosphorylation prevents mitochondrial import outside of G1/S as part of the decrease in mitochondrial replication generally. Schematic depiction of this model is presented in Figure 4.19A.

Alternatively, PrimPol's modification at S499 may be one of the modifications required to render PrimPol primase-active. This model would explain the lack of S499 phosphorylation on primase-deficient protein, and the toxicity induced by the protein in cells, as recruiting protein that is both "overactive" as a primase or inactive entirely would likely be toxic to cells. Additionally, while entirely primase active PrimPol during G2 and mitosis may seem counterintuitive, it should be remembered that PrimPol is chromatin excluded during G2 (Mouron et al., 2013, Chapter 3). However, this model would also imply that a large proportion of PrimPol is kept primase-inactive during DNA replication, which, considering the low levels of endogenous protein, may be counterproductive. Further support for this model may be found by full characterisation of cells expressing zinc finger mutant PrimPol, to determine if they have similar phenotypes to S499A mutant cells, and in characterisation of the S499/ZnKO double mutant cells.

A possible alternative model is that the upper or lower bands of PrimPol may represent inactive or sequestered protein. Another protein which is visualised as multiple bands on low percentage western blot is CDK1, with the upper band representing protein phosphorylated at T14/Y15. Both bands are present across the cell cycle until mitosis, when the inhibitory phosphorylation is removed, and the protein presents as a single lower band. In this example, a proportion of the protein is kept inactive throughout the cell cycle as a regulatory mechanism to prevent premature mitotic entry (Coulonval et al., 2011). It is possible that inactivation of PrimPol by S499 phosphorylation occurs in tandem with S538 phosphorylation to deactivate PrimPol as the cells enter G2, and protein is reactivated after mitotic exit. Again, however, this implies a subsection of PrimPol is inactive throughout replication, even when protein is expressed at endogenous levels. A schematic depiction of this model is presented in Figure 4.19C.

The difficulty with compiling the data described in this chapter into a cohesive model is that the nature of the two bands and their maintenance throughout S

phase, coupled with the toxicity generated by the mutant protein, imply that both bands of PrimPol are essential. While the pattern of phosphorylation across the cell cycle lends itself to a model whereby one band of PrimPol is inactive, data from the mutant cell lines suggests neither band alone is sufficient for proper DNA damage tolerance during replication. One vital future experiment would determine whether S499 phosphorylation cycles throughout G1 and S phase, with repeated phosphorylation and dephosphorylation of the protein leading to the visible two bands of PrimPol. This final speculative model could be visualised using inhibitors to CDK1 and may imply that phosphorylation allows for template DNA binding or association with incoming nucleotides.

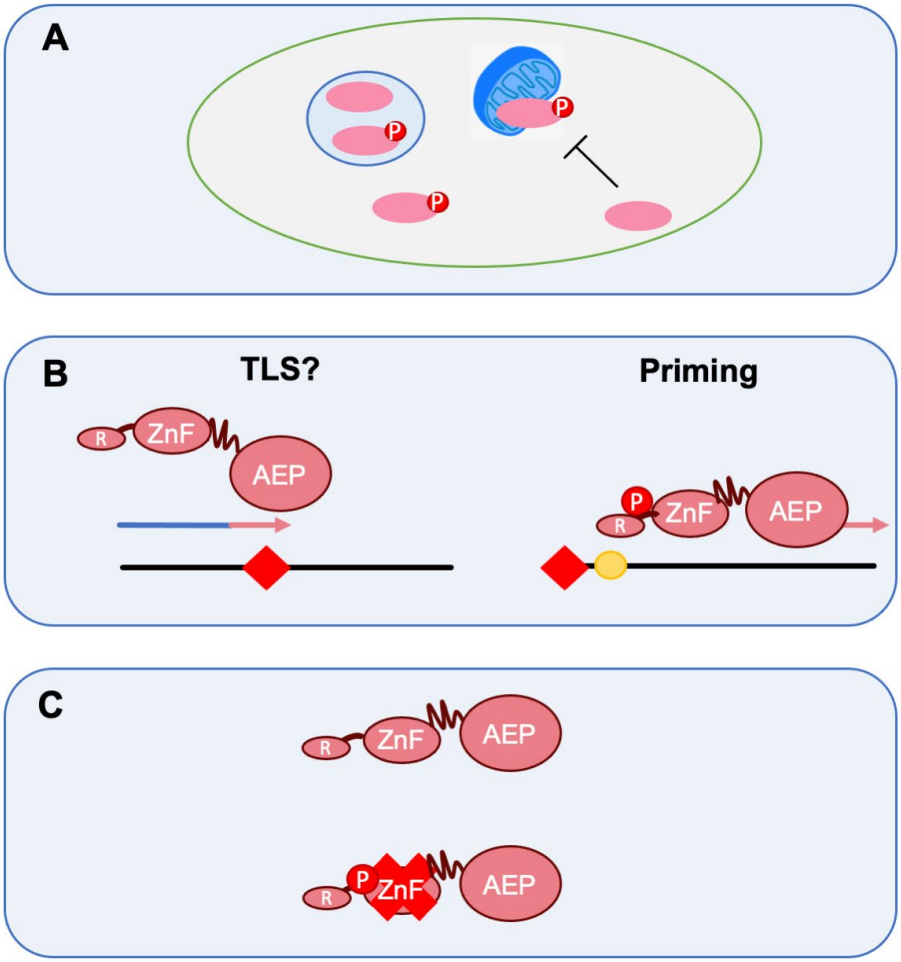

Figure 4.19. Potential models for the role of S499 phosphorylation in the regulation of PrimPol

A. Model 1: S499 phosphorylation controls cellular localisation of PrimPol, allowing transport to the mitochondria, or nuclear import. **B.** Model 2: S499 phosphorylation promotes primase activity of the protein. **C.** Model 3: Phosphorylation of S499 partially inactivates PrimPol through control over the zinc finger domain.

4.7.6 Further work

In addition to experiments to further explore sensitivity phenotypes identified in this chapter, an essential experiment for better understanding of S499 phosphorylation would be to identify the phosphatase enzyme responsible for dephosphorylating S499. While the mutant proteins allow for specific modification of this site without utilising inhibitors that would affect other proteins, control over the phosphorylation state of the protein in specific cell cycle stages, as opposed to complete deregulation, may be beneficial in elucidating the role of this phosphorylation. While difficult, work should also be performed to assess changes to the two bands of endogenous PrimPol across the cell cycle, as it may greatly differ from the overexpressed protein with respect to localisation or regulation.

Additional 2D gel electrophoresis, particularly on S499A and S499E mutant proteins, as well as protein treated with specific kinase inhibitors, would also elucidate exactly what isoforms of PrimPol are present during each cell cycle stage with greater clarity.

Overall, understanding of the role(s) of PrimPol S499 phosphorylation would also be improved by a more thorough examination of the exact genomic instability phenotypes generated by S499 mutant expression. For example, DNA fibre analysis and S1 nuclease assays would determine if both mutant forms of PrimPol are actually capable of repriming *in vivo*; while *in vitro* analysis showed that primase activity is unaffected (L. Bainbridge and A .Doherty, unpublished data), it is possible that the effect of S499 mutation *in vivo* does induce a change in activity. Other experimental approaches, such as iPOND, would allow for additional understanding of the modifications that allow PrimPol to be recruited to forks and determine if S499 mutation affects recruitment to active replication forks.

Additionally, it would be beneficial to examine the role of PrimPol and the S499 mutations in mitochondrial replication. The PrimPol S499 mutant cell lines are sensitive to stressors such as hydroxyurea (Chapter 4.4.3), aphidicolin (Chapter 4.4.4) and camptothecin (Chapter 4.4.6); while these drugs are often used to

induce nuclear replication stress, they would also stall mitochondrial replication, where PrimPol plays a somewhat elusive but key role (Bailey et al., 2019; Bailey and Doherty, 2017). Experiments in this chapter do not focus on the role of PrimPol in the mitochondria, but subsequent experiments could analyse the membrane potential of mitochondria, mitochondrial copy number or mitochondrial mutation rate, or utilise 2D gels to analyse mitochondrial replication directly, to determine the impact of PrimPol S499 mutation.

Finally, further analysis of the precise role of WT PrimPol in response to replication stress generated by genotoxins such as camptothecin, olaparib and aphidicolin, as well as further study of the effect of nucleotide depletion, would aid in understanding the sensitivity induced by S499 mutation, as well as improve understanding of damage tolerance during replication overall.

Chapter 5
Generation of tools to study PrimPol in RPE-1 cells

5.1 Introduction

Previous work on the phenotypes of PrimPol$^{-/-}$ cell lines has shown that - while they do not show overt sensitivity, as indicated by the minimal changes in cell survival - there are phenotypes that indicate replication in the absence of PrimPol leads to genomic instability. As RPE-1 cells are an immortalised, near “normal” diploid cell line, they are a good model to study the role of PrimPol, and a good candidate for genome editing. In this chapter, we utilised CRISPR-Cas9 genome editing to edit the PrimPol gene in the RPE-1 cell line, preventing protein expression and generating several knockout clones for analysis and characterisation. The generation of an RPE-1 PrimPol$^{-/-}$ cell line additionally allowed for the creation and preliminary characterisation of RPE-1 cells overexpressing WT, S538A and S538E mutant PrimPol, to allow for future experiments verifying phenotypes observed in the HEK-293 cells (Chapter 3).

Extensive previous study of PrimPol, conducted by the Doherty lab and others, has utilised systems where PrimPol protein is overexpressed. PrimPol is endogenously expressed in particularly low amounts within cells, which makes it difficult to detect by either western blot or immunofluorescence at endogenous levels (Beck et al., 2011). Overexpression of PrimPol allows for better visualisation by microscopy and circumvents issues with protein detection by commercial antibodies. In addition, our work on PrimPol’s regulation by phosphorylation suggests that the cell can correctly regulatee overexpressed PrimPol protein as it does endogenous protein, to prevent toxicity. Exogenous overexpression allows for the speedy analysis of mutant PrimPol proteins without having to undertake both genome editing and extensive screening. Additionally, systems such as the T-REx system where the promoter is doxycycline controlled allows for inducible protein expression; this is particularly important when working with mutant forms that disrupt genomic stability and can lead to poor cell survival.

This research has yielded crucial information on the role of PrimPol within cells. To supplement this work, we endeavoured to generate a novel cell line expressing fluorescent tagged PrimPol under its endogenous promoter, combining the effectiveness of tagged visualisation with the ability to better detect protein recruitment and dissociation more readily, as well as nuclear import and

export dynamics. We generated a cell line with a Clover-GFP tag at PrimPol's endogenous promoter as a tool for future analysis of PrimPol's distribution and dynamics within the cell.

5.2 Generation of RPE PrimPol$^{-/-}$ cell lines

RPE-1 cells were kindly gifted by Dr Helfrid Hochegger (University of Sussex). These cells were genetically modified to remove the puromycin selection cassette that is present in hTERT RPE-1 cells (N. Hégarat and H. Hochegger, unpublished data). PrimPol was knocked out of these cells using the Synthego Gene Knockout Kit v2. This kit provides 3 coordinated guideRNAs within the protein of interest that lead to the disruption of the genetic sequence by large fragment deletion, preventing protein production (Figure 5.1A). The three guideRNAs, listed in a table in Figure 5.1B, were targeted to Exon 7 of PrimPol. The ATG of PrimPol is within Exon 3. Exon 7 is the region downstream of the AEP of PrimPol, prior to the zinc finger.

RPE-1 cells were co-transfected with gRNAs and Cas9 nuclease at a ratio of 9:1 and left for 72 hours to grow in a 37°C incubator. 72 hours later, cells were trypsinised and plated as single cells in a 96 well plate and left for 2-3 weeks. A pool population was also grown for early analysis. PCR was performed around the region where the gRNAs were designed to cut. Figure 5.1C shows analysis of a pool population of cells treated with the guideRNAs, compared to a control population. The presence of several smaller bands indicates that the analysed region has been cut by the guides and been repaired with sections missing. Based on this, we concluded that the guideRNAs were effective in editing this region and continued with clonal isolation.

Viable, single cell clone lines were expanded until reaching approximately $1x10^5$ cells and were then harvested for genomic DNA isolation. PCR screening of these clones indicated several had homozygous deletions (Figure 5.1D, 1 and 2), while some had heterozygous deletions(H). Subsequent sequencing was performed by Eurofins SupremeRun and analysed using Synthego ICE Analysis (Hsiau et al., 2018). Results from this analysis are described in Figure 5.1E; Of the six clones with a 100% knockout (KO) score, two clones (Clone 1 and Clone 2) were taken

forward for initial analysis, with their characterisation forming the basis of this chapter. These clones each had large deletions of 149 base pairs, knocking out amino acids 199-248. Four clones were excluded for either slow or abnormal doubling times or sensitivity to passage, or were simply frozen down without further analysis.

Detecting endogenous PrimPol protein by western blot is particularly difficult, with the low levels of endogenous protein falling below most antibodies detection thresholds. However, we were able to visualise the characteristic two bands of PrimPol in parental cells by western blot and confirmed that the cell lines did not show detectable PrimPol protein (Figure 5.1F). This, combined with the sequencing results and PCR, made us confident these clones were PrimPol$^{-/-}$.

A

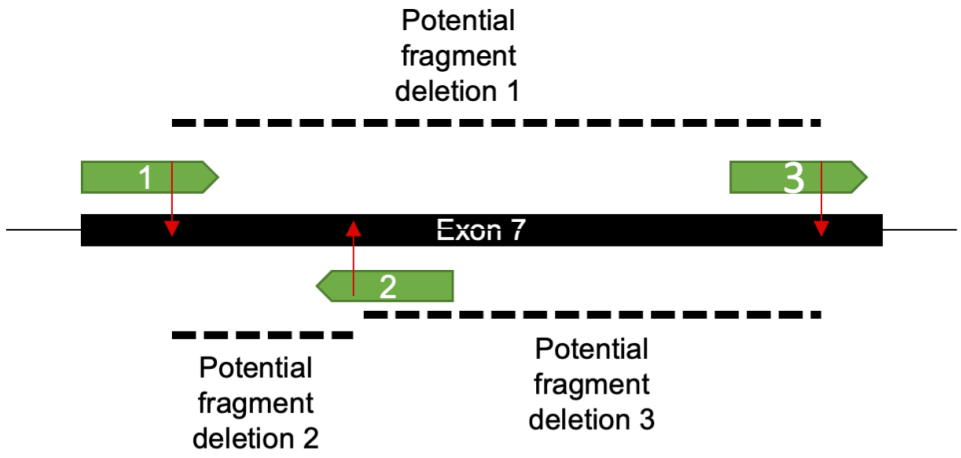

B

Name	GuideRNA Sequence
Synthego Guide 1	CCTGCTCTTGACTTGCT
Synthego Guide 2	CAGGTGCTTCTGAAAAA
Synthego Guide 3	ATCGAATTCAAAGAAAC

C

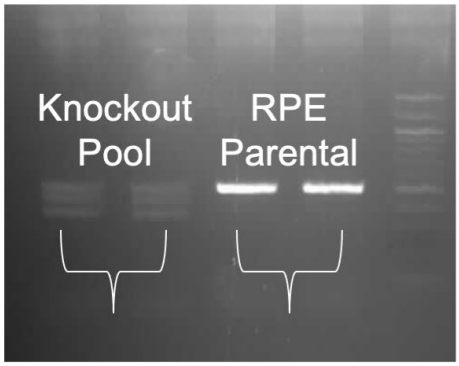

D

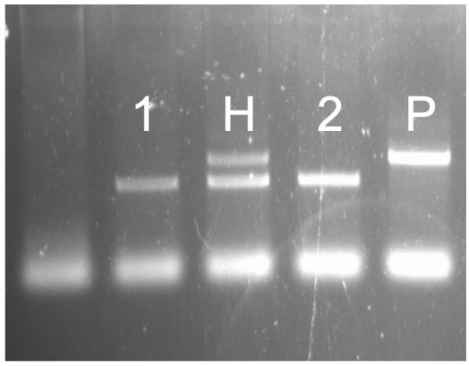

E

Label	ICE	KO-Score	ICE d	R Squared
Clone 1	100	100	98	1
Clone 2	100	100	98	1
Clone 3	45	41	99	0.45
Clone 4	99	99	100	0.99
Clone 5	82	78	100	0.82
Clone 6	100	100	100	1
Clone 7	9	9	100	0.09
Clone 8	100	100	98	1
Clone 9	100	100	98	1
Clone 10	95	95	100	0.95
Clone 11	67	63	95	0.67
Clone 12	74	64	100	0.74
Clone 13	98	98	97	0.98
Clone 14	100	100	98	1

F

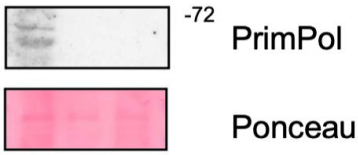

Figure 5.1. The generation of PrimPol$^{-/-}$ RPE-1 cells

A. A schematic describing the knockout method employed. Cells were transfected with multiple guideRNAs to Exon 7 of PrimPol to increase the efficiency. **B.** GuideRNAs targeted to Exon 7. **C.** PCR products from reactions performed on the genomic DNA of either a mixed knockout population, or control RPE parental cells, of a 1kb region within Exon 7 of PrimPol. **D.** PCR products from reactions performed on the genomic DNA of Clone 1 (1), Clone 2 (2) and a representative heterozygous clone and parental cell DNA as controls. **E.** Table showing knockout scores after ICE sequencing analysis. Green rows indicate Clone 1 and Clone 2, selected for further study. F. Western blot analysis of lysate from parental RPE-1 cells, Clone 1 and Clone 2. Protein was analysed with higher concentrations of PrimPol antibody than stated in Chapter 2 (1:500), with Ponceau stained membrane provided as protein loading control.

5.2.1 Generation of PrimPol$^{-/-}$ cells transfected to over-express WT PrimPol

As in previous experiments, we additionally generated a cell line over-expressing WT PrimPol. This was utilised to determine phenotypes observed in the RPE-1 PrimPol$^{-/-}$ cells could be reversed with the expression of PrimPol, and therefore that they were PrimPol specific and not generated by off-target effects of the guideRNAs. RPE-1 PrimPol$^{-/-}$ cell lines expressing PrimPol were generated using the Sleeping Beauty system. This system is comprised of the Sleeping Beauty transposase (SB100X) and a synthetic transposon plasmid vector, which contains the protein of interest flanked by two inverted terminal repeat sequences. This system leads to defined integration at particular loci, and allows for doxycycline inducible protein expression (Wu et al., 2016).

We initially generated cells overexpressing WT PrimPol, and verified that this was successful by inducing protein expression through the addition of doxycycline. Increasing concentrations of doxycycline were tested (Figure 5.2A) and in subsequent experiments, 500ng/ml doxycycline was utilised to induce protein expression, as it induced detectable levels of protein at similar levels to that induced by doxycycline in the HEK-293 cells.

5.3 Cellular phenotypes of RPE-1 PrimPol$^{-/-}$ cells

5.3.1 Micronuclei and abnormal mitosis in undamaged cells

To determine whether the absence of PrimPol induced genotoxic stress in RPE-1 cells, the number of micronuclei present was scored in WT parental RPE-1 cells and compared to the two PrimPol$^{-/-}$ clones. Presence of micronuclei is used to measure DNA lesions and genotoxicity, both prior to and after the addition of a DNA damaging compound (Luzhna et al., 2013). Initially cells were scored for micronuclei in undamaged conditions, where there was a significant increase in micronuclei in both PrimPol$^{-/-}$ clones, Clone 1 and 2, when compared to parental RPE-1 cells (Figure 5.2B). This increase was suppressed in both clones with the addition of WT PrimPol.

We additionally screened undamaged cells for the number of cells with hallmarks of abnormal mitosis, to determine whether this also increased alongside the number of cells with one or more micronuclei. We specifically analysed anaphase lagging chromosomes and anaphase bridging chromosomes, as they were the most common abnormal mitotic phenotype detected (Ganem and Pellman, 2012). To increase the percentage of cells undergoing mitosis when screened, cells were synchronised to mitosis using 500 nM nocodazole. Nocodazole synchronises RPE-1 cells to prometaphase with high efficiency (Scott et al., 2020). Cells were then released for 90 minutes to obtain an enhanced anaphase population, harvested and cytospun onto glass slides for analysis by microscopy. In this experiment, cells without PrimPol showed increased lagging or bridging chromosomes, and this was complemented by the addition of WT PrimPol (Figure 5.2C).

However, we considered that the number of abnormal mitotic cells may be partially inflated by the pre-treatment with nocodazole (Verdoodt et al., 1999). To verify that the PrimPol knockout cell line was not simply more sensitive to nocodazole treatment, we performed mitotic shake-off to isolate cells in mitosis from an unstalled population. While the overall number of cells undergoing abnormal mitosis decreased across all cell lines, there was still a statistically significant increase in the number of PrimPol$^{-/-}$ cells with lagging or bridging chromosomes (Figure 5.2D). This could be complemented by the over-expression of WT PrimPol, suggesting that presence of endogenous or overexpressed levels of PrimPol prevents accumulation of micronuclei, likely due to suppressing lagging chromosomes which go on to form them.

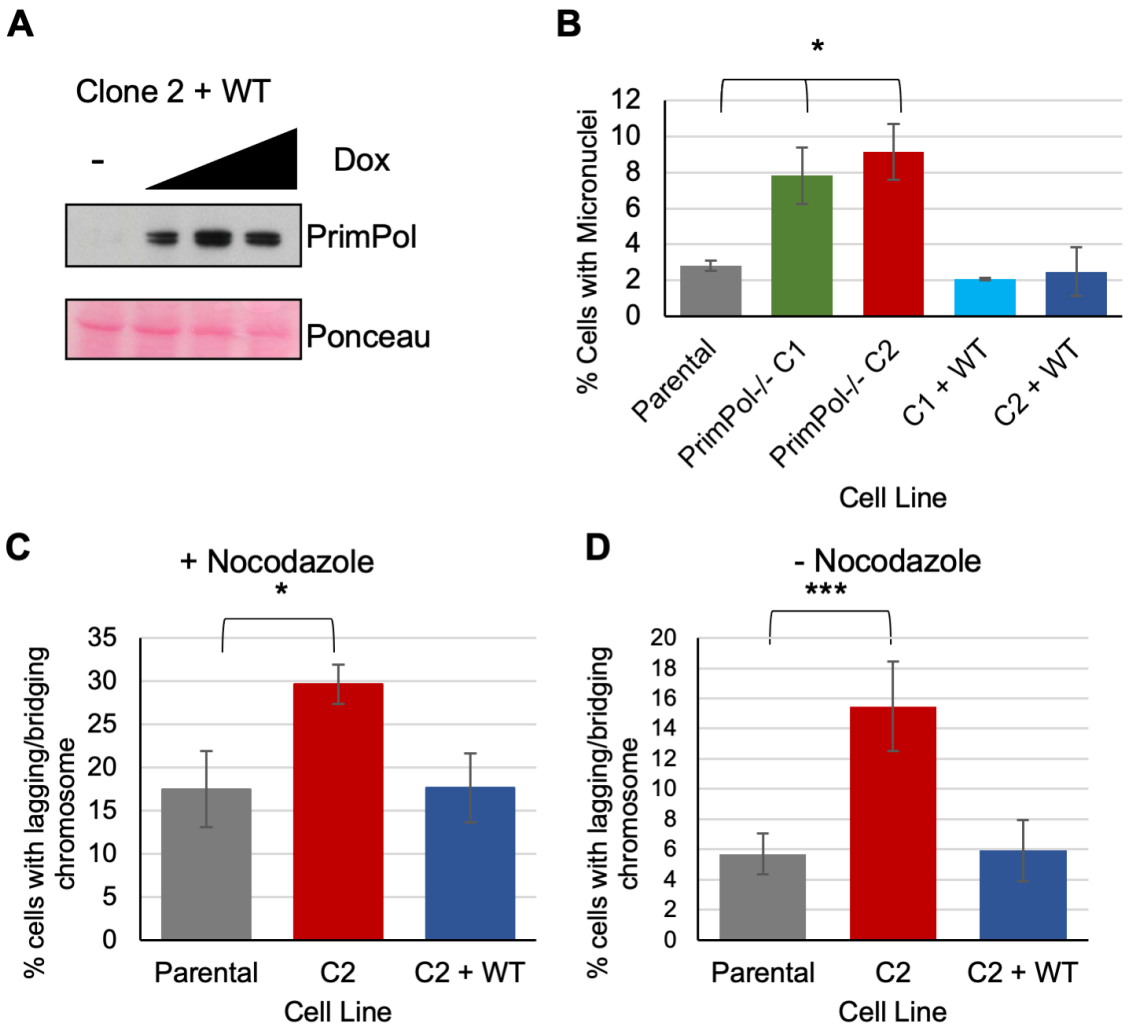

Figure 5.2. Evidence of mitotic abnormality in RPE-1 PrimPol$^{-/-}$ cells

A. Western blot of cell lysate from PrimPol $^{-/-}$ cells transfected to overexpress WT PrimPol. Cells were induced to express protein by increasing amounts (100,500 and 1000 ng/µl) doxycycline, or left uninduced, and lysate was probed with PrimPol and tubulin antibodies. **B.** Parental RPE-1 cells and RPE-1 PrimPol $^{-/-}$ cells with or without complementation with WT PrimPol, were counted 72 hours after plating (3 biological repeats with an n>400 cells). **C.** Parental RPE-1 cells and RPE-1 PrimPol $^{-/-}$ cells with or without complementation with WT PrimPol, were assessed for lagging chromosomes 90 minutes after nocodazole release (2 biological repeats, n>200). **D.** RPE-1 cells were assessed for lagging chromosomes (4 biological repeats, n>70).

5.3.2 Survival of RPE-1 PrimPol$^{-/-}$ cells after DNA damage

Previous work investigating the cellular response to the absence of repriming, performed in MRC-5 PrimPol knockout cells, has determined that while PrimPol is important for the bypass of UV-C damage, the absence of PrimPol does not induce significant UV sensitivity (Bailey et al., 2019). Additionally, loss of PrimPol in HEK-293 cells does not introduce overt UV-C sensitivity (L. Bailey and A. Doherty, unpublished data). We hypothesised that, as a cell line with a more normal karyotype, it may be possible to detect small survival changes in these cells in the absence of PrimPol.

In RPE-1 PrimPol$^{-/-}$ cells, we did see a significant UV-C sensitivity at 4 and 6J/m^2 (Figure 5.3A). This could be complemented by overexpression of WT PrimPol. This suggests that the RPE-1 cell lines may be more UV-C sensitive in the absence of PrimPol than either of the previously studied cell lines. Inherent cell line variability may explain this difference: it is possible that RPE-1 cells are increasingly dependent on repriming.

Similarly, damage by UV-C also increased the number of micronuclei in cells without PrimPol (Figure 5.3B), and this was complemented by overexpression of WT PrimPol, as described before in MRC-5 PrimPol$^{-/-}$ cells (Bailey et al., 2019).

5.3.3 Survival of PrimPol$^{-/-}$ cells after treatment with hydroxyurea

Additionally, PrimPol$^{-/-}$ Clone 2 was tested for sensitivity to high doses of hydroxyurea, a nucleotide depleting drug that stalls DNA replication. Previous evidence in this thesis has shown that cells overexpressing PrimPol protein are more likely to survive high doses of hydroxyurea than cells with endogenous levels, suggesting a role for increased PrimPol protein in recovery from fork stalling or collapse (Chapter 4). We additionally verified the same could be seen in RPE-1 cells. Interestingly, unlike HEK-293 cells, RPE-1 PrimPol$^{-/-}$ cells were sensitive to high doses of hydroxyurea. However, as before, the overexpression of WT Protein increased survival to above that of parental cells (Figure 5.3C).

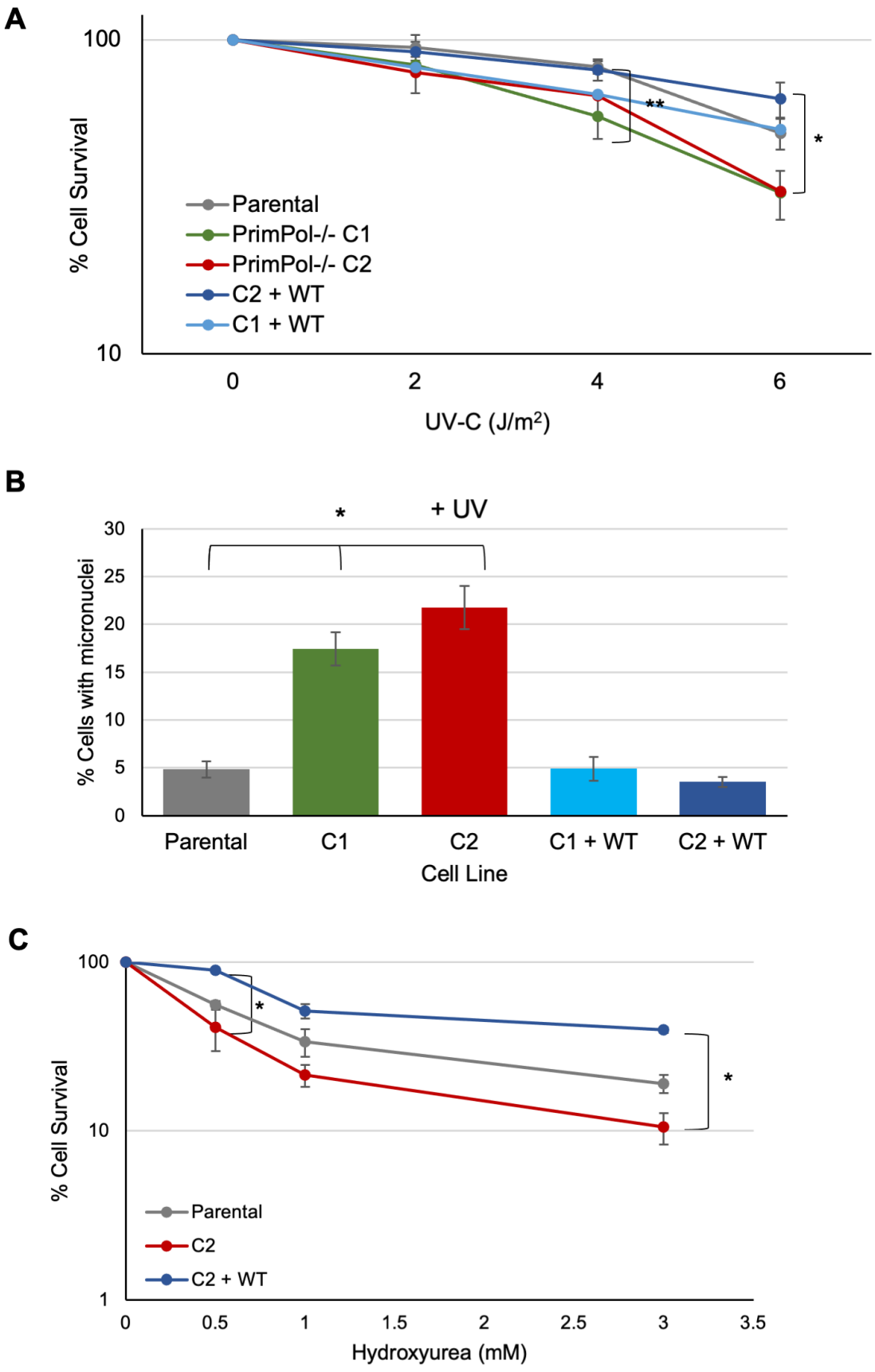

Figure 5.3. Survival of RPE-1 PrimPol$^{-/-}$ cells after DNA damage or replication stress

A. Colony survival assay measured sensitivity of RPE-1 parental cells, RPE-1 PrimPol$^{-/-}$ cells, or PrimPol$^{-/-}$ cells expressing WT PrimPol to increasing doses of UV-C damage. **B.** RPE-1 cells with 1 or more micronuclei were counted 72 hours after 5J/m^2 UV-C (3 biological repeats of n>400 cells). **C.** Colony survival assay measured sensitivity of RPE-1 parental cells, RPE-1 PrimPol$^{-/-}$ cells, or PrimPol$^{-/-}$ cells expressing WT PrimPol to increasing doses of hydroxyurea.

5.4 Phenotypes associated with expression of S538A mutant PrimPol are reproducible in RPE-1 cells

In Chapter 3, we described UV-C sensitivity phenotypes observed in the HEK-293 cells expressing S538A mutant PrimPol. These included increased micronuclei, and a decrease in survival after UV-C damage as measured by colony survival assays. RPE-1 PrimPol$^{-/-}$ cells were transfected with Sleeping Beauty vectors expressing PrimPol mutated at S538 to either alanine of glutamic acid (S538A and S538E) as before. Western blotting was performed to assess protein expression (Figure 5.4A), which verified that protein expressed in these cells was not bound by P-S538 antibody.

We performed colony survival assays in RPE-1 cells expressing WT, S538A or S538E mutant PrimPol to determine if the UV-C sensitivity phenotype was reproducible in another cell line. We found that S538A expression did induce a decrease in survival, greater than the sensitivity induced by the absence of PrimPol entirely (Figure 5.4C). S538E, as in HEK-293 cells, did not induce a change in survival. Cells expressing S538A also showed an increase in micronuclei in the absence of damage (Figure 5.4B).

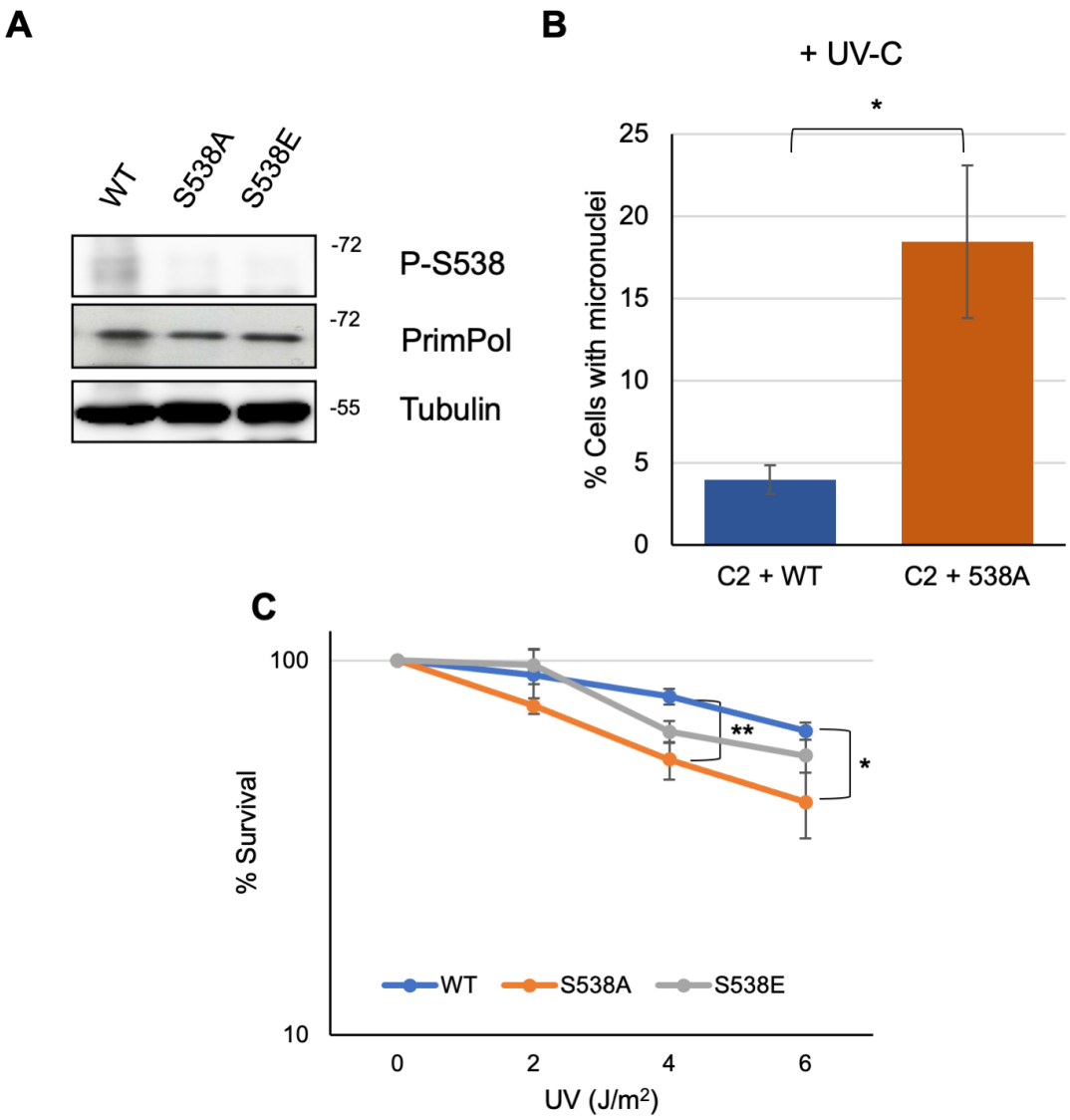

Figure 5.4. Phenotypes associated with PrimPol S538A expression are reproducible in RPE-1 cells

A. Western blot analysis of protein from RPE-1 PrimPol$^{-/-}$ cells transfected to express WT, S538A or S538E mutant PrimPol. Protein was probed with antibodies for P-S538, PrimPol and tubulin. **B.** RPE-1 PrimPol$^{-/-}$ cells expressing WT or S538A mutant PrimPol with 1 or more micronuclei were counted 72 hours after 5 J/m^2 UV-C (3 biological repeats of n>400 cells). **C.** Colony survival assay measured sensitivity of RPE-1 PrimPol$^{-/-}$ cells expressing WT, S538A or S538E mutant PrimPol to increasing doses of UV-C.

5.5 Generation of an RPE-1 cell line endogenously expressing GFP-tagged PrimPol

5.5.1 CRISPR-mediated tagging of endogenous PrimPol

When studying proteins with low expression, or mutant forms of a protein, it is beneficial to overexpress these proteins to aid in detection. Investigations into the role of PrimPol has thus far utilised overexpression techniques to study this lowly expressed protein. To aid in further investigation, we aimed to generate a cell line expressing GFP-tagged PrimPol at endogenous levels, as a tool to more precisely measure aspects such as recruitment and dissociation of the protein, in addition to triggers for nuclear import or export.

CRISPR-mediated gene knockout takes advantage of the NHEJ pathway (1.3.2.5). This pathway is active throughout the cell cycle and repairs double-strand breaks, such as those generated by Cas9 cutting, independent of a homologous template. This process can introduce indel mutations which in turn lead to gene knockout. An alternative mechanism of repair, which is exploited for knock-in, is homologous dependent repair (HDR). HDR can be used to introduce large exogenous sequences into genomic loci that then function as reporters for the activity or localisation of that protein (Roberts et al., 2017). This requires the presence of a donor template containing two regions of homology close to the cutting site, and only occurs in S phase or G2.

A vector was designed to introduce MClover3, a mutant form of GFP and one of the brightest fluorescent proteins (Campbell et al., 2018) at PrimPol's N-terminus. The donor vector contained two homology arms, homologous to 1kb regions before and after the start codon of PrimPol. In addition to the cDNA for PrimPol and the MClover3 tag, the vector also included a Neo/Kan resistance cassette under a PGK promoter.

The guideRNAs generated in tandem with the vector were inefficient at inducing cutting of the DNA (data not shown). However, the design of the vector's regions of homology, design to stretch 1kb close to the guideRNA's cutting site, meant that there were a small number of suitable guideRNAs available in intronic DNA.

As none of these guideRNA's cut efficiently, we generated a new set of guideRNAs which cut within Exon 3. We then mutated PrimPol within the donor vector so it was resistant to cutting by the guideRNA. While initial screening of these guideRNAs by surveyor assay did not show significant cutting by any guideRNA tested, one guideRNA (sequence in 2.2.3) was subsequently utilised to genetically modify the HEK-293 cells, generating large deletions in Exon 3 (Dr Laura Bailey, unpublished data). Therefore, this guideRNA was chosen for use in generating the endogenous tagged line. A schematic describing the experimental protocol is shown in Figure 5.5A.

To determine if the knock-in experiment was successful, multiple test PCRs were performed on clonal cell line genomic DNA. These tests utilised primers specific to PrimPol, MClover3 and the intronic region surrounding the integration site. Cell lines which indicated integration had occurred were then screened by FACS for GFP signal. However, the fluorescent signal from Clover expression under PrimPol's endogenous promoter was faint and led to a very small shift in fluorescence signal (Figure 5.5B). It was therefore not possible to use this technique to sort cells for successful integration.

After PCR determined that a clone contained the Clover-PrimPol construct integrated under PrimPol's endogenous promoter, western blotting was performed to determine if a GFP antibody would detect endogenous levels of PrimPol. Commercial antibodies to PrimPol are unable to detect endogenous PrimPol. Figure 5.5C shows that a band is present in the Clover-PrimPol cells at 100kDa, which is absent in both parental RPE cells and PrimPol$^{-/-}$ cells. We subsequently determined there were no overt phenotypes after this genomic editing, verifying there was no increase in micronuclei (Figure 5.5D) and no decrease in survival after UV-C damage (Figure 5.5E). Initial experiments were performed to determine whether endogenous PrimPol protein was detectable by microscopy and whether live cell or fixed imaging was optimal for PrimPol detection.

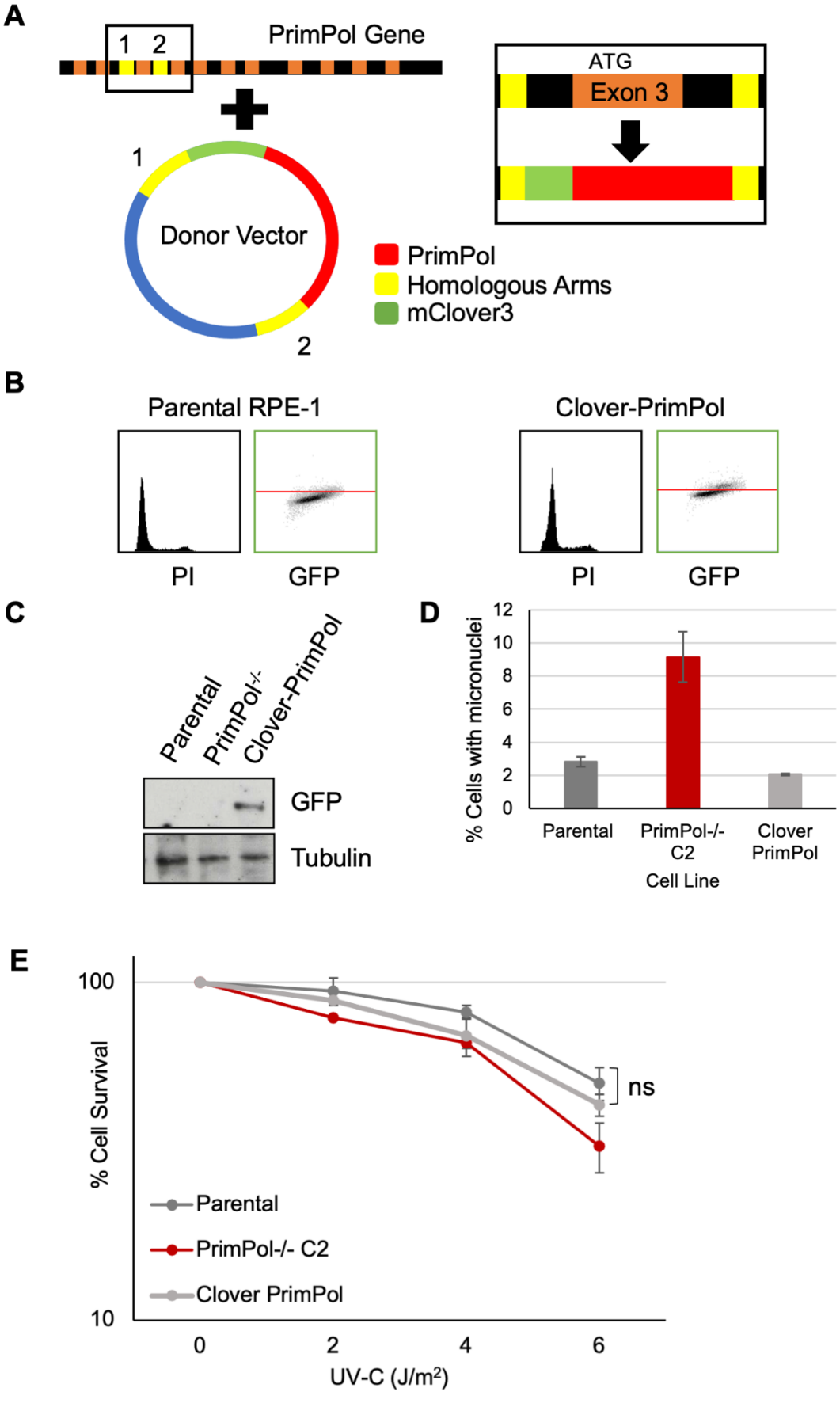
A
1 2
PrimPol Gene
1
Donor Vector
2
ATG
Exon 3
PrimPol
Homologous Arms
mClover3
B
Parental RPE-1
Clover-PrimPol
PI
GFP
PI
GFP
C
Parental
PrimPol-/-
Clover-PrimPol
GFP
Tubulin
D
% Cells with micronuclei
12
10
8
6
4
2
0
Parental
PrimPol-/- C2
Clover PrimPol
Cell Line
E
100
10
% Cell Survival
ns
Parental
PrimPol-/- C2
Clover PrimPol
0
2
4
6
UV-C (J/m2)

Figure 5.5. Generation of an RPE-1 cell line endogenously expressing fluorescently-tagged PrimPol

A. Schematic describing the experimental procedure for generating the endogenous tagged line. Parental RPE-1 cells were transfected with a guideRNA cloned into a Cas9 expression vector, which cut within the region of Exon 3 of PrimPol. Alongside this, cells were transfected with a donor vector containing two homology arms to the region surrounding the cut site, and Clover tagged PrimPol cDNA. **B.** FACS analysis of parental RPE-1 cells and Clover-PrimPol cells. Gates were applied to measure GFP fluorescence (FL1-A/FSC-A) and cells were stained with PI to determine DNA content. **C.** Western blot analysis of cell lysate from RPE-1 parental cells, PrimPol$^{-/-}$ cells (C2) and Clover-PrimPol RPE-1 cells, probed with GFP and tubulin antibodies. **D.** Parental RPE-1 cells, PrimPol$^{-/-}$ cells (C2) and Clover-PrimPol cells with 1 or more micronuclei were counted 72 hours after plating (3 biological repeats with an n>400 cells). **E.** Colony survival assay measured sensitivity of RPE-1 parental cells, RPE-1 PrimPol$^{-/-}$ cells, or Clover-PrimPol Cells to increasing doses of UV-C.

5.5.2 Detection of endogenous PrimPol protein through fixed and live cell microscopy

Initial work focused on determining whether endogenous levels of protein would be detectable by microscopy in the absence of antibodies or other detection agents. While using antibodies to endogenous PrimPol is possible, it is extremely difficult due in part to low specificity of these antibodies and difficulties detecting low amounts of protein. We initially fixed cells with either paraformaldehyde or methanol to determine if either method was preferable for visualisation of tagged protein. As seen in Figure 5.6A, both methods yielded adequate detection of Clover-PrimPol signal. Imaging was performed on the Zeiss LSM880 confocal microscope.

Additionally, the benefit of fluorescently tagged PrimPol is the option of tracking PrimPol by live cell imaging. Imaging cells on standard fluorescent microscopes such as an IX70 (Olympus) or an E400 (Nikon) was not possible, as the Clover-PrimPol signal was below the detection threshold. However, the Zeiss LSM880 confocal microscope was able to visualise cells with Clover-tagged PrimPol in cells. Representative images are shown below in Figure 5.6B. However, signal appeared much lower in live cell imaging in comparison to imaging after fixation, due to issues detecting adequate signal without bleaching the fluorescence.

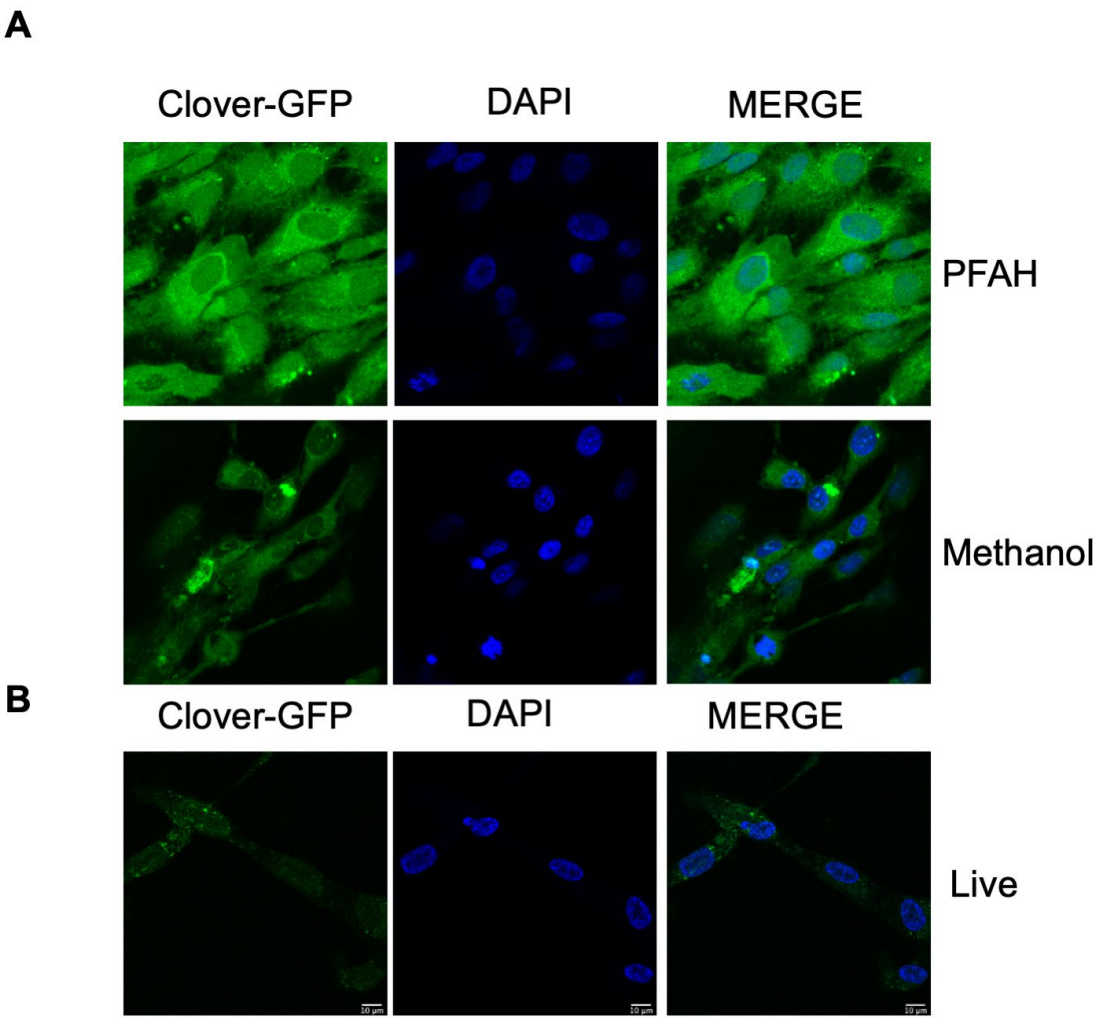

Figure 5.6. Detection of Clover-PrimPol signal by confocal microscopy

A. Representative images from microscopy analysis of RPE-1 Clover-PrimPol cells. Cells were fixed prior to analysis by either paraformaldehyde (upper panel) or 100% methanol (lower panel) and imaged on a Ziess LSM880 confocal microscope. **B.** Representative images from microscopy analysis of RPE-1 Clover-PrimPol cells. Cells were plated in CO_2-independent media and imaged on a Ziess LSM880 confocal microscope.

5.5.3 Fluorescently-tagged PrimPol does not visibly localise to the mitochondria in undamaged cells

To investigate the localisation of PrimPol to the mitochondria, cells were imaged in the presence of the mitochondrial stain Mitotracker Deep Red. Previous work has utilised cell fractionation experiments to determine that approximately 34% of PrimPol is found in the mitochondria in undamaged cells (García-Gómez et al., 2013), and that PrimPol mediated repriming is important, but not essential, for tolerance of replication stress and DNA damage and maintenance of normal DNA replication (Bailey et al., 2019; Torregrosa-Muñumer et al., 2017).

We investigated whether we could visualise endogenous levels of PrimPol protein localised to the mitochondria using our Clover-tagged cell line. We initially worked with fixed cells and could not visualise significant localisation to the mitochondria. We next tested co-localisation after 10 J/m^2 UV-C damage, and again did not see significant qualitative co-localisation, as visualised by yellow signal in images representing the presence of both Clover-PrimPol and red Mitotracker signal (Figure 5.7A). Due to the noise and background inherent to some fixed imaging, we next utilised the Mitotracker stain during live cell experiments. This reduced the background, but again, there was not significant qualitative co-localisation of signal (Figure 5.7B).

To determine whether the import to the mitochondria is affected by the Clover tag, future work will utilise cell fractionation techniques to obtain the mitochondrial fraction and use western blot analysis to determine that Clover-tagged protein can be detected.

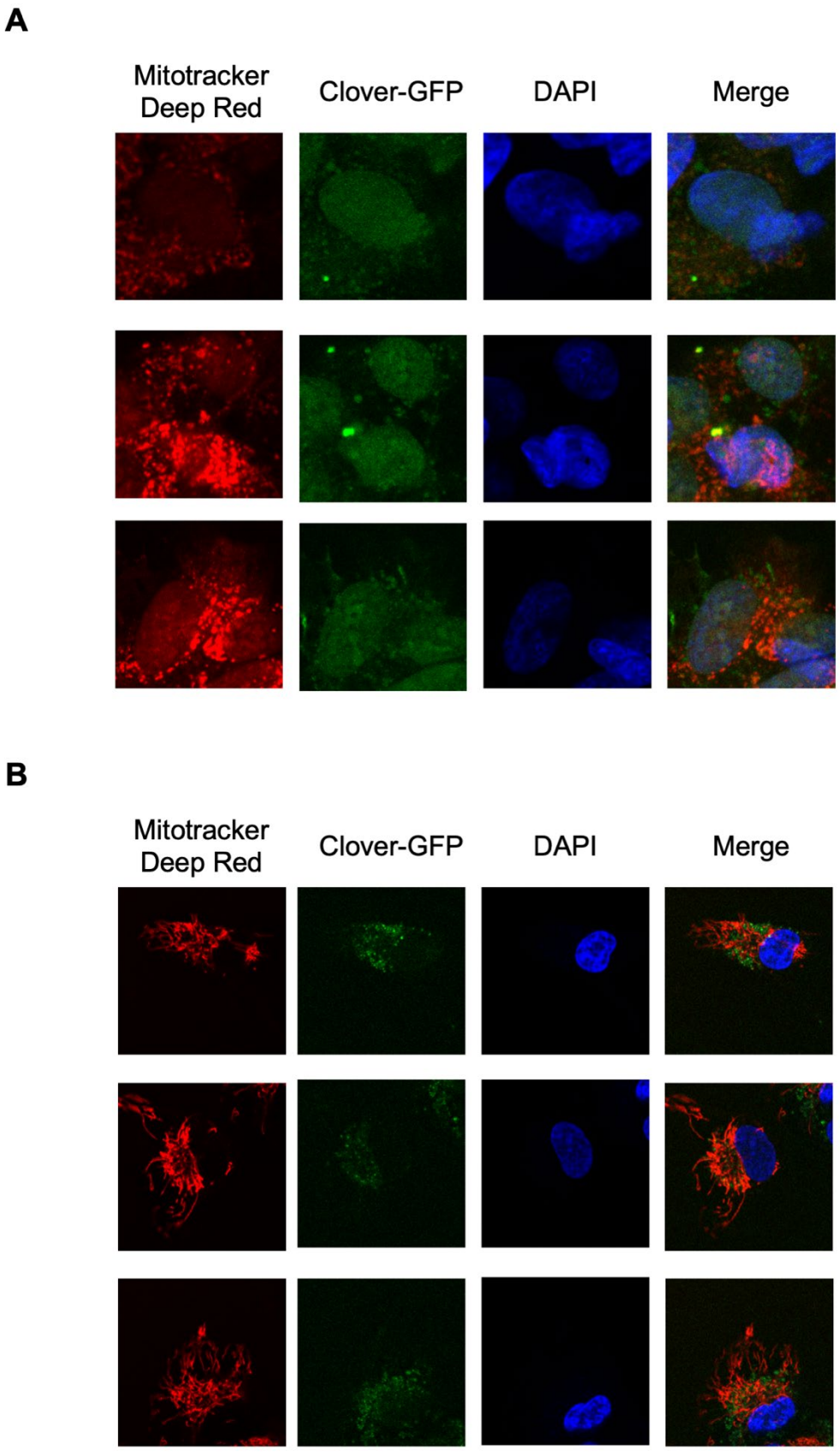

Figure 5.7. Clover-tagged PrimPol does not visibly localise to the mitochondria in undamaged RPE-1 cells

A. Cells were fixed by paraformaldehyde after treatment with Mitotracker Deep Red and imaged by confocal microscopy. DNA was stained with DAPI (blue) and Clover-GFP is shown in green. **B.** Cells were imaged live by confocal microscopy after treatment with Mitotracker Deep Red and Hoechst 33342 (DNA stain, blue). Clover-GFP is shown in green.

5.5.4 Hydroxyurea induces nuclear localisation of Clover-tagged PrimPol

While PrimPol protein is found within both the mitochondria and nucleus, in undamaged cells it is predominately cytoplasmic (Mourón et al., 2013). However, given that its major role is repriming stalled DNA replication, it is clear its primary activity must occur in the nucleus or mitochondria. Despite the absence of a canonical NLS, we hypothesise PrimPol may undergo a nuclear import-export cycle based on the cell cycle or in response to DNA damage or replication stress. In the nucleus, PrimPol protein has been shown to form foci after both UV-C damage and hydroxyurea treatment (Bianchi et al., 2013). For this reason, we performed preliminary experiments to determine if endogenous tagged PrimPol could be seen moving into the nucleus after hydroxyurea-induced replication stress.

2 mM hydroxyurea was added to cell media and cells were then incubated for 8 hours in a 37°C incubator. Cells were then washed several times with warm PBS before being released into fresh, drug free media for one hour. This was to allow recovery from the HU, including production of dNTPs to allow replication to resume. Cells were then harvested, and fixed, including a pre-extraction step to remove protein that was not bound to chromatin. Representative images can be seen in Figure 5.8A. Images were quantified for green PrimPol signal in DAPI positive regions, to represent nuclear protein. This quantification – of approximately 500 cells in one biological repeat – is represented in Figure 5.8B. This initial work suggests that one hour after release from HU, PrimPol is localised to the nucleus in greater amounts than in unstressed cells, potentially to aid in replication restart after fork collapse. However, it is also possible that the accumulation of protein in the nucleus during recovery is due to an increase in protein overall. As cells were pre-extracted, the cytoplasmic signal in both HU treated and undamaged cells is minimal, which may obscure an increase in total protein levels.

Future experiments investigating the effects of nucleotide depletion of PrimPol could omit the pre-extraction step of the protocol in order to precisely determine nuclear signal in comparison to cytoplasmic signal strength. Furthermore, additional work studying changes in PrimPol protein expression after HU

dependent fork stalling would also strengthen the hypothesis that fork stalling induces PrimPol localisation to the nucleus. As described in 3.5.4, PrimPol was seen binding to chromatin in higher amounts during a 16 hour stall, and decreased amounts after release. Therefore, further timepoints at the point of stalling, after significant stalling and after release and recovery will help elucidate the protein's localisation during nucleotide depletion and fork collapse.

5.5.5 UV-C damage induces localisation of PrimPol protein to the nucleus

Previous work has strongly implicated PrimPol in the bypass of UV-C induced damage during replication (Bailey et al., 2019; Bailey et al., 2016; Bianchi et al., 2013). Endogenous PrimPol is bound to chromatin in increased amounts after UV-C damage, and overexpressed PrimPol forms nuclear foci after UV-C damage; we therefore next tested whether nuclear import could be detected after UV damage. Given the issues with protein detection after pre-extraction, these experiments were conducted on live cells.

Representative images from preliminary experiments are shown in Figure 5.9A. Quantification of nuclear signal showed that cells which had been damaged by $10J/m^2$ UV-C, and had recovered for 45 minutes, had a higher level of fluorescence in the nucleus compared to undamaged cells (Figure 5.9B).

It has previously been reported that PrimPol protein and mRNA levels increase 24 hours after treatment with cisplatin or UV-C (Piberger et al., 2020), but only in BRCA-1 deficient cells: as RPE-1 cells are not BRCA1 deficient, we do not expect mRNA levels to change significantly, and therefore speculate that the nuclear localisation is independent of changes to protein level. However, it is possible that UV-C or HU mediated damage induced increase protein production, either in conjunction with or instead of nuclear import, contributing to the results presented here.

Further work is required to determine how quickly nuclear import happens after UV-C damage is detected and whether this is dependent on UV-C induced DNA damage signalling, such as ATR activation or RPA phosphorylation (Maréchal and Zou, 2013).

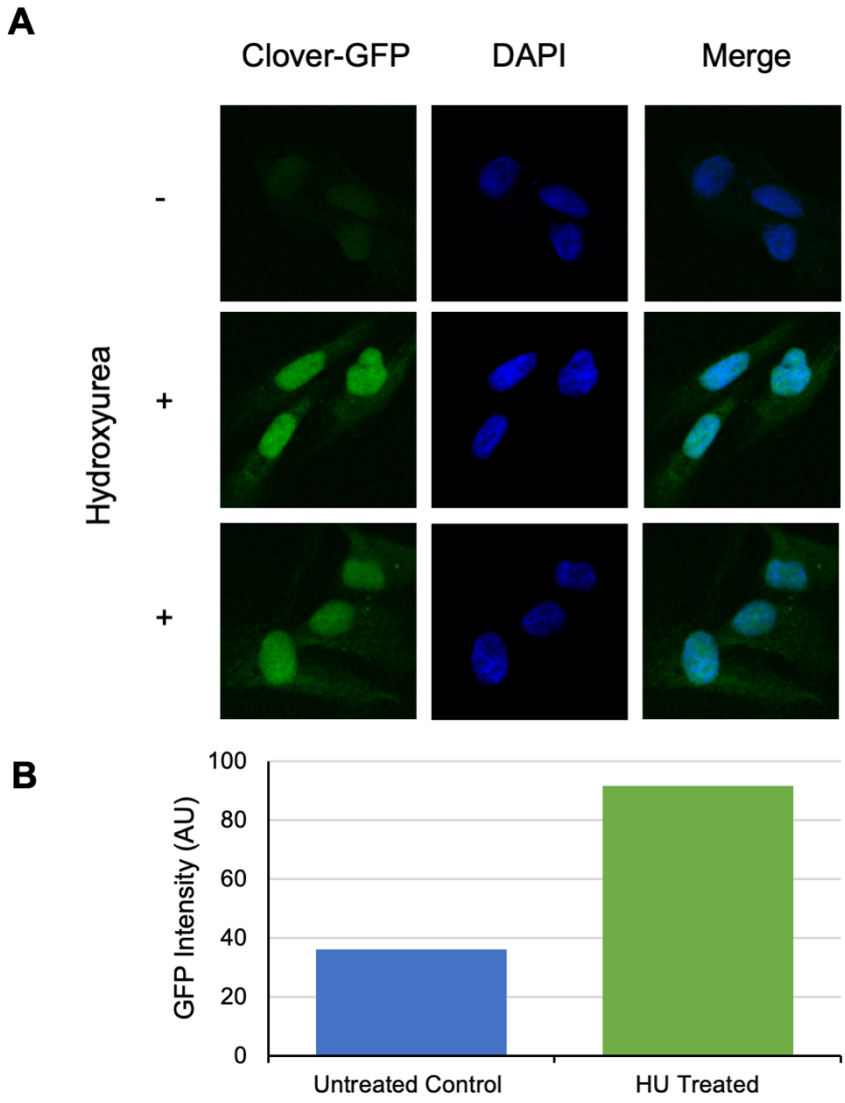

Figure 5.8. Hydroxyurea induced replication stress leads to increased nuclear PrimPol signal

A. 2 mM hydroxyurea was applied to cells for 8 hours before a 1 hour recovery period, before cells were harvested, pre-extracted and fixed, and imaged by confocal microscopy. Representative images from one biological repeat. **B.** Mean GFP intensity (AU) of approximately 100 cells of each condition in one biological repeat.

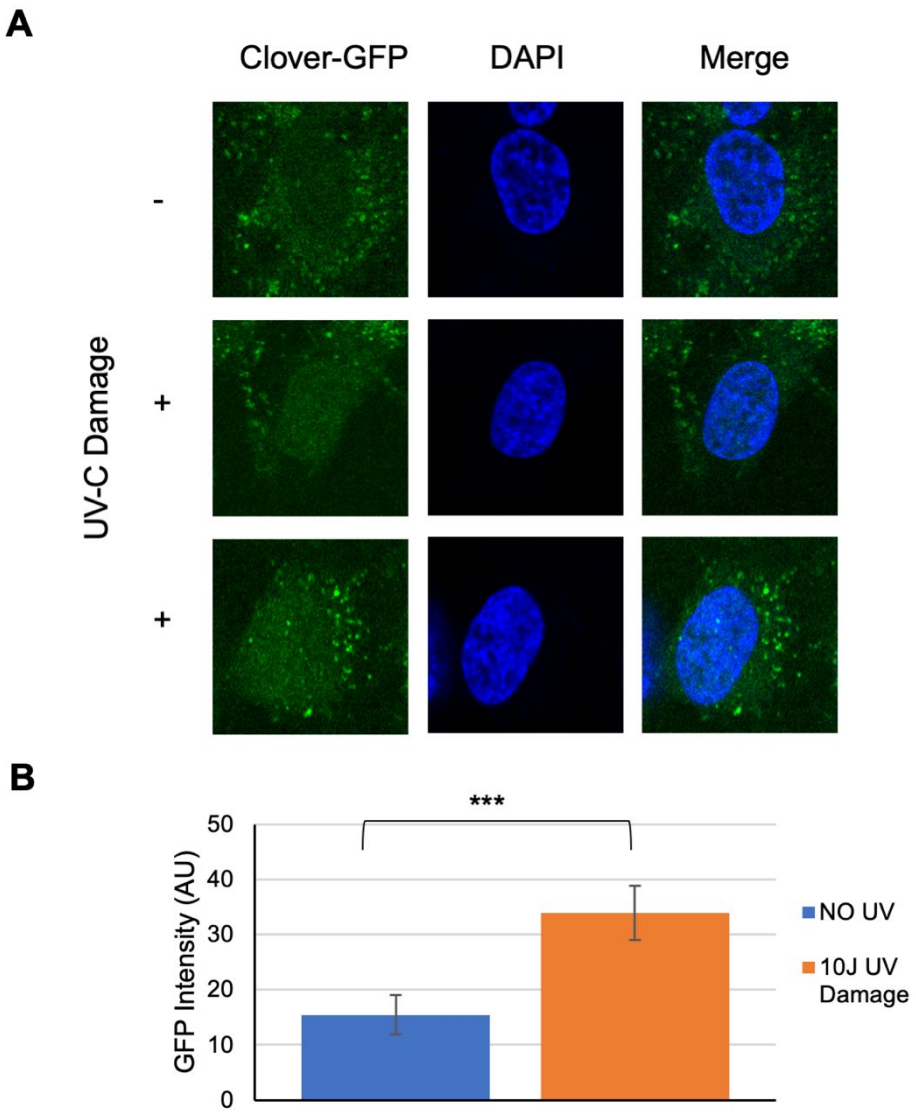

Figure 5.9. UV-C damage leads to an increase in nuclear PrimPol signal

A. 10 J/m^2 was applied to cells, which were left to recover for 45 minutes before cells were imaged by confocal microscopy. Representative images from one biological repeat. **B.** Mean GFP intensity (AU) from an average of >100 cells from one biological repeat, error bars showing standard deviation between cells.

5.6 Discussion

5.6.1 The absence of repriming and its effect on different cell lines

RPE-1 cells lacking PrimPol appear to be slightly UV-C sensitive, while HEK-293 cells and MRC-5 cells are not (Bailey et al., 2019, L. Bailey and A. Doherty, unpublished work). This difference could relate to the source of each cell line: while neither MRC-5 cells or HEK-293 cells are cancerous cells, MRC-5 cells are cancer associated fibroblasts, and HEK-293T cells have extremely aberrant karyotypes and abnormal p53 function (Lin et al., 2014b). For this reason, the closest example of a “normal” cell line examined for phenotypes related to PrimPol knockout may be the RPE-1 cells. Interestingly, recent work from the Cantor lab showed that several cancerous cell lines had developed a dependence on TLS polymerases not seen in non-cancerous lines (Nayak et al., 2020): it is possible that, across model cell lines, there are varying dependencies on different DDT pathways. Understanding whether cell lines have altered dependence on repriming or other pathways may aid in the investigation of cancer cells and help determine whether certain cancers can be sensitised – through the targeting of PrimPol or other competing pathways – to treatment. Preliminary work here also measures sensitivity of RPE-1 cells expressing S538A mutant PrimPol to UV-C, and future work will adress additional phenotypes observed in the HEK-293 cells.

5.6.2 Mitotic phenotypes associating with the loss of repriming

Investigation into the aberrant mitotic phenotype often seen in PrimPol$^{-/-}$ or mutant cells reveals that increased micronuclei may be generated by increased lagging or bridging chromosomes. Lagging or bridging chromosomes in anaphase can be generated by specific kinetochore-microtubule attachment errors (Thompson and Compton, 2011), which can be compounded by ssDNA breaks leading to more fragile chromosomes unable to withstand the separating forces (Ganem and Pellman, 2012). and micronuclei form when anaphase lagging chromosomes reassemble nuclear envelopes independent from the primary nucleus during telophase (Ganem and Pellman, 2012).

The presence of increased lagging chromosomes goes some way to explaining the increased micronuclei observed in PrimPol$^{-/-}$ cells previously (Bailey et al., 2019). It would be interesting to further investigate the effect of DNA damage tolerance in the absence of PrimPol on mitosis. Beyond the phenotypes detectable when screening for chromosomal abnormalities using DAPI staining alone, it is also worth remembering that additional mitotic phenotypes can be detected using more specialist markers. For example, catenanes at centromeres, replication stress and incomplete processing of replication intermediates, or replication stalling at telomeric regions, can lead to the generation of ultra-fine bridges (UFB). These are bridges that cannot be detected by DAPI staining, but instead require staining for proteins like the helicase BLM, RPA, or PLK1-interacting checkpoint helicase (PICH) (Chan et al., 2018). The precise nature of PrimPol's mitotic phenotypes could be better elucidated by screening for these markers and others, and quantifying the number of UFBs present in PrimPol$^{-/-}$ cells and determining their origin. Helpful clarification could be performed to determine if these cells generate a subtype of UFBs known as fragile site UFBs, marked by FANCD2 foci (Chan et al., 2009). If the bridges in PrimPol$^{-/-}$ cells were FANCD2 positive, this could indicate that the phenotypes are related to incomplete replication intermediates, due to the absence of a repriming pathway.

5.6.3 The observed localisation of PrimPol protein

The Clover-PrimPol cell line expresses Clover-tagged PrimPol cDNA under PrimPol's endogenous promoter, at the endogenous PrimPol locus. While expression levels of the tagged protein should mimic the levels seen in unedited cells, the presence of the fluorescent Clover tag along with potential differences due to the lack of splicing, mean that the Clover-PrimPol cell line may not be directly comparable to parental RPE-1 cells. One such difference is seen in localisation: while many previous studies have shown PrimPol localises to the mitochondria (Bailey et al., 2019; García-Gómez et al., 2013; Torregrosa-Muñumer et al., 2017), we did not observe clear localisation in our imaging attempts. It is possible that this is due to the imaging we performed, with low levels of PrimPol protein being obscured by strong Mitotracker signal or imperfect imaging parameters. It is also possible that the Clover-tagged PrimPol protein does not localise well to the mitochondria, and further experiments investigating

sub-cellular localisation through different means should be performed to determine this. A lack of visible mitochondrial localisation may also indicate that protein localisation changes across cell line, and unperturbed RPE-1 cells have lower requirements for PrimPol-mediated repriming in the mitochondria.

There was efficient nuclear import, and a clear difference in cytoplasmic and nuclear signal levels as has been described before (García-Gómez et al., 2013). Cytoplasmic signal appeared to form small foci or clusters within the cytoplasm, as has been seen before through IF imaging (Sean Rudd, PhD Thesis), while signal within the nucleus was pan-nuclear. Additional required research includes siRNA control experiments to validate the visible Clover signal definitely is PrimPol, and chromatin binding experiments to determine chromatin association is intact; these experiments must be performed before further research is done using this cell line.

5.6.4 Improving the efficiency of tagging PrimPol at its endogenous locus

The efficiency of the generation of the endogenous tagged line was impeded by some elements inherent to the specific problem being addressed. For example, we wanted to generate the cell line in a normal, non-cancerous cell line, and this meant accepting the inherently low levels of HDR RPE-1 cells perform (Ghetti et al., 2021). We were also working to tag a protein with extremely low expression levels (Beck et al., 2011), which meant that specific cell sorting techniques such as live cell FACS were not possible. Pool populations could still be tested by genomic PCR or western blot, but this only helped us determine that some cells had been edited as opposed to allowing us to enrich for the edited population.

Since the beginning of this project, genome editing techniques have improved significantly, and protocols now exist to improve the efficiency of knock-in experiments, even in difficult lines like RPE-1 cells. For example, experiments described here to generate the endogenous tagged line utilised a Cas9 expression vector containing the guide sequence, which was transfected into cells. However, there is extensive evidence to suggest the use of ribonucleoprotein improved efficiency and reduced editing kinetics, leading to reduced off target effects (Liang et al., 2015). Additionally, various techniques

exist that can increase the amount of HDR occurring in the cells. One example, which could be utilised is synchronising cells to ensure cutting occurs during S phase or G2, when HR is active (Lin et al., 2014a), though this technique would not be possible using our current method of Cas9 expression using a vector. Additionally, several approaches utilise inhibitors of key NHEJ factors such as Ku70/80 or the inhibition of 53BP1, to prevent NHEJ from taking place and therefore increasing HDR (Bischoff et al., 2020; Canny et al., 2018). Alongside strategies developed during the production of this cell line, such as transfection optimisation, these improvements would allow us to generate multiple cell lines for use in the study of PrimPol's localisation. Of particular interest is the generation of several cell lines expressing the phospho-mutants and other catalytic domain mutants described in earlier chapters.

Chapter 6

Discussion

6.1 The cellular regulation of human PrimPol

This thesis project set out to investigate the regulation of human PrimPol through post-translational modification. Human PrimPol is the second primase enzyme discovered in human cells, and differs significantly from the other human primase, Pol α: *in vitro,* PrimPol can initiate *de novo* DNA and RNA synthesis, DNA chain elongation, and has the capacity to bypass replisome stalling lesions by trans-lesion synthesis or origin-independent repriming. *In vivo,* it appears to predominately act to reprime stalled DNA synthesis, with no evidence it is actively utilised as a TLS polymerase (Keen et al., 2014b; Kobayashi et al., 2016).

Chapter Three of this thesis discusses the dynamic modification of a specific residue, S538, on the C-terminus of human PrimPol. This residue is phosphorylated by PLK1, and levels of phosphorylation change across the cell cycle, with low or absent levels in G1 and early S, and higher levels as cells progress from late S phase into G2 and mitosis. The onset of this phosphorylation can be delayed by the application of DNA damage or replication stress inducing agents - which in turn delay the cell cycle - or reversed if damage is applied once phosphorylation has occurred. Mutation of S538 to alanine, preventing its phosphorylation, induces catastrophic effects on cell survival and genomic stability, as indicated by plating deficiencies and genomic instability phenotypes in undamaged cells, and sensitivity to olaparib, camptothecin and UV-C damage. These phenotypes appear to be contingent on the primase activity of PrimPol and the protein's ability to bind RPA, but interestingly are not abrogated by total catalytic inactivation of the enzyme. Additionally, S538A mutant protein was found to associate with chromatin during G2, a cell cycle stage where PrimPol is usually excluded from chromatin (Mourón et al., 2013), but this association first requires significant UV-C damage, likely to generate a substrate for PrimPol to associate with in detectable amounts.

Chapter Four of this thesis centres around S499, which we found is the phosphorylation site responsible for the doublet appearance of PrimPol on an SDS-PAGE gel. Ablation of S499 phosphorylation, by mutation of the site, leads to decreases in cell survival after UV-C damage, and after replication stress induced by aphidicolin, dNTP depletion, olaparib or camptothecin. Its loss also

leads to increased micronuclei and mitotic abnormalities, which are rescued by the mutation of the RPA binding domain of PrimPol. Additionally, we show that phosphorylation of S499 is altered throughout the cell cycle, in accordance with the activity of the kinase responsible for its phosphorylation, CDK1. This phosphorylation is carefully maintained throughout the cell cycle, with full phosphorylation occurring in mitosis, but partial removal occurring throughout G1. Taken together, these results describe novel regulation pathways of PrimPol dependent on the activity of mitotic kinase enzymes.

Interestingly, we found that abrogation of the primase activity of PrimPol disrupts this phosphorylation. This could suggest that initiation of a priming reaction, such as nucleotide engagement, is required for S499 phosphorylation. It could also suggest that these mutations to the zinc finger domain of PrimPol change the secondary structure or protein stability so significantly that CDK1 can no longer interact. Additionally, both the S538 and S499 phenotypes are dependent on RPA binding: this suggests that the toxicity induced by these mutations first requires recruitment of PrimPol to sites of fork stalling.

Together, these data establish that regulation of PrimPol is crucial for cell survival and recovery from replication stress and damage. Understanding the cellular signals that initiate the utilisation or exclusion of PrimPol-mediated repriming is the first major step in defining the full function of PrimPol in DNA damage tolerance.

6.2 The regulation of repriming

PrimPol-dependent repriming offers many advantages as a mechanism for restarting arrested forks. It allows stalled DNA synthesis to resume, particularly on the leading strand, by bypassing a diverse range of impediments without necessity to interact with the obstacle itself, as in TLS. Additionally, when PrimPol mediates replication restart, it likely only incorporates a small number of nucleotides before disassociating due to its low processivity, minimising any mutagenic events.

There are, however, several obvious reasons why regulating PrimPol would be important for cells. Firstly, while it can incorporate dNTPs, evidence suggests that

it first incorporates an rNTP (Bianchi et al., 2013). As with the primers generated by Pol α, this rNTP must be removed. Regulating PrimPol's activity will also moderate rNTP incorporation; an accumulation of these bases in DNA can lead to genomic instability (Reijns et al., 2012).

It has recently been suggested that the gaps generated after repriming at bulky lesions are repaired by homologous recombination (Piberger et al., 2020). Piberger et al.'s work hypothesises that TLS polymerases may compete with HR factors for repair of PrimPol mediated ssDNA gaps, with the choice between the two potentially depending on the type of DNA lesion or the damage load the cells have. The repair of PrimPol induced ssDNA gaps is a potential cause for concern: it is currently not known at what distance from a lesion PrimPol will reprime, and therefore how large of a ssDNA gap will be left behind. This gap may include a lesion on the template strand, such as those induced by UV-C or BPDE, complicating its repair. After significant damage or stress, increased unregulated repriming in addition to the usual substrates for HR, may exhaust the HR machinery or the RPA pool.

Bai et al., (2020) suggested that an increase in repriming caused by the absence of HLTF, a fork reversal protein, causes unrestrained DNA replication and an increase in ssDNA gaps, which has been suggested by others to reduce cell fitness (Nayak et al., 2020). Similarly, in the absence of the protein CARM1, recently implicated in the organisation of fork reversal, fork speed increases, replication fidelity decreases alongside an increase in ssDNA gaps; indicative, the authors suggest, of an over-reliance on PrimPol mediated repriming (Genois et al., 2021). All these factors suggest that PrimPol's regulation is of vital importance in the cell, and that dysregulation of this could be harmful.

Interestingly, our lab has worked extensively with cells overexpressing PrimPol, and, when compared to cells expressing endogenous amounts, there have been very few detectable differences. We hypothesise this is due to the strict control over PrimPol in the cell to moderate PrimPol's usage. This thesis describes the first instance of overexpression of PrimPol inducing different phenotypes to cells expressing endogenous amounts: in Chapter Four, we observe significant increases in cell survival after high doses of HU when cells are overexpressing

WT PrimPol, suggesting that in the context of recovery from fork collapse, high levels of PrimPol protein can aid in cell survival. It will be interesting to determine what role PrimPol plays in cells undergoing dNTP depletion; it could be beneficial due to its ability to incorporate rNTPs, potentially generating primers at stalled forks that allow for the quick resumption of DNA synthesis after the replication stress is removed.

6.3 Regulation of PrimPol across the cell cycle

Beyond the requirement for general regulation of repriming, this thesis describes data that suggests regulation of PrimPol's activity across the cell cycle is vital for proper utilisation of the protein. The changes in both S538 and S499 phosphorylation across the cell cycle, and the effects of preventing that phosphorylation through mutation, suggest this type of regulation is essential for proper cell survival and tolerance of replication stress.

S538 phosphorylation occurs at the end of DNA replication, likely alongside the activation of PLK1, and remains high across G2 and mitosis. This phosphorylation appears to play a role in chromatin exclusion of the protein. Similarly, while a proportion of PrimPol is continuously S499 phosphorylated, this phosphorylation increases significantly as cells progress into G2, leading to full phosphorylation of PrimPol at S499, though the reason for this phosphorylation is unclear.

While the bulk of DNA replication is completed by the end of S phase, some does continue in G2. In kind, DNA damage tolerance is also employed during G2. While the cell cycle regulation of fork reversal is particularly poorly elucidated, the role of TLS during G2 is better established; it is suggested that alongside small amounts of DNA replication resumption, these polymerases also "patch up" ssDNA gaps left behind by alterative mechanisms such as repriming that occurred in S phase (Diamant et al., 2012). These gaps can also be repaired by HR-based mechanisms such as TS (Branzei and Foiani, 2010). Additionally, lesions within the DNA which had previously been bypassed, such as dimers generated by UV-C, can be repaired during G2 by post-replicative repair pathways like NER.

We hypothesise that, with these pathways in place to repair ssDNA gaps and aid in the resumption of DNA replication in the forks still progressing, PrimPol's presence would actually be a hinderance. If recruited, current information suggests it would only reprime to resume DNA synthesis, which a TLS polymerase could do equally well and is not likely to be a significant concern during G2, when most replication is complete. Recruitment of this protein to ssDNA in G2 could therefore block other pathways, like NER, and may generate new ssDNA gaps that require further repair.

We suggest, therefore, that PrimPol is phosphorylated by PLK1 at S538 in late S/G2 to prevent chromatin association. This data is supported by an increase in RPA foci, indicative of ssDNA, in non-replicating S538A cells compared to non-replicating WT cells (Bailey et al., 2021, Appendix B). As a primase, PrimPol has no clear role outside of DNA replication and as such, regulation controlling its activity outside of S phase is logical.

Additionally, S538 phosphorylation could serve to prevent PrimPol's association with common fragile sites, which are replicated late in S phase (Hellman et al., 2000; Le Beau et al., 1998). In the absence of this regulation, PrimPol may continue to bind to RPA and prime at stretches of ssDNA throughout late S and G2. Excessive repriming by S538A could lead to increased accumulation of ssDNA gaps and interfere with processes such as repair and transcription as cells progress towards mitosis. It may also interfere with the repair of ssDNA gaps it itself has generated during S phase.

While we have exclusively monitored S538 phosphorylation through use of a phospho-specific antibody and mutant protein, it is possible that further phosphorylation or additional modifications are involved in this process. This could be determined by mass spectrometry analysis of PrimPol protein phosphorylated and mutated at S538, to determine the subsequent effects of this phosphorylation. Potentially, PLK1 phosphorylation is followed by phosphorylation of other sites in this region in order to significantly change the charge of the region or sequester the protein from forks.

Cell cycle control over DNA repair pathways is not uncommon, most clearly exemplified in the control over DSB repair pathways (described in 1.3.3). While PLK1 has been implicated in the phosphorylation of several DNA repair proteins (Chabalier-Taste et al., 2016; Li et al., 2017), its role in the phosphorylation of BRCA2 is particularly noteworthy, as BRCA2's phosphorylation increases across G2 to a peak in mitosis, following the increased activity of PLK1, but can be prevented in response to DNA damage (Lee et al., 2004). CDK1 phosphorylation of BRCA2 also occurs in this manner, with increases in G2/M that follow decreased association with Rad51 (Esashi et al., 2005). In these examples, this phosphorylation in G2 promoted Rad51 filament disassembly, thus terminating recombination and promoting mitotic entry.

With many similar examples, it implies that a significant role for the phosphorylation of DNA repair proteins in G2 and mitosis is to prevent their activity and checkpoint activation during mitosis. Could this be the role for S499 phosphorylation – allowing or preventing association with a heretofore unknown PrimPol binding partner, signalling the end of repriming and promoting mitotic entry? A full analysis of the mutant protein's progression into mitosis or activation of the G2/M checkpoint may clarify this, though it is clear that further work is required to fully understand the role and function of S499 phosphorylation.

One unanswered question remains with regards to both S538 and S499 phosphorylation: what does PrimPol do in G1? It can bind chromatin in this stage, is unphosphorylated at S538 as in S phase, and the two bands of PrimPol representing S499 phosphorylated and unphosphorylated protein are present. Without ongoing replication, there is unlikely to be significant ssDNA: without this, as in G2, you would imagine there is minimal substrate for PrimPol binding. Investigation into PrimPol's association with replication fork machinery could help answer this question.

6.4 The dephosphorylation of PrimPol

The decrease in both S538 and S499 phosphorylation so soon after release from nocodazole implicates the activity of specific phosphatases at the point of mitotic exit. To counter the burst in phosphorylation that occurs to signal mitotic entry, a

small group of phosphatases are activated, the most abundant being PP1 and PP2A (Moura and Conde, 2019). Work in Chapter Three shows that S538 phosphorylation decreases very quickly after release from nocodazole, coinciding with mitotic exit. It stands to reason, therefore, that one of these phosphatases is responsible for S538 dephosphorylation. The status of S499 after nocodazole release is slightly more complex – while dephosphorylation does occur, it is more gradual and incomplete, with a small increase occurring 6 hours after release from nocodazole. Further study into the role of phosphatases in regulating S499 may shed some light on the role of this phosphorylation.

6.5 Consequences of dysregulation

One interesting aspect of this work is the significant impact of preventing proper regulation of both S499 and S538 phosphorylation. In both cases, the mutation of the serine residue to alanine, thereby preventing its phosphorylation, induced significant phenotypes in both undamaged cells and after damage or replication stress. S538A cells were sensitive to olaparib, camptothecin and UV-C, while both S499A and S499E - mutations mimicking both phosphorylation states - cells showed similar increased sensitivities to aphidicolin, olaparib and camptothecin compared to cells expressing WT PrimPol.

It is not clear what role S499 phosphorylation plays in the regulation of PrimPol, though the careful maintenance of the two bands across G1 and S phase suggests both isoforms play a role in DDT. It is clear from the phenotypes observed, alone and in combination with the AxA and RAB mutation, that these phenotypes are likely generated by the activity of PrimPol. The significant phenotypes associated with both the phosphomimic and phosphonull amino acid substitutions suggest that both isoforms are required together for full functionality. As ZnKO mutant PrimPol is not phosphorylated at S499, we can also infer that this phosphorylation is somehow linked to the zinc finger domain of PrimPol.

Interestingly, the phenotypes described above, showcasing the effect of disrupting PrimPol’s regulation, are significantly greater than phenotypes observed when PrimPol is missing. Similarly, this thesis highlights the toxicity of catalytically inactive (AxA)

PrimPol; cells expressing this mutant variant are also more sensitive than PrimPol$^{-/-}$ cells. Previous work analysing human PrimPol knockout cell lines has revealed that, overall, these cells show minimal overt phenotypes (Bailey et al., 2019), though DT40 chicken cells are sensitive (Bailey et al., 2016).

PrimPol that contains the RAB mutations, in their brief characterisation, have not showcased any phenotypes as severe as those seen after catalytic inactivation (AxA) or S538 mutation. We therefore suggest that it is the binding and recruitment, alongside potential changes in regulation, that induces decreased survival and evidence of genomic instability.

During DNA replication, there are multiple DNA damage tolerance pathways to employ when responding to replication stalling stress. It stands to reason that, in the absence of PrimPol, cells compensate for its loss by activating other pathways, such as fork reversal, template switching or TLS. However, in a normal cell with intact DDT pathways, it is increasingly unclear what mechanisms cells use to choose between these pathways. Work from the Cimprich group suggests that cells with competent HLTF promote fork reversal after treatment with low levels of hydroxyurea, inducing nucleotide depletion and replication stress. Only in the absence of this protein, as can occur in some cancers, does PrimPol mediated repriming occur in significant levels – as detected by ssDNA gap accumulation. Work described in Chapter Four of this thesis, suggests that overexpression PrimPol can increase survival after treatment with high doses of hydroxyurea, which lead to fork collapse (Chapter 4), suggesting a role for repriming here. Additionally, our work and that of others suggest that PrimPol may be the primary pathway for tolerance of certain bulky lesions (Piberger et al., 2020), though TLS is also employed to bypass lesions such as UV dimers. This suggests that the lesion type or damage load may play a key role in the regulation of pathway choice.

An increasing number of human disorders caused by defects in different components of the DNA-replication machinery have been described to date. Mutations in enzymes like Pol η can lead to diseases such as Xeroderma pigmentosum (Lehman et al., 1975; Lehmann et al., 2011). Similarly, there are very rare disorders characterised by mutations to Pol α, such as X-linked

intellectual disability (Van Esch et al., 2019). However, there are very few links to disease associated with PrimPol mutation. While it's possible that a PrimPol disorder has not been discovered, it's also possible that mutations to PrimPol that induce significant effects on the protein are not viable. An interesting next path for research into PrimPol's role in human cells could be to ascertain PrimPol's role in the early stages of development.

This work suggests that PrimPol's regulation by kinase enzymes, such as PLK1, are vitally important for the control of the protein, and errors in this control due to mutation are toxic to human cells. It also describes the strict cell cycle regulation of PrimPol protein, and the effects that certain drugs can have on this. This understanding will allow for a more complete picture of how cells choose between repriming, fork reversal and TLS: while an experiment looking into pathway choice may average out replication forks from across the cell cycle, our data suggests that forks in early S phase may undergo repriming after stalling while those in late S phase may not, due to S538 phosphorylation. Similarly, we know that, in tandem with delaying S phase completion, treatment with genotoxic drugs such as olaparib and camptothecin will stall S538 phosphorylation and potentially promote repriming. Further work examining how this pattern of modification fits in with our understanding of TLS and fork reversal, particularly as it relates to their regulation across the cell cycle and after damage or stress, is required.

Given our hypothesis regarding phosphorylation as a means of regulating repriming, an important next step will be to study the effects of this phosphorylation at endogenous levels. The Clover-PrimPol cell line is an exciting new tool to monitor the localisation and recruitment of PrimPol protein in human cells. This cell line, and additonal future lines, can investigate the recruitment of PrimPol protein to sites of damage using super-resolution microscopy, as has been performed recently with proteins involved DSB repair (Whelan and Rothenberg, 2021). It can also expand on preliminary experiments discussed in Chapter Five, examining the nuclear import and export of the protein. Finally, this cell line, and future versions, can be used to examine the endogenous effect of the phosphorylations described in Chapters Three and Four, to allow for more precise study of their role within cells.

6.6 Conclusion

This work focuses on the phosphorylation of PrimPol protein at two specific serine residues, S499 and S538. Our research has determined that the phosphorylation of these residues is reliant on the activity of the mitotic kinase enzymes PLK1 and CDK1, and that the phosphorylation of both residues is strictly controlled by the cell cycle (Figure 6.1). The phosphorylation of S538 can be impacted also by DNA damage or replication stress. Mutation of S538 to alanine, intended to mimic unphosphorylated protein, induces phenotypes indicative of genomic instability, though the mutation to glutamic acid has minimal effect. This mutation can also induce aberrant recruitment of PrimPol protein to chromatin outside of S phase. Mutation of S499 to alanine or glutamic acid also induces cell sensitivity phenotypes to a variety of stressors; though the cause of this sensitivity is unknown, it is more severe in HEK-293 cells than a lack of PrimPol, suggesting toxicity in the activity or binding of the protein more severe than the absence of repriming entirely.

Two new cell lines have been created to aid in the progression of this work. Several new PrimPol$^{-/-}$ RPE-1 clonal cell lines have been created, and the characterisation of several of them will allow for future study of the phosphorylation sites in this cell line. RPE-1 cells have a more stable karyotype than HEK-293 cells, and the Sleeping Beauty system means that a doxycycline inducible system can be utilised, making them beneficial for future study. Additionally, the creation of the Clover-PrimPol cell line allows for future imaging experiments to be conducted on endogenous levels of protein without the use of antibodies: this circumvents issues with poor performance of commercial antibodies, and allows for more complex imaging to be conducted, including super-resolution microscopy and live-cell imaging.

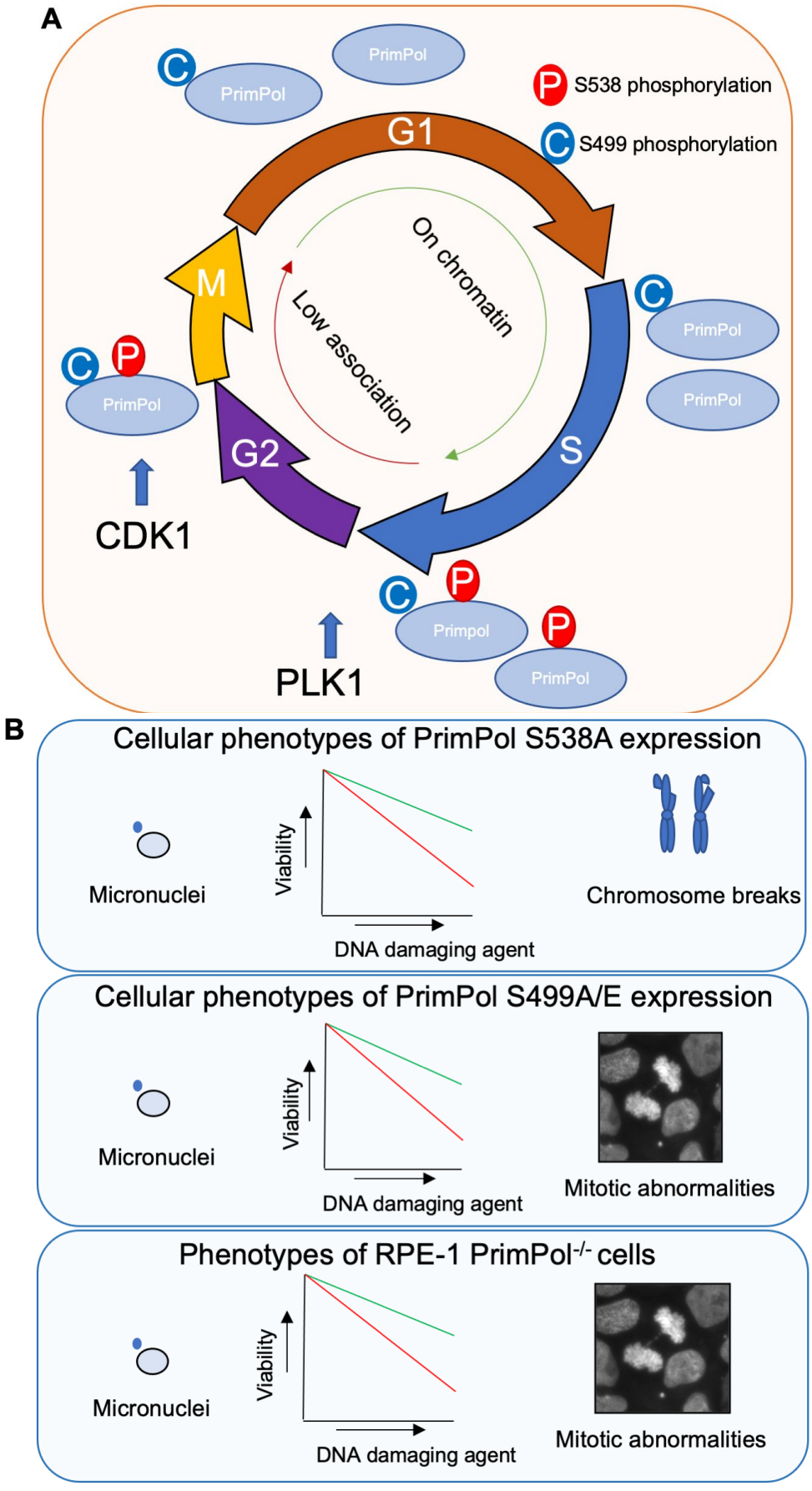
A
PrimPol
PrimPol
S538 phosphorylation
S499 phosphorylation
G1
On chromatin
Low association
M
S
G2
PrimPol
PrimPol
PrimPol
CDK1
Primpol
PrimPol
PLK1
B
Cellular phenotypes of PrimPol S538A expression
Micronuclei
Viability
DNA damaging agent
Chromosome breaks
Cellular phenotypes of PrimPol S499A/E expression
Micronuclei
Viability
DNA damaging agent
Mitotic abnormalities
Phenotypes of RPE-1 PrimPol-/- cells
Micronuclei
Viability
DNA damaging agent
Mitotic abnormalities

Figure 6.1 Changes to S499 and S538 phosphorylation across the cell cycle

A. A schematic describing the pattern of S538 and S499 phosphorylation across the cell cycle, and how it corresponds to chromatin association and PLK1 and CDK1 levels. **B.** Cellular phenotypes of HEK-293 cells expressing S538A or S499A/E mutant PrimPol protein, or RPE-1 PrimPol$^{-/-}$ cells.

References:

Abbotts, R., and Wilson III, D.M. (2017). Coordination of DNA single strand break repair. Free Radical Biology and Medicine *107*, 228-244.

Acharya, N., Khandagale, P., Thakur, S., Sahu, J.K., and Utkalaja, B.G. (2020). Quaternary structural diversity in eukaryotic DNA polymerases: monomeric to multimeric form. Current Genetics *66*, 635-655.

Agudo, R., Calvo, P.A., Martínez-Jiménez, M.I., and Blanco, L. (2017). Engineering human PrimPol into an efficient RNA-dependent-DNA primase/polymerase. Nucleic Acids Research *45*, 9046-9058.

Akopyan, K., Cascales, H.S., Hukasova, E., Saurin, A.T., Müllers, E., Jaiswal, H., Hollman, D.A., Kops, G.J., Medema, R.H., and Lindqvist, A. (2014). Assessing kinetics from fixed cells reveals activation of the mitotic entry network at the S/G2 transition. Molecular Cell *53*, 843-853.

Alberts, B., Johnson, A., Lewis, J., Raff, M., Roberts, K., and Walter, P. (2002). The initiation and completion of DNA replication in chromosomes. In Molecular Biology of the Cell. 4th edition (Garland Science).

Aleem, E., Kiyokawa, H., and Kaldis, P. (2005). Cdc2–cyclin E complexes regulate the G1/S phase transition. Nature Cell Biology *7*, 831-836.

Allison, D.F., and Wang, G.G. (2019). R-loops: formation, function, and relevance to cell stress. Cell Stress *3*, 38-46.

Amunugama, R., Willcox, S., Wu, R.A., Abdullah, U.B., El-Sagheer, A.H., Brown, T., McHugh, P.J., Griffith, J.D., and Walter, J.C. (2018). Replication fork reversal during DNA interstrand crosslink repair requires CMG unloading. Cell reports *23*, 3419-3428.

Arezi, B., and Kuchta, R.D. (2000). Eukaryotic DNA primase. Trends in Biochemical Sciences *25*, 572-576.

Bai, G., Kermi, C., Stoy, H., Schiltz, C.J., Bacal, J., Zaino, A.M., Hadden, M.K., Eichman, B.F., Lopes, M., and Cimprich, K.A. (2020). HLTF Promotes Fork Reversal, Limiting Replication Stress Resistance and Preventing Multiple Mechanisms of Unrestrained DNA Synthesis. Molecular Cell *78*, 1237-1251.e1237.

Bailey, L.J., Bianchi, J., and Doherty, A.J. (2019). PrimPol is required for the maintenance of efficient nuclear and mitochondrial DNA replication in human cells. Nucleic Acids Research *47*, 4026-4038.

Bailey, L.J., Bianchi, J., Hegarat, N., Hochegger, H., and Doherty, A.J. (2016). PrimPol-deficient cells exhibit a pronounced G2 checkpoint response following UV damage. Cell Cycle *15*, 908-918.

Bailey, L.J., and Doherty, A.J. (2017). Mitochondrial DNA replication: a PrimPol perspective. Biochemical Society Transactions *45*, 513-529.

Bainbridge, L.J., Teague, R., and Doherty, A.J. (2021). Repriming DNA synthesis: an intrinsic restart pathway that maintains efficient genome replication. Nucleic Acids Research *49*, 4831-4847.

Bakkenist, C.J., and Kastan, M.B. (2003). DNA damage activates ATM through intermolecular autophosphorylation and dimer dissociation. Nature *421*, 499-506.

Baretić, D., Jenkyn-Bedford, M., Aria, V., Cannone, G., Skehel, M., and Yeeles, J.T. (2020). Cryo-EM structure of the fork protection complex bound to CMG at a replication fork. Molecular Cell *78*, 926-940. e913.

Barr, F.A., Sillje, H.H., and Nigg, E.A. (2004). Polo-like kinases and the orchestration of cell division. Nat Rev Mol Cell Biol *5*, 429-440.

Bartek, J., and Lukas, J. (2003). Chk1 and Chk2 kinases in checkpoint control and cancer. Cancer Cell *3*, 421-429.

Bashir, T., and Pagano, M. (2005). Cdk1: the dominant sibling of Cdk2. Nature Cell Biology *7*, 779-781.

Bębenek, A., and Ziuzia-Graczyk, I. (2018). Fidelity of DNA replication—a matter of proofreading. Current Genetics *64*, 985-996.

Bebenek, K., and Kunkel, T.A. (2004). Functions of DNA polymerases. Advances in Protein Chemistry *69*, 137-165.

Beck, M., Schmidt, A., Malmstroem, J., Claassen, M., Ori, A., Szymborska, A., Herzog, F., Rinner, O., Ellenberg, J., and Aebersold, R. (2011). The quantitative proteome of a human cell line. Molecular Systems Biology *7*, 549.

Bemark, M., Khamlichi, A.A., Davies, S.L., and Neuberger, M.S. (2000). Disruption of mouse polymerase ζ (Rev3) leads to embryonic lethality and impairs blastocyst development in vitro. Current Biology *10*, 1213-1216.

Benada, J., Burdová, K., Lidak, T., von Morgen, P., and Macurek, L. (2015). Polo-like kinase 1 inhibits DNA damage response during mitosis. Cell Cycle *14*, 219-231.

Berti, M., Ray Chaudhuri, A., Thangavel, S., Gomathinayagam, S., Kenig, S., Vujanovic, M., Odreman, F., Glatter, T., Graziano, S., Mendoza-Maldonado, R*., et al.* (2013). Human RECQ1 promotes restart of replication forks reversed by DNA topoisomerase I inhibition. Nature Structural & Molecular Biology *20*, 347-354.

Bertoletti, F., Cea, V., Liang, C.-C., Lanati, T., Maffia, A., Avarello, M.D., Cipolla, L., Lehmann, A.R., Cohn, M.A., and Sabbioneda, S. (2017). Phosphorylation regulates human polη stability and damage bypass throughout the cell cycle. Nucleic Acids Research *45*, 9441-9454.

Bhat, K.P., and Cortez, D. (2018). RPA and RAD51: fork reversal, fork protection, and genome stability. Nature Structural & Molecular Biology *25*, 446-453.

Bianchi, J., Rudd, S.G., Jozwiakowski, S.K., Bailey, L.J., Soura, V., Taylor, E., Stevanovic, I., Green, A.J., Stracker, T.H., Lindsay, H.D*., et al.* (2013). PrimPol bypasses UV photoproducts during eukaryotic chromosomal DNA replication. Molecular Cell *52*, 566-573.

Bienko, M., Green, C.M., Sabbioneda, S., Crosetto, N., Matic, I., Hibbert, R.G., Begovic, T., Niimi, A., Mann, M., and Lehmann, A.R. (2010). Regulation of translesion synthesis DNA polymerase η by monoubiquitination. Molecular Cell *37*, 396-407.

Bischoff, N., Wimberger, S., Maresca, M., and Brakebusch, C. (2020). Improving Precise CRISPR Genome Editing by Small Molecules: Is there a Magic Potion? Cells *9*, 1318.

Blackford, A.N., and Jackson, S.P. (2017). ATM, ATR, and DNA-PK: the trinity at the heart of the DNA damage response. Molecular Cell *66*, 801-817.

Boddy, M.N., Gaillard, P.-H.L., McDonald, W.H., Shanahan, P., Yates 3rd, J.R., and Russell, P. (2001). Mus81-Eme1 are essential components of a Holliday junction resolvase. Cell *107*, 537-548.

Bouché, J., Zechel, K., and Kornberg, A. (1975). dnaG gene product, a rifampicin-resistant RNA polymerase, initiates the conversion of a single-stranded coliphage DNA to its duplex replicative form. Journal of Biological Chemistry *250*, 5995-6001.

Branzei, D., and Foiani, M. (2010). Maintaining genome stability at the replication fork. Nature Reviews Molecular Cell Biology *11*, 208-219.

Bryan, T.M. (2019). Mechanisms of DNA Replication and Repair: Insights from the Study of G-Quadruplexes. Molecules *24*, 3439-3454.

Bucknall, R., Moores, H., Simms, R., and Hesp, B. (1973). Antiviral effects of aphidicolin, a new antibiotic produced by Cephalosporium aphidicola. Antimicrobial Agents and Chemotherapy *4*, 294-298.

Bulavin, D.V., Higashimoto, Y., Popoff, I.J., Gaarde, W.A., Basrur, V., Potapova, O., Appella, E., and Fornace, A.J. (2001). Initiation of a G2/M checkpoint after ultraviolet radiation requires p38 kinase. Nature *411*, 102-107.

Burgers, P.M., Koonin, E.V., Bruford, E., Blanco, L., Burtis, K.C., Christman, M.F., Copeland, W.C., Friedberg, E.C., Hanaoka, F., Hinkle, D.C*., et al.* (2001). Eukaryotic DNA polymerases: proposal for a revised nomenclature. Journal of Biological Chemistry *276*, 43487-43490.

Burgers, P.M., and Kunkel, T.A. (2017). Eukaryotic DNA replication fork. Annual Review of Biochemistry *86*, 417-438.

Burkard, M.E., Santamaria, A., and Jallepalli, P.V. (2012). Enabling and disabling polo-like kinase 1 inhibition through chemical genetics. ACS Chemical Biology *7*, 978-981.

Burns, M.B., Temiz, N.A., and Harris, R.S. (2013). Evidence for APOBEC3B mutagenesis in multiple human cancers. Nature Genetics *45*, 977-983.

Byun, T.S., Pacek, M., Yee, M.-c., Walter, J.C., and Cimprich, K.A. (2005). Functional uncoupling of MCM helicase and DNA polymerase activities activates the ATR-dependent checkpoint. Genes & Development *19*, 1040-1052.

Caldecott, K.W. (2008). Single-strand break repair and genetic disease. Nature Reviews Genetics *9*, 619.

Caldecott, K.W. (2007). Mammalian single-strand break repair: mechanisms and links with chromatin. DNA Repair *6*, 443-453.

Calvo, P.A., Sastre-Moreno, G., Perpiñá, C., Guerra, S., Martínez-Jiménez, M.I., and Blanco, L. (2019). The invariant glutamate of human PrimPol DxE motif is critical for its Mn2+-dependent distinctive activities. DNA Repair *77*, 65-75.

Campbell, B.C., Petsko, G.A., and Liu, C.F. (2018). Crystal structure of green fluorescent protein clover and design of clover-based redox sensors. Structure *26*, 225-237. e223.

Canny, M.D., Moatti, N., Wan, L.C., Fradet-Turcotte, A., Krasner, D., Mateos-Gomez, P.A., Zimmermann, M., Orthwein, A., Juang, Y.-C., and Zhang, W. (2018). Inhibition of 53BP1 favors homology-dependent DNA repair and increases CRISPR–Cas9 genome-editing efficiency. Nature Biotechnology *36*, 95.

Carr, A.M., and Lambert, S. (2013). Replication stress-induced genome instability: the dark side of replication maintenance by homologous recombination. Journal of Molecular Biology *425*, 4733-4744.

Cervera, L., Gutiérrez, S., Gòdia, F., and Segura, M.M. (2011). Optimization of HEK 293 cell growth by addition of non-animal derived components using design of experiments. BMC Proc *5 Suppl 8*, P126-P126.

Chabalier-Taste, C., Brichese, L., Racca, C., Canitrot, Y., Calsou, P., and Larminat, F. (2016). Polo-like kinase 1 mediates BRCA1 phosphorylation and recruitment at DNA double-strand breaks. Oncotarget *7*, 2269.

Chan, K.L., Palmai-Pallag, T., Ying, S., and Hickson, I.D. (2009). Replication stress induces sister-chromatid bridging at fragile site loci in mitosis. Nature Cell Biology *11*, 753-760.

Chan, Y.W., Fugger, K., and West, S.C. (2018). Unresolved recombination intermediates lead to ultra-fine anaphase bridges, chromosome breaks and aberrations. Nature Cell Biology *20*, 92-103.

Chanut, P., Britton, S., Coates, J., Jackson, S.P., and Calsou, P. (2016). Coordinated nuclease activities counteract Ku at single-ended DNA double-strand breaks. Nature Communications *7*, 12889.

Chapard, C., Meraldi, P., Gleich, T., Bachmann, D., Hohl, D., and Huber, M. (2014). TRAIP is a regulator of the spindle assembly checkpoint. Journal of Cell Science *127*, 5149-5156.

Chatre, L., and Ricchetti, M. (2013). Prevalent coordination of mitochondrial DNA transcription and initiation of replication with the cell cycle. Nucleic Acids Research *41*, 3068-3078.

Chaudhuri, A.R., Hashimoto, Y., Herrador, R., Neelsen, K.J., Fachinetti, D., Bermejo, R., Cocito, A., Costanzo, V., and Lopes, M. (2012). Topoisomerase I poisoning results in PARP-mediated replication fork reversal. Nature Structural & Molecular Biology *19*, 417.

Chen, G., and Deng, X. (2018). Cell synchronization by double thymidine block. Bio-protocol *8*.

Chen, H., Lisby, M., and Symington, L.S. (2013). RPA coordinates DNA end resection and prevents formation of DNA hairpins. Molecular Cell *50*, 589-600.

Chen, Y., Carrington-Lawrence, S.D., Bai, P., and Weller, S.K. (2005). Mutations in the putative zinc-binding motif of UL52 demonstrate a complex interdependence between the UL5 and UL52 subunits of the human herpes simplex virus type 1 helicase/primase complex. Journal of Virology *79*, 9088-9096.

Chen, Y.-w., Cleaver, J.E., Hatahet, Z., Honkanen, R.E., Chang, J.-Y., Yen, Y., and Chou, K.-m. (2008). Human DNA polymerase η activity and translocation is regulated by phosphorylation. Proceedings of the National Academy of Sciences *105*, 16578-16583.

Cheng, X., Kanki, T., Fukuoh, A., Ohgaki, K., Takeya, R., Aoki, Y., Hamasaki, N., and Kang, D. (2005). PDIP38 associates with proteins constituting the mitochondrial DNA nucleoid. Journal of Biochemistry *138*, 673-678.

Cho, H.J., Oh, Y.J., Han, S.H., Chung, H.J., Kim, C.H., Lee, N.S., Kim, W.-J., Choi, J.-M., and Kim, H. (2013). Cdk1 protein-mediated phosphorylation of receptor-associated protein 80 (RAP80) serine 677 modulates DNA damage-induced G2/M checkpoint and cell survival. Journal of Biological Chemistry *288*, 3768-3776.

Ciccia, A., and Elledge, S.J. (2010). The DNA damage response: making it safe to play with knives. Molecular Cell *40*, 179-204.

Clausen, A.R., Lujan, S.A., Burkholder, A.B., Orebaugh, C.D., Williams, J.S., Clausen, M.F., Malc, E.P., Mieczkowski, P.A., Fargo, D.C., and Smith, D.J. (2015). Tracking replication enzymology in vivo by genome-wide mapping of ribonucleotide incorporation. Nature Structural & Molecular Biology *22*, 185-191.

Cooke, M.S., Evans, M.D., Dizdaroglu, M., and Lunec, J. (2003). Oxidative DNA damage: mechanisms, mutation, and disease. The FASEB Journal *17*, 1195-1214.

Copeland, W.C., Kasiviswanathan, R., and Longley, M.J. (2016). Analysis of translesion DNA synthesis by the mitochondrial DNA polymerase γ. Mitochondrial DNA, 19-26.

Cortez, D., Guntuku, S., Qin, J., and Elledge, S.J. (2001). ATR and ATRIP: partners in checkpoint signaling. Science *294*, 1713-1716.

Costanzo, V., Shechter, D., Lupardus, P.J., Cimprich, K.A., Gottesman, M., and Gautier, J. (2003). An ATR-and Cdc7-dependent DNA damage checkpoint that inhibits initiation of DNA replication. Molecular Cell *11*, 203-213.

Coulonval, K., Kooken, H., and Roger, P.P. (2011). Coupling of T161 and T14 phosphorylations protects cyclin B–CDK1 from premature activation. Molecular Biology of the Cell *22*, 3971-3985.

Cruet-Hennequart, S., Coyne, S., Glynn, M.T., Oakley, G.G., and Carty, M.P. (2006). UV-induced RPA phosphorylation is increased in the absence of DNA polymerase η and requires DNA-PK. DNA Repair *5*, 491-504.

Day, T.A., Palle, K., Barkley, L.R., Kakusho, N., Zou, Y., Tateishi, S., Verreault, A., Masai, H., and Vaziri, C. (2010). Phosphorylated Rad18 directs DNA polymerase η to sites of stalled replication. Journal of Cell Biology *191*, 953-966.

De Bont, R., and van Larebeke, N. (2004). Endogenous DNA damage in humans: a review of quantitative data. Mutagenesis *19*, 169-185.

Debatisse, M., Le Tallec, B., Letessier, A., Dutrillaux, B., and Brison, O. (2012). Common fragile sites: mechanisms of instability revisited. Trends in Genetics *28*, 22-32.

Deegan, T.D., and Diffley, J.F. (2016). MCM: one ring to rule them all. Current Opinion in Structural Biology *37*, 145-151.

Dephoure, N., Zhou, C., Villén, J., Beausoleil, S.A., Bakalarski, C.E., Elledge, S.J., and Gygi, S.P. (2008). A quantitative atlas of mitotic phosphorylation. Proceedings of the National Academy of Sciences *105*, 10762-10767.

Dewar, J.M., Low, E., Mann, M., Räschle, M., and Walter, J.C. (2017). CRL2Lrr1 promotes unloading of the vertebrate replisome from chromatin during replication termination. Genes & Development *31*, 275-290.

Dewar, J.M., and Walter, J.C. (2017). Mechanisms of DNA replication termination. Nature Reviews Molecular Cell Biology *18*, 507-516.

Diamant, N., Hendel, A., Vered, I., Carell, T., Reißner, T., De Wind, N., Geacinov, N., and Livneh, Z. (2012). DNA damage bypass operates in the S and G2 phases of the cell cycle and exhibits differential mutagenicity. Nucleic Acids Research *40*, 170-180.

Dianov, G.L., Sleeth, K.M., Dianova, I.I., and Allinson, S.L. (2003). Repair of abasic sites in DNA. Mutation Research/Fundamental and Molecular Mechanisms of Mutagenesis *531*, 157-163.

Díaz-Talavera, A., Calvo, P.A., González-Acosta, D., Díaz, M., Sastre-Moreno, G., Blanco-Franco, L., Guerra, S., Martínez-Jiménez, M.I., Méndez, J., and Blanco, L. (2019). A cancer-associated point mutation disables the steric gate of human PrimPol. Scientific Reports *9*, 1121.

Elvers, I., Johansson, F., Groth, P., Erixon, K., and Helleday, T. (2011). UV stalled replication forks restart by re-priming in human fibroblasts. Nucleic Acids Research *39*, 7049-7057.

Ercilla, A., Feu, S., Aranda, S., Llopis, A., Brynjólfsdóttir, S.H., Sørensen, C.S., Toledo, L.I., and Agell, N. (2020). Acute hydroxyurea-induced replication blockade results in replisome components disengagement from nascent DNA without causing fork collapse. Cellular and Molecular Life Sciences *77*, 735-749.

Esashi, F., Christ, N., Gannon, J., Liu, Y., Hunt, T., Jasin, M., and West, S.C. (2005). CDK-dependent phosphorylation of BRCA2 as a regulatory mechanism for recombinational repair. Nature *434*, 598-604.

Esposito, G., Godin, I., Klein, U., Yaspo, M.-L., Cumano, A., and Rajewsky, K. (2000). Disruption of the Rev3l-encoded catalytic subunit of polymerase ζ in mice results in early embryonic lethality. Current Biology *10*, 1221-1224.

Evrin, C., Clarke, P., Zech, J., Lurz, R., Sun, J., Uhle, S., Li, H., Stillman, B., and Speck, C. (2009). A double-hexameric MCM2-7 complex is loaded onto origin DNA during licensing of eukaryotic DNA replication. Proceedings of the National Academy of Sciences *106*, 20240-20245.

Fan, L., Bi, T., Wang, L., and Xiao, W. (2020). DNA-damage tolerance through PCNA ubiquitination and sumoylation. Biochemical Journal *477*, 2655-2677.

Fasching, C.L., Cejka, P., Kowalczykowski, S.C., and Heyer, W.-D. (2015). Top3-Rmi1 dissolve Rad51-mediated D loops by a topoisomerase-based mechanism. Molecular Cell *57*, 595-606.

Fragkos, M., and Naim, V. (2017). Rescue from replication stress during mitosis. Cell Cycle *16*, 613-633.

Franz, A., Orth, M., Pirson, P.A., Sonneville, R., Blow, J.J., Gartner, A., Stemmann, O., and Hoppe, T. (2011). CDC-48/p97 coordinates CDT-1 degradation with GINS chromatin dissociation to ensure faithful DNA replication. Molecular Cell *44*, 85-96.

Frit, P., Ropars, V., Modesti, M., Charbonnier, J.B., and Calsou, P. (2019). Plugged into the Ku-DNA hub: The NHEJ network. Progress in Biophysics and Molecular Biology *147*, 62-76.

Fu, D., Dudimah, F., Zhang, J., Pickering, A., Paneerselvam, J., Palrasu, M., Wang, H., and Fei, P. (2013). Recruitment of DNA polymerase eta by FANCD2 in the early response to DNA damage. Cell Cycle *12*, 803-809.

Fu, Yu V., Yardimci, H., Long, David T., Guainazzi, A., Bermudez, Vladimir P., Hurwitz, J., van Oijen, A., Schärer, Orlando D., and Walter, Johannes C. (2011). Selective Bypass of a Lagging Strand Roadblock by the Eukaryotic Replicative DNA Helicase. Cell *146*, 931-941.

Fumasoni, M., Zwicky, K., Vanoli, F., Lopes, M., and Branzei, D. (2015). Error-free DNA damage tolerance and sister chromatid proximity during DNA replication rely on the Polα/Primase/Ctf4 Complex. Molecular Cell *57*, 812-823.

Gambus, A., Jones, R.C., Sanchez-Diaz, A., Kanemaki, M., van Deursen, F., Edmondson, R.D., and Labib, K. (2006). GINS maintains association of Cdc45 with MCM in replisome progression complexes at eukaryotic DNA replication forks. Nature Cell Biology *8*, 358-366.

Ganem, N.J., and Pellman, D. (2012). Linking abnormal mitosis to the acquisition of DNA damage. Journal of Cell Biology *199*, 871-881.

García-Gómez, S., Reyes, A., Martínez-Jiménez, M.I., Chocrón, E.S., Mourón, S., Terrados, G., Powell, C., Salido, E., Méndez, J., and Holt, I.J. (2013). PrimPol, an archaic primase/polymerase operating in human cells. Molecular Cell *52*, 541-553.

Garinis, G.A., Van der Horst, G.T., Vijg, J., and Hoeijmakers, J.H. (2008). DNA damage and ageing: new-age ideas for an age-old problem. Nature Cell Biology *10*, 1241-1247.

Ge, X.Q., and Blow, J.J. (2010). Chk1 inhibits replication factory activation but allows dormant origin firing in existing factories. Journal of Cell Biology *191*, 1285-1297.

Ge, X.Q., Jackson, D.A., and Blow, J.J. (2007). Dormant origins licensed by excess Mcm2–7 are required for human cells to survive replicative stress. Genes & Development *21*, 3331-3341.

Genois, M.-M., Gagné, J.-P., Yasuhara, T., Jackson, J., Saxena, S., Langelier, M.-F., Ahel, I., Bedford, M.T., Pascal, J.M., and Vindigni, A. (2021). CARM1 regulates replication fork speed and stress response by stimulating PARP1. Molecular Cell, 784-800.

Georgescu, R.E., Schauer, G.D., Yao, N.Y., Langston, L.D., Yurieva, O., Zhang, D., Finkelstein, J., and O'Donnell, M.E. (2015). Reconstitution of a eukaryotic replisome reveals suppression mechanisms that define leading/lagging strand operation. Elife *4*, e04988.

Gheghiani, L., Loew, D., Lombard, B., Mansfeld, J., and Gavet, O. (2017). PLK1 activation in late G2 sets up commitment to mitosis. Cell Reports *19*, 2060-2073.

Ghetti, S., Burigotto, M., Mattivi, A., Magnani, G., Casini, A., Bianchi, A., Cereseto, A., and Fava, L.L. (2021). CRISPR/Cas9 ribonucleoprotein-mediated knockin generation in hTERT-RPE1 cells. STAR Protocols *2*, 100407.

Giannattasio, M., Follonier, C., Tourrière, H., Puddu, F., Lazzaro, F., Pasero, P., Lopes, M., Plevani, P., and Muzi-Falconi, M. (2010). Exo1 competes with repair synthesis, converts NER intermediates to long ssDNA gaps, and promotes checkpoint activation. Molecular Cell *40*, 50-62.

Glover, T.W., Berger, C., Coyle, J., and Echo, B. (1984). DNA polymerase α inhibition by aphidicolin induces gaps and breaks at common fragile sites in human chromosomes. Human Genetics *67*, 136-142.

Göhler, T., Sabbioneda, S., Green, C.M., and Lehmann, A.R. (2011). ATR-mediated phosphorylation of DNA polymerase η is needed for efficient recovery from UV damage. Journal of Cell Biology *192*, 219-227.

Goodman, M.F., and Woodgate, R. (2013). Translesion DNA polymerases. Cold Spring Harbor Perspectives in Biology *5*, a010363.

Gottlieb, T.M., and Jackson, S.P. (1993). The DNA-dependent protein kinase: requirement for DNA ends and association with Ku antigen. Cell *72*, 131-142.

Grawunder, U., Wilm, M., Wu, X., Kulesza, P., Wilson, T.E., Mann, M., and Lieber, M.R. (1997). Activity of DNA ligase IV stimulated by complex formation with XRCC4 protein in mammalian cells. Nature *388*, 492-495.

Gu, C., Zhang, Q., Yang, Z., Wang, Y., Zou, Y., and Wang, Y. (2006). Recognition and incision of oxidative intrastrand cross-link lesions by UvrABC nuclease. Biochemistry *45*, 10739-10746.

Guilliam, T.A., Bailey, L.J., Brissett, N.C., and Doherty, A.J. (2016). PolDIP2 interacts with human PrimPol and enhances its DNA polymerase activities. Nucleic Acids Research *44*, 3317-3329.

Guilliam, T.A., Brissett, N.C., Ehlinger, A., Keen, B.A., Kolesar, P., Taylor, E.M., Bailey, L.J., Lindsay, H.D., Chazin, W.J., and Doherty, A.J. (2017). Molecular basis for PrimPol recruitment to replication forks by RPA. Nature Communications *8*, 15222.

Guilliam, T.A., Jozwiakowski, S.K., Ehlinger, A., Barnes, R.P., Rudd, S.G., Bailey, L.J., Skehel, J.M., Eckert, K.A., Chazin, W.J., and Doherty, A.J. (2015). Human PrimPol is a highly error-prone polymerase regulated by single-stranded DNA binding proteins. Nucleic Acids Research *43*, 1056-1068.

Guilliam, T.A., and Yeeles, J.T. (2020). Reconstitution of translesion synthesis reveals a mechanism of eukaryotic DNA replication restart. Nature Structural & Molecular Biology *27*, 450-460.

Guo, C., Fischhaber, P.L., Luk-Paszyc, M.J., Masuda, Y., Zhou, J., Kamiya, K., Kisker, C., and Friedberg, E.C. (2003). Mouse Rev1 protein interacts with multiple DNA polymerases involved in translesion DNA synthesis. The EMBO Journal *22*, 6621-6630.

Haince, J.-F., McDonald, D., Rodrigue, A., Déry, U., Masson, J.-Y., Hendzel, M.J., and Poirier, G.G. (2008). PARP1-dependent kinetics of recruitment of MRE11 and NBS1 proteins to multiple DNA damage sites. Journal of Biological Chemistry *283*, 1197-1208.

Hanes, J.W., Thal, D.M., and Johnson, K.A. (2006). Incorporation and replication of 8-oxo-deoxyguanosine by the human mitochondrial DNA polymerase. Journal of Biological Chemistry *281*, 36241-36248.

Harbour, J.W., Luo, R.X., Dei Santi, A., Postigo, A.A., and Dean, D.C. (1999). Cdk phosphorylation triggers sequential intramolecular interactions that progressively block Rb functions as cells move through G1. Cell *98*, 859-869.

Harley, M.E., Murina, O., Leitch, A., Higgs, M.R., Bicknell, L.S., Yigit, G., Blackford, A.N., Zlatanou, A., Mackenzie, K.J., Reddy, K*., et al.* (2016). TRAIP promotes DNA damage response during genome replication and is mutated in primordial dwarfism. Nature Genetics *48*, 36-43.

Hedglin, M., Aitha, M., Pedley, A., and Benkovic, S.J. (2019). Replication protein A dynamically regulates monoubiquitination of proliferating cell nuclear antigen. Journal of Biological Chemistry *294*, 5157-5168.

Hedglin, M., Pandey, B., and Benkovic, S.J. (2016). Characterization of human translesion DNA synthesis across a UV-induced DNA lesion. Elife *5*, e19788.

Heller, R.C., and Marians, K.J. (2006). Replisome assembly and the direct restart of stalled replication forks. Nature Reviews Molecular Cell Biology *7*, 932-943.

Hellman, A., Rahat, A., Scherer, S.W., Darvasi, A., Tsui, L.-C., and Kerem, B. (2000). Replication delay along FRA7H, a common fragile site on human chromosome 7, leads to chromosomal instability. Molecular and Cellular Biology *20*, 4420-4427.

Hendel, A., Krijger, P.H., Diamant, N., Goren, Z., Langerak, P., Kim, J., Reißner, T., Lee, K.-y., Geacintov, N.E., and Carell, T. (2011). PCNA ubiquitination is important, but not essential for translesion DNA synthesis in mammalian cells. PLoS Genetics *7*.

Hochegger, H., Dejsuphong, D., Sonoda, E., Saberi, A., Rajendra, E., Kirk, J., Hunt, T., and Takeda, S. (2007). An essential role for Cdk1 in S phase control is revealed via chemical genetics in vertebrate cells. The Journal of Cell Biology *178*, 257-268.

Hoege, C., Pfander, B., Moldovan, G.-L., Pyrowolakis, G., and Jentsch, S. (2002). RAD6-dependent DNA repair is linked to modification of PCNA by ubiquitin and SUMO. Nature *419*, 135-141.

Hoeijmakers, J.H. (2009). DNA damage, aging, and cancer. New England Journal of Medicine *361*, 1475-1485.

Hoeijmakers, J.H. (2001). Genome maintenance mechanisms for preventing cancer. Nature *411*, 366-374.

Hoffmann, I., Draetta, G., and Karsenti, E. (1994). Activation of the phosphatase activity of human cdc25A by a cdk2-cyclin E dependent phosphorylation at the G1/S transition. The EMBO Journal *13*, 4302-4310.

Holloman, W.K. (2011). Unraveling the mechanism of BRCA2 in homologous recombination. Nature Structural & Molecular Biology *18*, 748-754.

Hsiau, T., Maures, T., Waite, K., Yang, J., Kelso, R., Holden, K., and Stoner, R. (2018). Inference of CRISPR edits from Sanger trace data. BioRxiv, 251082.

Hyun, S.-Y., Hwan, H.-I., and Jang, Y.-J. (2014). Polo-like kinase-1 in DNA damage response. BMB Reports *47*, 249.

Ira, G., Pellicioli, A., Balijja, A., Wang, X., Fiorani, S., Carotenuto, W., Liberi, G., Bressan, D., Wan, L., and Hollingsworth, N.M. (2004). DNA end resection, homologous recombination and DNA damage checkpoint activation require CDK1. Nature *431*, 1011-1017.

Iyama, T., and Wilson, D.M., 3rd (2013). DNA repair mechanisms in dividing and non-dividing cells. DNA Repair *12*, 620-636.

Iyer, D.R., and Rhind, N. (2017). The intra-S checkpoint responses to DNA damage. Genes *8*, 74.

Iyer, L.M., Koonin, E.V., Leipe, D.D., and Aravind, L. (2005). Origin and evolution of the archaeo-eukaryotic primase superfamily and related palm-domain proteins: structural insights and new members. Nucleic Acids Research *33*, 3875-3896.

Iyer, R.R., Pluciennik, A., Burdett, V., and Modrich, P.L. (2006). DNA mismatch repair: functions and mechanisms. Chemical Reviews *106*, 302-323.

Jazayeri, A., Falck, J., Lukas, C., Bartek, J., Smith, G.C., Lukas, J., and Jackson, S.P. (2006). ATM-and cell cycle-dependent regulation of ATR in response to DNA double-strand breaks. Nature Cell Biology *8*, 37-45.

Jia, N., Nakazawa, Y., Guo, C., Shimada, M., Sethi, M., Takahashi, Y., Ueda, H., Nagayama, Y., and Ogi, T. (2015). A rapid, comprehensive system for assaying DNA repair activity and cytotoxic effects of DNA-damaging reagents. Nature Protocols *10*, 12-24.

Johansson, E., and Dixon, N. (2013). Replicative DNA polymerases. Cold Spring Harbor Perspectives in Biology *5*, a012799.

Kanao, R., and Masutani, C. (2017). Regulation of DNA damage tolerance in mammalian cells by post-translational modifications of PCNA. Mutation Research/DNA Repair *803-805*, 82-88.

Karras, G.I., Fumasoni, M., Sienski, G., Vanoli, F., Branzei, D., and Jentsch, S. (2013). Noncanonical role of the 9-1-1 clamp in the error-free DNA damage tolerance pathway. Molecular Cell *49*, 536-546.

Kathe, S.D., Shen, G.-P., and Wallace, S.S. (2004). Single-stranded breaks in DNA but not oxidative DNA base damages block transcriptional elongation by RNA polymerase II in HeLa cell nuclear extracts. Journal of Biological Chemistry *279*, 18511-18520.

Kato, J.-Y., Matsuoka, M., Strom, D.K., and Sherr, C.J. (1994). Regulation of cyclin D-dependent kinase 4 (cdk4) by cdk4-activating kinase. Molecular and Cellular Biology *14*, 2713-2721.

Katsuno, Y., Suzuki, A., Sugimura, K., Okumura, K., Zineldeen, D.H., Shimada, M., Niida, H., Mizuno, T., Hanaoka, F., and Nakanishi, M. (2009). Cyclin A–Cdk1 regulates the origin firing program in mammalian cells. Proceedings of the National Academy of Sciences *106*, 3184-3189.

Kawabe, Y.-i., Branzei, D., Hayashi, T., Suzuki, H., Masuko, T., Onoda, F., Heo, S.-J., Ikeda, H., Shimamoto, A., and Furuichi, Y. (2001). A novel protein interacts with the Werner's syndrome gene product physically and functionally. Journal of Biological Chemistry *276*, 20364-20369.

Keen, B.A., Bailey, L.J., Jozwiakowski, S.K., and Doherty, A.J. (2014a). Human PrimPol mutation associated with high myopia has a DNA replication defect. Nucleic Acids Research *42*, 12102-12111.

Keen, B.A., Jozwiakowski, S.K., Bailey, L.J., Bianchi, J., and Doherty, A.J. (2014b). Molecular dissection of the domain architecture and catalytic activities of human PrimPol. Nucleic Acids Research *42*, 5830-5845.

Khare, V., and Eckert, K.A. (2002). The proofreading 3'→ 5' exonuclease activity of DNA polymerases: a kinetic barrier to translesion DNA synthesis. Mutation Research/Fundamental and Molecular Mechanisms of Mutagenesis *510*, 45-54.

Kim, Y.J., and Wilson, D.M., 3rd (2012). Overview of base excision repair biochemistry. Current Molecular Pharmacology *5*, 3-13.

Kingston, R.E., Chen, C.A., and Rose, J.K. (2003). Calcium phosphate transfection. Current Protocols in Molecular Biology *63*, 9.1. 1-9.1. 11.

Kinner, A., Wu, W., Staudt, C., and Iliakis, G. (2008). γ-H2AX in recognition and signaling of DNA double-strand breaks in the context of chromatin. Nucleic Acids Research *36*, 5678-5694.

Kitagawa, R., Bakkenist, C.J., McKinnon, P.J., and Kastan, M.B. (2004). Phosphorylation of SMC1 is a critical downstream event in the ATM–NBS1–BRCA1 pathway. Genes & Development *18*, 1423-1438.

Kobayashi, K., Guilliam, T.A., Tsuda, M., Yamamoto, J., Bailey, L.J., Iwai, S., Takeda, S., Doherty, A.J., and Hirota, K. (2016). Repriming by PrimPol is critical for DNA replication restart downstream of lesions and chain-terminating nucleosides. Cell Cycle *15*, 1997-2008.

Kothandapani, A., Sawant, A., Dangeti, V.S.M.N., Sobol, R.W., and Patrick, S.M. (2013). Epistatic role of base excision repair and mismatch repair pathways in mediating cisplatin cytotoxicity. Nucleic Acids Research *41*, 7332-7343.

Krupina, K., Goginashvili, A., and Cleveland, D.W. (2021). Causes and consequences of micronuclei. Current Opinion in Cell Biology *70*, 91-99.

Kuchta, R.D., and Stengel, G. (2010). Mechanism and evolution of DNA primases. Biochimica et Biophysica Acta (BBA)-Proteins and Proteomics *1804*, 1180-1189.

Kumar, M., Gouw, M., Michael, S., Sámano-Sánchez, H., Pancsa, R., Glavina, J., Diakogianni, A., Valverde, J.A., Bukirova, D., and Čalyševa, J. (2020). ELM—the eukaryotic linear motif resource in 2020. Nucleic Acids Research *48*, D296-D306.

Kuzminov, A. (2001). Single-strand interruptions in replicating chromosomes cause double-strand breaks. Proceedings of the National Academy of Sciences *98*, 8241-8246.

Lamers, M.H., and O'Donnell, M. (2008). A consensus view of DNA binding by the C family of replicative DNA polymerases. Proceedings of the National Academy of Sciences *105*, 20565-20566.

Lane, H.A., and Nigg, E.A. (1996). Antibody microinjection reveals an essential role for human polo-like kinase 1 (Plk1) in the functional maturation of mitotic centrosomes. Journal of Cell Biology *135*, 1701-1714.

Lau, W.C.Y., Li, Y., Zhang, Q., and Huen, M.S.Y. (2015). Molecular architecture of the Ub-PCNA/Pol η complex bound to DNA. Scientific Reports *5*, 15759.

Le Beau, M.M., Rassool, F.V., Neilly, M.E., Espinosa, R., III, Glover, T.W., Smith, D.I., and McKeithan, T.W. (1998). Replication of a Common Fragile Site, FRA3B, Occurs Late in S Phase and is Delayed Further Upon Induction: Implications for the Mechanism of Fragile Site Induction. Human Molecular Genetics *7*, 755-761.

Lee, K.S., Oh, D.Y., Kang, Y.H., and Park, J.E. (2008). Self-regulated mechanism of Plk1 localization to kinetochores: lessons from the Plk1-PBIP1 interaction. Cell Div *3*, 4.

Lee, M., Daniels, M.J., and Venkitaraman, A.R. (2004). Phosphorylation of BRCA2 by the Polo-like kinase Plk1 is regulated by DNA damage and mitotic progression. Oncogene *23*, 865-872.

Lee, M.G., and Nurse, P. (1987). Complementation used to clone a human homologue of the fission yeast cell cycle control gene cdc2. Nature *327*, 31-35.

Legros, F., Malka, F., Frachon, P., Lombès, A., and Rojo, M. (2004). Organization and dynamics of human mitochondrial DNA. Journal of Cell Science *117*, 2653-2662.

Lehman, A., Kirk-Bell, S., Arlett, C., Paterson, M., Lohman, P., de Weerd-Kastelein, E., and Bootsma, D. (1975). Xeroderma pigmentosum cells with normal levels of excision repair have a defect in DNA synthesis after UV-irradiation. Proceedings of the National Academy of Sciences *72*, 219-223.

Lehmann, A.R. (1972). Postreplication repair of DNA in ultraviolet-irradiated mammalian cells. Journal of Molecular Biology *66*, 319-337.

Lehmann, A.R., McGibbon, D., and Stefanini, M. (2011). Xeroderma pigmentosum. Orphanet Journal of Rare Diseases *6*, 70.

Lehmann, C.P., Jiménez-Martín, A., Branzei, D., and Tercero, J.A. (2020). Prevention of unwanted recombination at damaged replication forks. Current Genetics, 1-7.

Lei, M. (2005). The MCM complex: its role in DNA replication and implications for cancer therapy. Current Cancer Drug Targets *5*, 365-380.

Lemmens, B., Hegarat, N., Akopyan, K., Sala-Gaston, J., Bartek, J., Hochegger, H., and Lindqvist, A. (2018). DNA replication determines timing of mitosis by restricting CDK1 and PLK1 activation. Molecular Cell *71*, 117-128. e113.

Lénárt, P., Petronczki, M., Steegmaier, M., Di Fiore, B., Lipp, J.J., Hoffmann, M., Rettig, W.J., Kraut, N., and Peters, J.-M. (2007). The small-molecule inhibitor BI 2536 reveals novel insights into mitotic roles of polo-like kinase 1. Current Biology *17*, 304-315.

Li, H., Wang, Y., and Liu, X. (2008). Plk1-dependent phosphorylation regulates functions of DNA topoisomerase IIα in cell cycle progression. Journal of Biological Chemistry *283*, 6209-6221.

Li, S., and Wu, X. (2020). Common fragile sites: protection and repair. Cell & Bioscience *10*, 29.

Li, X., and Heyer, W.-D. (2008). Homologous recombination in DNA repair and DNA damage tolerance. Cell Research *18*, 99-113.

Li, Z., Li, J., Kong, Y., Yan, S., Ahmad, N., and Liu, X. (2017). Plk1 phosphorylation of Mre11 antagonizes the DNA damage response. Cancer Research *77*, 3169-3180.

Liang, X., Potter, J., Kumar, S., Zou, Y., Quintanilla, R., Sridharan, M., Carte, J., Chen, W., Roark, N., and Ranganathan, S. (2015). Rapid and highly efficient mammalian cell engineering via Cas9 protein transfection. Journal of Biotechnology *208*, 44-53.

Liao, H., Ji, F., Geng, X., Xing, M., Li, W., Chen, Z., Shen, H., and Ying, S. (2017). CDK1 promotes nascent DNA synthesis and induces resistance of cancer cells to DNA-damaging therapeutic agents. Oncotarget *8*, 90662.

Liao, H., Ji, F., Helleday, T., and Ying, S. (2018). Mechanisms for stalled replication fork stabilization: new targets for synthetic lethality strategies in cancer treatments. EMBO Reports *19*, e46263.

Liaw, H., Lee, D., and Myung, K. (2011). DNA-PK-dependent RPA2 hyperphosphorylation facilitates DNA repair and suppresses sister chromatid exchange. PloS One *6*.

Lin, S., Staahl, B.T., Alla, R.K., and Doudna, J.A. (2014a). Enhanced homology-directed human genome engineering by controlled timing of CRISPR/Cas9 delivery. elife *3*, e04766.

Lin, W., Xin, H., Zhang, Y., Wu, X., Yuan, F., and Wang, Z. (1999). The human REV1 gene codes for a DNA template-dependent dCMP transferase. Nucleic Acids Research *27*, 4468-4475.

Lin, Y.-C., Boone, M., Meuris, L., Lemmens, I., Van Roy, N., Soete, A., Reumers, J., Moisse, M., Plaisance, S., and Drmanac, R. (2014b). Genome dynamics of the human embryonic kidney 293 lineage in response to cell biology manipulations. Nature Communications *5*, 1-12.

Lindahl, T., and Barnes, D. (2000). Repair of endogenous DNA damage. In Cold Spring Harbor symposia on quantitative biology (Cold Spring Harbor Laboratory Press), pp. 127-134.

Lindon, C., and Pines, J. (2004). Ordered proteolysis in anaphase inactivates Plk1 to contribute to proper mitotic exit in human cells. The Journal of Cell Biology *164*, 233-241.

Liu, D., Davydenko, O., and Lampson, M.A. (2012). Polo-like kinase-1 regulates kinetochore–microtubule dynamics and spindle checkpoint silencing. Journal of Cell Biology *198*, 491-499.

Liu, L., Rodriguez-Belmonte, E.M., Mazloum, N., Xie, B., and Lee, M.Y. (2003). Identification of a novel protein, PDIP38, that interacts with the p50 subunit of DNA polymerase δ and proliferating cell nuclear antigen. Journal of Biological Chemistry *278*, 10041-10047.

Liu, Q., Guntuku, S., Cui, X.-S., Matsuoka, S., Cortez, D., Tamai, K., Luo, G., Carattini-Rivera, S., DeMayo, F., and Bradley, A. (2000). Chk1 is an essential kinase that is regulated by Atr and required for the G2/M DNA damage checkpoint. Genes & Development *14*, 1448-1459.

Livneh, Z., and Shachar, S. (2010). Multiple two-polymerase mechanisms in mammalian translesion DNA synthesis. Cell Cycle *9*, 729-735.

Lopes, M., Cotta-Ramusino, C., Pellicioli, A., Liberi, G., Plevani, P., Muzi-Falconi, M., Newlon, C.S., and Foiani, M. (2001). The DNA replication checkpoint response stabilizes stalled replication forks. Nature *412*, 557-561.

Lopes, M., Foiani, M., and Sogo, J.M. (2006). Multiple mechanisms control chromosome integrity after replication fork uncoupling and restart at irreparable UV lesions. Molecular Cell *21*, 15-27.

Lujan, S.A., Williams, J.S., and Kunkel, T.A. (2016). DNA polymerases divide the labor of genome replication. Trends in Cell Biology *26*, 640-654.

Lukášová, E., Řezáčová, M., Bačíková, A., Šebejová, L., Vávrová, J., and Kozubek, S. (2019). Distinct cellular responses to replication stress leading to apoptosis or senescence. FEBS Open bio *9*, 870-890.

Luzhna, L., Kathiria, P., and Kovalchuk, O. (2013). Micronuclei in genotoxicity assessment: from genetics to epigenetics and beyond. Frontiers in Genetics *4*, 131.

Ma, H.T., and Poon, R.Y. (2020). Aurora kinases and DNA damage response. Mutation Research/Fundamental and Molecular Mechanisms of Mutagenesis, 111716.

Ma, W., Westmoreland, J.W., and Resnick, M.A. (2013). Homologous recombination rescues ssDNA gaps generated by nucleotide excision repair and reduced translesion DNA synthesis in yeast G2 cells. Proceedings of the National Academy of Sciences *110*, E2895-E2904.

Maga, G., Frouin, I., Spadari, S., and Hübscher, U. (2001). Replication protein A as a "fidelity clamp" for DNA polymerase α. Journal of Biological Chemistry *276*, 18235-18242.

Mailand, N., Falck, J., Lukas, C., Syljuâsen, R.G., Welcker, M., Bartek, J., and Lukas, J. (2000). Rapid destruction of human Cdc25A in response to DNA damage. Science *288*, 1425-1429.

Malumbres, M., and Barbacid, M. (2009). Cell cycle, CDKs and cancer: a changing paradigm. Nature Reviews Cancer *9*, 153-166.

Malumbres, M., Sotillo, R.o., Santamaría, D., Galán, J., Cerezo, A., Ortega, S., Dubus, P., and Barbacid, M. (2004). Mammalian cells cycle without the D-type cyclin-dependent kinases Cdk4 and Cdk6. Cell *118*, 493-504.

Mandal, R., and Strebhardt, K. (2013). Plk1: unexpected roles in DNA replication. Cell Research *23*, 1251-1253.

Maréchal, A., and Zou, L. (2013). DNA damage sensing by the ATM and ATR kinases. Cold Spring Harbor Perspectives in Biology *5*, a012716.

Maric, M., Maculins, T., De Piccoli, G., and Labib, K. (2014). Cdc48 and a ubiquitin ligase drive disassembly of the CMG helicase at the end of DNA replication. Science *346*, 1253596.

Martínez-Jiménez, M.I., Calvo, P.A., García-Gómez, S., Guerra-González, S., and Blanco, L. (2018). The Zn-finger domain of human PrimPol is required to stabilize the initiating nucleotide during DNA priming. Nucleic Acids Research *46*, 4138-4151.

Martínez-Jiménez, M.I., Lahera, A., and Blanco, L. (2017). Human PrimPol activity is enhanced by RPA. Scientific Reports *7*, 1-8.

Mason, J.M., Chan, Y.-L., Weichselbaum, R.W., and Bishop, D.K. (2019). Non-enzymatic roles of human RAD51 at stalled replication forks. Nature Communications *10*, 4410.

Masutani, C., Kusumoto, R., Iwai, S., and Hanaoka, F. (2000). Mechanisms of accurate translesion synthesis by human DNA polymerase η. The EMBO journal *19*, 3100-3109.

Matsuda, T., Bebenek, K., Masutani, C., Hanaoka, F., and Kunkel, T.A. (2000). Low fidelity DNA synthesis by human DNA polymerase-η. Nature *404*, 1011-1013.

Matsuoka, S., Ballif, B.A., Smogorzewska, A., McDonald, E.R., Hurov, K.E., Luo, J., Bakalarski, C.E., Zhao, Z., Solimini, N., and Lerenthal, Y. (2007). ATM and ATR substrate analysis reveals extensive protein networks responsive to DNA damage. Science *316*, 1160-1166.

Maya-Mendoza, A., Moudry, P., Merchut-Maya, J.M., Lee, M., Strauss, R., and Bartek, J. (2018). High speed of fork progression induces DNA replication stress and genomic instability. Nature *559*, 279-284.

McGlynn, P., and Lloyd, R.G. (2002). Recombinational repair and restart of damaged replication forks. Nature Reviews Molecular Cell Biology *3*, 859-870.

McInerney, P., and O'Donnell, M. (2004). Functional Uncoupling of Twin Polymerases: Mechanism of Polymerase Dissociation From A Lagging Strand Block. Journal of Biological Chemistry *279*, 21543-21551.

McKinnon, P.J. (2009). DNA repair deficiency and neurological disease. Nat Rev Neurosci *10*, 100-112.

Mikule, K., Delaval, B., Kaldis, P., Jurcyzk, A., Hergert, P., and Doxsey, S. (2007). Loss of centrosome integrity induces p38—p53—p21-dependent G1—S arrest. Nature Cell Biology *9*, 160-170.

Miyabe, I., Kunkel, T.A., and Carr, A.M. (2011). The major roles of DNA polymerases epsilon and delta at the eukaryotic replication fork are evolutionarily conserved. PLoS Genetics *7*, e1002407.

Miyabe, I., Mizuno, K.I., Keszthelyi, A., Daigaku, Y., Skouteri, M., Mohebi, S., Kunkel, T.A., Murray, J.M., and Carr, A.M. (2015). Polymerase δ replicates both strands after homologous recombination–dependent fork restart. Nature Structural & Molecular Biology *22*, 932–938

Moreno, S.P., Bailey, R., Campion, N., Herron, S., and Gambus, A. (2014). Polyubiquitylation drives replisome disassembly at the termination of DNA replication. Science *346*, 477-481.

Moreno, S.P., and Gambus, A. (2020). Mechanisms of eukaryotic replisome disassembly. Biochemical Society Transactions *48*, 823-836.

Moreno, S.P., Jones, R.M., Poovathumkadavil, D., Scaramuzza, S., and Gambus, A. (2019). Mitotic replisome disassembly depends on TRAIP ubiquitin ligase activity. Life science alliance *2*.

Moura, M., and Conde, C. (2019). Phosphatases in mitosis: roles and regulation. Biomolecules *9*, 55.

Mourón, S., Rodriguez-Acebes, S., Martínez-Jiménez, M.I., García-Gómez, S., Chocrón, S., Blanco, L., and Méndez, J. (2013). Repriming of DNA synthesis at stalled replication forks by human PrimPol. Nature Structural & Molecular Biology *20*, 1383-1389.

Muñoz, S., and Méndez, J. (2017). DNA replication stress: from molecular mechanisms to human disease. Chromosoma *126*, 1-15.

Murai, J., Zhang, Y., Morris, J., Ji, J., Takeda, S., Doroshow, J.H., and Pommier, Y. (2014). Rationale for poly (ADP-ribose) polymerase (PARP) inhibitors in combination therapy with camptothecins or temozolomide based on PARP trapping versus catalytic inhibition. Journal of Pharmacology and Experimental Therapeutics *349*, 408-416.

Mutreja, K., Krietsch, J., Hess, J., Ursich, S., Berti, M., Roessler, F.K., Zellweger, R., Patra, M., Gasser, G., and Lopes, M. (2018). ATR-Mediated Global Fork Slowing and Reversal Assist Fork Traverse and Prevent Chromosomal Breakage at DNA Interstrand Cross-Links. Cell Reports *24*, 2629-2642.e2625.

Nakajima, H., Toyoshima-Morimoto, F., Taniguchi, E., and Nishida, E. (2003). Identification of a consensus motif for Plk (Polo-like kinase) phosphorylation reveals Myt1 as a Plk1 substrate. Journal of Biological Chemistry *278*, 25277-25280.

Nakamura, K., Kustatscher, G., Alabert, C., Hödl, M., Forne, I., Völker-Albert, M., Satpathy, S., Beyer, T.E., Mailand, N., and Choudhary, C. (2021). Proteome dynamics at broken replication forks reveal a distinct ATM-directed repair response suppressing DNA double-strand break ubiquitination. Molecular Cell *81*, 1084-1099. e1086.

Nayak, S., Calvo, J.A., Cong, K., Peng, M., Berthiaume, E., Jackson, J., Zaino, A.M., Vindigni, A., Hadden, M.K., and Cantor, S.B. (2020). Inhibition of the translesion synthesis polymerase REV1 exploits replication gaps as a cancer vulnerability. Science Advances *6*, eaaz7808.

Neelsen, K.J., and Lopes, M. (2015). Replication fork reversal in eukaryotes: from dead end to dynamic response. Nature Reviews Molecular Cell Biology *16*, 207-220.

Nemec, A.A., Wallace, S.S., and Sweasy, J.B. (2010). Variant base excision repair proteins: contributors to genomic instability. Seminars in Cancer Biology *20*, 320-328.

Noll, D.M., Mason, T.M., and Miller, P.S. (2006). Formation and repair of interstrand cross-links in DNA. Chemical Reviews *106*, 277-301.

O'Driscoll, M. (2012). Diseases associated with defective responses to DNA damage. Cold Spring Harbor Perspectives in Biology *4*, a012773.

Oakley, G.G., Patrick, S.M., Yao, J., Carty, M.P., Turchi, J.J., and Dixon, K. (2003). RPA Phosphorylation in Mitosis Alters DNA Binding and Protein− Protein Interactions. Biochemistry *42*, 3255-3264.

Ochi, T., Blackford, A.N., Coates, J., Jhujh, S., Mehmood, S., Tamura, N., Travers, J., Wu, Q., Draviam, V.M., and Robinson, C.V. (2015). PAXX, a paralog of XRCC4 and XLF, interacts with Ku to promote DNA double-strand break repair. Science *347*, 185-188.

Orlowska, K.P., Klosowska, K., Szczesny, R.J., Cysewski, D., Krawczyk, P.S., and Dziembowski, A. (2013). A new strategy for gene targeting and functional proteomics using the DT40 cell line. Nucleic Acids Research *41*, e167-e167.

Ortega, S., Prieto, I., Odajima, J., Martín, A., Dubus, P., Sotillo, R., Barbero, J.L., Malumbres, M., and Barbacid, M. (2003). Cyclin-dependent kinase 2 is essential for meiosis but not for mitotic cell division in mice. Nature genetics *35*, 25-31.

Pai, C.-C., Hsu, K.-F., Durley, S.C., Keszthelyi, A., Kearsey, S.E., Rallis, C., Folkes, L.K., Deegan, R., Wilkins, S.E., and Pfister, S.X. (2019). An essential role for dNTP homeostasis following CDK-induced replication stress. Journal of Cell Science *132*.

Pathania, S., Nguyen, J., Hill, S.J., Scully, R., Adelmant, G.O., Marto, J.A., Feunteun, J., and Livingston, D.M. (2011). BRCA1 is required for postreplication repair after UV-induced DNA damage. Molecular Cell *44*, 235-251.

Peddu, C., Zhang, S., Zhao, H., Wong, A., Lee, E.Y., Lee, M.Y., and Zhang, Z. (2018). Phosphorylation Alters the Properties of Pol η: Implications for Translesion Synthesis. iScience *6*, 52-67.

Peng, C.Y., Graves, P.R., Thoma, R.S., Wu, Z., Shaw, A.S., and Piwnica-Worms, H. (1997). Mitotic and G2 checkpoint control: regulation of 14-3-3 protein binding by phosphorylation of Cdc25C on serine-216. Science *277*, 1501-1505.

Petermann, E., Orta, M.L., Issaeva, N., Schultz, N., and Helleday, T. (2010). Hydroxyurea-stalled replication forks become progressively inactivated and require two different RAD51-mediated pathways for restart and repair. Molecular Cell *37*, 492-502.

Piberger, A.L., Bowry, A., Kelly, R.D.W., Walker, A.K., González-Acosta, D., Bailey, L.J., Doherty, A.J., Méndez, J., Morris, J.R., Bryant, H.E*., et al.* (2020). PrimPol-dependent single-stranded gap formation mediates homologous recombination at bulky DNA adducts. Nature Communications *11*, 5863.

Pilzecker, B., Buoninfante, O.A., Pritchard, C., Blomberg, O.S., Huijbers, I.J., van den Berk, P.C., and Jacobs, H. (2016). PrimPol prevents APOBEC/AID family mediated DNA mutagenesis. Nucleic Acids Research *44*, 4734-4744.

Pluciennik, A., Dzantiev, L., Iyer, R.R., Constantin, N., Kadyrov, F.A., and Modrich, P. (2010). PCNA function in the activation and strand direction of MutLα endonuclease in mismatch repair. Proceedings of the National Academy of Sciences *107*, 16066-16071.

Pommier, Y., Barcelo, J.M., Rao, V.A., Sordet, O., Jobson, A.G., Thibaut, L., Miao, Z.H., Seiler, J.A., Zhang, H., and Marchand, C. (2006). Repair of topoisomerase I-mediated DNA damage. Progress in Nucleic Acid Research and Molecular Biology *81*, 179-229.

Ponte-Sucre, A. (2016). An overview of Trypanosoma brucei infections: an intense host–parasite interaction. Frontiers in Microbiology *7*, 2126.

Prasad, C.B., Prasad, S.B., Yadav, S.S., Pandey, L.K., Singh, S., Pradhan, S., and Narayan, G. (2017). Olaparib modulates DNA repair efficiency, sensitizes cervical cancer cells to cisplatin and exhibits anti-metastatic property. Scientific Reports *7*, 1-15.

Quinet, A., Lemaçon, D., and Vindigni, A. (2017). Replication fork reversal: players and guardians. Molecular Cell *68*, 830-833.

Quinet, A., Tirman, S., Jackson, J., Šviković, S., Lemaçon, D., Carvajal-Maldonado, D., González-Acosta, D., Vessoni, A.T., Cybulla, E., and Wood, M. (2020). PRIMPOL-Mediated Adaptive Response Suppresses Replication Fork Reversal in BRCA-Deficient Cells. Molecular cell *77*, 461-474. e469.

Rajski, S.R., and Williams, R.M. (1998). DNA cross-linking agents as antitumor drugs. Chemical Reviews *98*, 2723-2796.

Ran, F.A., Hsu, P.D., Wright, J., Agarwala, V., Scott, D.A., and Zhang, F. (2013). Genome engineering using the CRISPR-Cas9 system. Nature Protocols *8*, 2281-2308.

Rane, S.G., Dubus, P., Mettus, R.V., Galbreath, E.J., Boden, G., Reddy, E.P., and Barbacid, M. (1999). Loss of Cdk4 expression causes insulin-deficient diabetes and Cdk4 activation results in β-islet cell hyperplasia. Nature Genetics *22*, 44-52.

Rass, U., Compton, S.A., Matos, J., Singleton, M.R., Ip, S.C., Blanco, M.G., Griffith, J.D., and West, S.C. (2010). Mechanism of Holliday junction resolution by the human GEN1 protein. Genes & Development *24*, 1559-1569.

Ravanat, J.-L., Douki, T., and Cadet, J. (2001). Direct and indirect effects of UV radiation on DNA and its components. Journal of Photochemistry and Photobiology B: Biology *63*, 88-102.

Rechkoblit, O., Gupta, Y.K., Malik, R., Rajashankar, K.R., Johnson, R.E., Prakash, L., Prakash, S., and Aggarwal, A.K. (2016). Structure and mechanism of human PrimPol, a DNA polymerase with primase activity. Science Advances *2*, e1601317.

Reijns, M.A., Rabe, B., Rigby, R.E., Mill, P., Astell, K.R., Lettice, L.A., Boyle, S., Leitch, A., Keighren, M., and Kilanowski, F. (2012). Enzymatic removal of ribonucleotides from DNA is essential for mammalian genome integrity and development. Cell *149*, 1008-1022.

Rey, L., Sidorova, J.M., Puget, N., Boudsocq, F., Biard, D.S., Monnat, R.J., Cazaux, C., and Hoffmann, J.-S. (2009). Human DNA polymerase η is required for common fragile site stability during unperturbed DNA replication. Molecular and Cellular BIology *29*, 3344-3354.

Roberts, B., Haupt, A., Tucker, A., Grancharova, T., Arakaki, J., Fuqua, M.A., Nelson, A., Hookway, C., Ludmann, S.A., and Mueller, I.A. (2017). Systematic gene tagging using

CRISPR/Cas9 in human stem cells to illuminate cell organization. Molecular Biology of the Cell *28*, 2854-2874.

Rogakou, E.P., Pilch, D.R., Orr, A.H., Ivanova, V.S., and Bonner, W.M. (1998). DNA double-stranded breaks induce histone H2AX phosphorylation on serine 139. Journal of Biological Chemistry *273*, 5858-5868.

Rothwell, P.J., and Waksman, G. (2005). Structure and mechanism of DNA polymerases. Advances in Protein Chemistry *71*, 401-440.

Rudd, S.G., Glover, L., Jozwiakowski, S.K., Horn, D., and Doherty, A.J. (2013). PPL2 translesion polymerase is essential for the completion of chromosomal DNA replication in the African trypanosome. Molecular Cell *52*, 554-565.

Rupp, W.D., and Howard-Flanders, P. (1968). Discontinuities in the DNA synthesized in an excision-defective strain of Escherichia coli following ultraviolet irradiation. Journal of Molecular Biology *31*, 291-304.

Sale, J.E., Lehmann, A.R., and Woodgate, R. (2012). Y-family DNA polymerases and their role in tolerance of cellular DNA damage. Nature Reviews Molecular Cell Biology *13*, 141-152.

Sanchez, M., Drechsler, M., Stark, H., and Lipps, G. (2009). DNA translocation activity of the multifunctional replication protein ORF904 from the archaeal plasmid pRN1. Nucleic Acids Research *37*, 6831-6848.

Santamaria, A., Wang, B., Elowe, S., Malik, R., Zhang, F., Bauer, M., Schmidt, A., Silljé, H.H., Körner, R., and Nigg, E.A. (2011). The Plk1-dependent phosphoproteome of the early mitotic spindle. Molecular & Cellular Proteomics *10*, M110. 004457.

Santamaría, D., Barrière, C., Cerqueira, A., Hunt, S., Tardy, C., Newton, K., Cáceres, J.F., Dubus, P., Malumbres, M., and Barbacid, M. (2007). Cdk1 is sufficient to drive the mammalian cell cycle. Nature *448*, 811-815.

Sarbajna, S., and West, S.C. (2014). Holliday junction processing enzymes as guardians of genome stability. Trends in Biochemical Sciences *39*, 409-419.

Schiavone, D., Guilbaud, G., Murat, P., Papadopoulou, C., Sarkies, P., Prioleau, M.N., Balasubramanian, S., and Sale, J.E. (2014). Determinants of G quadruplex-induced epigenetic instability in REV 1-deficient cells. The EMBO Journal *33*, 2507-2520.

Schiavone, D., Jozwiakowski, S.K., Romanello, M., Guilbaud, G., Guilliam, T.A., Bailey, L.J., Sale, J.E., and Doherty, A.J. (2016). PrimPol is required for replicative tolerance of G quadruplexes in vertebrate cells. Molecular Cell *61*, 161-169.

Scott, S.J., Suvarna, K.S., and D'Avino, P.P. (2020). Synchronization of human retinal pigment epithelial-1 cells in mitosis. Journal of Cell Science *133*.

Seol, J.-H., Shim, E.Y., and Lee, S.E. (2018). Microhomology-mediated end joining: Good, bad and ugly. Mutation Research/Fundamental and Molecular Mechanisms of Mutagenesis *809*, 81-87.

Shen, M., Cai, Y., Yang, Y., Yan, X., Liu, X., and Zhou, T. (2013). Centrosomal protein FOR20 is essential for S-phase progression by recruiting Plk1 to centrosomes. Cell Research *23*, 1284-1295.

Shorrocks, A.-M.K., Jones, S.E., Tsukada, K., Morrow, C.A., Belblidia, Z., Shen, J., Vendrell, I., Fischer, R., Kessler, B.M., and Blackford, A.N. (2021). The Bloom syndrome complex senses RPA-coated single-stranded DNA to restart stalled replication forks. Nature Communications *12*, 1-15.

Sinha, R.P., and Häder, D.-P. (2002). UV-induced DNA damage and repair: a review. Photochemical & Photobiological Sciences *1*, 225-236.

Sishc, B.J., and Davis, A.J. (2017). The role of the core non-homologous end joining factors in carcinogenesis and cancer. Cancers *9*, 81.

Sonneville, R., Moreno, S.P., Knebel, A., Johnson, C., Hastie, C.J., Gartner, A., Gambus, A., and Labib, K. (2017). CUL-2 LRR-1 and UBXN-3 drive replisome disassembly during DNA replication termination and mitosis. Nature Cell Biology *19*, 468-479.

Sørensen, C.S., Syljuåsen, R.G., Falck, J., Schroeder, T., Rönnstrand, L., Khanna, K.K., Zhou, B.B., Bartek, J., and Lukas, J. (2003). Chk1 regulates the S phase checkpoint by coupling the physiological turnover and ionizing radiation-induced accelerated proteolysis of Cdc25A. Cancer Cell *3*, 247-258.

Spivak, G. (2015). Nucleotide excision repair in humans. DNA Repair *36*, 13-18.

Stark, G.R., and Taylor, W.R. (2006). Control of the G2/M transition. Molecular Biotechnology *32*, 227-248.

Stary, A., Kannouche, P., Lehmann, A.R., and Sarasin, A. (2003). Role of DNA polymerase η in the UV mutation spectrum in human cells. Journal of Biological Chemistry *278*, 18767-18775.

Steitz, T.A., and Steitz, J.A. (1993). A general two-metal-ion mechanism for catalytic RNA. Proceedings of the National Academy of Sciences *90*, 6498-6502.

Stojkovič, G., Makarova, A.V., Wanrooij, P.H., Forslund, J., Burgers, P.M., and Wanrooij, S. (2016). Oxidative DNA damage stalls the human mitochondrial replisome. Scientific Reports *6*, 1-13.

Sumara, I., Giménez-Abián, J.F., Gerlich, D., Hirota, T., Kraft, C., de la Torre, C., Ellenberg, J., and Peters, J.-M. (2004). Roles of polo-like kinase 1 in the assembly of functional mitotic spindles. Current Biology *14*, 1712-1722.

Šviković, S., Crisp, A., Tan-Wong, S.M., Guilliam, T.A., Doherty, A.J., Proudfoot, N.J., Guilbaud, G., and Sale, J.E. (2019). R-loop formation during S phase is restricted by PrimPol-mediated repriming. The EMBO Journal *38*.

Taglialatela, A., Alvarez, S., Leuzzi, G., Sannino, V., Ranjha, L., Huang, J.-W., Madubata, C., Anand, R., Levy, B., and Rabadan, R. (2017). Restoration of replication fork stability in BRCA1-and BRCA2-deficient cells by inactivation of SNF2-family fork remodelers. Molecular Cell *68*, 414-430. e418.

Takeda, D.Y., and Dutta, A. (2005). DNA replication and progression through S phase. Oncogene *24*, 2827-2843.

Taylor, M.R., and Yeeles, J.T. (2018). The initial response of a eukaryotic replisome to DNA damage. Molecular Cell *70*, 1067-1080. e1012.

Terasawa, M., Shinohara, A., and Shinohara, M. (2014). Canonical non-homologous end joining in mitosis induces genome instability and is suppressed by M-phase-specific phosphorylation of XRCC4. PLoS Genetics *10*, e1004563.

Thompson, S.L., and Compton, D.A. (2011). Chromosome missegregation in human cells arises through specific types of kinetochore–microtubule attachment errors. Proceedings of the National Academy of Sciences *108*, 17974-17978.

Tiranti, V., Savoia, A., Forti, F., D'Apolito, M.-F., Centra, M., Rocchi, M., and Zeviani, M. (1997). Identification of the Gene Encoding the Human Mitochondrial RNA Polymerase (h-mtRPOL) by Cyberscreening of the Expressed Sequence Tags Database. Human Molecular Genetics *6*, 615-625.

Tissier, A., Janel-Bintz, R., Coulon, S., Klaile, E., Kannouche, P., Fuchs, R.P., and Cordonnier, A.M. (2010). Crosstalk between replicative and translesional DNA polymerases: PDIP38 interacts directly with Polη. DNA Repair *9*, 922-928.

Tissier, A., McDonald, J.P., Frank, E.G., and Woodgate, R. (2000). polι, a remarkably error-prone human DNA polymerase. Genes & Development *14*, 1642-1650.

Todd, A.K., Johnston, M., and Neidle, S. (2005). Highly prevalent putative quadruplex sequence motifs in human DNA. Nucleic Acids Research *33*, 2901-2907.

Torregrosa-Muñumer, R., Forslund, J.M., Goffart, S., Pfeiffer, A., Stojkovič, G., Carvalho, G., Al-Furoukh, N., Blanco, L., Wanrooij, S., and Pohjoismäki, J.L. (2017). PrimPol is required for replication reinitiation after mtDNA damage. Proceedings of the National Academy of Sciences *114*, 11398-11403.

Tsuda, M., Ogawa, S., Ooka, M., Kobayashi, K., Hirota, K., Wakasugi, M., Matsunaga, T., Sakuma, T., Yamamoto, T., and Chikuma, S. (2019). PDIP38/PolDIP2 controls the DNA damage tolerance pathways by increasing the relative usage of translesion DNA synthesis over template switching. PloS One *14*.

Ulrich, H.D., and Jentsch, S. (2000). Two RING finger proteins mediate cooperation between ubiquitin-conjugating enzymes in DNA repair. The EMBO Journal *19*, 3388-3397.

Vaisman, A., and Woodgate, R. (2017). Translesion DNA polymerases in eukaryotes: what makes them tick? Critical Reviews in Biochemistry and Molecular Biology *52*, 274-303.

Van Esch, H., Colnaghi, R., Freson, K., Starokadomskyy, P., Zankl, A., Backx, L., Abramowicz, I., Outwin, E., Rohena, L., and Faulkner, C. (2019). Defective DNA polymerase α-primase leads to X-linked intellectual disability associated with severe growth retardation, microcephaly, and hypogonadism. The American Journal of Human Genetics *104*, 957-967.

Vassilev, L.T., Tovar, C., Chen, S., Knezevic, D., Zhao, X., Sun, H., Heimbrook, D.C., and Chen, L. (2006). Selective small-molecule inhibitor reveals critical mitotic functions of human CDK1. Proceedings of the National Academy of Sciences *103*, 10660-10665.

Vassin, V.M., Anantha, R.W., Sokolova, E., Kanner, S., and Borowiec, J.A. (2009). Human RPA phosphorylation by ATR stimulates DNA synthesis and prevents ssDNA accumulation during DNA-replication stress. Journal of Cell Science *122*, 4070-4080.

Verdoodt, B., Decordier, I., Geleyns, K., Cunha, M., Cundari, E., and Kirsch-Volders, M. (1999). Induction of polyploidy and apoptosis after exposure to high concentrations of the spindle poison nocodazole. Mutagenesis *14*, 513-520.

Wan, L., Lou, J., Xia, Y., Su, B., Liu, T., Cui, J., Sun, Y., Lou, H., and Huang, J. (2013). hPrimpol1/CCDC111 is a human DNA primase-polymerase required for the maintenance of genome integrity. EMBO Reports *14*, 1104-1112.

Wang, W., Walmacq, C., Chong, J., Kashlev, M., and Wang, D. (2018). Structural basis of transcriptional stalling and bypass of abasic DNA lesion by RNA polymerase II. Proceedings of the National Academy of Sciences *115*, E2538-E2545.

Warbrick, E. (1998). PCNA binding through a conserved motif. Bioessays *20*, 195-199.

Waters, L.S., Minesinger, B.K., Wiltrout, M.E., D'Souza, S., Woodruff, R.V., and Walker, G.C. (2009). Eukaryotic Translesion Polymerases and Their Roles and Regulation in DNA Damage Tolerance. Microbiology and Molecular Biology Reviews *73*, 134-154.

Watson, J.D., and Crick, F.H.C. (1953). Molecular Structure of Nucleic Acids: A Structure for Deoxyribose Nucleic Acid. Nature *171*, 737-738.

Whelan, D.R., and Rothenberg, E. (2021). Super-resolution mapping of cellular double-strand break resection complexes during homologous recombination. Proceedings of the National Academy of Sciences *118*.

Wilhelm, T., Olziersky, A.-M., Harry, D., De Sousa, F., Vassal, H., Eskat, A., and Meraldi, P. (2019). Mild replication stress causes chromosome mis-segregation via premature centriole disengagement. Nature Communications *10*, 1-14.

Wittschieben, J., Shivji, M., Lalani, E., Jacobs, M., Marini, F., Gearhart, P., Rosewell, I., Stamp, G., and Wood, R. (2000). Disruption of the developmentally regulated Rev3l gene causes embryonic lethality. Current Biology *10*, 1217-1220.

Wohlschlegel, J.A., Dwyer, B.T., Dhar, S.K., Cvetic, C., Walter, J.C., and Dutta, A. (2000). Inhibition of eukaryotic DNA replication by geminin binding to Cdt1. Science *290*, 2309-2312.

Wold, M.S. (1997). Replication protein A: a heterotrimeric, single-stranded DNA-binding protein required for eukaryotic DNA metabolism. Annual Review of Biochemistry *66*, 61-92.

Wu, Y., Zhang, T.-Y., Fang, L.-l., Chen, Z.-X., Song, L.-W., Cao, J.-L., Yang, L., Yuan, Q., and Xia, N.-S. (2016). Sleeping Beauty transposon-based system for rapid generation of HBV-replicating stable cell lines. Journal of Virological Methods *234*, 96-100.

Yamamoto, J., Takahata, C., Kuraoka, I., Hirota, K., and Iwai, S. (2016). Chemical incorporation of chain-terminating nucleoside analogs as 3'-blocking DNA damage and their removal by human ERCC1-XPF endonuclease. Molecules *21*, 766.

Yan, Y., Xu, Z., Huang, J., Guo, G., Gao, M., Kim, W., Zeng, X., Kloeber, J.A., Zhu, Q., and Zhao, F. (2020). The deubiquitinase USP36 Regulates DNA replication stress and confers therapeutic resistance through PrimPol stabilization. Nucleic Acids Research *48*, 12711-12726.

Yata, K., Lloyd, J., Maslen, S., Bleuyard, J.-Y., Skehel, M., Smerdon, S.J., and Esashi, F. (2012). Plk1 and CK2 act in concert to regulate Rad51 during DNA double strand break repair. Molecular Cell *45*, 371-383.

Yazdi, P.T., Wang, Y., Zhao, S., Patel, N., Eva, Y.-H.L., and Qin, J. (2002). SMC1 is a downstream effector in the ATM/NBS1 branch of the human S-phase checkpoint. Genes & Development *16*, 571-582.

Yeeles, J.T., and Marians, K.J. (2013). Dynamics of leading-strand lesion skipping by the replisome. Molecular Cell *52*, 855-865.

Yeeles, J.T., and Marians, K.J. (2011). The Escherichia coli replisome is inherently DNA damage tolerant. Science *334*, 235-238.

Yoon, J.-H., Park, J., Conde, J., Wakamiya, M., Prakash, L., and Prakash, S. (2015). Rev1 promotes replication through UV lesions in conjunction with DNA polymerases η, ι, and κ but not DNA polymerase ζ. Genes & Development *29*, 2588-2602.

Yoshimura, A., Oikawa, M., Jinbo, H., Hasegawa, Y., Enomoto, T., and Seki, M. (2019). WRNIP1 Controls the Amount of PrimPol. Biological and Pharmaceutical Bulletin *42*, 764-769.

Zafar, M.K., Ketkar, A., Lodeiro, M.F., Cameron, C.E., and Eoff, R.L. (2014). Kinetic analysis of human PrimPol DNA polymerase activity reveals a generally error-prone enzyme capable of accurately bypassing 7, 8-dihydro-8-oxo-2'-deoxyguanosine. Biochemistry *53*, 6584-6594.

Zellweger, R., Dalcher, D., Mutreja, K., Berti, M., Schmid, J.A., Herrador, R., Vindigni, A., and Lopes, M. (2015). Rad51-mediated replication fork reversal is a global response to genotoxic treatments in human cells. Journal of Cell Biology *208*, 563-579.

Zhao, F., Wu, J., Xue, A., Su, Y., Wang, X., Lu, X., Zhou, Z., Qu, J., and Zhou, X. (2013). Exome sequencing reveals CCDC111 mutation associated with high myopia. Human Genetics *132*, 913-921.

Zhao, H., and Piwnica-Worms, H. (2001). ATR-mediated checkpoint pathways regulate phosphorylation and activation of human Chk1. Molecular and Cellular Biology *21*, 4129-4139.

Zheng, L., Baumann, U., and Reymond, J.-L. (2004). An efficient one-step site-directed and site-saturation mutagenesis protocol. Nucleic Acids Research *32*, e115-e115.

Zhu, B., Wang, L., Mitsunobu, H., Lu, X., Hernandez, A.J., Yoshida-Takashima, Y., Nunoura, T., Tabor, S., and Richardson, C.C. (2017). Deep-sea vent phage DNA polymerase specifically initiates DNA synthesis in the absence of primers. Proceedings of the National Academy of Sciences *114*, E2310-E2318.

Zou, L., and Elledge, S.J. (2003). Sensing DNA damage through ATRIP recognition of RPA-ssDNA complexes. Science *300*, 1542-1548.

Zou, L., and Nguyen, H.D. (2018). Getting a Genomic View of DNA Replication Stress. Molecular Cell *72*, 201-203.

Appendix

Appendix A: Lewis J Bainbridge, **Rebecca Teague**, Aidan J Doherty, Repriming DNA synthesis: an intrinsic restart pathway that maintains efficient genome replication, *Nucleic Acids Research*, Volume 49, Issue 9, 21 May 2021, Pages 4831–4847, https://doi.org/10.1093/nar/gkab176

Appendix B: Laura J Bailey, **Rebecca Teague**, Peter Kolesar, Lewis J Bainbridge, Aidan J Doherty, PLK1 regulates PrimPol-dependent repriming during the cell cycle, Resubmitted after revision, *Science Advances*.

Published online 21 March 2021

Nucleic Acids Research, 2021, Vol. 49, No. 9 ***4831–4847***
doi: 10.1093/nar/gkab176

SURVEY AND SUMMARY

Repriming DNA synthesis: an intrinsic restart pathway that maintains efficient genome replication

Lewis J. Bainbridge †, Rebecca Teague † and Aidan J. Doherty *

Genome Damage and Stability Centre, School of Life Sciences, University of Sussex, Brighton, BN1 9RQ, UK

Received January 19, 2021; Revised March 01, 2021; Editorial Decision March 02, 2021; Accepted March 05, 2021

ABSTRACT

To bypass a diverse range of fork stalling impediments encountered during genome replication, cells possess a variety of DNA damage tolerance (DDT) mechanisms including translesion synthesis, template switching, and fork reversal. These pathways function to bypass obstacles and allow efficient DNA synthesis to be maintained. In addition, lagging strand obstacles can also be circumvented by downstream priming during Okazaki fragment generation, leaving gaps to be filled post-replication. Whether repriming occurs on the leading strand has been intensely debated over the past half-century. Early studies indicated that both DNA strands were synthesised discontinuously. Although later studies suggested that leading strand synthesis was continuous, leading to the preferred semi-discontinuous replication model. However, more recently it has been established that replicative primases can perform leading strand repriming in prokaryotes. An analogous fork restart mechanism has also been identified in most eukaryotes, which possess a specialist primase called PrimPol that conducts repriming downstream of stalling lesions and structures. PrimPol also plays a more general role in maintaining efficient fork progression. Here, we review and discuss the historical evidence and recent discoveries that substantiate repriming as an intrinsic replication restart pathway for maintaining efficient genome duplication across all domains of life.

INTRODUCTION: THE EUKARYOTIC DNA REPLICATION MACHINERY

During the synthesis phase (S phase) of the cell cycle, genome replication is performed by the replisome. This multi-protein complex consists of the major replicative enzymes required to accurately duplicate DNA. Replisome proteins include the DNA polymerases α, δ and ε, the Cdc45–MCM–GINS (CMG) DNA helicase complex, as well as additional proteins such as AND-1 (yeast Ctf4), Timeless (Tof1), Claspin (Mrc1), Tipin (Csm3), Topoisomerase I, Mcm10, Replication Protein A (RPA) and FACT (1). Replisome assembly begins in G1 phase with the binding of the minichromosome maintenance (MCM) complex to defined loci known as origins of replication (2). Loading of the MCMs to origins is dependent on prior binding of the Origin Recognition Complex (ORC), comprised of ORC1–6, and the proteins Cdc6 and Cdt1 (3). The MCM replicative helicase is loaded as an inactive, double hexamer structure (4), and is activated when DNA replication begins at the start of S phase (reviewed in (5)). The activation process remodels the MCM complex into two active CMG complexes, one for each direction of synthesis. Encircling each leading DNA strand, the active complex moves away from the centre of the origin and allows for the assembly of the remaining replisome components on the resulting single-stranded DNA (ssDNA) (6).

While the bulk of synthesis is completed by the major replicative polymerases (Pol δ and Pol ε), these enzymes lack the ability to initiate DNA synthesis *de novo*. Therefore, a short ribonucleotide primer is required, from which 3′ extension can be continued by the replicative polymerases (7). In the conventional model, the initiating primers on both the leading and lagging strand are generated by the Pol α-primase complex. This primase synthesises a short RNA primer *de novo*, from which Pol α can extend using dNTPs to create an RNA-DNA primer. This is then further extended by a primary replicative polymerase with proofreading capacity, to ensure high fidelity synthesis. Polymerase

*To whom correspondence should be addressed. Tel: +44 1273877500; Fax: +44 1273678121; Email: a.j.doherty@sussex.ac.uk
†The authors wish it to be known that, in their opinion, the first two authors should be regarded as Joint First Authors.

usage throughout replication is well-coordinated, with the majority of leading strand synthesis undertaken by Pol ε, while Pol δ copies the lagging strand (8). However, this may not always be the case, as Pol δ can conduct synthesis on both strands in yeast, both during bulk replication and following replication restart (9,10). All polymerases exclusively synthesise DNA in a 5′ to 3′ direction. For this reason, the lagging strand is synthesised in short, discontinuous fragments, as the DNA is unwound to allow coupled unidirectional replication to occur (11,12). The Pri1/Pri2 (PriS/L) primase complex frequently synthesises ribonucleotide primers on the lagging strand template, from which Pol α and Pol δ can extend (13). The generally accepted model for leading strand synthesis involves continuous synthesis by Pol ε from the Pri1/Pri2 generated primer at the origin until termination (14). Pol ε is more processive than Pol δ, in keeping with its role of replicating the majority of the leading strand (15,16). Termination of DNA replication occurs either when converging replication forks meet or when the end of the chromosome is reached (17). The replication machinery is then unloaded by the ATPase p97 (cdc48 in yeast), to prevent re-replication of DNA (18). Unlike replication initiation, which is well studied in eukaryotes, replication termination has received significantly less attention. For this reason, the current understanding of replication termination is somewhat incomplete.

Replication stress: derailing the DNA replication machinery

During genome duplication, the replication fork encounters a myriad of conditions and obstacles that can affect the progression of DNA polymerases, resulting in replication stress. Pol δ and Pol ε operate with high fidelity to accurately copy DNA and stall at atypical bases or DNA structures, due to an inability to bypass distorted templates (19). Causes of polymerase stalling include unrepaired DNA lesions generated by both endogenous and exogenous sources (20), DNA secondary structures such as G4 quadruplexes (21) or R loops (22), proteins tightly bound to DNA (23), repetitive sequences, including common fragile sites (24), and increased expression of oncogenes (25,26). Replication stress occurs when the replisome encounters such features on the DNA template, causing slowing or stalling of the fork, which, in turn, can lead to slower or reduced synthesis, fork collapse, DNA breaks, and checkpoint activation (27). The intra-S checkpoint allows for fork stabilisation and the prevention of origin firing, as well as the further slowing of DNA replication. Mutations in the checkpoint response proteins reveal the severe effects of prolonged replication stress. For example, mutations in the Ataxia Telangiectasia and Rad3-related (ATR) gene can cause Seckel syndrome (microcephalic primordial dwarfism), characterised by microcephaly and intellectual disability (28).

To avoid replication fork collapse or mutagenesis, and ultimately maintain genome stability, stalling impediments must either be resolved or bypassed efficiently. DNA repair mechanisms, such as nucleotide excision repair (NER), can be employed outside of S phase to remove damaged DNA nucleotides before the onset of replication. NER is a multistep process that involves several proteins (reviewed in (29)) and is particularly important for the removal of bulky lesions, like those introduced by ultra-violet (UV) light. Importantly, NER is a relatively slow process that is not infallible, and, additionally, lesions can arise during S phase. Therefore, unrepaired lesions are frequently present in DNA during replication, where they have the potential to affect polymerase progression.

The consequences of stalling events vary, depending upon which strand the arresting structure or lesion resides on. It is generally accepted that the constant cycles of priming during discontinuous synthesis reduces the impact of lagging strand lesions on fork progression, as a downstream primer can readily be synthesised as part of this canonical replication process. Providing the replicative helicase is not impaired by a lagging strand barrier, the lagging strand polymerase (Pol δ) can dissociate and restart replication from a new primer, bypassing the impediment (30). In fact, overall fork progression is hardly affected by lagging strand damage in reconstituted replisome collisions (31). The repair of stalling lesions can subsequently be conducted in a post-replicative manner. In contrast, large stretches of ssDNA are generated by leading strand polymerase stalling, caused by the continued unwinding of the DNA template by the replicative helicase; this is known as helicase-polymerase uncoupling (32). ssDNA is fragile and prone to breakage and is therefore protected by the binding of RPA. RPA binding acts as a marker of replication stress and can trigger the S phase checkpoint response by activating the ATR-mediated DNA damage response cascade. This prevents cell cycle progression when replication is incomplete (33). A wide variety of DNA damaging agents, including UV damage, crosslinking agents, polymerase inhibitors or stalling-induced replication stress, can localise and activate ATR by generating stretches of ssDNA. This is bound by RPA, and the 5′ primer end can be bound by the Rad9-Rad1-Hus1 (9-1-1) complex (34). This pathway, therefore, orchestrates multiple branches of the cell's replication stress response. The activity of ATR in the stress response pathway is reviewed in (35). ATR also decreases origin firing elsewhere in the genome, which prevents excessive ssDNA formation that would exhaust cellular RPA resources (36).

Damage tolerance pathways: mechanisms to maintain active replication

DNA damage tolerance (DDT) mechanisms are employed during S phase to bypass DNA lesions, structures and other obstacles without removing them and these impediments will be resolved by a variety of post-replicative pathways. This prevents fork stalling and allows DNA replication to continue in a timely manner, preventing replication stress. There are several mechanisms that cells rely on to continue replication past damage, including, translesion synthesis, template switching, fork reversal and firing of dormant origins (Figure 1).

Virtually all polymerases can perform synthesis across damaged DNA to some degree, but polymerases with high fidelity are the least adept at this process and are therefore prone to stalling. To tolerate damage, atypical bases can be bypassed by specialised polymerases during translesion synthesis (TLS) (37). These specialised Y family TLS polymerases (Pol k, Pol ι, Pol η, Rev1, and Pol ζ) can re-

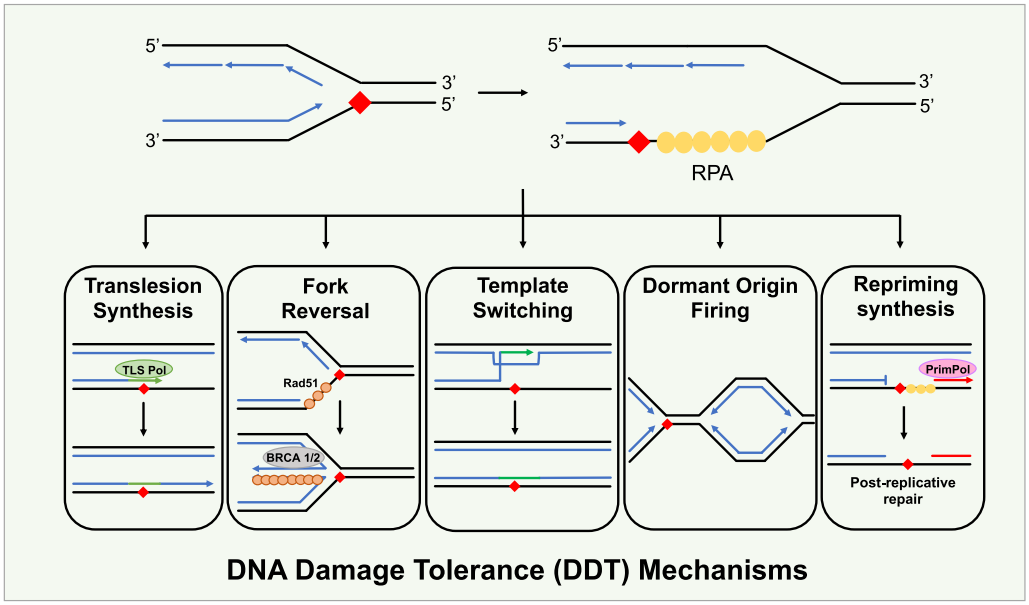

Figure 1. DNA damage tolerance pathways. Obstacles on the DNA template (red diamond) block ongoing DNA replication (blue arrows) and lead to fork stalling. This leads to helicase/polymerase uncoupling, generating tracts of ssDNA, which is bound by RPA (yellow circles). DNA damage tolerance mechanisms allow DNA replication to continue in the presence of such impediments. Translesion synthesis employs specialised polymerases (green oval) to insert bases opposite damaged templating bases (orange line indicates this insertion). Fork reversal begins as the recombinase Rad51 (orange circle) replaces RPA, and, along with the recruitment of additional factors, promotes the transient remodelling of a replication fork into a stabilised 'chicken foot' structure to allow for lesion repair or template switching. Rad51 and BRCA 1/2 (grey oval) are factors that prevent degradation of this reversed fork structure. Template switching requires strand invasion to use the newly replicated strand as a template instead of the damaged parental strand. Dormant origin firing is activated when the replication fork slows or stalls to ensure replication is completed in a timely manner. Dormant origin firing can occur alongside the other mechanisms of DDT. Finally, repriming requires *de novo* primer synthesis downstream of the lesion (red arrow) from which replication can be resumed by a replicative polymerase. In vertebrate cells, this is dependent on PrimPol (pink oval), which is recruited by RPA to ssDNA.

place the replicative polymerase in an attempt to continue replication. TLS polymerases are able to accommodate distorted bases because they are endowed with more open active sites than the replicative polymerases. Because of this, TLS polymerases display low processivity, fidelity and efficiency, as their larger active sites interact less securely with DNA templates (38). Despite their inherent low fidelity, each specialised TLS polymerase is able to bypass at least one specific kind of DNA damage with relatively high fidelity: for example, Pol η accurately replicates over UV-induced cyclobutene pyrimidine dimers (CPD) lesions but is very inefficient at bypassing 6–4 photoproducts *in vitro* (39). Rev1 can bypass abasic sites by incorporating deoxycytidine bases (40). TLS polymerases lack the 3′-5′ exonuclease activity found in Pol δ and Pol ε, and this absence of 'proofreading' allows these polymerases to avoid enzymatic idling, where the proofreading exonuclease would remove any incorrect bases incorporated by the polymerase (41). The regulation of TLS polymerase activity is tightly controlled, in part by the activity of Proliferating Cell Nuclear Antigen (PCNA), a DNA clamp that forms part of the replisome. Monoubiquitination of PCNA by Rad6/Rad18 is a signal for the recruitment of TLS polymerases. However, polyubiquitination of PCNA—remarkably at the same amino acid, K164 (42)—will signal for the assembly of a different DDT pathway: template switching.

Template switching is a recombination-mediated mechanism of fork restart and is therefore significantly more accurate than using TLS polymerases, as the correct sequence can be copied from an undamaged template (43). The process of template switching involves the initial steps of TLS, including recruitment of Rad18 by RPA and chromatin remodelling by INO80. However, at the point of PCNA ubiquitination by Rad6/Rad18, Rad18 may recruit MMS2-UBC13 and HTLF/SHPRH, which polyubiquitinates K164 to stimulate template switching (44–47). The 9–1–1 clamp is then loaded to the 5′ end of the ssDNA, leading to Exo1 recruitment (48), and Rad51/BRCA2/Dss1 mediated strand invasion of the sister chromatid (49). This facilitates the synthesis of the unreplicated sequence opposite the damaged template by Pol δ. After replication has been completed, the newly synthesised strand switches back to its original position, leaving no unreplicated DNA but instead a sister chromatid junction (SJC) that requires resolution by BLM (Sgs1)/TOP3α (Top3)/RMI1/2 (RMI1) (50). This process is complex and requires the timely recruitment of a significant number of proteins, the formation and resolution of a D-loop and the resolution of an SJC before replication can continue. Unlike TLS, this process is considered to be error-free.

Fork reversal is another mechanism by which replication of a damaged template can be avoided, by using the newly synthesised nascent strand as a template. Fork reversal leads to the formation of a regressed fork, which is commonly referred to as a 'chicken foot' structure (51,52). This provides the cell with the opportunity to remove the DNA lesion after fork regression but before replication restart, or, alternatively, to bypass it through template switching once

the fork restarts. Reversed forks can also converge with oncoming replication forks, bypassing the need for fork restart (53). Several factors have been implicated in protecting the reversed fork, including both BRCA1 and BRCA2, and the binding of Rad51 to RPA covered ssDNA. Fork reversal is dependent on the action of SMARCAL1, HLTF or ZRANB3 (54). The majority of fork reversal mechanisms have only recently been reported (reviewed in (55)) and further studies are required to fully elucidate the molecular mechanisms underpinning this process.

An additional method employed by cells to tolerate replication stress is dormant origin firing, a mechanism by which the inactive origins distributed throughout the genome are activated. In G1, when the MCM complex is loaded onto origins, significantly more origins are loaded with inactive complexes than are initially activated. The remaining inactivated origins can then be activated in response to replication stress, despite the activation of the ATR-dependent S phase checkpoint, which decreases late-stage origin firing (56). In fact, Chk1, required for the suppression of origin firing, is paradoxically required for the dormant origin activation by distinguishing between origins within currently active replication factories and those outside (57).

While all of these DDT pathways are now well established, the existence of another conserved mechanism for the bypass of replication fork barriers has been debated by the field for over half a century. The canonical model for discontinuous lagging strand synthesis has long been accepted and, in keeping with this, lesion bypass can be explained simply by constant cycles of priming. However, the existence of a bespoke pathway to reprime stalled leading strand synthesis has been the subject of much debate. Here, we review the available evidence for repriming as a canonical mechanism that promotes DNA damage tolerance and replication restart during leading strand duplication.

Early investigations to elucidate a model of DNA replication

In the years following the discovery of the structure of double-stranded DNA (dsDNA) by Watson and Crick, the field moved quickly to develop a model that described the mechanism of its duplication (58). The isolation of the first DNA polymerase (*Escherichia coli* DNA polymerase I) in the late 1950s provided the first example of an enzyme with the ability to catalyze the synthesis of new DNA strands (59). Interestingly, this polymerase synthesised DNA in a specific 5′ to 3′ direction, which has since been shown to be an inherent feature of all known polymerase enzymes (60). This directionality of synthesis posed an interesting question regarding the nature of replication of each of the antiparallel strands in dsDNA. While one strand could, theoretically, be replicated continuously as the DNA is unwound, the other strand must somehow be replicated backwards (3′ to 5′) to allow for coupled, unidirectional fork progression.

In a classic study investigating replication intermediates in *E. coli*, Okazaki *et al.* used alkaline sucrose gradient sedimentation approaches to uncover low molecular weight (LMW) DNA fragments (Okazaki fragments), synthesised during a quick pulse of radioactive labelling (61,62). The failure to detect any high molecular weight (HMW) molecules after short pulse times led to the postulation that all DNA is synthesised in small pieces. By adding a chase of unlabelled nucleotides into the protocol, the conversion of the radioactive LMW intermediates into fragments of HMW could be observed, hinting at the existence of a joining process and confirming that the small fragments observed were, in fact, intermediates of chromosomal DNA synthesis (61). Subsequent studies found that the newly synthesised DNA fragments were assembled into larger molecules by the further joining of additional fragments to the 3′ end of pre-existing material, as would be expected (63,64). The DNA ligase enzyme was later implicated in the joining of the small fragments, and, accordingly, almost all DNA is present in small molecules in cells expressing temperature-sensitive ligase mutants at non-permissive temperatures (65,66). DNA ligase was also shown to join these fragments in both *Saccharomyces cerevisiae* and *Schizosaccharomyces pombe* (67,68), and human DNA ligase I is now well characterised in this role (reviewed in (69)). *E. coli* harbouring mutations in DNA polymerase I (PolA) also displayed an impairment in the joining of LMW fragments into HMW molecules (70). This suggested a model where PolA fills in gaps between fragments before DNA ligase catalyses the formation of a phosphodiester bond to seal the individual pieces together.

Okazaki's findings offered a solution to the directionality problem, whereby the strand requiring synthesis in the 3′ to 5′ direction (now known as the lagging strand) could be synthesised in short, discontinuous fragments, which can subsequently be ligated into a completed product. Supporting this, the small fragments isolated by Okazaki *et al.* were shown to contain short stretches of RNA, which provided insights into the mechanism by which they are produced (71). Since DNA polymerases are incapable of *de novo* synthesis, short RNA primers would be required at frequent intervals on the exposed lagging strand to act as substrates for the initiation of DNA synthesis by the replicative polymerase. The presence of these RNA species signified that the short fragments are the result of true initiation events and established a model for lagging strand synthesis that allows replication to progress in the same direction as its anti-parallel partner strand, which is also replicated in a 5′ to 3′ direction (71).

Following these seminal studies, there was considerable debate regarding the nature of leading strand (5′ to 3′) synthesis; was it synthesised continuously from the origin to termination (semi-discontinuous model) or did synthesis frequently start and stop in a similar manner to the lagging strand (discontinuous model) (Figure 2A)? Logically, replication restart on the leading strand seems unnecessary, as continuous 5′ to 3′ synthesis from the origin until termination is mechanistically possible. In theory, the 3′-OH of the nascent leading strand can prime further replication and, in addition, discontinuous synthesis would be more energy- and time-consuming. However, all replication intermediates detected in Okazaki's studies were LMW fragments, supporting a discontinuous model where synthesis is reinitiated frequently on both strands. The evidence put forward to settle this debate over the coming decades was conflicting.

Despite the early evidence pointing towards a fully discontinuous model of replication, later studies introduced contradictory evidence that supported the simpler semi-

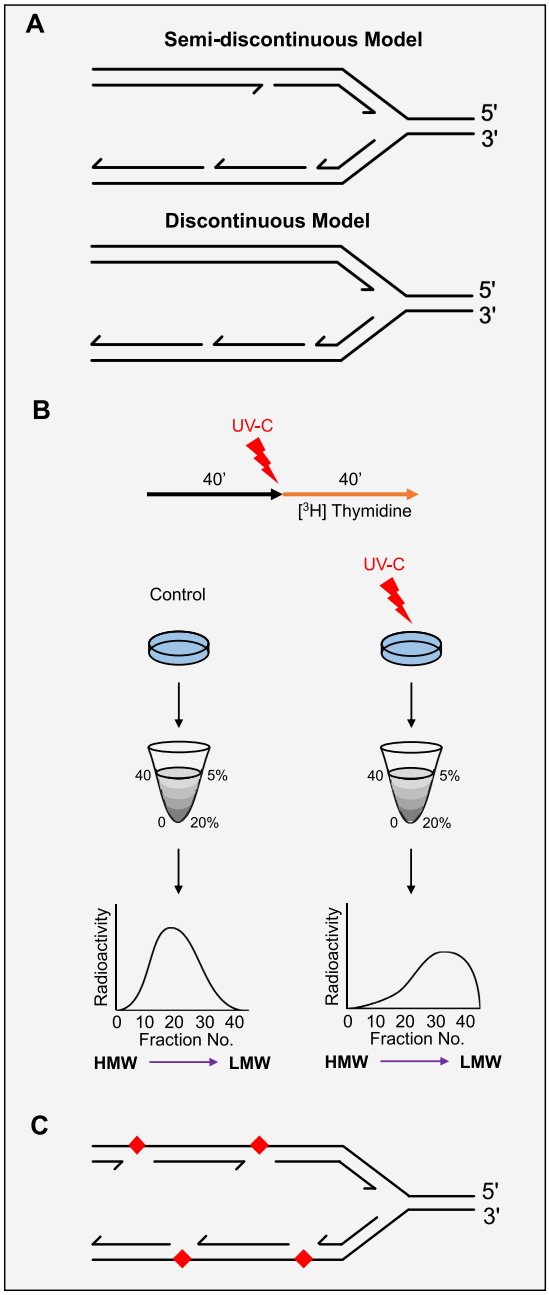

Figure 2. Uncovering models of DNA replication. (**A**) In the semi-discontinuous model of DNA replication, leading strand synthesis is continuous from origin to termination and the lagging strand is synthesised in short fragments. Theoretically, if ligation is prevented, two size classes of replication intermediates would be produced: a HMW continuous leading strand and LMW fragments from the lagging strand. In the discontinuous model, both strands of DNA are synthesised as fragments and all DNA initially consists of LMW fragments. (**B**) The protocol used in the seminal studies of Rupp and Howard–Flanders to investigate DNA replication intermediates in bacteria following UV damage. *Escherichia coli* cells were grown in unlabelled medium (black arrow) before being irradiated with UV-C and transferred to media containing radioactive thymidine (orange arrow). After 40 min of labeling, the cells were collected for analysis. DNA was harvested from either control or irradiated cultures and subject to alkaline sucrose gradient centrifugation. The sedimentation showed that DNA fragments extracted from irradiated cells were significantly smaller than those from control cells. (**C**) The results were interpreted to indicate that gaps were present in the nascent DNA opposite the CPDs (red) induced by UV irradiation.

discontinuous model which, perhaps due to its practical appeal, was well received by the field. The results of studies utilising an *in vitro E. coli* DNA synthesis system provided compelling evidence in support of continuous leading strand synthesis (72). Fragments of DNA produced in this system during ligase inhibition were reproducibly shown to fit into one of two distinct size classes; Okazaki fragments that were produced with a low sedimentation coefficient and a distinct class of larger labelled molecules. Interestingly, the distribution of DNA between the two classes was roughly equal and further investigation confirmed that fragments in one class were complementary to fragments in the other, a sign that they originated from opposing (leading or lagging) strands (73). These data were indicative of one strand being synthesised continuously while the other one was produced discontinuously, adding support to the semi-discontinuous model. In addition, multiple studies exploiting rolling circle-type DNA replication systems were able to produce long leading strand products of 40–500 kb in length, with no evidence of dissociation (74,75). Thus, the semi-discontinuous model of replication was well supported by *in vitro* studies (72–75).

The evidence regarding the nature of bacterial leading strand synthesis was often contradictory between the published *in vitro* and *in vivo* studies, with the latter usually supporting a fully discontinuous model. However, evidence supporting the use of a continuous mechanism of leading strand synthesis *in vivo* is provided in some early literature. Iyer and Lark investigated the mechanism of production of intermediate molecular weight and HMW replication intermediates that were generated during pulse labelling experiments (63). Their results showed nucleotides being added to the 3′ end of nascent DNA strands, suggesting continuous synthesis. Direct *in vivo* evidence for a semi-discontinuous model was later reported, however, this was dependent on the presence of PolA, which is now known to fill in gaps generated by discontinuous synthesis, as described earlier (76). The method of reaction termination (pyridine-KCN) used in the two studies presented above has since been called into question (77). The use of a pyridine-KCN termination pulse permits the ligation of nascent DNA fragments after application, and this is likely the source of the long 'continuous' fragments. By using a more rapid and robust method of termination, it was shown that all nascent DNA fragments were short *in vivo*, agreeing with previous studies and supporting a discontinuous model of replication (77).

Subsequent studies set out to explain the disparities between the *in vitro* results and those observed in biological systems. One possibility that had not been excluded by early studies was that the fragments observed *in vivo* could be a result of DNA processing or excision repair activities. Uracil is a common lesion present in DNA, resulting from either deamination of cytosine or misincorporation of deoxyuridine 5′-triphosphate nucleotide (dUTP). In order to maintain genomic integrity, uracil must be detected and removed by base excision repair (BER), a process that generates breaks, or gaps, in the backbone of the DNA chain. Examining DNA synthesis in *E. coli* lysates had previously uncovered two size classes of intermediates (72). Increasing the concentration of dUTP present in the lysate solution led to a decrease in the sedimentation coefficient of the larger

size class, representing the generation of smaller fragments (78). The addition of dUTP to *in vitro* reactions produced smaller DNA fragments with a sedimentation profile that was similar to DNA obtained from *in vivo* experiments. The conclusion was, therefore, that the small DNA fragments observed in previous experiments could be explained simply by dUTP incorporation and excision and it was deemed no longer necessary to consider possible leading strand reinitiation events. However, this conclusion was strongly refuted by other evidence published at the same time (79). Comparing the sedimentation profiles of DNA produced by ligase-deficient *E. coli* to DNA from a strain that was also deficient in excision-repair of uracil demonstrated little or no difference in the sizes of fragments produced by either strain *in vivo*. Subsequent studies also concluded that neither DNA processing nor uracil excision were found to affect the size of replication intermediates (80). While this added support to the idea of multiple initiation events on both strands, it was not direct evidence and the semi-discontinuous model was generally still considered to be the most convincing.

A recent study has revisited the questions surrounding the origin of replication intermediates in bacteria (81). Surprisingly, nearly all of the LMW leading strand products observed in earlier studies can be explained by fragmentation as part of excision-repair processes. Mutants deficient in BER, mismatch repair (MMR), NER and ribonucleotide excision repair (RER) were able to perform largely continuous synthesis on the leading strand, suggesting that these could be responsible for fragmenting DNA. In particular, the RER pathway is responsible for most fragmentation events, which could explain why earlier studies investigating dUTP excision failed to detect a noticeable effect (79,80). The implication of this work is, therefore, that all DNA is initially synthesised with a number of incorrect bases and requires extensive excision repair in order to become mature DNA. Such events generate discontinuities in the nascent chain that produce the DNA fragments detected in previous studies. Interestingly, their data did not show chromosome-length continuous fragments in the absence of any excision pathways, in fact, DNA fragmented in two size classes, with the largest class of fragments determined to be 50–70 kb. This supports Okazaki's original model for the discontinuous synthesis of both strands of DNA, albeit with two size classes of fragments, presumably originating independently from each of the DNA strands.

Studying replication after damage: new insights into the replication model

Although the studies described above helped to delineate a working model for the canonical mechanism of DNA replication in unperturbed conditions with normal amounts of fork stalling caused by endogenous sources, examining how DNA is copied following the application of fork stalling agents also provided critical insights into how this duplication process operates. In the late 1960s, Rupp and Howard-Flanders conducted a seminal study, which explored the fate of DNA when cells were permitted to replicate following UV damage (82). By utilising NER-deficient *E. coli* strains, UV-induced pyrimidine dimers could persist into S phase. At the time, it was unknown whether replication would be stalled by these photo-lesions or continue past this damage with minimal perturbation. By measuring tritiated thymidine incorporation following UV irradiation, they determined that each lesion caused ∼10-s delay to the replication fork, however, the lesions did not completely block replication. This observation prompted the central question of the study: was the bypass of UV lesions continuous or discontinuous in nature? To address this question, they utilised rapid pulses of radioactive labelling to mark newly synthesised DNA in damaged and undamaged cells that could be subjected to alkaline sucrose gradient centrifugation for comparison (Figure 2B). DNA originating from cultures that weren't exposed to UV sedimented in large pieces, however, strikingly, DNA synthesised following UV exposure sedimented in significantly smaller pieces; a sign of discontinuities in the nascent chains. The results were interpreted to indicate the presence of single-stranded gaps in the DNA of daughter strands following UV exposure. Interestingly, the gaps observed were spaced at distances roughly correlating to the predicted distance between CPDs produced at the specific UV dose used, suggesting the gaps may reside opposite damaged bases (Figure 2C). Further work demonstrated that these ssDNA gaps were ∼1000–2000 bp in length (83). Over time, the ssDNA gaps opposite CPDs were repaired by sister-chromatid exchange (SCE) to produce detectable full-length chromosomal DNA (84). The discovery of gaps in all nascent DNA following damage led to the postulation that replication restart downstream of polymerase-stalling damage could occur on both strands of DNA.

Repeating the initial experiments conducted by Rupp and Howard-Flanders in mammalian (Chinese hamster) cells produced ssDNA gaps similar to those observed in *E. coli*, which were also filled in over time (85). Gaps were later discovered in DNA from human cells following UV irradiation (86). In contrast to the results in *E. coli*, no evidence of gap-filling by an SCE mechanism could be found in mammalian cells; however, there was evidence of gap filling by DNA synthesis that was not coupled to SCE (87). The evidence for discontinuous synthesis after damage provided by these early studies suggested an inherent ability of the replisome to skip synthesis opposite a lesion or replicative impediment and restart replication downstream on both the leading and lagging strand. One model proposed to explain the observed results involved the generation of a *de novo* primer downstream of a stalling lesion, from which the replicative polymerase can resume synthesis, as occurs on the lagging strand.

Following the publication of these studies, there was little further work into resolving the questions surrounding discontinuous leading strand synthesis. Replication restart downstream of lesions was still considered unlikely and the leading strand was generally considered by the field to be synthesised continuously (88). The discovery of TLS polymerases in the late 1990s provided a compelling solution for lesion bypass that didn't require reinitiating synthesis on the leading strand (89–91). The ability of these enzymes to synthesise past damaged bases allowed the development of new models, which almost all involved polymerase switching to a TLS enzyme at the active fork, maintaining continuous synthesis of the nascent chain. The solutions offered by models

involving the newly discovered TLS pathways were preferable to models which went against the dogma of continuous leading strand synthesis.

In the early 2000s, the debate over continuous versus discontinuous leading strand synthesis was still ongoing (92), then, in 2006, two significant studies provided compelling evidence supporting a model where leading strand synthesis can be initiated downstream of a lesion, prompting a re-evaluation of the semi-discontinuous model. The first study combined 2D gel electrophoresis with electron microscopy to inspect DNA derived from UV-irradiated NER-deficient *S. cerevisiae* cells (93). Single-stranded DNA gaps in both strands were directly visualised behind the replication fork. In WT cells, the gaps were filled in over time. However, in cells deficient in TLS or homologous recombination, gaps persisted after completion of S phase suggesting they are repaired by a post-replicative repair mechanism(s). The second study provided the first mechanistic evidence supporting the existence of a repriming mechanism in *E. coli*, as Rupp and Howard-Flanders had originally proposed (94). By using a terminal 3′ dideoxynucleotide on the simulated nascent leading strand of a forked template, Heller & Marians showed that synthesis could resume downstream of the blocked end, without repair of the lesion; a process that would require *de novo* synthesis (94). This discontinuous synthesis was dependent on both the replicative primase (DnaG) and helicase (DnaB), suggesting that primer synthesis can take place on the leading strand to allow replication to resume after fork stalling events.

Roles of replicative primase enzymes in leading strand replication

As discussed above, both leading and lagging strand priming is performed by the replicative primase DnaG in *E. coli* (94,95). The roles of DnaG and DnaB (helicase) in repriming replication restart have now been also established (96,97). It is, however, important to note that although bacterial replisomes bear many mechanistic similarities to that of eukaryotes, both systems have seemingly evolved independently (reviewed in (98)). One key difference in their mechanisms is the direction of travel of their respective replicative helicases. In *E. coli*, DnaB traverses along the lagging strand in a 5′ to 3′ direction, while the eukaryotic MCM helicase moves 3′ to 5′, placing it on the leading strand (99,100). Furthermore, as discussed previously, the eukaryotic system divides the labour of bulk synthesis between Pol ε and Pol δ, whereas the majority of *E. coli* replication is conducted by multiple copies of the C-family polymerase, DNA Polymerase III (101). Interestingly, the primase enzymes of each domain of life are also distinct, despite their functional similarities. Bacterial DnaG primases are more closely related to topoisomerases, both having a common TOPRIM fold (102). In contrast, the so-called eukaryotic primases (Pri1/PriS) evolved from a primordial RNA recognition motif (RRM) with a diverse range of distantly related homologues found in all domains of life, albeit their specific roles in priming genome replication appears to be restricted to viruses, archaea and eukarya (103).

During eukaryotic replication, RNA-DNA primers are generated by the Pol α-primase complex, consisting of four distinct subunits: p180, p74, p58 and p48 (104). The primase is formed of the latter two subunits, with p48 (Pri1/PriS) acting as the catalytic subunit and p58 (Pri2/PriL) acting to stabilise the primase (105). A temperature-sensitive mutant of the budding yeast Pri1 subunit has allowed investigation of the role of the primase *in vivo* (106). DNA synthesis in the mutant is partially defective at the permissive temperature, however, at the restrictive temperature, DNA synthesis fails at an early step following release from G1 arrest. These results indicated that the primase is required to maintain ongoing DNA synthesis. Interestingly, cells expressing the mutant primase fail to slow the rate of S phase progression following methyl methanesulfonate (MMS)-induced DNA damage. Investigating this effect further revealed evidence suggesting a role for Pri1 in the Rad53p-dependent checkpoint pathways that regulate cell cycle progression in response to DNA damage. Pri1 mutants have recently been shown to experience an increase in premature sister chromatid separation (107).

Reconstituting the yeast replisome *in vitro* has facilitated further studies into the roles of Pol α-primase and provided insights into priming events on the leading strand. In one study, the Pol α-primase complex was shown to synthesise a primer on the leading strand of a forked substrate and then extend this using its polymerase activity, or hand over to Pol ε or Pol δ (108). Additionally, when a primer was provided, the enzyme complex preferentially extended this, rather than synthesise a *de novo* primer. The study found no evidence of repriming on the leading strand. In another recent study, lagging strand priming by Pol α-primase complex to bypass a CPD was found to be fast and efficient, while leading strand repriming was inefficient for re-establishing replication beyond the lesion (31). Interestingly, the efficiency of leading strand repriming was related to the availability of RPA, where depleting the pools of RPA increased priming efficiency. Pol α-primase has long been thought to prime the leading strand at the origins. However, a recent examination of the establishment of bi-directional leading strand synthesis in a reconstituted yeast system determined that leading strand synthesis is, in fact, initiated from a lagging strand primer on the opposite side of the origin (109). Overall, this evidence suggests that budding yeast Pol α-primase does not play a major role in priming leading strand synthesis, at least at origins, nor does it appear to efficiently reprime on this strand to promote damage tolerance.

While the availability of temperature-sensitive mutants and *in vitro* reconstituted replisome systems have allowed the study of some of the functions of the budding yeast primase, the mammalian enzyme has proven more difficult to study. In a similar manner to the yeast homologue, human Pol α-primase forms the replicative primase complex that is composed of the DNA polymerase α subunits (POLA1 and POLA2) and the DNA primase subunits PRIM1 and PRIM2 (110). There is currently no substantial evidence to suggest that the human Pol α-primase complex plays a role in DNA damage tolerance on the leading strand. Therefore, in contrast to prokaryotic cells, it is unlikely that stalled leading strand synthesis in eukaryotic cells can be restarted from downstream primers synthesised by the replicative primase.

The observations described above raise important questions regarding the strand-specific differences in priming efficiency displayed by Pol α-primase. What enables the enzyme to regularly prime the lagging strand efficiently, while priming on the leading strand is so inefficient? Most ssDNA is rapidly coated in RPA, which has been shown to inhibit Pol α-primase activity, however, despite this, the lagging strand is primed efficiently by this complex (31). During replisome progression, the CMG encircles and translocates along the leading strand, while the lagging strand is excluded (6). Pol α-primase is kept in close proximity to CMG via an interaction with Ctf4 (AND-1 in humans), and it is possible to consider that this proximity may prevent RPA from binding the lagging strand before it reaches the primase, allowing efficient priming to take place during Okazaki fragment generation (111). Outside of this specific scenario, for example during helicase uncoupling after leading strand stalling events, ssDNA is rapidly coated in RPA, which would prevent Pol α-primase from priming or repriming (31). Another possibility is that Pol α-primase could be regulated by auxiliary factors that limit its usage. For example, while the absence of Ctf4 in reconstituted yeast systems does not seem to affect lagging strand synthesis on chromatin *in vitro*, Ctf4 has been suggested to aid the maintenance of robust lagging strand priming when Pol α-primase activity is reduced *in vivo* (112,113). The human Ctf4-orthologue, AND-1, interacts with Pol α-primase via its C-terminal HMG box and displays DNA-binding activity, potentially providing a mechanism by which Pol α-primase is directed to the lagging strand (114).

Discovery of a new class of eukaryotic primase

In the past, DNA primase enzymes were thought to possess one specific function: synthesising short RNA primers during the initiation of DNA replication. However, more recently, this has been shown to be somewhat of a functional mis-annotation and nowhere is this more evident than in members of the archaeo-eukaryotic primase (AEP) superfamily (reviewed in (103)). Enzymes belonging to this superfamily can be found throughout all domains of life, where they have evolved specialist roles in replication, repair and DNA damage tolerance.

Perhaps the best-known family member is Pri1 (PriS) which, in complex with the large subunit (Pri2/PriL), synthesises RNA primers during canonical origin firing and lagging strand synthesis (13). In archaea, Pri1 can extend primers with dNTPs in a manner similar to Pol α, which is lacking from these organisms (115). Archaeal Pri1 can also conduct TLS over various helix-distorting lesions to facilitate DNA damage tolerance (116). Pri1 is not the only AEP discovered in archaea; for example, the archaeal cryptic plasmid pRN1 encodes an enzyme, ORF904, which contains a helicase/translocase domain in addition to the AEP domain that renders the protein proficient in both primase and polymerase activities (117). In fact, ORF904 can synthesise many kilobases of DNA when conducting bulk replication of pRN1 plasmids. In addition, many bacterial species possess various AEP orthologues. For example, RepB' and Rep are AEPs found on RSF1010 and ColE2 plasmids, respectively, that more conventionally generate short primers to initiate plasmid replication (118,119). Perhaps even more intriguing is the discovery of AEP proteins that are co-operonic with bacterial non-homologous end joining (NHEJ) protein Ku (120,121). Here, the AEP protein forms part of a larger DNA break repair complex known as Ligase D (LigD), which further associates with Ku (Ku-LigD complex) to facilitate prokaryotic NHEJ (122). In mycobacteria, Prim-PolC is co-operonic with Ligase C and plays a role in excision repair (123), binding to the short gaps produced as part of this excision process and conducting gap-repair synthesis (124). The AEP family has recently been renamed as Primase-Polymerases (Prim-Pols) to better reflect the more diverse origins and functions of this replicase superfamily (103).

In 2005, a bioinformatic study identified a variety of novel Prim-Pols, including a second Prim-Pol gene in the human genome called CCDC111 (125). This gene product was subsequently isolated and characterised (126–128). The protein was shown to be a DNA-dependent DNA polymerase that also possesses TLS-like activities on lesion-containing templates, such as 8-oxo-G and 6–4 pyrimidine dimers. In addition, the enzyme showed robust primase activity on DNA templates. However, in contrast to replicative primases, it utilises dNTPs much more efficiently than rNTPs (129). To reflect both of these capabilities, CCDC111 was renamed Primase-Polymerase (PrimPol). Human PrimPol is a monomeric enzyme (130), differing from replicative primase enzymes, which form heterodimers, such as the eukaryotic primase complex Pri1/Pri2 (131). PrimPol contains a characteristic N-terminal AEP domain containing three conserved motifs (I, II and III) that are essential for all catalytic activities. Motif I contains residues (DxE) that create a binding site for divalent metals (125) and mutating these residues ablates catalytic activity (126–128). A UL52-like zinc finger (ZnF) domain is located downstream of the catalytic domain. This domain contains a conserved sequence (Cys-His-Cys-Cys) that allows the coordination of a metal ion to form a zinc finger. The ZnF domain binds to ssDNA and appears to play a role in PrimPol's priming mechanism, as mutating/deleting it abolishes primase, but not polymerase, activity (130,132,133). The C-terminal domain (CTD) of PrimPol binds to the single-strand binding protein, replication protein A (RPA70) (128,134) and PrimPol foci formation is dependent on this interaction (135). A recent study elucidated the molecular basis of this interaction and identified two RPA binding motifs, RBM-A and RBM-B, contained within the CTD, which interact with the basic cleft of RPA70N (135). PrimPol also binds to PolDIP2 (PDIP38) and this enhances its polymerase, but not its priming, activities (136), although the specific cellular role of this complex remains to be established.

Establishing a role for PrimPol in vertebrate cells

Orthologues of PrimPol are found in most eukaryotic organisms, with a few notable exceptions, such as *S. cerevisiae, S. pombe, Caenorhabditis elegans* and *Drosophila melanogaster*. Our current understanding of the enzyme's *in vivo* functions comes predominantly from avian and human cell studies. PrimPol knockout avian cells (DT40) show a pronounced sensitivity to UV-C damage, 4NQO (a UV

mimetic), cisplatin, chain-terminating nucleotide analogues (CTNAs) and MMS, but no greater sensitivity to agents that induce double-strand breaks (126,137,138). These cells also exhibited a distinct G2-M checkpoint response after UV damage (137). In contrast to Pol η knock out cells, which also display UV-C sensitivity, no loss in post-replicative repair of UV-C damage was observed when PrimPol is depleted (130,137). Fork speeds and general fork progression are decreased in PrimPol's absence. This is especially prominent following UV damage, strongly suggesting a role for PrimPol in the maintenance of fork progression after DNA damage.

The importance of PrimPol in DNA damage tolerance was further supported by studies of human PrimPol$^{-/-}$ MRC-5 cells (139), which also showed decreased fork speeds and increased fork stalling after damage, although the damage sensitivity observed in avian cells was not observed in the human knock out (or knock down) cells (126). This discrepancy is likely due to the significantly shorter doubling time of DT40 cells compared to human cells – 11 hours compared to 24 hours (140,141). Human PrimPol$^{-/-}$ cells also exhibit a variety of phenotypes that highlight the important roles this protein plays in maintaining DNA stability in both the nucleus and mitochondria. These include increased micronuclei, sister chromatin exchanges and mutation frequency (139).

While PrimPol evidently plays an important role in tolerating lesions, it is important to acknowledge that PrimPol is also involved in maintaining replication during stress (Figure 3A). Hydroxyurea (HU) slows and stalls replication by inhibiting ribonucleotide reductase, thus depleting the cellular dNTP pool. Upon treatment with HU, human cells exhibit both an increase in chromatin-bound PrimPol and a relocalisation of PrimPol into subnuclear foci (126,132). In PrimPol depleted cells, HU treatment causes a decrease in fork progression, as measured by DNA fibre analysis, which can be rescued by expressing wild-type PrimPol, but not a primase-deficient version of the enzyme (132). A recent CRISPR screen implicated PrimPol in the response to resveratrol and its chemical analogue pterostilbene (142). Like HU treatment, Resveratrol also induces comparable dNTP depletion and fork speed decrease, highlighting the drug's ability to cause replication stress. Overall, these studies suggest that PrimPol also performs a more general 'house-keeping' role in maintaining unperturbed fork progression in response to replication slowing and endogenous fork stalling.

PrimPol reprimes downstream of lesions and stalling structures *in vivo*

Recent studies have begun to establish the roles that PrimPol plays *in vivo*, which ultimately underlie the phenotypes observed in its absence. Early studies noted that PrimPol was required to maintain replication fork speed following UV exposure and that this effect was dependent on its primase activity (Figure 3A) (126,130,132). Interestingly, previous studies had already suggested that UV-stalled forks were restarted via repriming in human cells (87,143). There is also evidence that PrimPol reprimes downstream of AP-sites, and this activity has been suggested to allow some cells to tolerate the mutagenic lesions produced by the APOBEC/AID family of cytosine deaminases (144). Using avian cells, it was shown that PrimPol also mediates tolerance to chain-terminating nucleoside analogues (CTNAs) (Figure 3A), which stall DNA replication (138). Cells deficient in PrimPol experienced a significant decrease in survival after treatment with CTNAs, which can be complemented by the introduction of WT PrimPol, but not a primase-deficient mutant. The mechanism underpinning the tolerance was supported by *in vitro* studies demonstrating that PrimPol could synthesise a *de novo* primer ∼14 nucleotides downstream of a CTNA present at the 3′ end of a primer strand (138). A depiction of replication restart mediated by PrimPol following fork stalling is shown in Figure 3B and Figure 3C.

PrimPol has additionally been implicated in the tolerance of DNA structures, such as G4-quadruplexes (Figure 3A) (145). Using histone recycling as a measurement of replisome uncoupling in DT40 cells, Schiavone *et al*. found local epigenetic instability in the absence of PrimPol around the *BU-1A* locus when a G4 structure was present on the leading strand. While PrimPol does not directly replicate G4′s, it was shown to reprime downstream of these structures, allowing rapid resumption of replication and preventing replisome uncoupling. The system was later adapted to study the potential role of PrimPol in R-loop bypass by replacing the G4 quadruplex sequence with R-loop forming purine-rich repeats of $(GAA)_n$ (146). In a WT background, short tracts of repeats ($n = 10$) did not affect the epigenetic stability, indicating that the replisome can move through the region unhindered. Strikingly, in PrimPol knock-out cells, the same short tracts caused a significant increase in the local epigenetic instability, indicative of fork stalling, which could only be rescued by expression of primase-proficient PrimPol.

The abilities of PrimPol demonstrated by the studies described above highlight its role in the tolerance of a myriad of fork-stalling lesions and structures (Figure 3A). Interestingly, while multiple studies of PrimPol have demonstrated TLS capabilities *in vitro*, evidence supporting its use *in vivo* remains to be established. Hence, the current consensus is that PrimPol's primary role *in vivo* is to reprime DNA synthesis; while a role in TLS cannot be ruled out, it can be assumed that the majority of phenotypes observed in the absence of PrimPol are caused by the cell's inability to reprime stalled DNA replication, particularly on the leading strand (126,127,130,132). Previously, there was no known mechanism to facilitate repriming on the leading strand in vertebrate cells; however, considering all of the evidence now available, it is apparent that PrimPol-mediated repriming provides cells with a highly flexible mechanism for restarting DNA synthesis and bypassing obstacles on the leading strand thus preventing replication stress. It should be noted that PrimPol may also prime on the lagging strand, however, this would seem redundant given the activity of Pol α-primase. The discovery and characterisation of a PrimPol-dependent repriming pathway also provides additional evidence to support a model for discontinuous synthesis on both strands during DNA synthesis.

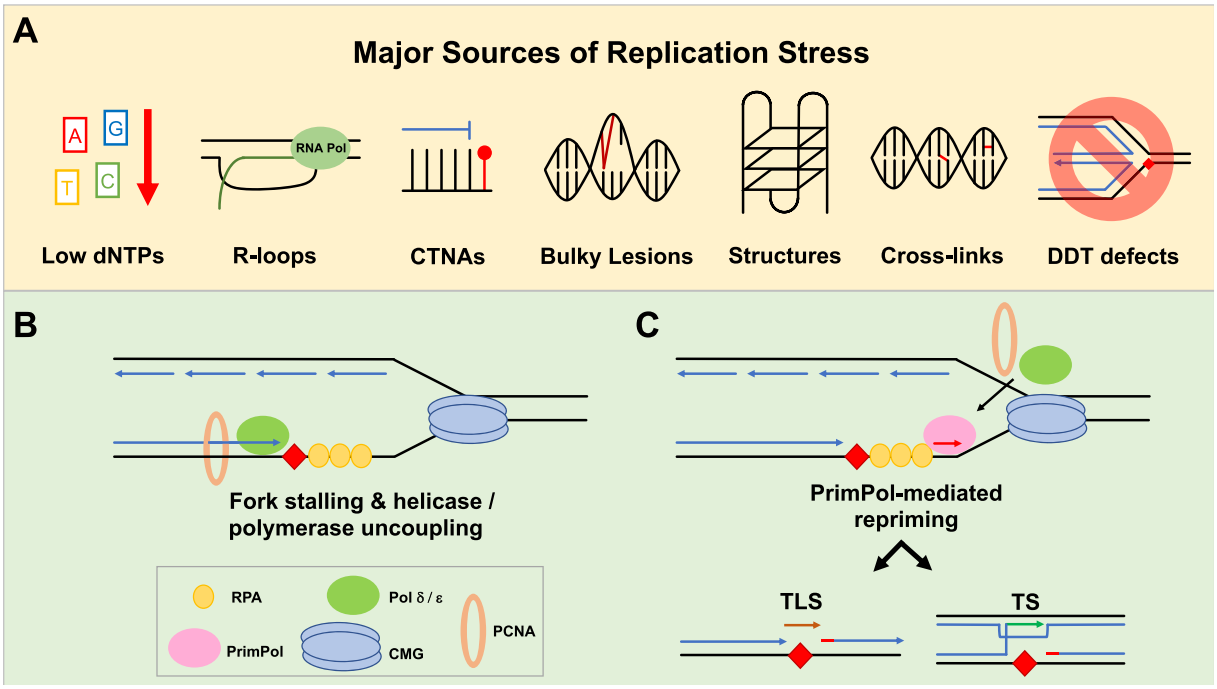

Figure 3. PrimPol-dependent repriming of stalled replication intermediates. (**A**) PrimPol-mediated repriming can assist in resolving fork stalling after many different kinds of lesions, including CTNAs, bulky lesions such as those generated by UV light, G-4 quadruplexes, R-loops, and intra/interstrand crosslinks. PrimPol can also be utilised when low dNTPs pools cause fork stalling. Additionally, the absence or loss of an alternative DDT pathway, such as fork reversal, can lead to the deployment of a PrimPol-dependent pathway. (**B**) Replication fork uncoupling occurs when lesions, or other sources of replication stress, transiently stall the replicative polymerase without impeding the rest of the replisome. This uncoupling generates stretches of ssDNA onto which RPA can bind. (**C**) PrimPol (pink oval) can be recruited to these tracts of RPA bound ssDNA to facilitate the restart of the uncoupled fork by repriming. From here, the replicative polymerase will take over to complete synthesis. The repriming depicted here occurs on the leading strand, with lagging strand machinery omitted for clarity.

Repriming DNA synthesis represents a canonical damage tolerance pathway

While evidence for the existence of DNA damage tolerance mechanisms that involve repriming downstream of replicase stalling obstacles has been invoked for over half a century, it is still rarely regarded as an actual canonical DDT pathway. This might be because the replicative primases of prokaryotes, and probably some other organisms too, have the intrinsic ability to reprime DNA synthesis and are, therefore, not considered to represent a distinct DDT pathway. Furthermore, the roles of other Prim-Pol enzymes in various other genome stability pathways have only recently been appreciated (103). In addition, the relatively mild phenotypes displayed by human cells depleted of PrimPol do not, at an initial glance, mark this out as a major pathway of DDT. While PrimPol deficient human cells do exhibit a change in cell cycle profile and modest slowing of replication forks, they do not display overt signs of distress or growth impediments (139). Interestingly, the effects of losing PrimPol seems to vary between organisms. For example, avian PrimPol$^{-/-}$ cells exhibit more pronounced phenotypes, specifically a sensitivity to fork stalling lesions, in addition to profound G2 stalling after UV damage that is only partially resolved by the application of Chk1 or p38 inhibitors (126,137). PrimPol$^{-/-}$ mice remain viable without displaying any overt phenotypes. Mouse embryonic fibroblasts (MEFs) lacking PrimPol display increased chromatid breaks, suggesting the generation of lesions during S phase (126,127). Depletion of a PrimPol orthologue, PPL2, in trypanosomes results in a lethal mitotic catastrophe-like phenotype, likely due to replication defects, highlighting an essential role for PrimPol in these protists (147).

An ever-increasing number of recent studies are reporting functional overlaps between repriming and other DDT pathways, suggesting that the impact of repriming is often underestimated, as its absence can be compensated for by other pathways. The first such overlap to be described was observed while studying PrimPol depletion in xeroderma pigmentosum variant (XP-V) cells (126,139). XP-V cells contain mutations in the *POLH* gene, which encodes the TLS polymerase Eta (Pol η) (91). Pol η provides tolerance to UV-induced damage by conducting error-free bypass of CPD lesions. Due to PrimPol's proficiency in conducting TLS-like bypass of UV-induced lesions (6–4 PPs) and extending from CPDs *in vitro*, it was hypothesised that the two enzymes could work in complementary pathways (126). To test this, PrimPol was depleted in both WT and XP-V cells before applying a dose of UV radiation. Both cell types exhibited increased RPA foci and a concurrent increase in phosphorylation of the intra-S checkpoint kinase Chk1 in response to UV-induced damage. Interestingly, in cells lacking both Pol η and PrimPol, levels of Chk1 phosphorylation remained elevated for significantly longer than cells deficient in only one enzyme, suggesting a complete deficiency in UV damage bypass when both enzymes are re-

moved. While both PrimPol-depleted fibroblasts and XP-V exhibited either absent or mild UV-C sensitivity, in the absence of caffeine, PrimPol-depleted XP-V cells become synergistically sensitive to UV irradiation, establishing a non-epistatic relationship between these distinct DDT pathways. PrimPol's role in DNA damage tolerance was also shown to be independent of Pol ζ in avian cells, where its absence exacerbated the phenotypes of Pol η/Pol ζ knockout cells (138). Notably, complementing PrimPol$^{-/-}$ cells with a primase defective, but polymerase/TLS active, PrimPol did not rescue their damage sensitivity, further supporting the notion that PrimPol's primary role *in vivo* is to reprime DNA synthesis (130,138). These studies demonstrate how the existence of complementary damage tolerance pathways can mask the effects of losing one mechanism alone.

Another proposed DDT mechanism involves fork reversal following a major replisome stalling event. The breast cancer-associated (BRCA) proteins (BRCA-1 and BRCA-2) have been suggested to protect reversed forks from nucleolytic degradation and therefore promote bypass of DNA lesions by homologous recombination (148,149). Mutations in these genes are the leading cause of familial breast and ovarian cancers (150). As BRCA proteins protect replication forks undergoing reversal from degradation, BRCA null cell lines may be susceptible to increased genomic instability brought on by extensive fork degradation (55). It was reported that the fork degradation phenotype typically displayed by BRCA1 deficient cells after a single dose of cisplatin is absent after treatment with multiple doses, with cells exhibiting increased replication fork speeds (151). Overexpressing WT PrimPol, but not catalytically- or primase-inactive mutants, protected against the degradation phenotype observed in BRCA deficient cells. These results suggest that cells may upregulate their PrimPol-dependent repriming pathway in order to compensate for the loss of fork reversal as an alternative mechanism of cisplatin tolerance. Supporting this, following multiple cisplatin doses, PrimPol mRNA levels were significantly elevated and chromatin-bound PrimPol increased in BRCA-1 deficient cells, but not in cells complemented with BRCA-1. The increase in mRNA was found to be regulated by ATR. Another recent study reported that the USP36 protease also possibly plays a role in regulating PrimPol protein levels (152), and the ATPase WRNIP1 has been suggested to target PrimPol protein for degradation (153). This suggests that multiple mechanisms exist that regulate PrimPol deployment in human cells. This is probably not surprising as a failure to suppress ssDNA gaps has been suggested to be a major hallmark of BRCA-deficient cancers and a cause of their sensitivity to chemotherapeutic agents (154). Uncontrolled repriming may lead to a similar increase in ssDNA gaps, decreasing cell fitness unless cells can compensate, e.g. by increasing TLS activity as observed in some cancer cells (155).

Another study by Bai *et al*. (156) investigating cells deficient in the fork remodeller HLTF reached similar conclusions to those of Quinet *et al*. (151). HLTF is an SWI/SNF family chromatin remodelling enzyme that promotes fork reversal and, in its absence, PrimPol is required to maintain efficient fork progression, leading to the accumulation of ssDNA gaps (157,158). PrimPol's action at the fork appears to confer replication stress resistance and allow S phase to continue without slowing of DNA synthesis. However, if HLTF is present and allowed to bind to the replication fork but contains an inactive HIRAN domain (the domain that binds the 3′-hydroxyl group of nascent DNA), PrimPol is outcompeted at the fork and does not act, and the role of S phase progression is undertaken by Rev1. Similar work has shown that in the absence of CARM1, a protein implicated in the stabilisation of reversed forks, PrimPol and TLS are both employed in restarting replication forks (159). The balance between these complementary DTT pathways therefore has the potential to mask the key roles that repriming undertakes *in vivo*.

Repriming is not the end of the story...

In eukaryotes, PrimPol's repriming activities allow replication to continue past lesions, structures and other impediments. However, once synthesised, the primer is likely to be some distance away from the CMG complex due to helicase uncoupling that accompanies leading-stand fork stalling (160). In order to restore efficient canonical replication, synthesis must be recoupled to the CMG. In the case of TLS, Pol δ conducts leading-strand synthesis following lesion bypass, which fits well with the previous reports of Pol δ replicating both strands after replication restart (9,10). PrimPol interacts with, and is stimulated by, Polymerase δ-interacting protein 2 (PolDIP2), which may facilitate a handoff from PrimPol to Pol δ, once primer synthesis is complete (136,161,162). Pol δ could then synthesise until replication can be recoupled to CMG-Pol ε, as is the case following TLS (9,163).

One of the major distinctions between the two human primases is that Pri1 produces an RNA primer, while PrimPol synthesises a predominantly DNA polymer. This preference to reprime using dNTPs may facilitate a more efficient restarting of DNA synthesis as high fidelity replicases preferentially copy B-form DNA templates, whereas priming with an RNA polymer produces an RNA–DNA hybrid that is a much poorer A-form substrate. In addition, it also eliminates the requirement for Pol α-dependent synthesis prior to primer handover to Pol δ/Pol ε. DNA primers may also be preferred to avoid introducing breaks on the leading strand. Following replication, RNA primers are subsequently excised (e.g. Fen1/Pol I) and then replaced with DNA to maintain genome integrity. However, during PrimPol-dependent repriming, it is likely that dNTPs are preferentially incorporated to prevent the processing and removal of the newly synthesised primers as this could result in undesirable strand breaks that are particularly dangerous on the leading strand. Notably, PrimPol incorporates a single initiating 5′ ribonucleotide during primer synthesis but this is likely removed by the RNase HII pathway in a post-replicative fashion (127,164).

Reinitiating DNA synthesis from a downstream primer generates a single-stranded gap in the nascent chain opposite the unresolved stalling lesion or structure. To complete replication, gaps must be filled in a manner that is independent of the global genome replication process. Interestingly, this event was not found to occur in any known DNA repair centres; instead, the majority of ssDNA accumulates in

post-replicative repair territories (PORTs) (165). Here, TLS or template-switching pathways facilitate the removal of the ssDNA gaps. TLS does not solely occur directly at an active fork - following the monoubiquitination of PCNA, TLS enzymes can synthesise over bypassed UV lesions in a post-replicative manner to fill gaps that result from repriming (166). A recent study has also implicated homologous recombination in the gap-filling process at PrimPol-mediated ssDNA gaps in human cells (167). As part of this process, MRE11 and EXO1 facilitate 3′ to 5′ resection of DNA gaps to expose sufficient ssDNA for the loading of the HR protein, Rad51. Subsequent template switching allows the replication of the gapped region by using the unimpaired sister chromatid as a template. Presumably, persistent fork-stalling DNA structures must be resolved using the canonical mechanisms before opposing gaps can be filled.

Coping without a bespoke repriming pathway

Since repriming represents a major canonical DDT pathway in most cells, how do organisms without specialised repriming mechanisms (e.g., budding/fission yeast, drosophila, *C. elegans*) deal with leading strand stalling events? As discussed, in prokaryotes this appears to be resolved by simply repurposing the replicative primases to also reinitiate replication. However, evidence to suggest that a similar process occurs in eukaryotic organisms is lacking. It is very likely that cells without a bespoke repriming pathway may simply rely on alternative DDT pathways and mechanisms to ultimately maintain genome stability without the requirement to conduct leading strand repriming. One such viable alternative pathway involves using TLS and, in fact, the budding yeast replisome has been shown to efficiently utilise Pol η to bypass leading strand lesions 'on the fly' (9). Additionally, recent findings indicate that the yeast replisome is itself inherently tolerant of oxidative damage (168). Upon encountering a leading strand thymine glycol or 8-oxo-G, Pol ε is switched for Pol δ, which conducts rapid, error-free synthesis over the lesion. There is also some evidence to potentially support a similar role for Pol δ in higher eukaryotes, although this mechanism remains to be established (169–171).

In addition, other functionally overlapping DDT pathways could also offer sufficient protection against the deleterious effects of leading strand lesions. For example, yeast cells display an abundance of recombination intermediates associated with fork reversal and temple-switching, in fitting with the preferential usage of recombination pathways by these organisms (reviewed in (172)). It is therefore likely that HR and other DDT pathways (e.g TLS, dormant origin firing) readily compensate for the lack of repriming mechanisms and these alternative mechanisms may even provide more efficient replication restart solutions for some organisms.

CONCLUDING REMARKS

Since the seminal studies of Rupp and Howard-Flanders, the precise nature of leading strand synthesis has been debated (82). The initial evidence pointed to a mechanism whereby all DNA was synthesised in small pieces, regardless of which strand, leading or lagging, the nascent chain originated. A plethora of conflicting publications made it difficult to draw concrete conclusions and it seems the field gravitated towards the mechanistically simpler model of continuous leading strand synthesis from origin to termination. The discovery of TLS enzymes made the continuous argument even more appealing, as these enzymes offered an explanation as to how lesions could be bypassed without breaking the continuous nascent chain (89–91). However, the idea of repriming was not forgotten and later studies provided some compelling evidence of leading strand repriming occurring in bacteria and yeast (88,93,94). The discovery and subsequent characterisation of a second primase enzyme in vertebrate cells (PrimPol) has now established that a similar process also occurs in most eukaryotic cells and represents a key additional DDT pathway for maintaining efficient fork progression (161). With more research being conducted into leading strand repriming, it is becoming apparent that it offers a flexible replication restart pathway that is an ideal solution for bypassing a wide variety of fork stalling impediments, that can subsequently be resolved in a post-replicative manner. This is most apparent in studies that demonstrate functional redundancies between repriming and a variety of specific pathways for tolerating damage (126,139). Thus, after examining all of the available evidence, it is clear that repriming on the leading strand should now be considered a canonical DDT pathway in a wide range of organisms, from bacteria to human cells. In fact, repriming may even represent the original DDT pathway as it is also required to maintain efficient DNA duplication during unperturbed replication.

Although the significance of repriming mechanisms in vertebrate cells is becoming more evident, much remains to be discovered about this process. Since aberrant priming on ssDNA is clearly undesirable, there are likely many undiscovered regulatory mechanisms to ensure that the usage of repriming pathways is strictly restricted to when and where they are required. Additionally, taking into account the diverse range of functions displayed by other Prim-Pol superfamily members (103), it seems plausible that PrimPol may undertake additional roles in DNA replication and repair, e.g. TLS or gap repair synthesis. Since PrimPol is involved in an important mechanism that maintains replication restart in human cells, defects in this pathway are likely to have a role in genetic diseases. A specific PrimPol mutation has already been identified as a susceptibility gene for high myopia (173), although its role in the development of this condition has not been established. Additionally, PrimPol alterations have been observed in cancers, with overexpression of PrimPol reported in glioblastoma and a point mutation identified in lung cancer (174,175). Interestingly, DNA primase (PRIM1) mutations have recently been linked to the development of Microcephalic Primordial Dwarfism (MPD) (176), further demonstrating the association of primase mutations with disease states and highlighting the need for further research into the exact mechanisms that underpin this canonical DNA replication-associated restart pathway.

DATA AVAILABILITY

No primary data is associated with this article.

ACKNOWLEDGEMENTS

We thank Dr Laura Bailey for her comments on the manuscript. We also thank past group members and collaborators who have made important contributions to studies cited in this review.

FUNDING

A.J.D.'s laboratory supported by grants from the Biotechnology and Biological Sciences Research Council (BBSRC) [BB/H019723/1, BB/M008800/1]; L.J.B. and R.T. were supported by PhD studentships funded by the Wellcome Trust ISSF and University of Sussex. The open access publication charge for this paper has been waived by Oxford University Press – *NAR* Editorial Board members are entitled to one free paper per year in recognition of their work on behalf of the journal

Conflict of interest statement. None declared.

REFERENCES

1. Gambus,A., Jones,R.C., Sanchez-Diaz,A., Kanemaki,M., van Deursen,F., Edmondson,R.D. and Labib,K. (2006) GINS maintains association of Cdc45 with MCM in replisome progression complexes at eukaryotic DNA replication forks. *Nat. Cell Biol.*, **8**, 358–366.
2. Lei,M. (2005) The MCM complex: its role in DNA replication and implications for cancer therapy. *Curr. Cancer Drug Targets*, **5**, 365–380.
3. Wohlschlegel,J.A., Dwyer,B.T., Dhar,S.K., Cvetic,C., Walter,J.C. and Dutta,A. (2000) Inhibition of eukaryotic DNA replication by geminin binding to Cdt1. *Science*, **290**, 2309–2312.
4. Evrin,C., Clarke,P., Zech,J., Lurz,R., Sun,J., Uhle,S., Li,H., Stillman,B. and Speck,C. (2009) A double-hexameric MCM2-7 complex is loaded onto origin DNA during licensing of eukaryotic DNA replication. *Proc. Natl. Acad. Sci. U.S.A.*, **106**, 20240–20245.
5. Deegan,T.D. and Diffley,J.F. (2016) MCM: one ring to rule them all. *Curr. Opin. Struct. Biol.*, **37**, 145–151.
6. Fu,YuV., Yardimci,H., Long,DT., Guainazzi,A., Bermudez,VP., Hurwitz,J., van Oijen,A., Schärer,OD. and Walter,J.C. (2011) Selective bypass of a lagging strand roadblock by the eukaryotic replicative DNA helicase. *Cell*, **146**, 931–941.
7. Kuchta,R.D. and Stengel,G. (2010) Mechanism and evolution of DNA primases. *Biochim. Biophys. Acta (BBA)-Proteins Proteomics*, **1804**, 1180–1189.
8. Clausen,A.R., Lujan,S.A., Burkholder,A.B., Orebaugh,C.D., Williams,J.S., Clausen,M.F., Malc,E.P., Mieczkowski,P.A., Fargo,D.C. and Smith,D.J. (2015) Tracking replication enzymology in vivo by genome-wide mapping of ribonucleotide incorporation. *Nat. Struct. Mol. Biol.*, **22**, 185–191.
9. Guilliam,T.A. and Yeeles,J.T. (2020) Reconstitution of translesion synthesis reveals a mechanism of eukaryotic DNA replication restart. *Nat. Struct. Mol. Biol.*, **27**, 450–460.
10. Miyabe,I., Mizuno,K.I., Keszthelyi,A., Daigaku,Y., Skouteri,M., Mohebi,S., Kunkel,T.A., Murray,J.M. and Carr,A.M. (2015) Polymerase δ replicates both strands after homologous recombination–dependent fork restart. *Nat. Struct. Mol. Biol.*, **22**, 932–938
11. Lujan,S.A., Williams,J.S. and Kunkel,T.A. (2016) DNA polymerases divide the labor of genome replication. *Trends Cell Biol.*, **26**, 640–654.
12. Miyabe,I., Kunkel,T.A. and Carr,A.M. (2011) The major roles of DNA polymerases epsilon and delta at the eukaryotic replication fork are evolutionarily conserved. *PLos Genet.*, **7**, e1002407.
13. Pellegrini,L. (2012) The Pol α-primase complex. *Eukaryotic Replisome*, **62**, 157–169.
14. Baker,T.A. and Wickner,S.H. (1992) Genetics and enzymology of DNA replication in *Escherichia coli*. *Annu. Rev. Genet.*, **26**, 447–477.
15. Dua,R., Levy,D.L., Li,C.M., Snow,P.M. and Campbell,J.L. (2002) In vivo reconstitution of *Saccharomyces cerevisiae* DNA polymerase ε in insect cells purification and characterisation *J. Biol. Chem.*, **277**, 7889–7896.
16. Chilkova,O., Stenlund,P., Isoz,I., Stith,C.M., Grabowski,P., Lundström,E.-B., Burgers,P.M. and Johansson,E. (2007) The eukaryotic leading and lagging strand DNA polymerases are loaded onto primer-ends via separate mechanisms but have comparable processivity in the presence of PCNA. *Nucleic Acids Res.*, **35**, 6588–6597.
17. Dewar,J.M. and Walter,J.C. (2017) Mechanisms of DNA replication termination. *Nat. Rev. Mol. Cell Biol.*, **18**, 507–516.
18. Franz,A., Orth,M., Pirson,P.A., Sonneville,R., Blow,J.J., Gartner,A., Stemmann,O. and Hoppe,T. (2011) CDC-48/p97 coordinates CDT-1 degradation with GINS chromatin dissociation to ensure faithful DNA replication. *Mol. Cell*, **44**, 85–96.
19. Bębenek,A. and Ziuzia-Graczyk,I. (2018) Fidelity of DNA replication—a matter of proofreading. *Curr. Genet.*, **64**, 985–996.
20. Mailand,N., Gibbs-Seymour,I. and Bekker-Jensen,S. (2013) Regulation of PCNA–protein interactions for genome stability. *Nat. Rev. Mol. Cell Biol.*, **14**, 269–282.
21. Bryan,T.M. (2019) Mechanisms of DNA replication and repair: insights from the study of G-quadruplexes. *Molecules*, **24**, 3439–3454.
22. Allison,D.F. and Wang,G.G. (2019) R-loops: formation, function, and relevance to cell stress. *Cell Stress*, **3**, 38–46.
23. Carr,A.M. and Lambert,S. (2013) Replication stress-induced genome instability: the dark side of replication maintenance by homologous recombination. *J. Mol. Biol.*, **425**, 4733–4744.
24. Debatisse,M., Le Tallec,B., Letessier,A., Dutrillaux,B. and Brison,O. (2012) Common fragile sites: mechanisms of instability revisited. *Trends Genet.*, **28**, 22–32.
25. Maya-Mendoza,A., Ostrakova,J., Kosar,M., Hall,A., Duskova,P., Mistrik,M., Merchut-Maya,J.M., Hodny,Z., Bartkova,J. and Christensen,C. (2015) Myc and Ras oncogenes engage different energy metabolism programs and evoke distinct patterns of oxidative and DNA replication stress. *Mol. Oncol.*, **9**, 601–616.
26. Kotsantis,P., Silva,L.M., Irmscher,S., Jones,R.M., Folkes,L., Gromak,N. and Petermann,E. (2016) Increased global transcription activity as a mechanism of replication stress in cancer. *Nat. Commun.*, **7**, 13087.
27. Muñoz,S. and Méndez,J. (2017) DNA replication stress: from molecular mechanisms to human disease. *Chromosoma*, **126**, 1–15.
28. O'Driscoll,M., Ruiz-Perez,V.L., Woods,C.G., Jeggo,P.A. and Goodship,J.A. (2003) A splicing mutation affecting expression of ataxia–telangiectasia and Rad3–related protein (ATR) results in Seckel syndrome. *Nat. Genet.*, **33**, 497–501.
29. Marteijn,J.A., Lans,H., Vermeulen,W. and Hoeijmakers,J.H.J. (2014) Understanding nucleotide excision repair and its roles in cancer and ageing. *Nat. Rev. Mol. Cell Biol.*, **15**, 465–481.
30. McInerney,P. and O'Donnell,M. (2004) Functional uncoupling of twin polymerases: mechanism of polymerase dissociation from a lagging strand block. *J. Biol. Chem.*, **279**, 21543–21551.
31. Taylor,M.R. and Yeeles,J.T. (2018) The initial response of a eukaryotic replisome to DNA damage. *Mol. Cell*, **70**, 1067–1080.
32. Byun,T.S., Pacek,M., Yee,M.-c., Walter,J.C. and Cimprich,K.A. (2005) Functional uncoupling of MCM helicase and DNA polymerase activities activates the ATR-dependent checkpoint. *Genes Dev.*, **19**, 1040–1052.
33. Zou,L. and Elledge,S.J. (2003) Sensing DNA damage through ATRIP recognition of RPA-ssDNA complexes. *Science*, **300**, 1542–1548.
34. Cimprich,K.A. and Cortez,D. (2008) ATR: an essential regulator of genome integrity. *Nat. Rev. Mol. Cell Biol.*, **9**, 616–627.
35. Saldivar,J.C., Cortez,D. and Cimprich,K.A. (2017) The essential kinase ATR: ensuring faithful duplication of a challenging genome. *Nat. Rev. Mol. Cell Biol.*, **18**, 622–636.
36. Toledo,L.I., Altmeyer,M., Rask,M.-B., Lukas,C., Larsen,D.H., Povlsen,L.K., Bekker-Jensen,S., Mailand,N., Bartek,J. and Lukas,J. (2013) ATR prohibits replication catastrophe by preventing global exhaustion of RPA. *Cell*, **155**, 1088–1103.

37. Sale,J.E., Lehmann,A.R. and Woodgate,R. (2012) Y-family DNA polymerases and their role in tolerance of cellular DNA damage. *Nat. Rev. Mol. Cell Biol.*, **13**, 141–152.
38. Vaisman,A. and Woodgate,R. (2017) Translesion DNA polymerases in eukaryotes: what makes them tick? *Crit. Rev. Biochem. Mol. Biol.*, **52**, 274–303.
39. Masutani,C., Kusumoto,R., Iwai,S. and Hanaoka,F. (2000) Mechanisms of accurate translesion synthesis by human DNA polymerase η. *EMBO J.*, **19**, 3100–3109.
40. Lin,W., Xin,H., Zhang,Y., Wu,X., Yuan,F. and Wang,Z. (1999) The human REV1 gene codes for a DNA template-dependent dCMP transferase. *Nucleic Acids Res.*, **27**, 4468–4475.
41. Khare,V. and Eckert,K.A. (2002) The proofreading 3′→ 5′ exonuclease activity of DNA polymerases: a kinetic barrier to translesion DNA synthesis. *Mut. Res./Fundam. Mol. Mech. Mutagen.*, **510**, 45–54.
42. Haracska,L., Torres-Ramos,C.A., Johnson,R.E., Prakash,S. and Prakash,L. (2004) Opposing effects of ubiquitin conjugation and SUMO modification of PCNA on replicational bypass of DNA lesions in *Saccharomyces cerevisiae*. *Mol. Cell. Biol.*, **24**, 4267–4274.
43. Lehmann,C.P., Jiménez-Martín,A., Branzei,D. and Tercero,J.A. (2020) Prevention of unwanted recombination at damaged replication forks. *Curr. Genet.*, **66**, 1045–1051.
44. Ulrich,H.D. and Jentsch,S. (2000) Two RING finger proteins mediate cooperation between ubiquitin-conjugating enzymes in DNA repair. *EMBO J.*, **19**, 3388–3397.
45. Hoege,C., Pfander,B., Moldovan,G.-L., Pyrowolakis,G. and Jentsch,S. (2002) RAD6-dependent DNA repair is linked to modification of PCNA by ubiquitin and SUMO. *Nature*, **419**, 135–141.
46. Fan,L., Bi,T., Wang,L. and Xiao,W. (2020) DNA-damage tolerance through PCNA ubiquitination and sumoylation. *Biochem. J.*, **477**, 2655–2677.
47. Kanao,R. and Masutani,C. (2017) Regulation of DNA damage tolerance in mammalian cells by post-translational modifications of PCNA. *Mutat. Res.*, **803–805**, 82–88.
48. Karras,G.I., Fumasoni,M., Sienski,G., Vanoli,F., Branzei,D. and Jentsch,S. (2013) Noncanonical role of the 9-1-1 clamp in the error-free DNA damage tolerance pathway. *Mol. Cell*, **49**, 536–546.
49. Holloman,W.K. (2011) Unraveling the mechanism of BRCA2 in homologous recombination. *Nat. Struct. Mol. Biol.*, **18**, 748–754.
50. Fasching,C.L., Cejka,P., Kowalczykowski,S.C. and Heyer,W.-D. (2015) Top3-Rmi1 dissolve Rad51-mediated D loops by a topoisomerase-based mechanism. *Mol. Cell*, **57**, 595–606.
51. Lopes,M., Cotta-Ramusino,C., Pellicioli,A., Liberi,G., Plevani,P., Muzi-Falconi,M., Newlon,C.S. and Foiani,M. (2001) The DNA replication checkpoint response stabilizes stalled replication forks. *Nature*, **412**, 557–561.
52. Neelsen,K.J. and Lopes,M. (2015) Replication fork reversal in eukaryotes: from dead end to dynamic response. *Nat. Rev. Mol. Cell Biol.*, **16**, 207–220.
53. McGlynn,P. and Lloyd,R.G. (2002) Recombinational repair and restart of damaged replication forks. *Nat. Rev. Mol. Cell Biol.*, **3**, 859–870.
54. Taglialatela,A., Alvarez,S., Leuzzi,G., Sannino,V., Ranjha,L., Huang,J.-W., Madubata,C., Anand,R., Levy,B. and Rabadan,R. (2017) Restoration of replication fork stability in BRCA1-and BRCA2-deficient cells by inactivation of SNF2-family fork remodelers. *Mol. Cell*, **68**, 414–430.
55. Quinet,A., Lemaçon,D. and Vindigni,A. (2017) Replication fork reversal: players and guardians. *Mol. Cell*, **68**, 830–833.
56. Ge,X.Q., Jackson,D.A. and Blow,J.J. (2007) Dormant origins licensed by excess Mcm2–7 are required for human cells to survive replicative stress. *Genes Dev.*, **21**, 3331–3341.
57. Ge,X.Q. and Blow,J.J. (2010) Chk1 inhibits replication factory activation but allows dormant origin firing in existing factories. *J. Cell Biol.*, **191**, 1285–1297.
58. Watson,J.D. and Crick,F.H. (1953) Molecular structure of nucleic acids: a structure for deoxyribose nucleic acid. *Nature*, **171**, 737–738.
59. Lehman,I.R., Bessman,M.J., Simms,E.S. and Kornberg,A. (1958) Enzymatic synthesis of deoxyribonucleic acid I. Preparation of substrates and partial purification of an enzyme from Escherichia coli. *J. Biol. Chem.*, **233**, 163–170.
60. Richardson,C.C., Schildkraut,C.L. and Kornberg,A. (1963) In: *Cold Spring Harbor Symposia on Quantitative Biology*. Cold Spring Harbor Laboratory Press, Vol. **28**, pp. 9–19.
61. Sakabe,K. and Okazaki,R. (1966) A unique property of the replicating region of chromosomal DNA. *Biochim. Biophys. Acta*, **129**, 651–654.
62. Okazaki,R., Okazaki,T., Sakabe,K., Sugimoto,K. and Sugino,A. (1968) Mechanism of DNA chain growth. I. Possible discontinuity and unusual secondary structure of newly synthesized chains. *Proc. Natl. Acad. Sci. U.S.A.*, **59**, 598–605.
63. Iyer,V. and Lark,K. (1970) DNA replication in *Escherichia coli*: location of recently incorporated thymidine withi molecules of high molecular weight DNA. *Proc. Natl. Acad. Sci. U.S.A.*, **67**, 629–636.
64. Okazaki,T. and Okazaki,R. (1969) Mechanism of DNA chain growth. IV. Direction of synthesis of T4 short DNA chains as revealed by exonucleolytic degradation. *Proc. Natl. Acad. Sci. U.S.A.*, **64**, 1242–1248.
65. Konrad,E.B., Modrich,P. and Lehman,I. (1973) Genetic and enzymatic characterization of a conditional lethal mutant of *Escherichia coli* K12 with a temperature-sensitive DNA ligase. *J. Mol. Biol.*, **77**, 519–529.
66. Sugimoto,K., Okazaki,T. and Okazaki,R. (1968) Mechanism of DNA chain growth. II. Accumulation of newly synthesized short chains in *E. coli* infected with ligase-defective T4 phages. *PNAS*, **60**, 1356–1362.
67. Johnston,L.H. and Nasmyth,K.A. (1978) Saccharomyces cerevisiae cell cycle mutant cdc 9 is defective in DNA ligase. *Nature*, **274**, 891–893.
68. Nasmyth,K.A. (1977) Temperature-sensitive lethal mutants in the structural gene for DNA ligase in the yeast *Schizosaccharomyces pombe*. *Cell*, **12**, 1109–1120.
69. Sallmyr,A., Rashid,I., Bhandari,S.K., Naila,T. and Tomkinson,A.E. (2020) Human DNA ligases in replication and repair. *DNA Repair (Amst.)*, **93**, 102908.
70. Kuempel,P.L. and Veomett,G.E. (1970) A possible function of DNA polymerase in chromosome replication. *Biochem. Biophys. Res. Commun.*, **41**, 973–980.
71. Sugino,A., Hirose,S. and Okazaki,R. (1972) RNA-linked nascent DNA fragments in Escherichia coli. *Proc. Natl. Acad. Sci.*, **69**, 1863–1867.
72. Olivera,B. and Bonhoeffer,F. (1972) Discontinuous DNA replication in vitro. I. Two distinct size classes of intermediates. *Nat. New Biol.*, **240**, 233–235.
73. Herrmann,R., Huf,J. and Bonhoeffer,F. (1972) II. Cross hybridization and rate of chain elongation of the two classes of DNA intermediates. *Nat. New Biol.*, **240**, 235–237.
74. Nakai,H. and Richardson,C. (1988) Leading and lagging strand synthesis at the replication fork of bacteriophage T7. Distinct properties of T7 gene 4 protein as a helicase and primase. *J. Biol. Chem.*, **263**, 9818–9830.
75. Wu,C., Zechner,E. and Marians,K. (1992) Coordinated leading-and lagging-strand synthesis at the Escherichia coli DNA replication fork. I. Multiple effectors act to modulate Okazaki fragment size. *J. Biol. Chem.*, **267**, 4030–4044.
76. Louarn,J.-M. and Bird,R.E. (1974) Size distribution and molecular polarity of newly replicated DNA in Escherichia coli. *Proc. Natl. Acad. Sci. U.S.A.*, **71**, 329–333.
77. Sternglanz,R., Wang,H.F. and Donegan,J.J. (1976) Evidence that both growing DNA chains at a replication fork are synthesized discontinuously. *Biochemistry*, **15**, 1838–1843.
78. Olivera,B.M. (1978) DNA intermediates at the Escherichia coli replication fork: effect of dUTP. *Proc. Natl. Acad. Sci. U.S.A.*, **75**, 238–242.
79. Tye,B.-K., Chien,J., Lehman,I., Duncan,B.K. and Warner,H.R. (1978) Uracil incorporation: a source of pulse-labeled DNA fragments in the replication of the *Escherichia coli* chromosome. *Proc. Natl. Acad. Sci. U.S.A.*, **75**, 233–237.
80. Amado,L. and Kuzminov,A. (2006) The replication intermediates in *Escherichia coli* are not the product of DNA processing or uracil excision. *J. Biol. Chem.*, **281**, 22635–22646.
81. Cronan,G.E., Kouzminova,E.A. and Kuzminov,A. (2019) Near-continuously synthesized leading strands in *Escherichia coli* are broken by ribonucleotide excision. *Proc. Natl. Acad. Sci. U.S.A.*, **116**, 1251–1260.

82. Rupp,W.D. and Howard-Flanders,P. (1968) Discontinuities in the DNA synthesized in an excision-defective strain of *Escherichia coli* following ultraviolet irradiation. *J. Mol. Biol.*, **31**, 291–304.
83. Iyer,V. and Rupp,W. (1971) Usefulness of benzoylated naphthoylated DEAE-cellulose to distinguish and fractionate double-stranded DNA bearing different extents of single-stranded regions. *Biochim. Biophys. Acta (BBA)-Nucleic Acids Protein Synth.*, **228**, 117–126.
84. Rupp,W.D., Wilde,C.E. III, Reno,D.L. and Howard-Flanders,P. (1971) Exchanges between DNA strands in ultraviolet-irradiated Escherichia coli. *J. Mol. Biol.*, **61**, 25–44.
85. Cleaver,J. and Thomas,G. (1969) Single strand interruptions in DNA and the effects of caffeine in Chinese hamster cells irradiated with ultraviolet light. *Biochem. Biophys. Res. Commun.*, **36**, 203–208.
86. Meneghini,R. (1976) Gaps in DNA synthesized by ultraviolet light-irradiated WI38 human cells. *Biochim. Biophys. Acta (BBA)-Nucleic Acids Protein Synth.*, **425**, 419–427.
87. Lehmann,A.R. (1972) Postreplication repair of DNA in ultraviolet-irradiated mammalian cells. *J. Mol. Biol.*, **66**, 319–337.
88. Lehmann,A.R. and Fuchs,R.P. (2006) Gaps and forks in DNA replication: rediscovering old models. *DNA Repair (Amst.)*, **5**, 1495–1498.
89. Johnson,R.E., Prakash,S. and Prakash,L. (1999) Efficient bypass of a thymine-thymine dimer by yeast DNA polymerase, Polη. *Science*, **283**, 1001–1004.
90. Nelson,J.R., Lawrence,C.W. and Hinkle,D.C. (1996) Thymine-thymine dimer bypass by yeast DNA polymerase ζ. *Science*, **272**, 1646–1649.
91. Masutani,C., Kusumoto,R., Yamada,A., Dohmae,N., Yokoi,M., Yuasa,M., Araki,M., Iwai,S., Takio,K. and Hanaoka,F. (1999) The XPV (xeroderma pigmentosum variant) gene encodes human DNA polymerase η. *Nature*, **399**, 700–704.
92. Wang,T.C.V. (2005) Discontinuous or semi-discontinuous DNA replication in Escherichia coli? *Bioessays*, **27**, 633–636.
93. Lopes,M., Foiani,M. and Sogo,J.M. (2006) Multiple mechanisms control chromosome integrity after replication fork uncoupling and restart at irreparable UV lesions. *Mol. Cell*, **21**, 15–27.
94. Heller,R.C. and Marians,K.J. (2006) Replisome assembly and the direct restart of stalled replication forks. *Nat. Rev. Mol. Cell Biol.*, **7**, 932–943.
95. Bouché,J., Zechel,K. and Kornberg,A. (1975) dnaG gene product, a rifampicin-resistant RNA polymerase, initiates the conversion of a single-stranded coliphage DNA to its duplex replicative form. *J. Biol. Chem.*, **250**, 5995–6001.
96. Yeeles,J.T. and Marians,K.J. (2011) The *Escherichia coli* replisome is inherently DNA damage tolerant. *Science*, **334**, 235–238.
97. Yeeles,J.T. and Marians,K.J. (2013) Dynamics of leading-strand lesion skipping by the replisome. *Mol. Cell*, **52**, 855–865.
98. Yao,N. and O'Donnell,M. (2016) Bacterial and eukaryotic replisome machines. *JSM Biochem. Mol. Biol.*, **3**, 1013.
99. LeBowitz,J.H. and McMacken,R. (1986) The Escherichia coli dnaB replication protein is a DNA helicase. *J. Biol. Chem.*, **261**, 4738–4748.
100. Moyer,S.E., Lewis,P.W. and Botchan,M.R. (2006) Isolation of the Cdc45/Mcm2-7/GINS (CMG) complex, a candidate for the eukaryotic DNA replication fork helicase. *Proc. Natl. Acad. Sci. U.S.A.*, **103**, 10236–10241.
101. McInerney,P., Johnson,A., Katz,F. and O'Donnell,M. (2007) Characterization of a triple DNA polymerase replisome. *Mol. Cell*, **27**, 527–538.
102. Podobnik,M., McInerney,P., O'Donnell,M. and Kuriyan,J. (2000) A TOPRIM domain in the crystal structure of the catalytic core of *Escherichia coli* primase confirms a structural link to DNA topoisomerases. *J. Mol. Biol.*, **300**, 353–362.
103. Guilliam,T.A., Keen,B.A., Brissett,N.C. and Doherty,A.J. (2015) Primase-polymerases are a functionally diverse superfamily of replication and repair enzymes. *Nucleic Acids Res.*, **43**, 6651–6664.
104. Plevani,P., Foiani,M., Falconi,M.M., Pizzagalli,A., Santocanale,C., Francesconi,S., Valsasnini,P., Comedini,A., Piatti,S. and Lucchini,G. (1988) The yeast DNA polymerase-primase complex: genes and proteins. *Biochim. Biophys. Acta (BBA)-Gene Struct. Expression*, **951**, 268–273.
105. Nasheuer,H.P. and Grosse,F. (1988) DNA polymerase alpha-primase from calf thymus. Determination of the polypeptide responsible for primase activity. *J. Biol. Chem.*, **263**, 8981–8988.
106. Marini,F., Pellicioli,A., Paciotti,V., Lucchini,G., Plevani,P., Stern,D.F. and Foiani,M. (1997) A role for DNA primase in coupling DNA replication to DNA damage response. *EMBO J.*, **16**, 639–650.
107. Fumasoni,M., Zwicky,K., Vanoli,F., Lopes,M. and Branzei,D. (2015) Error-free DNA damage tolerance and sister chromatid proximity during DNA replication rely on the Polα/Primase/Ctf4 complex. *Mol. Cell*, **57**, 812–823.
108. Georgescu,R.E., Schauer,G.D., Yao,N.Y., Langston,L.D., Yurieva,O., Zhang,D., Finkelstein,J. and O'Donnell,M.E. (2015) Reconstitution of a eukaryotic replisome reveals suppression mechanisms that define leading/lagging strand operation. *Elife*, **4**, e04988.
109. Aria,V. and Yeeles,J.T.P. (2018) Mechanism of bidirectional leading-strand synthesis establishment at eukaryotic DNA replication origins. *Mol. Cell*, **73**, 199–211.
110. Lehman,I. and Kaguni,L. (1989) DNA polymerase alpha. *J. Biol. Chem.*, **264**, 4265–4268.
111. Sun,J., Shi,Y., Georgescu,R.E., Yuan,Z., Chait,B.T., Li,H. and O'Donnell,M.E. (2015) The architecture of a eukaryotic replisome. *Nat. Struct. Mol. Biol.*, **22**, 976–982.
112. Kurat,C.F., Yeeles,J.T.P., Patel,H., Early,A. and Diffley,J.F.X. (2017) Chromatin controls DNA replication origin selection, lagging-strand synthesis, and replication fork rates. *Mol. Cell*, **65**, 117–130.
113. Porcella,S.Y., Koussa,N.C., Tang,C.P., Kramer,D.N., Srivastava,P. and Smith,D.J. (2020) Separable, Ctf4-mediated recruitment of DNA Polymerase α for initiation of DNA synthesis at replication origins and lagging-strand priming during replication elongation. *PLoS Genet.*, **16**, e1008755.
114. Kilkenny,M.L., Simon,A.C., Mainwaring,J., Wirthensohn,D., Holzer,S. and Pellegrini,L. (2017) The human CTF4-orthologue AND-1 interacts with DNA polymerase α/primase via its unique C-terminal HMG box. *Open Biol.*, **7**, 170217.
115. Bocquier,A.A., Liu,L., Cann,I.K., Komori,K., Kohda,D. and Ishino,Y. (2001) Archaeal primase: bridging the gap between RNA and DNA polymerases. *Curr. Biol.*, **11**, 452–456.
116. Jozwiakowski,S.K., Gholami,F.B. and Doherty,A.J. (2015) Archaeal replicative primases can perform translesion DNA synthesis. *Proc. Natl. Acad. Sci. U.S.A.*, **112**, E633–E638.
117. Lipps,G., Röther,S., Hart,C. and Krauss,G. (2003) A novel type of replicative enzyme harbouring ATPase, primase and DNA polymerase activity. *EMBO J.*, **22**, 2516–2525.
118. Scherzinger,E., Bagdasarian,M.M., Scholz,P., Lurz,R., Rückert,B. and Bagdasarian,M. (1984) Replication of the broad host range plasmid RSF1010: requirement for three plasmid-encoded proteins. *Proc. Natl. Acad. Sci. U.S.A.*, **81**, 654–658.
119. Scherzinger,E., Haring,V., Lurz,R. and Otto,S. (1991) Plasmid RSF1010 DNA replication in vitro promoted by purified RSF1010 RepA, RepB and RepC proteins. *Nucleic Acids Res.*, **19**, 1203–1211.
120. Aravind,L. and Koonin,E.V. (2001) Prokaryotic homologs of the eukaryotic DNA-end-binding protein Ku, novel domains in the Ku protein and prediction of a prokaryotic double-strand break repair system. *Genome Res.*, **11**, 1365–1374.
121. Weller,G.R. and Doherty,A.J. (2001) A family of DNA repair ligases in bacteria? *FEBS Lett.*, **505**, 340–342.
122. Della,M., Palmbos,P.L., Tseng,H.-M., Tonkin,L.M., Daley,J.M., Topper,L.M., Pitcher,R.S., Tomkinson,A.E., Wilson,T.E. and Doherty,A.J. (2004) Mycobacterial Ku and ligase proteins constitute a two-component NHEJ repair machine. *Science*, **306**, 683–685.
123. Płociński,P., Brissett,N.C., Bianchi,J., Brzostek,A., Korycka-Machała,M., Dziembowski,A., Dziadek,J. and Doherty,A.J. (2017) DNA ligase C and Prim-PolC participate in base excision repair in mycobacteria. *Nat. Commun.*, **8**, 1251.
124. Brissett,N.C., Zabrady,K., Płociński,P., Bianchi,J., Korycka-Machała,M., Brzostek,A., Dziadek,J. and Doherty,A.J. (2020) Molecular basis for DNA repair synthesis on short gaps by mycobacterial primase-polymerase C. *Nat. Commun.*, **11**, 4196.
125. Iyer,L.M., Koonin,E.V., Leipe,D.D. and Aravind,L. (2005) Origin and evolution of the archaeo-eukaryotic primase superfamily and related palm-domain proteins: structural insights and new members. *Nucleic Acids Res.*, **33**, 3875–3896.

126. Bianchi,J., Rudd,S.G., Jozwiakowski,S.K., Bailey,L.J., Soura,V., Taylor,E., Stevanovic,I., Green,A.J., Stracker,T.H., Lindsay,H.D. *et al.* (2013) PrimPol bypasses UV photoproducts during eukaryotic chromosomal DNA replication. *Mol. Cell*, **52**, 566–573.
127. García-Gómez,S., Reyes,A., Martínez-Jiménez,M.I., Chocrón,E.S., Mourón,S., Terrados,G., Powell,C., Salido,E., Méndez,J. and Holt,I.J. (2013) PrimPol, an archaic primase/polymerase operating in human cells. *Mol. Cell*, **52**, 541–553.
128. Wan,L., Lou,J., Xia,Y., Su,B., Liu,T., Cui,J., Sun,Y., Lou,H. and Huang,J. (2013) hPrimpol1/CCDC111 is a human DNA primase-polymerase required for the maintenance of genome integrity. *EMBO Rep.*, **14**, 1104–1112.
129. Wang,T., Hu,S. and Korn,D. (1984) DNA primase from KB cells. Characterization of a primase activity tightly associated with immunoaffinity-purified DNA polymerase-alpha. *J. Biol. Chem.*, **259**, 1854–1865.
130. Keen,B.A., Jozwiakowski,S.K., Bailey,L.J., Bianchi,J. and Doherty,A.J. (2014) Molecular dissection of the domain architecture and catalytic activities of human PrimPol. *Nucleic Acids Res.*, **42**, 5830–5845.
131. Arezi,B. and Kuchta,R.D. (2000) Eukaryotic DNA primase. *Trends Biochem. Sci.*, **25**, 572–576.
132. Mourón,S., Rodriguez-Acebes,S., Martínez-Jiménez,M.I., García-Gómez,S., Chocrón,S., Blanco,L. and Méndez,J. (2013) Repriming of DNA synthesis at stalled replication forks by human PrimPol. *Nat. Struct. Mol. Biol.*, **20**, 1383–1389.
133. Martínez-Jiménez,M.I., Calvo,P.A., García-Gómez,S., Guerra-González,S. and Blanco,L. (2018) The Zn-finger domain of human PrimPol is required to stabilize the initiating nucleotide during DNA priming. *Nucleic Acids Res.*, **46**, 4138–4151.
134. Guilliam,T.A., Jozwiakowski,S.K., Ehlinger,A., Barnes,R.P., Rudd,S.G., Bailey,L.J., Skehel,J.M., Eckert,K.A., Chazin,W.J. and Doherty,A.J. (2015) Human PrimPol is a highly error-prone polymerase regulated by single-stranded DNA binding proteins. *Nucleic Acids Res.*, **43**, 1056–1068.
135. Guilliam,T.A., Brissett,N.C., Ehlinger,A., Keen,B.A., Kolesar,P., Taylor,E.M., Bailey,L.J., Lindsay,H.D., Chazin,W.J. and Doherty,A.J. (2017) Molecular basis for PrimPol recruitment to replication forks by RPA. *Nat. Commun.*, **8**, 15222.
136. Guilliam,T.A., Bailey,L.J., Brissett,N.C. and Doherty,A.J. (2016) PolDIP2 interacts with human PrimPol and enhances its DNA polymerase activities. *Nucleic Acids Res.*, **44**, 3317–3329.
137. Bailey,L.J., Bianchi,J., Hegarat,N., Hochegger,H. and Doherty,A.J. (2016) PrimPol-deficient cells exhibit a pronounced G2 checkpoint response following UV damage. *Cell Cycle*, **15**, 908–918.
138. Kobayashi,K., Guilliam,T.A., Tsuda,M., Yamamoto,J., Bailey,L.J., Iwai,S., Takeda,S., Doherty,A.J. and Hirota,K. (2016) Repriming by PrimPol is critical for DNA replication restart downstream of lesions and chain-terminating nucleosides. *Cell Cycle*, **15**, 1997–2008.
139. Bailey,L.J., Bianchi,J. and Doherty,A.J. (2019) PrimPol is required for the maintenance of efficient nuclear and mitochondrial DNA replication in human cells. *Nucleic Acids Res.*, **47**, 4026–4038.
140. Orlowska,K.P., Klosowska,K., Szczesny,R.J., Cysewski,D., Krawczyk,P.S. and Dziembowski,A. (2013) A new strategy for gene targeting and functional proteomics using the DT40 cell line. *Nucleic Acids Res.*, **41**, e167–e167.
141. Cervera,L., Gutiérrez,S., Gòdia,F. and Segura,M.M. (2011) Optimization of HEK 293 cell growth by addition of non-animal derived components using design of experiments. *BMC Proc*, **5**, P126.
142. Benslimane,Y., Bertomeu,T., Coulombe-Huntington,J., McQuaid,M., Sánchez-Osuna,M., Papadopoli,D., Avizonis,D., Russo,M.D.S.T., Huard,C. and Topisirovic,I. (2020) Genome-wide screens reveal that resveratrol induces replicative stress in human cells. *Mol. Cell*, **79**, 846–856.
143. Elvers,I., Johansson,F., Groth,P., Erixon,K. and Helleday,T. (2011) UV stalled replication forks restart by re-priming in human fibroblasts. *Nucleic Acids Res.*, **39**, 7049–7057.
144. Pilzecker,B., Buoninfante,O.A., Pritchard,C., Blomberg,O.S., Huijbers,I.J., van den Berk,P.C. and Jacobs,H. (2016) PrimPol prevents APOBEC/AID family mediated DNA mutagenesis. *Nucleic Acids Res.*, **44**, 4734–4744.
145. Schiavone,D., Jozwiakowski,S.K., Romanello,M., Guilbaud,G., Guilliam,T.A., Bailey,L.J., Sale,J.E. and Doherty,A.J. (2016) PrimPol is required for replicative tolerance of G quadruplexes in vertebrate cells. *Mol. Cell*, **61**, 161–169.
146. Šviković,S., Crisp,A., Tan-Wong,S.M., Guilliam,T.A., Doherty,A.J., Proudfoot,N.J., Guilbaud,G. and Sale,J.E. (2019) R-loop formation during S phase is restricted by PrimPol-mediated repriming. *EMBO J.*, **38**, e99793.
147. Rudd,S.G., Glover,L., Jozwiakowski,S.K., Horn,D. and Doherty,A.J. (2013) PPL2 translesion polymerase is essential for the completion of chromosomal DNA replication in the African trypanosome. *Mol. Cell*, **52**, 554–565.
148. Schlacher,K., Christ,N., Siaud,N., Egashira,A., Wu,H. and Jasin,M. (2011) Double-strand break repair-independent role for BRCA2 in blocking stalled replication fork degradation by MRE11. *Cell*, **145**, 529–542.
149. Schlacher,K., Wu,H. and Jasin,M. (2012) A distinct replication fork protection pathway connects Fanconi anemia tumor suppressors to RAD51-BRCA1/2. *Cancer Cell*, **22**, 106–116.
150. Mavaddat,N., Peock,S., Frost,D., Ellis,S., Platte,R., Fineberg,E., Evans,D.G., Izatt,L., Eeles,R.A. and Adlard,J. (2013) Cancer risks for BRCA1 and BRCA2 mutation carriers: results from prospective analysis of EMBRACE. *J. Natl. Cancer Inst.*, **105**, 812–822.
151. Quinet,A., Tirman,S., Jackson,J., Šviković,S., Lemaçon,D., Carvajal-Maldonado,D., González-Acosta,D., Vessoni,A.T., Cybulla,E., Wood,M. *et al.* (2020) PRIMPOL-mediated adaptive response suppresses replication fork reversal in BRCA-deficient cells. *Mol. Cell*, **77**, 461–474.
152. Yan,Y., Xu,Z., Huang,J., Guo,G., Gao,M., Kim,W., Zeng,X., Kloeber,J.A., Zhu,Q. and Zhao,F. (2020) The deubiquitinase USP36 regulates DNA replication stress and confers therapeutic resistance through PrimPol stabilization. *Nucleic Acids Res.*, **48**, 12711–12726.
153. Yoshimura,A., Oikawa,M., Jinbo,H., Hasegawa,Y., Enomoto,T. and Seki,M. (2019) WRNIP1 controls the amount of PrimPol. *Biol. Pharm. Bull.*, **42**, 764–769.
154. Panzarino,N.J., Krais,J.J., Cong,K., Peng,M., Mosqueda,M., Nayak,S.U., Bond,S.M., Calvo,J.A., Doshi,M.B., Bere,M. *et al.* (2020) Replication gaps underlie BRCA-deficiency and therapy response. *Cancer Res.*, **81**, 1388–1397.
155. Nayak,S., Calvo,J.A., Cong,K., Peng,M., Berthiaume,E., Jackson,J., Zaino,A.M., Vindigni,A., Hadden,M.K. and Cantor,S.B. (2020) Inhibition of the translesion synthesis polymerase REV1 exploits replication gaps as a cancer vulnerability. *Sci. Adv.*, **6**, eaaz7808.
156. Bai,G., Kermi,C., Stoy,H., Schiltz,C.J., Bacal,J., Zaino,A.M., Hadden,M.K., Eichman,B.F., Lopes,M. and Cimprich,K.A. (2020) HLTF promotes fork reversal, limiting replication stress resistance and preventing multiple mechanisms of unrestrained DNA synthesis. *Mol. Cell*, **78**, 1237–1251.
157. Kile,A.C., Chavez,D.A., Bacal,J., Eldirany,S., Korzhnev,D.M., Bezsonova,I., Eichman,B.F. and Cimprich,K.A. (2015) HLTF's ancient HIRAN domain binds 3′ DNA ends to drive replication fork reversal. *Mol. Cell*, **58**, 1090–1100.
158. Peng,M., Cong,K., Panzarino,N.J., Nayak,S., Calvo,J., Deng,B., Zhu,L.J., Morocz,M., Hegedus,L. and Haracska,L. (2018) Opposing roles of FANCJ and HLTF protect forks and restrain replication during stress. *Cell Rep.*, **24**, 3251–3261.
159. Genois,M.-M., Gagné,J.-P., Yasuhara,T., Jackson,J., Saxena,S., Langelier,M.-F., Ahel,I., Bedford,M.T., Pascal,J.M. and Vindigni,A. (2021) CARM1 regulates replication fork speed and stress response by stimulating PARP1. *Mol. Cell*, **81**, 784–800.
160. Taylor,M.R. and Yeeles,J.T. (2019) Dynamics of replication fork progression following helicase–polymerase uncoupling in eukaryotes. *J. Mol. Biol.*, **431**, 2040–2049.
161. Guilliam,T.A. and Doherty,A.J. (2017) PrimPol—prime time to reprime. *Genes*, **8**, 20.
162. Tsuda,M., Ogawa,S., Ooka,M., Kobayashi,K., Hirota,K., Wakasugi,M., Matsunaga,T., Sakuma,T., Yamamoto,T. and Chikuma,S. (2019) PDIP38/PolDIP2 controls the DNA damage tolerance pathways by increasing the relative usage of translesion DNA synthesis over template switching. *PLoS One*, **14**, e0213383.
163. Guilliam,T.A. and Yeeles,J.T. (2020) An updated perspective on the polymerase division of labor during eukaryotic DNA replication. *Crit. Rev. Biochem. Mol. Biol.*, **55**, 469–481.
164. Rydberg,B. and Game,J. (2002) Excision of misincorporated ribonucleotides in DNA by RNase H (type 2) and FEN-1 in cell-free extracts. *Proc. Natl. Acad. Sci. U.S.A.*, **99**, 16654–16659.

165. Wong,R.P., García-Rodríguez,N., Zilio,N., Hanulová,M. and Ulrich,H.D. (2020) Processing of DNA polymerase-blocking lesions during genome replication is spatially and temporally segregated from replication forks. *Mol. Cell*, **77**, 3–16.
166. Daigaku,Y., Davies,A.A. and Ulrich,H.D. (2010) Ubiquitin-dependent DNA damage bypass is separable from genome replication. *Nature*, **465**, 951–955.
167. Piberger,A.L., Bowry,A., Kelly,R.D., Walker,A.K., González-Acosta,D., Bailey,L.J., Doherty,A.J., Méndez,J., Morris,J.R. and Bryant,H.E. (2020) PrimPol-dependent single-stranded gap formation mediates homologous recombination at bulky DNA adducts. *Nat. Commun.*, **11**, 5863.
168. Guilliam,T.A. and Yeeles,J.T. (2021) The eukaryotic replisome tolerates leading-strand base damage by replicase switching. *EMBO J.*, **40**, e107037.
169. Hirota,K., Tsuda,M., Mohiuddin, Tsurimoto,T., Cohen,I.S., Livneh,Z., Kobayashi,K., Narita,T., Nishihara,K., Murai,J. *et al.* (2016) In vivo evidence for translesion synthesis by the replicative DNA polymerase δ. *Nucleic Acids Res.*, **44**, 7242–7250.
170. Hirota,K., Yoshikiyo,K., Guilbaud,G., Tsurimoto,T., Murai,J., Tsuda,M., Phillips,L.G., Narita,T., Nishihara,K., Kobayashi,K. *et al.* (2015) The POLD3 subunit of DNA polymerase δ can promote translesion synthesis independently of DNA polymerase ζ. *Nucleic Acids Res.*, **43**, 1671–1683.
171. Narita,T., Tsurimoto,T., Yamamoto,J., Nishihara,K., Ogawa,K., Ohashi,E., Evans,T., Iwai,S., Takeda,S. and Hirota,K. (2010) Human replicative DNA polymerase δ can bypass T-T (6-4) ultraviolet photoproducts on template strands. *Genes Cells*, **15**, 1228–1239.
172. Meng,X. and Zhao,X. (2017) Replication fork regression and its regulation. *FEMS Yeast Res.*, **17**, fow110.
173. Zhao,F., Wu,J., Xue,A., Su,Y., Wang,X., Lu,X., Zhou,Z., Qu,J. and Zhou,X. (2013) Exome sequencing reveals CCDC111 mutation associated with high myopia. *Hum. Genet.*, **132**, 913–921.
174. Yan,X., Ma,L., Yi,D., Yoon,J.-g., Diercks,A., Foltz,G., Price,N.D., Hood,L.E. and Tian,Q. (2011) A CD133-related gene expression signature identifies an aggressive glioblastoma subtype with excessive mutations. *Proc. Natl. Acad. Sci. U.S.A.*, **108**, 1591–1596.
175. Liu,J., Lee,W., Jiang,Z., Chen,Z., Jhunjhunwala,S., Haverty,P.M., Gnad,F., Guan,Y., Gilbert,H.N. and Stinson,J. (2012) Genome and transcriptome sequencing of lung cancers reveal diverse mutational and splicing events. *Genome Res.*, **22**, 2315–2327.
176. Parry,D.A., Tamayo-Orrego,L., Carroll,P., Marsh,J.A., Greene,P., Murina,O., Uggenti,C., Leitch,A., Káposzta,R. and Merő,G. (2020) PRIM1 deficiency causes a distinctive primordial dwarfism syndrome. *Genes Dev.*, **34**, 1520–1533.

PLK1 regulates the PrimPol damage tolerance pathway during the cell cycle

Laura J. Bailey[1, §], Rebecca Teague[1, §], Peter Kolesar[1], Lewis J. Bainbridge[1], Howard D. Lindsay[2] & Aidan J. Doherty[1*]

[1]Genome Damage and Stability Centre, University of Sussex, Falmer, Brighton, BN1 9RQ

[2] Lancaster Medical School, Faculty of Health and Medicine, Lancaster University, Lancaster, LA1 4YQ, UK

[§] These authors contributed equally

* Corresponding author: ajd21@sussex.ac.uk

Keywords: Primase; PrimPol; Repriming; DNA Replication; Replication stress; PLK1; damage tolerance

Abstract

Replication stress and DNA damage stalls replication forks and impedes genome synthesis. During S-phase, damage tolerance pathways allow bypass of impediments to ensure efficient genome duplication. These mechanisms include repriming, translesion synthesis and fork reversal. Repriming allows for DNA synthesis downstream of stalling lesions and is performed by Primase-Polymerase (PrimPol) in human cells. However, the mechanisms by which PrimPol is regulated are poorly understood. Here, we demonstrate that human PrimPol is phosphorylated by Polo-like Kinase 1 (PLK1) at a conserved residue between PrimPol's RPA binding motifs. This serine phosphorylation is differentially modified throughout the cell cycle, which prevents aberrant recruitment of PrimPol to chromatin. Phosphorylation can also be delayed and reversed in response to replication stress. The absence of PLK1-dependent regulation of PrimPol induces phenotypes including chromosome breaks, micronuclei and decreased survival after treatment with camptothecin, cisplatin, olaparib and UV-C. Together, these findings establish that deregulated repriming leads to genomic instability, highlighting the importance of appropriately restricting this DNA damage tolerance pathway following replication fork stalling and throughout the cell cycle.

Teaser

PrimPol is regulated by PLK1 phosphorylation to restrict repriming and prevent genomic instability.

Introduction

The DNA replication machinery regularly encounters obstacles that slow or stall its progression. The causes of replicase stalling are varied and include DNA lesions and structures, nucleotide depletion and other forms of genotoxic stress (*1*). In order to complete replication, cells must bypass such impediments, as unresolved forks are susceptible to degradation and may induce double-strand breaks. Cells have evolved several DNA damage tolerance (DDT) pathways to maintain ongoing replication in perturbed conditions, whose usage is dependent on the environment, type of blockage and available resources.

One such DDT pathway involves repriming DNA synthesis downstream of obstacles to enable stalled replication to resume. Repriming in human cells is dependent on Primase-Polymerase (PrimPol) an enzyme involved in the maintenance of nuclear and mitochondrial DNA replication (*2, 3*). PrimPol can reprime DNA synthesis on the leading strand after the fork encounters stalling lesions, such as cyclopyrimidine dimers (CPDs) and structured DNA (e.g. G4 quadruplexes), as well as chain terminators (*4-7*). PrimPol can also perform translesion synthesis (TLS) polymerase, replicating across DNA lesions (e.g. 8-oxoG, 6-4 photoproducts) that stall replicative polymerases (*6, 7*).

Specialised DNA polymerases, such as Pol Eta (η), can also perform translesion synthesis (*8, 9*). This allows for continuous replication and lesion bypass, at the expense of fidelity (*10*). Another DDT pathway is fork reversal, which allows the strand adjacent to the lesion to be copied from the sister chromatid and allowing for error-free lesion bypass (*11*). With many DDT pathways available during DNA replication, it is essential that cells utilise the optimal restart pathway to efficiently reinitiate genome synthesis.

The availability of alternative overlapping pathways means that, despite its importance in maintaining active replication forks, cells lacking PrimPol are viable and grow normally. However, these cells have delayed recovery times after UV-C damage and hallmarks of replication stress, such as increased micronuclei and elevated mutation frequencies (*6, 12, 13*). These phenotypes are further exacerbated when other DDT pathways are disrupted, such as in the absence of Pol η, where PrimPol-null cells

exhibit an overt UV-C sensitivity (*4, 6, 12*) . Recent studies have also shown that in the absence of HLTF, an enzyme involved in fork reversal, PrimPol mediated repriming or TLS is utilised to rescue stalled forks (*14*). Similarly, in the absence of CARM1 / PRMT4, implicated in the stabilisation of reversed forks, PrimPol and TLS are both employed to restart replication forks (*15*). PrimPol also plays a role in DNA damage tolerance when cells lack BRCA1, with PrimPol protein levels increasing after multiple cisplatin doses, leading to suppressed fork reversal (*16*).

While PrimPol can act when other pathways are unavailable, it is unknown how PrimPol is prevented from acting when repriming would be undesirable. PrimPol must be tightly regulated during DNA replication to avoid aberrant repriming, fork speeding and chromosomal breaks (*15*), and such regulation would therefore need to be dynamic in order to respond to DNA damage or changes in DDT pathway availability. While recent studies have shown that PrimPol protein levels are tightly controlled by ATR activity and can be regulated by WRNIP1 levels (*16-18*), there is currently no evidence for a more responsive mode of regulation.

Post-translational modifications (PTMs) provide a dynamic and reversible form of regulation that is known to play roles in regulating DDT pathways. TLS polymerases, such as Pol η, are highly regulated by PTMs, such as phosphorylation, ubiquitination and SUMOylation (*19-22*). To control phosphorylation, cells employ a number of specific kinases and phosphatases to regulate progression through the cell cycle and the cell's response to replication stress. One such kinase is Polo-like kinase 1 (PLK1), which has a critical role in mitotic progression and has also been implicated in the DNA damage response (*23-25*). PLK1 regulates many DNA damage response proteins, including Rad51 and BRCA2, and can lead to inhibition of protein loading at sites of damage, for example MRE11 (*26-28*). PLK1 itself is also regulated by a defined methylation / phosphorylation switch, important for the timely removal of RPA2 and Rad51 from DNA damage sites (*29*).

Here we report that PrimPol is phosphorylated by PLK1 on a highly conserved serine residue, located between two RPA binding sites at its C-terminus. Phosphorylation by PLK1 occurs at the end of S-phase, though it can be modulated in response to high levels of replication stress, such as that induced by the PARP inhibitor olaparib or the

topoisomerase poison camptothecin. Deregulation of this PLK1-dependent phosphorylation leads to damage sensitivity and the onset of cellular phenotypes associated with genomic instability, including micronuclei, chromosome breaks and mitotic defects. Together, these findings establish that PLK1 provides regulatory control over PrimPol during the cell cycle to restrict its activity outside of S-phase, where it is required for restarting stalled forks to ensure that DNA replication proceeds in a timely and efficient manner.

Results

PrimPol is phosphorylated at a conserved serine located between the RPA binding motifs

Despite recent progress, little is known about how PrimPol's activity and recruitment are regulated throughout the cell cycle. Given its interaction with RPA is requisite for PrimPol's functionality at stalled forks, PTMs in the C-terminus may play a role in its regulation. We carried out mass spectrometry analysis on Flag-tagged PrimPol from human cells to detect potential modifications that may play roles in regulating its activity. We identified a number of phosphorylation sites (Fig. S1A), including a serine residue (S538) located between the two RPA binding motifs (RBMs) in human PrimPol. We also identified phosphorylation of a homologous residue on the C-terminus of *Xenopus laevis* PrimPol, and found this modification is conserved with the duplication of the RPA binding motif B (Fig. S1A). As this residue is also highly conserved in other eukaryotes, we hypothesised that it may play a role in PrimPol's regulation (Fig. 1A). To study the significance of this phosphorylation in human cells, we generated a phospho-specific antibody, raised against a peptide containing phosphorylated S538 (P-S538). To confirm this antibody's specificity, we tested it against whole cell extracts from HEK293 cells expressing PrimPol, or mutants PrimPol^{S538A} and PrimPol^{S538E} (Fig. 1B). While S538 phosphorylation was observed for wild type protein, no binding was observed when S538 was mutated. In addition, antibody binding was also lost when cell lysate was treated with λ phosphatase (Fig. S1B).

Disruption of S538 phosphorylation affects cell growth and genome stability

To analyse the significance of S538 phosphorylation, we examined the effects that disrupting this modification had in cultured human cells. We first generated several PrimPol$^{-/-}$ clones in a Flp-In HEK293 T-REx cell line, denoted ΔPP-1-3. These cells all carried biallelic PrimPol deletions, which lead to downstream gene disruption, with no observed PrimPol protein production (Fig. S1C). ΔPP cells exhibited phenotypes

similar to those observed previously in MRC5 PrimPol$^{-/-}$ cells, namely normal growth and no UV-C sensitivity, but delayed cell cycle recovery after UV damage (Fig. S1D-G) (*12*). N-terminal FLAG-tagged PrimPol, or PrimPol containing S538 mutations, were stably introduced into the Flp-In T-REx site in these cells and expressed using doxycycline (*30*) (Fig.1B, S2A). To analyse any defect arising from the expression of mutant PrimPol, we used colony formation assays in the presence or absence of doxycycline to assess plating efficiency. While PrimPol and PrimPol^{S538E} expression had no effect on plating efficiency, PrimPol^{S538A} caused a significant decreased in colony formation (Fig. 1C). In addition, whilst expression of PrimPol had little effect on growth rates, PrimPol^{S538A} caused a small but significant increase in doubling times, suggesting that this modification may play a role in PrimPol's ability to maintain cell cycle progression or cell viability (Fig. S2B). We also observed a similar effect on plating efficiency when we expressed PrimPol^{S538A} in parental cells carrying endogenous PrimPol protein, indicating that this mutation has a dominant negative effect (Fig. 1C). However, we found no significant changes in cell cycle populations 48 hrs after protein induction (Fig. S2C).

As S538 resides between the RPA binding motifs, it may regulate PrimPol's interaction with RPA and thus its recruitment and retention on ssDNA. However, when we analysed the binding of the C-terminal region of wild type or mutant PrimPol with RPA70N by analytical gel filtration, we observed no overt changes in the interactions between PrimPol and RPA *in vitro* (Fig. S3A). We also found no changes in PrimPol and RPA interaction *in vivo* after mutation of the S538 residue when analysed by immunoprecipitation (Fig. S3B). Additionally, mutation of S538 did not affect PrimPol's chromatin association *in vivo* (Fig. 1D). Notably, biochemical analysis also showed that neither PrimPol^{S538A} or PrimPol^{S538E} altered primase or polymerase activities or fidelity *in vitro* (Fig. S3C, D).

To understand further the impact of mutating the S538 phosphorylation site, we examined markers of genomic instability. Cells expressing PrimPol^{S538A} showed an increase in micronuclei under unperturbed conditions (Fig. 1E) and substantially more chromosomal breaks (Fig. 1F). As with PrimPol$^{-/-}$ MRC5 cells, ΔPP cells exhibited increased sister chromatid exchanges (SCEs) that could be rescued by expression of

PrimPol or PrimPol^{S538E}, but not PrimPol^{S538A} (Fig. 1G) (*12*). Together, these results indicate that PrimPol^{S538A} expression leads to an increase in genomic instability.

PrimPol^{S538A} decreases cell viability after UV-C induced DNA damage

As PrimPol is required for repriming DNA replication after fork stalling lesions and structures, we examined the role of S538 phosphorylation in maintaining DNA replication and cell viability after DNA damage (*4, 5, 7*). After treatment with UV-C, we observed a significant increase in damage sensitivity in cells expressing the phospho-null mutant (PrimPol^{S538A}) compared to ΔPP cells (Fig. 2A), establishing that expressing PrimPol^{S538A} is more harmful than the absence of PrimPol. To confirm this was not an artefact of an individual clone, we carried out UV-C survival assays on three independent PrimPol knockout clones complemented with PrimPol^{S538A} and obtained consistent results (Fig S4A). Additionally, we observed a decrease in UV-C survival, when we expressed PrimPol^{S538A} in parental cells carrying endogenous protein, indicating that endogenous levels of PrimPol are not able to overcome the toxicity of PrimPol^{S538A} (Fig. S4A). Moreover, cells expressing PrimPol^{S538A} also showed a sensitivity to the crosslinking agent cisplatin (Fig. 2A, S4A). As previously reported, PrimPol$^{-/-}$ cells exhibit delayed recovery after UV-C (*12*); we therefore measured the ability of the different PrimPol proteins to complement this defect. As in MRC5 PrimPol$^{-/-}$ cells, we observed that expression of PrimPol and PrimPol^{S538E} decreased the delay in recovery time 24 hours after UV-C damage. While cells expressing PrimPol^{S538A} showed less stalling than ΔPP cells, there was an increase in late S / G2-M stalling (Fig. 2B, S4B). We also examined hallmarks of genome instability and found a significant increase in micronuclei after UV-C damage in cells expressing PrimPol^{S538A}, compared to those expressing PrimPol or PrimPol^{S538E} (Fig. 2C, S4C). To confirm PrimPol^{S538A} toxicity was not specific to HEK293 cells, we expressed PrimPol in RPE cells using a Sleeping Beauty transposon expression system (*31*) (Fig. S4D). We found that PrimPol^{S538A} expression caused a similar decrease in survival after UV-C damage, along with hallmarks of genomic instability such as increased micronuclei both with and without UV-C damage (Fig. S4E, F).

In asynchronous cells damaged with UV-C (6J/m^2), there was no detectable difference in the amount of mutant PrimPol bound to chromatin, compared to PrimPol (Fig. S5A). To look more directly at the effects of PrimPol^{S538A} at the replication fork, we used a DNA fibre assay to analyse ongoing replication after UV damage. Despite the increased UV-C sensitivity, both PrimPol^{S538A} and PrimPol^{S538E} had minimal effect on fork stalling (Fig. 2D) This suggests that the genotoxic effects of PrimPol^{S538A} may be initiated outside of S-phase replication.

Additionally, we found that PrimPol^{S538A} expression caused a decrease in replication fork speed in undamaged conditions (Fig. 2E, S5B). We observed a small but significant increase in replication fork speeds with PrimPol^{S538E} expression, suggesting this mutant is also capable of causing changes in fork progression, potentially through alteration of pathway choice at stalled or slowed forks (Fig. 2E). This was also observed in parental cells containing endogenous PrimPol (Fig. S5B). To examine if PrimPol's activity was inhibited after loss of phosphorylation, we looked at restart of stalled forks after HU or camptothecin treatment and identified a decrease in fork restart in the absence of PrimPol. However, mutation of S538 did not affect the ability of the protein to complement this, confirming that - as observed *in vitro* - the protein remains functional in the absence of S538 phosphorylation (Fig. S5C).

PrimPol^{S538A} induced genotoxicity is rescued by mutation of RPA-binding motifs

To confirm whether PrimPol^{S538A}'s phenotype was due directly to its activity on DNA, we investigated whether impairing PrimPol's recruitment to chromatin, by mutation of PrimPol's RPA binding motifs, could abolish these phenotypes. RBM-A and RBM-B, the two motifs responsible for RPA association and therefore recruitment to ssDNA, were mutated to generate PrimPol^{RAB} in the presence or absence of the S538 mutations (Fig. S5D) (*30*). When expressed alone in ΔPP cells, PrimPol^{RAB} had little effect on UV-C survival and rescued PrimPol^{S538A}'s UV sensitivity (Fig. 2F, S5E). In addition, complete loss of both RPA binding sites (PrimPol^{RAB}) completely reversed the genomic instability phenotypes observed with PrimPol^{S538A}, as evident by no increase in chromosome breaks or micronuclei (Fig. 2G, S5F). Together, these

findings establish that the genotoxicity induced by PrimPol^{S538A} requires PrimPol's RPA-dependent interaction with chromatin.

PrimPol^{S538A} causes sensitivity to olaparib and camptothecin

Recent studies have shown that repriming and fork reversal are distinct DDT mechanisms that rescue stalled replication forks. Changes in the levels of fork reversal proteins, such as HLTF and PARP, have been suggested to alter the balance between these pathways and therefore the requirement for PrimPol following stalling (*14, 15*). Therefore, we used the drug olaparib to inhibit PARP and determine if the S538A mutation affected the availability of PrimPol for repriming at stalled forks. When we examined colony formation in the presence of low doses of olaparib, we observed that expression of PrimPol^{S538A} caused a significant increase in sensitivity, similar to that observed with other damaging agents (Fig. 3A, S6A). However, in addition to affecting the availability of the fork reversal pathway, PARP is also utilised in the resolution of single-stranded and double stranded breaks (SSBs & DSBs) – it therefore follows that the use of olaparib leads to an increase in SSBs and DSBs (*32, 33*). We investigated this possibility by employing the Top1 poison camptothecin, which has been shown to cause an increase in SSBs (*34*). Indeed, we observed that, whilst little sensitivity was evident in cells lacking PrimPol, cells expressing PrimPol^{S538A} showed a significant decrease in cell survival after the addition of camptothecin (Fig. 3A, S6B). These combined sensitivities suggest that this is due largely to an increase in breaks and fork stalling itself, rather than the loss of fork reversal, as this is not affected by camptothecin treatment.

We then inspected for other signs of genomic instability and stress after treatment with olaparib or camptothecin and again found an increase in micronuclei 48 hrs after treatment only in cells expressing PrimPol^{S538A} (Fig. 3B, S6C). We also observed a similar increase in mitotic cells showing abnormalities, such as lagging or misaligned chromosomes (Fig. 3C, S6D). In addition, we noted a significant increase in chromosomes with breaks in cells expressing PrimPol^{S538A} 48 hrs after treatment with camptothecin or olaparib (Fig. 3D, S6E).

A small change in cell cycle population was observed after olaparib treatment, with cells expressing PrimPol^{S538A} stalling in G2/M more compared to cells expressing PrimPol or PrimPol^{S538A} (Fig. 3E, S6F). As olaparib treatment causes an increase in replication speed (*35*), we investigated if PrimPol may be involved in this process. While fork speeds increased after olaparib treatment, only minor differences were observed in cells expressing PrimPol^{S538A}, suggesting that S538 phosphorylation does not play a significant role in this increase in replication fork speed (Fig. 3F). This is similar to other studies, where no changes in fibre length were observed in the absence of PrimPol after olaparib treatment (*15*). Camptothecin is known to cause fork stalling due to DNA torsional restraint (*36*). However, although we observed an increase in CldU/IdU after addition of 50 nM camptothecin with the second label compared to untreated cells, no additional sensitivity was observed in cells expressing PrimPol^{S538A} (Fig. 3F). Again, this confirms that changes in S538 phosphorylation does not significantly impact its role during replication perturbation in S-phase, and supports an effect in G2/M.

Mutation of the Zn finger significantly rescues cellular defects caused by PrimPol^{S538A}

As our data suggests the S538A mutation may only have very minor affects during unperturbed S-phase, we next examined if the phenotypes induced by expression of PrimPol^{S538A} were dependent on PrimPol's primase activity. PrimPol's zinc finger is required for its primase function and may be important for stabilisation of the incoming nucleotide, primer translocation and extension (*7, 37*). Therefore, to further investigate the cause of PrimPol^{S538A}-induced cell toxicity, we generated a disruptive zinc finger (ZF) mutant (C419A, H426A, hereafter PrimPol^{ZF}) in the PrimPol^{S538A} background (Fig. S7A). Expression of PrimPol^{ZF} alone did not alter plating efficiency but mutation of the zinc finger rescued the plating deficiency observed in PrimPol^{S538A} (Fig. S7B). Expression of PrimPol^{ZF} also caused a small decrease in survival after treatment with UV-C, olaparib, camptothecin or cisplatin, suggesting its primase activity is required for restart after such damage (Fig. 4A). The combined PrimPol$^{ZF, S538A}$ mutant was able to partially rescue the S538A induced decrease in survival after damage but was still

less viable than ΔPP or PrimPol^{ZF} expressing cells. In addition, PrimPol^{ZF} was able to largely rescue the increase in chromosomal breaks, micronuclei and abnormal mitotic cells observed after expression of PrimPol^{S538A} in both damaged and undamaged cells (Fig. 4 B-D, S7C-E). However, although levels of micronuclei and breaks were significantly lower, they were still consistently higher in PrimPol$^{ZF,\ S538A}$ expressing lines compared with those expressing PrimPol. Although substantial loss of genomic instability was observed after the addition of PrimPol^{ZF}, we noted that PrimPol, PrimPol^{ZF} and PrimPol$^{ZF\ S538A}$ all proficiently bound chromatin in undamaged cells and cells damaged by UV-C, suggesting recruitment is maintained (Fig. S7F).

Serine 538 is phosphorylated by PLK1 in human cells

As ablation of PrimPol S538 phosphorylation clearly has significant effects on cellular viability, it appears likely that this modification is tightly regulated. To identify the kinase responsible for this phosphorylation, we analysed the sequence motifs around S538 using the Eukaryotic Linear Motif (ELM) database (*38*) and identified that it resides within a signature motif characteristic of a PLK1 site (*39, 40*). This PLK1 motif is also highly conserved in PrimPol across a diverse range of higher eukaryotes (Fig. 5A). To determine if the proposed motif containing S538 represents a *bona fide* PLK1 phosphorylation site, we purified recombinant PrimPol and performed kinase assays by incubating it with PLK1 and ATP. Using the P-S538 specific antibody, we showed that PrimPol, but not PrimPol^{S538A}, was specifically phosphorylated by PLK1 at residue S538 *in vitro* (Fig. 5B).

To confirm if this residue was also modified by PLK1 *in vivo*, we utilised the PLK-specific inhibitor BI2536 (*41*). Addition of BI2536 resulted in an absence of S538 phosphorylation, as identified using the phospho-specific antibody (Fig. 5C). To verify that S538 is specifically phosphorylated by PLK1 in cells, we utilised RPE1 PLK1-as cells (*42*). These cells contain a mutant form of PLK1, which can be inactivated using an ATP analogue. Cells were stably transfected to express PrimPol before treated with the ATP analogue 3-MBPP1 to inactivate PLK1. In the absence of active PLK1, S538 phosphorylation was not detected, establishing a specific role for PLK1 kinase in phosphorylating PrimPol (Fig. 5C).

Phosphorylation of PrimPol serine 538 is cell cycle regulated

PLK1 activity changes dramatically throughout the cell cycle (*43-45*). Therefore, we examined PrimPol's S538 phosphorylation levels across the cell cycle using thymidine synchronisation. Phosphorylation of S538 was lost in cells synchronised at the G1/S border. Phosphorylation was then detectable by late S-phase, reaching a peak in G2 (Fig. 5D). This phosphorylation was retained throughout mitosis before decreasing in G1. A similar pattern of S538 phosphorylation as cells enter late S-phase / G2 was also observed in RPE cells expressing PrimPol (Fig. S8A). This pattern of phosphorylation matched that of known PLK1 substrates, such as TCTP (Fig. 5D) (*46*). This establishes that S538 phosphorylation is tightly regulated across the cell cycle, which suggests it may be employed to regulate PrimPol during different cell cycle stages.

To confirm the importance of PLK1 phosphorylation in the regulation of PrimPol activity *in vivo*, we again utilised the PLK1 inhibitor BI2536 (*41*). Cells were synchronised using a thymidine block, stalling cells at the G1/S border. Cells were then released into media containing nocodazole, and additionally containing olaparib or camptothecin, in the presence of absence of BI2536. Mitotic cells were collected and spread to analyse the accumulation of chromosome breaks. As observed previously, cells expressing PrimPol^{S538A} had an increased number of breaks in all conditions compared to ΔPP cells or those expressing PrimPol (Fig. 5E, S8B). The addition of the PLK1 inhibitor did not further increase chromosomal breaks in PrimPol^{S538A} cells, nor did it increase the number of breaks in ΔPP cells, suggesting that the inhibition of PLK1 alone did not induce breaks. However, breaks increased in cells expressing PrimPol to levels similar to PrimPol^{S538A} cells. These findings suggest that preventing active phosphorylation of PrimPol by PLK1 is able to phenocopy the genotoxicity caused by the S538A mutation.

PrimPol^{S538A} phenotypes are caused by its dysregulation across the cell cycle

As S538 phosphorylation is largely restricted to G2 and mitosis, PrimPol^{S538A} expressed in these cell cycle stages may be a potential cause of genotoxicity. To investigate changes in genomic stability across different cell cycle stages, we examined the formation of micronuclei. Cells were first labelled with EdU to identify those in S-phase and then immediately treated with 0 or 5 J/m^2 UV-C and allowed to recover for up to 48hrs. Cells expressing PrimPol^{S538A} had a significantly higher percentage of EdU positive cells with micronuclei, 48 hrs after labelling, suggesting they may be retained by the cell for longer. When UV-C treated cells were analysed, we observed that in ΔPP-1 cells, and those expressing PrimPol or PrimPol^{S538E}, the majority of micronuclei were found in cells that were in S-phase when they were damaged (Fig. 6A, S9A). EdU negative cells - cells damaged by UV-C outside of S-phase – showed little increase in micronuclei, even 48 hrs post UV-C damage. This confirms that damage in non-replicating cells is not a major cause of micronuclei in ΔPP-1 cells, or those expressing PrimPol or PrimPol^{S538E}. In contrast, cells expressing PrimPol^{S538A} showed a significant increase in micronuclei in both EdU positive and negative cells. These data show that expression of PrimPol^{S538A} after UV-C damage leads to micronuclei, regardless of whether the damage occurred in replicating or non-replicating cells.

To examine changes in the recruitment of PrimPol^{S538A} outside of S-phase, we analysed cell stage-specific chromatin binding. Cells were first synchronised using a double thymidine block and released to progress through the cell cycle before being treated with 0 or 20 J/m^2 UV-C. Cells were allowed to recover for 1 hr before chromatin isolation. UV-C damage induced an increase in chromatin bound RPA32, and RPA32 phosphorylated at S33, an ATR dependent modification induced by DNA damage (*47*)**.** PrimPol is observed binding to chromatin in G1 and S-phase, with no observable binding in G2 as reported previously (Fig. 6B, S9B) (42). However, 1 hr after 20 J/m^2 UV-C damage, PrimPol^{S538A} was found to be chromatin associated in G2, while PrimPol and PrimPol^{S538E} were not observably recruited (Fig. 6B). We also followed PrimPol's chromatin dissociation across the cell cycle and found loss of chromatin binding as cells progressed into G2, which correlates with S538 phosphorylation changes described earlier (Fig. S9C, 5D). Together, these data indicate that S538

phosphorylation may play an important role in the regulation of PrimPol's recruitment to chromatin.

In addition, we observed an increase in RPA foci in cells expressing PrimPol^{S538A} in both undamaged and UV-C treated conditions suggesting a possible increase in ssDNA (Fig. 6C, S9D). To look more closely at this, we analysed levels of native CldU incorporated into DNA to look more specifically for ssDNA. We observed a minor increase in CldU signal in cells expressing mutant forms of PrimPol and this was also seen with damage (Fig.6D, S9E, F). However, this difference was decreased when cells were first treated with BI2536 to inhibit PLK1 with cells expressing PrimPol and PrimPol^{S538A} showing little differences (Fig. 6D, S9E, F).

In addition, we assessed levels of ssDNA gaps during replication, using the S1 fibre assay to detect repriming events. In asynchronous conditions we observed little difference between cell lines (data not shown). However, when cells were synchronised to late S-phase, we noted increased fibre shortening after S1 treatment in cells expressing PrimPol^{S538A}, suggesting increased repriming (Fig. 6E). To look at the impact of PLK1 phosphorylation on late S-phase repriming, we released cells from thymidine into BI2536 to prevent S538 phosphorylation. Cells were allowed to progress into late S-phase, at which point we again measured S1 nuclease cutting. We found that all cell lines showed an increase in replication fork length distribution after PLK1 inhibition and that expression of PrimPol now also lead to a significant decrease in fork length after S1 treatment, mimicking PrimPol^{S538A} expression.

Phosphorylation of S538 is actively regulated in response to fork stalling

As well as cell cycle changes, PLK1 has previously been shown to regulate protein activity via phosphorylation in response to DNA damage (*27, 28*). We therefore analysed whether PrimPol may also be regulated in response to damage / fork stalling by PLK1, through its phosphorylation of S538. When cells were allowed to progress synchronously through the cell cycle in the presence of damage, S538 phosphorylation was delayed along with the cell cycle but phosphorylation was still detected once the bulk of cells entered G2 (Fig. S10A-B). This confirmed that S538

phosphorylation is tightly maintained with cell cycle stage and constitutively activated upon completion of S-phase.

To determine if active dephosphorylation of S538 was possible in response to damage, we first synchronised cells to the G1/S boundary using thymidine and released synchronously for 5 hrs to late S-phase, the point where S538 phosphorylation begins to appear. Cells were then treated with sufficient doses of UV-C, olaparib or camptothecin to slow the S-phase completion, but still ultimately allow cells to progress to mitosis. We found a small but consistent decrease in phosphorylation shortly after damage, compared with unperturbed cells (Fig. 7A, S10C). This was most prominent 1 hr after camptothecin treatment and, in all cases, was resolved around 5 hrs after damage induction when most cells where in G2 or mitosis. However, FACS analysis revealed that 5 hrs after release, a large proportion of cells had already entered G2 and were therefore unlikely to encounter stalled replication forks. This suggested that we were unable to visualise damage induced dephosphorylation due to increased phosphorylation in G2 cells.

To address this, we repeated the experiment with the addition of the PLK1 inhibitor BI2536, preventing further phosphorylation by PLK1. Cells were released from a thymidine block into late S-phase as before, but this time prior to damage cells were treated with BI2536 and allowed to progress through the cell cycle for a further 5 hrs at which point the majority of cells had reached mitosis (Fig. 7B). In the absence of BI2536, damaged cells showed a similar increase in phosphorylation to untreated cells (Fig. 7B). In contrast, where PLK1 was inhibited, no increase in phosphorylation was observed upon G2 / M entry in the absence of damage. Strikingly, cells treated with olaparib, camptothecin or UV-C showed a significant loss of S538 phosphorylation (Fig 7B). This indicates that PrimPol is actively dephosphorylated in response to damage in late S-phase. We hypothesise that this dephosphorylation is important for proper utilisation of PrimPol in late S-phase, where it may only be required after damage due to an excess abundance of stalled forks.

Discussion

PrimPol-dependent repriming offers many advantages as a mechanism for restarting arrested forks. It allows stalled DNA synthesis to resume on the leading strand by bypassing a diverse range of impediments, without interaction with the obstacle itself, as occurs in TLS. Additionally, when PrimPol mediates replication restart, it likely only incorporates a small number of nucleotides before disassociating due to its low processivity, minimising any mutagenic events. However, PrimPol-mediated repriming must be tightly regulated, as excessive repriming could lead to increased accumulation of ssDNA gaps and interfere with processes such as repair and transcription.

In this study, we establish that PrimPol is regulated by PLK1 phosphorylation and that the levels of this modification change throughout the cell cycle (Fig. 5D). Phosphorylation increases as DNA replication is completed, coinciding with a suppression of PrimPol's recruitment as cells progress into G2 (Fig. 6B). Preventing S538 phosphorylation leads to decreased survival after DNA damage or replication stress, an increase in genomic instability in both damaged and unperturbed cells (Fig. 2A, 3A-B), and PrimPol's recruitment is deregulated outside of S-phase. These phenotypes can be entirely rescued by mutation of the RPA binding domains to prevent chromatin binding (Fig. 2F-G) and partially rescued by mutations to the zinc finger domain (Fig. 4A-D). PLK1-dependent phosphorylation can also be delayed or removed when cells experience replication stress (Fig. 7A-B). These findings support a model whereby PrimPol usage at stalled replication forks is dynamically regulated by phosphorylation (Fig. 7C). Together, these results highlight the importance of regulating repriming and maintaining balance between the multiple DDT pathways.

Regulation of PrimPol by PLK1 alters pathway availability

The role of PLK1 as a highly conserved regulator of mitosis is well established (*48*). Outside of mitosis, PLK1 has been suggested to play roles in S-phase, though recent evidence suggests that DNA replication itself suppresses PLK1 activity and PLK1 levels do not increase until the bulk of DNA synthesis is complete (*25, 43, 48, 49*). Phosphorylation of PrimPol by PLK1 closely aligns with this profile. PrimPol displays

low levels of S538 phosphorylation in early S-phase and higher levels in late S/G2 (Fig. 5D). Phosphorylation at the end of S-phase may potentially operate to keep PrimPol away from replication forks in common fragile sites, which are replicated in late S-phase (*50*). Following a similar pattern, PLK1 has also been shown to phosphorylate BRCA2 as cells complete S-phase, with phosphorylation levels peaking during mitosis (*26*). As with PrimPol, the cell cycle-dependent phosphorylation of BRCA2 can be suppressed by the application of DNA damaging agents.

As it possesses potential genotoxic primase activity, the cell's requirements for PrimPol are likely to significantly change throughout the cell cycle. Our data supports a model where phosphorylation by PLK1 at the end of S-phase negatively regulates PrimPol's activities as cells enter G2. Loss of this regulation leads to inappropriate PrimPol usage outside of S-phase. This likely leads to unscheduled repriming events causing increased ssDNA gaps that interfere with G2 pathways, such as HR, as well as at transcription bubbles. Cell cycle-dependent phosphorylation provides an innate regulatory mechanism whereby proteins can be dynamically and reversibly regulated, without the need to be degraded and resynthesized. Our study has demonstrated that although PrimPol is gradually repressed towards the end of S-phase, if cells experience significant replication stress in late S-phase, PrimPol can be reactivated by dephosphorylation (Fig. 7C). This implies the usage of one or more phosphatases working in concert with PLK1 to regulated PrimPol, although more work is required to uncover this regulatory mechanism.

The outcomes of PrimPol deregulation

Cells expressing PrimPol^{S538A}, which cannot be phosphorylated, are sensitive to olaparib, camptothecin, UV-C and cisplatin (Fig. 2A, 3A-B). These treatments induce replication stress, which leads fork stalling and the generation of ssDNA. ssDNA is particularly sensitive to damage and hypermutation, due to greater exposure of the bases to oxidative and chemical damage (*51*). Therefore, ssDNA is bound by RPA for protection during replication and repair. Without regulation, PrimPol may be aberrantly recruited to these regions of ssDNA through its interaction with RPA, when alternative

mechanisms of DDT may be better suited. As a result, an increase in ssDNA is observed in PrimPol^{S538A} cells (Fig. 6C-E).

A recent study indicated that the ssDNA gaps left behind by PrimPol-mediated repriming are repaired by Rad51-dependent HR pathways (*52*). To maintain cell survival and suppress DSB formation, ssDNA gaps must be repaired before the cell progresses through the cell cycle and a dramatic increase in gaps is likely to require much of the cell's HR machinery. In addition, excess ssDNA may potentially deplete the cell's RPA pool, leaving ssDNA exposed, sensitive to further damage and, ultimately, replication catastrophe (*16, 53, 54*). Recent work has also suggested that cancer cell survival depends, in part, on a shift in the balance between DDT pathways, with cancer cells increasingly dependent on TLS polymerases to suppress excessive ssDNA gap formation (*55*). This recent study lends support to a hypothesis that deregulation of PrimPol leads to increased recruitment in late S/G2, leading to increased gap formation and decreased cell fitness and genomic stability.

In addition to DNA damaging agents, loss of PrimPol regulation also causes sensitivity to the PARP inhibitor olaparib. PARP plays multiple roles in the maintenance of genomic stability, including repair of SSBs and unligated Okazaki fragments, as well as promoting replication fork reversal (*33, 36, 56*). It has been reported that PARP1 acts in conjunction with CARM1 to promote fork reversal and its inhibition by olaparib leads to increased utilisation of PrimPol (*15*). Our findings also show that replication fork speeds increased after olaparib treatment, though strikingly this was not increased further in PrimPol^{S538A} cells. We observed similar sensitives with camptothecin but have shown that all mutants are able to reinitiate replication after stalling in S-phase. This suggests that regulation of PrimPol by PLK1-dependent phosphorylation is less important in S-phase and mainly acts to regulate PrimPol once the bulk of replication is completed.

PrimPol^{S538A} phenotypes require RPA binding and only partially dependent on the zinc finger

Although we show that phosphorylation of PrimPol regulates its activities throughout the cell cycle, the details of how this is achieved are still to be determined. The location of this PLK1 modification between the RPA binding motifs initially implied S538 phosphorylation may regulate PrimPol's RPA interaction. However, we observed no difference in the interaction of PrimPol^{S538A} or PrimPol^{S538E} with chromatin, or with RPA70 *in vivo* or *in vitro*. However, PrimPol's interactions with RPA at stalled forks may be dependent on other modifications or binding partners that are yet to be uncovered. Genomic instability phenotypes induced by PrimPol^{S538A} expression are, however, dependent on RPA binding and recruitment to chromatin (Fig. 2F).

While PrimPol^{ZF} mutant cannot initiate *de novo* primer synthesis, it retains polymerase activity and can extend existing primers (*7, 37*). The majority of PrimPol^{S538A} genotoxicity was lost by the mutation of the zinc finger domain; these cells showed increased survival after genotoxic stress and decreased chromosome breaks compared to PrimPol^{S538A} alone. This aligns with observations from other *in vivo* complementation studies, where it has been found that most phenotypes observed upon PrimPol depletion are not complemented by PrimPol^{ZF} (*4, 7, 57*). These data suggest that PrimPol^{S538A} genotoxicity is largely due to PrimPol's repriming activity. However, cells expressing PrimPol^{ZF,S538A} are still more damage sensitive than PrimPol^{ZF} (Fig. 4). We hypothesise this is likely to be due to the aberrant recruitment of PrimPol^{S538A} to chromatin, which is maintained after the addition of the ZF mutations (Fig. S7F). Aberrant recruitment, without the ability to reprime, may block alternative mechanisms of DDT or repair and delay fork restart, leading to this partial phenotype.

In summary, this study establishes that PLK1-dependent phosphorylation of PrimPol prevents aberrant recruitment and repriming that could otherwise lead to significant genomic instability. Our data highlights the importance of appropriately regulating PrimPol's recruitment following replication fork stalling, and throughout the cell cycle. While this study identifies that PrimPol is specifically regulated by PLK1, it is likely that additional mechanisms also regulate PrimPol, and other DDT pathways, to ensure that cells respond appropriately in the immediate aftermath of replication stress. The discovery of PLK1's role in regulating PrimPol's deployment underscores other

important functions this major cell cycle kinase undertakes outside of mitosis, emphasising its status as a key regulator of genome stability.

Materials and Methods

In vitro kinase assay

To confirm PLK1 phosphorylation of PrimPol, 1 μg purified PrimPol (WT or S538A) was incubated in a 20 μl reaction with NEB protein Kinase buffer, 500 μM ATP and 20 μg PLK1 (Merck). The reaction was incubated at 30 ºC for 2 hrs before addition of Laemmli sample buffer and boiling. Samples were then analysed by western blot with a total PrimPol and P-S538 specific antibodies.

Plasmids and mutagenesis

pCDNA5 containing N-terminally Flag tagged PrimPol was used to express PrimPol in HEK293 cells as has been described previously (*30*). PrimPol was cloned into the sleeping beauty plasmid pSB*tet* following PCR amplification with primers PP SB using NEBuilder HiFi DNA assembly cloning kit (New England Biolabs) (*31*). A range of mutants were generated by site directed mutagenesis as described previously (*6, 7, 30*), briefly PCR was carried out with Phusion (New England Biolabs) along with the relevant primers described Table S1 and products were transformed into *E. coli.* Plasmids were purified and the generation of the desired mutation was confirmed by Sanger sequencing (GATC).

Human cell culture

HEK293 cells were grown at 37 °C, 5 % CO_2 in DMEM supplemented with 10 % fetal calf serum, 1 % L-glutamine and 1 % penicillin/streptomycin. RPE cells were grown in DMEM/F12 supplemented with 10 % fetal calf serum, 1 % L-glutamine and 1 % penicillin/streptomycin.

To generate PrimPol knockout cell lines guide oligos, 1,5'-TTATCATCCGTATACAGGCCAAGATTGTCCAAGCCAGAAGAACCAC-3' or 2, 5'-CCATCTATATGGAGGCTGTTTCATCGACAAGCTCAAGCTTTTAATTTTG -3' targeted to the first exon of PrimPol, were cloned into plasmid pSpCas9(BB) as described (*58*). These plasmids were transfected into Flp-In HEK293 T-REx cells

which were separated to single cells in 96 well plates at 3 days after transfection and grown to form single colonies. Single colonies were selected and expanded, and a proportion were taken for PCR across the target region. PCR was carried out with primers sets KO1, across the guide targeted site and KO2 far away in exon 7. Clones which showed a change in product size or loss of the target site product whilst the exon 7 product was unchanged were expanded further and tested for loss of PrimPol by western blotting with a PrimPol specific antibody (*12*). The genetic change was also confirmed by sequencing of the PCR product generated across the deleted region.

To generate cell lines expressing mutant forms of PrimPol Flp-In HEK293 T-Rex were co transfected with pOG44 and pCDNA5 containing flag tagged PrimPol using calcium phosphate (*59*). Cells were selected with 100 ug/ml hygromycin and 15 ug/ml blasticidin for approximately 2 weeks and the resulting resistant clones were pooled. PrimPol was then expressed in these cells by the addition of 10 ng/ml doxycycline.

Growth rate of different cell lines were calculated in the presence of 10 ng/ml doxycycline by counting cells at approximately 24 hr intervals using a haemocytometer, growth curves were then used to calculate the doubling time using an online tool (*60*).

In vivo PLK1 disruption

To inhibit PLK1, 10 nM BI2536 (Merck) was added to cell media for 16 hours before protein induction by 10 ng/ml doxycycline. Phosphorylation of protein after BI2536 treatment was assessed by western blot.

RPE1 PLK1-AS (*42*) cells were co-transfected with 2 µg pSB*tet*-PrimPol and 100 ng transposase enzyme plasmid pSB-100X by electroporation and selected for 10 days using 2 µg/ml puromycin. Cells were split to single cells to generate clonal cells lines and screened for incorporation of BFP. To inactive PLK1 in these cells, cells were treated with 1 µM 3-MB-PP1, followed by induction of protein expression using 100 ng/ml doxycycline.

Western blotting and Antibodies

To check protein expression cells were induced by the addition of 10 ng/ml doxycycline for 24 hrs and 30 μg total cell lysate was analysed by western blotting with a PrimPol antibody in comparison to α-tubulin controls. To look specifically at PrimPol phosphorylation a phospho-peptide antibody was generated (Eurogentec). Antibodies were raised in rabbits to the peptide ac- ELAEAAEN-S*(PO3H2)*-LLS+C –conh2 and affinity purified. The specificity of the antibody was confirmed by western blotting of phosphatase treated cell lysate. Briefly, cells were lysed in RIPA buffer. 5 μl of PMP buffer (New England Biolabs) and $MnCl_2$ (New England Biolabs) were then added to 40 μl of protein sample, and then incubated at 30 °C for 1 hour with or without 400 U λ phosphatase. The specificity of the antibody was assessed by western blot.

Immunoprecipitation

PrimPol was isolated from HEK293 cells as described previously (29). Briefly, approximately 1x 10^7 cells expressing Flag-tagged PrimPol were lysed in NETN buffer (150 mM NaCl, 30 mM Tris pH 7.5, 0.5 % NP-40, 2.5 mM $MgCl_2$, 100 μg/ml DNase I) for 30 mins at 4˚C. Cell lysate was incubated with Anti-Flag M2 magnetic beads (Merck) for 2 hrs at 4 ˚C before beads were washed 3 times with wash buffer (150 mM NaCl, 30 mM Tris pH 7.5, 0.1 % NP-40). Proteins and interacting partners were eluted with 50 μl elution buffer (25 mM Tris-HCl pH 7.5, 150 mM NaCl, 1 mM PMSF, 200 μg/mL 3xFLAG peptide (Merck)) and analysed against input cell lysate by western blot.

For mass spectrometry analysis 10 x 10^7 cells expressing Flag-tagged PrimPol were lysed in RIPA buffer. Protein was bound by Anti-Flag M2 magnetic beads (Merck) for 2 hrs at 4 ˚C before being washed 3 x in 50 mM ammonium bicarbonate. After overnight on-bead digestion at 37 ˚C by Glu-C protease, the peptides were analysed on Orbitrap Exploris 480 (with FAIMS) mass spectrometer by the Proteomics Core Facility at CEITEC (Brno, Czech Republic).

Analysis of *Xenopus* PrimPol C-terminal Domain (CTD)

The *Xenopus laevis* PrimPol CTD sequence (corresponding to amino acids 511-676) was gene synthesised (Eurofins) and cloned into the GST expression vector pGEX-KGH. The protein was expressed in BL21 *E.coli* and purified on glutathione agarose (Sigma). Purified protein was dialysed into XB buffer and incubated with *Xenopus* egg extract treated with aphidicolin (100 μg/ml). Sperm pronuclei were added (5 x 10^3 /ml extract) and incubated at 21 °C for 80 minutes. Extract and nuclei were diluted with XB buffer containing 0.25 % Triton-X100 and chromatin was recovered by centrifugation though 30 % sucrose. The chromatin pellet was washed extensively with XB buffer and resuspended in XB buffer containing benzonase (2 U/μl). Insoluble material was pelleted by centrifugation and the soluble supernatant was applied to glutathione agarose beads. Protein was separated by SDS PAGE and in gel digested with trypsin and chymotrypsin (Promega) overnight at 37 ˚C before analysis by mass spectrometry, (LTQ Orbitrap XL/ETD).

Cell synchronisation

To analyse or carry out experiments on cells within a specific cell cycle stage cells were synchronised with a double thymidine block. Cells were treated with 4 mM thymidine for 16 hrs before being washed 3 x in PBS and returned to normal media to continue cycling for 8 hrs. Cells were then blocked again with 4 mM thymidine for 16 hrs, cells were washed 3 x in PBS and then utilised immediately at G1/early S-phase or allowed to progress through the cell cycle in standard media for 2 hrs, S-phase, 6 hrs, G2 or 14 hrs G1. To analyse the effects of damage on phosphorylation cells were released into media containing 1 μM nocodazole to prevent them from progressing through to the next round of the cell cycle. Cells were then treated at relevant timepoints with 10 μM olaparib, 50 nM camptothecin or 20 J/m^2 UV-C and samples were later collected at relevant timepoints for chromosome spreads, protein or Facs analysis. To look at the effect of PLK1 inhibition 100 nM BI2536 was included.

Where PrimPol expression was required doxycycline was included in the media throughout. Cells treated in parallel were tested by flow cytometry to confirm synchronisation and cell populations.

Plating efficiency and colony survival assays

200 cells or a serial expansion dependent on expected toxicity were plated with the addition of 10 ng/ml doxycycline if protein expression was required and allowed to attach for approximately 16 hrs. Cells were then left untreated to analyse plating efficiency or treated with increasing doses of UV-C using a G6T5 Germicidal 9" 6W T5 UVC lamp (General Lamps Ltd.), or relevant concentrations of drugs were added. In the case of cisplatin, drugs were washed off after 6 hrs. Colonies were allowed to form for approximately 10 days and cells were stained with 1 % methylene blue for counting. Sensitivity was measured in relation to plating efficiency calculated from undamaged controls.

Chromatin Binding Analysis

DNA bound protein populations were analysed by chromatin assay as described previously (*6*). Approximately 7 x 10^6 cells were grown in 10 ng/ml doxycycline for at least 16 hrs before being treated with 0 or 20 J/m^2 UV-C and allowed to recover for 6 hrs. Cells were collected and ¼ were resuspended in 50 μl NETN buffer (150 mM NaCl, 5 mM EDTA, 50 mM Tris pH 7.5, 0.5 % NP-40). The remaining ¾ was incubated in 150 µl CSK buffer (100 mM NaCl, 300 mM sucrose, 3 mM MgCl2, 10 mM PIPES pH 6.8, 1 mM EGTA, 0.2 % (v/v) Triton X-100) on ice for 5 minutes before being pelleted at 4°C with the supernatant containing soluble proteins. The pellet containing chromatin bound proteins was washed twice in PBS and resuspended in 150 µl Laemmli sample buffer and boiled for 10 minutes. Proteins were analysed by western blotting relative to whole cell fraction using antibodies.

RPA foci

Cells were plated on poly-lysine coated coverslips in 10 ng/ml doxycycline for at least 16 hrs. Cells were either left undamaged or treated with 6 J/m^2 UV-C and allowed to recover for 24 hrs. Cells were pre-extracted with CSK buffer (100 mM NaCl, 300 mM

sucrose, 3 mM $MgCl_2$, 10 mM PIPES pH 6.8, 1 mM EGTA, 0.2 % (v/v) Triton X-100) for 10 mins on ice before being fixed with 3 % paraformaldehyde. Cells were stained with the relevant antibodies, mouse anti-RPA2 and anti-mouse Alexa Fluor 488 and EdU was labelled by click chemistry, slides were mounted in VectorShield with DAPI (Vectorlabs) (Table S2). Slides were analysed on an Olympus IX70 fluorescent microscope and analysed using ImageJ.

ssDNA staining

Cells were plated on poly-lysine coated coverslips in 10 ng/ml doxycycline and 10 μM CldU for 48 hrs. Cells were washed before being labelled with 10 μM Edu in the absence or presence of 10 μM olaparib or 50 nM Camptothecin for 2 hrs. Where PLK1 inhibition was required cells were treated prior to this and throughout with 100 nM BI2536 for 1 hr. Cells were pre-extracted with 2x CSK buffer (100 mM NaCl, 300 mM sucrose, 3 mM $MgCl_2$, 10 mM PIPES pH 6.8, 1 mM EGTA, 0.4 % (v/v) Triton X-100) for 10 mins on ice before being fixed with 3 % paraformaldehyde. Cells were stained with the relevant antibodies, Rat anti-BrdU and anti-rat Alexa Fluor 488, before click chemistry was used to label EdU and slides were mounted in VectorShield with DAPI (Table S2). Slides were analysed on an Olympus IX70 fluorescent microscope and analysed using ImageJ.

Micronuclei assays

To analyse micronuclei cells were plated in 10 ng/ml doxycycline for 16 hrs before being treated with 0 or 5 J/m^2 UV-C, 0.5 μM olaparib or 10 nM camptothecin. 48 hrs after treatment, cells were cytospun onto glass slides, fixed with paraformaldehyde and mounted in Vectorshield with DAPI (Vectorlabs). Cells were analysed for the presence of a micronuclei on a Nikon E400 fluorescent microscope. To analyse the effect of cell cycle position at the time of damage cells were plated overnight as before in doxycycline. They were then labelled with 10 μM EdU for 30 mins before being treated with 0 or 5 J/m^2 UV-C. Cells were either collected immediately or allowed to recover for 24 or 48 hrs before being cytospun and fixed in paraformaldehyde. EdU

incorporation was labelled using the click-it reaction using sulfo-CY5 azide (Jena Biosciences) as described previously (*12, 61*).

Chromosome Spreads

To analyse the occurrence of chromosome breaks cells were first grown for 96 hrs in the presence of 10 ng/ml doxycycline alone or 48 hrs with 0.5 μM olaparib or 10 nM camptothecin. 1 μM nocodazole was added for the final 16 hrs before the cells now largely stalled in mitosis were collected. Cells were swollen in 75 mM KCl at 37 °C before being fixed in 3:1 methanol: acetic acid. Cells were dropped onto glass slides and after drying chromosomes were stained with Giemsa (Merck) and mounted in Eukitt Quick-hardening mounting medium (Merck). Slides were analysed on a Nikon E400 fluorescent microscope.

To look in more detail at chromosome disruption sister chromatid exchanges were analysed as described previously (*62*). Briefly cells were grown in 10 ng/ml doxycycline, 10 μM BrdU for 48 hrs. Cells were blocked in mitosis and collected, spread and dried as described above. Chromosomes were then stained with 10 μg/ml Hoechst before being washed in SSC, (150 mM Sodium Chloride, 15mM Sodium Citrate) and exposed to UV light for 1 hr, then incubated in SSC buffer for a further 1 hr at 60 °C. Slides were then stained with Giemsa and mounted and viewed as described above.

Fibre Assays

Replication fork speed and stalling was analysed on DNA fibres as described previously (*6*). Briefly, approximately 10 x10^4 cells were incubated in 10 ng/ml doxycycline for at least 16 hrs, cells were then labelled with 25 μM CldU for 20 minutes followed by 250 μM IdU for a further 20 minutes. For fork stalling assays, a pulse of 20 J/m^2 UV-C was given in between the two labels. Where the effects of damage were analysed cells were either first treated with 10 μM Olaparib for 2hrs and throughout the labelling or 50 nM camptothecin was added along with IdU label. For analysis of

fork restart cells were labelled as normal with 25 μM CldU for 20 minutes before the addition of 4 mM HU for 16 hrs or 5 μM camptothecin for 1 hr. Drugs were washed off and cells were released into media containing 250 μM IdU for 60 minutes. Cells were collected into 150 μl PBS and 2.5 μl were lysed directly on slides with 7.5 μl lysis buffer (20 mM Tris pH 7.5, 50 mM EDTA, 0.5 % SDS). DNA was spread down slides using gravity before being fixed with 3:1 methanol: acetic acid. After rehydration, fibres were stained with antibodies to the specific labels, rat anti-BrdU [BU1/75 (ICR1)], mouse anti-BrdU Clone B44, anti-rat Alexa Fluor 488, anti-mouse Alexa Fluor 594 (Table S2). Slides were mounted with Fluoromount (Sigma-Aldrich) and imaged on an Olympus IX70 fluorescent microscope and analysed using OMERO. The S1 fibre assay was adapted from previous protocols (*63*), cells were labelled as above before being collected and treated with CSK buffer on ice for 10 mins. Nuclei were pelleted and treated with 0 or 20 U/ml S1 (Promega) for 30 mins at 37 ˚C before being washed and spread as above.

Flow cytometry

Cell cycle populations were analysed using flow cytometry. To confirm synchronisation cells were collected at desired time points and fixed in 70 % ethanol at -20°C. To label replicating DNA cells were treated with 10 μM EdU prior to collection. EdU positive cells were then labelled using Click chemistry and sulfo-CY5 azide (Jena Biosciences)(*12, 61*). Cells were then washed in PBS and labelled with 5 μg/ml propidium iodide and RNA was degraded with 150 μg/ml RNAse A. To follow progression into mitosis samples were additionally stained for P-H3. After fixation cells were permeabilised with 0.2 % triton in PBS for 10 mins before blocking in 3 % BSA and staining with antibodies to P-H3 followed by anti-Rat 488 green (Table S2). Cells were then stained for EdU and PI as above. Samples were analysed using a BD Accuri C6 flow cytometer and approximately 10,000 cells were quantified using BD CSampler Software. To follow cell cycle progression after damage cells were first plated in 10 ng/ml doxycycline for at least 16 hrs before being treated with 0 or 5 J/m^2 UV-C. Cells were allowed to recover for increasing times before being labelled with 10 μM EdU for 30 mins and collected as above.

Purification of Recombinant Proteins

Full-length human PrimPol and S538A/E mutants were purified as described previously (*7*). Briefly, the proteins were expressed in SHuffle® T7 *Escherichia coli* cells (New England Biolabs) overnight at 16 °C. Following sonication and isolation by centrifugation, the proteins were purified by affinity chromatography using Ni-NTA affinity resin (Generon), then separated by charge by affinity exchange chromatography on a Hi-Trap Heparin HP column (GE Healthcare) and finally subject to size exclusion chromatography on a Superdex 75 gel filtration column (GE Healthcare).

PrimPol CTD ($PrimPol_{480-560}$) and corresponding S538A/E mutants were purified as described previously (*30*). Briefly, the proteins were expressed in BL21 *E. coli* cells overnight at 20 °C. Following sonication and isolation by centrifugation, the proteins were purified by affinity chromatography using Ni-NTA affinity resin (Generon), followed by separation by Q Sepharose (GE Healthcare) and size exclusion chromatography on a Superdex 75 gel filtration column (GE Healthcare).

RPA70N ($RPA70_{1-120}$) was purified as described previously (*30*). Briefly, the protein was expressed in BL21 *E. coli* cells overnight at 20 °C. Following sonication and isolation by centrifugation, RPA70N was purified using Ni-NTA affinity resin (Generon) with a gradient elution. The polyhistidine tag was cleaved by thrombin overnight at room temperature and the product passed through Ni-NTA affinity resin (Generon) to separate the protein from the tag. Finally, the protein was polished by a size exclusion chromatography step on a Superdex 75 gel filtration column (GE Healthcare).

Analytical Size-Exclusion Chromatography

Protein interactions were analysed by analytical size-exclusion chromatography as described previously (*29*). Briefly, a Superdex 75 10/300 GL gel filtration column (GE

Healthcare) was pre-equilibriated in a buffer containing 50mM Tris-HCl, 100 mM NaCl and 2 mM TCEP. Firstly, individual proteins were loaded at a concentration of 35 μM to provide baseline elution volumes for each. To test protein interactions, the CTD variants were mixed with RPA70N at 35 μM. Interactions were identified by a shift in the chromatograph peaks relative to the respective baseline elution volumes.

Primase Assays

Increasing concentrations of protein (0.5 µM, 1 µM, 2 µM and 4 µM) were incubated in 20 μl reactions containing 10 µM ssDNA template (Cy5-CCAACCTTTATATTGCCAATCTCTAACCTTTTTCCCATTTACATATAGTddG) with 100 µM dNTPs, 2.5 μM FAM-y-GTP, 10 mM Bis-Tris-Propane-HCl (pH 7), 10 mM NaCl, 2 mM MnCl, 0.5 mM TCEP. The reaction was carried out at 37 °C for 30 minutes and stopped by the addition of 15 µl stop buffer (60 % formamide, 5 mM EDTA, 0.025 % SDS, 0.09 % xylene cyanol and 6 M urea). Excess labelled NTP was removed by ethanol precipitation. Primers were resuspended in 20 μl loading dye (95 % formamide with 0.25 % bromophenol blue and xylene cyanol). Samples were boiled and resolved on a 20 % polyacrylamide/7 M urea/TBE gel at 25 W for 2 hours. Fluorescently labelled primers were detected using a Fujifilm FLA-5100 image reader.

Polymerase Assays

A template oligonucleotide (GACTACTATCTCGACTATATACTATTGCTTCTACGAAGACCTTCA) was annealed to a complementary fluorescently labelled DNA primer (FAM-TGAAGGTCTTCGTAGAAGC). 50 nm of protein was incubated with 30 nM annealed primer-template substrate, 10 mM Bis-Tris-Propane-HCl (pH 7), 10 mM MgCl, 10 mM NaCl, 0.5 mM TCEP and 100 µM dNTPs to a final volume of 20 µl. The reactions were performed at 37 °C and stopped at 2, 5, 10 and 15 minutes by the addition of 20 μl stop buffer (60 % formamide, 5 mM EDTA, 0.025 % SDS, 6 M urea). For fidelity assays, similar conditions were used, except for 20 nM primer-template substrate, 100 µM PrimPol, 200 µM dNTPs and a 30 minute reaction time. Samples were boiled and

resolved on a 15 % polyacrylamide/7 M urea/TBE gel at 25 W for 1.5 hours. Fluorescently labelled oligonucleotides were detected using a Fujifilm FLA-5100 image reader.

Data Analyses

Charts show independent experiments with error bars showing standard deviation, colony survivals represent 3 or more independent experiments. Significance was determined using a students T-test, or Mann-Whitney for fibres and foci, $P \leq 0.05$ *, ≤ 0.01 **, ≤ 0.001 ***, ≤ 0.0001 ****. For fibres experiments the black line represents the mean of the data where approximately 300 fibres were measured across three independent experiments unless stated otherwise. For cell analysis approximately 500 cells were counted per independent experiment, for chromosome spreads this was 100, or 300 for SCEs. Data analysis was carried out using GraphPad and images were quantified with Image J and OMERO.

References

1. M. K. Zeman, K. A. Cimprich, Causes and consequences of replication stress. *Nat Cell Biol* **16**, 2-9 (2014).
2. T. A. Guilliam, A. J. Doherty, PrimPol-Prime Time to Reprime. *Genes* **8**, (2017).
3. L. J. Bailey, A. J. Doherty, Mitochondrial DNA replication: a PrimPol perspective. *Biochemical Society transactions* **45**, 513-529 (2017).
4. K. Kobayashi *et al.*, Repriming by PrimPol is critical for DNA replication restart downstream of lesions and chain-terminating nucleosides. *Cell cycle* **15**, 1997-2008 (2016).
5. D. Schiavone *et al.*, PrimPol Is Required for Replicative Tolerance of G Quadruplexes in Vertebrate Cells. *Molecular Cell* **61**, 161-169 (2016).
6. J. Bianchi *et al.*, PrimPol bypasses UV photoproducts during eukaryotic chromosomal DNA replication. *Molecular Cell* **52**, 566-573 (2013).
7. B. A. Keen, S. K. Jozwiakowski, L. J. Bailey, J. Bianchi, A. J. Doherty, Molecular dissection of the domain architecture and catalytic activities of human PrimPol. *Nucleic Acids Res* **42**, 5830-5845 (2014).
8. J. E. Sale, Translesion DNA synthesis and mutagenesis in eukaryotes. *Cold Spring Harb Perspect Biol* **5**, a012708 (2013).
9. M. F. Goodman, R. Woodgate, Translesion DNA polymerases. *Cold Spring Harb Perspect Biol* **5**, a010363 (2013).
10. S. D. McCulloch *et al.*, Preferential cis-syn thymine dimer bypass by DNA polymerase eta occurs with biased fidelity. *Nature* **428**, 97-100 (2004).
11. A. Quinet, D. Lemacon, A. Vindigni, Replication Fork Reversal: Players and Guardians. *Molecular Cell* **68**, 830-833 (2017).
12. L. J. Bailey, J. Bianchi, A. J. Doherty, PrimPol is required for the maintenance of efficient nuclear and mitochondrial DNA replication in human cells. *Nucleic Acids Res* **47**, 4026-4038 (2019).
13. L. J. Bailey, J. Bianchi, N. Hegarat, H. Hochegger, A. J. Doherty, PrimPol-deficient cells exhibit a pronounced G2 checkpoint response following UV damage. *Cell Cycle* **15**, 908-918 (2016).
14. G. Bai *et al.*, HLTF Promotes Fork Reversal, Limiting Replication Stress Resistance and Preventing Multiple Mechanisms of Unrestrained DNA Synthesis. *Molecular Cell* **78**, 1237-1251 e1237 (2020).
15. M. M. Genois *et al.*, CARM1 regulates replication fork speed and stress response by stimulating PARP1. *Molecular Cell*, (2020).
16. A. Quinet *et al.*, PRIMPOL-Mediated Adaptive Response Suppresses Replication Fork Reversal in BRCA-Deficient Cells. *Mol Cell* **77**, 461-474 e469 (2020).
17. V. N. Duong *et al.*, Identifying the role of PrimPol in TDF-induced toxicity and implications of its loss of function mutation in an HIV+ patient. *Scientific Reports* **10**, 9343 (2020).
18. A. Yoshimura *et al.*, WRNIP1 Controls the Amount of PrimPol. *Biol Pharm Bull* **42**, 764-769 (2019).
19. E. Despras *et al.*, Rad18-dependent SUMOylation of human specialized DNA polymerase eta is required to prevent under-replicated DNA. *Nature Communications* **7**, 13326 (2016).
20. F. Bertoletti *et al.*, Phosphorylation regulates human poleta stability and damage bypass throughout the cell cycle. *Nucleic Acids Res* **45**, 9441-9454 (2017).
21. C. Peddu *et al.*, Phosphorylation Alters the Properties of Pol eta: Implications for Translesion Synthesis. *iScience* **6**, 52-67 (2018).
22. M. Bienko *et al.*, Regulation of translesion synthesis DNA polymerase eta by monoubiquitination. *Molecular Cell* **37**, 396-407 (2010).

23. G. Combes, I. Alharbi, L. G. Braga, S. Elowe, Playing polo during mitosis: PLK1 takes the lead. *Oncogene* **36**, 4819-4827 (2017).
24. S. Y. Hyun, H. I. Hwang, Y. J. Jang, Polo-like kinase-1 in DNA damage response. *BMB Rep* **47**, 249-255 (2014).
25. K. Nakamura *et al.*, Proteome dynamics at broken replication forks reveal a distinct ATM-directed repair response suppressing DNA double-strand break ubiquitination. *Molecular Cell* **81**, 1084-1099 e1086 (2021).
26. M. Lee, M. J. Daniels, A. R. Venkitaraman, Phosphorylation of BRCA2 by the Polo-like kinase Plk1 is regulated by DNA damage and mitotic progression. *Oncogene* **23**, 865-872 (2004).
27. Z. Li *et al.*, Plk1 Phosphorylation of Mre11 Antagonizes the DNA Damage Response. *Cancer research* **77**, 3169-3180 (2017).
28. K. Yata *et al.*, Plk1 and CK2 act in concert to regulate Rad51 during DNA double strand break repair. *Molecular Cell* **45**, 371-383 (2012).
29. W. Li *et al.*, A methylation-phosphorylation switch determines Plk1 kinase activity and function in DNA damage repair. *Science Advances* **5**, eaau7566 (2019).
30. T. A. Guilliam *et al.*, Molecular basis for PrimPol recruitment to replication forks by RPA. *Nature communications* **8**, 15222 (2017).
31. E. Kowarz, D. Loscher, R. Marschalek, Optimized Sleeping Beauty transposons rapidly generate stable transgenic cell lines. *Biotechnol J* **10**, 647-653 (2015).
32. R. Aleksandrov, R. Hristova, S. Stoynov, A. Gospodinov, The Chromatin Response to Double-Strand DNA Breaks and Their Repair. *Cells* **9**, (2020).
33. A. Ray Chaudhuri, A. Nussenzweig, The multifaceted roles of PARP1 in DNA repair and chromatin remodelling. *Nature reviews. Molecular Cell Biology* **18**, 610-621 (2017).
34. K. P. Jakobsen, A. H. Andersen, L. Bjergbaek, Abortive activity of Topoisomerase I: a challenge for genome integrity? *Current Genetics* **65**, 1141-1144 (2019).
35. A. Maya-Mendoza *et al.*, High speed of fork progression induces DNA replication stress and genomic instability. *Nature* **559**, 279-284 (2018).
36. A. Ray Chaudhuri *et al.*, Topoisomerase I poisoning results in PARP-mediated replication fork reversal. *Nature Structural & Molecular Biology* **19**, 417-423 (2012).
37. M. I. Martinez-Jimenez, P. A. Calvo, S. Garcia-Gomez, S. Guerra-Gonzalez, L. Blanco, The Zn-finger domain of human PrimPol is required to stabilize the initiating nucleotide during DNA priming. *Nucleic Acids Res* **46**, 4138-4151 (2018).
38. N. E. Davey *et al.*, Attributes of short linear motifs. *Mol Biosyst* **8**, 268-281 (2012).
39. H. Nakajima, F. Toyoshima-Morimoto, E. Taniguchi, E. Nishida, Identification of a consensus motif for Plk (Polo-like kinase) phosphorylation reveals Myt1 as a Plk1 substrate. *Journal of Biological Chemistry* **278**, 25277-25280 (2003).
40. A. Santamaria *et al.*, The Plk1-dependent phosphoproteome of the early mitotic spindle. *Mol Cell Proteomics* **10**, M110 004457 (2011).
41. G. Lian *et al.*, BI2536, a potent and selective inhibitor of polo-like kinase 1, in combination with cisplatin exerts synergistic effects on gastric cancer cells. *Int J Oncol* **52**, 804-814 (2018).
42. M. E. Burkard, A. Santamaria, P. V. Jallepalli, Enabling and disabling polo-like kinase 1 inhibition through chemical genetics. *ACS Chem Biol* **7**, 978-981 (2012).
43. B. Lemmens *et al.*, DNA Replication Determines Timing of Mitosis by Restricting CDK1 and PLK1 Activation. *Molecular Cell* **71**, 117-128 e113 (2018).
44. L. Macurek *et al.*, Polo-like kinase-1 is activated by aurora A to promote checkpoint recovery. *Nature* **455**, 119-123 (2008).
45. K. Akopyan *et al.*, Assessing kinetics from fixed cells reveals activation of the mitotic entry network at the S/G2 transition. *Molecular Cell* **53**, 843-853 (2014).

46. U. Cucchi *et al.*, Phosphorylation of TCTP as a marker for polo-like kinase-1 activity in vivo. *Anticancer Res* **30**, 4973-4985 (2010).
47. V. M. Vassin, R. W. Anantha, E. Sokolova, S. Kanner, J. A. Borowiec, Human RPA phosphorylation by ATR stimulates DNA synthesis and prevents ssDNA accumulation during DNA-replication stress. *Journal of Cell Science* **122**, 4070-4080 (2009).
48. F. A. Barr, H. H. Sillje, E. A. Nigg, Polo-like kinases and the orchestration of cell division. *Nature reviews. Molecular Cell Biology* **5**, 429-440 (2004).
49. R. Mandal, K. Strebhardt, Plk1: unexpected roles in DNA replication. *Cell Res* **23**, 1251-1253 (2013).
50. S. Li, X. Wu, Common fragile sites: protection and repair. *Cell Biosci* **10**, 29 (2020).
51. N. Saini, D. A. Gordenin, Hypermutation in single-stranded DNA. *DNA Repair* **91-92**, 102868 (2020).
52. A. L. Piberger *et al.*, PrimPol-dependent single-stranded gap formation mediates homologous recombination at bulky DNA adducts. *Nature Communications* **11**, 5863 (2020).
53. L. I. Toledo *et al.*, ATR prohibits replication catastrophe by preventing global exhaustion of RPA. *Cell* **155**, 1088-1103 (2013).
54. L. Toledo, K. J. Neelsen, J. Lukas, Replication Catastrophe: When a Checkpoint Fails because of Exhaustion. *Molecular Cell* **66**, 735-749 (2017).
55. S. Nayak *et al.*, Inhibition of the translesion synthesis polymerase REV1 exploits replication gaps as a cancer vulnerability. *Science Advances* **6**, eaaz7808 (2020).
56. H. Hanzlikova *et al.*, The Importance of Poly(ADP-Ribose) Polymerase as a Sensor of Unligated Okazaki Fragments during DNA Replication. *Molecular Cell* **71**, 319-331 e313 (2018).
57. S. Mouron *et al.*, Repriming of DNA synthesis at stalled replication forks by human PrimPol. *Nature Structural & Molecular Biology* **20**, 1383-1389 (2013).
58. F. A. Ran *et al.*, Genome engineering using the CRISPR-Cas9 system. *Nature Protocols* **8**, 2281-2308 (2013).
59. M. Jordan, A. Schallhorn, F. M. Wurm, Transfecting mammalian cells: optimization of critical parameters affecting calcium-phosphate precipitate formation. *Nucleic Acids Res* **24**, 596-601 (1996).
60. V. Roth, Doubling Time Computing. *Available from: http://www.doubling-time.com/compute.php*, (2006).
61. N. Jia *et al.*, A rapid, comprehensive system for assaying DNA repair activity and cytotoxic effects of DNA-damaging reagents. *Nature Protocols* **10**, 12-24 (2015).
62. D. M. Stults, M. W. Killen, A. J. Pierce, The sister chromatid exchange (SCE) assay. *Methods Mol Biol* **1105**, 439-455 (2014).
63. A. Quinet, D. Carvajal-Maldonado, D. Lemacon, A. Vindigni, DNA Fiber Analysis: Mind the Gap! *Methods in Enzymology* **591**, 55-82 (2017).

Acknowledgements

AJD's laboratory supported by grants from the Biotechnology and Biological Sciences Research Council (BBSRC: BB/H019723/1 and BB/M008800/1). RT and LJB were supported by PhD studentships funded by the University of Sussex and Wellcome Trust ISSF, respectively. Thanks to Dr Helfrid Hochegger for pSB*tet* and pSB100X plasmids and Dr Chris Chan and Dr Mark Burkard for RPE1 PLK1-as cells. Thanks to the Proteomics Core Facility at CEITEC (Brno, Czech Republic) for mass spectrometry analysis.

The authors declare that they have no competing interests. All data needed to evaluate the conclusions in the paper are present in the paper and/or the Supplementary Materials.

Author Contributions

Conceptualization, L.J.B. and A.J.D; **Methodology**, L.J.B and A.J.D.; **Investigation**, L.J.B., R.T., P.K., L.J.B., H.D.L.; **Writing – Original Draft,** L.J.B., R.T. and A.J.D.; **Writing – Review & Editing,** L.J.B., R.T., and A.J.D.; **Funding Acquisition, Project Administration and Supervision,** A.J.D.

Figures

Figure 1. PrimPol is modified by phosphorylation and loss of the highly conserved serine 538 phosphorylation causes genomic instability

(**A**) Alignment of the C-terminal region of PrimPol containing the RPA binding domains. Hs, *Homo sapien (Human);* Tt, *Tursiops truncatus (Atlantic bottle-nosed dolphin);* Ts, *Tarsius syrichta (Philippine tarsier);* Hg, *Heterocephalus glaber (Naked mole rat);* Cp, *Cavia porcellus (Guinea pig);* Mm, *Mus musculus (Mouse);* Md, *Monodelphis domestica (Gray short-tailed opossum);* Gg*, Gallus Gallus (Chicken);* Xt*, Xenopus tropicalis (Western Clawed frog);* Ap*, Anas platyrhynchos (Northern mallard)*; Ci, *Ciona intestinalis (Vase tunicate.)* (**B**) Whole cell lysate from HEK293 cells where PrimPol was expressed by addition of doxycycline for 24 hrs analysed by western blotting. (**C**) Plating efficiency of different cell lines expressing PrimPol variants compared to no doxycycline controls. (**D**) ΔPP-1 cells expressing PrimPol, PrimPol^{S538A} or PrimPol^{S538E} were collected and detergent resistant chromatin fractions were separated from soluble proteins before being separated by western blot. (**E**) Quantification of cells with 1 or more micronuclei 48 hrs after PrimPol expression. (**F**) PrimPol was expressed for 96 hrs in HEK293 cells before being stalled in mitosis with nocodazole. Chromosomes were spread and those containing one or more chromosome with a break were quantified as a percentage of the population. (**G**) To analyse sister chromatid exchanges cells were grown 10 μM BrdU for 48 hrs before being blocked in mitosis. Cells were spread and stained with Hoescht and Geimsa and the number of chromosomes with one or more crossovers were counted as a percentage of the total population.

Figure 2. Loss of PrimPol S538 phosphorylation affects genomic stability after UV-C damage and is dependent on RPA interaction.

(**A**) Damage sensitivity was measured by colony survival after increasing doses of UV-C, or cisplatin. (**B**) Quantification of cell cycle recovery after damage was measured by flow cytometry, by EdU and PI labelling 24 hrs after treatment with 5 J/m^2 UV-C, images shown in Fig. S4B. (**C**) Cells with 1 or more micronuclei were counted 48 hrs

after 5 J/m^2 UV-C treatment. (**D**) CldU/IdU ratios show replication changes where a pulse of 20 J/m^2 UV-C was given between labels**.** (**E**) Undamaged replication fork speed was measured in the different cell lines at least 16 hrs after PrimPol expression by labelling cells consecutively with CldU and IdU. (**F**) UV sensitivity was analysed by colony survival in ΔPP-1 cells expressing RAB mutated forms of PrimPol also carrying the 538 mutations. (**G**) Micronuclei were analysed 48 hrs after 5 J/m^2 in cells expressing protein additionally carrying the RAB mutations.

Figure 3. Cells expressing PrimPol^{S538A} are sensitive to genotoxic agents camptothecin and olaparib.

(**A**) Sensitivity to olaparib and camptothecin was measured by colony survival approximately 10 days after the addition of drugs**.** Changes in levels of micronuclei (**B**) or cells undergoing abnormal mitotic segregation (**C**), were analysed 48 hrs after treatment with camptothecin or olaparib. (**D**) Chromosome breaks were analysed 48 hrs after treatment with olaparib or camptothecin. (**E**) Effects of olaparib and camptothecin were quantified after 48 hrs by flow cytometry, see images in Fig. S6F. (**F**) The effect on replication in the presence of these drugs was analysed by measuring DNA fibres. Cells were treated with 10 μM olaparib for 2 hrs before and during fibre analysis or 50 nM camptothecin was added with IdU labelling.

Figure 4. Mutation of PrimPol's Zinc finger reduces PrimPol^{S538A} induced genomic instability.

(**A**) Damage sensitivity changes caused by the addition of the ZF mutations in PrimPol were measured by colony survival with increasing doses of UV-C, cisplatin, olaparib and camptothecin. Cells with one or more chromosome breaks were counted 96 hrs after PrimPol expression (**B)**, or after 48 hrs incubation with olaparib or camptothecin (**C**). (**D**) Micronuclei were counted 48 hrs after recovery from 0 or 5 J/m^2 UV-C, or 48 hrs incubation with olaparib or camptothecin.

Figure 5. PrimPol S538 phosphorylation is cell cycle regulated by PLK1

(**A**) Alignment of the region of PrimPol containing a potential PLK1 site in different species, residue 538 in human protein. Hs, *Homo sapien (Human);* Tt, *Tursiops truncatus (Atlantic bottle-nosed dolphin);* Ts, *Tarsius syrichta (Philippine tarsier);* Hg, *Heterocephalus glaber (Naked mole rat);* Cp, *Cavia porcellus (Guinea pig).* (**B**) PLK1 *in vitro* kinase assay where PrimPol was incubated with recombinant PLK1 and the resulting protein phosphorylation analysed for by western blotting. (**C**) HEK293 ΔPP-1 cells expressing PrimPol were treated with increasing concentrations BI2536 or mock treated. RPE PLK1-as cells expressing PrimPol were treated with 3-MB-PP1 and whole cell lysate was subject to western blotting (left and right panels respectively). (**D**) HEK293 ΔPP-1 cells expressing PrimPol were released from a double thymidine block for increasing times or left untreated as an asynchronous control and analysed for cell cycle synchronisation by flow cytometry. Whole cell extract from cells at each time point was subjected to western blotting. (**E**) Chromosome breaks were analysed after synchronisation, cells were released from a double thymidine block into nocodazole with or without the addition of PLK1 inhibitor BI2536, olaparib or camptothecin and allowed to progress to mitosis.

Figure 6. Dysregulation throughout the cell cycle drives PrimPol^{S538A} genotoxic phenotypes.

(**A**)To quantify micronuclei in cells, they were first labelled with EdU, to distinguish those in S-phase. Cells were treated with 0 or 5 J/m^2 UV-C and allowed to recover for 48 hrs before being analysed for micronuclei and EdU. (**B**) Cells were synchronised by double thymidine block and released into respective cell cycle stages before being UV-C damaged and allowed to recover for 1 hr. Chromatin fractions were then isolated and analysed by western blotting. (**C**) RPA2 foci were quantified in undamaged cells or 24 hrs after UV-C treatment, representative images shown in Fig. S9D. (**D**). Cells were labelled with CldU for 48 hrs before being washed and left untreated or treated with 10 μM Olaparib for 2hrs. Cells were then stained for CldU under native conditions to analyse ssDNA. Images were quantified in Image J, n=3 (olaparib N=2), examples shown in Fig. S9F. (**E**) Cells were synchronised with a double thymidine block before

being released for 6 hrs with or without BI2536. Cells were labelled with CldU and IdU before S1 nuclease treatment, total fibre length was measured to assess nuclease cutting, n=2.

Figure 7. S538 phosphorylation of PrimPol changes in response to DNA damage and cell cycle progression.

(**A**) Cells were released from a double thymidine block into nocodazole containing media for 5 hrs allowing them to reach late S-phase before the addition of damage and analysed by western blot. (**B**) Cells were released from a double thymidine into media containing nocodazole for 5 hrs, before the addition of damage in the absence or presence of the PLK1 inhibitor for a further 5 hrs. Whole cell lysates were analysed by western blotting and progression into mitosis by P-H3 staining for flow cytometry. (**C**) A model showing the roles of S538 phosphorylation in the regulation of PrimPol throughout the cell cycle and in response to fork stalling damage.

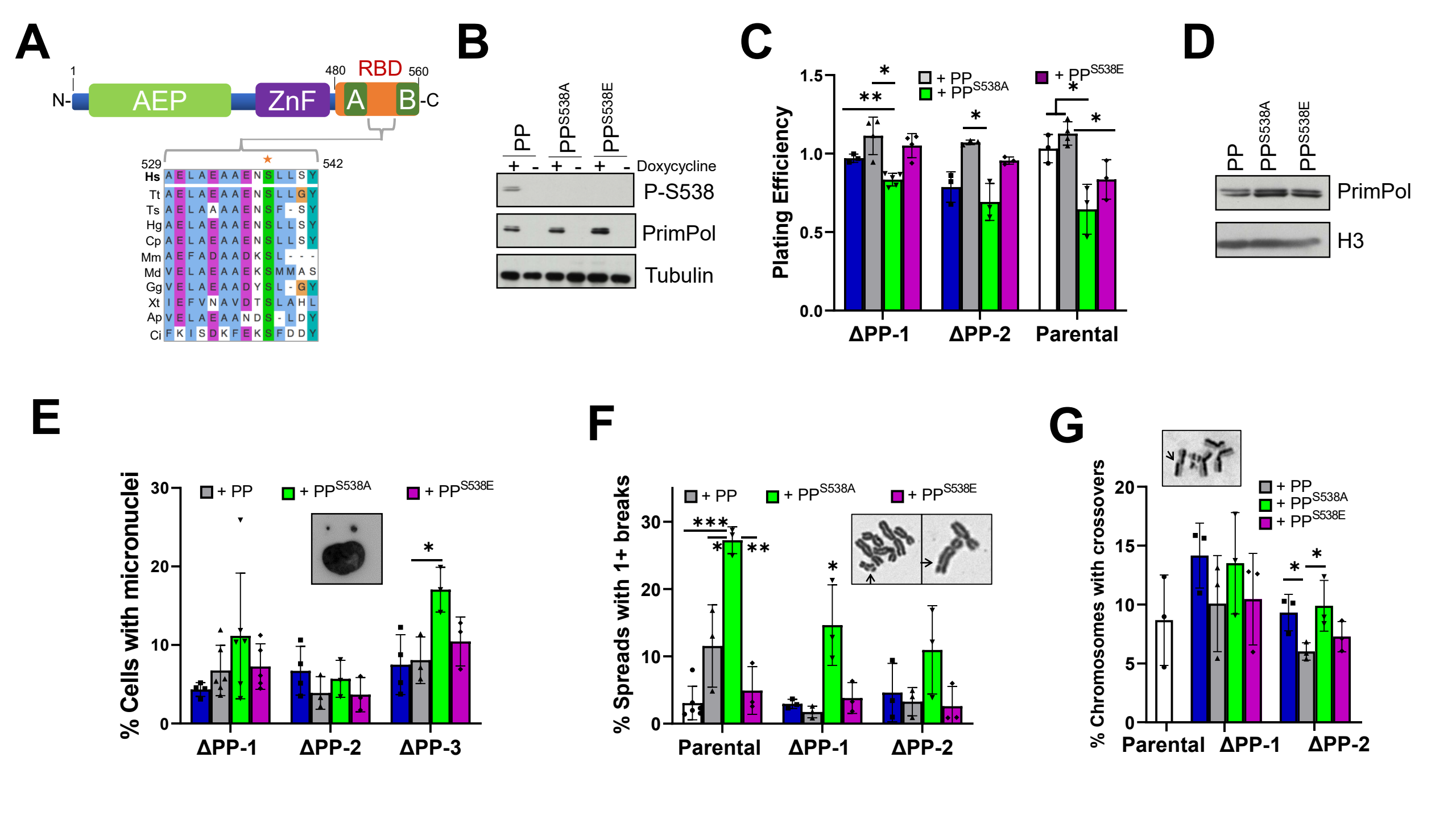
A
1
480
RBD
560
N-
AEP
ZnF
A
B
-C
529
542
Hs AELAEAAENSLLSY
Tt AELAEAAENSLLGY
Ts AELAAAAENSF-SY
Hg AELAEAAENSLLSY
Cp AELAEAAENSLLSY
Mm AEFADAADKSL----
Md VELAEAAEKSMMAS
Gg VELAEAADYSL-GY
Xt IEFVNAVDTSLAHL
Ap VELAEAANDS-LDY
Ci FKISDKFEKSFDDY
B
PP
PPS538A
PPS538E
+ - + - + -
Doxycycline
P-S538
PrimPol
Tubulin
C
Plating Efficiency
1.5
1.0
0.5
0.0
+ PP
+ PPS538A
+ PPS538E
ΔPP-1
ΔPP-2
Parental
D
PP
PPS538A
PPS538E
PrimPol
H3
E
% Cells with micronuclei
30
20
10
0
+ PP
+ PPS538A
+ PPS538E
ΔPP-1
ΔPP-2
ΔPP-3
F
% Spreads with 1+ breaks
30
20
10
0
+ PP
+ PPS538A
+ PPS538E
Parental
ΔPP-1
ΔPP-2
G
% Chromosomes with crossovers
20
15
10
5
0
+ PP
+ PPS538A
+ PPS538E
Parental
ΔPP-1
ΔPP-2

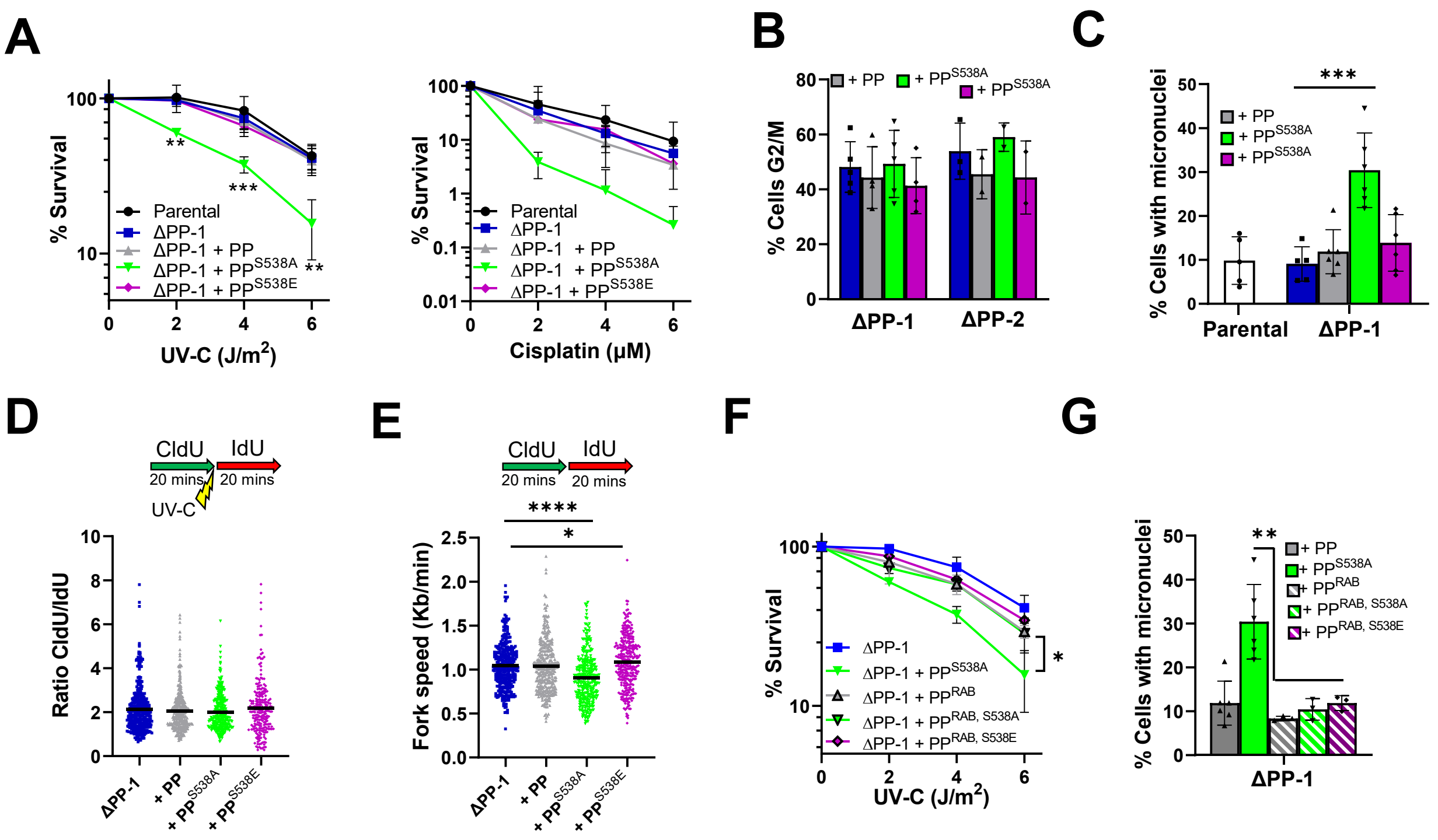
A
% Survival
UV-C (J/m2)
Cisplatin (μM)
Parental
ΔPP-1
ΔPP-1 + PP
ΔPP-1 + PPS538A
ΔPP-1 + PPS538E
B
% Cells G2/M
+ PP
+ PPS538A
+ PPS538A
ΔPP-1
ΔPP-2
C
% Cells with micronuclei
***
+ PP
+ PPS538A
+ PPS538A
Parental
ΔPP-1
D
CldU
IdU
20 mins
20 mins
UV-C
Ratio CldU/IdU
ΔPP-1
+ PP
+ PPS538A
+ PPS538E
E
CldU
IdU
20 mins
20 mins
****
*
Fork speed (Kb/min)
ΔPP-1
+ PP
+ PPS538A
+ PPS538E
F
% Survival
UV-C (J/m2)
ΔPP-1
ΔPP-1 + PPS538A
ΔPP-1 + PPRAB
ΔPP-1 + PPRAB, S538A
ΔPP-1 + PPRAB, S538E
*
G
% Cells with micronuclei
**
+ PP
+ PPS538A
+ PPRAB
+ PPRAB, S538A
+ PPRAB, S538E
ΔPP-1

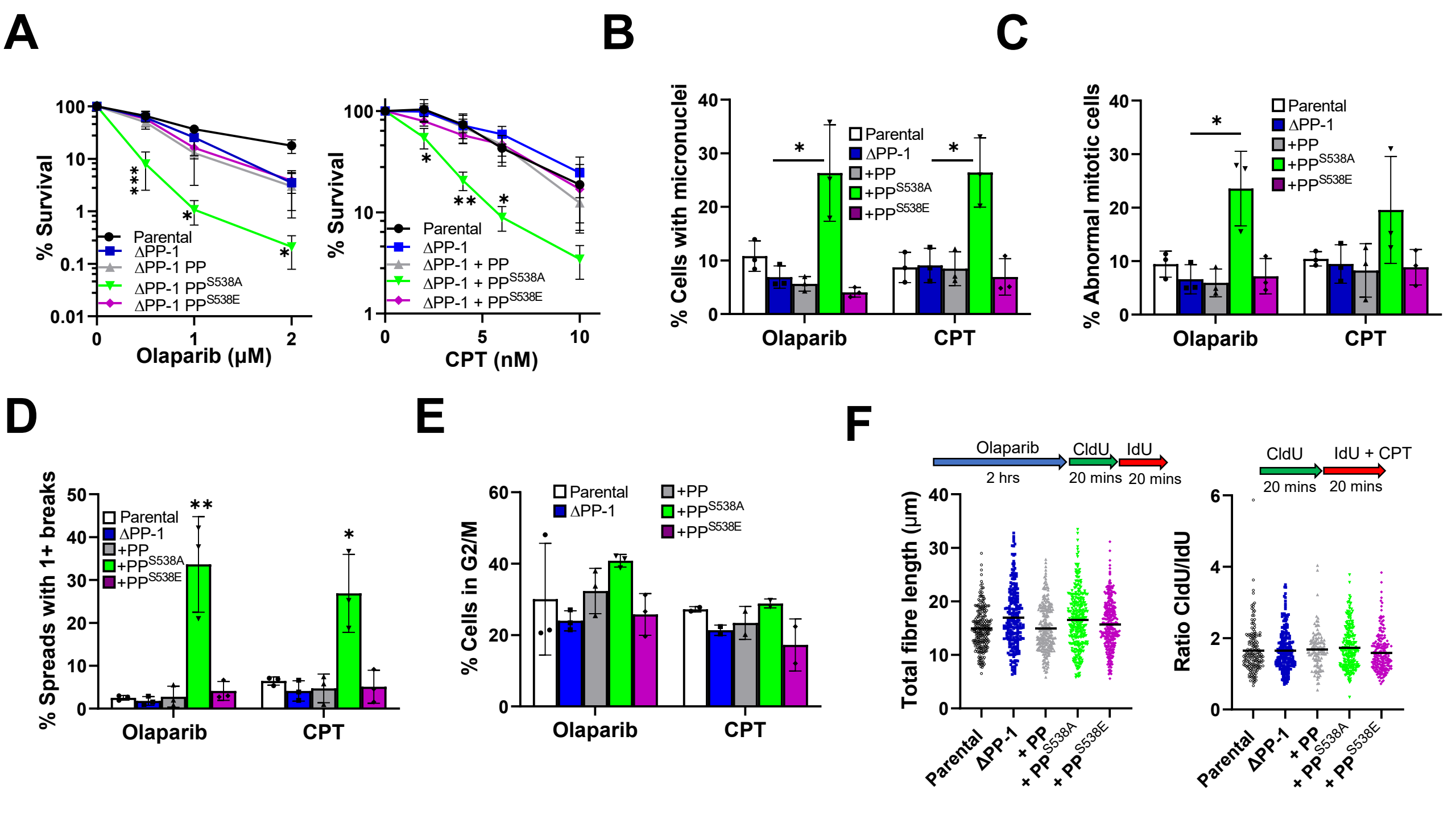
A
% Survival
Olaparib (μM)
CPT (nM)
Parental
ΔPP-1
ΔPP-1 PP
ΔPP-1 PP^S538A
ΔPP-1 PP^S538E
ΔPP-1 + PP
ΔPP-1 + PP^S538A
ΔPP-1 + PP^S538E
B
% Cells with micronuclei
Olaparib
CPT
+PP
+PP^S538A
+PP^S538E
C
% Abnormal mitotic cells
D
% Spreads with 1+ breaks
E
% Cells in G2/M
F
Olaparib
2 hrs
CldU
20 mins
IdU
20 mins
IdU + CPT
Total fibre length (μm)
Ratio CldU/IdU

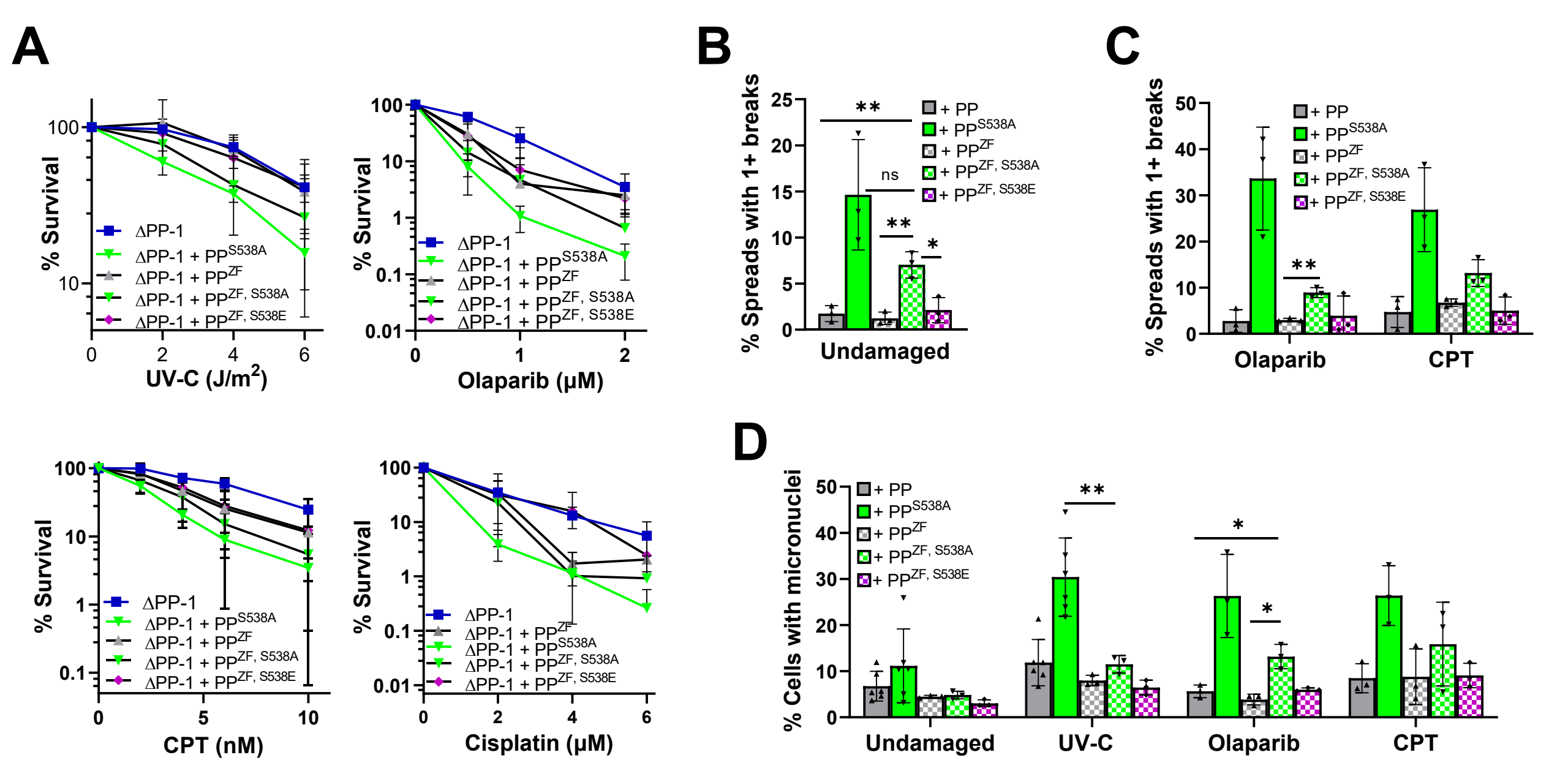
A
% Survival
UV-C (J/m2)
Olaparib (μM)
CPT (nM)
Cisplatin (μM)
ΔPP-1
ΔPP-1 + PPS538A
ΔPP-1 + PPZF
ΔPP-1 + PPZF, S538A
ΔPP-1 + PPZF, S538E
B
% Spreads with 1+ breaks
Undamaged
ns
+ PP
+ PPS538A
+ PPZF
+ PPZF, S538A
+ PPZF, S538E
C
% Spreads with 1+ breaks
Olaparib
CPT
D
% Cells with micronuclei
Undamaged
UV-C
Olaparib
CPT

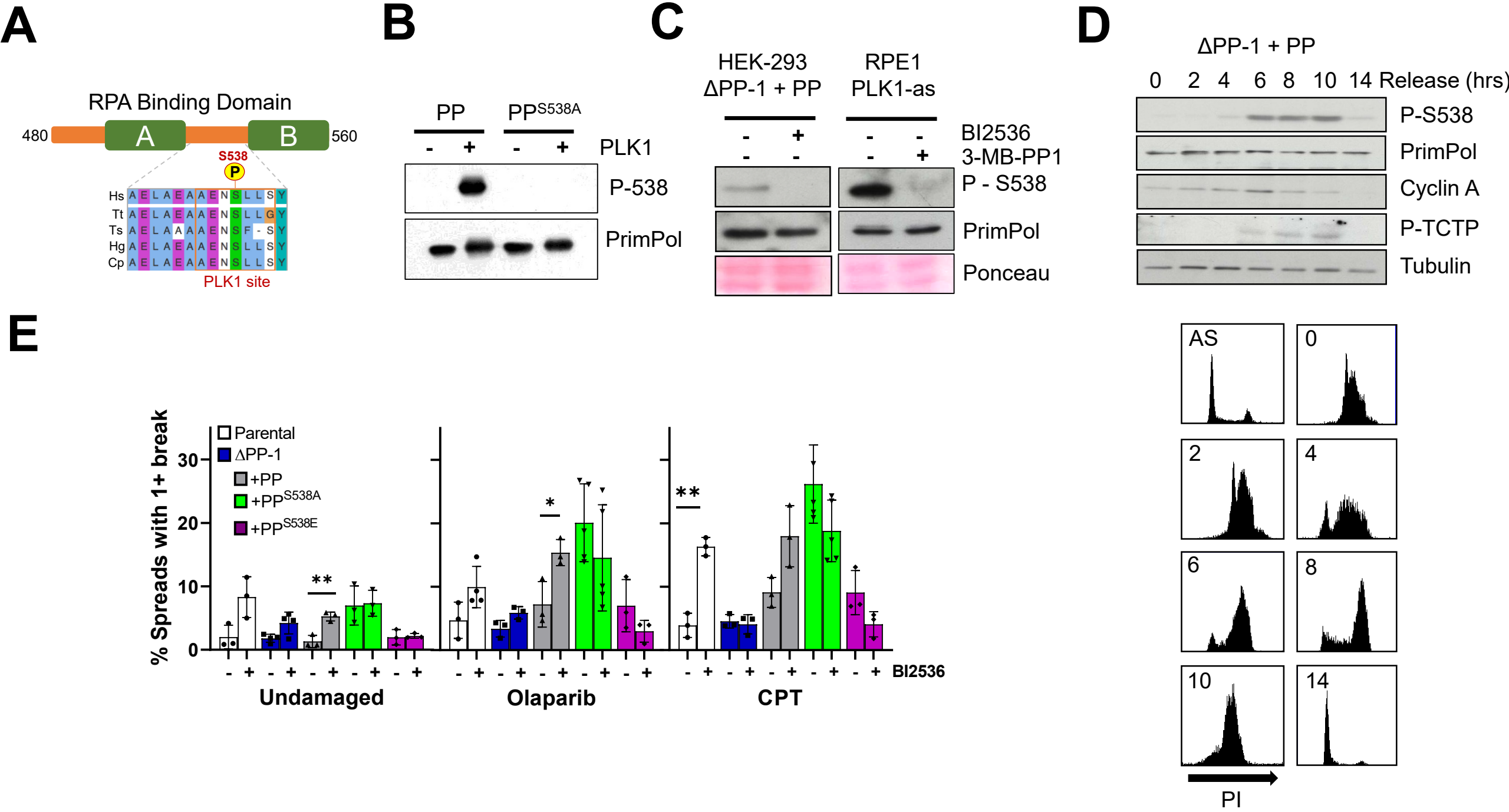
A
RPA Binding Domain
480
A
B
560
S538
P
Hs AELAEAAENSLLSY
Tt AELAEAAENSLLGY
Ts AELAAAAENSF-SY
Hg AELAEAAENSLLSY
Cp AELAEAAENSLLSY
PLK1 site
B
PP
PPS538A
PLK1
P-538
PrimPol
C
HEK-293
ΔPP-1 + PP
RPE1
PLK1-as
BI2536
3-MB-PP1
P - S538
PrimPol
Ponceau
D
ΔPP-1 + PP
0 2 4 6 8 10 14 Release (hrs)
P-S538
PrimPol
Cyclin A
P-TCTP
Tubulin
E
% Spreads with 1+ break
Parental
ΔPP-1
+PP
+PPS538A
+PPS538E
Undamaged
Olaparib
CPT
BI2536
AS
0
2
4
6
8
10
14
PI

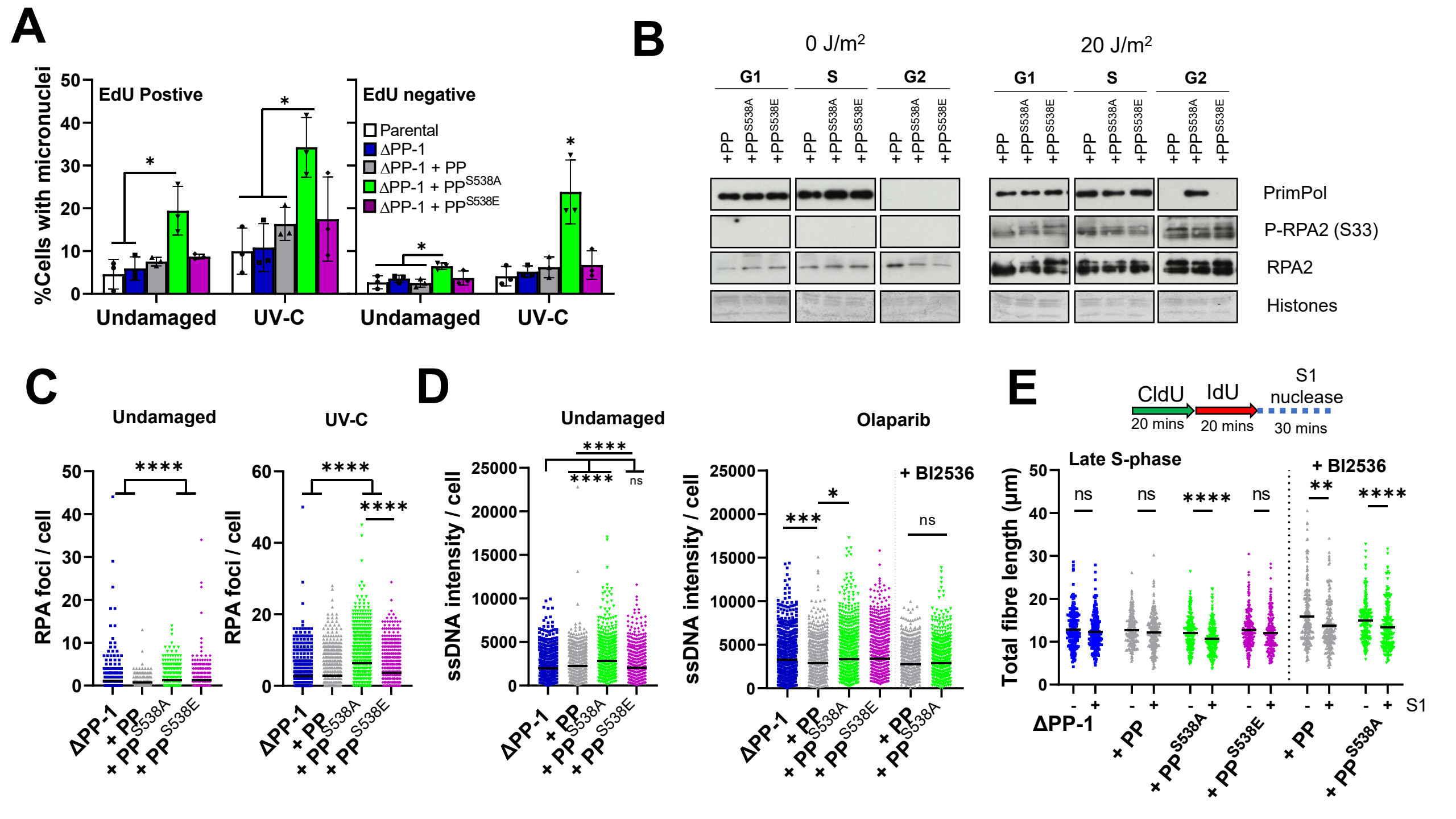
A
EdU Postive
EdU negative
%Cells with micronuclei
Parental
ΔPP-1
ΔPP-1 + PP
ΔPP-1 + PP S538A
ΔPP-1 + PP S538E
Undamaged
UV-C
Undamaged
UV-C
B
0 J/m2
20 J/m2
G1
S
G2
+PP
+PP S538A
+PP S538E
PrimPol
P-RPA2 (S33)
RPA2
Histones
C
Undamaged
UV-C
RPA foci / cell
D
Undamaged
Olaparib
+ BI2536
ssDNA intensity / cell
E
CldU
IdU
S1 nuclease
20 mins
20 mins
30 mins
Late S-phase
+ BI2536
Total fibre length (μm)
S1

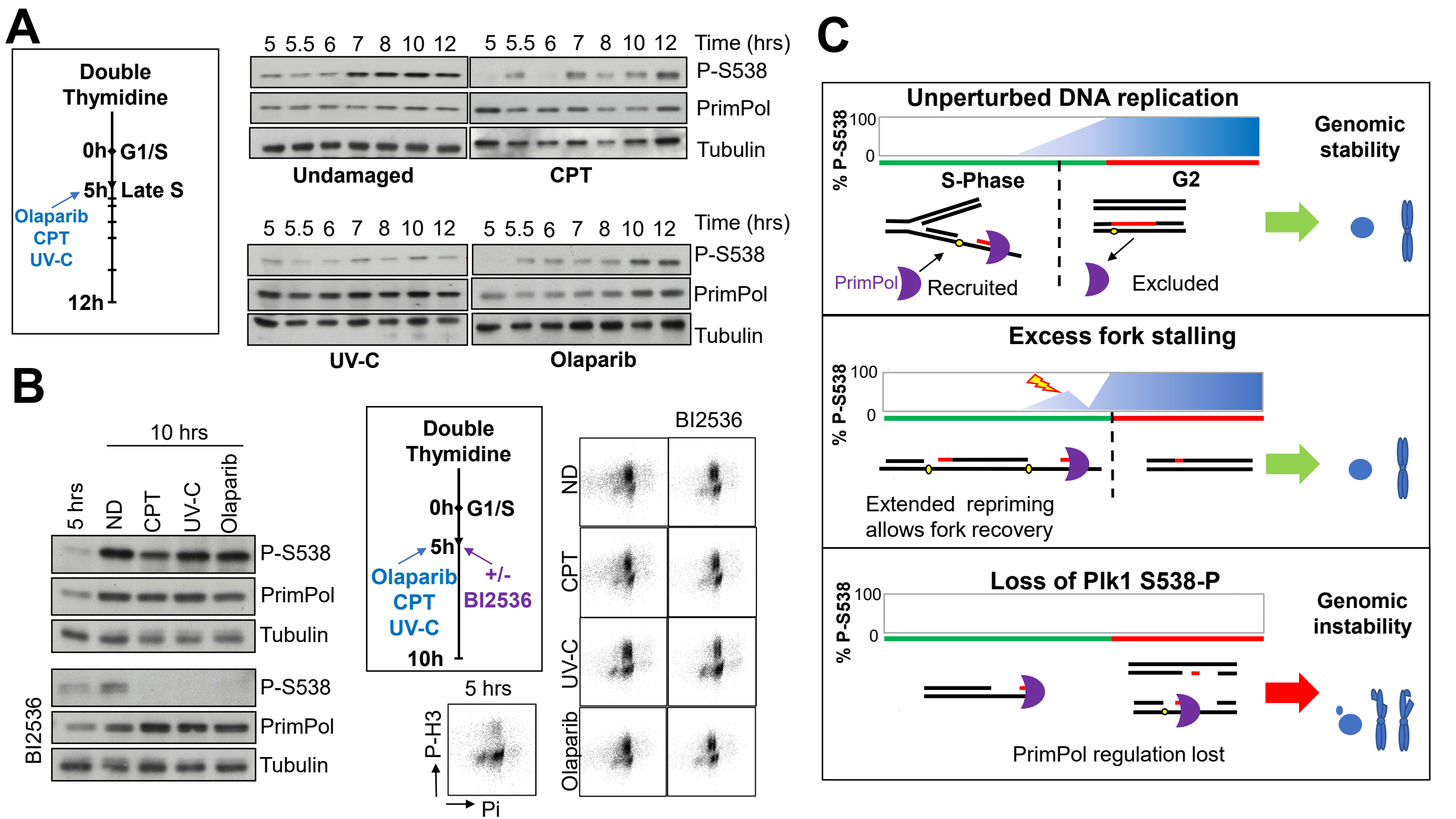
A
Double Thymidine
0h G1/S
5h Late S
Olaparib
CPT
UV-C
12h
5 5.5 6 7 8 10 12
Time (hrs)
P-S538
PrimPol
Tubulin
Undamaged
CPT
UV-C
Olaparib
B
10 hrs
5 hrs
ND
CPT
UV-C
Olaparib
BI2536
Double Thymidine
0h G1/S
5h
Olaparib
CPT
UV-C
+/-
BI2536
10h
5 hrs
P-H3
Pi
C
Unperturbed DNA replication
% P-S538
100
0
S-Phase
G2
Genomic stability
PrimPol
Recruited
Excluded
Excess fork stalling
Extended repriming
allows fork recovery
Loss of Plk1 S538-P
Genomic instability
PrimPol regulation lost

Supplementary Materials for

PLK1 regulates the PrimPol damage tolerance pathway during the cell cycle

Laura J. Bailey, Rebecca Teague, Peter Kolesar, Lewis J. Bainbridge,

Howard D. Lindsay & Aidan J. Doherty*

* Corresponding author: ajd21@sussex.ac.uk

The PDF file includes:
Supplementary Figs. S1 to S10
Tables S1 and S2

Figure S1

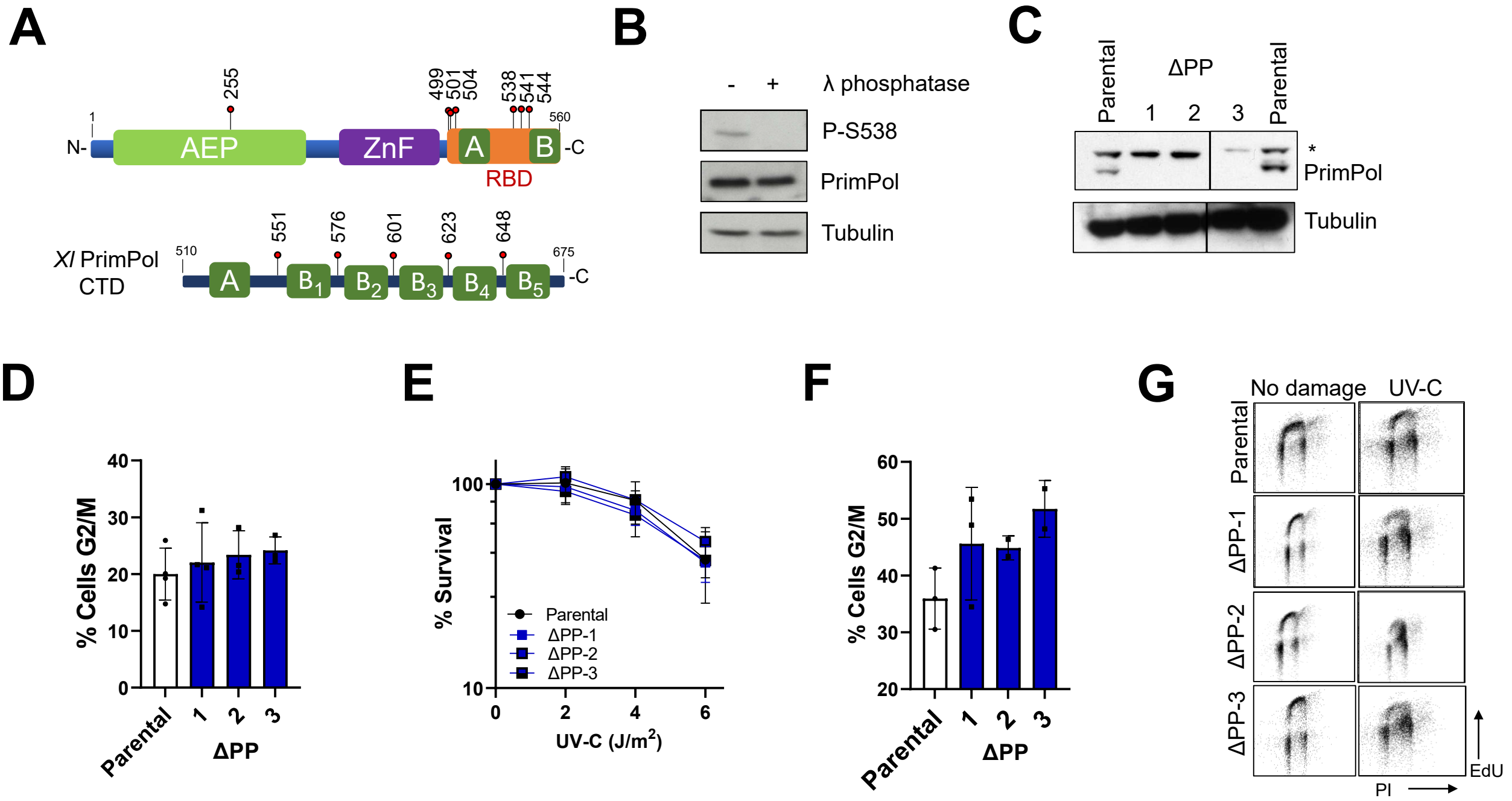
A
255
499
501
504
538
541
544
1
560
N-
AEP
ZnF
A
B
-C
RBD
Xl PrimPol
CTD
510
551
576
601
623
648
675
A
B1
B2
B3
B4
B5
-C
B
- + λ phosphatase
P-S538
PrimPol
Tubulin
C
Parental
ΔPP
1 2 3
Parental
*
PrimPol
Tubulin
D
% Cells G2/M
40
30
20
10
0
Parental 1 2 3
ΔPP
E
% Survival
100
10
0 2 4 6
UV-C (J/m2)
Parental
ΔPP-1
ΔPP-2
ΔPP-3
F
% Cells G2/M
60
50
40
30
20
Parental 1 2 3
ΔPP
G
No damage
UV-C
Parental
ΔPP-1
ΔPP-2
ΔPP-3
EdU
PI

Supplementary Figure 1. Generation and analysis of PrimPol knockout HEK 293 cells, ΔPP1-3, and a P-S538 antibody.

(**A**) Phosphorylation sites identified on human and the C-terminal domain (CTD) of *Xenopus laevis* PrimPol by mass spectrometry. (**B**) The specificity of the P-S538 peptide antibody was tested using western blotting of whole cell lysates treated or untreated with λ protein phosphatase. (**C**) Loss of PrimPol protein from individual clones was confirmed by western blotting of whole cell lysate using a total PrimPol antibody in relation to a tubulin total protein marker, * indicates a non-specific band. (**D**) Cell cycle populations were analysed by flow cytometry of PI and EdU labelled cells and figure shows proportion of cells in G2 in an asynchronous population. (**E**) UV-C sensitivity was measured in different clones by colony survival in comparison with parental HEK 293 cells. (**F**) Changes in recovery time after UV-C damage was analysed in parental and ΔPP cell lines by flow cytometry. G2 populations were quantified 24 hrs after 0 or 5 J/m^2 UV-C. Representative images shown and quantified in (**G)**.

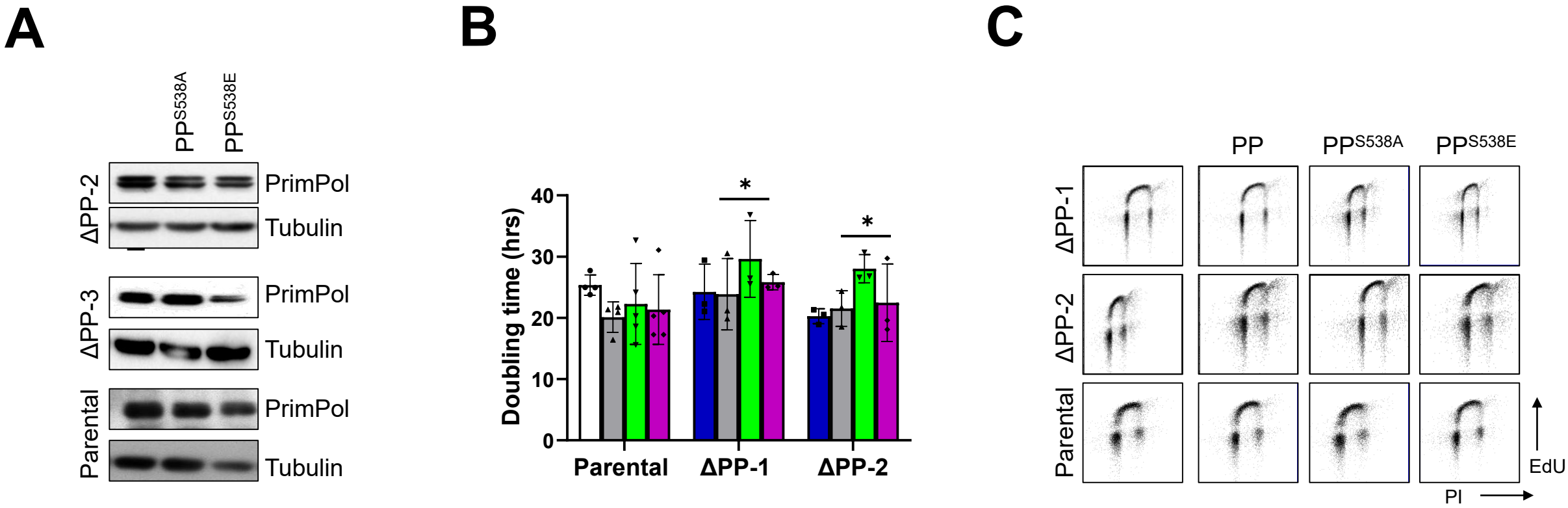
A
PPS538A
PPS538E
ΔPP-2
PrimPol
Tubulin
ΔPP-3
PrimPol
Tubulin
Parental
PrimPol
Tubulin
B
Doubling time (hrs)
40
30
20
10
0
*
*
Parental
ΔPP-1
ΔPP-2
C
PP
PPS538A
PPS538E
ΔPP-1
ΔPP-2
Parental
EdU
PI

Supplementary Figure 2. Expression of PrimPol in 293 ΔPP cells

Flag-tagged PrimPol was stably integrated into the HEK293 system using a doxycycline promoter with either no changes or S538A or S538E mutations. Expression was induced with 10 ng/ml doxycycline for 24 hrs and expression was compared in parental HEK293 and ΔPP cell lines by western blotting. (**A**) Growth rates of cell lines expressing different PrimPol constructs was analysed by counting cell numbers every 24 hrs to generate growth curves. (**B**) Figure shows average doubling times for n = 3 independent experiments. (**C)** Representative images from flow cytometry analyses to assess cell cycle in cells expressing different forms of PrimPol.

Figure S3

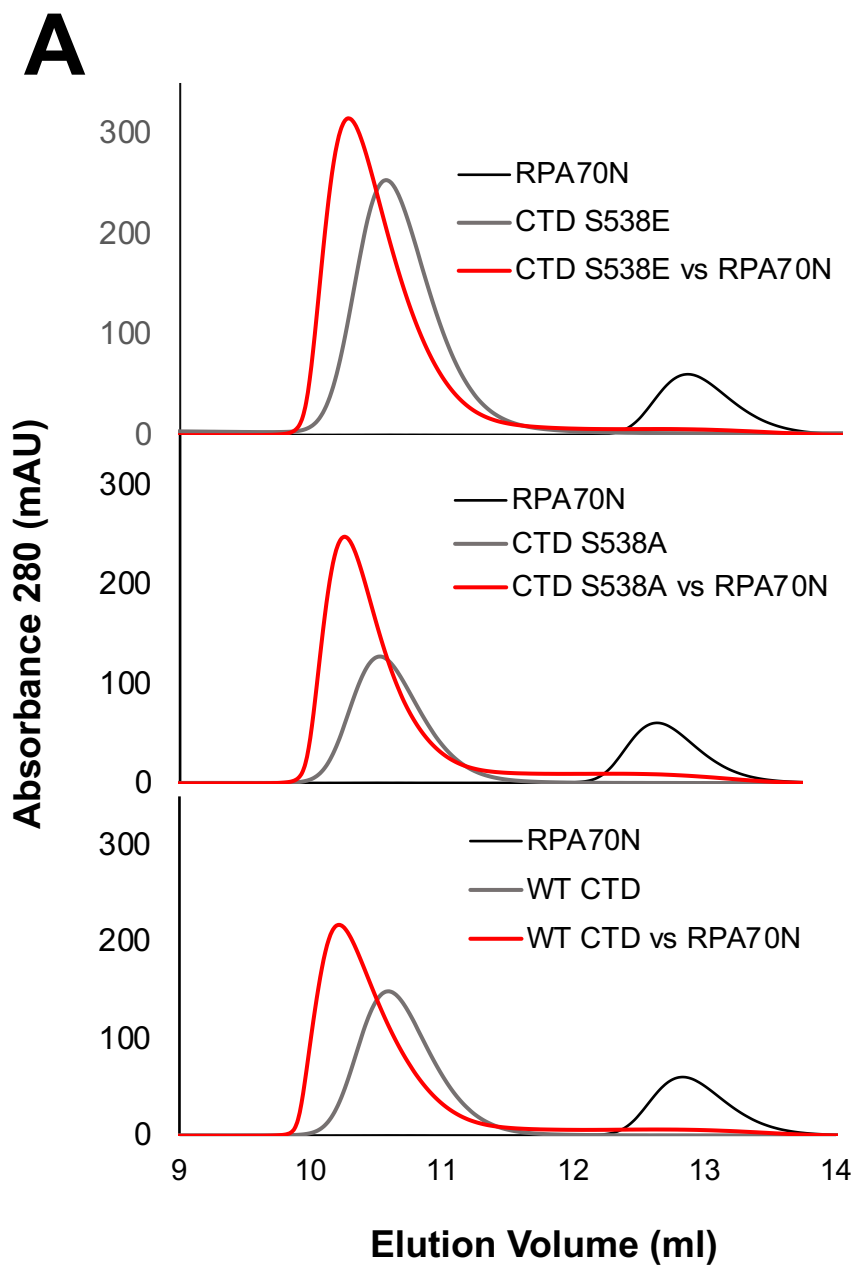
A
Absorbance 280 (mAU)
300
200
100
0
RPA70N
CTD S538E
CTD S538E vs RPA70N
RPA70N
CTD S538A
CTD S538A vs RPA70N
RPA70N
WT CTD
WT CTD vs RPA70N
9
10
11
12
13
14
Elution Volume (ml)

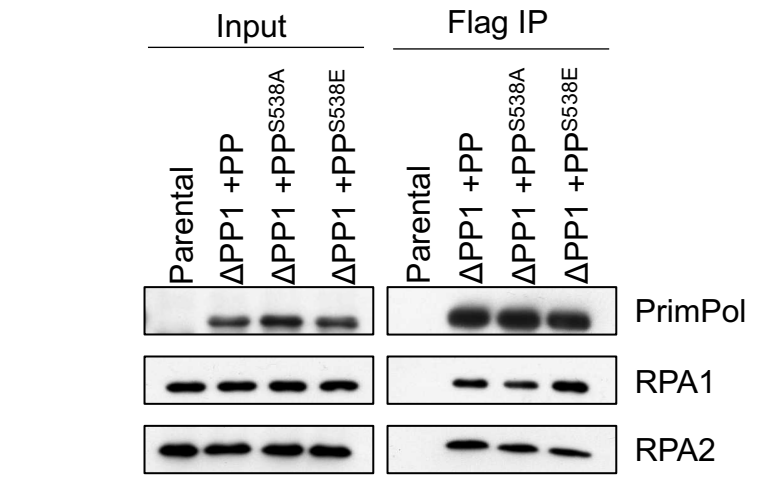
B
Input
Flag IP
Parental
ΔPP1 +PP
ΔPP1 +PPS538A
ΔPP1 +PPS538E
PrimPol
RPA1
RPA2

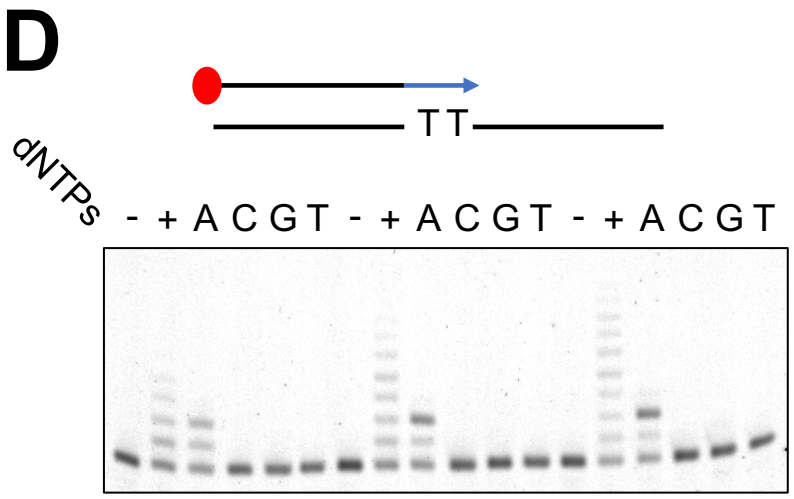
D
dNTPs
- + A C G T - + A C G T - + A C G T
T T

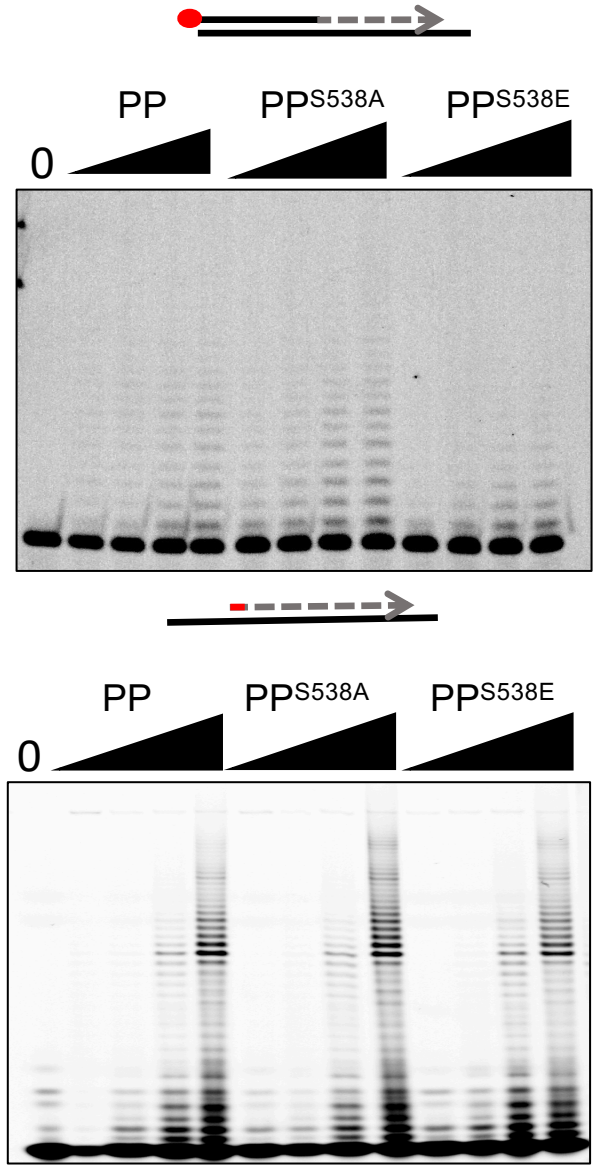
C
PP
PPS538A
PPS538E
0
PP
PPS538A
PPS538E
0

Supplementary Figure 3. PrimPol^{S538A} mutation does not affect RPA interaction or primase/polymerase activity.

(**A**) WT, S538A and S538E mutated PrimPol CTD were purified from *E.coli* and their interactions with RPA70N assessed by analytical gel filtration. (**B**) Proteins were immunoprecipitated from doxycycline induced ΔPP 293 cells, expressing flag-tagged PrimPol or parental with only endogenous protein, using flag magnetic beads and eluted proteins were analysed alongside input material by western blotting using antibodies specific to PrimPol and RPA. (**C**) PrimPol, PrimPol^{S538A} and PrimPol^{S538E} were purified from *E.coli* and polymerase (top panel) and primase (bottom panel) activities of the different proteins compared using fluorescently labelled primers or dNTPs. (**D**) Fidelity of PrimPol incorporation was analysed by looking at utilisation different dNTPs in polymerase extension of a DNA primer opposite TT nucleotides.

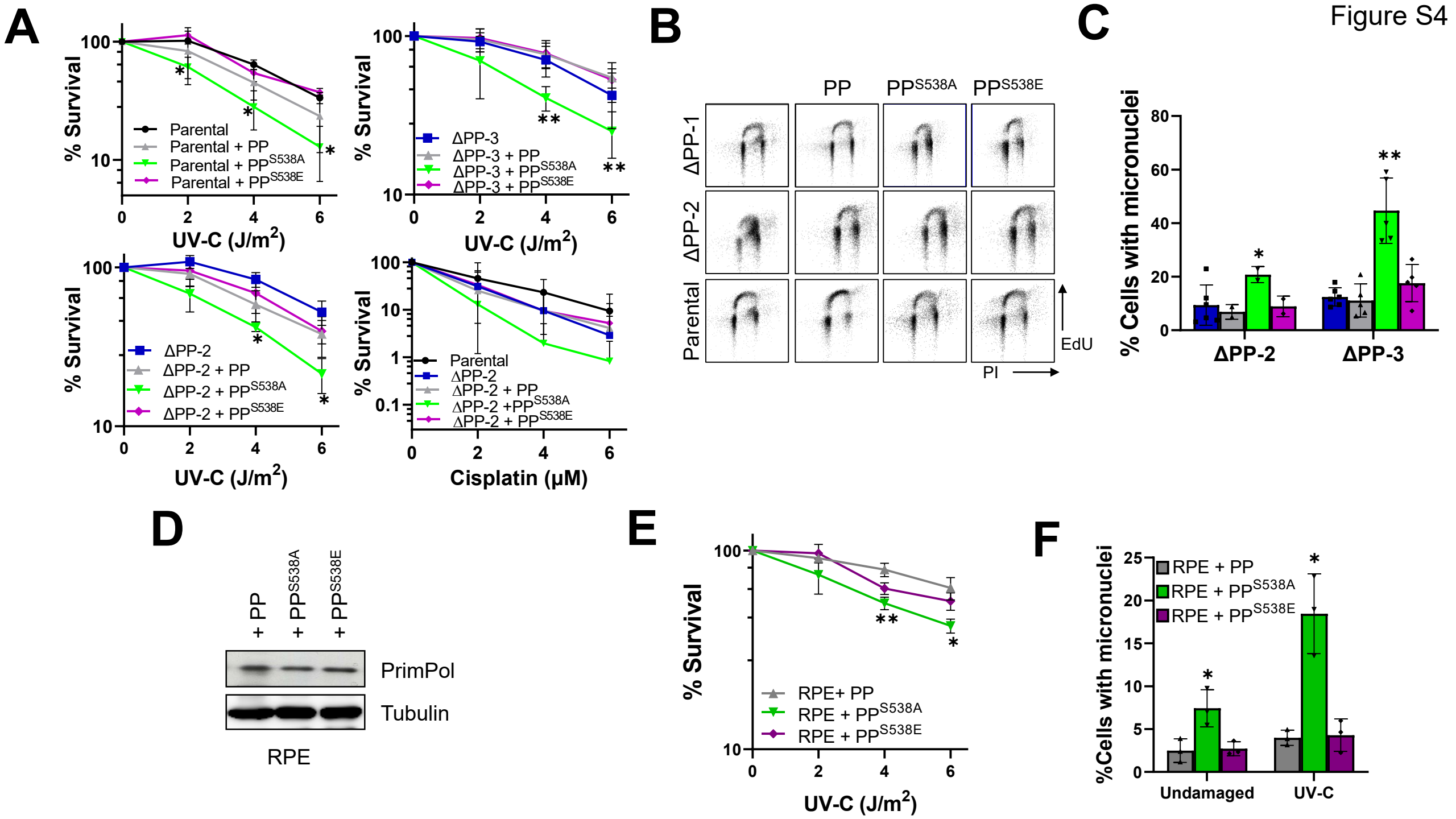
A
% Survival
UV-C (J/m2)
Parental
Parental + PP
Parental + PPS538A
Parental + PPS538E
ΔPP-3
ΔPP-3 + PP
ΔPP-3 + PPS538A
ΔPP-3 + PPS538E
ΔPP-2
ΔPP-2 + PP
ΔPP-2 + PPS538A
ΔPP-2 + PPS538E
Cisplatin (μM)
ΔPP-2 +PPS538A
B
PP
PPS538A
PPS538E
ΔPP-1
ΔPP-2
Parental
EdU
PI
C
% Cells with micronuclei
ΔPP-2
ΔPP-3
D
+ PP
+ PPS538A
+ PPS538E
PrimPol
Tubulin
RPE
E
RPE+ PP
RPE + PPS538A
RPE + PPS538E
F
%Cells with micronuclei
Undamaged
UV-C

Supplementary Figure 4. Expression of PrimPol^{S538A} effects cell survival and genomic stability.

(**A**) Cell survival was compared in additional cell lines expressing different PrimPol constructs in response to UV-C and cisplatin. (**B**) Representative data showing flow cytometry analysis of cells labelled with EdU and PI 24 hrs after 0 or 5 J/m^2 UV-C treatment, quantification shown in Fig. 2B. (**C**) Percentage of cells with 1 or more micronuclei, 48 hrs after 5 J/m^2 UV-C treatment, compared in different ΔPP clones expressing different PrimPol proteins. (**D**) Analysis of whole cell lysate from RPE cells showing expression of PrimPol by western blot. (**E**) Colony survival after UV-C damage in RPE cells expressing WT or mutant PrimPol. (**F**) After expression of WT or mutant PrimPols, percentage of cells containing micronuclei 48 hrs after treatment with 0 or 6 J/m^2 UV-C was analysed by DAPI staining and microscopy.

Figure S5

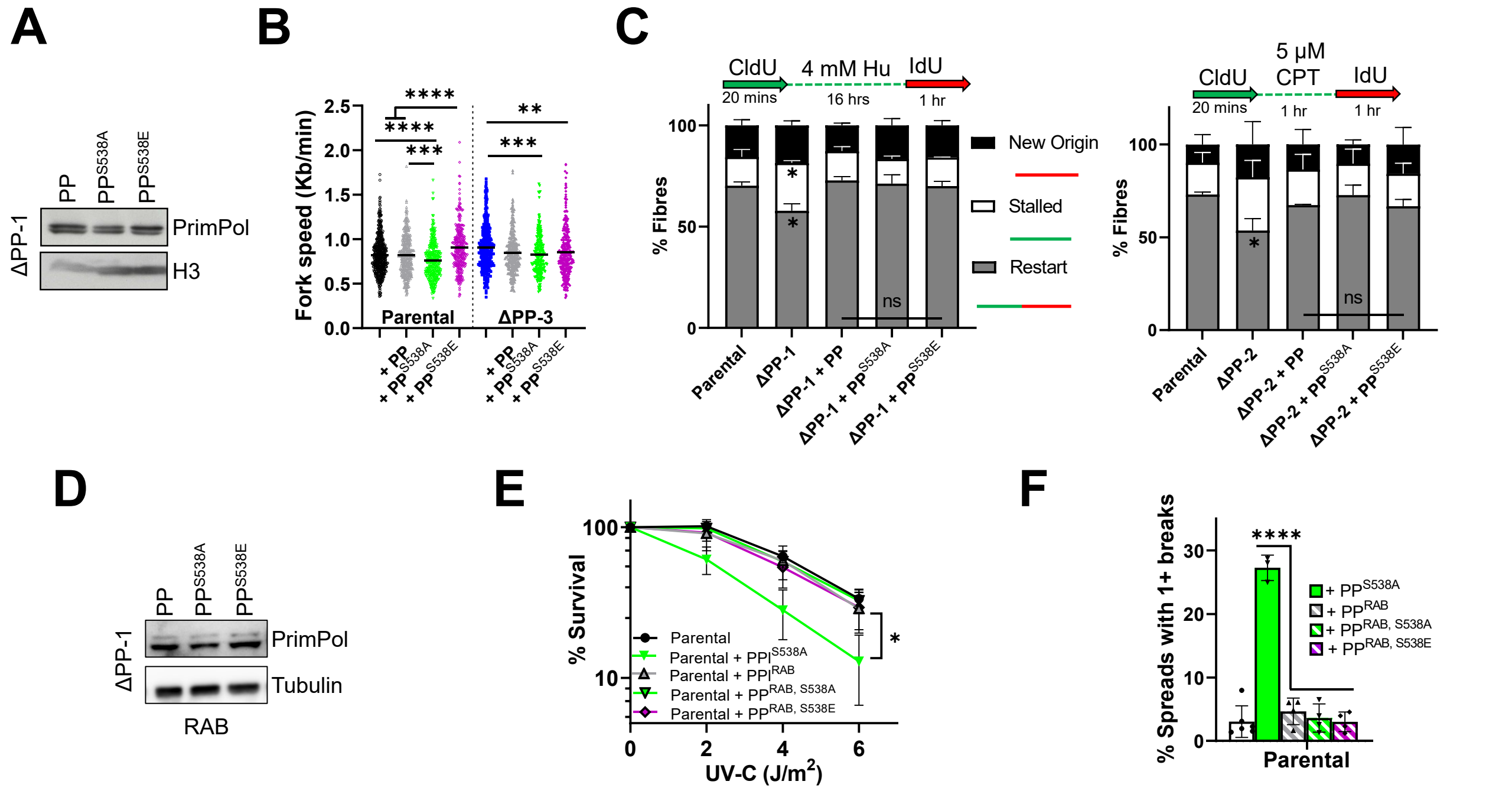
A
PP
PPS538A
PPS538E
ΔPP-1
PrimPol
H3
B
Fork speed (Kb/min)
Parental
ΔPP-3
+ PP
+ PPS538A
+ PPS538E
C
CldU
20 mins
4 mM Hu
16 hrs
IdU
1 hr
% Fibres
New Origin
Stalled
Restart
ns
Parental
ΔPP-1
ΔPP-1 + PP
ΔPP-1 + PPS538A
ΔPP-1 + PPS538E
5 μM
CPT
ΔPP-2
ΔPP-2 + PP
ΔPP-2 + PPS538A
ΔPP-2 + PPS538E
D
Tubulin
RAB
E
% Survival
UV-C (J/m2)
Parental + PPIS538A
Parental + PPIRAB
Parental + PPRAB, S538A
Parental + PPRAB, S538E
F
% Spreads with 1+ breaks
+ PPS538A
+ PPRAB
+ PPRAB, S538A
+ PPRAB, S538E

Supplementary Figure 5. PrimPol S538A mutation does not affect chromatin binding or fork restart and its toxicity is abolished by loss of RPA binding sites.

(**A**) Cells were treated with 20 J/m^2 and allowed to recover for 6 hrs before chromatin bound proteins were isolated and analysed by western blot. (**B**) Replication fork speed was analysed in additional ΔPP clones and parental cells. Forks were labelled with CldU and IdU for 20 mins each before being spread and labelled. Chart shows data from at least 300 fibres over 3 or more independent experiments, red line represents mean of data. (**C**) Fork restart after HU or CPT stalling was analysed by fibre analysis measuring the number of green only, stalled fibres, restarted, red and green or new origins, red only fibres. (**D**) Flag-tagged PrimPol carrying the RAB mutations alone or in combination with S538A or S538E were stably transfected into parental or ΔPP cells under a doxycycline inducible promoter. Protein was expressed for 24 hrs with 10 ng/ml doxycycline and whole cell extracts were analysed by western blot. (**E**) Parental cells were analysed for UV-C sensitivity when expressing $PrimPol^{RAB}$ mutants by colony survival and the occurrence of chromosome breaks in the absence of damage (**F**).

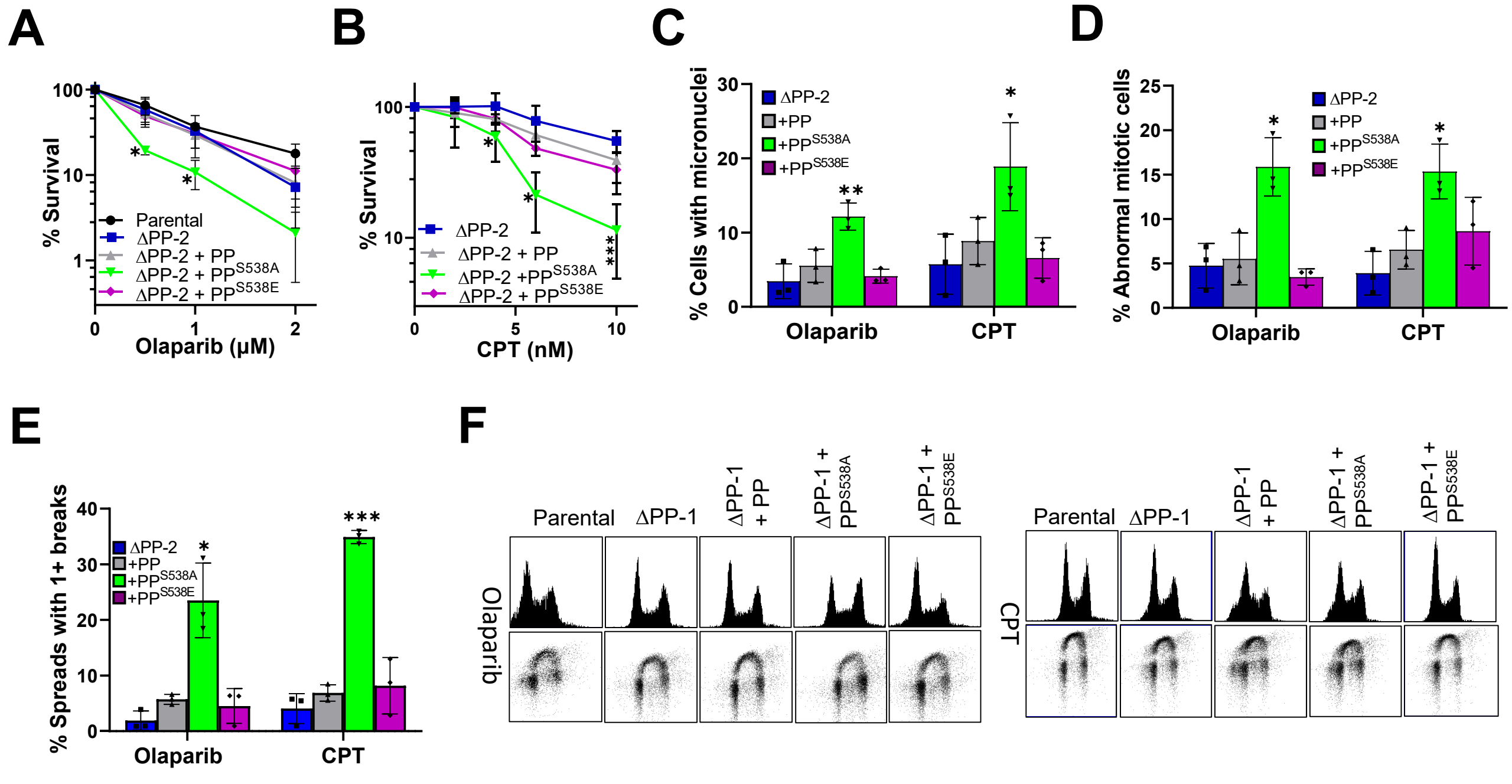
A
% Survival
Olaparib (μM)
Parental
ΔPP-2
ΔPP-2 + PP
ΔPP-2 + PPS538A
ΔPP-2 + PPS538E
B
% Survival
CPT (nM)
ΔPP-2
ΔPP-2 + PP
ΔPP-2 +PPS538A
ΔPP-2 + PPS538E
C
% Cells with micronuclei
ΔPP-2
+PP
+PPS538A
+PPS538E
Olaparib
CPT
D
% Abnormal mitotic cells
ΔPP-2
+PP
+PPS538A
+PPS538E
Olaparib
CPT
E
% Spreads with 1+ breaks
ΔPP-2
+PP
+PPS538A
+PPS538E
Olaparib
CPT
F
Parental
ΔPP-1
ΔPP-1 + PP
ΔPP-1 + PPS538A
ΔPP-1 + PPS538E
Olaparib
CPT

Supplementary Figure 6. PrimPol S538A mutation sensitises cells to olaparib and camptothecin.

Cell survival after olaparib (**A**) or camptothecin (**B**) was analysed in ΔPP-2 cells expressing different forms of PrimPol. Presence of micronuclei (**C)**, abnormal mitotic cells (**D**), and chromosome breaks (**E**)**,** 48 hrs after olaparib or camptothecin treatment was analysed in ΔPP-2 cells. (**F**) Examples of EdU, PI FACs profiles for cells treated with 2 μM olaparib or 10 nM camptothecin for 48 hrs and quantified in Fig. 3E.

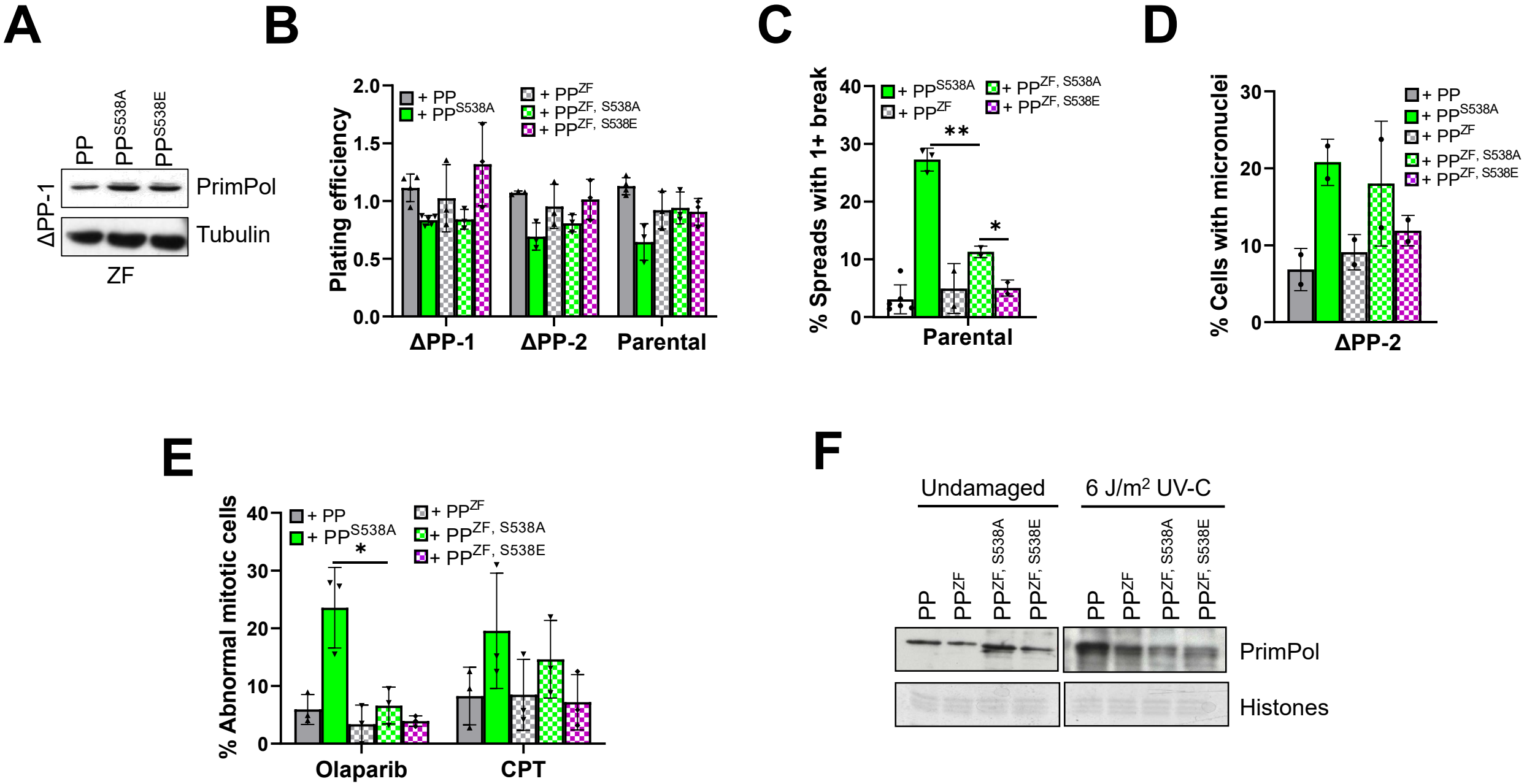
A
PP
PPS538A
PPS538E
ΔPP-1
PrimPol
Tubulin
ZF
B
Plating efficiency
2.0
1.5
1.0
0.5
0.0
+ PP
+ PPS538A
+ PPZF
+ PPZF, S538A
+ PPZF, S538E
ΔPP-1
ΔPP-2
Parental
C
% Spreads with 1+ break
40
30
20
10
0
+ PPS538A
+ PPZF
+ PPZF, S538A
+ PPZF, S538E
**
*
Parental
D
% Cells with micronuclei
30
20
10
0
+ PP
+ PPS538A
+ PPZF
+ PPZF, S538A
+ PPZF, S538E
ΔPP-2
E
% Abnormal mitotic cells
40
30
20
10
0
+ PP
+ PPS538A
+ PPZF
+ PPZF, S538A
+ PPZF, S538E
*
Olaparib
CPT
F
Undamaged
6 J/m2 UV-C
PP
PPZF
PPZF, S538A
PPZF, S538E
PrimPol
Histones

Supplementary Figure 7. Effects of ZF mutation on PrimPol^{S538A} toxicity.

(**A**) Flag-tagged PrimPol carrying ZF**,** mutations alone or in combination with S538A or S538E were stably transfected into Parental or ΔPP cells under a doxycycline inducible promoter. Protein was expressed for 24 hrs with 10 ng/ml doxycycline and whole cell extracts were analysed by western blot. (**B**) Plating efficiency was used to measure the effects of over expressing different forms of PrimPol in different cell clones. (**C**) Cells expressing PrimPol^{ZF} mutants were grown for 96 hrs before spreading and number of cells with 1 or more chromosome breaks were counted. Data is shown beside that shown previously for cells expressing WT PrimPol mutants. (**D**) Cells expressing PrimPol^{ZF} variants were analysed for percentage with 1 or more micronuclei 48 hrs after 5 J/m^2 UV-C in relation to WT PrimPol mutants shown previously. (**E**) Abnormal mitotic cells were analysed 48 hrs after the addition of camptothecin or olaparib in cells expressing PrimPol^{Zn} in comparison to WT PrimPol. (**F**) Cells expressing PrimPol were treated with 0 or 20 J/m^2 UV-C and allowed to recover for 6 hrs before isolation of chromatin bound proteins and analysis by western blotting.

Figure S8

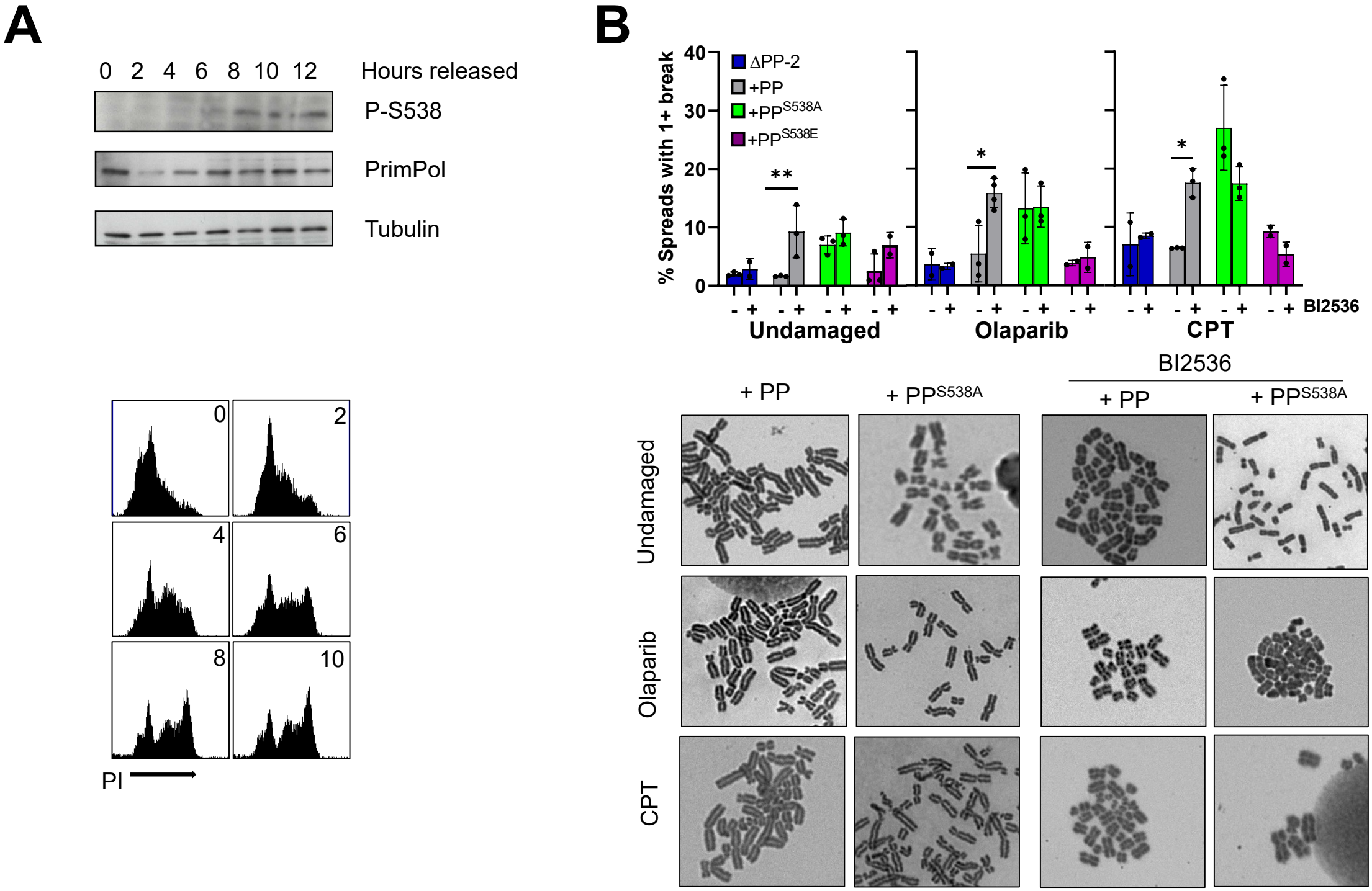
A
0 2 4 6 8 10 12
Hours released
P-S538
PrimPol
Tubulin
0
2
4
6
8
10
PI
B
% Spreads with 1+ break
ΔPP-2
+PP
+PPS538A
+PPS538E
**
*
*
- + - + - + - + - + - + - + - + - + - +
BI2536
Undamaged
Olaparib
CPT
BI2536
+ PP
+ PPS538A
+ PP
+ PPS538A
Undamaged
Olaparib
CPT

Supplementary Figure 8. PrimPol phosphorylation is cell cycle regulated and becomes toxic in the absence of PLK1.

(**A**) RPE cells expressing PrimPol were synchronised by double thymidine block before being released into nocodazole. Cell cycle progression was monitored by Facs, lower panel, and the same samples were analysed by western blot for changes in 538 phosphorylation and total PrimPol, alongside tubulin. (**B**) PLK1-dependent toxicity was confirmed in a second clone. Cells were released from a double thymidine block into media containing nocodazole with or without PLK1 inhibitor and camptothecin, olaparib, UV-C or undamaged. After 10 hrs mitotic cells were collected and analysed for chromosome breaks, representative images shown below.

Figure S9

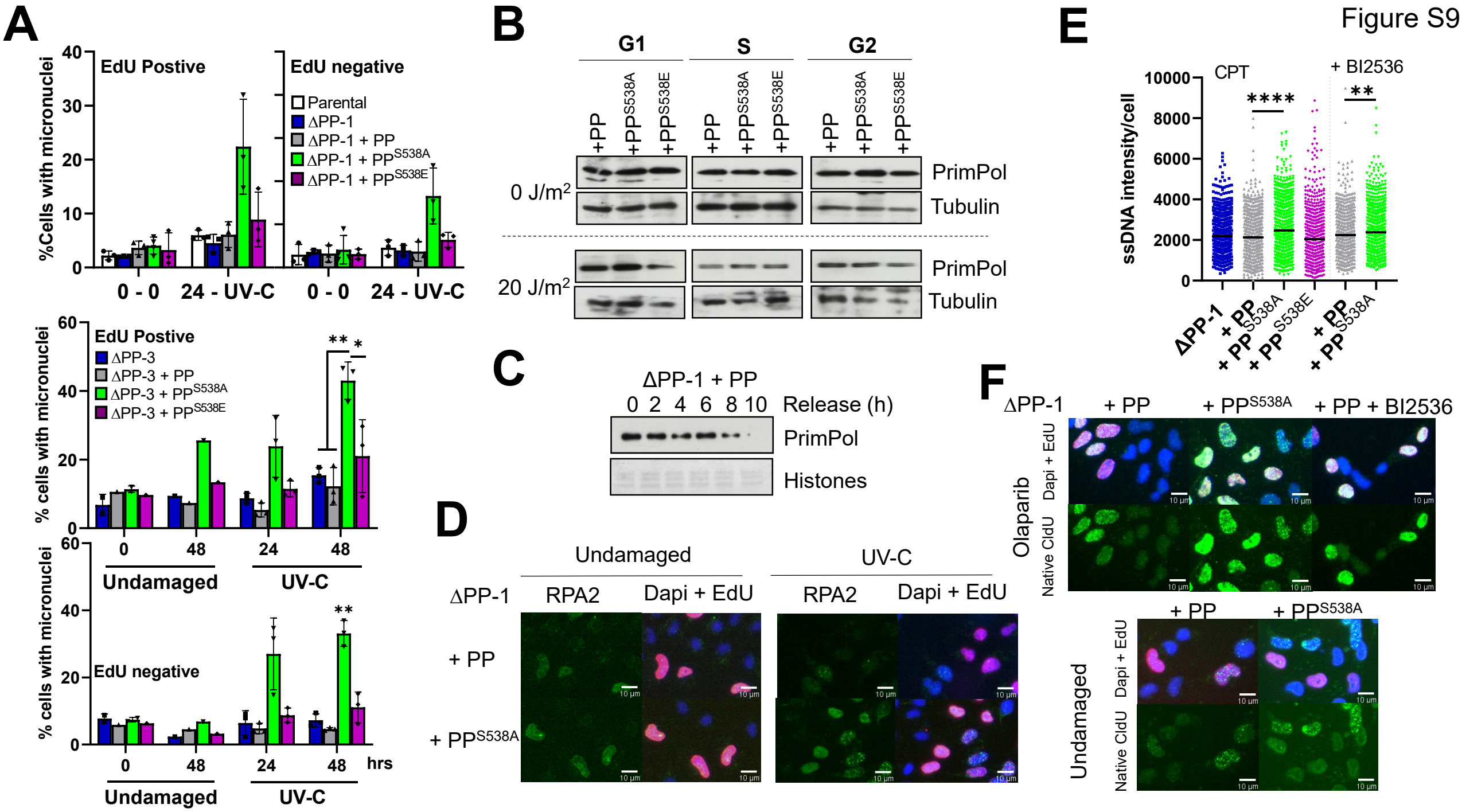
A
%Cells with micronuclei
EdU Postive
EdU negative
Parental
ΔPP-1
ΔPP-1 + PP
ΔPP-1 + PP^S538A
ΔPP-1 + PP^S538E
0 - 0
24 - UV-C
0 - 0
24 - UV-C
% cells with micronuclei
EdU Postive
ΔPP-3
ΔPP-3 + PP
ΔPP-3 + PP^S538A
ΔPP-3 + PP^S538E
**
*
0
48
24
48
Undamaged
UV-C
% cells with micronuclei
EdU negative
**
0
48
24
48
hrs
Undamaged
UV-C
B
G1
S
G2
+PP
+PP^S538A
+PP^S538E
0 J/m2
PrimPol
Tubulin
20 J/m2
PrimPol
Tubulin
C
ΔPP-1 + PP
0 2 4 6 8 10 Release (h)
PrimPol
Histones
D
Undamaged
UV-C
ΔPP-1
RPA2
Dapi + EdU
RPA2
Dapi + EdU
+ PP
+ PP^S538A
10 μm
E
CPT
+ BI2536
ssDNA intensity/cell
10000
8000
6000
4000
2000
0
****
**
ΔPP-1
+ PP
+ PP^S538A
+ PP^S538E
+ PP
+ PP^S538A
F
ΔPP-1
+ PP
+ PP^S538A
+ PP + BI2536
Olaparib
Dapi + EdU
Native CldU
+ PP
+ PP^S538A
Undamaged
Dapi + EdU
Native CldU
10 μm

Supplementary Figure 9. Unphosphorylated PrimPol is toxic outside of S-phase and leads to increased ssDNA. (**A**) To analyse the effect of UV-C on different cell cycle stages, ΔPP-1 or ΔPP-3 cells were labelled with EdU followed by 0 or 5 J/m^2 UV-C. Cells either, EdU positive or negative, were analysed for the presence of 1 or more micronuclei, immediately after damage, 24 or 48 hrs later. (**B**) whole cell blots from the chromatin samples shown in Fig. 6B. (**C**) Chromatin association of PrimPol was monitored across the cell cycle. ΔPP-1 cells expressing PrimPol were synchronised by double thymidine block and were released to progress through the cell, samples were collected and chromatin associated PrimPol was analysed by western blot alongside histones. (**D**) Representative images showing RPA foci, quantified in Fig. 6C. (**E**) Quantification of native ssDNA signal after 2 hrs treatment with 50 nM camptothecin with or without BI2536. (**F**) Representative images of native CldU staining for ssDNA, quantified in Fig. 6D.

Figure S10

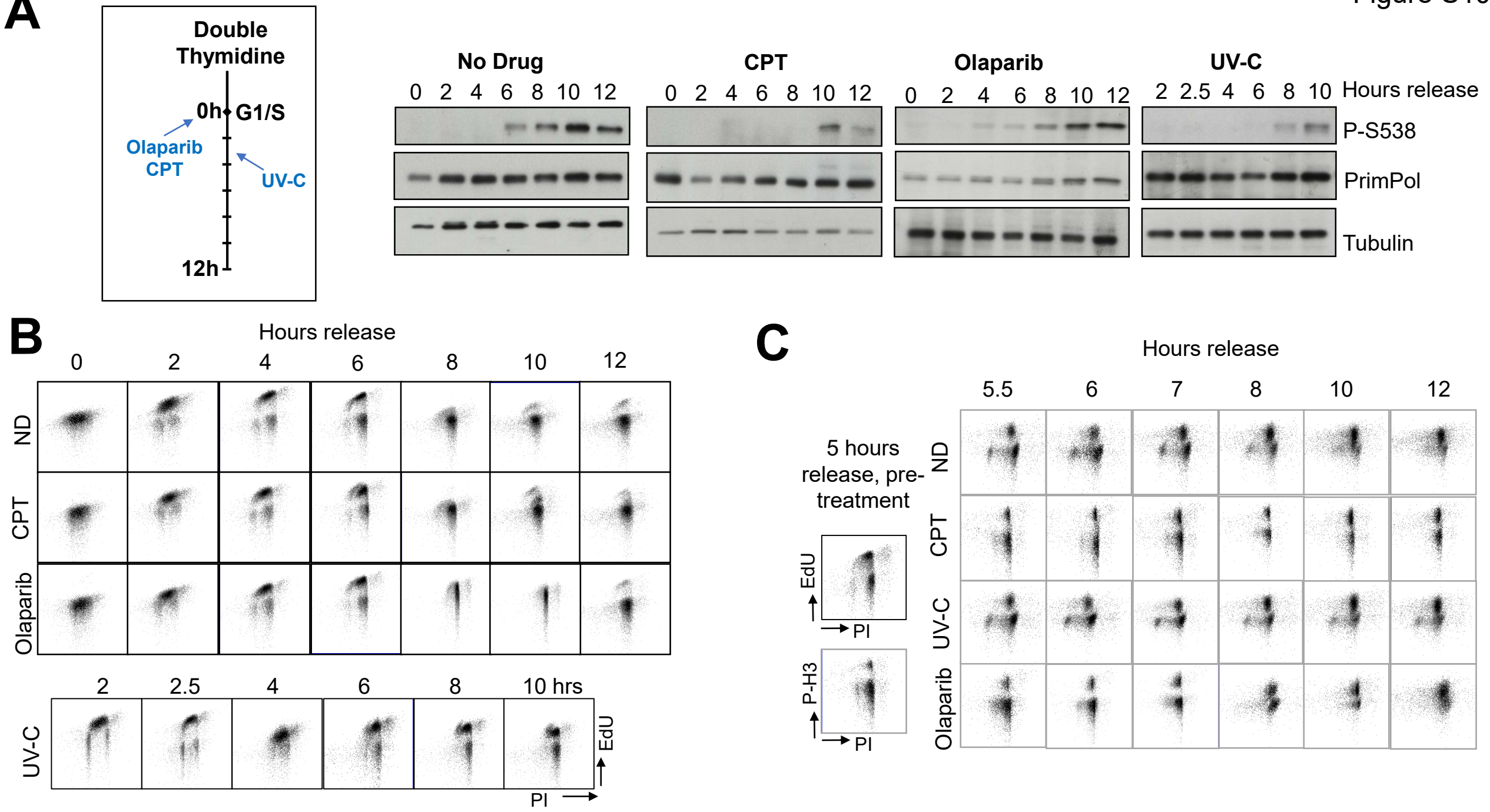
A
Double Thymidine
0h
G1/S
Olaparib
CPT
UV-C
12h
No Drug
CPT
Olaparib
UV-C
0 2 4 6 8 10 12
2 2.5 4 6 8 10
Hours release
P-S538
PrimPol
Tubulin
B
Hours release
0 2 4 6 8 10 12
ND
CPT
Olaparib
2 2.5 4 6 8 10 hrs
UV-C
EdU
PI
C
Hours release
5.5 6 7 8 10 12
5 hours release, pre-treatment
EdU
PI
P-H3
PI
ND
CPT
UV-C
Olaparib

Supplementary Figure 10. PrimPol S538 phosphorylation is tightly linked with cell cycle procession.

(**A**) Cells were released from a double thymidine block into media containing nocodazole and either immediately treated with olaparib or camptothecin or UV-C irradiated 2 hrs later. Samples were collected over the following 12 hrs and whole cell lysate was analysed by western blot to assess changes in phosphorylation levels. (**B**) Cells were also labelled with Edu and analysed by flow cytometry follow the progression through the cell cycle. (**C**) P-H3 labelling and flow cytometry were used to follow entry of cells into mitosis in synchronised cells where damage was administered at 5 hrs, western blot Fig. 7A.

Table S1 : DNA primers used in this study

Name	Sequence (5'-3')
S538A fwd	CAGAGAACGCTCTTCTCAGTTATAACAGTGAAGTG
S538A rev	CTGAGAAGAGCGTTCTCTGCAGCTTCAGC
S538E fwd	CAGAGAACGAGCTTCTCAGTTATAACAGTGAAGTG
S538E rev	CTGAGAAGCTCGTTCTCTGCAGCTTCAGC
ZN fwd	GTAAATATCGGTGGGCTGAAAACATTGGAAGAGCCGCTAAGAGTAATAATATAATG
Zn rev	CTCTTAGCGGCTCTTCCAATGTTTTCAGCCCACCGATATTTACAAATATCATAAACCAGTAATTC
RA fwd	GGCATTGATCGTGCTTATGCTTTAGAAGCTACTGAAGATGC
RA rev	GCTTCTAAAGCATAAGCACGATCAATGCCATTATCCCAGAC
RB fwd	GAAATTCCTCGTGAACTAGCTATAGAAGTATTACAAGAG
RB rev	CTTCTATAGCTAGTTCACGAGGAATTTCATCCACTTCAC
KO1 fwd	ATGAATAGAAAATGGGAAGCAAAACTG
KO1 rev	GCTTGTCGATGAAATAGTCTCCAGATG
KO2 fwd	GCTTGGCAGTGAAGATGATGATAGC
KO2 rev	GCTTCTCTCCCATGTTATTCTTCACAAC
PP SB fwd	GAAAGGCCTCTGAGGCCACCATGAATAGAAAATGGGAAGC
PP SB rev	ATCTTATCATGTCTATCGATCTACTCTTGTAATACTTCTATAATTAGTTC

Table S2: Antibodies used in this study

Antibody	**Supplier**
Rabbit anti - PrimPol	(*6*)
Rabbit anti - PrimPol	Antibodie Genie (#PACO0022224-100)
Rabbit anti - PrimPol P-S538	Eurogentech- this publication
Mouse anti - tubulin	Merck (T5168)
Rabbit anti - H3	Abcam (ab1791)
Rat anti - P-H3 (HTA28)	Abcam (ab10543)
Rat anti-BrdU [BU1/75 (ICR1)]	Abcam (ab6326)
Mouse anti-BrdU Clone B44	BD (347580)
Mouse anti – RPA1	Calbiochem (Na 13)
Mouse anti - RPA2	Calbiochem (Na 18)
Rabbit anti-P(S33)RPA2	Novus Biologicals (NB100-544)
Mouse anti-Cyclin A2	Abcam (ab16720)
Rabbit anti-P(S46)TCTP	Cell Signalling #5251
Anti - rabbit HRP	Abcam (ab6721)
Anti - mouse HRP	Abcam (ab6728)
anti-mouse Alexa Fluor 594	Invitrogen Molecular Probes (A31624)
anti-mouse Alexa Fluor 488	Invitrogen Molecular Probes (A31620)
anti-rat Alexa Fluor 488	Invitrogen Molecular Probes (A21208)